

FILE HISTORY

US 5,880,976

PATENT: 5,880,976

INVENTORS: DiGioia III, Anthony M.  
Simon, David A.  
Jaramaz, Branislav  
Blackwell, Michael K.  
Morgan, Frederick M.  
O'Toole, Robert V.  
Kanade, Takeo

TITLE: Apparatus and method for facilitating the  
implantation of artificial components in  
joints

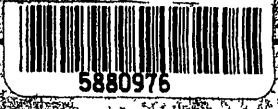
APPLICATION NO: US1997803993A

FILED: 21 FEB 1997

ISSUED: 09 MAR 1999

COMPILED: 03 SEP 2014

5880976



UTILITY SERIAL NUMBER: 364  
PATENT DATE: MAR 09 1998  
PATENT NUMBER: 5880976

SERIAL NUMBER: 364  
FILING DATE: [blank]  
CLASS: [blank]  
SUBCLASS: 516  
GROUP ART UNIT: 2763  
EXAMINER: FRED

APPLICANTS: [faded text]  
RF / [signature]

Foreign priority claimed 35 USC 119 conditions met:  yes  no  
Verified and Acknowledged: [initials]  
AS FILED: [arrow]  
STATE OR COUNTRY: [blank]  
SHEETS DRWGS: [blank]  
TOTAL CLAIMS: [blank]  
INDEP CLAIMS: [blank]  
FILING FEE RECEIVED: [blank]  
ATTORNEY'S DOCKET NO: [blank]

ADDRESS: [faded text]

TITLE: [faded text]

U S DEPT OF COMM./PAT & TM—PTO-436L (Rev 12-84)

PARTS OF APPLICATION FILED SEPARATELY		Patsy Harrod Applications Examiner	
NOTICE OF ALLOWANCE MAILED		CLAIMS ALLOWED	
6-24-98		Total Claims	Print Claim
Russell W FRED Assistant Examiner		24	1
ISSUE FEE: A-S GROUP-2700		DRAWING	
Amount Due	Date Paid	Sheets Drwg	Figs Drwg
660.00	9/29/98	10/11	20
Label Area		ISSUE BATCH NUMBER: F89	
PREPARED FOR ISSUE		VINCENT N. TRANS PRIMARY EXAMINER [Signature] Primary Examiner	
WARNING: The information disclosed herein may be restricted. Unauthorized disclosure may be prohibited by the United States Code Title 35 Sections 122, 181, and 368. Possession outside the U.S. Patent & Trademark Office is restricted to authorized employees and contractors only.			

ISSUE FEE IN FILE

Form PTO-436A (Rev 8/92)

SCANNED  
RF  
KOB

5,880,976

**APPARATUS AND METHOD FOR FACILITATING THE IMPLANTATION OF  
ARTIFICIAL COMPONENTS IN JOINTS**

**Transaction History**

<b>3/24/1997</b>	<b>Initial Exam Team nn</b>
<b>6/5/1997</b>	<b>Notice Mailed Application Incomplete Filing Date Assigned</b>
<b>9/8/1997</b>	<b>Application Is Now Complete</b>
<b>9/12/1997</b>	<b>Application Dispatched from OIPE</b>
<b>9/12/1997</b>	<b>IFW Scan &amp; PACR Auto Security Review</b>
<b>11/4/1997</b>	<b>Case Docketed to Examiner in GAU</b>
<b>5/13/1998</b>	<b>Case Docketed to Examiner in GAU</b>
<b>6/24/1998</b>	<b>Mail Notice of Allowance</b>
<b>6/24/1998</b>	<b>Notice of Allowance Data Verification Completed</b>
<b>9/22/1998</b>	<b>Issue Fee Payment Verified</b>
<b>9/22/1998</b>	<b>Mailroom Date of Drawing(s)</b>
<b>9/30/1998</b>	<b>Application Ordered to Match Drawing(s)</b>
<b>9/30/1998</b>	<b>Drawing(s) Received at Publications</b>
<b>12/14/1998</b>	<b>Application Received to Match Drawing(s)</b>
<b>12/14/1998</b>	<b>Preexamination Location Change</b>
<b>12/23/1998</b>	<b>Drawing(s) Matched to Application</b>
<b>12/29/1998</b>	<b>Drawing(s) Processing Completed</b>
<b>2/1/1999</b>	<b>Issue Notification Mailed</b>
<b>3/9/1999</b>	<b>Recordation of Patent Grant Mailed</b>
<b>10/7/1999</b>	<b>Applicant Has Filed a Verified Statement of Small Entity Status in Compliance with 37 CFR 1 27</b>

08/803993

APPROVED FOR LICENSE

PATENT APPLICATION



08803993

INITIALS: APR 0 1979

Date Entered or Counted

CONTENTS

Date Received or Mailed

	1	Application <u>1</u> papers	
	2	<u>1st- Dec</u>	<u>6/5/97</u>
	3	<u>Final Art</u>	<u>5/20/97</u>
	4	<u>McSES Quichy</u>	<u>8/5/97</u>
	5	<u>FDS</u>	<u>5-20-97</u>
<u>6-22</u>	6	<u>Notice of allowability</u>	<u>6-24-98</u>
	7	<u>Letter</u>	<u>6/25/98</u>
<u>12/21/98</u>	8	<u>Formal Drawing (11 sheets) set 1</u>	<u>9/22/98</u>
	9	<u>PTO GRANT MAR 09 1998</u>	
	10	<u>Small entity status</u>	
	11		
	12		
	13		
	14		
	15		
	16		
	17		
	18		
	19		
	20		
	21		
	22		
	23		
	24		
	25		
	26		
	27		
	28		
	29		
	30		
	31		
	32		

(FRONT)



PATENT NUMBER		ORIGINAL CLASSIFICATION	
		CLASS 364	SUBCLASS 5.78
APPLICATION SERIAL NUMBER 08/803,993		CROSS REFERENCE(S)	
APPLICANT'S NAME (PLEASE PRINT) DIGIOTA III ET AL		CLASS 623	SUBCLASS 22 (ONE SUBCLASS PER BLOCK)
IF REISSUE ORIGINAL PATENT NUMBER			
INTERNATIONAL CLASSIFICATION			
A61F		2 B2	
A61F		2 B4	
A61F		2 B6	
		2.763	
GROUP ART UNIT		ASSISTANT EXAMINER (PLEASE STAMP OR PRINT FULL NAME) RUSSELL W. FRED	
		PRIMARY EXAMINER (PLEASE STAMP OR PRINT FULL NAME) VINCENT N. TRAVIS	

PTO 270  
(REV 5-81)

ISSUE CLASSIFICATION SLIP

U.S. DEPARTMENT OF COMMERCE  
PATENT AND TRADEMARK OFFICE

Staple Issue Slip Here

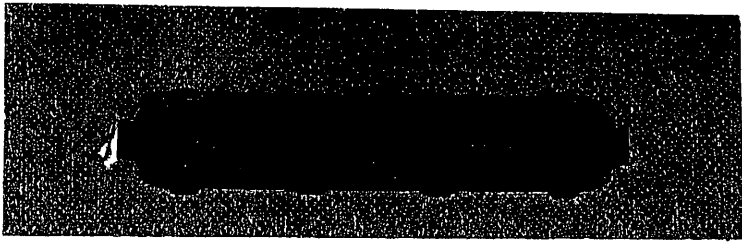
POSITION	ID NO	DATE
CLASSIFIER	32	4/11/97
EXAMINER	704	6-3
TYPIST	704	6-3
VERIFIER		
CORPS CORR		
SPEC HAND		
FILE MAINT		
DRAFTING		

INDEX OF CLAIMS

Claim		Date			
Final	Original				
1	1				
2	2				
3	3				
4	4				
5	5				
6	6				
7	7				
8	8				
9	9				
10	10				
11	11				
12	12				
13	13				
14	14				
15	15				
16	16				
17	17				
18	18				
19	19				
20	20				
21	21				
22	22				
23	23				
24	24				
25					
26					
27					
28					
29					
30					
31					
32					
33					
34					
35					
36					
37					
38					
39					
40					
41					
42					
43					
44					
45					
46					
47					
48					
49					
50					

Claim		Date			
Final	Original				
	51				
	52				
	53				
	54				
	55				
	56				
	57				
	58				
	59				
	60				
	61				
	62				
	63				
	64				
	65				
	66				
	67				
	68				
	69				
	70				
	71				
	72				
	73				
	74				
	75				
	76				
	77				
	78				
	79				
	80				
	81				
	82				
	83				
	84				
	85				
	86				
	87				
	88				
	89				
	90				
	91				
	92				
	93				
	94				
	95				
	96				
	97				
	98				
	99				
	100				

SYMBOLS  
 ✓ Rejected  
 = Allowed  
 (Through numeral) Canceled  
 + Restricted  
 N Non-elected  
 I Interference  
 A Appeal  
 O Objected



漢

SEARCHED			
Class	Sub	Date	Exmr
344	578	6/11/98	RF
606	86		
{	89		
{	90		
{	91		
623	11		
{	22		
{	23		

SEARCH NOTES		
	Date	Exmr
APS SEARCH	6/11/98	RF
TELE SEARCH	6/11/98	RF

INTERFERENCE SEARCHED			
Class	Sub	Date	Exmr
344	578	6/12/98	RF
623	22		



US005880976A

United States Patent [19]  
DiGioia III et al

[11] Patent Number 5,880,976  
[45] Date of Patent Mar 9, 1999

[54] APPARATUS AND METHOD FOR FACILITATING THE IMPLANTATION OF ARTIFICIAL COMPONENTS IN JOINTS  
[75] Inventors Anthony M DiGioia III Pittsburgh Pa David A Simon Boulder Colo Branislav Jaramaz Michael K Blackwell both of Pittsburgh Pa Frederick M Morgan Quincy Robert V O'Toole Brookline both of Mass Takeo Kanade Pittsburgh Pa

[73] Assignee Carnegie Mellon University Pittsburgh Pa

[21] Appl No 803,993

[22] Filed Feb 21, 1997

[51] Int Cl<sup>6</sup> A61F 2/32 A61F 2/34 A61F 2/36

[52] U S Cl 364/578 623/22

[58] Field of Search 364/578 606/86 606/89 90 91 623/11 22 23

[56] References Cited

U S PATENT DOCUMENTS

4 341 220	7/1982	Perry	128/630
4 905 148	2/1990	Crawford	364/413 1
5 007 936	4/1991	Woolson	623/23
5 086 401	2/1992	Glassman et al	395/94
5 242 455	9/1993	Skeens et al	606/130
5 251 127	10/1993	Raab	364/413 13
5 299 288	3/1994	Glassman et al	395/80
5 305 203	4/1994	Raab	364/413 13
5 383 454	1/1995	Bucholz	128/653 1
5 389 101	2/1995	Heilbrun et al	606/130
5 408 409	4/1995	Glassman et al	364/413 13
5 517 990	5/1996	Kalfas et al	128/653 1

OTHER PUBLICATIONS

A M DiGioia M D D A Simon B Jaramaz M Blackwell F Morgan R V O Toole B Colgan E Kischell HipNav Pre-operative Planning and Intra-operative Navi

gational Guidance for Acetabular Implant Placement in Total Hip Replacement Surgery Proceeding of Computer Assisted Orthopedic Surgery Bern Switzerland (1996) Robert J Krushell M D Denis W Burke M D and Wilham H Harris M D Range of Motion in Contemporary Total Hip Arthroplasty pp 97-101 The Journal of Arthroplasty vol 6 No 2 Jun 1991 Robert J Krushell M D Dennis w Burke M D and Wilham H Harris M D Elevated-rim Acetabular Components pp 1-6 The Journal of Arthroplasty vol 6 Oct 1991

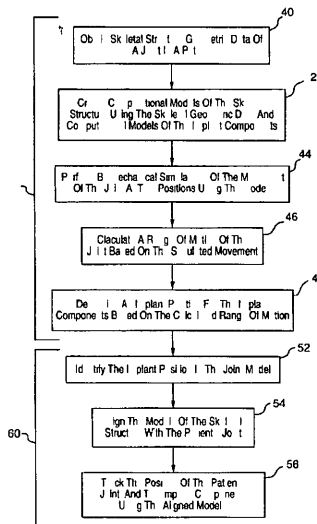
(List continued on next page )

Primary Examiner—Vincent N Trans  
Assistant Examiner—Russell W Frejd  
Attorney Agent or Firm—Kirkpatrick & Lockhart LLP

[57] ABSTRACT

Apparatuses and methods are disclosed for determining an implant position for at least one artificial component in a joint and facilitating the implantation thereof The apparatuses and methods include creating a joint model of a patient s joint into which an artificial component is to be implanted and creating a component model of the artificial component The joint and artificial component models are used to simulate movement in the patient s joint with the artificial component in a test position The component model and the joint model are used to calculate a range of motion in the joint for at least one test position based on the simulated motion An implant position including angular orientation in the patient s joint is determined based on a predetermined range of motion and the calculated range of motion In a preferred embodiment the implant position can be identified in the joint model and the joint model aligned with the joint by registering positional data from discrete points on the joint with the joint model Such registration also allows for tracking of the joint during surgical procedures A current preferred application of the invention is for determining the implant position and sizing of an acetabular cup and femoral implant for use in total hip replacement surgery

24 Claims, 11 Drawing Sheets



## OTHER PUBLICATIONS

- George E Lewinnek M D Jack L Lewis Ph D Richard Tarr M S Clinton L Compere M D and Jerald R Zimmerman B S Dislocations After Total Hip-Replacement Arthroplasties pp 217-220 vol 60-A No 2 Mar 1978 The Journal of Bone and Joint Surgery Incorporated
- Harlan C Amstutz M D R M Lodwig D J Schurman M D and A G Hodgson Range of Motion Studies for Total Hip Replacements pp 124-130 Clinical Orthopaedics and Related Research #111 Sep 1975
- T K Cobb M D B F Morrey M D and D M Ilstrup M S The Elevated-rim Acetabular Liner in Total Hip Arthroplasty Relationship to Postoperative Dislocation pp 80-86 The Journal of Bone and Joint Surgery 1996
- D A Simon R V O Toole M Blackwell F Morgan A M DiGirola and T Kanade Accuracy Validation in Image-Guided Orthopaedic Surgery 2<sup>d</sup> Annual Symposium on Medical Robotics and Computer Assisted Surgery Baltimore MD Nov 4-7<sup>1</sup> 1995
- David A Simon Martial Hebert and Takeo Kanade Techniques for Fast and Accurate Intrasurgical Registration Journal of Image Guided Surgery 1 17-29 (1995)
- Donald E McCollum M D and William J Gray M D Dislocation After Total Arthroplasty pp 159-170 Clinical Orthopaedics and Related Research No 261 Dec 1990
- David A Simon Martial Hebert and Takeo Kanade Real-time 3-D Pose Estimation Using a High-Speed Range Sensor pp 1-14 Carnegie Mellon University Robotics Institute Technical Report CMU-RI-TR-93-24 Nov 1993
- T A Maxian T D Brown D R Pedersen J J Callaghan Femoral Head Containment in Total Hip Arthroplasty Standard vs Extended Lip Liners p 420 42<sup>d</sup> Annual Meeting Orthopaedic Research Society Feb 19-22 Atlanta Georgia
- T A Maxian T D Brown D R Pedersen and J J Callaghan Finite Element Modeling of Dislocation Propensity in Total Hip Arthroplasty pp 259-344 42<sup>d</sup> Annual Meeting 1996 Atlanta Georgia
- Vincent Dessenne Stephane Lavallee Remi Julliard Rachel Orti Sandra Martelli Philippe Cinquin Computer-Assisted Knee Anterior Cruciate Ligament Reconstruction First Clinical Tests Journal of Image Guided Surgery 1 59-64 (1995)
- Ali Hamadeh Stephane Lavallee Richard Szeliski Philippe Cinquin Olivier Peria Anatomy-based Registration for Computer-integrated Surgery pp 212-218 Program of 1 International Conference on Computer Version Virtual Reality Robotics in Medicine 1995 Nice France
- K Rademacher H W Staudte G Rau Computer Assisted Orthopedic Surgery by Means of Individual Templates Aspects and Analysis of Potential Applications pp 42-48
- Lutz-P Nolte Lucia J Zamorano Zhaowei Jiang Qinghai Wang Frank Langlotz Erich Arm Heiko Visarius A Novel Approach to Computer Assisted Spine Surgery pp 323-328
- Robert Rohling Patrice Munger John M Hollerbach Terry Peters Comparison of Relative Accuracy Between a Mechanical and an Optical Position Tracker for Image-guided Neurosurgery Journal of Image Guided Surgery 1 30-34 (1995)
- E Grimson T Lozano-Perez W Wells G Ettinger S White R Kikinis Automated Registration for Enhanced Reality Visualization in Surgery pp 26-29
- S Lavallee P Sautot J Troccaz P Cinquin P Merloz Computer-Assisted Spine Surgery A Technique for Accurate Transpedicular Screw Fixation Using CT Data and a 3-D Optical Localizer Journal of Image Guided Surgery 1 65-73 (1995)
- Russell H Taylor Brent D Mittelstadt Howard A Paul William Hanson Peter Kazanzides Joel F Zuhars Bill Williamson Bela L Musits Edward Glassman William L Bargar An Image-Directed Robotic System for Precise Orthopaedic Surgery IEEE Transactions on Robotics and Automation vol 10 No 3 Jun 1994

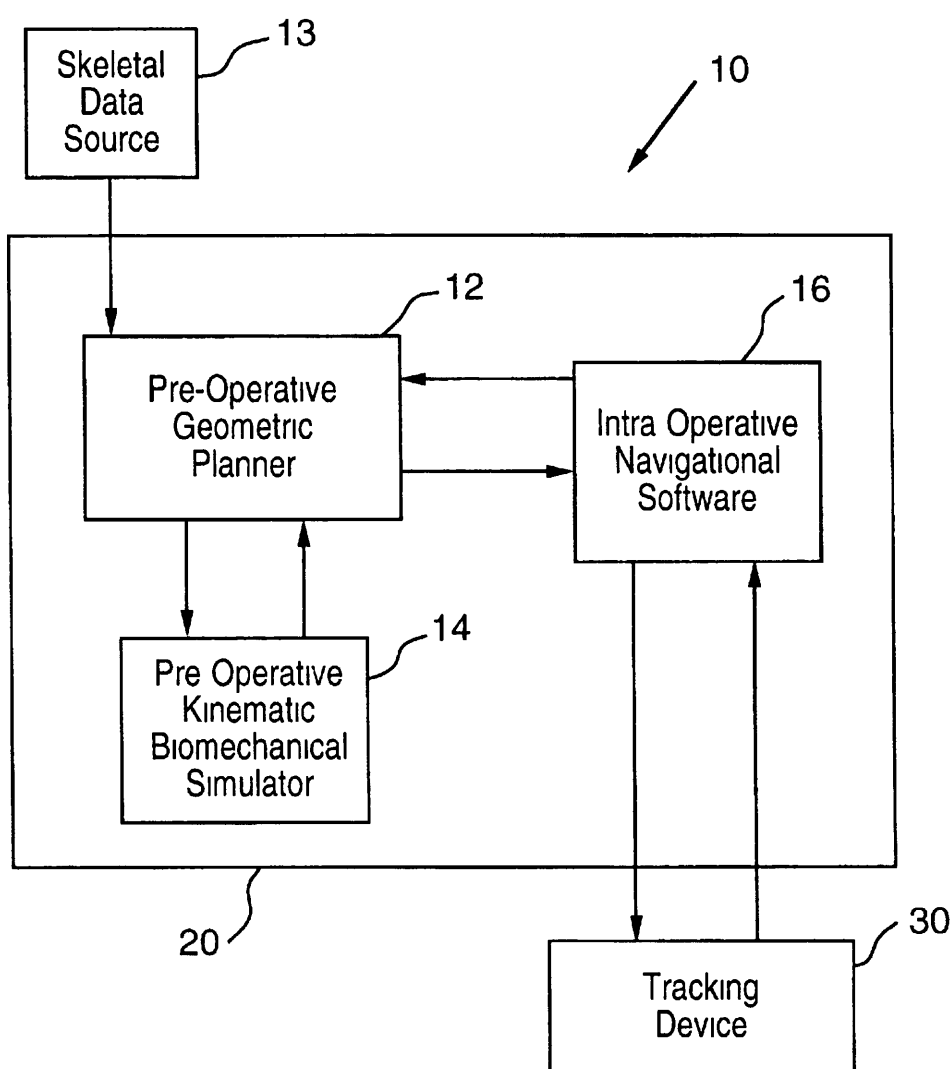


FIG 1

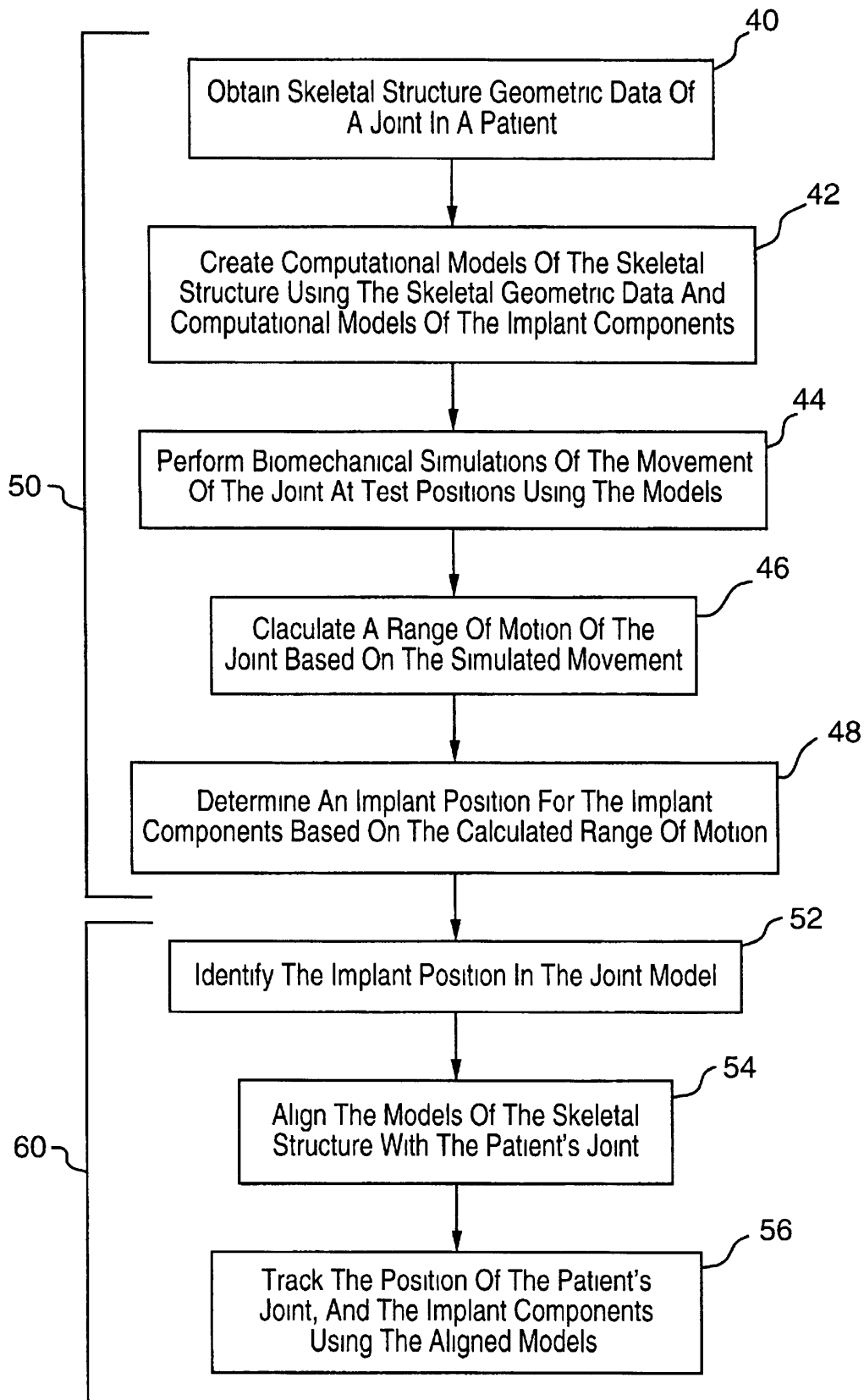


FIG 2

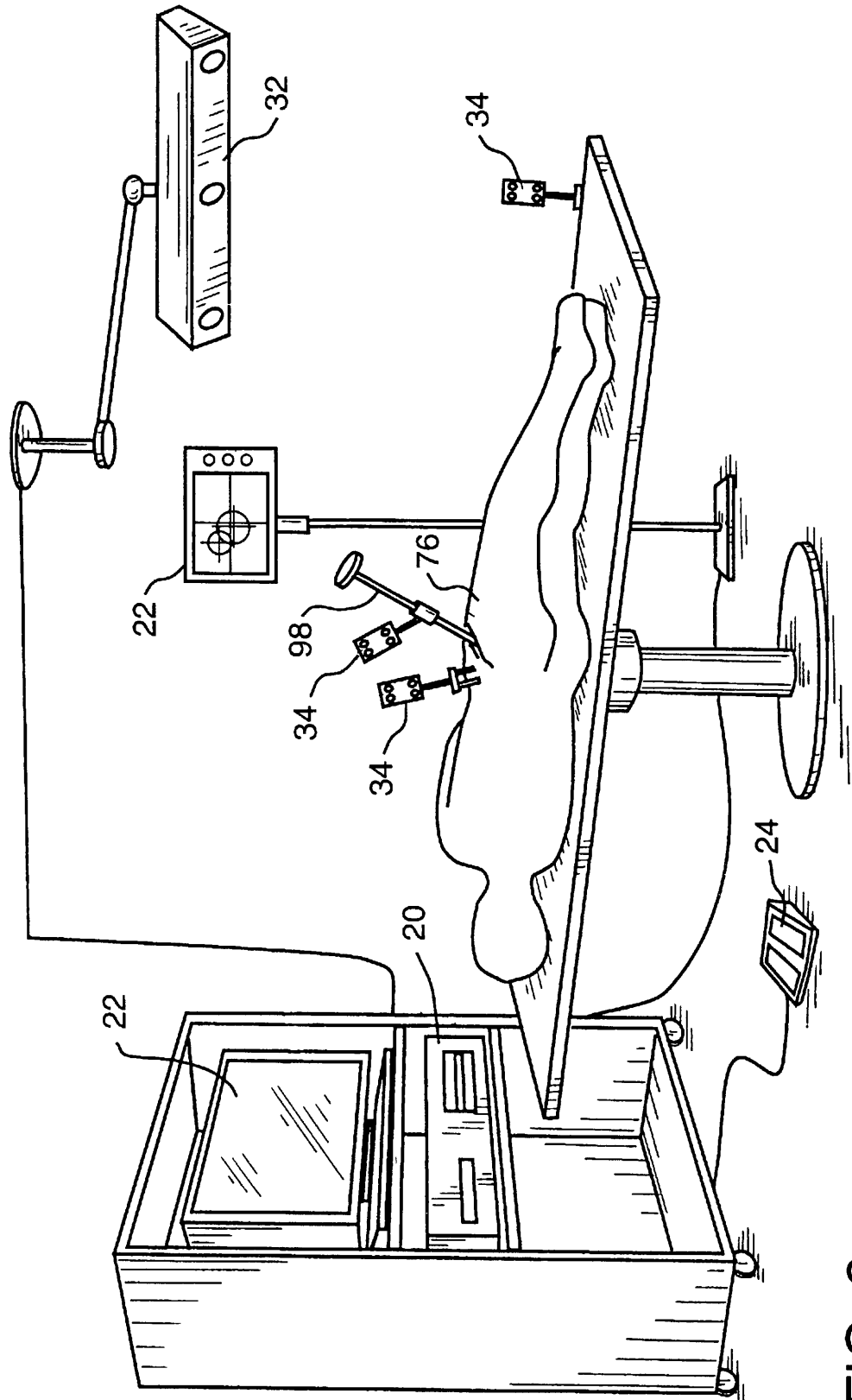


FIG 3



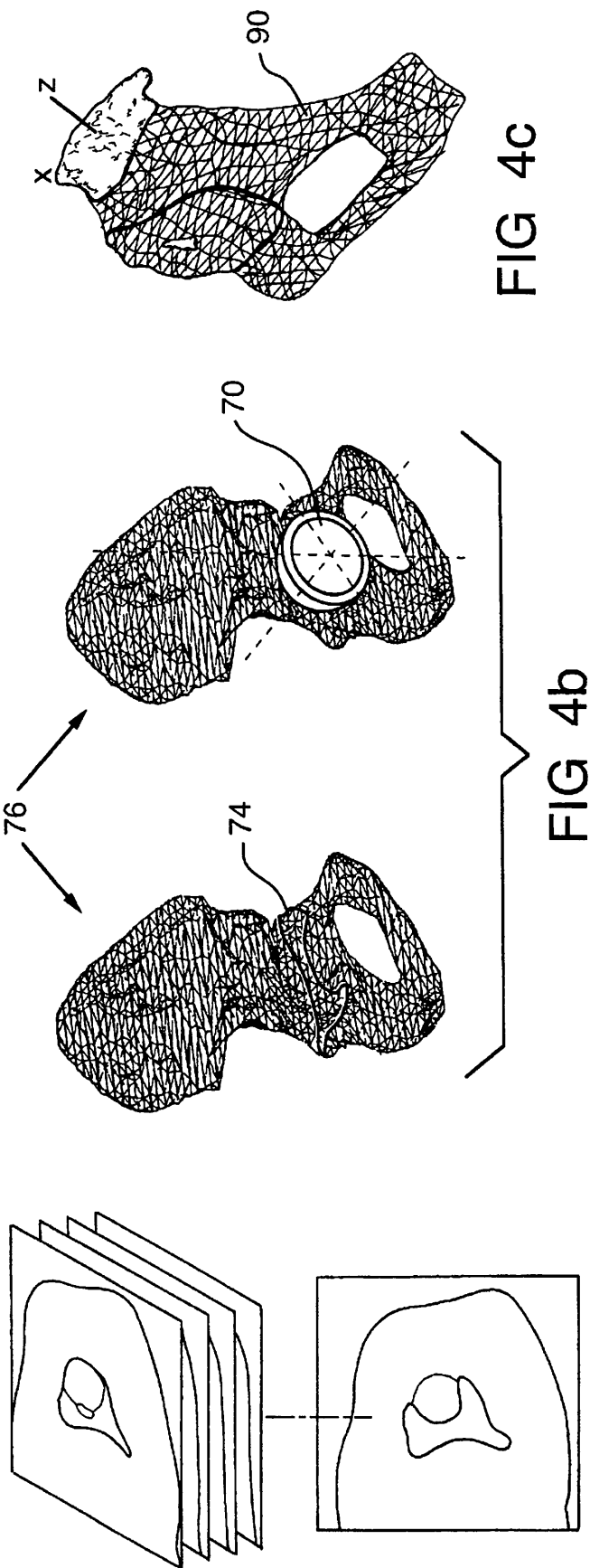


FIG 4a

FIG 4c

FIG 4b

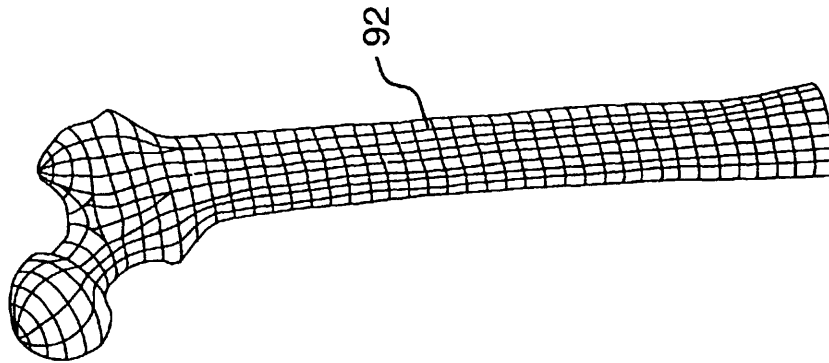


FIG. 5c

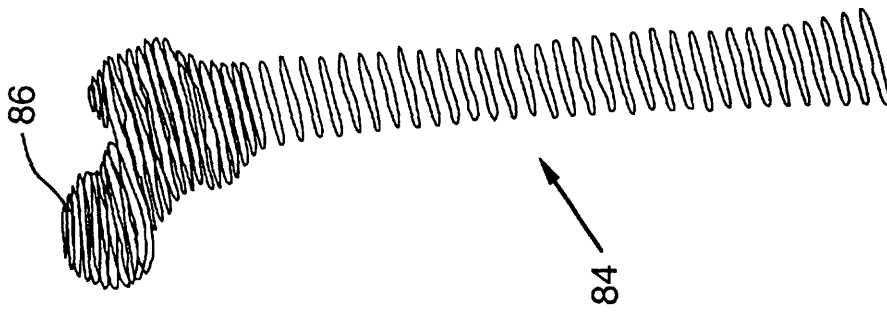


FIG 5b

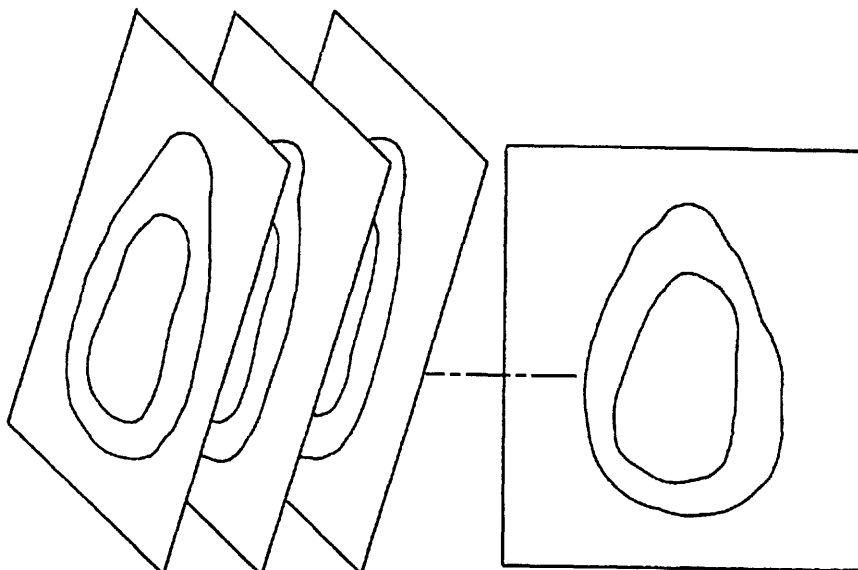


FIG 5a

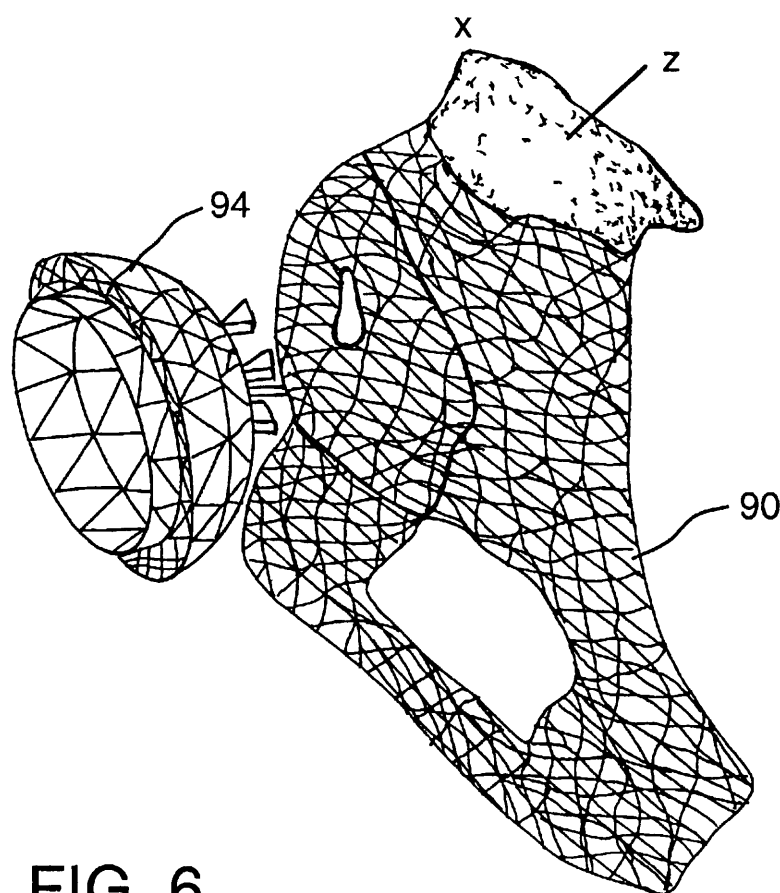
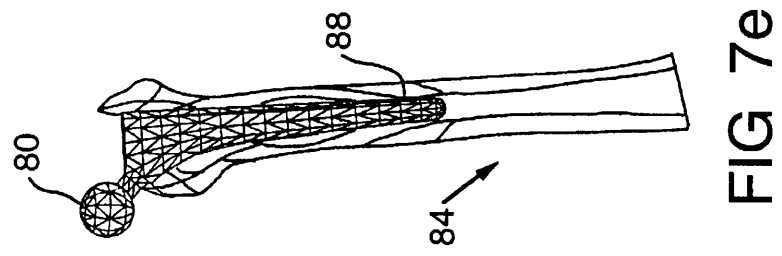
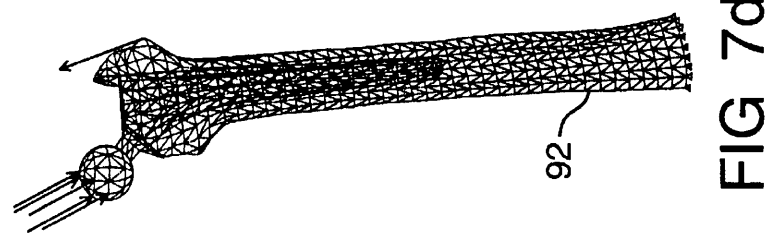
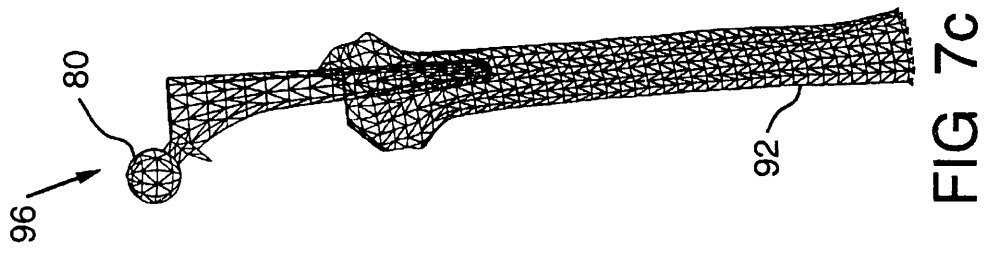
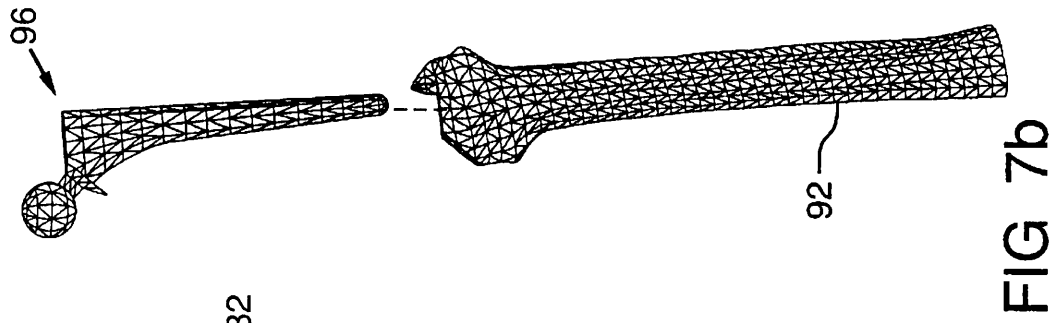
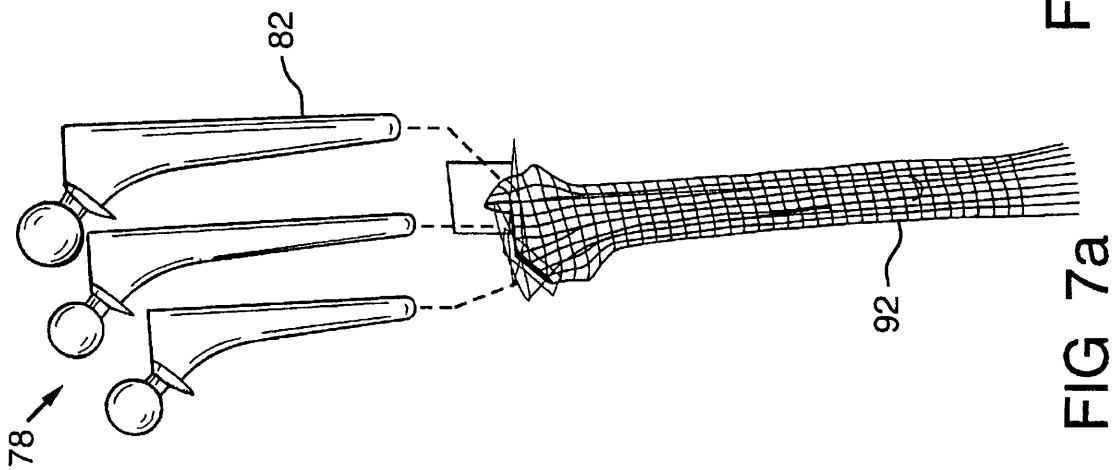


FIG 6



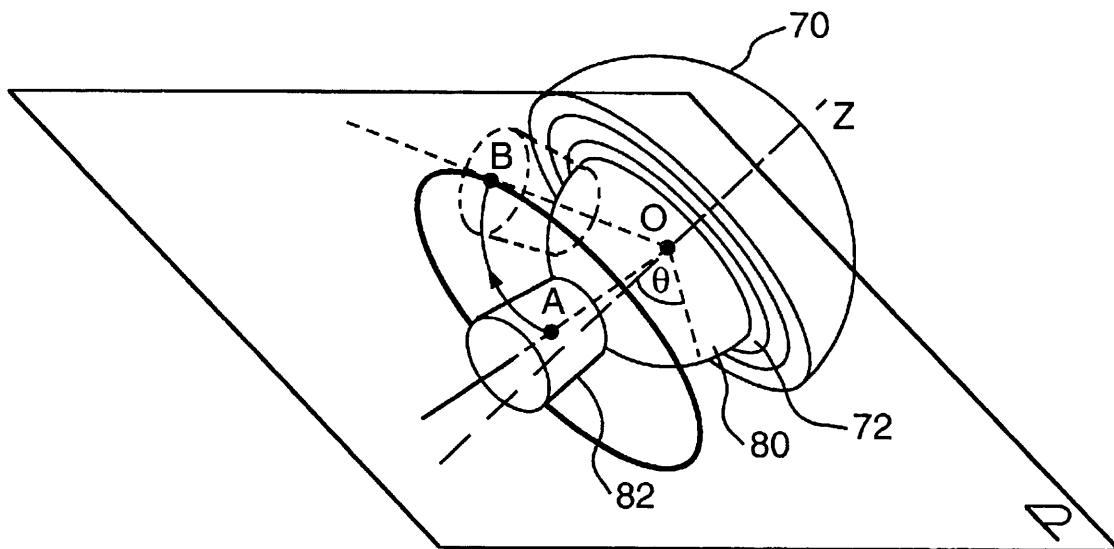


FIG 8

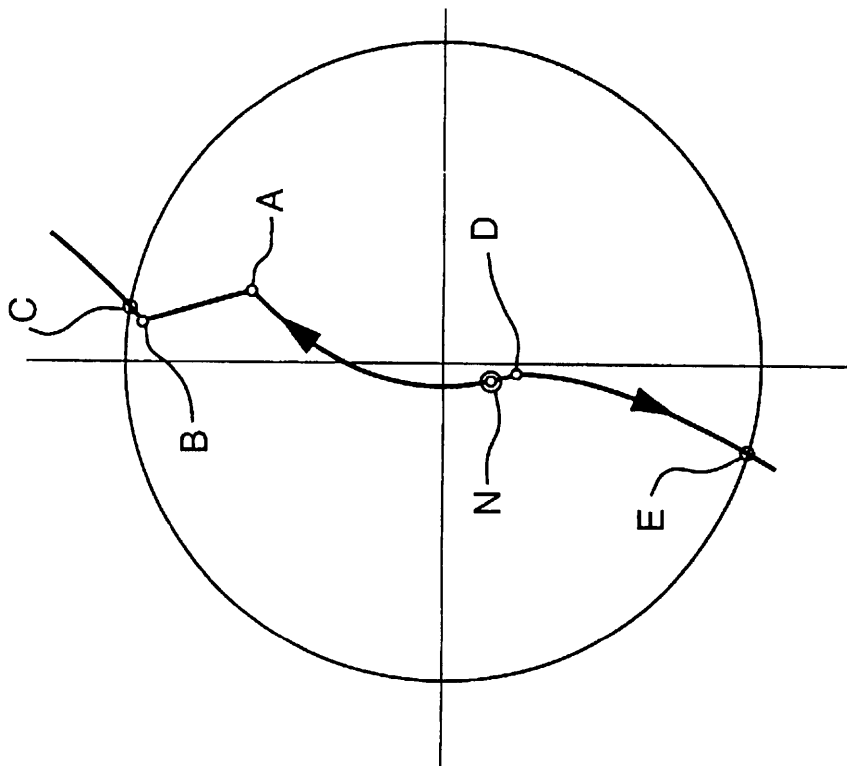


FIG. 9a

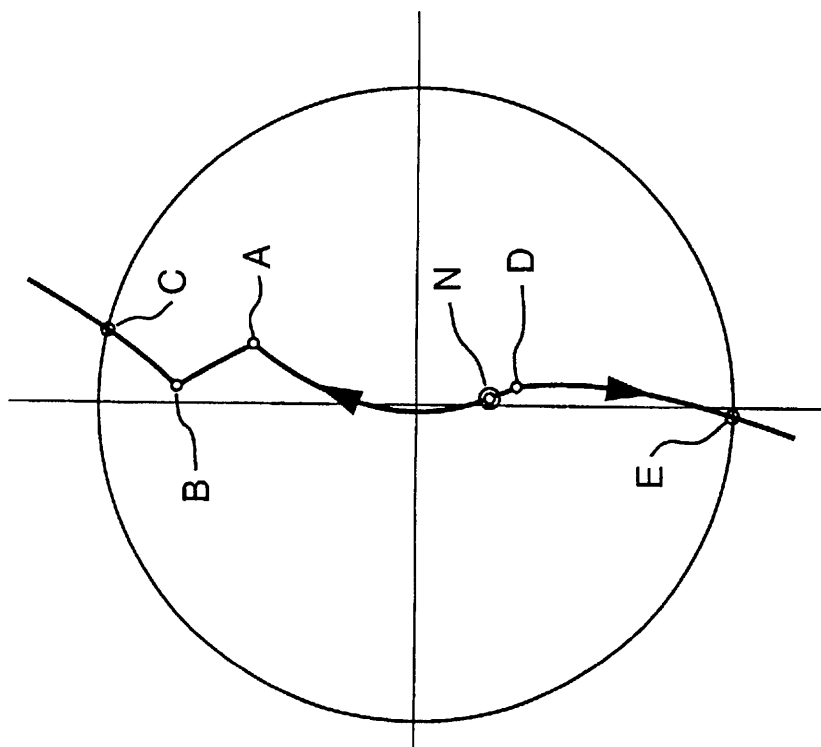


FIG. 9b

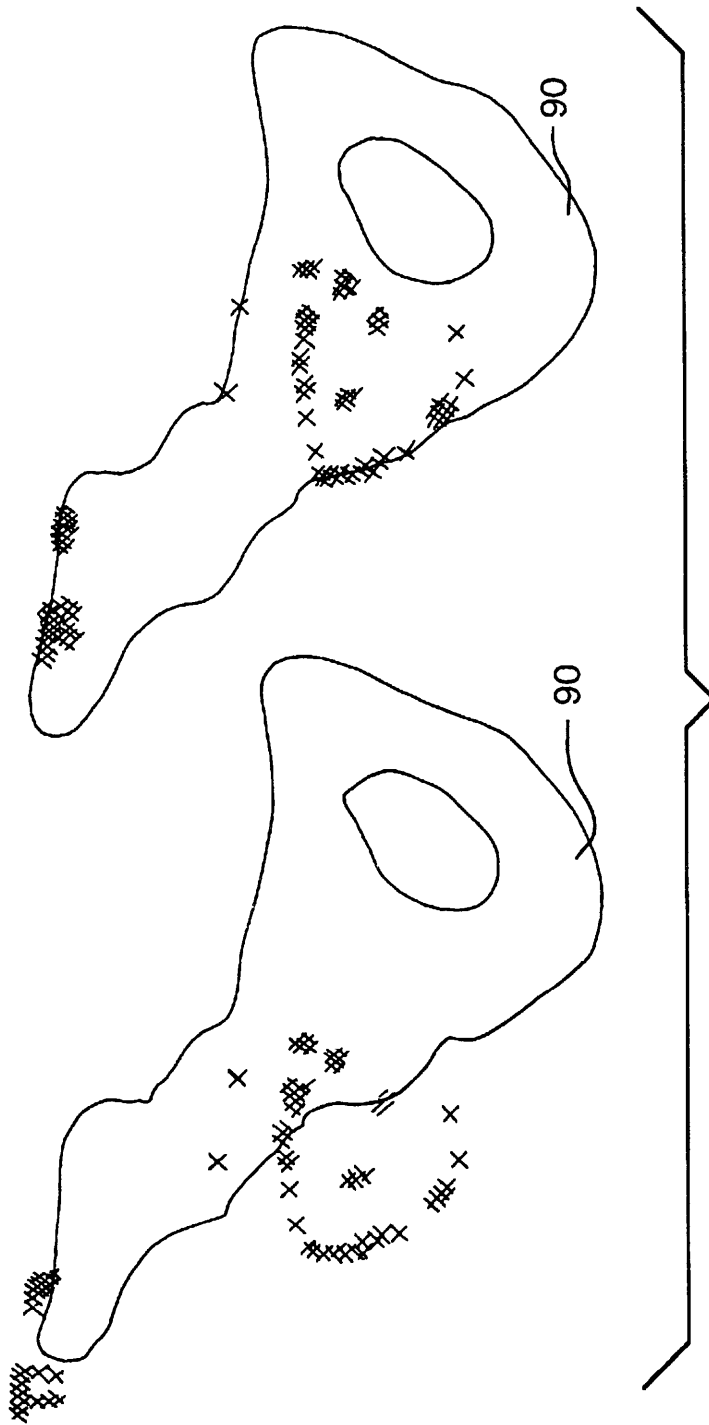


FIG 10a

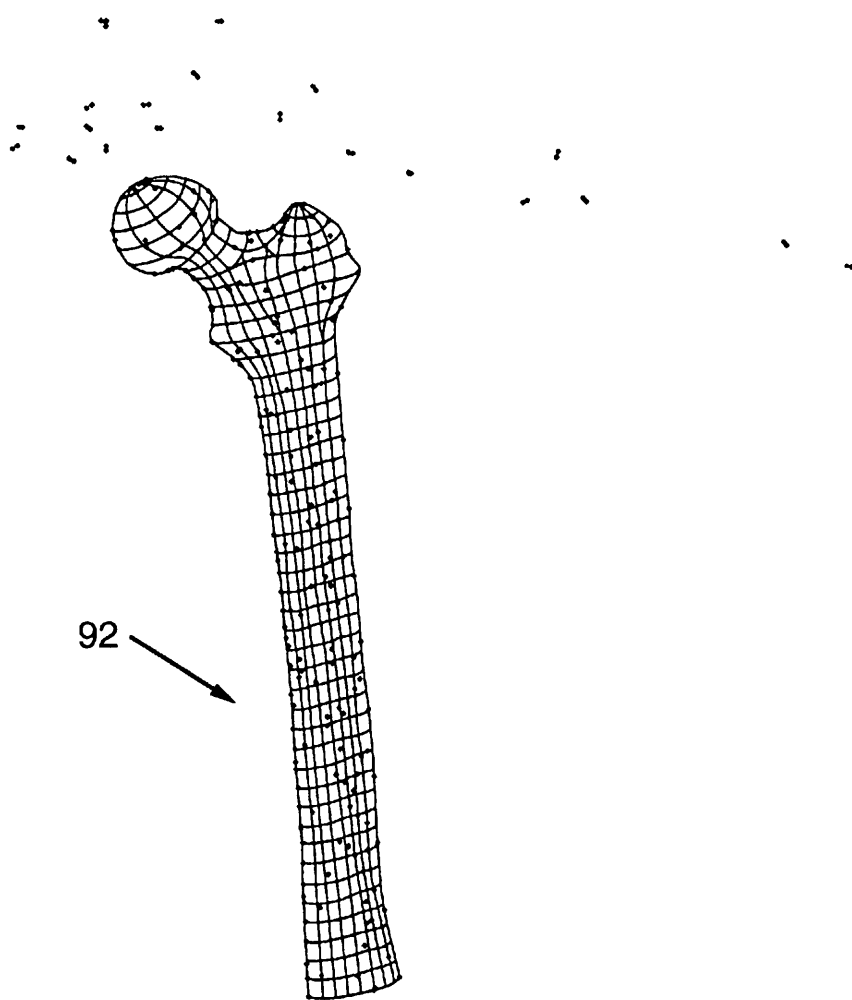


FIG 10b



1

**APPARATUS AND METHOD FOR  
FACILITATING THE IMPLANTATION OF  
ARTIFICIAL COMPONENTS IN JOINTS**

**STATEMENT REGARDING FEDERALLY  
SPONSORED RESEARCH OR DEVELOPMENT**

This work was supported in part by a National Challenge grant from the National Science Foundation Award IRI 9422734

**CROSS REFERENCE TO RELATED  
APPLICATIONS**

Not Applicable

**BACKGROUND OF THE INVENTION**

The present invention is directed generally to the implantation of artificial joint components and more particularly to computer assisted surgical implantation of artificial acetabular and femoral components during total hip replacement and revision procedures

Total hip replacement (THR) or arthroplasty (THA) operations have been performed since the early 1960s to repair the acetabulum and the region surrounding it and to replace the hip components such as the femoral head that have degenerated. Currently approximately 200,000 THR operations are performed annually in the United States alone of which approximately 40,000 are redo procedures otherwise known as revisions. The revisions become necessary due to a number of problems that may arise during the lifetime of the implanted components such as dislocation, component wear and degradation and loosening of the implant from the bone.

Dislocation of the femoral head from the acetabular component or cup is considered one of the most frequent early problems associated with THR because of the sudden physical and emotional hardship brought on by the dislocation. The incidence of dislocation following the primary THR surgery is approximately 2-6% and the percentage is even higher for revisions. While dislocations can result from a variety of causes such as soft tissue laxity and loosening of the implant, the most common cause is impingement of the femoral neck with either the rim of an acetabular cup implant or the soft tissue or bone surrounding the implant. Impingement most frequently occurs as a result of the malposition of the acetabular cup component within the pelvis.

Some clinicians and researchers have found incidence of impingement and dislocations can be lessened if the cup is oriented specifically to provide for approximately 15° of anteversion and 45° of abduction however this incidence is also related to the surgical approach. For example McCollum et al cited a comparison of THAs reported in the orthopaedic literature that revealed a much higher incidence of dislocation in patients who had THAs with a posterolateral approach. McCollum D E and W J Gray Dislocation after total hip arthroplasty (causes and prevention) Clinical Orthopaedics and Related Research Vol 261 p 159-170 (1990). McCollum's data showed that when the patient is placed in the lateral position for a posterolateral THA approach the lumbar lordotic curve is flattened and the pelvis may be flexed as much as 35°. If the cup was oriented at 15°-20° of flexion with respect to the longitudinal axis of the body when the patient stood up and the postoperative lumbar lordosis was regained the cup could be retroverted as much as 10°-15° resulting in an unstable cup placement.

2

Lewinnek et al performed a study taking into account the surgical approach utilized and found that the cases falling in the zone of 15° ± 10° of anteversion and 40° ± 10° of abduction have an instability rate of 1.5% compared with a 6% instability rate for the cases falling outside this zone. Lewinnek G E et al Dislocation after total hip replacement arthroplasties Journal of Bone and Joint Surgery Vol 60 A No 2 p 217-220 (March 1978). The Lewinnek work essentially verifies that dislocations can be correlated with the extent of malpositioning as would be expected. The study does not address other variables such as implant design and the anatomy of the individual both of which are known to greatly affect the performance of the implant.

The design of the implant significantly affects stability as well. A number of researchers have found that the head to neck ratio of the femoral component is the key factor of the implant impingement. See Amstutz H C et al Range of Motion Studies for Total Hip Replacements Clinical Orthopaedics and Related Research Vol 111 p 124-130 (September 1975). Krushell et al additionally found that certain long and extra long neck designs of modular implants can have an adverse effect on the range of motion. Krushell R J, Burke D W and Harris W H Range of motion in contemporary total hip arthroplasty (the impact of modular head neck components) The Journal of Arthroplasty Vol 6 p 97-101 (February 1991). Krushell et al also found that an optimally oriented elevated rim liner in an acetabular cup implant may improve the joint stability with respect to implant impingement. Krushell R J, Burke D W and Harris W H Elevated rim acetabular components Effect on range of motion and stability in total hip arthroplasty The Journal of Arthroplasty Vol 6 Supplement p 1-6 (October 1991). Cobb et al have shown a statistically significant reduction of dislocations in the case of elevated rim liners compared to standard liners. Cobb T K, Morrey B F, Ilstrup D M The elevated rim acetabular liner in total hip arthroplasty Relationship to postoperative dislocation Journal of Bone and Joint Surgery Vol 78 A No 1 p 80-86 (January 1996). The two year probability of dislocation was 2.19% for the elevated liner compared with 3.85% for standard liner. Initial studies by Maxian et al using a finite element model indicate that the contact stresses and therefore the polyethylene wear are not significantly increased for elevated rim liners however points of impingement and subsequent angles of dislocation for different liner designs are different as would be expected. Maxian T A et al Femoral head containment in total hip arthroplasty Standard vs extended hip liners 42nd Annual meeting Orthopaedic Research society p 420 Atlanta Ga (Feb 19-22 1996) and Maxian T A et al Finite element modeling of dislocation propensity in total hip arthroplasty 42nd Annual meeting Orthopaedic Research society p 259-64 Atlanta Ga (Feb 19-22 1996).

An equally important concern in evaluating the dislocation propensity of an implant are variations in individual anatomies. As a result of anatomical variations there is no single optimal design and orientation of hip replacement components and surgical procedure to minimize the dislocation propensity of the implant. For example the pelvis can assume different positions and orientations depending on whether an individual is lying supine (as during a CT scan or routine X rays) in the lateral decubitus position (as during surgery) or in critical positions during activities of normal daily living (like bending over to tie shoes or during normal gait). The relative position of the pelvis and leg when defining a neutral plane from which the angles of movement anteversion abduction etc are calculated will

3

significantly influence the measured amount of motion permitted before impingement and dislocation occurs. Therefore, it is necessary to uniquely define both the neutral orientation of the femur relative to the pelvis for relevant positions and activities and the relations between the femur with respect to the pelvis of the patient during each segment of leg motion.

Currently, most planning for acetabular implant placement and size selection is performed using acetate templates and a single anterior-posterior x-ray of the pelvis. Acetabular templating is most useful for determining the approximate size of the acetabular component; however, it is only of limited utility for positioning of the implant because the x-rays provide only a two-dimensional image of the pelvis. Also, the variations in pelvic orientation can not be more fully considered as discussed above.

Intra-operative positioning devices currently used by surgeons attempt to align the acetabular component with respect to the sagittal and coronal planes of the patient. B. F. Morrey, editor, *Reconstructive Surgery of the Joints*, chapter Joint Replacement Arthroplasty, pages 605-608, Churchill Livingstone, 1996. These devices assume that the patient's pelvis and trunk are aligned in a known orientation and do not take into account individual variations in a patient's anatomy or pelvic position on the operating room table. These types of positioners can lead to a wide discrepancy between the desired and actual implant placement, possibly resulting in reduced range of motion, impingement, and subsequent dislocation.

Several attempts have been made to more precisely prepare the acetabular region for the implant components. U.S. Pat. No. 5,007,936 issued to Woolson is directed to establishing a reference plane through which the acetabulum can be reamed and generally prepared to receive the acetabular cup implant. The method provides for establishing the reference plane based on selecting three reference points, preferably the 12 o'clock position on the superior rim of the acetabulum and two other reference points, such as a point in the posterior rim and the inner wall, that are a known distance from the superior rim. The location of the superior rim is determined by performing a series of computed tomography (CT) scans that are concentrated near the superior rim and other reference locations in the acetabular region.

In the Woolson method, calculations are then performed to determine a plane in which the rim of the acetabular cup should be positioned to allow for a predetermined rotation of the femoral head in the cup. The distances between the points and the plane are calculated, and an orientation jig is calibrated to define the plane when the jig is mounted on the reference points. During the surgical procedure, the surgeon must identify the 12 o'clock orientation of the superior rim and the reference points. In the preferred mode, the jig is fixed to the acetabulum by drilling a hole through the reference point on the inner wall of the acetabulum and affixing the jig to the acetabulum. The jig incorporates a drill guide to provide for reaming of the acetabulum in the selected plane.

A number of difficulties exist with the Woolson method. For example, the preferred method requires drilling a hole in the acetabulum. Also, visual recognition of the reference points must be required, and precision placement on the jig on reference points is performed in a surgical setting. In addition, proper alignment of the reaming device does not ensure that the implant will be properly positioned, thereby establishing a more lengthy and costly procedure with no

4

guarantees of better results. These problems may be a reason why the Woolson method has not gained widespread acceptance in the medical community.

In U.S. Pat. Nos. 5,251,127 and 5,305,203 issued to Raab, a computer-aided surgery apparatus is disclosed in which a reference jig is attached to a double self-indexing screw previously attached to the patient to provide for a more consistent alignment of the cutting instruments similar to that of Woolson. However, unlike Woolson, Raab et al. employ a digitizer and a computer to determine and relate the orientation of the reference jig and the patient during surgery with the skeletal shapes determined by tomography.

Similarly, U.S. Pat. Nos. 5,086,401, 5,299,288 and 5,408,409 issued to Glassman et al. disclose an image-directed surgical robotic system for reaming a human femur to accept a femoral stem and head implant using a robot cutter system. In the system, at least three locating pins are inserted in the femur, and CT scans of the femur in the region containing the locating pins are performed. During the implanting procedure, the locating pins are identified on the patient as discussed in col. 9, lines 19-68 of Glassman's 401 patent. The location of the pins during the surgery are used by a computer to transform CT scan coordinates into the robot cutter coordinates, which are used to guide the robot cutter during reaming operations.

While the Woolson, Raab, and Glassman patents provide methods and apparatuses that further offer the potential for increased accuracy and consistency in the preparation of the acetabular region to receive implant components, there remain a number of difficulties with the procedures. A significant shortcoming of the methods and apparatuses is that when used for implanting components in a joint, there are underlying assumptions that the proper position for the placement of the components in the joints has been determined and provided as input to the methods and apparatuses that are used to prepare the site. As such, the utility and benefit of the methods and apparatuses are based upon the correctness and quality of the implant position provided as input to the methods.

In addition, both the Raab and Glassman methods and apparatuses require that fiducial markers be attached to the patient prior to performing tomography of the patient. Following the tomography, the markers must either remain attached to the patient until the surgical procedure is performed or the markers must be reattached at the precise locations to allow the transformation of the tomographic data to the robotic coordinate system, either of which is undesirable and/or difficult in practice.

Thus, the need exists for apparatuses and methods which overcome, among others, the above-discussed problems so as to provide for the proper placement and implantation of the joint components to provide an improved range of motion and usage of the joint following joint reconstruction, replacement, and revision surgery.

#### BRIEF SUMMARY OF THE INVENTION

The above objectives and others are accomplished by methods and apparatuses in accordance with the present invention. The apparatuses and methods include creating a joint model of a patient's joint into which an artificial component is to be implanted and creating a component model of the artificial component. The joint and artificial component models are used to simulate movement of the patient's joint with the artificial component in a test position. The component model and the joint model are used to calculate a range of motion of the joint for at least one test

5

position based on the simulated movement. An implant position including angular orientation for the artificial component is determined based on a predetermined range of motion and the calculated range of motion. A goal of the simulation process is to find the implant position which optimizes the calculated range of motion using the predetermined range of motion as a basis for optimization. In practice, the predetermined range of motion is determined based on desired functional motions selected by a medical practitioner on a patient specific basis (e.g., sitting requires flexion of 90°). In a preferred embodiment, the implant position can be identified in the joint model. During surgery, the joint model can be aligned with the joint by registering positional data from discrete points on the joint with the joint model. Such registration also allows for tracking of the joint during the surgical procedures.

A current preferred application of the invention is for determining the implant position and sizing of an acetabular cup and femoral implant for use in total hip replacement surgery. Also in a preferred embodiment, alignment of the joint model with the patient's joint is performed using surface based registration techniques. The tracking of the pelvis, the acetabular cup, femoral implant, and surgical instrument is preferably performed using an emitter/detector optical tracking system.

The present invention provides the medical practitioner a tool to precisely determine an optimal size and position of artificial components in a joint to provide a desired range of motion of the joint following surgery and to substantially lessen the possibility of subsequent dislocation. Accordingly, the present invention provides an effective solution to problems heretofore encountered with precisely determining the proper sizing and placement of an artificial component to be implanted in a joint. In addition, the practitioner is afforded a less invasive method for executing the surgical procedure in accordance with the present invention. These advantages and others will become apparent from the following detailed description.

#### BRIEF DESCRIPTION OF THE DRAWINGS

A preferred embodiment of the invention will now be described by way of example only with reference to the accompanying figures wherein like members bear like reference numerals and wherein:

FIG. 1 is a system overview of a preferred embodiment of the present invention.

FIG. 2 is a flow chart illustrating the method of the present invention.

FIG. 3 is a schematic layout of the apparatus of the present invention being used in a hip replacement procedure.

FIGS. 4(a-c) show the creation of the pelvic model using two dimensional scans of the pelvis (a) from which skeletal geometric data is extracted as shown in (b) and used to create the pelvic model (c).

FIGS. 5(a-c) show the creation of the femur model using two dimensional scans of the femur (a) from which skeletal geometric data is extracted as shown in (b) and used to create the femur model (c).

FIG. 6 shows the sizing of the acetabular cup in the pelvic model.

FIGS. 7(a-e) show the creation of different sized femoral implant models (a) and the fitting of the femoral implant model into a cut femur (b-e).

FIG. 8 is a schematic drawing showing the range of motion of a femoral shaft and the impingement (in dotted lines) of a femoral shaft on an acetabular cup.

6

FIGS. 9(a-b) shows the range of motion results from biomechanical simulation of two respective acetabular cup orientations and

FIGS. 10 (a) and (b) show the registration of the pelvis and femur.

#### DETAILED DESCRIPTION OF THE INVENTION

The apparatus 10 of the present invention will be described generally with reference to the drawings for the purpose of illustrating the present preferred embodiments of the invention only and not for purposes of limiting the same. A system overview is provided in FIG. 1 and general description of the method of the present invention is presented in flow chart form in FIG. 2. The apparatus 10 includes a geometric pre-operative planner 12 that is used to create geometric models of the joint and the components to be implanted based on geometric data received from a skeletal structure data source 13. The pre-operative planner 12 is interfaced with a pre-operative kinematic biomechanical simulator 14 that simulates movement of the joint using the geometric models for use in determining implant positions including angular orientations for the components. The implant positions are used in conjunction with the geometric models in intra-operative navigational software 16 to guide a medical practitioner in the placement of the implant components at the implant positions.

The pre-operative geometric planner 12, the pre-operative kinematic biomechanical simulator 14, and the intra-operative navigational software are implemented using a computer system 20 having at least one display monitor 22 as shown in FIG. 3. For example, applicants have found that a Silicon Graphics 02 workstation (Mountain View, Calif.) can be suitably employed as the computer system 20; however, the choice of computer system 20 will necessarily depend upon the resolution and calculational detail sought in practice. During the pre-operative stages of the method, the display monitor 22 is used for viewing and interactively creating and/or generating models in the pre-operative planner 12 and displaying the results of the biomechanical simulator 14. The pre-operative stages of the method may be carried out on a computer (not shown) remote from the surgical theater.

During the intra-operative stages of the method, the computer system 20 is used to display the relative locations of the objects being tracked with a tracking device 30. The medical practitioner preferably can control the operation of the computer system 20 during the procedure such as through the use of a foot pedal controller 24 connected to the computer system 20. The tracking device 30 can employ any type of tracking method as may be known in the art, for example, emitter/detector systems including optic acoustic or other wave forms, shape based recognition tracking algorithms, or video based mechanical, electro magnetic and radio frequency (RF) systems. In a preferred embodiment, schematically shown in FIG. 3, the tracking device 30 is an optical tracking system that includes at least one camera 32 that is attached to the computer system 20 and positioned to detect light emitted from a number of special light emitting diodes or targets 34. The targets 34 can be attached to bones, tools, and other objects in the operating room equipment to provide precision tracking of the objects. One such device that has been found to be suitable for performing the tracking function is the Optotrak™ 3020 system from Northern Digital Inc., Ontario, Canada, which is advertised as capable of achieving

accuracies of roughly 0.1 mm at speeds of 100 measurements per second or higher

The apparatus 10 of FIG 1 is operated in accordance with the method illustrated in FIG 2. The skeletal structure of the joint is determined at step 40 using tomographic data (three dimensional) or computed tomographic data (pseudo three dimensional data produced from a series of two dimensional scans) or other techniques from the skeletal data source 13. Commonly used tomographic techniques include computed tomography (CT), magnetic resonance imaging (MRI), positron emission tomographic (PET) or ultrasound scanning of the joint and surrounding structure. The tomographic data from the scanned structure generated by the skeletal data source 13 is provided to the geometric planner 12 for use in producing a model of the skeletal structure. It should be noted that in a preferred embodiment there is no requirement that fiducial markers be attached to the patient in the scanned region to provide a reference frame for relating the tomography scans to intra operative position of the patient although markers can be used as a cross reference or for use with other alternative embodiments.

At step 42 a surface model is created or constructed from the skeletal geometric data using techniques such as those described by B. Geiger in "Three dimensional modeling of human organs and its application to diagnosis and surgical planning" Ph.D. thesis Ecole des Mines de Paris April 1993. The geometric models constructed from the skeletal data source 13 can be manually generated and input to the geometric planner 12 but it is preferable that the data be used to create the geometric models in an automated fashion.

Also at step 42 geometric models of the artificial components to be implanted into the joint are created/generated. The geometric models can be created in any manner as is known in the art including those techniques described for creating joint models. The geometric models of the artificial components can be used in conjunction with the joint model to determine an initial static estimate of the proper size of the artificial components to be implanted.

In step 44 the geometric models of the joint and the artificial components are used to perform biomechanical simulations of the movement of the joint containing the implanted artificial components. The biomechanical simulations are preferably performed at a number of test positions to dynamically optimize the size, position and orientation of the artificial components in the patient's joint to achieve a predetermined range of motion following surgery. The predetermined range of motion for a particular patient is determined based on the expected activities of the patient following surgery. For example, with regard to hip functions, daily activities such as getting out of bed, walking, sitting and climbing stairs that are performed by individuals requiring different ranges of motion as will be discussed in further detail below.

The size and orientations of the implant component and movements simulated at various test positions used in step 44 can be fully automated or manually controlled. In a preferred embodiment the selection and test process would be automated so as to be more fully optimizable to a predetermined range of motion either generally or for predetermined activity. However, because it is necessary that medical practitioners be comfortable and develop confidence in the system, manual control is provided over the selection of the implant components and the test positions in the biomechanical simulator 14.

In step 46 the simulated movement of the joint at various implant positions is used to calculate a range of motion for

each implant position. In step 48 the calculated ranges of motion are compared to the predetermined range of motion to select an implant position for the artificial components. A goal of the simulation process is to find the implant position which optimizes the calculated range of motion using the predetermined range of motion as a basis for optimization. In practice the predetermined range of motion is determined based on desired functional motions selected by a medical practitioner on a patient specific basis (e.g. sitting requires flexion of 90°). The determination of the implant position can be further influenced by other factors such as the variation in the calculated range of motion as a function of implant component orientation. This criterion is useful for determining the surgical margin of error that is available to the medical practitioner without a substantial diminution in the range of motion of the joint.

Steps 40, 42, 44, 46 and 48 represent a pre-operative procedure 50 which is performed so that the artificial components can be properly sized and implant positions can be properly determined. The remainder of the steps in FIG 2, steps 52, 54 and 56 comprise a procedure 60 which enables a surgeon to realize the desired implant position in the surgical theater.

In step 52 the implant positions determined using procedure 50 are then identified by marking or incorporating the information in some appropriate manner in the geometric model of the joint. The geometric models of the joint and the artificial components can then be used in conjunction with positional data obtained from the joint and the artificial components during a surgical procedure to provide intra-operative guidance for the implantation of the artificial components.

In step 54 the joint model based on the skeletal data is aligned with the intra-operative position of the patient's joint. In a preferred embodiment step 54 is performed using a technique known as three dimensional (3D) surface registration. In 3D surface registration discrete registration points are obtained from the joint skeletal structure to define the intra-operative position of the patient's joint. The registration points are fitted to the joint model of the skeletal structure to determine a coordinate transformation that is used to align the joint model with the intra-operative position of the patient's joint. Once the transformation is established the intra-operative position of the patient's joint can be tracked using the joint model by obtaining positional data from a point on the joint that provides spatial correspondence between the pre-operative models and the intra-operative measurements. A more thorough description of the surface registration procedure is discussed in D.A. Simon, M. Hebert and T. Kanade, "Real time 3-D Pose Estimation Using a High Speed Range Sensor", Carnegie Mellon University Robotics Institute Technical Report CMU RI-TR 93-24 (November 1993); D.A. Simon, M. Hebert and T. Kanade, "Techniques for fast and accurate intra-surgical registration", *Journal of Image Guided Surgery* 1(1) 17-29 (April 1995) and D.A. Simon et al., "Accuracy validation in image guided orthopaedic surgery", *Proc 2nd Int'l Symp MRCAS Baltimore* (Nov 1995) which are incorporated herein by reference.

The physical location of the intra-operative registration points on the joint from which the positional data is obtained will determine the amount of positional data required to uniquely determine and align the geometric model with the registration points. For example, it is desirable to obtain positional data from the joint that will maximize the constraint on the possible solutions to the alignment problem and provide high level of sensitivity to variations in the

position including orientation of the joint as discussed above in the Simon et al references. The goal of the registration process is to determine a registration transformation which best aligns the discrete points that provide the spatial position and orientation of the joint with the joint models. Preferably an initial estimate of this transformation is first determined using manually specified anatomical landmarks to perform corresponding point registration. Once this initial estimate is determined the surface based registration algorithm uses the pre- and intra-operative data to refine the initial transformation estimate.

Alternatively step 54 can be implemented using registration systems that employ fiducial markers to align the pre-operative data with the intra-operative position of the patient's joint. In those methods the fiducial markers must be surgically implanted into the skeletal structure before pre-operative images are acquired in step 40. The intra-operative position of the fiducial markers are compared to the pre-operative data to determine the position of the patient's joint. An example of such a fiducial marker system is discussed in R. H. Tylor et al. "An image directed robotic system for precise orthopaedic surgery." *IEEE Trans on Robotics and Automation* 10(3) 261-275 June 1994. In addition step 54 can be implemented using other registration systems that do not require the pre-operative use of fiducial markers.

In step 56 the position of the joint and the implant components are tracked and compared in near real time to the implant position identified in the joint model. In this step the tracking device 30 provides the positional data representative of the position of the patient's joint to the computer system 20. The computer system 20 employs registration routines within the intra-operative navigational software 16 to determine the position and orientation of the joint and then displays the relative positions of the artificial component and the implant position. The tracking device 30 can also be used to track and provide positional data representative of the position of other physical objects in the operating room such as surgical instruments. Additional details of the methods and apparatuses are presented in "HipNav: Pre-operative Planning and Intra-operative Navigational Guidance for Acetabular Implant Placement in Total Hip Replacement Surgery." DiGioia et al. 2<sup>d</sup> CAOS Symposium Bern Switzerland 1996 which is incorporated herein by reference.

The operation of the apparatus 10 will now be discussed with reference to its use in a THR procedure. Generally an acetabular cup 70 (FIG 8) having a cup liner 72 in a convex portion thereof is implanted in an acetabulum 74 (FIG 4b) of a pelvis 76. In addition a femoral implant 78 (FIG 7) having a head or ball 80 and a neck or shaft 82 is implanted into a femur 84. The femur 84 has a head portion 86 (FIG 5) that is removed to facilitate the implantation. A bore 88 is drilled in the femur 84 into which the femoral implant 78 is placed. The femoral neck 82 is secured in the bore 88 in a position to allow the femoral head 80 to cooperate with the cup liner 72 in the acetabular cup 70.

In accordance with step 40 skeletal structure data is obtained on the femur and pelvic regions of the patient preferably via CT scans as shown in FIGS 4(a) and 5(a) respectively from the skeletal data source 13. The CT scans are either manually or automatically inputted in the computer system 20 (FIGS 4(b) and 5(b)) and used to create geometric surface models 90 and 92 of the patient's pelvis 76 and femur 84 (FIGS 4(c) and 5(c)) respectively as per step 42.

Geometric models 94 and 96 of the acetabular cup 70 and a femoral implant 78 shown in FIGS 6 and 7 respectively

are created either manually or in an automated fashion using conventional computer assisted design modelling techniques with implant design or manufacturing data. The size of the acetabular cup 70 can be determined automatically based on the size of the acetabulum 74 determined from the pelvis model 90 the skeletal data or can be manually input. Similarly the femoral implant 78 can be manually sized to cooperate with the selected acetabular cup 70 using standard implant components or the sizing of the head 80 and neck 82 of the femoral implant 78 can be customized to fit the femur 84 using the femoral implant model 96 and the femur model 92 as shown in FIGS 7(a-e). One skilled in the art will appreciate that the computer system 20 in performing step 42 can be programmed using separate or combined software routines to create the geometric surface models of the patient's anatomy and the implant components.

The computer system 20 uses the geometric model 90 of the patient's pelvis 76 the model 92 of the patient's femur the model 94 of the acetabular cup 70 and model 96 of the femoral implant 78 to perform simulated biomechanical testing of the acetabular cup 70 and the femoral implant 78 implanted at various test positions in the acetabulum 74 and femur 84 respectively according to step 44. For example in the case of femoral neck 82—cup liner 72 impingement shown in FIG 8 the important parameters in evaluating the prosthetic range of motion are the head 80 to neck 82 ratio of the femoral implant 78 the position including angular orientation of the acetabular cup 70 and the relative position of the femoral implant 78 with respect to the cup 70.

While the present invention is applicable to non-axisymmetric acetabular implants (i.e. hooded liners non-neutral liners) and femoral necks (i.e. non-symmetric cross sections) the following discussion of an axisymmetric acetabular cup and femoral neck alignment case is presented to ease the explanation of the concepts. If the center of rotation in the acetabular cup 70 coincides with the center of the head 80 of the femoral implant 78 as shown in FIG 8 the angle  $\theta$  between the axis of symmetry Z of the acetabular cup 70 and the line of impingement OB defines the allowable angle of motion. The limits of impingement create a cone within which the axis of the femoral neck (line OA) can move without the femoral neck impinging upon the cup liner 72.

The position of the neck axis with respect to the cone can be evaluated by observing its intersection with a plane P placed at an arbitrary distance normal to the Z axis. The cross section of the cone defines the impingement circle (if as stated above both the liner 72 and the neck 82 are axisymmetric) and the path of the axis of the femoral neck 82 defines a curve in the plane P. In FIG 8 the axis of the femoral neck 82 begins at point A and moves along the path AB to point B at which point the femoral neck 82 impinges upon the cup liner 72.

The motion of the femoral neck 82 can be derived from (and expressed as a function of) the physiological movement of the leg described in terms of combined flexion extension abduction adduction and external and internal rotation. FIGS 9(a) and 9(b) show an example of range of motion (ROM) simulation for two different cup orientations and for two identical sets of ROM exercises (I) 90 flexion (A)+15 adduction (B)+maximum internal rotation (C) and (II) 10 extension (D)+maximum external rotation (E). As a result of reorienting the cup from 45 abduction+15 flexion (FIG 9(a)) to 50 abduction+5 flexion (FIG 9(b)) maximum internal rotation at the impingement point C is reduced from 15.7 to 4.3 in exercise I and maximum external rotation at the impingement point E is increased from 45.8

## 11

to 55 8 in the exercise II In accordance with step 48 the implant position is determined by comparison of the calculated range of motion of the femoral implant 78 in the acetabular cup 70 with the predetermined range of motion See Simulation of Implant Impingement and Dislocation in Total Hip Replacement Jaramaz et al Computer Assisted Radiology 10<sup>th</sup> International Symposium and Exhibition Paris June 1996 which is incorporated herein by reference

In the execution of the intra operative procedure 60 the implant position is identified in the pelvic model 90 prior to surgery as in step 52 During the surgical procedure the pelvis 76 of the patient is exposed One of the tracking targets 34 a pelvic target is attached to the pelvic region as shown in FIG 3 Preferably the target 34 is attached in close proximity to the acetabulum 74 to provide data as close to the area of interest as possible without becoming an impediment to the surgical procedure The close proximate placement of the target 34 provides an additional benefit of minimizing the extent to which the pelvis must be exposed during the procedure Positional data from discrete locations on the patient's pelvis 76 and femur 84 are taken and provided as input to the navigational guidance software 16 according to step 54

The intra operative positional data is registered with the pelvic model 90 and femur model 92 as shown in FIGS 10(a) and (b) to align the models with the intra operative position of the patient's pelvis 76 and femur 84 respectively During the acquisition of discrete registration point positional data from the pelvis 76 the tracking device 30 via camera 32 is used to track the pelvic target The pelvic target position data is used in combination with the transformation developed using the registration data provide a spatial correspondence between pre operative CT coordinates (i.e. pelvic model) and the intra operative coordinates (i.e. measurements of the patient's pelvis relative to the pelvic target) Intra operative tracking of the acetabular cup 70 is also performed relative to the pelvic target

The position of the acetabular cup 70 prior to implantation is preferably tracked by attaching at least one other tracking target 34 a second target to a cup insertion tool 98 as shown in FIG 3 and mathematically relating the position of the second target 34 to the position of the cup 70 In this manner the potential for damage to the cup 70 from directly mounting the target 34 to the cup 70 is eliminated In addition the target 34 can be placed on the tool 98 so as to not obscure the medical practitioner's view of the surgical area Preferably a third or reference target 34 is positioned to allow for spatial orientation of the operating room

Guidance in the placement of the acetabular cup 70 is provided by the navigational software 16 in the computer 20 which displays on the monitor 22 near real time position tracking of the cup 70 relative to the to the pre operatively specified implant position Once the cup 70 is aligned with the implant position the cup 70 is in the pre operatively planned orientation

A series of tests were developed and performed to assess the ability of the apparatus 10 to correctly predict the impingement of the femoral neck 82 with acetabular cup liner 72 The series of tests were developed because the testing described in available references did not include experimental parameters such as neck size and the orientation of the femoral neck axis necessary to evaluate the biomechanical simulator The testing was performed using a laboratory prototype of the apparatus 10 known as the HipNav™ system Details of the testing are presented in Jaramaz et al Range of Motion After Total Hip Arthro

## 12

plasty Experimental Verification of the Analytical Simulator Carnegie Mellon University Robotics Institute Technical Report CMU RI TR 97 09 (February 1997) and Jaramaz et al Simulation of Implant Impingement and Dislocation in Total Hip Replacement Computer Assisted Radiology 10<sup>th</sup> International Symposium and Exhibition Paris June 1996 both of which are incorporated herein by reference

Although the present invention has been described with specific examples directed to hip replacement and revision those skilled in the art will appreciate that the method and apparatus may be employed to implant a component in any joint The skilled artisan will further appreciate that any number of modifications and variations can be made to specific aspects of the method and apparatus of the present invention without departing from the scope of the present invention Such modifications and variations are intended to be covered by the foregoing specification and the following claims

What is claimed is

1 A computer system for determining an implant position of at least one artificial component in a patient's joint comprising

means for creating a joint model of a patient's joint into which an artificial component is to be implanted

means for creating a component model of the artificial component

means for simulating movement of the patient's joint with the artificial component in a test position using the component model and the joint model

means for calculating a range of motion of the joint at the test position based on the simulated movement and

means for determining an implant position for the artificial component based on a predetermined range of motion and the calculated range of motion

2 The computer system of claim 1 wherein said means for creating a joint model comprises means for creating a joint model using skeletal geometric data derived from the joint

3 The computer system of claim 2 wherein said means for creating a joint model comprises means for creating a joint model using tomographic data derived from the joint

4 The computer system of claim 2 wherein said means for creating a joint model comprises means for creating a joint model using computed tomographic data derived from the joint

5 The computer system of claim 1 wherein said means for determining comprises means for determining an implant position in the patient's joint based on a predetermined range of motion for a predetermined activity and the calculated range of motion

6 The computer system of claim 1 wherein said means for simulating comprises means for simulating movement of the artificial component in a test position in the patient's joint using the component model and the joint model

7 An apparatus for facilitating the implantation of artificial components in joints comprising

a tracking device for providing positional tracking data representative of the position of a patient's joint and an artificial component and

a computer system comprising

means for creating a joint model of the patient's joint into which the artificial component is to be implanted

means for creating a component model of the artificial component

13

means for simulating movement of the patient's joint with the artificial component in a test position using the component model and the joint model

means for calculating a range of motion of the joint for said test position based on the simulated movement

means for determining an implant position of the artificial component in the patient's joint based on a predetermined range of motion and the calculated range of motion

means for identifying the determined implant position in the joint model and

means for aligning the joint model with the patient's joint and the artificial component model with the corresponding artificial component based on said positional tracking data

8 The apparatus of claim 7 wherein said computer system further comprises

means for calculating the position of the artificial component relative to the implant position and

a display system attached to said computer system to provide a display of the position of the artificial component with respect to the implant position

9 The apparatus of claim 7 wherein said tracking device comprises an optical tracking system

10 The apparatus of claim 9 wherein said optical tracking system comprises at least one camera positioned to track the position of the patient's joint and the artificial component

11 The apparatus of claim 9 wherein said optical tracking system comprises

tracking targets attached to the patient and the artificial component and

at least one camera positioned to track the position of said tracking targets

12 The apparatus of claim 7 wherein said tracking device is selected from the group consisting of an acoustic tracking system shape based recognition tracking system video based tracking system mechanical tracking system electro magnetic tracking system and radio frequency tracking system

13 The apparatus of claim 7 wherein said means for aligning comprises

means for determining spatial coordinates of discrete points on the joint and

means for calculating a coordinate transformation to align the joint model with the discrete points on the joint

14 A computer system for determining an implant position of an artificial acetabular cup in a patient's acetabulum and an artificial femoral head and shaft component in the patient's femur to provide for cooperation between the artificial femoral head and the acetabular cup said computer system comprising

means for creating a pelvic model of a patient's pelvis into which an artificial acetabular cup component is to be implanted

means for creating an acetabular cup model of the artificial acetabular cup

means for creating a femoral model of a patient's femur into which an artificial femoral head and shaft component is to be implanted

means for creating a femoral head and shaft model of the artificial femoral head and shaft component

means for simulating movement of the patient's hip joint with the artificial femoral head cooperating with the acetabular cup in a test position using the femoral head

14

and shaft and acetabular cup models and the pelvic and femoral models

means for calculating a range of motion of the femoral head and shaft component in the acetabular cup for the test position based on the simulated movement and

means for determining an implant position for the artificial acetabular cup and femoral component based on a predetermined range of motion and the calculated range of motion

15 A method of determining an implant position for artificial components in a joint comprising

creating a joint model of a patient's joint into which an artificial component is to be implanted

creating a component model of the artificial component

simulating movement of the patient's joint with the artificial component in a test position using the component model and the joint model

calculating a range of motion of the joint for said test position based on the simulated movement and

determining an implant position for the artificial component based on a predetermined range of motion and the calculated range of motion

16 A method of facilitating the implantation of artificial components in joints comprising

creating a joint model of a patient's joint into which an artificial component is to be implanted

creating a component model of the artificial component

simulating movement of the patient's joint with the artificial component in a test position using the component model and the joint model

calculating a range of motion of the joint for said test position based on the simulated movement

determining an implant position for the artificial component based on a predetermined range of motion and the calculated range of motion

identifying the implant position in the joint model

aligning the joint model with the patient's joint and the artificial component model with the corresponding artificial component based on positional tracking data representative of the position of the joint and the artificial component and

tracking the artificial component and the joint to maintain alignment of the joint model with the joint and to determine the artificial component position relative to the implant position in the joint

17 The method of claim 16 wherein said step of aligning further comprises

determining spatial coordinates of selected points on the joint and

calculating a coordinate transformation to align the joint model with the points on the joint

18 The method of claim 17 wherein said step of aligning further comprises providing a stationary marker to provide a frame of reference for said step of determining spatial coordinates

19 The method of claim 16 wherein said step of tracking further comprises the step of determining the position of surgical instruments relative to the joint

20 A computerized method of facilitating the implantation of an artificial acetabular cup in an acetabulum of a pelvis comprising

creating a three dimensional pelvic model based on skeletal geometric data of a pelvis and acetabulum into which an artificial acetabular cup is to be implanted



15

creating a three dimensional component model of the artificial acetabular cup and a femoral component  
simulating movement of the patient s hip joint with the artificial femoral head cooperating with the acetabular cup in a test position using the femoral head and shaft and acetabular cup models and the pelvic and femoral models

calculating a range of motion of the femoral head and shaft component in the acetabular cup for the test position based on the simulated movement

determining an implant position for the artificial acetabular cup and femoral component based on a predetermined range of motion and the calculated range of motion

identifying the implant position in the pelvic model  
aligning the pelvic model with the patient s pelvis and the acetabular cup model with the acetabular cup based on positional tracking data providing the position of the pelvis and the acetabular cup and

tracking the acetabular cup and the pelvis to maintain alignment of the pelvic model with the pelvis and to determine the acetabular cup position relative to the implant position in the hip

21 The method of claim 20 wherein

said step of creating further comprises creating a three dimensional femur model of a femur from skeletal data

said step of interfacing further comprises interfacing the femur model with the femoral component model at a femoral implant position

said step of simulating further comprises simulating movement of the artificial femoral component in the acetabular cup at the femoral test position using the artificial component and pelvic models

said step of identifying further comprises identifying the femoral implant position in the femur model

said step of aligning further comprises aligning femoral points on the femur to align the femoral model with the femur and

said step of tracking further comprises tracking the femoral component and the femur to maintain alignment of the femur model with the femur and to determine femoral component position relative to the femoral implant position and the acetabular cup

22 A computer readable medium containing instructions for determining an implant position for artificial components in a joint wherein said instructions comprise instructions for

16

creating a joint model of a patient s joint into which an artificial component is to be implanted

creating a component model of the artificial component  
simulating movement of the patient s joint with the artificial component in a test position using the component model and the joint models

calculating a range of motion of the joint for at least one test position based on the simulated movement and

determining an implant position for the artificial component based on a predetermined range of motion and the calculated range of motion

23 A computer readable medium containing instructions for facilitating the implantation of an artificial acetabular cup in an acetabulum of a pelvis wherein said instructions comprise instructions for

creating a joint model of a patient s joint into which an artificial component is to be implanted

creating a component model of the artificial component  
simulating movement of the patient s joint with the artificial component in a test position using the component model and the joint model

calculating a range of motion of the joint for at least one test position based on the simulated movement

determining an implant position for the artificial component based on a predetermined range of motion and the calculated range of motion

identifying the implant position in the joint model

aligning the joint model with the patient s joint and the artificial component model with the corresponding artificial component based on positional tracking data representative of the position of the joint and the artificial component and

tracking the artificial component and the joint to maintain alignment of the joint model with the joint and to determine the artificial component position relative to the implant position in the joint

24 The computer readable medium of claim 23 wherein said step instruction for aligning comprises instructions for determining spatial coordinates of discrete points on the joint and

calculating a coordinate transformation to align the joint model with the discrete points on the joint

\* \* \* \* \*



PATENT APPLICATION SERIAL NO 08/803993

U S DEPARTMENT OF COMMERCE  
PATENT AND TRADEMARK OFFICE  
FEE RECORD SHEET

PTO-1556  
(5/87)

010 TL 03/28/97 08F03 93  
1 101 1,258 00 LN 97012

087807073



Attorney's Docket No 97012

**PATENT**

**IN THE UNITED STATES PATENT AND TRADEMARK OFFICE**

Box Patent Application  
Assistant Commissioner for Patents  
Washington, D C 20231

**NEW APPLICATION TRANSMITTAL**

Transmitted herewith for filing is the patent application of

Inventor(s) <sup>100</sup> Anthony M / DiGloia, <sup>200</sup> David A / Simon, <sup>300</sup> Branislav Jaramaz,  
<sup>400</sup> Mike K / Blackwell, <sup>500</sup> Frederick Morgan, <sup>600</sup> Robert V / O'Toole,  
and <sup>700</sup> Takeo Kanade

**WARNING** Patent must be applied for in the name(s) of all of the actual inventor(s) 37 CFR 1 41(a) and 1 53(b)

For (title)

**APPARATUS AND METHOD FOR FACILITATING THE IMPLANTATION OF ARTIFICIAL COMPONENTS IN JOINTS**

**CERTIFICATION UNDER 37 CFR 1 10**

I hereby certify that this New Application Transmittal and the documents referred to as enclosed therein are being deposited with the United States Postal Service on this date February 21, 1997 in an envelope as Express Mail Post Office to Addressee Mailing Label Number E1374889661US addressed to the Assistant Commissioner for Patents Washington D C 20231

Beth H Retort

(type or print name of person mailing paper)

Signature of person mailing paper

**NOTE** Each paper or fee referred to as enclosed herein has the number of the Express Mail mailing label placed thereon prior to mailing 37 CFR 1 10(b)

**WARNING** Certificate of mailing (first class) or facsimile transmission procedures of 37 CFR 1 8 cannot be used to obtain a date of mailing or transmission for this correspondence

(Application Transmittal [4 1]—page 1 of 9)

**1 Type of Application**

This new application is for a(n)

(check one applicable item below)

- Original (nonprovisional)
- Design
- Plant

**WARNING** Do not use this transmittal for a completion in the U S of an International Application under 35 U S C 371(c)(4) unless the International Application is being filed as a divisional continuation or continuation in part application

**WARNING** Do not use this transmittal for the filing of a provisional application

**NOTE** If one of the following 3 items apply then complete and attach ADDED PAGES FOR NEW APPLICATION TRANSMITTAL WHERE BENEFIT OF A PRIOR U S APPLICATION CLAIMED and a NOTIFICATION IN PARENT APPLICATION OF THE FILING OF THIS CONTINUATION APPLICATION

- Divisional
- Continuation
- Continuation-in-part (C-I-P)

**2 Benefit of Prior U S Application(s) (35 U S C 119(e), 120 or 121)**

**NOTE** If the new application being transmitted is a divisional continuation or a continuation in part of a parent case or where the parent case is an International Application which designated the U S or benefit of a prior provisional application is claimed then check the following item and complete and attach ADDED PAGES FOR NEW APPLICATION TRANSMITTAL WHERE BENEFIT OF PRIOR U S APPLICATION(S) CLAIMED

**WARNING** If an application claims the benefit of the filing date of an earlier filed application under 35 U S C 120 121 or 365(c) the 20-year term of that application will be based upon the filing date of the earliest U S application that the application makes reference to under 35 U S C 120 121 or 365(c) (35 U S C 154(a)(2) does not take into account for the determination of the patent term any application on which priority is claimed under 35 U S C 119 365(a) or 365(b)) For a c-i-p application applicant should review whether any claim in the patent that will issue is supported by an earlier application and if not the applicant should consider canceling the reference to the earlier filed application The term of a patent is not based on a claim by claim approach See Notice of April 14 1995 60 Fed Reg 20 195 at 20 205

**WARNING** When the last day of pendency of a provisional application falls on a Saturday Sunday or Federal holiday within the District of Columbia any nonprovisional application claiming benefit of the provisional application must be filed prior to the Saturday Sunday or Federal holiday within the District of Columbia See 37 C F R § 1 78(a)(3)

- The new application being transmitted claims the benefit of prior U S application(s) Enclosed are ADDED PAGES FOR NEW APPLICATION TRANSMITTAL WHERE BENEFIT OF PRIOR U S APPLICATION(S) CLAIMED

**3 Papers Enclosed That Are Required for Filing Date under 37 C F R 1 53(b) (Regular) or 37 C F R 1 153 (Design) Application**

- 21 Pages of specification
- 12 Pages of claims
- 1 Pages of Abstract
- 10 Sheets of drawing
- formal
- informal

(Application Transmittal [4-1]—page 2 of 9)

**WARNING DO NOT** submit original drawings. A high quality copy of the drawings should be supplied when filing a patent application. The drawings that are submitted to the Office must be on strong white smooth and non shiny paper and meet the standards according to § 1.84. If corrections to the drawings are necessary they should be made to the original drawing and a high quality copy of the corrected original drawing then submitted to the Office. Only one copy is required or desired. Comments on proposed new 37 CFR 1.84 Notice of March 9 1988 (1990 O.G. 57.62)

**NOTE** Identifying indicia if provided should include the application number or the title of the invention inventor's name docket number (if any) and the name and telephone number of a person to call if the Office is unable to match the drawings to the proper application. This information should be placed on the back of each sheet of drawing a minimum distance of 1.5 cm (5/8 inch) down from the top of the page. 37 C.F.R. 1.84(c)

(complete the following, if applicable)

- The enclosed drawing(s) are photograph(s), and there is also attached a 'PETITION TO ACCEPT PHOTOGRAPH(S) AS DRAWING(S)' 37 C.F.R. 1.84(b)

**4 Additional papers enclosed**

- Preliminary Amendment  
 Information Disclosure Statement (37 C.F.R. 1.98)  
 Form PTO-1449 (PTO/SB/08A and 08B)  
 Citations  
 Declaration of Biological Deposit  
 Submission of "Sequence Listing" computer readable copy and/or amendment pertaining thereto for biotechnology invention containing nucleotide and/or amino acid sequence  
 Authorization of Attorney(s) to Accept and Follow Instructions from Representative  
 Special Comments  
 Other

**5 Declaration or oath**

- Enclosed  
Executed by

(check all applicable boxes)

- inventor(s)  
 legal representative of inventor(s)  
37 CFR 1.42 or 1.43  
 joint inventor or person showing a proprietary interest on behalf of inventor who refused to sign or cannot be reached  
 This is the petition required by 37 CFR 1.47 and the statement required by 37 CFR 1.47 is also attached. See item 13 below for fee

Not Enclosed

**WARNING** Where the filing is a completion in the U.S. of an International Application but where a declaration is not available or where the completion of the U.S. application contains subject matter in addition to the International Application the application may be treated as a continuation or continuation in part as the case may be utilizing ADDED PAGE FOR NEW APPLICATION TRANSMITTAL WHERE BENEFIT OF PRIOR U.S. APPLICATION CLAIMED

(Application Transmittal [4 1]—page 3 of 9)

- Application is made by a person authorized under 37 C F R 1 41(c) on behalf of all the above named inventor(s)

*(The declaration or oath, along with the surcharge required by 37 CFR 1 16(e) can be filed subsequently)*

*NOTE It is important that all the correct inventor(s) are named for filing under 37 CFR 1 41(c) and 1 53(b)*

- Showing that the filing is authorized  
*(not required unless called into question 37 CFR 1 41(d))*

## 6 Inventorship Statement

**WARNING** *If the named inventors are each not the inventors of all the claims an explanation including the ownership of the various claims at the time the last claimed invention was made should be submitted*

The inventorship for all the claims in this application are

- The same

or

- Not the same An explanation including the ownership of the various claims at the time the last claimed invention was made,  
 is submitted  
 will be submitted

## 7 Language

*NOTE An application including a signed oath or declaration may be filed in a language other than English. A verified English translation of the non English language application and the processing fee of \$130 00 required by 37 CFR 1 17(k) is required to be filed with the application or within such time as may be set by the Office 37 CFR 1 52(d)*

*NOTE A non English oath or declaration in the form provided or approved by the PTO need not be translated 37 CFR 1 69(b)*

- English  
 Non-English  
 The attached translation is a verified translation 37 C F R 1 52(d)

## 8 Assignment

- An assignment of the invention to \_\_\_\_\_  
\_\_\_\_\_  
 is attached A separate  "COVER SHEET FOR ASSIGNMENT (DOCUMENT) ACCOMPANYING NEW PATENT APPLICATION or  FORM PTO 1595 is also attached  
 will follow

*NOTE If an assignment is submitted with a new application send two separate letters one for the application and one for the assignment Notice of May 4 1990 (1114 O G 77 78)*

**WARNING** *A newly executed CERTIFICATE UNDER 37 CFR 3 73(b) must be filed when a continuation in part application is filed by an assignee Notice of April 30 1993 1150 O G 62 64*

(Application Transmittal [4 1]—page 4 of 9)

**9 Certified Copy**

Certified copy(les) of application(s)

Country	Appln no	Filed
Country	Appln no	Filed
Country	Appln no	Filed

from which priority is claimed

- is (are) attached
- will follow

*NOTE The foreign application forming the basis for the claim for priority must be referred to in the oath or declaration 37 CFR 1 55(a) and 1 63*

*NOTE This item is for any foreign priority for which the application being filed directly relates. If any parent U S application or International Application from which this application claims benefit under 35 U S C 120 is itself entitled to priority from a prior foreign application then complete item 18 on the ADDED PAGES FOR NEW APPLICATION TRANSMITTAL WHERE BENEFIT OF PRIOR U S APPLICATION(S) CLAIMED*

**10 Fee Calculation (37 C F R 1 16)**

A  Regular application

CLAIMS AS FILED						
Number filed		Number Extra		Rate		Basic Fee 37 C F R 1 16(a) \$770 00
Total Claims (37 CFR 1 16(c))	24 - 20 =	4	×	\$ 22 00		88 00
Independent Claims (37 CFR 1 16(b))	8 - 3 =	5	×	\$ 80 00		400 00
Multiple dependent claim(s), if any (37 CFR 1 16(d))			+	\$260 00		

- Amendment cancelling extra claims is enclosed
- Amendment deleting multiple-dependencies is enclosed
- Fee for extra claims is not being paid at this time

*NOTE If the fees for extra claims are not paid on filing they must be paid or the claims cancelled by amendment prior to the expiration of the time period set for response by the Patent and Trademark Office in any notice of fee deficiency 37 CFR 1 16(d)*

Filing Fee Calculation \$ 1,258 00

(Application Transmittal [4 1]—page 5 of 9)

B  Design application  
(\$320.00—37 CFR 1.16(f))

Filing Fee Calculation \$ \_\_\_\_\_

C  Plant application  
(\$530.00—37 CFR 1.16(g))

Filing fee calculation \$ \_\_\_\_\_

**11 Small Entity Statement(s)**

Verified Statement(s) that this is a filing by a small entity under 37 CFR 1.9 and 1.27 is (are) attached

**WARNING** Status as a small entity in one application or patent does not affect any other application or patent including applications or patents which are directly or indirectly dependent upon the application or patent in which the status has been established. A nonprovisional application claiming benefit under 35 U.S.C. 119(e), 120, 121 or 365(c) of a prior application may rely on a verified statement filed in the prior application if the nonprovisional application includes a reference to a verified statement in the prior application or includes a copy of the verified statement filed in the prior application if status as a small entity is still proper and desired. 37 CFR § 1.28(a)

(complete the following, if applicable)

Status as a small entity was claimed in prior application

\_\_\_\_\_ / \_\_\_\_\_, filed on \_\_\_\_\_, from which benefit is being claimed for this application under

- 35 U.S.C.  119(e),  
 120,  
 121  
 365(c),

and which status as a small entity is still proper and desired

A copy of the verified statement in the prior application is included

Filing Fee Calculation (50% of A, B or C above)

\$ \_\_\_\_\_

**NOTE** Any excess of the full fee paid will be refunded if a verified statement and a refund request are filed within 2 months of the date of timely payment of a full fee. The two month period is not extendable under § 1.136. 37 CFR 1.28(a)

**12 Request for International-Type Search (37 CFR 1.104(d))**

(complete if applicable)

Please prepare an international-type search report for this application at the time when national examination on the merits takes place

(Application Transmittal [4 1]—page 6 of 9)

13 Fee Payment Being Made at This Time

- Not Enclosed
  - No filing fee is to be paid at this time  
(This and the surcharge required by 37 C F R 1 16(e) can be paid subsequently)

Enclosed

- Basic filing fee \$ 1,258 00
- Recording assignment  
(\$40 00, 37 C F R 1 21(h))  
(See attached "COVER SHEET FOR  
ASSIGNMENT ACCOMPANYING NEW  
APPLICATION') \$ \_\_\_\_\_
- Petition fee for filing by other than all the  
inventors or person on behalf of the inventor  
where inventor refused to sign or cannot be  
reached  
(\$130 00, 37 C F R 1 47 and 1 17(h)) \$ \_\_\_\_\_
- For processing an application with a  
specification in  
a non-English language  
(\$130 00, 37 C F R 1 52(d) and 1 17(k)) \$ \_\_\_\_\_
- Processing and retention fee  
(\$130 00 37 C F R 1 53(d) and 1 21(l)) \$ \_\_\_\_\_
- Fee for international-type search report  
(\$40 00 37 C F R 1 21(e)) \$ \_\_\_\_\_

NOTE 37 CFR 1 21(l) establishes a fee for processing and retaining any application that is abandoned for failing to complete the application pursuant to 37 CFR 1 53(d) and this as well as the changes to 37 CFR 1 53 and 1 78 indicate that in order to obtain the benefit of a prior US application either the basic filing fee must be paid or the processing and retention fee of § 1 21(l) must be paid within 1 year from notification under § 53(d)

Total fees enclosed \$ 1,258 00

14 Method of Payment of Fees

- Check in the amount of \$ 1,258 00
- Charge Account No \_\_\_\_\_ in the amount of \$ \_\_\_\_\_

A duplicate of this transmittal is attached

NOTE Fees should be itemized in such a manner that it is clear for which purpose the fees are paid 37 CFR 1 22(b)

(Application Transmittal [4 1]—page 7 of 9)



**15 Authorization to Charge Additional Fees**

**WARNING** If no fees are to be paid on filing the following items should not be completed

**WARNING** Accurately count claims especially multiple dependent claims to avoid unexpected high charges if extra claim charges are authorized

The Commissioner is hereby authorized to charge the following additional fees by this paper and during the entire pendency of this application to Account No 11-1110

37 C F R 1 16(a), (f) or (g) (filing fees)

37 C F R 1 16(b) (c) and (d) (presentation of extra claims)

**NOTE** Because additional fees for excess or multiple dependent claims not paid on filing or on later presentation must only be paid or these claims cancelled by amendment prior to the expiration of the time period set for response by the PTO in any notice of fee deficiency (37 CFR 1 16(d)) it might be best not to authorize the PTO to charge additional claim fees except possibly when dealing with amendments after final action

37 C F R 1 16(e) (surcharge for filing the basic filing fee and/or declaration on a date later than the filing date of the application)

37 C F R 1 17 (application processing fees)

**WARNING** While 37 CFR 1 17(a) (b) (c) and (d) deal with extensions of time under § 1 136(a) this authorization should be made only with the knowledge that Submission of the appropriate extension fee under 37 C F R 1 136(a) is to no avail unless a request or petition for extension is filed (Emphasis added) Notice of November 5 1985 (1060 O G 27)

37 C F R 1 18 (issue fee at or before mailing of Notice of Allowance pursuant to 37 C F R 1 311(b))

**NOTE** Where an authorization to charge the issue fee to a deposit account has been filed before the mailing of a Notice of Allowance the issue fee will be automatically charged to the deposit account at the time of mailing the notice of allowance 37 CFR 1 311(b)

**NOTE** 37 CFR 1 28(b) requires Notification of any change in loss of entitlement to small entity status must be filed in the application prior to paying or at the time of paying issue fee From the wording of 37 CFR 1 28(b) (a) notification of change of status must be made even if the fee is paid as other than a small entity and (b) no notification is required if the change is to another small entity


**16 Instructions as to Overpayment**

Credit Account No \_\_\_\_\_

Refund

Reg No 29,688

Tel No ( 412 ) 355-8645

  
\_\_\_\_\_  
**SIGNATURE OF ATTORNEY**  
Edward L. Pencoske  
\_\_\_\_\_  
(type or print name of attorney)  
Kirkpatrick & Lockhart LLP  
\_\_\_\_\_  
P O Address 1500 Oliver Building  
Pittsburgh, PA 15222  
\_\_\_\_\_

**Incorporation by reference of added pages**

*(check the following item if the application in this transmittal claims the benefit of prior U S application(s) (including an international application entering the U S stage as a continuation divisional or C I-P application) and complete and attach the ADDED PAGES FOR NEW APPLICATION TRANSMITTAL WHERE BENEFIT OF PRIOR U S APPLICATION(S) CLAIMED)*

- Plus Added Pages for New Application Transmittal Where Benefit of Prior U S Application(s) Claimed

Number of pages added \_\_\_\_\_

- Plus Added Pages for Papers Referred to in Item 4 Above

Number of pages added \_\_\_\_\_

- Plus "Assignment Cover Letter Accompanying New Application

Number of pages added \_\_\_\_\_

**Statement Where No Further Pages Added**

*(if no further pages form a part of this Transmittal, then end this Transmittal with this page and check the following item)*

- This transmittal ends with this page

10

1258-101 A  
08/803993



TITLE OF THE INVENTION

Apparatus and Method for Facilitating the Implantation of Artificial Components in Joints

CROSS-REFERENCE TO RELATED APPLICATIONS

Not Applicable

STATEMENT REGARDING FEDERALLY SPONSORED RESEARCH OR DEVELOPMENT

10 This work was supported in part by a National Challenge grant from the National Science Foundation Award IRI 9422734

BACKGROUND OF THE INVENTION

15 The present invention is directed generally to the implantation of artificial joint components and, more particularly, to computer assisted surgical implantation of artificial acetabular and femoral components during total hip replacement and revision procedures

20 Total hip replacement (THR) or arthroplasty (THA) operations have been performed since the early 1960s to repair the acetabulum and the region surrounding it and to replace the hip components, such as the femoral head, that have degenerated. Currently, approximately 200,000 THR  
25 operations are performed annually in the United States alone, of which approximately 40,000 are redo procedures, otherwise known as revisions. The revisions become necessary due to a number of problems that may arise during the lifetime of the implanted components, such as dislocation, component wear and  
30 degradation, and loosening of the implant from the bone

Dislocation of the femoral head from the acetabular component, or cup, is considered one of the most frequent early problems associated with THR, because of the sudden physical, and emotional, hardship brought on by the  
35 dislocation. The incidence of dislocation following the

RECEIVED

2

primary THR surgery is approximately 2-6% and the percentage is even higher for revisions. While dislocations can result from a variety of causes, such as soft tissue laxity and loosening of the implant, the most common cause is

5 impingement of the femoral neck with either the rim of an acetabular cup implant, or the soft tissue or bone surrounding the implant. Impingement most frequently occurs as a result of the malposition of the acetabular cup component within the pelvis.

10 Some clinicians and researchers have found incidence of impingement and dislocations can be lessened if the cup is oriented specifically to provide for approximately 15° of anteversion and 45° of abduction, however, this incidence is also related to the surgical approach. For example, McCollum

15 et al. cited a comparison of THAs reported in the orthopaedic literature that revealed a much higher incidence of dislocation in patients who had THAs with a posterolateral approach. McCollum, D E and W J Gray, "Dislocation after total hip arthroplasty (causes and prevention)", Clinical

20 Orthopaedics and Related Research, Vol 261, p 159-170 (1990). McCollum's data showed that when the patient is placed in the lateral position for a posterolateral THA approach, the lumbar lordotic curve is flattened and the pelvis may be flexed as much as 35°. If the cup was oriented

25 at 15-20° of flexion with respect to the longitudinal axis of the body, when the patient stood up and the postoperative lumbar lordosis was regained, the cup could be retroverted as much as 10°-15° resulting in an unstable cup placement.

Lewinnek et al. performed a study taking into account the

30 surgical approach utilized and found that the cases falling in the zone of 15°±10° of anteversion and 40°±10° of abduction have an instability rate of 1.5%, compared with a 6% instability rate for the cases falling outside this zone.

Lewinnek G E, et al., "Dislocation after total hip-

35 replacement arthroplasties", Journal of Bone and Joint Surgery, Vol 60-A, No 2, p 217-220 (March 1978). The

Lewinnek work essentially verifies that dislocations can be correlated with the extent of malpositioning, as would be expected. The study does not address other variables, such as implant design and the anatomy of the individual, both of which are known to greatly affect the performance of the implant.

The design of the implant significantly affects stability as well. A number of researchers have found that the head-to-neck ratio of the femoral component is the key factor of the implant impingement, see Amstutz H C , et al , "Range of Motion Studies for Total Hip Replacements", Clinical Orthopaedics and Related Research Vol 111, p 124-130 (September 1975). Krushell et al additionally found that certain long and extra long neck designs of modular implants can have an adverse effect on the range of motion. Krushell, R J , Burke D W , and Harris W H , "Range of motion in contemporary total hip arthroplasty (the impact of modular head-neck components)", The Journal of Arthroplasty, Vol 6, p 97-101 (February 1991). Krushell et al also found that an optimally oriented elevated-rim liner in an acetabular cup implant may improve the joint stability with respect to implant impingement. Krushell, R J , Burke D W , and Harris W H , "Elevated-rim acetabular components Effect on range of motion and stability in total hip arthroplasty", The Journal of Arthroplasty, Vol 6 Supplement, p 1-6, (October 1991). Cobb et al have shown a statistically significant reduction of dislocations in the case of elevated-rim liners, compared to standard liners. Cobb T K , Morrey B F , Ilstrup D M , "The elevated-rim acetabular liner in total hip arthroplasty Relationship to postoperative dislocation", Journal of Bone and Joint Surgery, Vol 78-A, No 1, p 80-86, (January 1996). The two-year probability of dislocation was 2.19% for the elevated liner, compared with 3.85% for standard liner. Initial studies by Maxian et al using a finite element model indicate that the contact stresses and therefore the polyethylene wear are not significantly increased for

EXHIBIT 1003

4

elevated rim liners, however, points of impingement and subsequent angles of dislocation for different liner designs are different as would be expected Maxian T A , et al "Femoral head containment in total hip arthroplasty Standard vs extended lip liners", 42nd Annual meeting, Orthopaedic Research society, p 420, Atlanta, Georgia (February 19-22, 1996), and Maxian T A , et al "Finite element modeling of dislocation propensity in total hip arthroplasty", 42nd Annual meeting, Orthopaedic Research society, p 259-64, Atlanta, Georgia (February 19-22, 1996)

An equally important concern in evaluating the dislocation propensity of an implant are variations in individual anatomies As a result of anatomical variations, there is no single optimal design and orientation of hip replacement components and surgical procedure to minimize the dislocation propensity of the implant For example, the pelvis can assume different positions and orientations depending on whether an individual is lying supine (as during a CT-scan or routine X-rays), in the lateral decubitus position (as during surgery) or in critical positions during activities of normal daily living (like bending over to tie shoes or during normal gait) The relative position of the pelvis and leg when defining a "neutral" plane from which the angles of movement, anteversion, abduction, etc , are calculated will significantly influence the measured amount of motion permitted before impingement and dislocation occurs Therefore, it is necessary to uniquely define both the neutral orientation of the femur relative to the pelvis for relevant positions and activities, and the relations between the femur with respect to the pelvis of the patient during each segment of leg motion

Currently, most planning for acetabular implant placement and size selection is performed using acetate templates and a single anterior-posterior x-ray of the pelvis Acetabular templating is most useful for determining the approximate size of the acetabular component, however, it

is only of limited utility for positioning of the implant because the x-rays provide only a two dimensional image of the pelvis Also, the variations in pelvic orientation can not be more fully considered as discussed above

5 Intra-operative positioning devices currently used by surgeons attempt to align the acetabular component with respect to the sagittal and coronal planes of the patient B F Morrey, editor, "Reconstructive Surgery of the Joints", chapter Joint Replacement Arthroplasty, pages 605-608, 10 Churchill Livingstone, 1996 These devices assume that the patient's pelvis and trunk are aligned in a known orientation, and do not take into account individual variations in a patient's anatomy or pelvic position on the operating room table These types of positioners can lead to 15 a wide discrepancy between the desired and actual implant placement, possibly resulting in reduced range of motion, impingement and subsequent dislocation

Several attempts have been made to more precisely prepare the acetabular region for the implant components 20 U S Patent No 5,007,936 issued to Woolson is directed to establishing a reference plane through which the acetabulum can be reamed and generally prepared to receive the acetabular cup implant The method provides for establishing the reference plane based on selecting three reference 25 points, preferably the 12 o'clock position on the superior rim of the acetabulum and two other reference points, such as a point in the posterior rim and the inner wall, that are a known distance from the superior rim The location of the superior rim is determined by performing a series of computed 30 tomography (CT) scans that are concentrated near the superior rim and other reference locations in the acetabular region

In the Woolson method, calculations are then performed to determine a plane in which the rim of the acetabular cup should be positioned to allow for a predetermined rotation of 35 the femoral head in the cup The distances between the points and the plane are calculated and an orientation jig is

11-1-96 10:00 AM

6

calibrated to define the plane when the jig is mounted on the reference points. During the surgical procedure, the surgeon must identify the 12 o'clock orientation of the superior rim and the reference points. In the preferred mode, the jig is  
5 fixed to the acetabulum by drilling a hole through the reference point on the inner wall of the acetabulum and affixing the jig to the acetabulum. The jig incorporates a drill guide to provide for reaming of the acetabulum in the selected plane.

10 A number of difficulties exist with the Woolson method. For example, the preferred method requires drilling a hole in the acetabulum. Also, visual recognition of the reference points must be required and precision placement on the jig on reference points is performed in a surgical setting. In  
15 addition, proper alignment of the reaming device does not ensure that the implant will be properly positioned, thereby establishing a more lengthy and costly procedure with no guarantees of better results. These problems may be a reason why the Woolson method has not gained widespread acceptance  
20 in the medical community.

In U.S. Patent Nos. 5,251,127 and 5,305,203 issued to Raab, a computer-aided surgery apparatus is disclosed in which a reference jig is attached to a double self-indexing screw, previously attached to the patient, to provide for a  
25 more consistent alignment of the cutting instruments similar to that of Woolson. However, unlike Woolson, Raab et al. employ a digitizer and a computer to determine and relate the orientation of the reference jig and the patient during surgery with the skeletal shapes determined by tomography.

30 Similarly, U.S. Patent Nos. 5,086,401, 5,299,288 and 5,408,409 issued to Glassman et al. disclose an image directed surgical robotic system for reaming a human femur to accept a femoral stem and head implant using a robot cutter system. In the system, at least three locating pins are  
35 inserted in the femur and CT scans of the femur in the region containing the locating pins are performed. During the

1002202-0000

7



implanting procedure, the locating pins are identified on the patient, as discussed in col 9, lines 19-68 of Glassman's '401 patent. The location of the pins during the surgery are used by a computer to transform CT scan coordinates into the robot cutter coordinates, which are used to guide the robot cutter during reaming operations

While the Woolson, Raab and Glassman patents provide methods and apparatuses that further offer the potential for increased accuracy and consistency in the preparation of the acetabular region to receive implant components, there remain a number of difficulties with the procedures. A significant shortcoming of the methods and apparatuses is that when used for implanting components in a joint there are underlying assumptions that the proper position for the placement of the components in the joints has been determined and provided as input to the methods and apparatuses that are used to prepare the site. As such, the utility and benefit of the methods and apparatuses are based upon the correctness and quality of the implant position provided as input to the methods

In addition, both the Raab and Glassman methods and apparatuses require that fiducial markers be attached to the patient prior to performing tomography of the patients. Following the tomography, the markers must either remain attached to the patient until the surgical procedure is performed or the markers must be reattached at the precise locations to allow the transformation of the tomographic data to the robotic coordinate system, either of which is undesirable and/or difficult in practice

Thus, the need exists for apparatuses and methods which overcome, among others, the above-discussed problems so as to provide for the proper placement and implantation of the joint components to provide an improved range of motion and usage of the joint following joint reconstruction, replacement and revision surgery

CONFIDENTIAL

8

BRIEF SUMMARY OF THE INVENTION

The above objectives and others are accomplished by methods and apparatuses in accordance with the present invention. The apparatuses and methods include creating a joint model of a patient's joint into which an artificial component is to be implanted and creating a component model of the artificial component. The joint and artificial component models are used to simulate movement of the patient's joint with the artificial component in a test position. The component model and the joint model are used to calculate a range of motion of the joint for at least one test position based on the simulated movement. An implant position, including angular orientation, for the artificial component is determined based on a predetermined range of motion and the calculated range of motion. A goal of the simulation process is to find the implant position which optimizes the calculated range of motion using the predetermined range of motion as a basis for optimization. In practice, the predetermined range of motion is determined based on desired functional motions selected by a medical practitioner on a patient specific basis (e.g. sitting requires flexion of 90°). In a preferred embodiment, the implant position can be identified in the joint model. During surgery the joint model can be aligned with the joint by registering positional data from discrete points on the joint with the joint model. Such registration also allows for tracking of the joint during the surgical procedures.

A current preferred application of the invention is for determining the implant position and sizing of an acetabular cup and femoral implant for use in total hip replacement surgery. Also in a preferred embodiment, alignment of the joint model with the patient's joint is performed using surface based registration techniques. The tracking of the pelvis, the acetabular cup, femoral implant, and surgical

9

instrument is preferably performed using an emitter/detector optical tracking system

The present invention provides the medical practitioner a tool to precisely determine an optimal size and position of artificial components in a joint to provide a desired range of motion of the joint following surgery and to substantially lessen the possibility of subsequent dislocation. Accordingly, the present invention provides an effective solution to problems heretofore encountered with precisely determining the proper sizing and placement of an artificial component to be implanted in a joint. In addition, the practitioner is afforded a less invasive method for executing the surgical procedure in accordance with the present invention. These advantages and others will become apparent from the following detailed description.

#### BRIEF DESCRIPTION OF THE DRAWINGS

A preferred embodiment of the invention will now be described, by way of example only, with reference to the accompanying figures wherein like members bear like reference numerals and wherein

Fig 1 is a system overview of a preferred embodiment of the present invention,

Fig 2 is a flow chart illustrating the method of the present invention,

Fig 3 is a schematic layout of the apparatus of the present invention being used in a hip replacement procedure,

Figs 4(a-c) show the creation of the pelvic model using two dimensional scans of the pelvis (a), from which skeletal geometric data is extracted as shown in (b) and used to create the pelvic model (c),

Figs 5(a-c) show the creation of the femur model using two dimensional scans of the femur (a), from which skeletal geometric data is extracted as shown in (b) and used to create the femur model (c),

10

Fig 6 shows the sizing of the acetabular cup in the pelvic model,

Figs 7(a-e) show the creation of different sized femoral implant models (a) and the fitting of the femoral implant model into a cut femur (b-e),

Fig 8 is a schematic drawing showing the range of motion of a femoral shaft and the impingement (in dotted lines) of a femoral shaft on an acetabular cup,

Figs 9(a-b) shows the range of motion results from biomechanical simulation of two respective acetabular cup orientations, and

Figs 10 (a) and (b) show the registration of the pelvis and femur

15 DETAILED DESCRIPTION OF THE INVENTION

The apparatus 10 of the present invention will be described generally with reference to the drawings for the purpose of illustrating the present preferred embodiments of the invention only and not for purposes of limiting the same. A system overview is provided in Figure 1 and general description of the method of the present invention is presented in flow chart form in Figure 2. The apparatus 10 includes a geometric pre-operative planner 12 that is used to create geometric models of the joint and the components to be implanted based on geometric data received from a skeletal structure data source 13. The pre-operative planner 12 is interfaced with a pre-operative kinematic biomechanical simulator 14 that simulates movement of the joint using the geometric models for use in determining implant positions, including angular orientations, for the components. The implant positions are used in conjunction with the geometric models in intra-operative navigational software 16 to guide a medical practitioner in the placement of the implant components at the implant positions.

The pre-operative geometric planner 12, the pre-operative kinematic biomechanical simulator 14 and the intra-operative navigational software are implemented using a computer system 20 having at least one display monitor 22, as shown in Figure 3. For example, applicants have found that a Silicon Graphics O2 workstation (Mountain View, CA) can be suitably employed as the computer system 20, however, the choice of computer system 20 will necessarily depend upon the resolution and calculational detail sought in practice. During the pre-operative stages of the method, the display monitor 22 is used for viewing and interactively creating and/or generating models in the pre-operative planner 12 and displaying the results of the biomechanical simulator 14. The pre-operative stages of the method may be carried out on a computer (not shown) remote from the surgical theater.

During the intra-operative stages of the method, the computer system 20 is used to display the relative locations of the objects being tracked with a tracking device 30. The medical practitioner preferably can control the operation of the computer system 20 during the procedure, such as through the use of a foot pedal controller 24 connected to the computer system 20. The tracking device 30 can employ any type of tracking method as may be known in the art, for example, emitter/detector systems including optic, acoustic or other wave forms, shape based recognition tracking algorithms, or video-based, mechanical, electro-magnetic and radio frequency (RF) systems. In a preferred embodiment, schematically shown in Figure 3, the tracking device 30 is an optical tracking system that includes at least one camera 32 that is attached to the computer system 20 and positioned to detect light emitted from a number of special light emitting diodes, or targets 34. The targets 34 can be attached to bones, tools, and other objects in the operating room equipment to provide precision tracking of the objects. One such device that has been found to be suitable for performing the tracking function is the Optotrak™ 3020 system from

12

Northern Digital Inc , Ontario, Canada, which is advertised as capable of achieving accuracies of roughly 0.1 mm at speeds of 100 measurements per second or higher

5 The apparatus 10 of Fig 1 is operated in accordance with the method illustrated in Fig 2. The skeletal structure of the joint is determined at step 40 using tomographic data (three dimensional) or computed tomographic data (pseudo three dimensional data produced from a series of two dimensional scans) or other techniques from the skeletal data source 13. Commonly used tomographic techniques include 10 computed tomography (CT), magnetic resonance imaging (MRI), positron emission tomographic (PET), or ultrasound scanning of the joint and surround structure. The tomographic data from the scanned structure generated by the skeletal data source 13 is provided to the geometric planner 12 for use in 15 producing a model of the skeletal structure. It should be noted that, in a preferred embodiment, there is no requirement that fiducial markers be attached to the patient in the scanned region to provide a reference frame for relating the tomography scans to intra-operative position of 20 the patient, although markers can be used as a cross reference or for use with other alternative embodiments.

At step 42, a surface model is created, or constructed, from the skeletal geometric data using techniques, such as 25 those described by B. Geiger in "Three-dimensional modeling of human organs and its application to diagnosis and surgical planning", Ph D thesis, Ecole des Mines de Paris, April 1993. The geometric models constructed from the skeletal data source 13 can be manually generated and input to the geometric planner 12, but it is preferable that the data be 30 used to create the geometric models in an automated fashion.

Also at step 42, geometric models of the artificial components to be implanted into the joint are created/generated. The geometric models can be created in 35 any manner as is known in the art including those techniques described for creating joint models. The geometric models of

the artificial components can be used in conjunction with the joint model to determine an initial static estimate of the proper size of the artificial components to be implanted

5 In step 44, the geometric models of the joint and the artificial components are used to perform biomechanical simulations of the movement of the joint containing the implanted artificial components. The biomechanical simulations are preferably performed at a number of test positions to dynamically optimize the size, position and orientation of the artificial components in the patient's joint to achieve a predetermined range of motion following surgery. The predetermined range of motion for a particular patient is determined based on the expected activities of the patient following surgery. For example, with regard to hip functions, daily activities, such as getting out of bed, walking, sitting and climbing stairs, that are performed by individuals requiring different ranges of motion, as will be discussed in further detail below.

20 The size and orientations of the implant component, and movements simulated at various test positions used in step 44 can be fully automated or manually controlled. In a preferred embodiment, the selection and test process would be automated so as to be more fully optimizable to a predetermined range of motion, either generally, or for predetermined activity. However, because it is necessary that medical practitioners be comfortable and develop confidence in the system, manual control is provided over the selection of the implant components and the test positions in the biomechanical simulator.

30 In step 46, the simulated movement of the joint at various implant positions is used to calculate a range of motion for each implant position. In step 48, the calculated ranges of motion are compared to the predetermined range of motion to select an implant position for the artificial components. A goal of the simulation process is to find the implant position which optimizes the calculated range of

14

motion using the predetermined range of motion as a basis for optimization. In practice, the predetermined range of motion is determined based on desired functional motions selected by a medical practitioner on a patient specific basis (e.g. sitting requires flexion of 90°). The determination of the implant position can be further influenced by other factors such as the variation in the calculated range of motion as a function of implant component orientation. This criterion is useful for determining the surgical margin of error that is available to the medical practitioner without a substantial diminution in the range of motion of the joint.

Steps 40, 42, 44, 46 and 48 represent a pre-operative procedure 50 which is performed so that the artificial components can be properly sized and implant positions can be properly determined. The remainder of the steps in Fig. 2, steps 52, 54, and 56 comprise a procedure 60 which enables a surgeon to realize the desired implant position in the surgical theater.

In step 52, the implant positions determined using procedure 50 are then identified, by marking or incorporating the information in some appropriate manner in the geometric model of the joint. The geometric models of the joint and the artificial components can then be used in conjunction with positional data obtained from the joint and the artificial components during a surgical procedure to provide intra-operative guidance for the implantation of the artificial components.

In step 54, the joint model based on the skeletal data is aligned with the intra-operative position of the patient's joint. In a preferred embodiment, step 54 is performed using a technique known as three dimensional (3D) surface registration. In 3D surface registration, discrete registration points are obtained from the joint skeletal structure to define the intra-operative position of the patient's joint. The registration points are fitted to the joint model of the skeletal structure to determine a

15



coordinate transformation that is used to align the joint model with the intra-operative position of the patient's joint. Once the transformation is established, the intra-operative position of the patient's joint can be tracked using the joint model by obtaining positional data from a point on the joint that provides spatial correspondence between the pre-operative models and the intra-operative measurements. A more thorough description of the surface registration procedure is discussed in D A Simon, M Hebert, and T Kanade, "Real-time 3-D Pose Estimation Using a High-Speed Range Sensor", Carnegie Mellon University, Robotics Institute Technical Report CMU-RI-TR-93-24 (November 1993), D A Simon, M Hebert, and T Kanade, "Techniques for fast and accurate intra-surgical registration", Journal of Image Guided Surgery, 1(1) 17-29, (April 1995), and D A Simon, et al, "Accuracy validation in image-guided orthopaedic surgery", Proc 2nd Int'l Symp MRCAS, Baltimore, (Nov 1995), which are incorporated herein by reference.

The physical location of the intra-operative registration points on the joint from which the positional data is obtained will determine the amount of positional data required to uniquely determine and align the geometric model with the registration points. For example, it is desirable to obtain positional data from the joint that will maximize the constraint on the possible solutions to the alignment problem and provide high level of sensitivity to variations in the position, including orientation, of the joint, as discussed above in the Simon et al references. The goal of the registration process is to determine a "registration transformation" which best aligns the discrete points that provide the spatial position and orientation of the joint with the joint models. Preferably, an initial estimate of this transformation is first determined using manually specified anatomical landmarks to perform corresponding point registration. Once this initial estimate is determined, the

EXHIBIT 1003

Up

surface-based registration algorithm uses the pre- and intra-operative data to refine the initial transformation estimate

Alternatively, step 54 can be implemented using registration systems that employ fiducial markers, to align  
5 the pre-operative data with the intra-operative position of the patient's joint. In those methods, the fiducial markers must be surgically implanted into the skeletal structure before pre-operative images are acquired in step 40. The  
10 intra-operative position of the fiducial markers are compared to the pre-operative data to determine the position of the patient's joint. An example of such a fiducial marker system is discussed in R. H. Taylor, et al., "An image-directed  
15 robotic system for precise orthopaedic surgery", IEEE Trans on Robotics and Automation, 10(3) 261-275, June 1994. In addition, step 54 can be implemented using other registration systems that do not require the pre-operative use of fiducial markers.

In step 56, the position of the joint and the implant components are tracked and compared in near real time to the  
20 implant position identified in the joint model. In this step, the tracking device 30 provides the positional data representative of the position of the patient's joint to the computer system 20. The computer system 20 employs  
25 registration routines within the intra-operative navigational software 16 to determine the position and orientation of the joint and then displays the relative positions of the artificial component and the implant position. The tracking device 30 can also be used to track and provide positional  
30 data representative of the position of other physical objects in the operating room, such as surgical instruments. Additional details of the methods and apparatuses are presented in "HipNav: Pre-operative Planning and Intra-operative Navigational Guidance for Acetabular Implant  
35 Placement in Total Hip Replacement Surgery" DiGioia et al., 2<sup>nd</sup> CAOS Symposium, Bern, Switzerland, 1996, which is incorporated herein by reference.

The operation of the apparatus 10 will now be discussed with reference to its use in a THR procedure. Generally, an acetabular cup 70 (Fig 8) having a cup liner 72 in a convex portion thereof is implanted in an acetabulum 74 (Fig 4b) of a pelvis 76. In addition, a femoral implant 78 (Fig 7) having a head, or ball, 80 and a neck, or shaft, 82 is implanted into a femur 84. The femur 84 has a head portion 86 (Fig 5) that is removed to facilitate the implantation. A bore 88 is drilled in the femur 84 into which the femoral implant 78 is placed. The femoral neck 82 is secured in the bore 88 in a position to allow the femoral head 80 to cooperate with the cup liner 72 in the acetabular cup 70.

In accordance with step 40, skeletal structure data is obtained on the femur and pelvic regions of the patient, preferably via CT scans as shown in Figure 4(a) and 5(a), respectively, from the skeletal data source 13. The CT scans are either manually or automatically inputted in the computer system 20 (Figs 4(b) and 5(b)) and used to create geometric surface models 90 and 92 of the patient's pelvis 76 and femur 84 (Figs 4(c) and 5(c)), respectively as per step 42.

Geometric models 94 and 96 of the acetabular cup 70 and an femoral implant 78, shown in Figures 6 and 7, respectively, are created either manually or in an automated fashion using conventional computer assisted design modelling techniques with implant design or manufacturing data. The size of the acetabular cup 70 can be determined automatically based on the size of the acetabulum 74 determined from the pelvis model 90, the skeletal data or can be manually input. Similarly, the femoral implant 78 can be manually sized to cooperate with the selected acetabular cup 70 using standard implant components or the sizing of the head 80 and neck 82 of the femoral implant 78 can be customized to fit the femur 84 using the femoral implant model 96 and the femur model 92 as shown in Figures 7(a-e). One skilled in the art will appreciate that the computer system 20 in performing step 42 can be programmed using separate or combined software.

14

routines to create the geometric surface models of the patient's anatomy and the implant components

The computer system 20 uses the geometric model 90 of the patient's pelvis 76, the model 92 of the patient's femur, the model 94 of the acetabular cup 70, and model 96 of the femoral implant 78 to perform simulated biomechanical testing of the acetabular cup 70 and the femoral implant 78 implanted at various test positions in the acetabulum 74 and femur 84, respectively, according to step 44. For example, in the case of femoral neck 82 - cup liner 72 impingement, shown in Figure 8, the important parameters in evaluating the prosthetic range of motion are the head 80 to neck 82 ratio of the femoral implant 78, the position, including angular orientation, of the acetabular cup 70 and the relative position of the femoral implant 78 with respect to the cup 70

While the present invention is applicable to non-axisymmetric acetabular implants (i.e. hooded liners, non-neutral liners) and femoral necks (i.e. non-symmetric cross sections), the following discussion of an axisymmetric acetabular cup and femoral neck alignment case is presented to ease the explanation of the concepts. If the center of rotation in the acetabular cup 70 coincides with the center of the head 80 of the femoral implant 78, as shown in Figure 8, the angle  $\Theta$  between the axis of symmetry Z of the acetabular cup 70 and the line of impingement OB defines the allowable angle of motion. The limits of impingement create a cone within which the axis of the femoral neck (line OA) can move without the femoral neck impinging upon the cup liner 72

The position of the neck axis with respect to the cone can be evaluated by observing its intersection with a plane P placed at an arbitrary distance normal to the Z axis. The cross section of the cone defines the impingement circle (if, as stated above, both the liner 72 and the neck 82 are axisymmetric), and the path of the axis of the femoral neck

19

82 defines a curve in the plane P In Figure 8, the axis of the femoral neck 82 begins at point A and moves along the path AB to point B at which point the femoral neck 82 impinges upon the cup liner 72

5 The motion of the femoral neck 82 can be derived from (and expressed as a function of) the physiological movement of the leg, described in terms of combined flexion, extension, abduction, adduction, and external and internal rotation Figs 9(a) and 9(b) show an example of range of  
10 motion (ROM) simulation for two different cup orientations and for two identical sets of ROM exercises (I) 90° flexion (A) + 15° adduction (B) + maximum internal rotation (C) and (II) 10° extension (D) + maximum external rotation (E) As a result of reorienting the cup from 45° abduction + 15°  
15 flexion (Fig 9(a)) to 50° abduction + 5° flexion (Fig 9(b)), maximum internal rotation at the impingement point C is reduced from 15 7° to 4 3° in exercise I and maximum external rotation at the impingement point E is increased from 45 8° to 55 8° in the exercise II In accordance with  
20 step 48, the implant position is determined by comparison of the calculated range of motion of the femoral implant 78 in the acetabular cup 70 with the predetermined range of motion See "Simulation of Implant Impingement and Dislocation in Total Hip Replacement", Jaramaz et al , Computer Assisted  
25 Radiology, 10<sup>th</sup> International Symposium and Exhibition, Paris, June, 1996, which is incorporated herein by reference

In the execution of the intra-operative procedure 60, the implant position is identified in the pelvic model 90 prior to surgery as in step 52 During the surgical  
30 procedure, the pelvis 76 of the patient is exposed One of the tracking targets 34, a pelvic target, is attached to the pelvic region, as shown in Figure 3 Preferably, the target 34 is attached in close proximity to the acetabulum 74 to provide data as close to the area of interest as possible  
35 without becoming an impediment to the surgical procedure The close proximate placement of the target 34 provides an

additional benefit of minimizing the extent to which the  
pelvis must be exposed during the procedure Positional data  
from discrete locations on the patient's pelvis 76 and femur  
84 are taken and provided as input to the navigational  
5 guidance software 16 according to step 54

The intra-operative positional data is registered with  
the pelvic model 90 and femur model 92, as shown in Figs  
10(a) and (b), to align the models with the intra-operative  
position of the patient's pelvis 76 and femur 84,  
10 respectively During the acquisition of discrete registration  
point positional data from the pelvis 76, the tracking device  
30, via camera 32, is used to track the pelvic target The  
pelvic target position data is used in combination with the  
transformation developed using the registration data provide  
15 a spatial correspondence between pre-operative CT coordinates  
(i.e. pelvic model) and the intra-operative coordinates (i.e.  
measurements of the patient's pelvis relative to the pelvic  
target) Intra-operative tracking of the acetabular cup 70  
is also performed relative to the pelvic target

The position of the acetabular cup 70 prior to  
20 implantation is preferably tracked by attaching at least one  
other tracking target 34, a second target, to a cup insertion  
tool 98, as shown in Figure 3, and mathematically relating  
the position of the second target 34 to the position of the  
25 cup 70 In this manner, the potential for damage to the cup  
70 from directly mounting the target 34 to the cup 70 is  
eliminated In addition, the target 34 can be placed on the  
tool 98 so as to not obscure the medical practitioner's view  
of the surgical area Preferably, a third, or reference,  
30 target 34 is positioned to allow for spatial orientation of  
the operating room

Guidance in the placement of the acetabular cup 70 is  
provided by the navigational software 16 in the computer 20  
which displays on the monitor 22 near real time position  
35 tracking of the cup 70 relative to the to the pre-operatively  
specified implant position Once the cup 70 is aligned with

21

the implant position, the cup 70 is in the pre-operatively planned orientation

A series of tests were developed and performed to assess the ability of the apparatus 10 to correctly predict the  
5 impingement of the femoral neck 82 with acetabular cup liner 72. The series of tests were developed because the testing described in available references did not include experimental parameters, such as neck size and the orientation of the femoral neck axis, necessary to evaluate  
10 the biomechanical simulator. The testing was performed using a laboratory prototype of the apparatus 10, known as the HipNav™ system. Details of the testing are presented in Jaramaz et al., "Range of Motion After Total Hip Arthroplasty: Experimental Verification of the Analytical  
15 Simulator", Carnegie Mellon University, Robotics Institute Technical Report CMU-RI-TR-97-09 (Feb 1997) and Jaramaz et al., "Simulation of Implant Impingement and Dislocation in Total Hip Replacement", Computer Assisted Radiology, 10<sup>th</sup> International Symposium and Exhibition, Paris, June, 1996,  
20 both of which are incorporated herein by reference.

Although the present invention has been described with specific examples directed to hip replacement and revision, those skilled in the art will appreciate that the method and apparatus may be employed to implant a component in any  
25 joint. The skilled artisan will further appreciate that any number of modifications and variations can be made to specific aspects of the method and apparatus of the present invention without departing from the scope of the present invention. Such modifications and variations are intended to  
30 be covered by the foregoing specification and the following claims.

22

CLAIMS

What is claimed is

- 1 A computer system for determining an implant position of at least one artificial component in a patient's joint, comprising
  - means for creating a joint model of a patient's joint into which an artificial component is to be implanted,
  - means for creating a component model of the artificial component,
  - means for simulating movement of the patient's joint with the artificial component in a test position using the component model and the joint model,
  - means for calculating a range of motion of the joint at the test position based on the simulated movement, and
  - means for determining an implant position for the artificial component based on a predetermined range of motion and the calculated range of motion

- 2 The computer system of claim 1, wherein said means for creating a joint model comprises means for creating a joint model using skeletal geometric data derived from the joint

- 3 The computer system of claim 2, wherein said means for creating a joint model comprises means for creating a joint model using tomographic data derived from the joint

- 4 The computer system of claim 2, wherein said means for creating a joint model comprises means for creating a joint model using computed tomographic data derived from the joint

23



5 The computer system of claim 1, wherein said means for determining comprises means for determining an implant position in the patient's joint based on a predetermined range of motion for a predetermined activity and the calculated range of motion

6 The computer system of claim 1, wherein said means for simulating comprises means for simulating movement of the artificial component in a test position in the patient's joint using the component model and the joint model

2008-08-28 10:56:56

24

7 An apparatus for facilitating the implantation of artificial components in joints, comprising

a tracking device for providing positional tracking data representative of the position of a patient's joint and an artificial component, and

a computer system comprising,

means for creating a joint model of the patient's joint into which the artificial component is to be implanted,

means for creating a component model of the artificial component,

means for simulating movement of the patient's joint with the artificial component in a test position using the component model and the joint model,

means for calculating a range of motion of the joint for said test position based on the simulated movement,

means for determining an implant position of the artificial component in the patient's joint based on a predetermined range of motion and the calculated range of motion,

means for identifying the determined implant position in the joint model, and

means for aligning the joint model with the patient's joint and the artificial component model with the corresponding artificial component based on said positional tracking data

8 The apparatus of claim 7, wherein said computer system further comprises

means for calculating the position of the artificial component relative to the implant position, and,

a display system attached to said computer system to provide a display of the position of the artificial component with respect to the implant position

25

9 The apparatus of claim 7, wherein said tracking device comprises an optical tracking system

10 The apparatus of claim 9, wherein said optical tracking system comprises at least one camera positioned to track the position of the patient's joint and the artificial component

9  
11 The apparatus of claim 9, wherein said optical tracking system comprises  
tracking targets attached <sup>to</sup> the patient and the artificial component, and,  
at least one camera positioned to track the position of said tracking targets

12 The apparatus of claim 7, wherein said tracking device is selected from the group consisting of an acoustic tracking system, shape based recognition tracking system, video-based tracking system, mechanical tracking system, electro-magnetic tracking system and radio frequency tracking system

13 The apparatus of claim 7, wherein said means for aligning comprises  
means for determining spatial coordinates of discrete points on the joint, and  
means for calculating a coordinate transformation to align the joint model with the discrete points on the joint

B

14 A computer system for determining an implant position of an artificial acetabular cup in a patient's acetabulum ~~and a~~<sup>and an</sup> artificial femoral head and shaft component in the patient's femur to provide for cooperation between the artificial femoral head and the acetabular cup, said computer system comprising

means for creating a pelvic model of a patient's pelvis into which an artificial acetabular cup component is to be implanted,

means for creating an acetabular cup model of the artificial acetabular cup,

means for creating a femoral model of a patient's femur into which an artificial femoral head and shaft component is to be implanted,

means for creating a femoral head and shaft model of the artificial femoral head and shaft component,

means for simulating movement of the patient's hip joint with the artificial femoral head cooperating with the acetabular cup in a test position using the femoral head and shaft and acetabular cup models and the pelvic and femoral models,

means for calculating a range of motion of the femoral head and shaft component in the acetabular cup for the test position based on the simulated movement, and

means for determining an implant position for the artificial acetabular cup and femoral component based on a predetermined range of motion and the calculated range of motion

27

15 A method of determining an implant position for artificial components in a joint, comprising  
creating a joint model of a patient's joint into which an artificial component is to be implanted,  
creating a component model of the artificial component,  
simulating movement of the patient's joint with the artificial component in a test position using the component model and the joint model,  
calculating a range of motion of the joint for said test position based on the simulated movement, and  
determining an implant position for the artificial component based on a predetermined range of motion and the calculated range of motion

24

CLAIMS SECTION

16 A method of facilitating the implantation of artificial components in joints, comprising

- creating a joint model of a patient's joint into which an artificial component is to be implanted,
- creating a component model of the artificial component,
- simulating movement of the patient's joint with the artificial component in a test position using the component model and the joint model,
- calculating a range of motion of the joint for said test position based on the simulated movement,
- determining an implant position for the artificial component based on a predetermined range of motion and the calculated range of motion,
- identifying the implant position in the joint model,
- aligning the joint model with the patient's joint and the artificial component model with the corresponding artificial component based on positional tracking data representative of the position of the joint and the artificial component, and,
- tracking the artificial component and the joint to maintain alignment of the joint model with the joint and to determine the artificial component position relative to the implant position in the joint

17 The method of claim 16, wherein said step of aligning further comprises

- determining spatial coordinates of selected points on the joint, and
- calculating a coordinate transformation to align the joint model with the points on the joint

29



20 A computerized method of facilitating the implantation of an artificial acetabular cup in an acetabulum of a pelvis, comprising

creating a three dimensional pelvic model based on skeletal geometric data of a pelvis and acetabulum into which an artificial acetabular cup is to be implanted,

creating a three dimensional component model of the artificial acetabular cup and a femoral component,

simulating movement of the patient's hip joint with the artificial femoral head cooperating with the acetabular cup in a test position using the femoral head and shaft and acetabular cup models and the pelvic and femoral models,

calculating a range of motion of the femoral head and shaft component in the acetabular cup for the test position based on the simulated movement,

determining an implant position for the artificial acetabular cup and femoral component based on a predetermined range of motion and the calculated range of motion,

identifying the implant position in the pelvic model,

aligning the pelvic model with the patient's pelvis and the acetabular cup model with the acetabular cup based on positional tracking data providing the position of the pelvis and the acetabular cup, and,

tracking the acetabular cup and the pelvis to maintain alignment of the pelvic model with the pelvis and to determine the acetabular cup position relative to the implant position in the hip









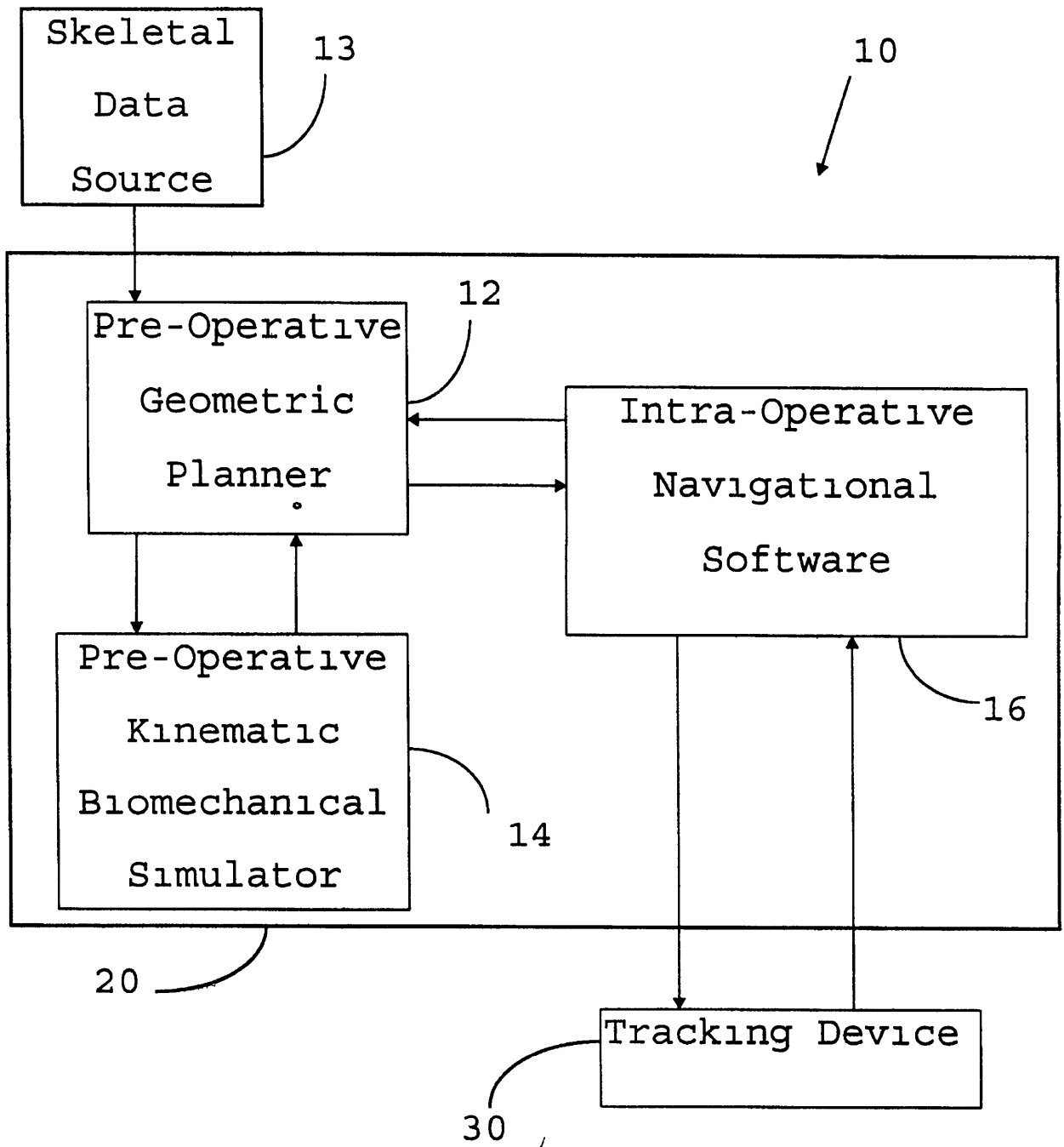
08/803,993

ABSTRACT OF THE DISCLOSURE

Apparatuses and methods are disclosed for determining an  
implant position for at least one artificial component in a  
5 joint and facilitating the implantation thereof. The  
apparatuses and methods include creating a joint model of a  
patient's joint into which an artificial component is to be  
implanted and creating a component model of the artificial  
component. The joint and artificial component models are  
10 used to simulate movement in the patient's joint with the  
artificial component in a test position. The component model  
and the joint model are used to calculate a range of motion  
in the joint for at least one test position based on the  
simulated motion. An implant position, including angular  
15 orientation, in the patient's joint is determined based on a  
predetermined range of motion and the calculated range of  
motion. In a preferred embodiment, the implant position can  
be identified in the joint model and the joint model aligned  
with the joint by registering positional data from discrete  
20 points on the joint with the joint model. Such registration  
also allows for tracking of the joint during surgical  
procedures. A current preferred application of the invention  
is for determining the implant position and sizing of an  
acetabular cup and femoral implant for use in total hip  
25 replacement surgery.

ABSTRACT OF THE DISCLOSURE

Fig. 1



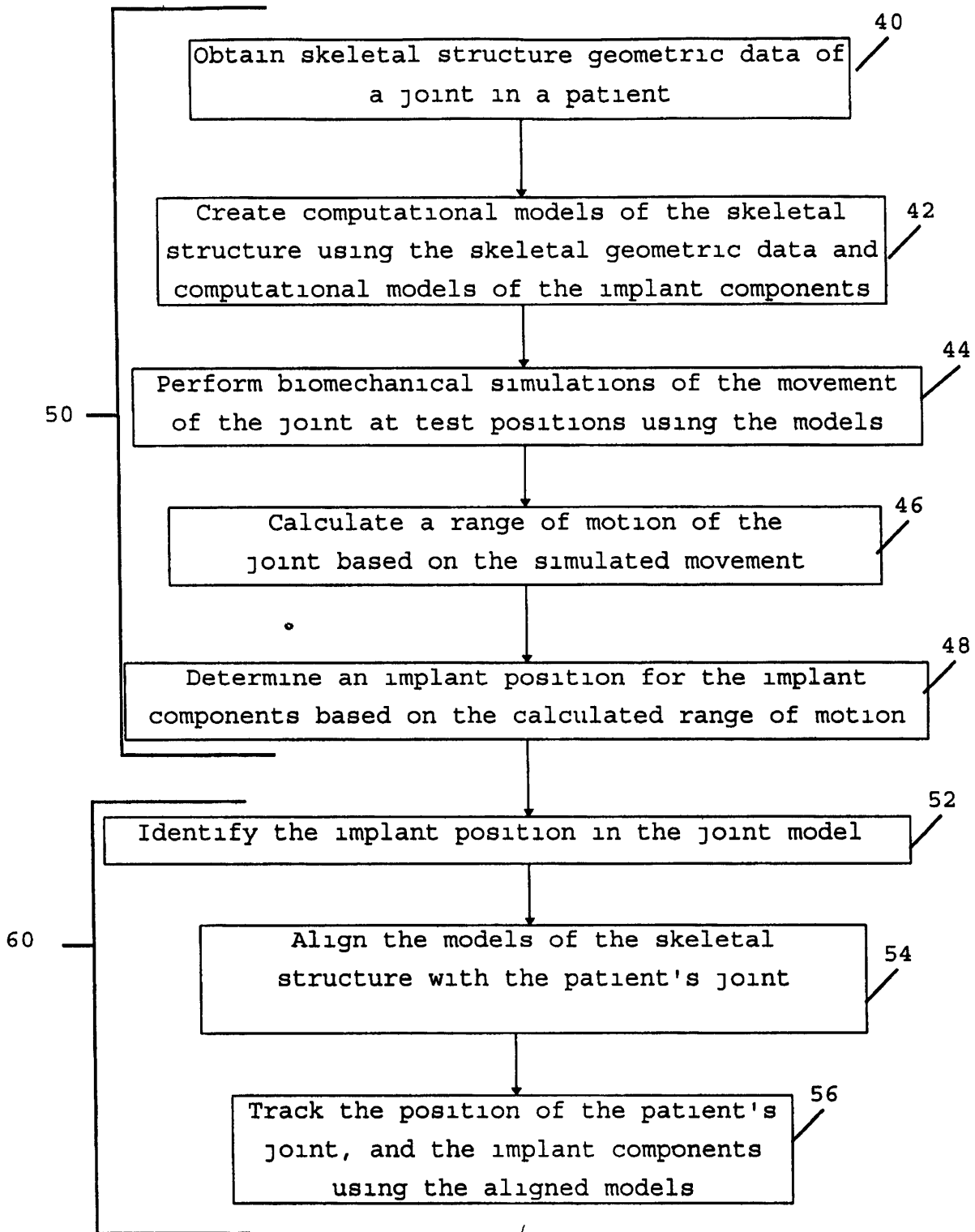
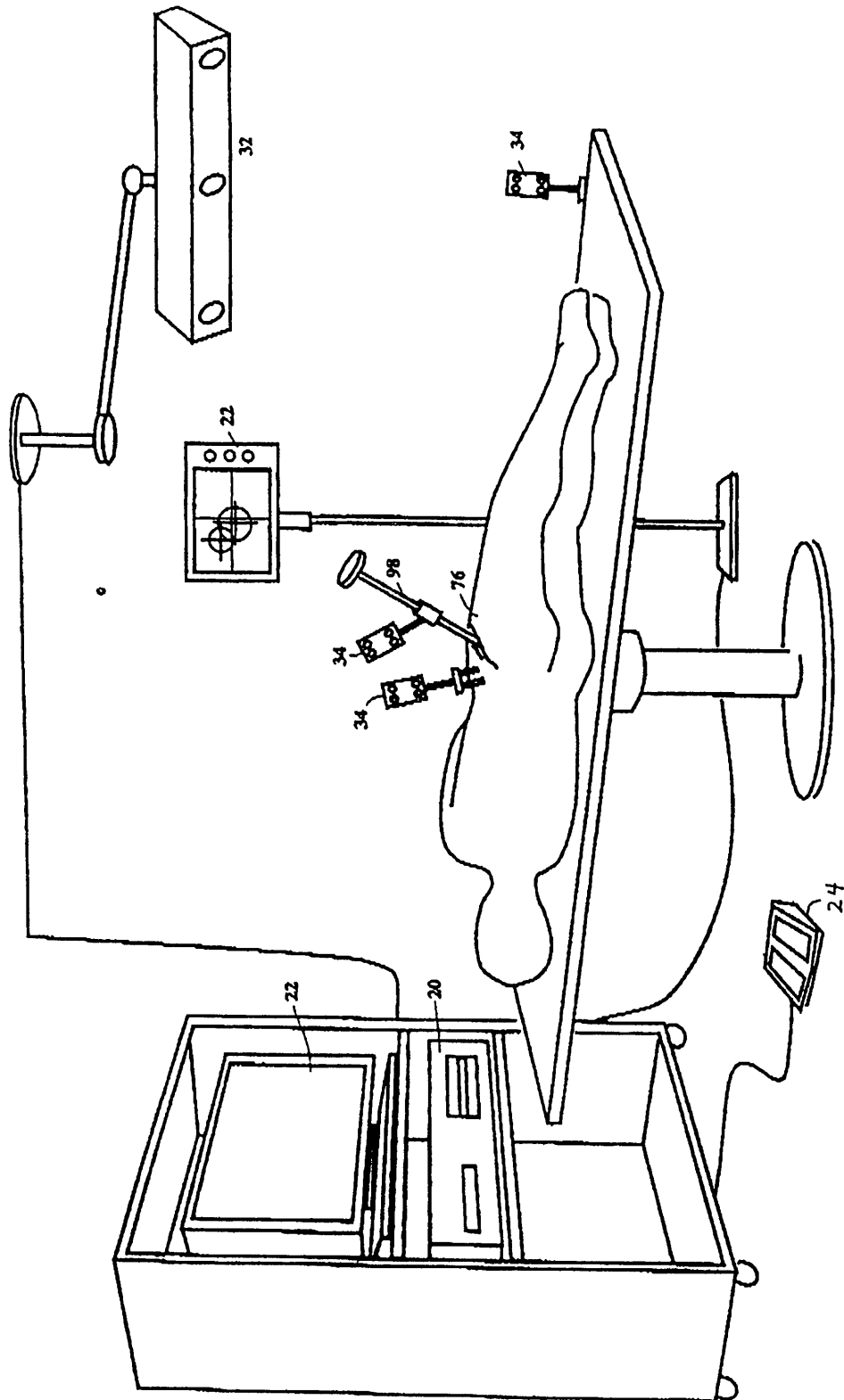


Fig 2

FIG 3







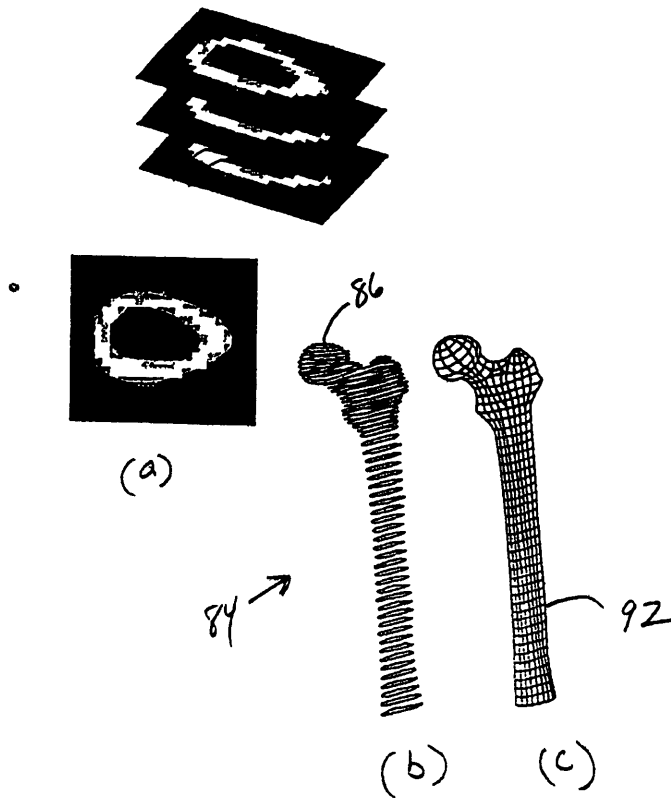


Fig 5

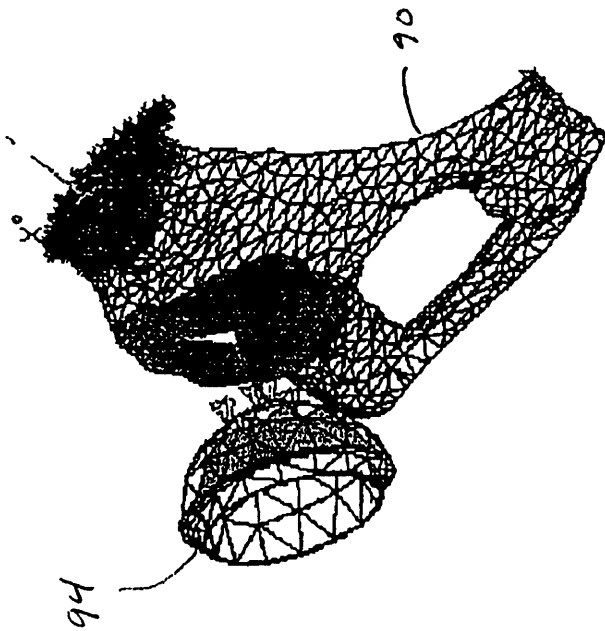
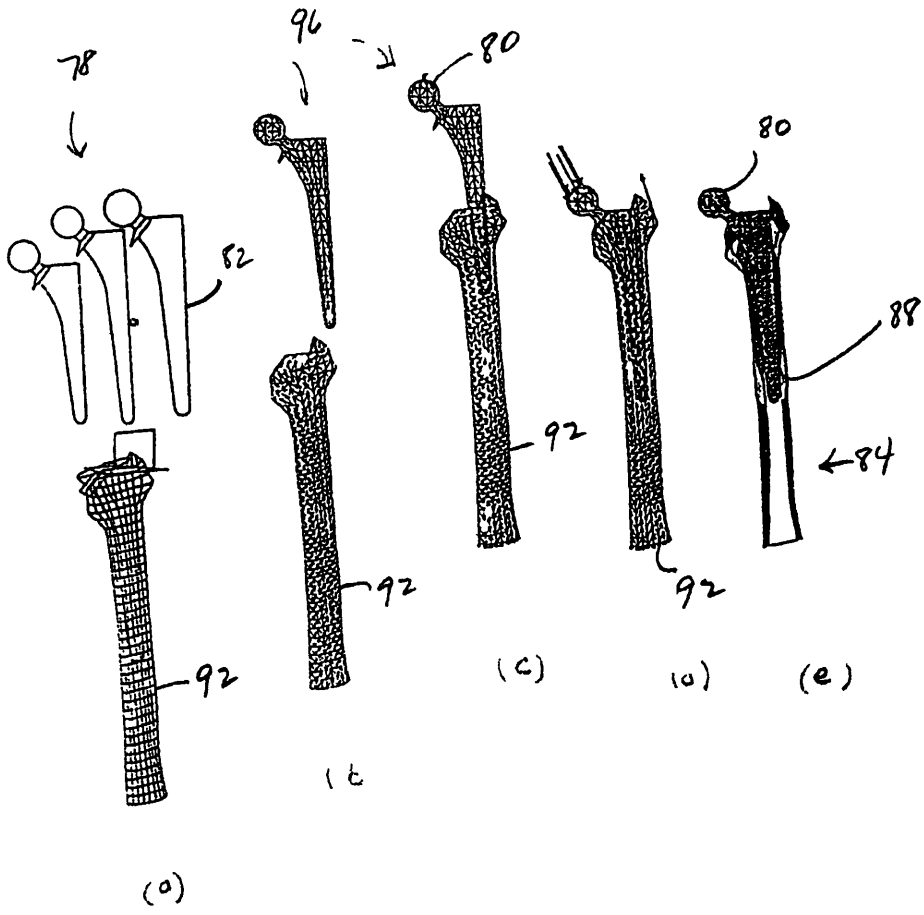
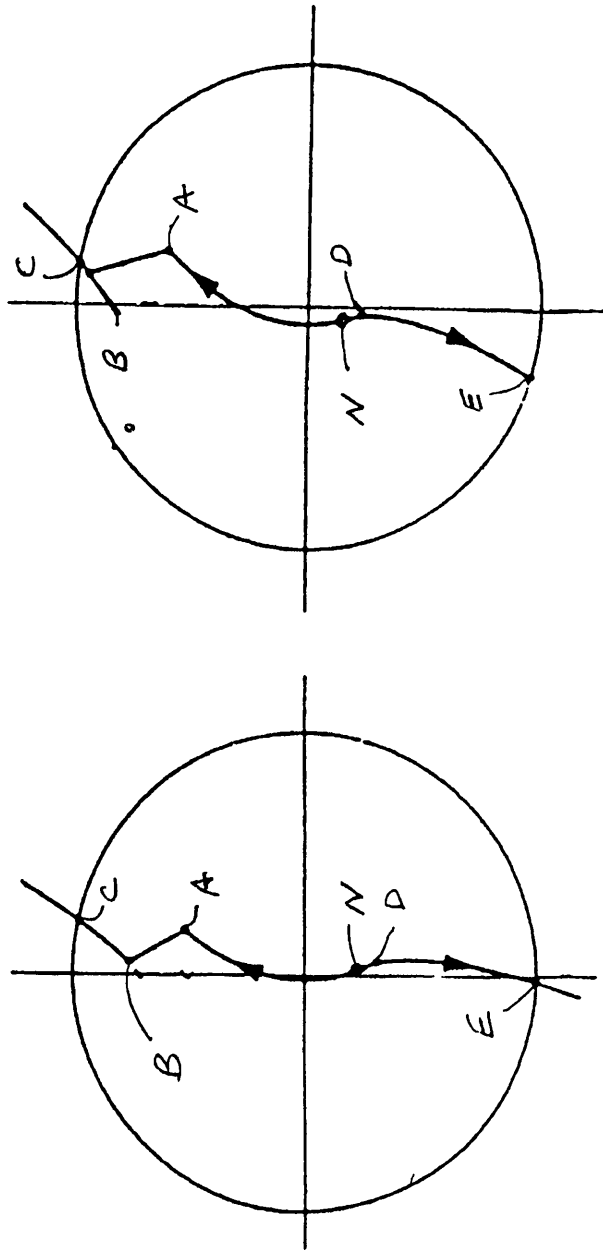


Fig. 6

Fig 7







(b)

Fig 9

(a)

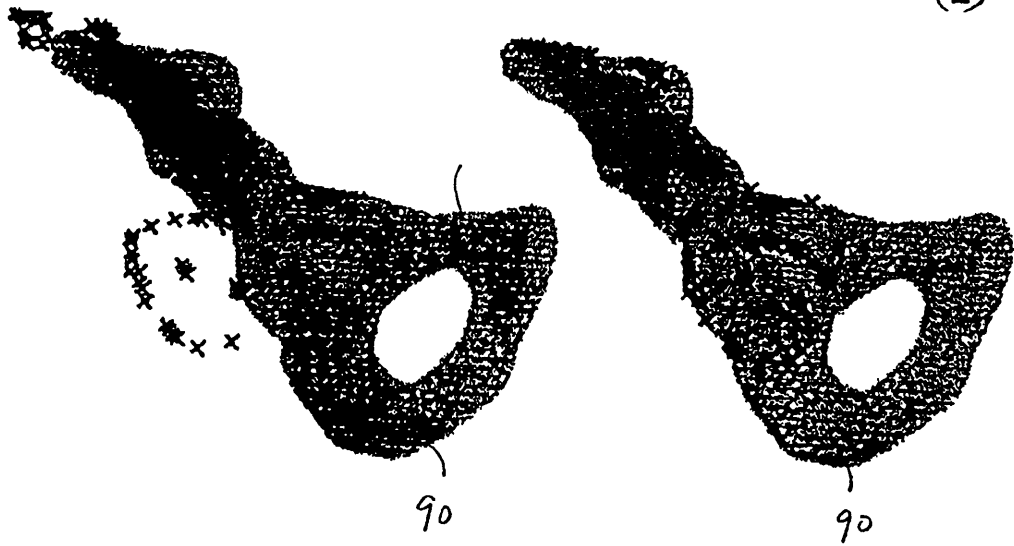
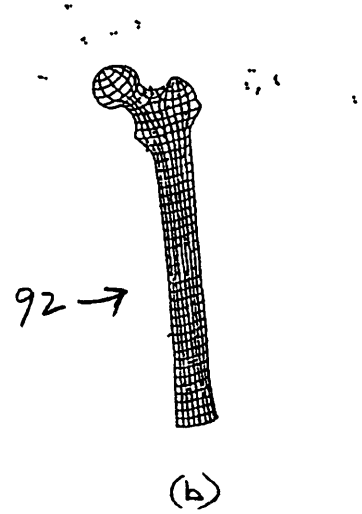


Fig 10

68975 U S PTO  
05/20/97

0360

~~Teammate~~  
#3  
PATENT IDS  
M. [Signature]  
11/3/97

IN THE UNITED STATES PATENT AND TRADEMARK OFFICE

Art Unit	Title
Examiner	APPARATUS AND METHOD FOR
In re application of	FACILITATING THE IMPLANTATION OF
A M DiGloia, et al	ARTIFICIAL COMPONENTS IN JOINTS
Serial No 08/803,993	Group
Filed February 21, 1997	

° INFORMATION DISCLOSURE STATEMENT

Pittsburgh, Pennsylvania 15222  
May 15, 1997

Commissioner of Patents  
and Trademarks  
Washington, D C 20231

Sir

Applicants, in accordance with the duty of disclosure pursuant to 37 C F R § 1 56, hereby advise the United States Patent and Trademark Office of the references listed on the accompanying form PTO 1449 "Information Disclosure Citation" A copy of each of the references cited therein is herewith enclosed

Applicants note that although the cited references may be relevant to the examination of the above-referenced application, under 37 C F R § 1 97(h), the filing of this Information Disclosure Statement "shall not be construed to be an admission that the information cited in the statement is, or is considered to be, material to patentability as defined in § 1 56(b) "

Respectfully submitted,

*Michael C Antone*

Michael C Antone  
Registration No 39,094  
Attorney for Applicant

Kirkpatrick & Lockhart LLP  
1500 Oliver Building  
Pittsburgh, PA 15222-2312  
(412) 355-8375

I hereby certify that this correspondence is being deposited with the United States Postal Service as first class mail in an envelope addressed to Commissioner of Patents and Trademarks Washington DC 20231, on 5/15/97  
*Michael C Antone*

Form PTO-1449 (Rev 12/92)  U S DEPARTMENT OF COMMERCE PATENT AND TRADEMARK OFFICE  INFORMATION DISCLOSURE STATEMENT BY APPLICANT  (Use several sheets if necessary)	Atty Docket No 97012	Serial No 08/803,993
	Applicant A M DiGloia, et al	
	Filing Date 2-21-97	Group 2763

U S PATENT DOCUMENTS

Examiner Initial	Document Number	Issue Date	Patentee	Class	Sub-Class	Filing Date
RF	4,341,220	Jul 27 1982	Perry	128	630	
RF	4,905,148	Feb 27, 1990	Crawford	364	413 1	
RF	5,007,936	Apr 16, 1991	Woolson	623	23	
RF	5 086,401	Feb 4, 1992	Glassman et al	395	94	
RF	5,242,455	Sep 7, 1993	Skeens et al	606	130	
RF	5,251,127	Oct 5 1993	Raab	364	413.13	
RF	5,299,288	Mar 29, 1994	Glassman et al	395	80	
RF	5 305,203	Apr 19, 1994	Raab	364	413 13	
RF	5,383,454	Jan 24 1995	Bucholz	128	653 1	
RF	5,389,101	Feb 14, 1995	Heilbrun et al	606	130	
RF	5,408,409	Apr 18, 1995	Glassman et al	364	413 13	
RF	5,517,990	May 21, 1996	Kalfas et al	128	653.1	

FOREIGN PATENT OR PUBLISHED FOREIGN PATENT APPLICATION

Examiner Initial	Document Number	Public Date	Country or Patent Office	Class	Sub-Class	Transl Y N

Examiner Initial	OTHER DOCUMENTS (Including Author, Title, Date, Relevant Pages Place of Publication)
RF	A M DiGloia, M D , D A Simon, B Jaramaz, M Blackwell, F Morgan, R V O'Toole, B Colgan, E Kischell, <b>HipNav Pre-operative Planning and Intra-operative Navigational Guidance for Acetabular Implant Placement in Total Hip Replacement Surgery</b> , Proceeding of Computer Assisted Orthopedic Surgery, Bern, Switzerland (1996)



Examiner Initial		OTHER DOCUMENTS (Including Author Title, Date, Relevant Pages, Place of Publication)
RF	2	Robert J Krushell, M D , Denis W Burke, M D and William H Harris, M D , <b>Range of Motion in Contemporary Total Hip Arthroplasty</b> , pgs 97-101, The Journal of Arthroplasty, <del>Vol 6, No 2</del> , June, 1991
RF	3	Robert J Krushell, M D , Dennis w Burke, M D and William H Harris, M D , <b>Elevated-rim Acetabular Components</b> , pages <del>1-6</del> , The Journal of Arthroplasty, Vol 6, October, 1991
RF	4	George E Lewinnek, M D , Jack L Lewis, Ph D , Richard Tarr, M S , Clinton L Compere, M D and Jerald R Zimmerman, B S , <b>Dislocations After Total Hip-Replacement Arthroplasties</b> , pgs <del>21-20</del> , Vol 60-A, No 2, March, 1978, The Journal of Bone and Joint Surgery, Incorporated
RF	5	Harlan C Amstutz, M D , R M Ludwig, D J Schurman, M D and A G Hodgson, <b>Range of Motion Studies for Total Hip Replacements</b> , pgs <del>124-130</del> , Clinical Orthopaedics and Related Research, #111, September, 1975
RF	6	T K Cobb, M D , B F Morrey, M D and D M Ilstrup, M S , <b>The Elevated-Rim Acetabular Liner in Total Hip Arthroplasty Relationship to Postoperative Dislocation</b> , pgs <del>80-86</del> , The Journal of Bone and Joint Surgery, 1996
RF	7	D A Simon, R V O'Toole, M Blackwell, F Morgan, A M DiGirola and T Kanade, <b>Accuracy Validation in Image-Guided Orthopaedic Surgery</b> , 2 <sup>nd</sup> Annual Symposium on Medical Robotics and Computer Assisted Surgery, Baltimore, MD, November 4-7 <sup>th</sup> , 1995
RF	8	David A Simon, Martial Hebert and Takeo Kanade, <b>Techniques for Fast and Accurate Intrasurgical Registration</b> , Journal of Image Guided Surgery, <del>1-17-29</del> (1995 )
RF	9	Donald E McCollum, M D and William J Gray, M D , <b>Dislocation After Total Arthroplasty</b> , pgs <del>159-170</del> , Clinical Orthopaedics and Related Research, No 261, December, 1990
RF	10	David A Simon, Martial Hebert and Takeo Kanade, <b>Real-time 3-D Pose Estimation Using a High-Speed Range Sensor</b> , pgs 1-14, Carnegie Mellon University, Robotics Institute, Technical Report, CMU-RI-TR-93-24, November, 1993
RF	11	T A Maxian, T D Brown, D R Pedersen, J J Callaghan, <b>Femoral Head Containment in Total Hip Arthroplasty Standard vs Exended Lip Liners</b> , page 420, 42 <sup>nd</sup> Annual Meeting, Orthopaedic Research Society, February 19-22, Atlanta, Georgia

Examiner Initial		OTHER DOCUMENTS (Including Author, Title, Date, Relevant Pages, Place of Publication)
RF	12	T A Maxian, T D Brown, D R Pederson and J J Callaghan, <b>Finite Element Modeling of Dislocation Propensity in Total Hip Arthroplasty</b> , pg 259-44, 42 <sup>nd</sup> Annual Meeting, Orthopaedic Research Society, February 19-22, 1996, Atlanta, Georgia
RF	13	Vincent Dessenne, Stephane Lavallee, Remi Julliard, Rachel Ort, Sandra Martelli, Philippe Cinquin, , <b>Computer-Assisted Knee Anterior Cruciate Ligament Reconstruction First Clinical Tests</b> , Journal of Image Guided Surgery 1 59-64 (1995)
RF	14	Ali Hamadeh, Stephane Lavallee, Richard Szeliski, Philippe Cinquin, Olivier Peria, <b>Anatomy-based Registration for Computer-integrated Surgery</b> , pgs 212-218, Program of 1 <sup>st</sup> International Conference on Computer Version Virtual Reality "Robotics in Medicine" 1995, Nice, France
RF	15	K Rademacher, H W Staudte, G Rau, <b>Computer Assisted Orthopedic Surgery by Means of Individual Templates Aspects and Analysis of Potential Applications</b> , pgs 42-48
RF	16	Lutz-P Nolte, Lucia J Zamorano, Zhaowei Jiang, Qinghai Wang, Frank Langlotz, Erich Arm, Heiko Visarius, <b>A Novel Approach to Computer Assisted Spine Surgery</b> , pgs 323-328
RF	17	Robert Rohling, Patrice Munger, John M Hollerbach, Terry Peters, <b>Comparison of Relative Accuracy Between a Mechanical and an Optical Position Tracker for Image-Guided Neurosurgery</b> , Journal of Image Guided Surgery, 1 30-34 (1995)
RF	18	E Grimson, T Lozano-Perez, W Wells, G Ettinger, S White, R Kikinis, <b>Automated Registration for Enhanced Reality Visualization in Surgery</b> , pgs 26-29
RF	19	S Lavallee, P Sautot, J Troccaz, P Cinquin, P Merloz, <b>Computer-Assisted Spine Surgery A Technique for Accurate Transpedicular Screw Fixation Using CT Data and a 3-D Optical Localizer</b> , Journal of Image Guided Surgery 1 65-73 (1995)

Examiner Initial			OTHER DOCUMENTS (Including Author, Title, Date, Relevant Pages, Place of Publication)
RF	19	✓	Russell H Taylor, Brent D Mittelstadt, Howard A Paul, William Hanson, Peter Kazanzides, Joel F Zuhars, Bill Williamson, Bela L Musits, Edward Glassman, William L Bargar, <b>An Image-Directed Robotic System for Precise Orthopaedic Surgery</b> , IEEE Transactions on Robotics and Automation, Vol 10, No 3, June, 1994
Examiner <b>RUSSELL FREJD</b>			Date Considered <b>11-Jun-98</b>
EXAMINER Initial citation considered Draw line through citation if not in conformance and not considered Include copy of this form with next communication to applicant			

To Appear in Proceedings of CAOS '96 - Bern, Switzerland

## HipNav: Pre-operative Planning and Intra-operative Navigational Guidance for Acetabular Implant Placement in Total Hip Replacement Surgery

A M DiGioia MD<sup>1,2</sup>, D A Simon<sup>1,2</sup>, B Jaramaz<sup>1,2</sup>, M Blackwell<sup>2</sup>, F Morgan<sup>2</sup>,  
R V O'Toole<sup>3</sup>, B Colgan<sup>1</sup>, E Kischell<sup>2</sup>

<sup>1</sup>Center for Orthopaedic Research  
Shadyside Hospital  
Pittsburgh PA 15232

<sup>2</sup>Robotics Institute  
Carnegie Mellon University  
Pittsburgh, PA 15213

<sup>3</sup>Harvard Medical School  
25 Shattuck St  
Boston MA 02115

### Abstract

*The Hip Navigation or HipNav system allows a surgeon to determine optimal patient specific acetabular implant placement and accurately achieve the desired acetabular implant placement during surgery. Hip Nav includes three components: a pre-operative planner, a range of motion simulator, and an intra-operative tracking and guidance system. The goals of the current HipNav system are to: 1) reduce dislocations following total hip replacement due to acetabular malposition; 2) determine and potentially increase the 'safe' range of motion; and 3) track in real time the position of the pelvis and acetabulum during surgery. This information will help the surgeon achieve more reliable and accurate positioning of the acetabular cup and take into account specific anatomy for individual patients. The HipNav system provides for a new class of research tools that can be used intra-operatively to permit surgeons to re-examine commonly held assumptions concerning bone and implant motion, range of motion testing, and the "optimal" alignment of acetabular cups.*

**Keywords:** computer assisted surgery, total hip replacement, navigational guidance

## 1 Introduction

The incidence of dislocation following primary total hip replacement (THR) surgery is between 2-6% and even higher following revisions [5] [4]. It is therefore, one of the most commonly occurring complications following hip replacement surgery. Dislocation of a total hip replacement causes significant distress to the patient and physician and is associated with significant additional costs in order to relocate the hip. Another complication of THR surgery is impingement between the neck of the femoral implant and the rim of the acetabular component, as shown in Figure 1. Impingement can lead to advanced wear of the acetabular rim resulting in polyethylene wear debris shown to accelerate loosening of implant bone interfaces. The position at which impingement occurs is determined by the design and geometry of the implants (such as the size of the femoral head, the width of the neck, and the design of the acetabular liner), and more importantly by the relative position of the femoral and acetabular implants. In certain cases, impingement may result in dislocation, as seen in the X-Ray of Figure 2. The causes of dislocation following total hip replacement are multi-factorial and include not only malposition of the implants causing impingement, but also soft tissue and bone impingement, and soft tissue laxity [5]. The most common cause of both impingement and dislocation is malposition of the acetabular component [5].

A system has been developed to permit accurate placement of the acetabular component during surgery. As shown in Figure 3, the Hip Navigation or HipNav system includes three components: a pre-operative

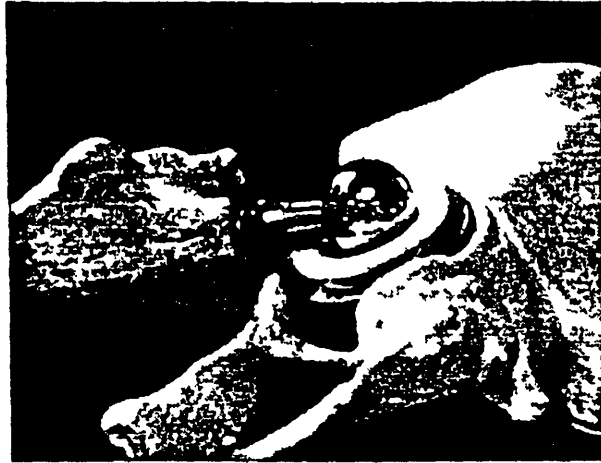


**Figure 1 Implant Impingement.**



**Figure 2 X-Ray showing pelvic dislocation**

planner, a range of motion simulator, and an intra-operative tracking and guidance system. The pre-operative planner allows the surgeon to manually specify the position of the acetabular component within the pelvis based upon pre-operative CT images. The range of motion simulator estimates femoral range of motion based upon the implant placement parameters provided by the pre-operative planner. The feedback provided by the simulator can aid the surgeon in determining optimal, patient specific acetabular implant placement. The intra-operative tracking and guidance system is used to accurately place the implant in the predetermined optimal position regardless of the position of the patient on the operating room table.

By accurately placing the acetabular component in an optimally selected position, the HipNav system has the potential to reduce the risk of dislocations and the generation of wear debris caused by impingement resulting from malpositioned components and increase the "safe" range of motion.

## **2 Current Practice**

Current planning for acetabular implant placement and size selection is performed using acetate templates and a single anterior-posterior X-Ray of the pelvis. Acetabular templating is most commonly performed



Figure 3 HipNav system overview

to determine the approximate size of the acetabular component, but there is little effort to accurately determine the ideal position of the implant

The intra-operative positioning devices currently used by surgeons attempt to align the acetabular component with respect to the sagittal and coronal planes of the patient [6]. These devices assume that the patient's pelvis and trunk are aligned in a known orientation, and do not take into account individual variations in a patient's anatomy or pelvic position on the operating room table. Use of this type of positioner can lead to a wide discrepancy between the desired and actual implant placement, possibly resulting in reduced range of motion, impingement and subsequent dislocation.

### 3 System Description

The first step in using the HipNav system is the pre-operative CT scan which is used to determine the patient's specific bony geometry. The CT images are used in the pre-operative planner which allows the surgeon to determine appropriate implant size and placement. In the current version of the planner, the surgeon can position cross sections of the acetabular implant upon orthogonal views of the pelvis, as seen in Figure 4. We are investigating other methods of presenting CT data to the surgeon, including an approach which displays implant placement on multiple CT cross sections, each of which passes through the acetabulum's central axis (the axis which passes through the center of pelvic rotation and which is perpendicular to the plane of the acetabular rim).

Once the surgeon has selected the position of the acetabular implant, the range of motion simulator is used to determine the femoral positions (in terms of extension/flexion, abduction/adduction and internal/external rotation) at which impingement would occur for that specific implant design and position. Based upon this range of motion information, the surgeon may choose to modify the selected position in an attempt to achieve the "optimal" cup position for the specific patient. The range of motion simulator performs a kinematic analysis which determines an "envelope" of the safe range of motion, as seen in Figure 5. A more detailed description of the range of motion simulator appears in [3].

The optimal patient specific plan is used by the HipNav System in the operating room on the day of surgery. HipNav permits the surgeon to determine where the pelvis and acetabulum are in "operating room coordinates" at all times during surgery. Knowing the position of the pelvis during all phases of surgery and especially during preparation and implantation of the acetabular implant, permits the surgeon to accu-

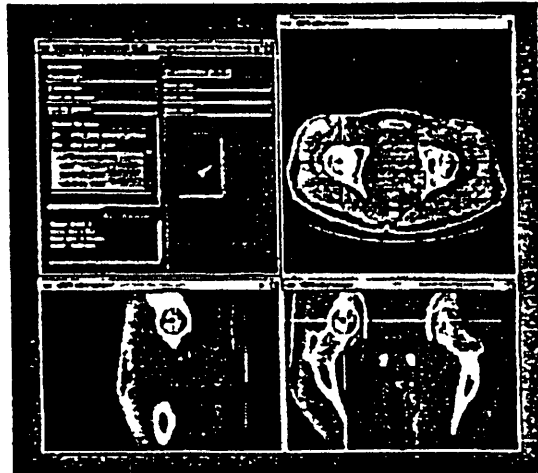


Figure 4 Pre-operative planner

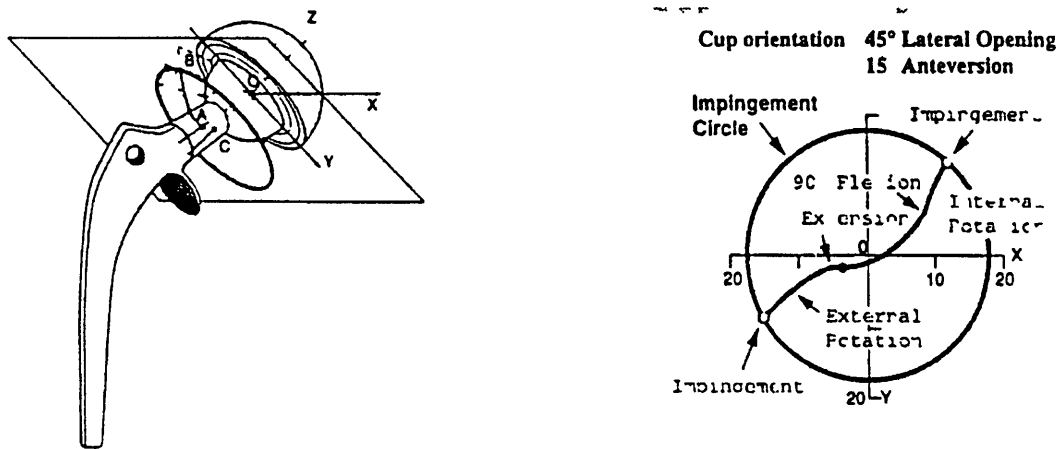
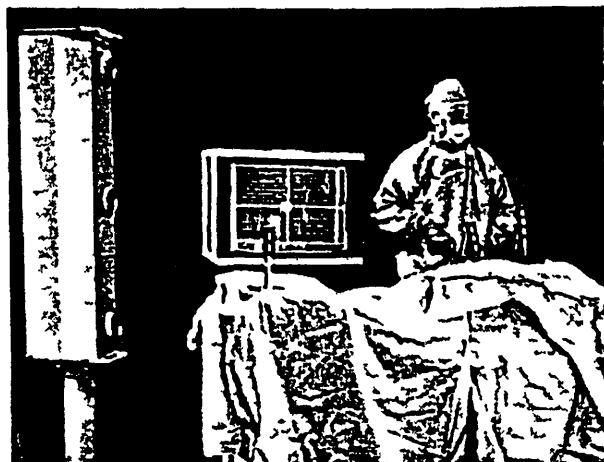


Figure 5 Kinematic simulations Left - implant geometry Right - motion envelope

rately and precisely position the cup according to the pre-operative plan. Alternately, using HipNav the surgeon can align the component to an accepted standard such as "true" 45 degrees of abduction and 20 degrees of anteversion.

There are several high-technology devices that are used intra-operatively to allow the surgeon to accurately execute the pre-operative plan, as seen in Figure 6. One such device is an 'Optotrak' optical tracking camera (Northern Digital Inc., Ontario, Canada) which is capable of tracking the position of special light emitting diodes or "LEDs". These LEDs can be attached to bones, tools, or other pieces of operating room equipment to allow highly reliable tracking. Optotrak can achieve accuracies of roughly 0.1mm at speeds of 100 measurements per second or higher.

In order to determine the location of the pelvis and the acetabular implant during surgery, Optotrak targets are attached to several conventional surgical tools, as seen in Figure 7. The pelvis is tracked by attaching a target to the pelvic portion of a Harris leg length caliper (Zimmer, Inc., Warsaw, IN), and inserting this device into the wing of the ilium. The acetabular implant is tracked by attaching a second target to the handle of an HGP II acetabular cup holder and positioner (Zimmer, Inc., Warsaw, IN). A third Optotrak target



**Figure 6 Intra-operative execution**

is required by the HipNav system to determine operating room coordinates (i.e., left, right, up and down with respect to the surgeon)

Several key steps are necessary to use the HipNav intra-operative guidance system. One of the most important is the registration of pre-operative information (i.e., the CT scan and pre-operative plan) to the position of the patient on the operating room table. One limitation of current registration systems used in orthopaedics is the need for pins to be surgically implanted into bone before pre-operative images are acquired (e.g. [9]). An alternative technique being investigated within our group uses surface geometry to perform registration [8] [7]. In this approach, the surfaces of a bone (such as the pelvis or acetabulum) can be used to accurately align the intra-operative position of the patient to the pre-operative plan without the use of pins or other invasive procedures. Using this technique, it is necessary to sense multiple points on the surface of the bone with a digitizing probe during surgery. These "intra-operative data points" are then matched to a geometric description of the bony surface of the patient derived from the CT images used to plan the surgery.

The registration process is illustrated in Figure 8. The pelvic surface model was constructed from CT data using techniques described in [1]. The discrete points were collected using a digitizing probe which was physically touched to the indicated points. The goal of the process is to determine a "registration transfor-

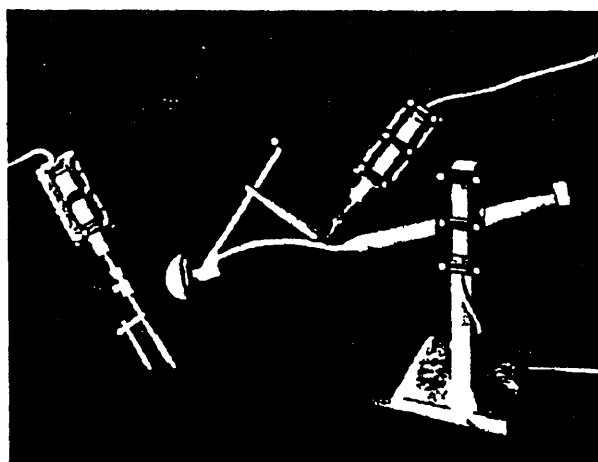


**Figure 7 Standard surgical tools instrumented with optical tracking targets**



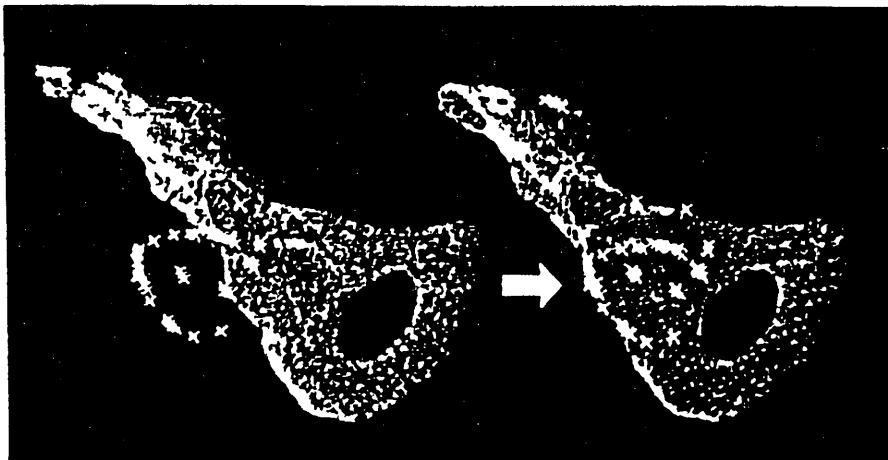


**Figure 8 Surface-based registration**

mation which best aligns the discrete points with the surface model. An initial estimate of this transformation is first determined using manually specified anatomical landmarks to perform corresponding point registration [2]. Once this initial estimate is determined, the surface-based registration algorithm described in [8] uses the pre- and intra-operative data to refine the initial transformation estimate.

Once the location of the pelvis is determined via registration, navigational feedback can be provided to the surgeon on a television monitor, as seen in Figure 9. This feedback is used by the surgeon to accurately position the acetabular implant within the acetabular cavity. To accurately align the cup within the acetabulum in the position determined by the pre-operative plan, the cross hairs representing the tip of the implant and the top of the handle must be aligned at the fixed cross hair in the center of the image. Once aligned, the implant is in the pre-operatively planned position and orientation.

Registration also allows the position of the pelvis to be tracked during surgery using the Optotrak system as demonstrated in Figure 10. This eliminates the need for rigid fixation of the pelvis. In addition, this tracking ability allows us to record the position of the pelvis during surgery, and especially at key times such as at the time of implantation of the acetabular component or during range of motion testing.

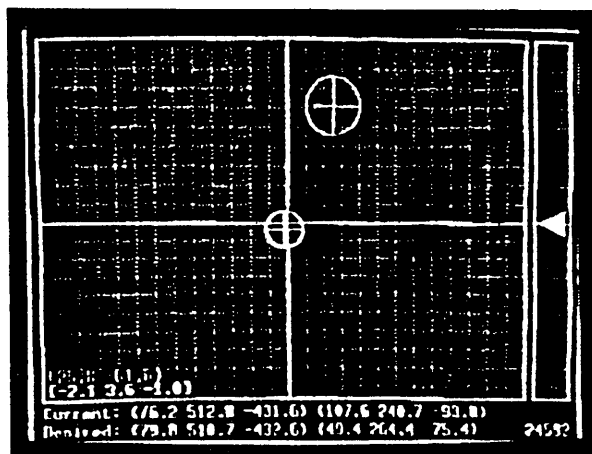


**Figure 9 Navigational feedback**

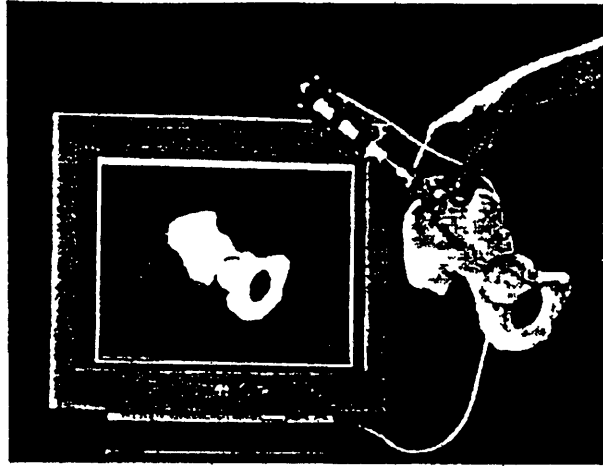


Figure 10 Real-time tracking of the pelvis

## 4 Conclusions

The goals of the HipNav system are to 1) reduce dislocations following total hip replacement due to impingement, 2) determine and potentially increase the 'safe' range of motion, and 3) track in real time the position of the pelvis and acetabulum during surgery. This information will help the surgeon achieve more reliable and accurate positioning of the acetabular cup and take into account specific anatomy for individual patients.

HipNav will also provide clinicians and researchers with a new class of tools for critically examining common assumptions concerning range of motion, bone motion, and 'optimal' alignment. For example, the pelvis can be tracked during surgery to determine its position at key times such as prior to dislocation, following dislocation, and during acetabular component implantation. Using these tools, we can evaluate the efficacy of the HipNav system in placing the acetabular implant compared to traditional techniques and critically examine commonly held beliefs of optimal acetabular position (i.e., 45 degrees of abduction, 20 degrees of anteversion).

The HipNav system holds the promise of reducing dislocation rates in primary and revision total hip replacement by optimizing the relative position of the acetabular implants and minimizing impingement. In addition, it will provide a new category of "smart" tools that will be useful to study issues in total hip replacement and ultimately other procedures.

## References

- [1] B. Geiger, *Three dimensional modeling of human organs and its application to diagnosis and surgical planning*, PhD thesis, Ecole des Mines de Paris, April 1993.
- [2] B. K. P. Horn, Closed form solution of absolute orientation using unit quaternions, *Journal of the Optical Society of America A*, 4(4) 629-642, April 1987.
- [3] B. Jaramaz, S. M. Kladakis, A. M. Digiorgio, L. F. Kallivokas, and O. Ghattas, Simulation of implant impingement and dislocation in total hip replacement. In *Computer Assisted Radiology 10th International Sympo*

*sium and Exhibition Paris June 1996*

- [4] D E McCollum M D and W J Gray M D Dislocation after total hip arthroplasty *Clinical Orthopaedics* (261) 159-170 1990
- [5] B F Morrey editor *Reconstructive Surgery of the Joints*, chapter 91- Dislocation pages 1247-1260 Churchill Livingstone 1996
- [6] B F Morrey editor *Reconstructive Surgery of the Joints* chapter Joint Replacement Arthroplasty pages 605-608 Churchill Livingstone 1996
- [7] D A Simon M Hebert and T Kanade Real-time 3-d pose estimation using a high-speed range sensor In *Proceedings of IEEE International Conference on Robotics and Automation*, pages 2235-2241 San Diego CA May 1994 IEEE
- [8] D A Simon M Hebert and T Kanade Techniques for fast and accurate intra-surgical registration *Journal of Image Guided Surgery* 1(1) 17-29 April 1995
- [9] R H Taylor B D Mittelstadt H A Paul W Hanson P Kazanzides J F Zuhars B Williamson B L Musits E Glassman and W L Bargar An image directed robotic system for precise orthopaedic surgery *IEEE Transactions on Robotics and Automation*, 10(3) 261-275 June 1994

# Range of Motion in Contemporary Total Hip Arthroplasty

## The Impact of Modular Head-Neck Components

Robert J. Krushell MD\* Dennis W. Burke MD† and  
William H. Harris MD\*

---

**Abstract** The prosthetic range of motion (PROM) of two modular total hip arthroplasty (THA) systems and one older nonmodular comparison system was evaluated. The head-neck geometry of the modular systems resulted in a smaller PROM than the nonmodular system. Longer head-neck components commonly had flanges which caused the greatest reduction in PROM. This effect became more pronounced as head size decreased. Modular head-neck components offer recognized benefits but can be associated with notably smaller ROM and increased risk of prosthetic impingement. The surgeon should be aware that in modern systems PROM decreases when neck width is increased. Moreover, in cases of prosthetic instability, the potential role of the flange of a modular head should be evaluated. Methods are suggested for maximizing PROM clinically through preoperative planning, optimal femoral neck resection, and implant utilization. **Key words:** modular femoral prosthesis, range of motion.

---

Range of motion (ROM) is a critical feature in the design of total hip arthroplasties (THA) (1, 2). Conceptually, in the absence of undue soft tissue laxity, the motion between the femoral and acetabular components will continue freely until either prosthetic or bone impingement occurs. Motion beyond this point of impingement will cause progressive subluxation until dislocation occurs. Prosthetic impingement can also lead to increased wear debris and increased stress and micromotion at the implant-cement-bone or bone-metal interfaces of the hip ar-

throplasty. Prosthetic impingement and ROM are markedly influenced by the configuration of the head-neck region of the femoral component (1, 2). Most contemporary THA systems have incorporated into the geometry of the femoral neck two features not found in previous designs: (1) a Morse taper which conveys the major advantage of allowing the use of modular femoral head components of varying neck lengths, and (2) a flange or skirt on many modular femoral head components with longer neck lengths (Fig. 1).

These changes in contemporary implant geometry can measurably affect the prosthetic range of motion (PROM), yet the magnitude of these effects has not previously been studied. In this paper, we report on ROM and impingement in two contemporary modular hip designs in comparison with a traditional nonmodular control. Methods to optimize ROM using contemporary modular systems are discussed.

---

*From the Department of Orthopaedics, Brigham and Women's Hospital, Boston, Massachusetts, and †Department of Orthopaedics, Massachusetts General Hospital, Boston, Massachusetts.*

Reprint requests: Dr. William H. Harris, Biomechanics Laboratory, Jackson 1126, Massachusetts General Hospital, Boston, MA 02114.

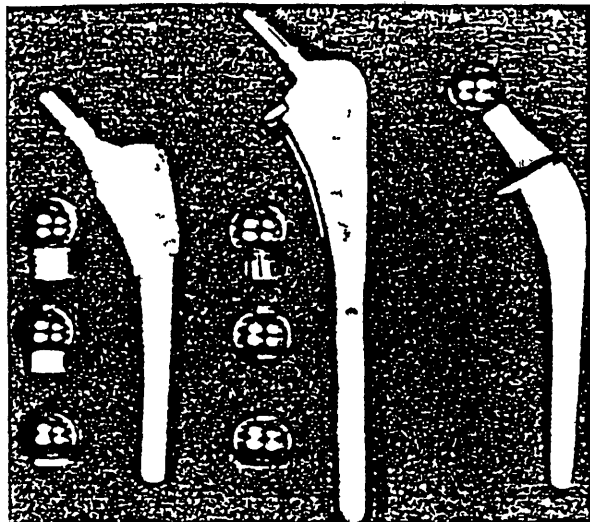


Fig 1 Femoral components tested shown together with their modular 26 mm head components (from left to right) PCA HGP and nonmodular HD 2. A flange or skirt is present on many lower neck modular head components. This flange fits over the end of the Morse taper of the femoral component and in effect widens the neck of the femoral component.

### Materials and Methods

An apparatus was constructed to incorporate a three dimensional protractor that allowed THAs to be inserted in consistent alignment and simulated a compressive force across the hip joint. ROM and stability were tested with anatomic bone models and

with special fixtures that held the implants allowing tests of the isolated PROM (Fig 2)

Two contemporary modular THA systems were studied (Zimmer HGP and Howmedica PCA) as well as an older nonmodular design for historical comparison (Howmedica HD 2) (Fig 1). Each femoral component was tested with its corresponding acetabular component and all acetabular components were of comparable geometry. For each modular system the ROM using 26-mm head components was measured. In addition head sizes of 22 mm and 32 mm were tested using the HGP system.

Each acetabular component was inserted in 30° of abduction and 20° of forward flexion. Femoral components were inserted in 15° of anteversion with a femoral anatomic axis of 8°. All implants were tested in four positions in neutral abduction, maximum flexion in neutral rotation (FLEX), maximum extension in neutral rotation (EXT), maximum internal rotation in 90° flexion (IRF) and maximum external rotation in 0° extension (ERE). As the implants were tested in each of these four positions, a record was made of the point at which prosthetic impingement and subluxation first occurred.

### Results

We defined the total flexion arc as the ROM in degrees measured with the hip in neutral rotation and abduction from full flexion to full extension before prosthetic impingement-subluxation occurred.

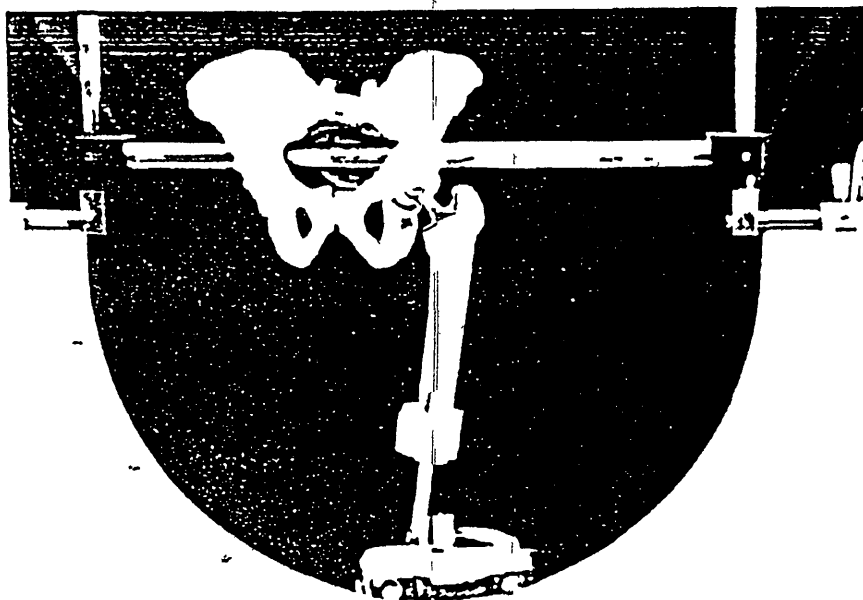


Fig 2 Test apparatus shown with bone model. Fixtures to secure the components can be substituted for testing isolated prosthetic ROM.

Table 1 Effect of Head Size on Prosthetic ROM

HGP	Max Flexion - Max Extension			Head Size	Internal Rotation (90 Flex)		
	2 mm	6 mm	32mm		2 mm	6 mm	32 mm
Flange (Long)	106	117	134	Flange (Long)	-5	14	27
No Flange (Med)	125	137	150	No Flange (Med)	0	14	27

The HGP with 22 mm, 6 mm and 32 mm heads of medium (no flange) and long (flange) neck length

The largest flexion arc measured was that of the nonmodular HD 2 and was 152°. Among the modular components without a flange on the head-neck piece the total flexion arc for the PCA (neck length +0) was 134° and for the HGP (medium neck) was 137°. In contrast among the longer neck components with flanges the ROM was considerably reduced. The total arc from maximum flexion to maximum extension was 113° for the PCA (+5 neck length) and 117 degrees for the HGP (long neck length).

Notable differences were also present when internal rotation in 90° flexion was evaluated (measured with the hip in 90° flexion and neutral abduction as the number of degrees from neutral rotation to maximum internal rotation before prosthetic impingement-subluxation). The nonmodular HD 2 had 27° of internal rotation. Among modular systems without flanges the PCA (+0 neck length) had 15° of internal rotation and the HGP (medium neck) had 18°. Systems with longer neck lengths with flanges had noticeably less internal rotation. The PCA (+5 neck) had 0° of internal rotation and the HGP (medium neck) 2° of internal rotation before prosthetic impingement-subluxation.

The effect of head size on prosthetic range of motion is shown in Table 1. The 22 mm head component in the long neck size which has a flange had the smallest ROM recorded: a total flexion arc of 106° and internal rotation of -5°. In contrast a 32 mm headpiece without a flange had the largest PROM recorded among the modular components with a total flexion arc of 150° degrees and internal rotation of 27°.

### Discussion

The ability to interchange head-neck pieces in modular total hip replacement designs has well recognized benefits. It offers the potential for reduced femoral implant inventory and the possibility of changing neck length after the femoral component has been inserted either at the time of original im-

plantation or during revision. What may be less well recognized is the negative impact these design changes have had upon implant geometry and prosthetic range of motion. There is a marked difference between the neck geometry of the modular femoral components tested and that of the nonmodular HD 2. This is particularly true of the anterior-posterior dimensions of the neck, a region that has a significant impact on ROM (Figs 3 and 4).

The neck of the HD 2 is flat along its anterior and posterior surface, whereas the Morse taper systems have round necks. More important, the flange of the longer head-neck components in both systems substantially widens the neck of the femoral component and decreases the head-neck ratio, thereby adversely affecting ROM.

This observation raises a theoretical concern regarding adverse effects from increased impingement such as wear debris or implant micromotion associated with the use of head-neck components with flanges. The data suggest that impingement and slight subluxation of heads with flanges during daily activities might not be unusual. Implants with flanges would also appear to allow the surgeon a narrower tolerance for positioning the implants so as to avoid subluxation or dislocation. These figures for PROM represent a theoretical maximum that may be achieved with the implant aligned as noted. Soft tissues might of course increase the influence of non prosthetic impingement on ROM and stability.

It is well recognized that if the ROM of a nonmodular THA is limited by bone impingement, this may be improved during surgery by using a longer neck component. However, with modular systems it is theoretically possible for range of motion actually

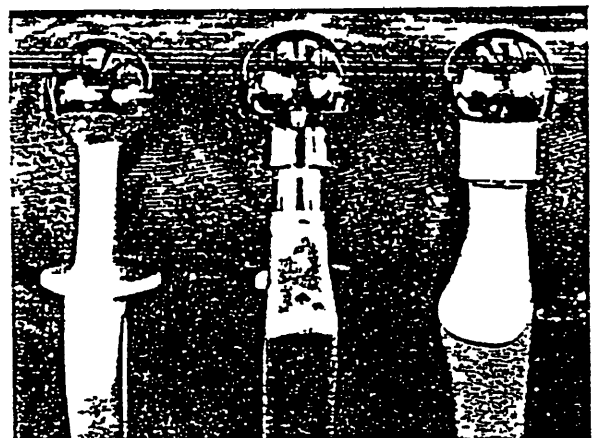


Fig 3 Head-neck geometry in modular vs nonmodular THAs tested (right to left): HD 2, HGP, PCA. Note the increased neck diameter in the modular systems associated with cylindrical necks and most notably with flanges on some head components.

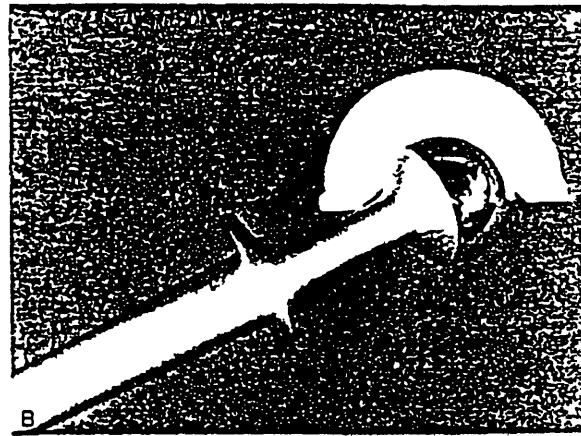
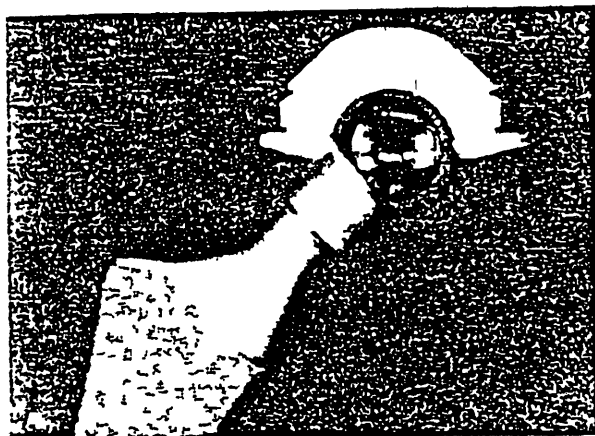


Fig 4 The impact of contemporary design on the geometry of the femoral neck and ROM (A) The neck of the HD 2 has a flattened anterior and posterior surface which allows greater ROM here illustrated in flexion (B) The modular systems (example shown PCA) have cylindrical necks as well as flanges on longer head-neck pieces which notably decrease prosthetic ROM

to decrease if a shorter head-neck component without a flange is replaced by a longer head-neck component with a flange.

Previous authors have demonstrated that large neck diameter decreases PROM and in contrast larger head size increases PROM (1). In the modular systems tested increasing the head size did in fact compensate for the decreased PROM associated with a flange. The use of a larger head size carries with it other features that must be considered in any given case but if PROM is limited by a flange a larger head size represents one alternative for addressing this problem.

We feel that the important advantages offered by modular femoral designs can be retained while reducing the potential for negative effects. This can be achieved by optimizing both implant design and surgical planning. Hip systems vary in the number of head-neck components they have with flanges. In the design of femoral components if the neck length is maximized within the limits of the prosthetic material the number of head-neck pieces with flanges can be minimized.

For the clinician it is important to be sure that the trial head-neck pieces used to test ROM provisionally have the same neck diameter as the corresponding real component. Only then can ROM be assessed accurately prior to inserting the definitive implant. Preoperative and intraoperative planning should provide for a femoral neck resection level that will allow the use of a head-neck component without a flange whenever possible. Some systems have an additional femoral component available with an extra

long or lateralized neck that may eliminate the need for a flanged head-neck component in some cases (Fig 5).

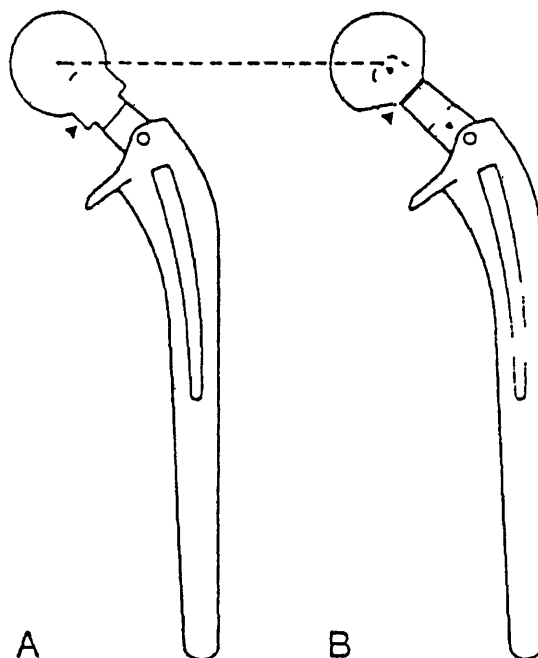


Fig 5 The identical femoral neck length can be achieved with either (A) a standard femoral component together with a long head-neck component that has a flange or (B) an extra long neck femoral component used together with a medium neck component thereby eliminating the need for a flange (Example—diagrammatic outline of Zimmer Precoat standard and extra long neck femoral components)

Finally when an unstable <sup>( )</sup>s encountered during surgery the possibility of prosthetic impingement should be investigated and if present the potential contribution of flanges on head-neck components should be borne in mind so that appropriate action can be taken. If such instability is noted during reduction of trial components surgical options would include component repositioning use of a longer neck femoral component in combination with a shorter head-neck component without a flange or if the size of the acetabulum is sufficiently large use of a larger sized femoral head.

#### References

- 1 Amstutz HC Ludwig RM Schuurman DJ Hodgson AG Range of motion studies for total hip replacement a comparative study with a new experimental apparatus Clin Orthop 111 124 1975
- 2 Chandler DR Glousman R Hull D et al Prosthetic hip range of motion and impingement the effects of head and neck geometry Clin Orthop 166 284 1982
- 3 Johnson RC Smidt GL Hip motion measurements for selected activities of daily living Clin Orthop 72 103 1970



Finally when an unstable <sup>( )</sup>s encountered during surgery the possibility of prosthetic impingement should be investigated and if present the potential contribution of flanges on head-neck components should be borne in mind so that appropriate action can be taken. If such instability is noted during reduction of trial components surgical options would include component repositioning use of a longer neck femoral component in combination with a shorter head-neck component without a flange or if the size of the acetabulum is sufficiently large use of a larger sized femoral head.

#### References

- 1 Amstutz HC Ludwig RM Schuurman DJ Hodson AG Range of motion studies for total hip replacement a comparative study with a new experimental apparatus Clin Orthop 111 124 1975
- 2 Chandler DR Glousman R Hull D et al Prosthetic hip range of motion and impingement the effects of head and neck geometry Clin Orthop 166 284 1982
- 3 Johnson RC Smidt GL Hip motion measurements for selected activities of daily living Clin Orthop 72 103 1970

# Elevated-rim Acetabular Components

## Effect on Range of Motion and Stability in Total Hip Arthroplasty

Robert J Krushell MD \* Dennis W Burke MD \* and  
William H Harris MD\*†

**Abstract** The effect of elevated rim (ER) acetabular components on pro-  
thetic range of motion (ROM) and stability was studied in a laboratory simulator  
using three contemporary total hip arthroplasty (THA) systems. Acetabular com-  
ponents were tested in positions simulating both normal alignment and excess  
abduction. The geometry of the implants differed between systems—two types  
were cement fixed and their effect on ROM in comparison with their corresponding  
plain liners were quantified. The ability of the liners to improve instability ap-  
peared to be dependent on the cause of instability, the orientation of the metal  
shell and ER liner and the ER liner geometry. The routine use of ER liners in  
otherwise satisfactorily positioned acetabular components appeared to offer no  
demonstrable benefit and raised concern over theoretical disadvantages. The  
primary indication for these implants appeared to be in cases of instability due  
to acetabular malposition in which the metal shell is already well fixed by cement  
or bone ingrowth or cannot be readily changed. **Key words** hip prosthesis  
hip arthroplasty dislocation range of motion prosthesis design biomaterials

A major objective of total hip arthroplasty (THA) design is to maximize range of motion (ROM), and stability. Amstutz et al (1), and Chandler et al (2) evaluated factors that affected ROM in various older implant designs. Since that time modular acetabular components which allow the surgeon to select from among both plain and extended rim elevated rim (ER) polyethylene acetabular liners have be-

come commonplace. Some systems have as many as four acetabular liners.

While these ER liners are being used clinically either on a routine basis or in cases of instability their actual effect on ROM and stability has never been reported. Differences in geometry among these implants are not well defined. We have examined the differences in the geometry of ER liners in three contemporary THA systems and the effect on im-  
plant ROM and stability.

From the Orthopaedic Biomechanics Laboratory and Hip and  
Implant Surgery Unit, Massachusetts General Hospital, Boston, Mas-  
sachusetts.

Supported in part by the William H. Harris Foundation, Boston, Massachusetts.

Reprint request: William H. Harris, MD, Orthopaedic Biomechanics Laboratory, Massachusetts General Hospital, Harvard Medical School, Boston, MA 02114.

### Materials and Methods

A three dimensional protractor was built that simulates bone anatomy around the hip applies a compressive force across the joint and allows the

THA to be maintained in consistent alignment while ROM and stability are measured (Fig 1) Tests were run with the acetabular components inserted in an anatomical synthetic plastic pelvis (Sawbones) and in specially designed acetabular fixtures. The fixtures ensured that each component maintained consistent alignment while the position of the elevated rim within the metal shell was sequentially varied.

Three contemporary modular THA systems were studied (Zimmer HGP Howmedica PCA Joint Medical) (Fig 2). All available neck lengths for the 26 mm head components of the HGP and PCA systems and the closest available head size from Joint Medical namely 28 mm were tested with the standard and elevated rim liners. Each acetabular component was tested in two positions: a standard position of 30° of abduction and 20° of forward flexion and malposition of 70° of abduction and 20° of forward flexion. Femoral components were inserted in 15° of anteversion and the femur aligned with an 8° femoral varus (anatomic) axis.

All implants were tested in four clinically relevant positions in neutral abduction: (1) maximum flexion in neutral rotation (FLEX), (2) maximum extension in neutral rotation (EXT), (3) maximum internal rotation in 90° flexion (IRF), and (4) maximum external rotation in 0° extension (ER). In each case the position of bone or prosthetic impingement and subluxation was noted. Motion of the hip was then continued until dislocation occurred; this position was also recorded. All tests were repeated three times.

The tests made with the acetabulum in the standard position were planned to assess the routine use of ER liners on a normally positioned component. All tests made with the acetabulum in this standard alignment utilized the elevated rim in a posterior position that maximized coverage of the

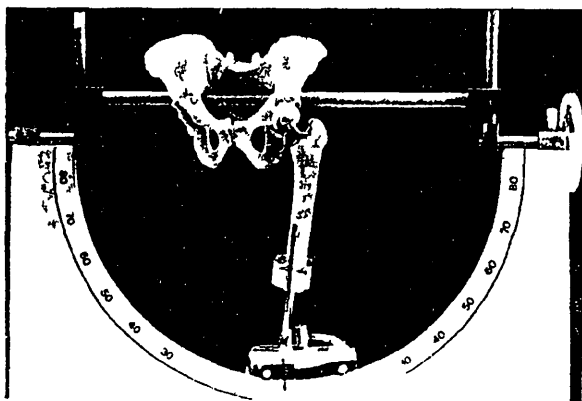


Fig 1 Test apparatus shown with anatomic bone models

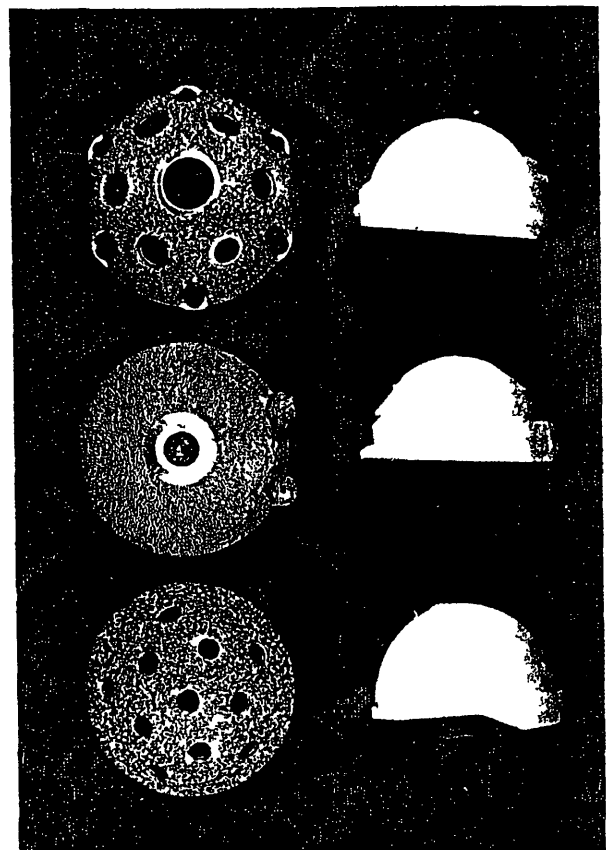


Fig 2 Acetabular implants tested: top to bottom Joint Medical, Howmedica PCA, Zimmer HGP. Left column: the metal shells; right: ER liners (Joint Medical ER size +15 shown).

femoral head during flexion and during internal rotation in flexion.

With the acetabulum malpositioned, the effect of rim orientation on stability was assessed. The apex of the liner was tested sequentially in four positions from 12 o'clock (directly cephalad) to 3 o'clock (directly posterior) in 30° increments. These tests assessed the degree to which an ER liner can improve the stability of an excessively abducted acetabular shell. Subsequent to this testing, the polyethylene liners were imbedded in plastic and sectioned with a microtome to facilitate analysis of their geometry.

## Results

In analyzing the results of this study, it became apparent that two different types of implant geometry could be used to create an ER liner (Fig 3). We defined type 1 ER liners as those in which the standard coaxial relationship between the acetabular

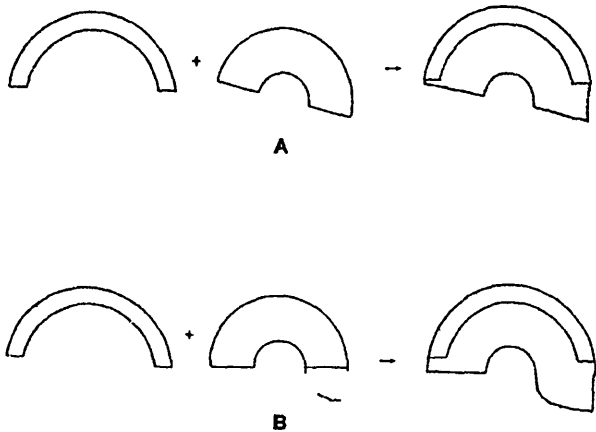


**Fig 3** Type 1 vs type 2 liner design. Diagrammatic representation in cross section through apex of the elevated rim (A) If the metal acetabular shell is taken as the reference orientation, the orientation of the type 1 ER liner is shifted in relation to the metal shell, but in geometry is otherwise similar to a plain liner. (B) The type 2 ER liner geometry and orientation to the metal shell is the same as that of a plain liner with the addition of an elevated rim in one sector.

liner and the metal shell was shifted in effect reorienting the liner within the metal shell. The Joint Medical and PCA liners appeared to function primarily in this way. In contrast, type 2 liners maintained the normal orientation between the acetabular liner and the metal shell; instead, an extra lip of polyethylene is added to just one section of the rim. The HGP liner had this type of design. All tests were repeated three times. The mechanical nature of these tests rendered results that were quite consistent. Measurements were found to be consistently reproducible within  $\pm 3^\circ$  for dislocation. Average

values for each measurement are reported. Results will be reported based on implant type and orientation of the acetabular component.

**Standard Position**

The type 1 liners reoriented the axes of the acetabular component in comparison to the plain liner from the same system. When the elevated rim was placed posteriorly, it had an effect similar to positioning the acetabular components in additional forward flexion; no additional support is given to the head once it subluxes. The PCA and Joint Medical liners had the overall effect of increasing flexion and decreasing extension, increasing internal rotation in flexion and decreasing external rotation in extension (Fig 4A, B).

The lip of the type 2 liner functioned by providing support for the femoral head after it reached the normal point of subluxation. Therefore, the point of subluxation in flexion or internal rotation in flexion is not altered by this type of ER liner; only the point of dislocation is affected. Range of motion was decreased in some planes due to the presence of the lip. When placed posteriorly, the HGP liner had the overall effect of increasing internal rotation in flexion and decreasing both extension and external rotation in extension, without notable effect on flexion in neutral rotation (Fig 5).

**Malposition**

The type 1 liners displayed the ability to reorient the liner in relation to the metal shell. The impact

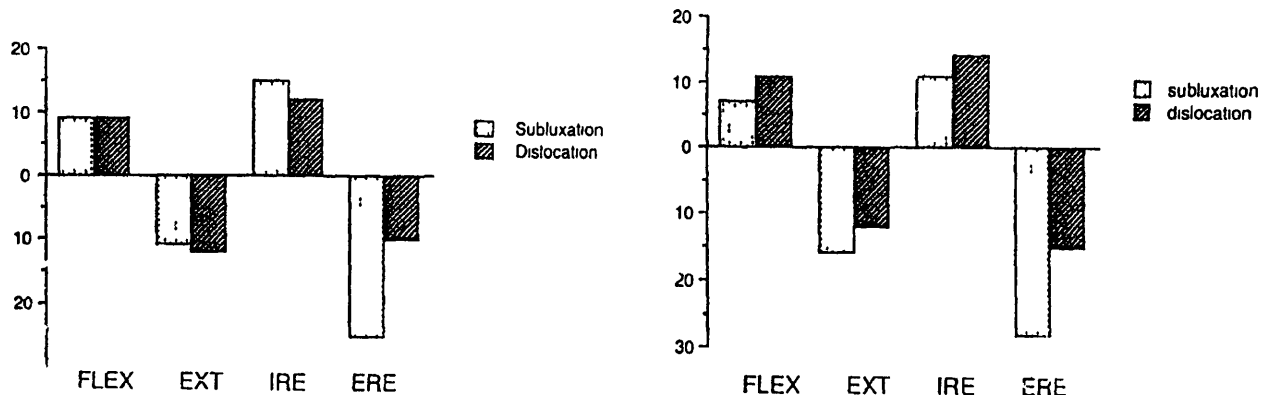


**Fig 4** Type 1 liner in standard position of  $30^\circ$  abduction and  $20^\circ$  forward flexion. The ROM of the plain liner is taken as the x-axis; the bar graphs show the increase or decrease in ROM of the ER liner in comparison with its corresponding plain liner in the same system. For each graph, the head-neck component is held constant. Changes in impingement/subluxation and dislocation are indicated. (A) Joint Medical +6 neck, 28 mm head, +10 ER liner. (B) PCA +5 neck, 26 mm head ER liner.

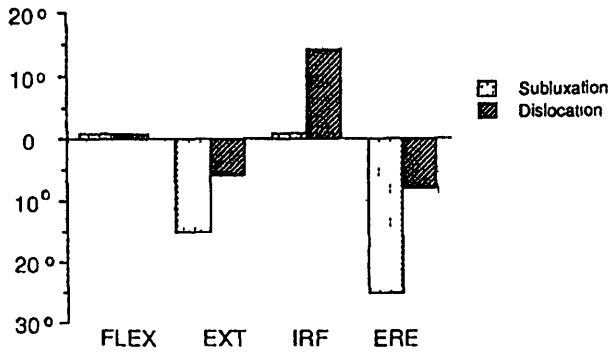


Fig 5 Type 2 liner standard position of 30° abduction and 20 forward flexion. The ROM of the plain liner is taken as the x axis. The bar graphs represent the increase or decrease in ROM of the ER liner in comparison with its corresponding plain liner. Changes in impingement/subluxation and dislocation are indicated. Shown here HGP with 26 mm head long neck and ER liner.

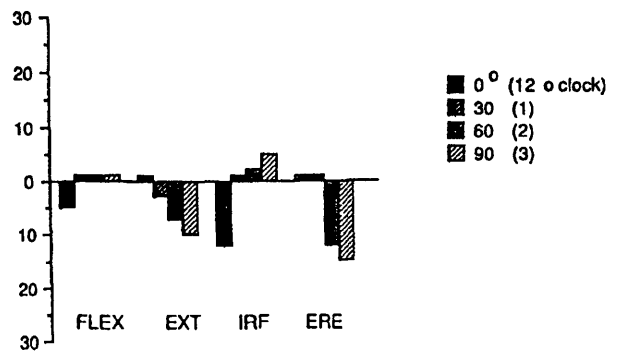


Fig 7 Effect of rotation of the elevated rim in type 2 liner—shell in malposition of 70° abduction 20 forward flexion. ROM of the plain liner is taken as the x axis. The bar graphs represent the increase or decrease in ROM of the ER liner in comparison with the plain liner. Shown here HGP with the 26 mm long neck and ER liner.

of these liners was highly dependent on the position in which the elevated rim was placed. Differences of 30° in the position of the apex of the elevated rim within the metal shell (eg from 1 o'clock to 2 o'clock) had a noticeable impact on the change in ROM provided by the ER liner (Fig 6A B). With the apex of the ER liner located at 12 o'clock, extension and external rotation in extension are generally increased and conversely flexion and internal rotation in 90° of flexion are decreased. As the apex of the ER liner is moved posteriorly (toward 3 o'clock) flexion and internal rotation in 90° flexion are increased and conversely extension and external rotation in extension progressively decrease.

The type 2 liner displayed some increase in stability over the plain liner in internal rotation in 90° of these liners was highly dependent on the position in which the elevated rim was placed. Differences of

flexion when placed posteriorly but the effect was far less marked than the type 1 liners and no additional support in flexion was noted (Fig 7).

All of the ER liners tested shared the common characteristic of relatively little improvement in stability when dislocation was due to bony impingement or the acetabular components in 30° abduction with the rim placed posteriorly. The average increase in internal rotation in flexion from the ER liners was 15° when dislocation was due to prosthetic impingement and 3° when due to bony impingement. Similarly for the acetabular components positioned in 70° abduction, apex of rim posterior the mean increase in IRF with type 1 ER liners was 20° when dislocation was due to prosthetic impingement and 3° when dislocation was due to bony impingement.

This appeared to be due to the relatively long lever

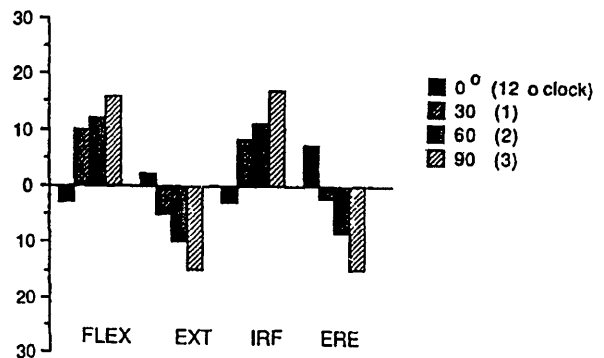
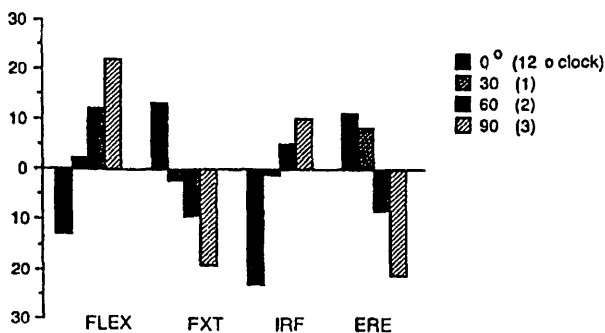


Fig 6 Effect of rotation of the elevated rim in type 1 liners—shell in malposition of 70° of abduction and 20 forward flexion. ROM of the plain liner is taken as the x axis. The bar graphs represent the increase or decrease in ROM of the ER liner in comparison with the plain liner. (A) Joint Medical 28 mm head +0 neck +20 ER liner. (B) PCA 26 mm head long neck and ER liner.

arm that exists between the point of impingement and the center of the femoral head in bone vs prosthetic impingement. Hence for bony impingement a relatively small rotation of the limb about the point of impingement produced a relatively large subluxation of the femoral head out of the acetabular component. In contrast when an equally small rotation of the limb occurred about a point of prosthetic impingement a smaller displacement of the head was produced.

### Discussion

In contrast with previous studies the evaluation of ER liners requires not only the measurement of ROM until impingement but the dislocation of the component. Like previous authors we noted that the point of impingement could be consistently measured within 1°. However the point of dislocation not measured in earlier studies was slightly less consistent and varied by up to 3° when the same tests were repeated in sequence.

As Chandler et al observed previously we noted that impingement occurred between acetabular rim and femoral neck or between bone and bone not between bone and implant. Impingement due to bone occurred between greater trochanter and ilium/pubis in FLEX and IRF and between greater trochanter and ischium in ERE. As neck length increases the role of bony impingement decreases and a change from bone to prosthetic impingement can result in a marked change in the ROM. While the experimental data sheds light on the geometry of these implants and the way in which they impact on ROM some factors clearly differ between the experimental and clinical settings. The presence of soft tissues in vivo would tend to increase the significance of bony impingement over that observed experimentally. The measurement of dislocation requires the simulation of compressive forces across the hip joint and the experimental apparatus cannot fully simulate the complex and changing force vectors of the hip joint musculature during ROM.

Nonetheless several observations appear relevant. All the ER acetabular liners share the common characteristic of simultaneously increasing ROM in some directions and decreasing ROM in complementary directions. When used in an acetabular shell that is not malpositioned their net effect is to reorient the axes of the acetabular liner away from the normal relationship with the metal shell. They do not in any global sense provide greater ROM than a plain liner. Therefore the routine use of an ER liner in acetabular

ular components that are otherwise well positioned does not appear to have a sound basis.

If for example the surgeon normally seeks to have the acetabular component in 20° of forward flexion and has positioned the implant in this desired position the addition of a posterior ER liner will effectively increase the forward flexion of the implant. If the implant is already positioned satisfactorily this change in orientation would seem undesirable. If the surgeon wishes to routinely have the implant in additional forward flexion it would be preferable to place the acetabular shell in this orientation and then use a plain liner for reasons outlined below.

When faced with an unstable THA the geometry of the liner and the cause of the dislocation will determine whether an ER liner will improve stability. The most common causes of THA instability are malposition, soft tissue laxity and bone/soft tissue impingement. This study suggests that ER liners will not be of significant benefit in the latter two situations.

On the other hand if instability is due to an acetabular component that is malaligned the results suggest that an optimally oriented ER liner may improve stability. This study also suggests that a type 1 liner design will be more effective in this setting than a type 2 liner design. The orientation and size of ER liner that will achieve maximal improvement in stability without notable impingement in other directions may not be immediately obvious. At times it may not be possible to place the ER liner in the optimal orientation without repositioning the metal shell since some shell designs allow a liner to rotate in only 60° increments.

If instability is due to acetabular malposition we feel it is preferable if possible to reposition the component rather than to use an ER liner based on the following observations: (1) ER liners have rims of unsupported polyethylene that may be exposed to high loads. Of interest the repeated impingements and dislocations were noted to take a toll on the implants. Some ER liners had to be replaced during testing when loss of fixation between the liner and the shell occurred due to torsional forces acting on the rim over the course of multiple dislocations. Liners showed visible deformation after multiple impingements. Of course the number of dislocations performed on these implants was large but the forces were probably lower than those occurring clinically. (2) The effect of the liner is sensitive to the exact position of the elevated rim yet the positioning of the ER liner may be less precise than positioning the acetabular component with a positioning guide. Larger and more accurate corrections in each plane are possible if the entire component is shifted. (3)

Many ER liners are more prominent than would be the case if the acetabular shell were repositioned and used with a plain liner. This raises concern about difficulty of reduction if a THA dislocates. We also have noted that many ER liners do not have a clearly visible radiopaque marker that identifies their presence on radiograph meaning that the surgeon treating the dislocation may not be aware of the presence of an ER liner.

It appears that the use of an ER liner on a routine basis has no clear advantage or rationale over the use of a plain liner. In cases of instability when the cause is soft tissue laxity or bony impingement measures other than inserting an ER liner would seem to offer the greatest likelihood for achieving a stable result.

This study suggests that the role of ER liners should be limited to specific cases in which instability is due to prosthetic malposition and the acetabular component cannot be readily changed for example if it is already well fixed with cement or bony ingrowth. In this setting type 1 liner designs would appear to be more effective than type 2 liner designs. The apex of the ER liner should be carefully marked before it is placed into the wound so that its orientation can be controlled during insertion. It should be recognized that the optimal position for the elevated rim

varies with the malposition of the acetabular component and that it may be necessary to test the ER liner with the rim in more than one orientation. The hip should be tested in flexion extension flexion plus internal rotation and extension plus external rotation in order to ensure that the elevated rim does not create excessive impingement or instability in an unanticipated direction.

### Acknowledgments

The authors thank the Zimmer and Joint Medical Products Corporations for providing their implants for this study.

### References

- 1 Amstutz HC Ludwig RM Schuurman DJ Hodgson AG Range of motion studies for total hip replacement a comparative study with a new experimental apparatus Clin Orthop 111 124 1975
- 2 Chandler DR Glousman R Hull D et al Prosthetic hip range of motion and impingement the effects of head and neck geometry Clin Orthop 166 284 1982

Copyright 1978 by The J. F. B. and J. S. G. I. P. D.

# Dislocations after Total Hip-Replacement Arthroplasties\*

BY GEORGE E. LEWINNEK, M.D.†, JACK L. LEWIS, Ph.D.‡, RICHARD TARR, M.S.‡, CLINTON L. COMPERE, M.D.† AND JERALD R. ZIMMERMAN, B.S.‡, CHICAGO, ILLINOIS

From the Northwestern Memorial Hospital, Chicago

**ABSTRACT** In a series of 300 total hip replacements, nine (3 per cent) dislocated. Precise measurements of the orientation of the acetabular cup were made and it was found that anterior dislocations were associated with increased acetabular component anteversion. There was no significant correlation between cup orientation angle and posterior dislocation. The dislocation rate for cup orientation with anteversion of  $15 \pm 10$  degrees and lateral opening of  $40 \pm 10$  degrees was 1.5 per cent, while outside this "safe" range the dislocation rate was 6.1 per cent. Other factors that were documented include time after surgery (with the greatest risk in the first thirty days) and surgical history (with a greater risk in hips that have had prior surgery).

### Material and Methods

Information about the patient's age, diagnosis, and acetabular component orientation was obtained for all nine hips with dislocation and for 113 of the 291 hips in which the prosthetic components did not dislocate. Detailed study of the remaining 178 hips was not possible because the roentgenograms required could not be obtained. The detailed data on hips with dislocations are listed in Table I. The 113 non-dislocated hips had diagnoses of osteoarthritis in fifty-nine and failure of previous surgery in sixteen (nine femoral prostheses, three cup arthroplasties, three osteotomies, and one fracture nailing). The other diagnoses were rheumatoid arthritis (fourteen), ankylosing spondylitis (three), avascular necrosis (seven), congenital dislocation of the hip (six), and others (eight).

Between January 1972 and June 1975, 300 total hip replacement procedures were performed by five surgeons

The standard technique used by the five surgeons was to approach the hip posterolaterally through a modification

TABLE I  
PATIENTS WITH DISLOCATED TOTAL HIP REPLACEMENTS

Case	Age (Yrs)	Sex	Diagnosis*	Time to Dislocation	Angle $\theta$ (Deg)	Angle $\alpha$ (Deg)	Direction of Dislocation
1	71	F	RS	20 days	54	25	Ant
2	70	F	RS	23 days	54	43	Ant
3	55	M	FA	30 days	40	31	Ant
4	78	F	RS	9 days	42	22	Post
5	66	M	RS	13 days	60	24	Post
6	63	F	RS	51 days	36	26	Post
7	35	M	RA	110 days	48	9	Post
8	72	F	RS	3 1/2 years	36	15	Post
9	88	F	OA	6 days	60	13	?

FA = fractured acetabulum, OA = osteoarthritis, RA = rheumatoid arthritis, and RS = revision of previous surgery

on the orthopaedic service of Northwestern Memorial Hospital. Dislocation of the femoral component from the acetabular cup occurred in nine patients. Five patients required a secondary operation and two had significant cardiopulmonary complications. The incidence of dislocation was 3 per cent, which is within the range reported from other centers (1 to 8 per cent)<sup>8, 10, 13, 15, 16</sup>. In order to understand this complication better, we undertook a study of our 300 cases.

of the Gibson incision. The trochanter and gluteus medius muscle insertion were left intact. The capsule was incised posteriorly, usually leaving the anterior capsule intact. One surgeon, who performed 190 of the operations in the study, used Aufranc-Turner prostheses. This surgeon reattached the external rotators during closure whenever possible. The other surgeons in the study used either Aufranc-Turner or Charnley-Mueller prostheses and did not regularly reattach the external rotators.

This work was supported by Grant SRS 73 P 55898 from the Rehabilitation Services Administration, 233 East Erie Street, Chicago, Illinois 60611. ‡ 345 East Superior Street, Room 1441, Chicago, Illinois 60611.

The orientation of the radiolucent cup was determined from the elliptical appearance of the circular marker wire on precisely oriented anteroposterior postoperative roent





FIG 1 A



FIG 1 B

Figs 1 A and 1 B Anterior dislocation of a total hip replacement

genograms (Fig 3) The lateral opening angle  $\theta$  was measured directly. The anteversion angle  $\alpha$  was calculated from the ratio between the lengths of the minor and major axes of the ellipse.

To determine whether the acetabular component was anteverted or retroverted the ellipse was closely scrutinized. Anteversion was diagnosed if the lateral arc of the ellipse was more sharply defined than the medial and vice versa.

A device with three legs and a bubble level was used to position the pelvis parallel to the film. The patient was positioned supine as for a routine roentgenogram and the feet held in the device were directly and firmly pressed



FIG 2 A



FIG 2 B

Figs 2 A and 2 B Posterior dislocation of a total hip replacement

over the anterior superior iliac spines and the symphysis pubis. The patient was instructed to reposition himself until the bubble level was horizontal. A small lead marker was placed on the patient along the midline of the body to mark the center of the x-ray beam.

A correction factor for distortion caused by the divergent x-ray beam was necessary.<sup>9</sup> Preliminary studies on a laboratory skeleton demonstrated that 5 degrees added to the apparent angle  $\alpha$  yielded the true  $\alpha$  and that  $\theta$  was correct as measured.

The roentgenographic technique was used on most of the 113 patients for whom data are presented. For patients on whom it was not possible to use the technique the av-

PELVIC COORDINATE STEM

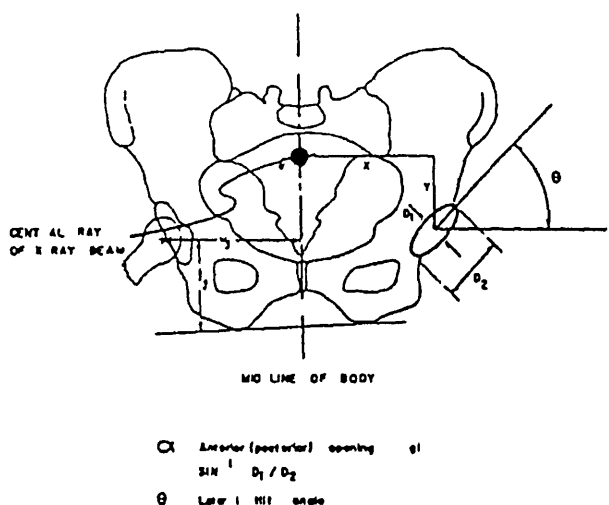


FIG 3

In order to measure the orientation of the acetabular component those portions of the wire marker that are obscured by the femoral component are drawn in with the aid of a draftsman's French curve. Measurement of  $D_1$  and  $D_2$  permit calculation of  $\alpha$ . Angle  $\theta$  is measured directly.

average of at least three routine anteroposterior roentgenograms was used but only when the several sets revealed reproducible measurements ( $\pm 3$  degrees).

The anteversion angle  $\alpha$  corresponds to rotation around an artificial axis which projects onto an x ray as the major axis of the marker wire ellipse. The Aufranc Turner cup positioner is designed so that the surgeon can control rotation about the anatomical transverse axis<sup>1</sup>. The amount of rotation in this sense may be called angle  $\phi$ . In contrast the Charnley Mueller positioner is designed to control angle  $\alpha$ <sup>14</sup>. Angle  $\phi$  may be calculated from the relationship  $\tan \alpha = \tan \phi \cos \theta$ . Angle  $\phi$  is 3 to 6 degrees larger than the anteversion angle  $\alpha$  for the usually recommended cup orientations.

In addition to the measurements on all nine of the dislocations adequate data were available on 113 of the 291 hips that remained stable. The total of 122 patients was not a random sample in that it included all nine of the dislocations. This provided more information than would have been available in a true random sample. With caution it was possible to apply the Fisher Irwin Yates exact test and tests on normalized variables to the available statistics<sup>1, 11</sup>.

Analysis of Data

The average age of the 122 patient study group was 63.1 years while the average age of the nine patients with dislocations was 66.4 years which is not significantly different. A significantly larger percentage of patients whose hips dislocated had had prior surgery on the same hip as compared with the control group. Of the nine patients whose hips dislocated six had had prior surgery. Of the 113 patients whose hips remained stable only fifteen had had prior surgery. This difference is significant at the 1 per cent level (Fisher exact test).

When dislocation occurred it tended to be early in the convalescent period. Six of the nine dislocations were seen within thirty days of the total hip replacement and these dislocations occurred while the patient was in bed or walking or during other normal activities. Two dislocations were caused by falls outside the hospital and these occurred more than thirty days after the operation. In one patient (Case 9) the hip dislocated more than three years after the operation, while she was bending over to tie her shoe. She was the only patient who had a late dislocation without significant trauma.

The relationship between the orientation of the acetabular component of the prosthesis and the dislocation (Fig 4) shows that the three anterior dislocations (Cases 1, 2, and 3) occurred with  $\alpha$  angles of 25 degrees or more as compared with an average of  $15.6 \pm 8.5$  degrees for the study group. The increased angle is significantly different from that of the stable group at the 1 per cent level of statistical significance. The three hips with anterior dislocation had an average  $\theta$  of 49.3 degrees which was not significantly different from the  $\theta$  of the stable group  $44.4 \pm 7.5$  degrees. The five posterior dislocations (Cases 4 through 9) had an average  $\alpha$  of 19.2 degrees and an average  $\theta$  of 44.4 degrees. Neither of these values were significantly different from the corresponding angles in the control group.

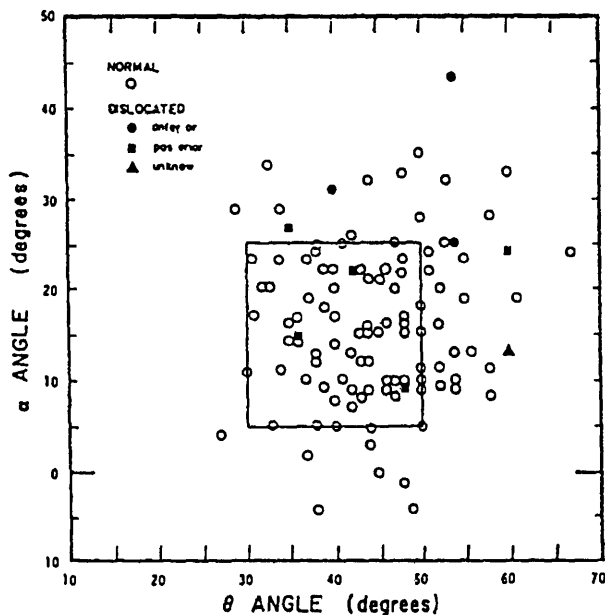


FIG 4

A scatter-diagram summary of the orientation of the acetabular components.

When all nine dislocations were considered together there seemed to be a tendency for the dislocations to be associated with large deviations from the average angles. This suggests that there is a relatively safe range of orientations for the cup. A number of such ranges were investigated and the range of  $\theta = 40 \pm 10$  degrees and  $\alpha = 15 \pm 10$  degrees proved most satisfactory. This range is a practical one because it is sufficiently large to allow the sur

geon reasonable leeway in the placement of the acetabular cup and is such that it allows adequate motion in the implanted prosthesis. The difference between the dislocation rate within this safe region and outside it is statistically significant ( $p < 4.5$  per cent). A projection of the data from the study group to the entire group of 300 patients shows that the predicted dislocation rate will be 1.5 per cent when acetabular-component orientation is within the safe range versus 6.1 per cent when safe orientation is not achieved.

The effect of shifts in the position of the acetabulum was studied as regards medial lateral and superior inferior translocations. The shifts did not correlate with dislocation. An attempt was made to correlate the treatment of the initial dislocation with the final result and we discovered no simple relationship between time in traction or casts and subsequent stability in this group of nine dislocations.

#### Discussion

Our data on the incidence of dislocation are similar to those reported by others as mentioned and the tendency of this complication to occur early in convalescence also has been noted previously. Of 929 patients followed by Nicholson for three months twenty had dislocations (2.1 per cent) and of 580 patients followed for twenty four months only five had dislocations (0.9 per cent). After twenty four months the dislocation rate fell still further (one of 295).

Our study suggests that the position of the acetabular

cup relative to the body's axis is important and in particular that anterior dislocation is associated with anteversion. We expected that decreased anteversion would lead to posterior dislocation and that an increased lateral opening angle would lead to superior or iliac dislocation but our clinical studies did not support either of these hypotheses.

In one study<sup>3</sup> half of the dislocations were associated with retroversion of the acetabular component of between 7 and 10 degrees. All of these dislocations were posterior. None of the acetabular components in the present series were retroverted more than 4 degrees. We therefore infer that while excessive retroversion may lead to posterior dislocation safe orientation of the acetabular component will not necessarily prevent such dislocations.

Acetabular component orientation has been shown in this study to be a significant factor in avoiding dislocations. It is not the only factor as demonstrated by the fact that the most experienced surgeon in this study had only one dislocation in 190 cases (0.5 per cent). He did not place a significantly greater number of acetabular cups within the safe range than did the other surgeons. He attributed his success to a number of factors such as adjustment of soft tissue tension to achieve clinical stability at the time of surgery and avoiding adduction for six weeks after surgery. Such elements could not be measured with satisfactory precision even though clinical experience indicates their importance in minimizing the risk of dislocation.

#### References

- 1 ARMITAGE P. *Statistical Methods in Medical Research*. New York: John Wiley, 1971.
- 2 BERGSTROM BJORN, LINDBERG LARS, PERSSON B M and ONNERFALT ROLF. Complications after Total Hip Arthroplasty According to Charnley in a Swedish Series of Cases. *Clin Orthop* 9: 91-95, 1973.
- 3 CHARNLEY JOHN. The Long Term Results of Low Friction Arthroplasty of the Hip Performed as a Primary Intervention. *J Bone and Joint Surg* 54 B: 61-76, Feb 1972.
- 4 CHARNLEY JOHN and CUPIC ZORAN. The Nine and Ten Year Results of the Low Friction Arthroplasty of the Hip. *Clin Orthop* 9: 9-25, 1973.
- 5 COVENTRY M B, BECKENBAUGH R D, NOLAN D R and ILSTRUP D M. 2,012 Total Hip Arthroplasties: A Study of Postoperative Course and Early Complications. *J Bone and Joint Surg* 56 A: 773-784, March 1974.
- 6 EFTEKHAR N S and STINCHFIELD F E. Experience with Low Friction Arthroplasty: A Statistical Review of Early Results and Complications. *Clin Orthop* 95: 60-68, 1973.
- 7 EFTEKHAR N S, SMITH D M, HENRY J H and STINCHFIELD F E. Revision Arthroplasty Using Charnley Low Friction Arthroplasty Technique With Reference to Specifics of Technique and Comparison of Results with Primary Low Friction Arthroplasty. *Clin Orthop* 9: 48-59, 1973.
- 8 EVANSKI P M, WAUGH T R and OROFINO C F. Total Hip Replacement with the Charnley Prosthesis. *Clin Orthop* 95: 69-72, 1973.
- 9 GOERGEV T G and RESNICK D. Evaluation of Acetabular Anteversion Following Total Hip Arthroplasty: Necessity of Proper Centring. *British J Radiol* 48: 259-260, 1975.
- 10 HARRIS W H. Preliminary Report of Results of Harris Total Hip Replacement. *Clin Orthop* 95: 168-173, 1973.
- 11 HILL A B. *Principles of Medical Statistics*, Ed 7. New York: Oxford University Press, 1961.
- 12 HOWMEDICA INC. *Vitalium Aufranc Turner Total Hip Prosthesis*, No 3 5199, January 1973.
- 13 LAZANSKY M G. Complications Revisited: The Debit Side of Total Hip Replacement. *Clin Orthop* 95: 96-103, 1973.
- 14 MULLER M E. Total Hip Prostheses. *Clin Orthop* 77: 46-68, 1970.
- 15 MURRAY W R. Results in Patients with Total Hip Replacement Arthroplasty. *Clin Orthop* 95: 80-90, 1973.
- 16 NICHOLSON O R. Total Hip Replacement: An Evaluation of the Results and Technics, 1967-1972. *Clin Orthop* 9: 217-223, 1973.

# Range of Motion Studies for Total Hip Replacements

## A Comparative Study with a New Experimental Apparatus

HARLAN C AMSTUTZ, MD,\* R M LODWIG,  
D J SCHURMAN, MD, AND A G HODGSON

The primary objectives of hip joint replacement (THR) are not only to relieve pain, but to improve motion and patient function, the total hip prostheses which provide an adequate range of motion (ROM) should also provide long-term joint stability. The ROM following THR depends on three factors: (1) the etiology of the hip disease, the related severity and type of capsular scarring, and/or the fibrosis within or between muscle fibers, (2) the prosthesis used, and (3) the technique of insertion.

Stability of THR depends upon motion of hip during activities of daily living or unintentional excesses which produce subluxation. Repeated impingement and subluxation of THR components may lead to rim wear, dislocation and force transmission to the acrylic-bone interface. Prosthesis geometry, technical error of insertion with excessive socket inclination or femoral component anteversion are factors which contribute to increased probability of repeated neck socket impingement.

A three dimensional protractor was constructed at UCLA to assess *in vitro* ROM of various THR components and the importance of component orientation. Analysis of factors involved may decrease the incidence of early postoperative and late dislocation and develop guidelines for future THR designs.

### METHODS AND MATERIALS

Prior to this study we measured ROM on a protractor similar to that described by Charnley.<sup>3</sup> The precision of these measurements was inadequate to resolve the differences in ROM between various THR designs. Therefore, a new protractor (Fig 1) was designed which would accept a human pelvis and femur, allow a direct visualization of the anatomical relationships and prosthesis while precisely measuring the *in vitro* ROM of the prosthetic components. This apparatus provided a precision of  $\pm 1^\circ$  in each angular setting or measurement. Stimulated range of motion studies were performed using 7 types with various head and neck diameters (Table 1). Components were inserted in the pelvis and femur and mounted in the ROM apparatus.

The pelvis was mounted in the apparatus with the anterior superior spines and the pubis in a vertical plane. To permit a direct comparison of the data the socket of each prosthesis was placed in the same position of  $42^\circ$  lateral opening from the horizontal plane with

Received October 14 1974

\* Professor of Surgery Chief Division of Orthopaedic Surgery School of Medicine 76-125 Health Sciences University of California Los Angeles Los Angeles California 90024

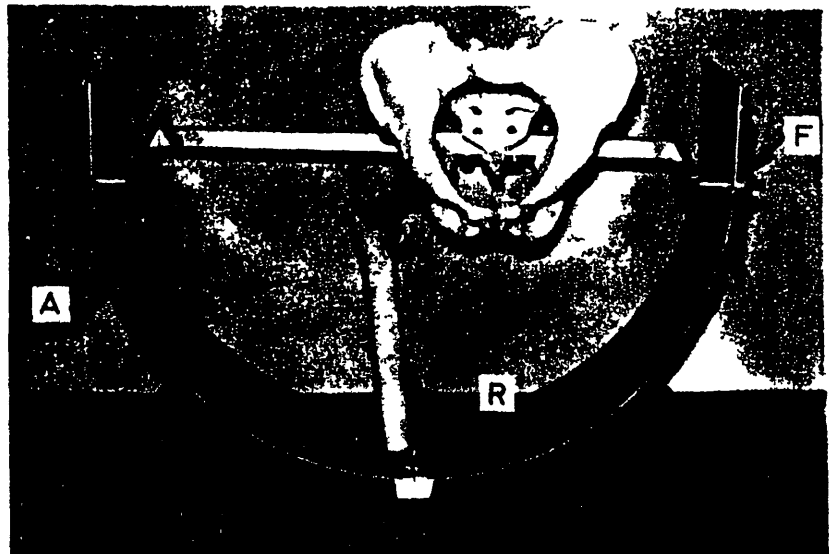


FIG 1 ROM apparatus

the patient upright and 20° of anteversion. The Charnley was also evaluated in 0° of anteversion. The degree of version was determined by inserting a pin into the distal condylar axis at the junction of the upper and middle thirds of the femur using the posterior surfaces of the condyles as 0° version.<sup>2</sup> The distal portion of the femur was then removed so that the femur would fit into the apparatus and a plaster jig was constructed to insert the prosthesis in the correct degree of version. The angle of the lateral opening of the socket

was indicated on protractor A by placing a ruler across the rim. Anteversion was determined with the pelvis flexed 90° at F.

Range of motion was recorded by the protractors A and R. Hip flexion and rotation in flexion were determined by flexing the pelvis at F. Flexion with external rotation and abduction was evaluated for the Trapezoidal 28 and the Mueller. To simulate the effects of wear the Charnley and Trapezoidal 28 sockets were deepened 2, 4, and 6 mm and ROM recorded.

TABLE 1 Types of Total Hip Replacement Prostheses Studied

Type of Prosthesis	Head Diameter (mm)	( $\frac{\text{Head Diameter}}{\text{Neck Diameter}}$ ) Ratio
Charnley (Standard Thackray)	22	1.74
Bechtol (1 3/4 inch neck, regular 3/8 inch width stem Richards)	25.4	1.95
Harris (Long neck Howmedica)	26	2.03
Trapezoidal 28 (Standard Zimmer)		
Short neck	28	2.01 to 3.24
Medium neck	28	1.97 to 2.97
Long neck	28	1.97 to 2.97
Extra long neck	28	1.77 to 3.00
Aufranc Turner (Regular Howmedica)	32	2.00 to 2.37
Mueller (Standard neck Standard stem Zimmer)	32	1.98
McKee Farrar (1 5/8 inch Standard Howmedica)	41	1.77

TABLE 2 Neck-socket Contact Angles of Various Hip Replacement Systems

Type of THR	Charnley	Charnley	McKee Farrar	Mueller	Harris	Bechtol	Aufranc Turner	Trapezoidal 28
Femoral component type (0° anteversion)	Standard	Standard	1 5/8" std	Standard	Long neck	Standard	32 mm Standard	Long neck Large stem
Acetabular component type (lateral opening 42°)	Standard	Standard	Standard	Standard	Standard	Standard	Standard	Medium
Anteverson	20	0	20	20	20	20	20	20
Flexion at 0° Abduction	80	63	105	96	93	93	101	114
Flexion at 10° abduction	86	67	114	103	99	99	109	123
Abduction in 90° flexion	38*	39*	59	66	58	51	72	79
Abduction in 90° flexion	0*	0*	19	6	2	4	12	26
Internal Rotator in 90° Flexion	0*	0*	14	6	3	2	14	36
External rotation in 90° flexion	85*	83*	102	99	103	94	108	119
Arc of rotation in 90° flexion	85*	83*	116	105	106	96	122	155
Extension	36	57	57	54	53	49	60	76
Abduction in Extension	42	46	48	57	57	45	56	60
Adduction in extension	40	44	37	42	40	47	41	41
Internal rotation in extension	87	69	106	110	107	97	118	120
External Rotator in Extension	42	62	54	68	66	52	69	74
Arc of rotation in extension	129	131	160	178	173	149	187	194

Note All numbers are in degrees Variable anatomy and bone impingement may significantly reduce rotation and other movements  
\* Measured at maximum flexion at 0° abduction

TABLE 3 Maximum Flexion and Abduction of Trapezoidal-28 as a Function of Socket Position\*

	Flexion (degrees)			Abduction (degrees)		
	10	20	30	10	20	30
Anteversion (degrees)						
Lateral opening (degrees)						
36	102	108	117	57	54	53
42	106	114	120	61	60	59
48	110	119	127	67	65	64

\* Long neck large stem prosthesis with medium socket and femoral anteversion held at 0 degrees

### RESULTS

The results of the ROM measurements are presented in Table 2. The angles reported are maximum values. The effects of muscle and other soft tissues were not included in this study.

Comparative analyses indicate that there are significant differences between designs in the clinically important parameters of flexion, internal rotation in flexion, and external rotation in extension. The Mueller design provides an increase in flexion of 16° over the Charnley design, this represents a 20 per cent increase. There also has been an increase observed in abduction in extension. Other "second generation" (post-Charnley) designs also provide improved ROM without neck-socket contact.

Flexion for the Trapezoidal-28 was 114°, which represented a 42 per cent increase over the Charnley, internal rotation in flexion varied from 0° for the Charnley and 2° for the Bechtol up to 36° for the Trapezoidal-28. Abduction in extension varied from 42° to 72°. The design factors responsible for these differences have been analyzed.

#### EFFECTS OF COMPONENT ORIENTATION

**Socket Orientation** The maximum flexion arc changes with lateral socket opening and anteversion. For the Trapezoidal-28, each degree of increase of lateral opening between 36° and 48° permitted about 0.8° of additional flexion (Table 3). Between 10° and 30°, each degree of in-

creased anteversion permits about 0.8° of additional flexion. As expected, small decreases in abduction are observed as anteversion is increased. External rotation in extension is relatively unaffected by changes in socket lateral opening in the positions tested, but is reduced as socket anteversion increases.

**Femoral Prosthesis Orientation** Anteversion of the femoral neck will increase flexion. For prosthesis such as the Mueller which have a circular neck cross section, the increase is approximately degree for degree. The gain in flexion for the Trapezoidal-28 is less (0.8 per degree) because of the optimized neck shape in flexion.

In both the normal and the prosthetic hip joints, the maximum flexion angle is increased by abduction and external rotation (Fig 2). Although there are small differences between the various types of prostheses, at abduction angles near zero approximately one degree of flexion is gained for each degree of external rotation. Similarly about one degree of flexion is gained for each degree of abduction for abduction angles near 10° and external rotation angles near 10°. However, at greater external rotation angles, the gain in flexion with further external rotation is smaller than the gain at lesser external rotation angles.

**Effects of Wear** The results of deepened sockets of the Charnley and Trapezoidal-28 designs are shown in Table 4. The direction of the "wear simulation" was determined by using the 17° angle from the

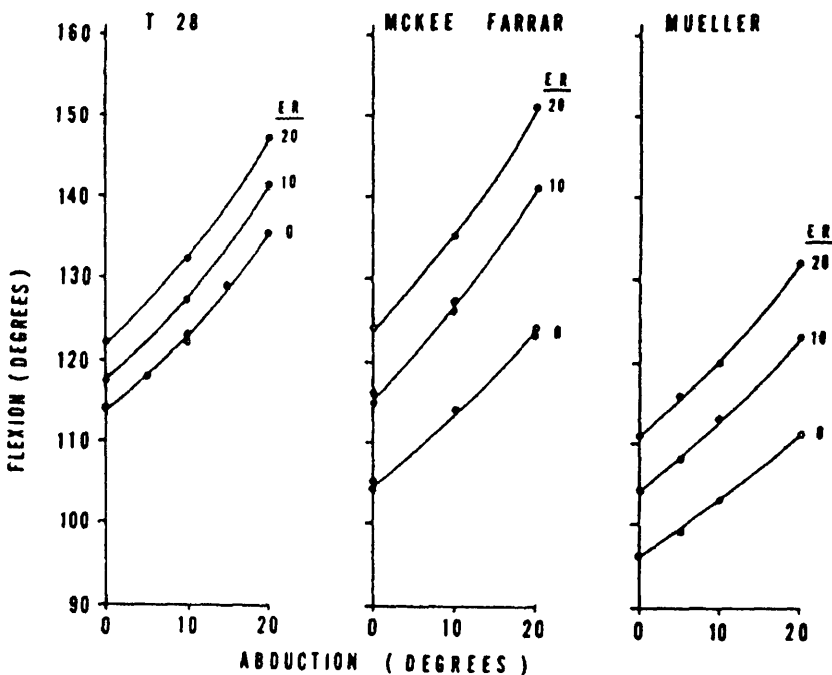


FIG 2 Relationship of flexion to limb abduction and external rotation

vertical<sup>5</sup> as determined by Rydell, when the socket was oriented in the standard position of 42° lateral opening and 20° anteversion in the pelvis

There was 19° less flexion with the Trapezoidal-28 4 mm deepened socket, and a 23° loss with the Charnley design

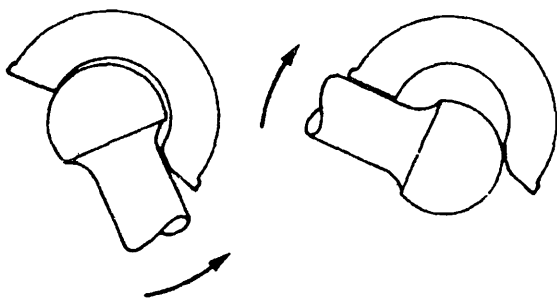
DISCUSSION

The increased ROM observed for various prostheses has been accomplished by (1) greater head diameter to neck diameter ratio, (2) smaller socket depth to ball radius ratio, and (3) optimization of the

geometry of neck<sup>4</sup> and socket rim<sup>1</sup> Preferential increases in flexion, internal rotation and abduction in flexion, and external rotation in extension were observed from two THR s with non-circular neck cross sections—the Aufranc-Turner with an elliptical neck cross section and the Trapezoidal-28 with a trapezoidal neck cross section

Results indicate a penalty in ROM for the deepening of the socket to provide additional stability, e.g. the Charnley design is deepened 2 mm beyond the ball radius to increase the stability with a loss of approximately 10° in flexion. Wear will also deepen the socket and diminish ROM of a THR prosthesis and this is more pronounced if the ROM is already marginal. Wear of the socket rim due to impingement may facilitate dislocation by reducing the containment of the femoral component (Figs 3A and B)

With the Trapezoidal-28, the increased flexion for a change in external rotation is slightly less than the gains for the Mueller or the McKee-Farrar. This occurs because the impingement of the socket rim with the flat side of the trapezoidal neck is near the



FIGS 3A and B A Wear of rim due to impingement may reduce subluxation but B facilitates dislocation with opposite position



FIG 4 Effects of component orientation on ROM

Change in Component Orientation	Flexion	Internal Rotation in Flexion	External Rotation in Extension	Abduction in Extension
↑ Socket anteversion or Femoral anteversion	↑	↑	↓	↓
↑ Socket lateral opening	↑	↑	↑	↑

optimum configuration in relation to the socket at the given flexion angles. Because of the optimization of the neck shape, the flexion values of the Trapezoidal-28 at zero degrees abduction and external rotation are greater than the flexion values of the other prostheses.

Johnston and Smidt<sup>4</sup> observed in their electrogoniometry study of normal subjects that an average of 104° of flexion was required for sitting, 112° to rise from sitting to standing, 114° to squat, and 125° to crouch to pick up an object from the floor. It is apparent that most total hip units would not permit these functions without subluxation, pelvic flexion, abduction or external rotation of the limb, or combinations of all these motions.

Preliminary data from our laboratory studies on normal, standing persons indicate that the orientation of the iliac spines—

pubis plane varies from 4° to 15° in ante-flexion (pubis anterior to iliac spines). The ROM data reported here are based upon an angle of zero degrees. The effect of the pelvic ante-flexion in the standing position is to increase flexion in the standing position by the amount of pelvic ante-flexion on a degree for degree basis.

Flexion can also be enhanced if the limb is abducted and externally rotated. Protection from possible subluxation or dislocation during sitting and squatting can be afforded THR patients by advising them to externally rotate and abduct their limbs during these activities.

Patients who have had post-traumatic complications of osteonecrosis are more likely to develop a free ROM and neck-socket impingement. The restricted ROM which follows take-down of arthrodesis is often related to the length of time the hip

TABLE 4 Restriction of Motion Due to Wear\*

	Trapezoidal 28			Charnley	
	2	4	6	2	4
Depth of Socket Wear (mm)	2	4	6	2	4
Loss of flexion (degrees)	9	19	29	11	23
Loss of abduction in extension (degrees)	7	16	23	13	23
Loss of external rotation in extension (degrees)	11	16	28	8	15
Loss of internal rotation in flexion (degrees)	5	19	30	—	—

\* Wear simulated by deepening the socket at angle of 17° to simulate the resultant angle determined by Rydell. Socket is oriented open 42° laterally and 20° anteverted.

has been immobilized. Any free ROM in excess of that permitted by the components without neck-socket impingement increases the risk of subluxation and dislocation, especially if the musculature is weak. Repeated contact of the socket rim will cause wear and permit additional ROM without contact, but the force necessary to dislocate the prosthesis may lessen. Neck-socket impingement has been also causally implicated in the loosening of the McKee-Farrar and other all-metal total hip replacements.

Subluxation and dislocation may also occur from gravitational forces on the limb, these may become greater than the capsular or muscular resisting forces during gait or when the ball is levered out of the socket by impingement of bony prominences. These forces can be partially controlled by attention to detail at surgery using trochanteric advancement to tighten the abductor mechanism and/or the insertion of a femoral component with a longer neck and removal of bony prominences.

#### SUMMARY

Significant differences in ROM exist between different THR prosthesis designs. Several of the prosthesis designs tested are marginal in flexion, several millimeters of socket wear will decrease the ROM. The results also emphasize the importance of proper component orientation at surgery.

The surgeon has less latitude in orienting the components of a THR with limited ROM. Subluxation and dislocation due to rim contact can be minimized with most prosthetic units by instructing the patients to abduct and/or externally rotate their hips during acute flexion. Analyses suggest that impingement of prosthesis neck and socket rim may lead to increased risk of dislocation and increased rim wear. Prostheses with adequate ROM for everyday activities should provide stability, less frequent neck and socket contact with decreased rim wear, less force transmission to acrylic-bone interface, and less diminution of ROM with wear of the socket wall.

#### REFERENCES

- 1 Amstutz H C and Markolf K. Design features in total hip replacement. Scheduled for publication in *The Hip*. St Louis, C V Mosby 1975.
- 2 Backman S. The proximal end of the femur. *Acta Radiol Supplement* 146, 1957.
- 3 Charnley J. Factors in the design of an artificial hip joint, *Proc Instn Mech Eng* 181 3 104 1966-7.
- 4 Johnston R C and Smidty G L. Hip motion measurement for selected activities of daily living. *Clin Orthop* 72 205 1970.
- 5 Rydell N W. Forces acting on the femoral head prosthesis. *Acta Orthop Scand* 37, Suppl 88, 1966.

Copyright © 1993 by JBJS, Inc. All rights reserved.

# The Elevated-Rim Acetabular Liner in Total Hip Arthroplasty: Relationship to Postoperative Dislocation\*

BY T. K. COBB, MD†, B. F. MORREY, MD†, AND D. M. ILSTRUP, MS, ROCHESTER, MINNESOTA

*Investigation performed at the Mayo Clinic, Rochester*

**ABSTRACT** Although an acetabular component with an elevated rim is thought to improve the postoperative stability of a total hip prosthesis, the actual clinical value has not yet been demonstrated. To address this question, we reviewed the results of 5167 total hip arthroplasties that had been performed at our institution from April 1, 1985, through December 31, 1991. The prostheses included 2469 acetabular components with an elevated rim liner (10 degrees of elevation) and 2698 with a standard liner. The cumulative probability of dislocation was estimated as a function of time since the operation with use of the Kaplan-Meier survivorship method. Forty-eight of the 2469 hips that had the elevated rim acetabular liner dislocated within two years, compared with 101 of the 2698 hips that had the standard acetabular liner. The two-year probability of dislocation was 2.19 per cent for the hip with the elevated rim liner and 3.85 per cent for those with the standard liner ( $p = 0.001$ ). A similar trend was seen at five years; however, because of a smaller sample, the difference was not significant. Increased stability at two years was also demonstrated for the hips with the elevated rim liner when the hips were analyzed according to the operative approach, the mode of fixation, the sex of the patient, and the type of total hip arthroplasty (primary or revision). Although these data demonstrate improved stability after total hip arthroplasty when an elevated liner is used, particularly in hips that are at greater risk for dislocation of the prosthesis, the long-term effect of this elevated liner on wear and loosening remains unknown but is of considerable concern. The elevated liner deserves additional study to clarify its effect on wear and loosening.

metrical build up of these components is thought to provide additional support in regions of compromised stability.<sup>1</sup> The orientation of the augmented rim can be individualized depending on the unique anatomy of each patient, with the built-up region placed where it is most needed (usually posteriorly and superiorly).

Although the theoretical attractions of the elevated rim are obvious and have been widely accepted, the clinical advantages have not been demonstrated to our knowledge. To address this issue, we retrospectively reviewed the cumulative probability of dislocation in 5167 total hip replacements inserted at the Mayo Clinic from 1985 through 1991. Our purpose was to determine the effect of an augmented acetabular component on the cumulative probability of dislocation after total hip arthroplasty.

### Materials and Methods

The results of all total hip arthroplasties performed at the Mayo Clinic from April 1, 1985, through December 31, 1991, were reviewed. Of the 7105 hip procedures, those that involved use of a bipolar prosthesis, fixed head endoprosthesis, custom design prosthesis, or acetabular liner with a rim elevated 15 or 20 degrees, as well as those performed for reconstruction after resection of a tumor, were excluded from the review. With use of these selection criteria, 5167 hips were enrolled in the study: 2469 with an elevated rim acetabular component and 2698 with a standard (neutral) acetabular component. The relative percentage of elevated rim acetabular liners used each year increased from 10 per cent in 1985 to more than 80 per cent in 1991. The critical variables relating to stability of the hip have been prospectively gathered and recorded in the Total Joint Registry. Dislocation treated with reduction by a physician was used as the discrete failure end point. The group that had a dislocation was analyzed according to the operative approach, the type of arthroplasty (primary or revision), the sex of the patient, and the type of fixation. The risk of dislocation was assessed on the basis of the design of the acetabular cup. Follow-up data were obtained by physical examination for 2739 hips (53 per cent), questionnaire for 1808 (35 per cent), and a telephone survey for 620 (12 per cent). Dislocation can be adequately assessed by any of these modes of evaluation.<sup>4</sup> Only

An elevated rim acetabular liner is used as a potential means of improving stability after total hip arthroplasty. An elevated rim on a high density polyethylene acetabular liner is currently available from most manufacturers. An implant with this design was first used by Charnley in the early 1970s to decrease the tendency for posterior dislocation of the femoral head.<sup>1</sup> The asym-

No benefits in any form have been received or will be received from a commercial party related directly or indirectly to the subject of this article. No funds were received in support of this study.  
†Mayo Clinic, 200 First Street S.W., Rochester, Minnesota 55905

TABLE I  
DISLOCATION AT TWO YEARS ACCORDING TO THE DESIGN  
OF THE ACETABULAR CUP AND THE OPERATIVE APPROACH

	Rim of Acetabular Cup		P Value
	Standard	Elevated	
Anterior approach (no)	2320	1919	
Dislocations (no)	79	35	
Probability of dislocation (per cent)	3.47	2.09	0.01
Posterior approach (no)	243	454	
Dislocations (no)	11	12	
Probability of dislocation (per cent)	4.62	2.33	0.03
Transstrochanteric approach (no)	120	91	
Dislocations (no)	9	1	
Probability of dislocation* (per cent)	7.63	1.14	0.01

\*The approach was not known for twenty hips

†The probability of dislocation two years after total hip arthroplasty as shown by Kaplan Meier analysis

years) Of the 3204 patients who were operated on before 1990 3089 (96 per cent) were followed for at least two years Only fifteen patients who were alive and had an intact implant that had not dislocated were followed for less than two years Of the 1385 hips that had been operated on at least five years before our analysis 1324 (96 per cent) were followed for at least five years

## Results

### Instability

One hundred and forty nine of the over all group of 5167 hips included in this study were complicated by dislocation within two years after the total hip arthroplasty Forty eight of the 2469 hips with the elevated rim acetabular liner had a dislocation of the femoral prosthesis within two years compared with 101 of the 2698 hips with the standard acetabular liner The two year Kaplan Meier probability of dislocation was 2.19 per cent for the hips with the elevated rim liner and 3.85 per cent for those with the standard liner (Fig 1 A) This difference was significant (log rank test  $p = 0.001$ )

A similar trend was seen at five years however the difference was not significant The subgroup analyzed at five years consisted of 1385 hips Of the 173 with the elevated rim acetabular liner five were complicated by dislocation Of the 1212 with the standard acetabular liner fifty three were complicated by dislocation The five year Kaplan Meier probability of dislocation was 2.97 per cent in the group with the elevated rim acetabular liner and 4.46 per cent in the group with the standard liner ( $p = 0.34$ ) (Fig 1 B)

### Primary Total Hip Arthroplasty

Of the 1949 primary total hip arthroplasties in which the elevated rim acetabular liner was used twenty five were complicated by a dislocation compared with fifty of the 2168 primary total hip arthroplasties in which the

standard liner was used (Fig 2 A) The cumulative probability of dislocation was 2.35 per cent for the hips with the standard liner and 1.43 per cent for those with the elevated rim liner ( $p = 0.04$ )

### Revision Total Hip Arthroplasty

There were twenty three dislocations within two years after the arthroplasty in the 520 hips that had had a revision with the elevated rim acetabular component after a previous total hip arthroplasty and fifty one dislocations in the 530 hips that had had a revision with the standard liner (Fig 2 B) The two year cumulative probability of dislocation was significantly lower ( $p = 0.005$ ) in the hips with the elevated rim liner (5.02 per cent) compared with that in the hips with the standard liner (10.03 per cent)

### Operative Approach

Three operative approaches (anterior posterior and transtrochanteric) which have been previously described<sup>19</sup> were used at our institution during this study Regardless of the approach that had been employed the hips with the elevated rim acetabular liner were more frequently stable at two years than those with the standard liner (Table I) This difference was signifi-

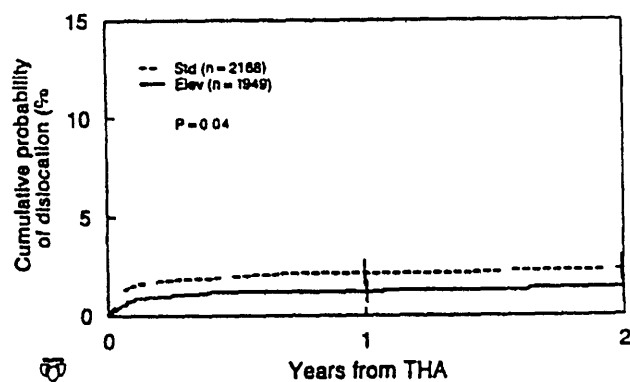


FIG 2 A

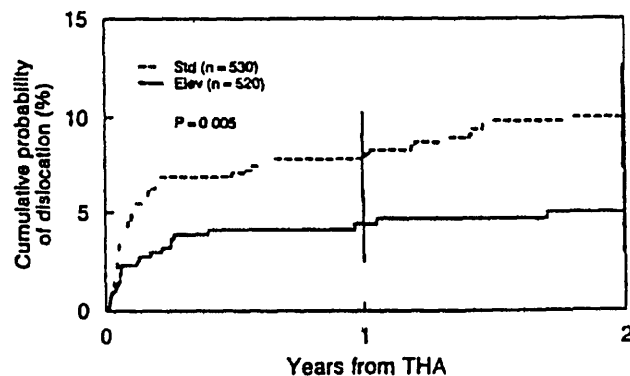


FIG 2 B

Figs 2 A and 2 B Kaplan Meier cumulative probability of dislocation for the elevated rim and standard acetabular components after primary total hip arthroplasty (Fig 2 A) and after revision total hip arthroplasty (Fig 2 B) THA = total hip arthroplasty

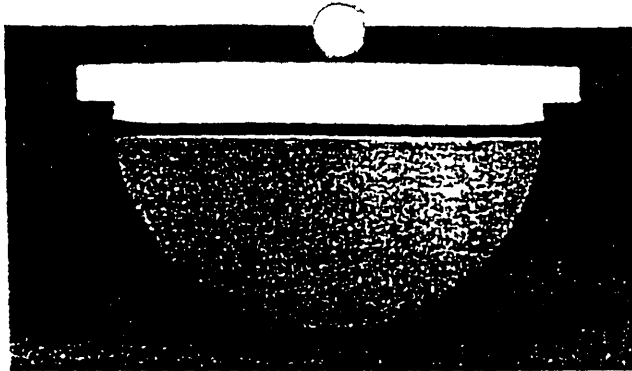


FIG 3 A

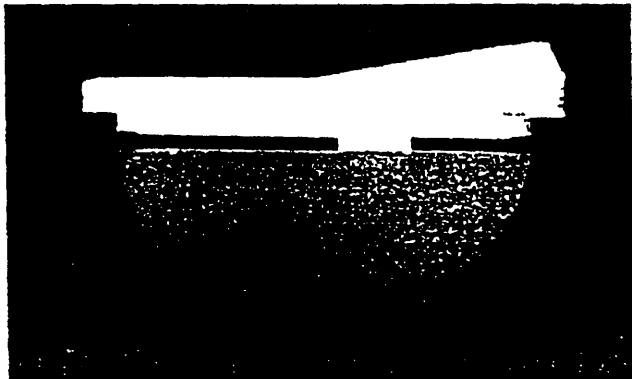


FIG 3 B

Figs. 3 A and 3 B Photographs of high density polyethylene neutral (Fig 3 A) and 10 degree elevated rim (Fig 3 B) acetabular liners for modular implants.

of instability. Olerud and Karlström reported success with this method in six patients who had recurrent dislocation. Other reports have been of limited numbers of patients and have described variable success.<sup>13,17,19</sup>

More recently various elevated liners have been incorporated into many systems of total hip arthroplasty (Figs 3 A and 3 B). For example, of the implants used commonly at our institution, one has for many years allowed the surgeon the option of using or not using an elevated rim liner, as well as options regarding the degree of augmentation. One attractive feature of the modular design of the current implants is that the augmented segment can be rotated into the desired position, theoretically enhancing stability.<sup>1</sup>

There has been concern about the long term effect of the enhanced stability derived from a more constrained articulation. Two worrisome complications could develop: increased wear debris from the high density polyethylene elevated rim, and loosening from the increased rotatory moment introduced by force being transmitted at the point of contact with the augmented rim (Fig 4).<sup>13</sup>

An additional limitation of the elevated rim design is that several biomechanical studies have shown that it is associated with a decreased arc of motion (Fig 5).<sup>1</sup> Krushell et al demonstrated that the stable arc of motion was not increased but rather reoriented with the use of an elevated rim. When the elevated rim was

placed posteriorly, stability was increased with the hip in flexion and in flexion with internal rotation with some designs, and only in internal rotation in flexion with other designs. Extension and external rotation in extension were decreased by elevated rim liners. Therefore, the range of motion was increased in some directions and decreased in complementary directions. The results of their study are supported by our clinical findings. A greater percentage of dislocations occurred anteriorly in the hips that had the elevated liner (eleven of thirty-seven, 30 per cent) compared with the percentage in the hips that had the standard liner (twelve of seventy-four, 16 per cent). This most likely resulted from impingement of the femoral neck on the elevated portion of the liner during extension of the hip.

Malorientation of one or both components has been shown to be the cause of approximately one half of dislocations after total hip arthroplasty.<sup>4</sup> The instability caused by malorientation is theoretically overcome by proper placement of an augmented acetabular liner. However, our analysis demonstrated less than a 1 degree difference between the anteversion of the standard acetabular cups and that of the elevated rim cups in the dislocated and non dislocated groups, which demonstrates that anteversion did not appear to play a role in the difference in stability observed between these two designs of component.

Charnley reported erosion of his elevated rim components. This worrisome complication was confirmed in a recent study by Murray who found severe erosion of four of ten elevated rim acetabular liners obtained at the time of revision. Similar problems with wear have been observed by the senior one of us (B. F. M.). Deformation and wear of the polyethylene liner is not only of concern from the standpoint of loss of mechanical sup-

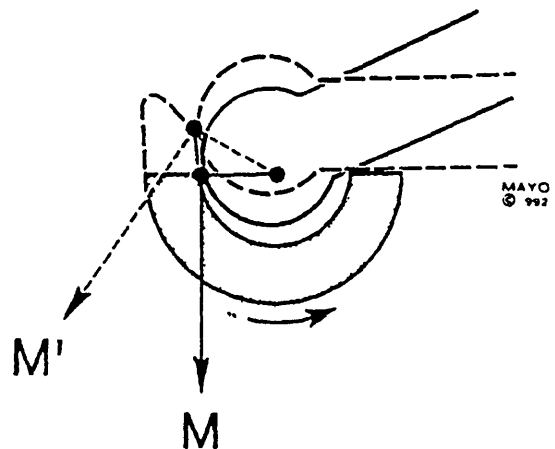


FIG 4

Illustration demonstrating a theoretical explanation of how stability is enhanced by the elevated rim design. The prosthesis is maintained within the acetabular cup during extremes of motion directed away from the elevated portion of the rim. However, the extended portion of the cup serves to increase the moment arm and therefore the torsional forces on the implant bone interface.  $M$  = the moment of the standard liner, and  $M'$  = the moment of the elevated rim liner.

eration was performed to one-third of all dislocations. Therefore, an estimated two patients per 100 revision total hip arthroplasties may be spared a subsequent operation by using an elevated-rim liner.

However, it must again be emphasized that additional studies are warranted regarding the possibility of

excessive polyethylene wear or increased torque causing loosening of the acetabular component. Because of the lack of data concerning these theoretical disadvantages, the senior one of us (B. F. M.) does not advocate the routine insertion of an acetabular component with an elevated rim liner at this time.

### References

1. Bosco J. A. and Benjamin J. B.: Loosening of a femoral stem associated with the use of an extended hip acetabular cup liner. A case report. *J Arthroplast* 8:91-9, 1993.
2. Charnley J.: *Low Friction Arthroplasty of the Hip: Theory and Practice*. New York: Springer, 1979.
3. Cox D. R.: Regression models and life tables. *J Roy Statist Soc. Series B* 4:147-220, 1972.
4. Daly P. J. and Murray B. F.: Operative correction of an unstable total hip arthroplasty. *J Bone and Joint Surg*, 74 A:1414-4, Oct 1992.
5. Elftokhar N. S.: Dislocation and instability complicating low friction arthroplasty of the hip joint. *Clin Orthop* 121:120-122, 1976.
6. Graham G. P., Jenkins A. I. R. and Mintowt Czys W.: Recurrent dislocation following hip replacement. brief report. *J Bone and Joint Surg* 70 B(4):675, 1988.
7. Kaplan E. L. and Meier P.: Nonparametric estimation from incomplete observations. *J Am Statist Assn* 53:457-481, 1958.
8. Krushell R. J., Burke D. W. and Harris W. H.: Elevated rim acetabular components. Effect on range of motion and stability in total hip arthroplasty. *J Arthroplast* 6 (Supplement) S33-S58, 1991.
9. Livermore J., Ilstrup D. and Morrey B.: Effect of femoral head size on wear of the polyethylene acetabular component. *J Bone and Joint Surg* 72 A:518-528, April 1990.
10. McCollum D. E. and Gray W. J.: Dislocation after total hip arthroplasty. Causes and prevention. *Clin Orthop* 261:159-170, 1990.
11. Morgensen B., Arnason H. and Jonsson G. T.: Socket wall addition for dislocating total hip. Report of two cases. *Acta Orthop Scandinavica* 57:573-574, 1986.
12. Morrey B. F. (editor): *Acetabulum In Joint Replacement Arthroplasty*, pp 569-572. New York: Churchill Livingstone, 1991.
13. Murray D. W.: Impingement and loosening of the long posterior wall acetabular implant. *J Bone and Joint Surg* 74 B(5):577-79, 1992.
14. Nicholas R. M., Orr J. F., Mollan R. A. B., Calderwood J. W., Nixon J. R. and Watson P.: Dislocation of total hip replacements. A comparative study of standard long posterior wall and augmented acetabular components. *J Bone and Joint Surg* 72 B(2):418-422, 1990.
15. Olerud S. and Karlstrom G.: Recurrent dislocation after total hip replacement. Treatment by fixing an additional sector to the acetabular component. *J Bone and Joint Surg* 67 B(3):402-405, 1985.
16. Peto R. and Peto J.: Asymptotically efficient rank invariant test procedures. *J Roy Statist Soc. Series A* 135:185-206, 1972.
17. Williamson J. B., Galasko C. S., and Rowley D. I.: Failure of acetabular augmentation for recurrent dislocation after hip arthroplasty. Report of three cases. *Acta Orthop Scandinavica* 60:676-677, 1989.
18. Woo R. Y. G. and Morrey B. F.: Dislocations after total hip arthroplasty. *J Bone and Joint Surg* 64 A:1295-1306, Dec 1982.

# File History Content Report

The following content is missing from the original file history record obtained from the United States Patent and Trademark Office. No additional information is available.

Document Date - 1997-05-20

Document Title - Non-Patent Literature

Page(s) - 81,83,85

## Accuracy Validation in Image-Guided Orthopaedic Surgery

D A Simon<sup>1</sup>, R V O'Toole<sup>2,1</sup>, M Blackwell<sup>1</sup>, F Morgan<sup>1</sup>, A M DiGioia<sup>2,1</sup>, T Kanade<sup>1</sup>  
das@ri.cmu.edu, rvo@ri.cmu.edu, mkb@ri.cmu.edu, fxm@ri.cmu.edu, digioia@ri.cmu.edu, tk@ri.cmu.edu

<sup>1</sup>Robotics Institute  
Carnegie Mellon University  
Pittsburgh, PA 15213

<sup>2</sup>Center for Orthopaedic Research  
Shadyside Hospital  
Pittsburgh, PA 15232

### Abstract

*Validating the accuracy of image guided surgical systems is a challenging and important problem which has received little attention in the literature. Potential sources of inaccuracy include CT imaging noise, model generation errors, errors introduced by fixturing, intra-operative data noise, registration errors, and inaccuracies in surgical tools and actions. In this paper we discuss our experience in validating an example image guided application in orthopaedic surgery. Various sources of inaccuracy are identified and approaches for mitigating their effects are suggested. The difficult problem of generating a reliable ground truth for evaluating the accuracy of surgical registration is discussed and surface based registration accuracy results are presented. A fiducial marker design which can be used to establish highly accurate ground truth correspondence between pre and intra-operative data is offered. Finally, the need for better accuracy metrics in image guided surgery is noted and shortcomings of metrics which are commonly used in the literature are illustrated.*

**Keywords:** image guided surgery, accuracy validation, surface based registration, accuracy metrics, fiducial marker design

### 1 Introduction

In image guided surgery pre-operative medical data are used to plan, simulate, guide or otherwise assist a surgeon in performing a medical procedure. In orthopaedic surgery possible sources of pre-operative data include CT, MRI or X Ray images. Using this data a surgeon may develop a pre-operative plan which specifies how one or more tasks are to be performed during surgery. The plan is constructed in a coordinate system relative to the pre-operative data. The surgical procedure is performed in a coordinate system relative to the patient. Surgical registration is the process of establishing a transformation between the pre-operative data and plan and the patient. Registration allows any 3 D point specified in the plan's coordinate system to be precisely located on the patient. Surgical execution is performed using either passive methods in which the surgeon is guided by information from the pre-operative plan or active methods in which a semi autonomous device such as a robot performs surgical tasks under the supervision of a surgeon.

This work was supported in part by a National Challenge grant from the National Science Foundation (award ECS 9422734)

A critical step required before the widespread clinical use of any novel image guided surgical technique is the evaluation and validation of the method. While several researchers have addressed the validation problem in the context of particular systems [6][17] very little formal research has been done in this area. In this paper we focus on the accuracy validation of pre-operative data and plans, registration methods, and surgical execution.

One difficulty in evaluating image guided techniques is the need for highly accurate ground truth. For example, to validate a registration technique it is necessary to have a high quality estimate of the true registration transformation. Depending on the requirements this can be a non-trivial problem requiring localization of complex patient anatomy with sub millimeter accuracy.

In the literature there has been little discussion of metrics for quantifying surgical task accuracy. Accuracy requirements and results are often reported as translational errors in distance units (e.g., mm) and rotational errors in degrees. In this paper we argue that there are potential ambiguities associated with these metrics due to a dependence upon the selected coordinate system. We propose that any meaningful measure of accuracy should be designed relative to the underlying task. For example, if the clinical goal is to cut a precise cavity in a femur ultimately we are interested in whether the actual position of the cavity is within certain tolerances of the desired position.

This paper presents an overview of methods used in our lab for validating an image guided application in orthopaedic surgery. We discuss sources of noise and error which arise in this system and suggest approaches for dealing with these errors. Finally we present accuracy validation results for the registration component of our system.

### 2 Prototypical System Overview

Figure 1 outlines the steps in a typical image-guided surgical system using total hip replacement as the example application [24]. Initially pre-operative data are acquired from the relevant patient anatomy. In our application this data is acquired from a CT imager. After acquisition, the data is fed to a computer workstation where a surgeon can interactively generate a patient specific pre-operative plan, potentially with the assistance of analysis and simulation tools. Since we



use a *surface based* registration technique [22] the pre operative data are also used to generate bounding surfaces of specified anatomical structures. Each of these processes are performed off-line before surgery.

During surgery the operations in the lower half of Figure 1 are performed. First the relevant patient anatomy is either 1) rigidly fixtured to prevent motion, as in [24], or 2) affixed with a tracking device that will allow the system to compensate for motion as in [4][15]. Second, registration data are acquired from the relevant anatomy using a suitable sensor (e.g. digitizing probe, ultrasound). Third, the registration process determines the transformation between the surface model (in the coordinate system of the pre-operative plan) and the intra-operative surface data (in the coordinate system of the intra-operative sensor). Once this key transformation has been determined, the pre-operative plan may be executed within the reference frame that describes the patient's anatomy at the time of the surgery. Intra-operative actions may be performed either manually or autonomously. For manual actions, navigational guidance can be provided to the surgeon based on measurements of current tool locations and knowledge of desired tool locations from the pre-operative plan. For autonomous actions, execution is performed by a tool such as a robot under the surgeon's supervision.

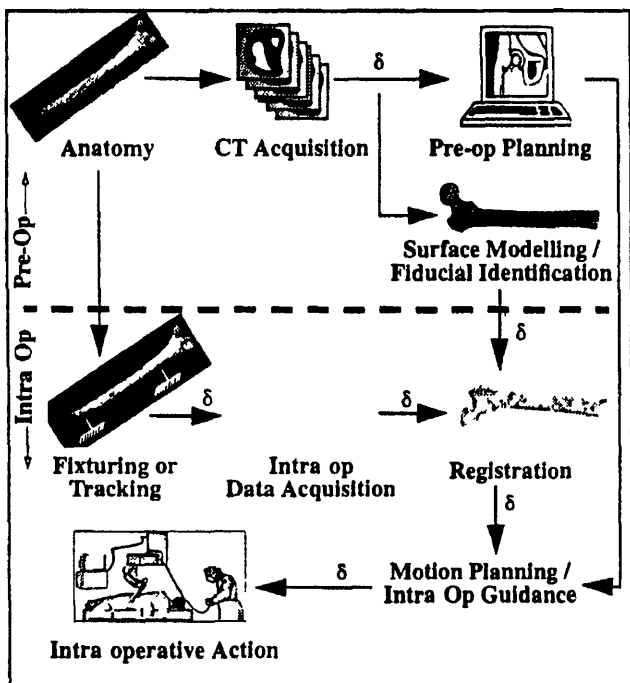


Figure 1 Image Guided Surgical System Components

### 3 System Error Analysis

As with any complex system, there are many potential sources of error and noise in an image-guided surgical system. In Figure 1, a  $\delta$  at the output of a component process indicates that the preceding operation may be a source of errors or noise. These errors include:

- CT imaging errors
- Surface model generation errors
- Errors introduced by fixturing
- Intra-operative data noise
- Registration errors
- Inaccuracies in surgical tools and actions

Each of these error sources has an impact upon the accuracy of the executed task. The first goal of system validation is to measure overall task accuracy (e.g. how well does a cavity cut in a femur match the planned cavity location). The second goal is to understand how each of the component processes contributes to the final error. The remainder of this section discusses each of the aforementioned error sources.

#### 3.1 CT Imaging Errors

During CT image creation, there are many opportunities for added error or noise [13]. Limitations in spatial and contrast resolution place bounds on the veracity of the resulting images. Artifacts caused by phenomena such as beam hardening, partial voluming, and patient motion can make it difficult to interpret the underlying data. For our purposes, these sources of error are relevant because of their effect on the accuracy of the resulting surface models.

While we are not actively pursuing research in CT image formation, we are acutely aware of the potential for noise in this process. For the results in this paper, we acquired high-quality data from a General Electric High Speed Advantage clinical CT imager (0.29mm x 0.29mm in slice resolution, 1.0mm slice thickness, acquired at various inter-slice separations). To estimate the quality of the resulting data, we rely on evaluation of downstream operations. In Section 3.2, we describe an approach for validating surface model accuracy. In Section 4.2, we describe a method for analyzing the locations of fiducial markers extracted from images of a precisely known phantom. From these analyses, we can indirectly estimate the accuracy of the underlying CT data.

Many parameters can be specified in clinical CT imagers. In-slice and inter-slice resolutions, beam power, and choice of reconstruction method all influence the resulting CT images. We are currently studying the effect of CT parameters on the resulting surface model accuracy. We are currently designing CT acquisition protocols tailored to the problem of constructing surface models of bones. The challenge is to minimize the amount of CT data acquired (and thus radiation exposure to the patient) while ensuring sufficient accuracy of the resulting surface models.

#### 3.2 Surface Model Generation Errors

Although there exist many techniques for creating surface models from medical images [12], little has been published about the validation of surface model accuracy. In medicine, surface models were originally used for diagnostic visualization tasks in which visual appearance, not geometric accuracy,

cy was important. With the recent expansion of image guided surgical techniques, surface model accuracy has taken on new importance [5][19].

In order to rigorously investigate error in surface models, a ground truth is needed. There are two methods for determining accurate ground truth: precisely manufacturing shapes for which a model exists, or accurately generating a computer surface model using an optical range sensor or other high accuracy measurement tool. Figure 2 shows a proposed extension to a method for analyzing the accuracy of surface models which was originally proposed by Geiger in [5]. Geiger argues that metrics such as difference volumes, Hausdorff distances, and measures of surface normal variation are useful for describing surface model accuracy. The primary difference between Geiger's original work and our proposed extension [19] is the use of real (as opposed to synthetic) CT data.

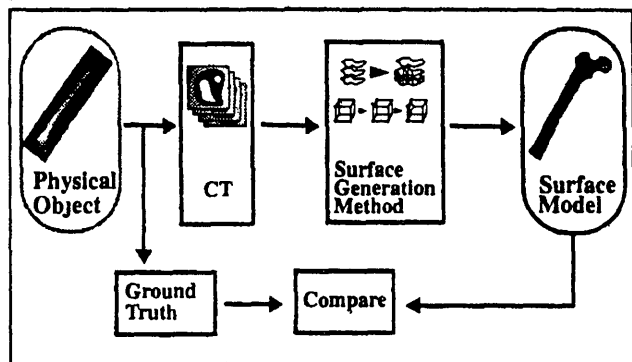


Figure 2 Schematic of surface model validation

### 3.3 Errors Introduced by Fixturing

Fixturing to patient anatomy establishes a fixed transformation between a patient attached coordinate system and that of computer assisted tools and sensors. Rigid fixturing ensures that the transformation between the pre-operative plan and the patient remains fixed during the procedure. An alternate approach is to rigidly fix a tracking device to the anatomy and use that device to accommodate movements of the anatomy which occur during surgery.

The rigid fixation and tracking methods both rely on a firm connection to the patient anatomy. If there is movement between the anatomy and the fixation device or target, the registration result is no longer valid. Sensitive motion detectors can be used to ensure that there is no motion between the anatomy and a fixed coordinate system [24]. This technique is less practical when the tracking method is used. Guaranteeing that a tracking target has not moved relative to the anatomy during surgery (e.g. from contact with the surgeon) is difficult, since it is impossible to differentiate motions of the target from motions of the anatomy.

An additional error source arises from the potential to deform the anatomy with the fixation device. This is of concern with the relatively massive external fixator devices used in orthopaedics. While tightening such devices onto the bone, it is

possible that the bone will undergo large stresses and therefore deform. For surgeries where submillimeter accuracy is required, such deformations can impact the overall accuracy of the procedure, since pre-operative surface models will no longer accurately represent the anatomy.

### 3.4 Intra-operative Data Noise

Data collected from patient anatomy during surgery are used by the registration process to establish the transformation between the patient and the pre-operative data. Noise present in this data will have a potentially harmful effect upon registration accuracy.

Several types of sensors have been used for acquiring intra-operative registration data. Research groups have reported on the use of X-Ray imagers [14], ultrasonic sensors [1], optical digitizers [4][15][21][22], mechanical digitizers [10], optical range imagers [6][20][22], video cameras [3], and robots [24]. For our current applications, we are using an optical digitizer to provide intra-operative data (Optotrak - Northern Digital Inc.). While other groups have used this sensor in medical applications, little has been published regarding details of its use. Rohling et al. conducted a study comparing the accuracy of the Optotrak sensor to a mechanical digitizer [21]. We have independently verified many of the results presented in that paper [16]. Northern Digital has also published a technical report which discusses accuracy issues related to the use of several types of digitizing probes [18].

A potential source of error from Optotrak involves probe tip geometry. As explained in [18], Northern Digital uses a pivoting calibration to determine a probe's end tip location. In order to minimize calibration errors due to motion during calibration, it is suggested to use ball point rather than sharp point probe tips. Ball point tips also have the advantage that they are less likely to penetrate the surface of an object being digitized. However, due to the finite radius of a ball point, data acquired using these probes are displaced from the true surface by a distance proportional to the ball radius. Depending upon the accuracy requirements of an application, these errors may or may not be significant. A possible fix for this problem is to acquire data such that the probe tip is well aligned with the underlying surface normal. In this case, measurements can be corrected to compensate for the ball radius; however, this approach may place an undue burden upon the data collector.

In our applications, intra-operative data are used solely for registration. Ideally, intra- and pre-operative data collected from the same underlying anatomy should be geometrically similar (i.e. if the two data sets are aligned via registration, overlapping data regions should be coincident). For several reasons, this condition may not be met in practice. Spatial resolution differences between the underlying sensors (i.e. CT and Optotrak) may cause certain features to be visible in one modality but not in the other. For example, small indentations present on bony surfaces may not be present in surface models generated from CT, but may be visible to an Op

totrak point-tip probe To compensate for this a ball probe tip can be used to spatially filter the intra-operative data (thus eliminating the surface indentations) It should be noted that it is more important that the two registration data sets be geometrically similar to each other than it is for either data set to faithfully represent the underlying anatomy

Other potential sources of Optotrak error which we have observed include

- Displacement of apparent target (LED) centroids as a function of target rotation
- Data acquisition near the sensor's field of view boundary

While some effects of intra surgical data noise can be removed via outlier elimination during registration other noise (e.g., biases from finite diameter ball probes) are difficult to remove Therefore, it is important to carefully design the data acquisition process to minimize noise in the collected data

### 3.5 Registration Errors

A key requirement in any registration process is the ability to extract and identify corresponding landmarks or features from the data sets being registered This process may be facilitated using synthetic fiducial markers attached to the patient which are easily located in both pre- and intra-operative data Fiducial based registration has a number of clinical disadvantages including attachment of markers may require additional surgery and additional patient trauma at or near the marker attachment site Therefore, many researchers have attempted to eliminate the need for fiducials by using landmarks which are intrinsic to the data itself [3][6][7][8][11] Intrinsic landmarks used in registration include bounding contours ridge lines discrete points and surfaces In the current work we use a surface based registration method described in [22]

The registration process is capable of introducing large errors into an image guided surgical system These errors may be caused by factors including

- Convergence of the registration algorithm to local minima in the space of possible transformations
- Poor geometric constraint between registration data sets [22] This results in reduced sensitivity of the registration cost metric and thus reduced accuracy

In addition registration accuracy is highly dependent upon the quality of the underlying data Noisy data will often result in poor registration accuracy In order to account for these factors we take the following precautions during registration

- Initial pose estimates should be as accurate as practical Manually specified anatomical landmark correspondence provides one way to establish initial pose estimates When good initial pose estimates are not available precautions should be taken to ensure convergence to the global minima [2]

- Careful selection of intra-operative data can increase the sensitivity of the registration cost metric and thus the resulting accuracy [22] This is especially important when limited amounts of data are available or the costs of data acquisition are high
- Outlier elimination should be used to reduce the effect of noisy data upon registration We are currently studying a constraint based outlier elimination method which builds upon the work in [22]
- On line, per use verification checks of registration are highly desirable For example manual selection of landmarks on the patient followed by automatic identification of those landmarks in CT data provides a means for verification

### 3.6 Inaccuracies in Surgical Tools and Actions

The pre-operative plan manifests itself in the operating room as either semi-autonomous robotic motion or as manual tool movements by a surgeon with the assistance of navigational guidance In both cases the resolution and accuracy with which a tool can be tracked impacts the precision of the executed procedure Although manipulators have impressive repeatability specifications calibration is usually needed to demonstrate high global accuracies When the tool is manually controlled by a surgeon based upon visual guidance execution inaccuracies may be large

Tool errors become more significant when disturbance forces are encountered If a robot is used for milling only small cutting forces are tolerable as these forces produce deflections in the robot which are challenging to counteract Since cutting or drilling forces increase with the speed of motion a trade off exists in some applications between speed and accuracy

## 4 Estimating Ground Truth

Figure 3 illustrates how we use ground truth to validate registration accuracy Generating accurate ground truth is critical for reliable validation however, it is also a difficult problem due to the submillimeter accuracies required

Our approach is to compare surface based to fiducial based registration results As with any fiducial based registration approach it is necessary to accurately extract the locations of fiducial markers from both pre-operative (CT) and intra-operative (Optotrak) data Therefore fiducial markers should be designed to facilitate accurate acquisition of this information In our case there were three primary fiducial marker design parameters material shape and size

### 4.1 Fiducial Design

*Fiducial Material* Choice of material was based on the goal of minimizing artifacts induced in CT while still being sufficiently hard and rigid so as not to deform (i.e. during data acquisition or from humidity/temperature variations) Since validation was not performed on humans biocompatibility was not an issue We chose an aluminum alloy (2017 T4) as

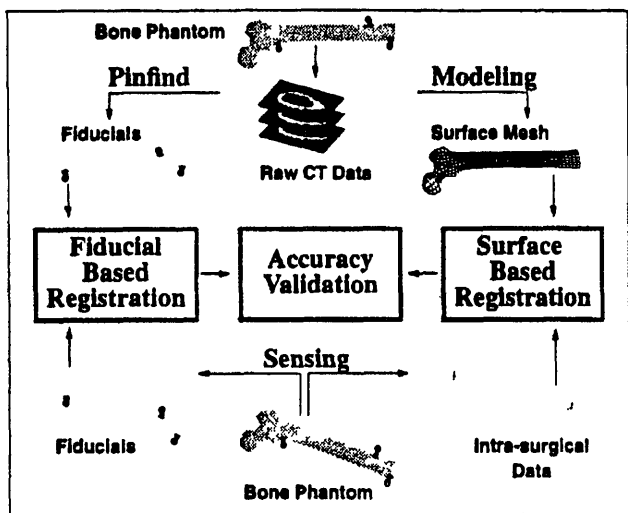


Figure 3 Validating Registration Accuracy

a material which avoids the imaging artifacts of harder materials (e.g. steel) while being more rigid and stable than softer materials (e.g. plastics). Aluminum's relatively high density also facilitates segmentation of the fiducials from CT data.

**Fiducial Shape** The shape of a fiducial was selected to facilitate the accurate estimation of a fixed point on the fiducial from both pre- and intra-operative data. Due to data noise, it is difficult to accurately extract a single point directly from the data. Rather, large quantities of data are used to infer a fixed point (i.e. centroid of a sphere, apex of a cone).

In CT, we observe that most of the error in locating a fiducial is due to beam hardening and partial volume artifacts [13]. To limit the effects of partial voluming (which occurs when an image voxel only partially contains the fiducial), it is desirable to minimize the relative number of voxels on the surface of the fiducial. Thus, we seek a shape which minimizes the ratio of surface area to total volume (for a given size).

Beam hardening and pluming artifacts in CT are influenced by shape and material of the imaged object. Thicker and denser materials result in larger potential for artifacts. However, small fiducials tend to have a high ratio of partial volume to non-partial volume voxels (approaching infinity as fiducial size approaches zero). Therefore, a trade-off exists between beam hardening and partial volume effects as a function of fiducial size.

We considered three possible fiducial shapes: cones, spheres, and cylinders. Spheres have many advantages, and for our application, they clearly outperform cones and cylinders. Estimating sphere centroids from both CT and intra-operative data is straightforward. While artifacts in CT may change the apparent radius of a sphere, the sphere centroid tends to remain unchanged due to symmetry. The same is not true of cones or cylinders, whose centroids (or other reference points) shift significantly as a result of artifacts. Spheres also have the smallest surface area for a given volume and are therefore less sensitive to partial voluming effects. Furthermore,

spheres are much easier than cones or cylinders to localize intra-operatively, as described in Section 4.3.

**Fiducial Description** A CT image of our final fiducial design mounted on a cadaver femur is shown in Figure 4. It is an aluminum sphere, 12.7 mm in diameter ( $\pm 25 \mu\text{m}$ ), mounted on a hollow Delrin cylinder which can be attached to bone using a screw or epoxy. The relatively large sphere diameter together with the moderate density of aluminum provides a trade-off between partial voluming and beam hardening/pluming. The Delrin mount provides a standoff between bone and aluminum, thus simplifying the CT segmentation task. The mounts have small holes which allow water to enter the hollow cylindrical mounts. Thus, the spheres can be almost completely surrounded by water during CT acquisition.



Figure 4 CT Image of a Fiducial Marker on Bone

## 4.2 Fiducial Locations from CT

We extract fiducial centroids from CT using a manual cropping procedure followed by an automatic threshold-based segmentation. The centroid can then be calculated directly from the thresholded data. We have experimented with several centroid location schemes which better utilize partial volume information; however, due to the spherical symmetry of our fiducials, these techniques did not significantly improve the result.

We tested the accuracy of CT fiducial localization by creating a phantom with three fiducials and measuring the centroid locations with a Coordinate Measuring Machine (CMM) to within  $10 \mu\text{m}$ . Inter-sphere distances averaged 49.6 mm with a maximum of 63.6 mm. After CT scanning the phantom at 1 mm slice intervals, we compared the extracted inter-fiducial distances to the corresponding known distances from the CMM. The average distance error was 0.1 mm, while the maximum distance error was 0.15 mm. We also performed fiducial registration between the two data sets using the technique described in [9]. The resulting maximum residual error was 0.11 mm, while the RMS residual error was 0.08 mm. This sub-voxel accuracy was sufficient for our application and verifies the strength of the fiducial design and localization method.

Nolte et al. [17] have proposed an optimization technique which perturbs extracted fiducial locations from CT data so that the inter-fiducial distances agree with the corresponding

distances from a known ground truth. We are currently investigating this technique to determine whether it will improve our ground truth results.

### 4.3 Fiducial Locations from Intra Operative Sensor

Using Optotrak, it is trivial to directly measure sphere centroids. Using a hollow cylindrical probe tip such as the one shown in Figure 5, a pivoting calibration [18] can be performed using a fiducial to provide the center of rotation. After calibration, the sensor will directly measure sphere centroids when the probe tip is mated to the sphere surface. By acquiring a large number of data points (e.g. 15), very good centroid estimates are possible.



Figure 5 Centroid Locating Probe Tip

Using the phantom and techniques described in Section 4.2, we have compared fiducial centroids measured by Optotrak with CMM based ground truth. The average distance error was 0.03mm, while the maximum distance error was 0.05mm. Using the fiducial based registration method, the maximum residual error was 0.03mm, while the RMS residual error was 0.03mm.

A second test of intra-operative fiducial localization was performed by estimating the centroids of 6 fiducials mounted on a bone phantom, performed twice, accomplished without moving the bone. Since the transformation between the first and second data sets should be null, we can use the results to estimate the repeatability of our measurements. Using fiducial based registration, the maximum residual error was 0.09mm, while the RMS residual error was 0.05mm. This resulted in an apparent motion of the bone of 0.09mm in translation and 0.03 degrees of rotation about a coordinate system located at the centroid of all six fiducials.

### 4.4 Overall Accuracy of the Ground Truth

As a final measure of fiducial based ground truth accuracy, we examined the residuals which resulted by registering CT and Optotrak fiducial centroids extracted from the bone phantom. The maximum resulting residual was 0.12mm, with an RMS error of 0.09mm.

## 5 Registration Validation Results

As outlined in Figure 3, we can use fiducial based registration to estimate the accuracy of surface based registration. For the purposes of discussing registration accuracy, we created a pre-operative plan for the placement of a femoral implant in total hip replacement surgery. Figure 6 is a schematic of a pre-operative plan which we have constructed using CT data from a cadaver bone. The goal of the planning process is

to determine the proper position of the implant with respect to the femur in the CT coordinate system. The plan is constructed manually via a graphical user interface which overlays a model of the implant upon the CT data.

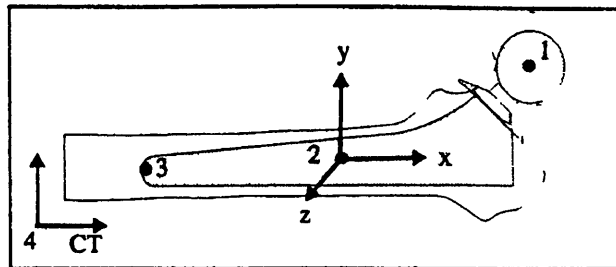


Figure 6 Pre Operative Plan

As mentioned in the introduction, we believe that all accuracy results and requirements should be specified using metrics which have direct physical meaning to the task being performed. To demonstrate this concept, registration accuracy results are presented below using two different metrics.

In the first experiment, we constructed a surface model from CT images of a cadaveric femur scanned in water. 100 intra-surgical data points were collected within a roughly 65mm region of the proximal femur using Optotrak. Data collection was limited to areas of the bone which are clinically accessible during total hip replacement surgery. Surface based registration was applied to the data in order to estimate the registration transformation. Fiducial based registration was performed using 6 markers to calculate ground truth.

Table 1 summarizes the results of this experiment using the conventional method of representing error. Each row of the table contains the registration error (i.e. difference between the fiducial based and surface based result) expressed as a transformation about a given coordinate system. The first column indicates the coordinate system, while the second and third columns indicate the magnitudes of the translation and rotation errors, respectively. Coordinate systems 1, 3 are all parallel with the X axis in the direction of the implant shaft's central axis, the Y axis defined by the projection of the femoral head centroid onto the X axis, and the Z axis defined as the cross product of the first two. The origin of each coordinate system is a point selected for its relevance to the implant placement task (centroid of the prosthetic femoral head centroid of the implant and distal tip of the implant, numbered 1, 3, respectively in Figure 6). The fourth coordinate system in Table 1 is the one used by the CT imager.

In the table, the magnitude of the translation error component is a function of the coordinate system, while the magnitude of the rotation component is constant. An explanation of this result is presented in the next paragraph. The important point is that each of the results in Table 1 refers to the *same transformation error*. This example demonstrates the potential ambiguity of this error metric. When using this metric, it is crucial that the selected coordinate system have a physically meaningful relation to the task being performed. Depending upon the selected coordinate system, the accuracy of our surface

**Table 1 Registration Errors Translation / Rotation**

Coordinate System	$\ T\ $ (mm)	$\ R\ $ (deg)
1 - Head Centroid	0.25	0.97
2 - Implant Centroid	0.31	0.97
3 - Implant Distal Tip	0.17	0.97
4 CT	1.77	0.97

based registration could either be reported as 0.17mm in translation or 1.77mm in translation a factor of 10 difference (Fortunately meaningful error values for this task are closer to the smaller value)

The schematic in Figure 7 provides insight into the results of Table 1. In the left half of the figure, the two lines labeled 1 and 2 represent a misalignment error such as that resulting from registration. With respect to a coordinate system positioned at point a, this error can be described as a pure rotation. In order to describe the same error with respect to a coordinate system positioned at point b, line 2 must first be rotated about point b to line 3, and then shifted back to point a. The angle of rotation about either point a or b is the same, however the translation differs. This same phenomenon applies to the results of Table 1, and explains the difference in translation magnitudes as a function of coordinate system.

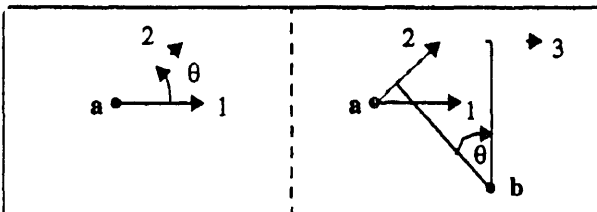


**Figure 7 Error Dependence on Coordinate Frame**

The second metric used to describe the results of the above experiment expresses registration error as a displacement induced at selected points on the implant. For each of the points numbered 1-3 in Figure 6, we calculated the displacement (i.e. change in position measured as a Euclidean distance) of the point which results by applying the registration error transformation of Table 1. These displacements are independent of the coordinate system about which the error is represented. Since this metric requires explicit specification of physically meaningful landmarks, it is potentially less ambiguous than the first metric. The resulting displacements are shown in Table 2 and can be interpreted as the implant misalignment at each point which would result if the implant were actually positioned using the registration transformation found above. It is no coincidence that the point displacement magnitudes are the same as the corresponding translation magnitudes from Table 1. (On the right side of Figure 7, the translation required to realign line 3 with line 1 is the same as the displacement which would be induced at point b by rotating line 2 together with point b about point a into line 1.)

**Table 2 Registration Errors Point Displacement**

Point Number	$\ D\ $ (mm)
1 - Head Centroid	0.25
2 - Implant Centroid	0.31
3 - Implant Distal Tip	0.17
4 Extremum Point	0.54

The fourth point in Table 2 was selected to provide an upper bound on displacement among all points on the implant surface. This point was found by determining the screw axis representation of the error [23] (the axis about which the transformation can be expressed as a rotation about the axis coupled with a translation along it). The extremum point was then selected as the implant surface point farthest from the axis. The projection of this screw axis onto the pre-operative plan is shown in Figure 8. Note that the point displacements of Table 2 are a function of the distance between the axis and each of the points. We have found 3-D graphical renderings of the screw axis superimposed on the relevant anatomy to be quite useful in visually interpreting registration error.

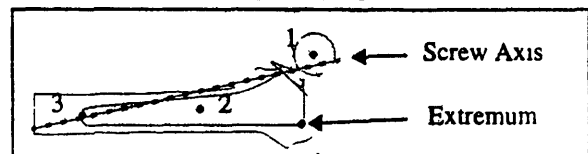


**Figure 8 Screw Axis Representation of Error**

## 6 Conclusions

We have presented several issues related to the accuracy validation of an image guided surgical system. We believe that many of the issues discussed with respect to our example task of total hip replacement have application to a broader set of image guided surgical problems.

A major issue which remains to be addressed is the specification of accuracy requirements for image guided surgical applications. Fundamental questions remain to be answered:

What are the best clinically meaningful measures of accuracy for a given task?

- How should accuracy specifications / tolerances for a given task and a given metric be determined?
- Are additional analysis tools required to allow clinicians to analyze task accuracy requirements? If so what form should these tools take?

The consequences of underestimating accuracy requirements in an image guided surgical application could be potentially catastrophic. Accuracy requirements which are too strict may have negative consequences as well. In general, achieving higher accuracy will have higher associated monetary costs (i.e. additional pre-operative data, more accurate intra-operative

tive sensors and tools longer times spent in surgery acquiring data etc ) Given the current economic climate in medicine we can not afford to waste limited resources on unnecessary accuracy

## 7 Acknowledgments

The authors wish to thank Rich Wallace of Shadyside Hospital for his invaluable help acquiring CT data Jesse Easudes generated CAD models of the surgical implants used to construct pre-operative plans Drew Shefman created much of the artwork in this paper Lori Gregor and Nate Walk helped with data collection and experimental tasks

## 8 References

- [1] Barbe C Troccaz J Mazier B and Lavallee S Using 2.5D Echography in Computer Assisted Spine Surgery *IEEE Engineering in Medicine and Biology Society Proceedings* pp 160 161 IEEE San Diego 1993
- [2] Besl PJ and McKay ND A Method for Registration of 3 D Shapes *IEEE Transactions on Pattern Analysis and Machine Intelligence* 14(2) 239 256 February 1992
- [3] Betting F Feldman J Ayache N and Devernay F A New Framework for Fusing Stereo Images with Volumetric Medical Images Ayache N (ed) *Proc CVRMed 95* pp 30 39 Springer Verlag Nice France April 1995
- [4] Dessenne V Lavallee S Julliard R Orti R Martelli S and Cinquin P Computer Assisted Knee Anterior Cruciate Ligament Reconstruction First Clinical Tests *J of Image Guided Surgery* 1(1) 59 64 April 1995
- [5] Geiger B *Three dimensional modeling of human organs and its application to diagnosis and surgical planning* PhD thesis Ecole des Mines de Paris April 1993
- [6] Grimson WEL Ettinger GJ White SJ Gleason PL Lozano Perez T Wells WM and Kikinis R Evaluating and Validating an Automated Registration System for Enhanced Reality Visualization in Surgery Ayache N (ed) *Proc CVRMed 95* pp 3 12 Springer Verlag Nice France April 1995
- [7] Hamadeh A Lavallee S Szeliski R Cinquin P and Pena O Anatomy based Registration for Computer Integrated Surgery Ayache N (ed) *Proc CVRMed 95* pp 212 218 Springer Verlag Nice France April 1995
- [8] Henri CJ Colchester ACF Zhao J Hawkes DJ Hill DLG and Evans RL Registration of 3 D Surface Data for Intra Operative Guidance and Visualization in Frameless Stereotactic Neurosurgery Ayache N (ed) *Proc CVRMed 95* pp 3 12 Springer Verlag Nice France April 1995
- [9] Horn BKP Closed Form Solution of Absolute Orientation Using Unit Quaternions *J of the Optical Society of America A* 4(4) 629 642 April 1987
- [10] ISG Technologies Inc *Viewing Wand Operator's Guide* ISG Technologies Inc Mississauga Canada 1993
- [11] Jiang H Robb RA and Holton KS A New Approach to 3 D Registration of Multimodality Medical Images by Surface Matching *Visualization in Biomedical Computing SPIE Vol 1808* pp 196 213 SPIE 1992
- [12] Kalvin AD *A survey of algorithms for constructing surfaces from 3D volume data* IBM Research Report RC 17600 IBM January 1992
- [13] Krestel E *Imaging Systems for Medical Diagnostics* Siemens Aktiengesellschaft Berlin 1990
- [14] Lavallee S and Szeliski R Recovering the Position and Orientation of Free Form Objects from Image Contours Using 3D Distance Maps *IEEE Trans PAMI* 17(4) 378 390 April 1995
- [15] Lavallee S Sautot P Troccaz J Cinquin P and Merloz P Computer-Assisted Spine Surgery A Technique for Accurate Transpedicular Screw Fixation Using CT Data and a 3 D Optical Localizer *J Image Guided Surgery* 1(1) 65 73 April 1995
- [16] Morgan F O Toole RV Simon DA and Blackwell MK *Opiotrak Validation Experiments* Technical Report CMU RI TR 95 26 Carnegie Mellon University Pittsburgh Pennsylvania 15213 July 1995
- [17] Nolte LP Zamorano LJ Zhaowei J Wang Q Langlotz F Arm E and Visarius H A Novel Approach to Computer Assisted Spine Surgery *Proc MRCAS 94* pp 323 328 Pittsburgh PA September 1994
- [18] Northern Digital Inc *Accuracy of Digitizing Probes* Technical Report 3 Northern Digital Inc Ontario CAN May 1992
- [19] O'Toole RV Simon DA Jaramaz B Ghattas O Blackwell MK Kallivokas L Morgan F Visnic C DiGirola AM and Kanade T Towards More Capable and Less Invasive Robotic Surgery in Orthopaedics *Proc CVRMed '95* pp 123 130 Springer Verlag Nice France April 1995
- [20] Pena O Francois Joubert A Lavallee S Champeboux G Cinquin P and Grand S Accurate registration of SPECT and MR brain images of patients suffering from epilepsy or tumor *Proc MRCAS 94* pp 58 62 Pittsburgh PA September 1994
- [21] Rohling R Munger P Hollerbach J and Peters T Comparison of Relative Accuracy Between a Mechanical and an Optical Position Tracker for Image Guided Neurosurgery *Proc MRCAS 94* pp 277 282 Pittsburgh PA September 1994
- [22] Simon DA Hebert M and Kanade T Techniques for Fast and Accurate Intra Surgical Registration *J Image Guided Surgery* 1(1) 17 29 April, 1995
- [23] Spoor CW and Veldpaus FE Rigid body motion calculated from spatial coordinates of markers *J Biomechanics* 13 391 393 1980
- [24] Taylor RH Mittelstadt BD Paul HA Hanson W Kazanides P Zuhars JF Williamson B Musits BL Glassman E and Bargar WL An Image Directed Robotic System for Precise Orthopaedic Surgery *IEEE Trans Robotics and Automation* 10(3) 261 275 June, 1994

*Laboratory Investigations***Techniques for Fast and Accurate Intrasurgical Registration**

David A. Simon, Martial Hebert, and Takeo Kanade  
*Robotics Institute, Carnegie Mellon University, Pittsburgh, Pennsylvania*

**ABSTRACT** The goal of intrasurgical registration is to establish a common reference frame between presurgical and intrasurgical three-dimensional data sets that correspond to the same anatomy. This paper presents two novel techniques that have application to this problem, high-speed pose tracking and intrasurgical data selection. In the first part of this paper, we describe an approach for tracking the pose of arbitrarily shaped rigid objects at rates up to 10 Hz. Static accuracies on the order of 1 mm in translation and 1° in rotation have been achieved. We have demonstrated the technique on a human face using a high-speed VLSI range sensor, however, the technique is independent of the sensor used or the anatomy tracked. In the second part of this paper, we describe a general purpose approach for selecting near-optimal intrasurgical registration data. Because of the high costs of acquisition of intrasurgical data, our goal is to minimize the amount of data acquired while ensuring registration accuracy. We synthesize near-optimal intrasurgical data sets, based on an analysis of differential surface properties of presurgical data. We demonstrate, using data from a human femur, that discrete-point data sets selected using our method are superior to those selected by human experts in terms of the resulting pose-refinement accuracy. *J Image Guid Surg* 1 17-29 (1995)  
 ©1995 Wiley Liss Inc

**Key words** 3-D registration, pose estimation, high-speed pose tracking, geometric constraint-based data selection

**INTRODUCTION**

A growing number of surgical procedures require the establishment of a common reference frame between presurgical volumetric data and the corresponding patient anatomy. This requires the solution of the three-dimensional (3-D) registration problem. Once a common reference frame is determined, presurgical data can be used in guiding robotic tool movements<sup>15,30</sup>, guiding or constraining a surgeon's tool movements<sup>5,16,22,24</sup>, superimposing graphical overlays of internal anatomy upon a surgeon's view of the patient<sup>6</sup>, or guiding the position of radiosurgical equipment<sup>26</sup>.

Current approaches to 3-D registration in medicine require manual specification of corresponding

points in presurgical and intrasurgical data sets.<sup>5</sup> Establishing correspondence is simplified by patient attached fiducial markers, the locations of which can be extracted from both data sets. Recent approaches to 3-D registration attempt to eliminate the need for fiducials and manual specification of correspondences by using features that are intrinsic to the data. For example, researchers have attempted to match intrinsic features such as bounding contours to surfaces,<sup>17</sup> ridge lines to ridge lines,<sup>8</sup> surfaces to surfaces,<sup>12</sup> and discrete points to surfaces.<sup>6,16,22,28</sup>

When the patient anatomy being registered is fixed in space, 3-D registration is performed only once to establish a common reference frame. How

Received original January 15, 1995; accepted February 20, 1995.

Address correspondence/reprint requests to David A. Simon, Robotics Institute, Carnegie Mellon University, Pittsburgh, PA 15213; e-mail address: das@ri.cmu.edu.

©1995 Wiley Liss Inc



ever, a recent trend in medical technology is to reduce the need for invasive and uncomfortable fixturing devices (e.g., stereotactic neurosurgical frames). Without the use of rigid fixation, the relevant anatomy is free to move. Thus, it becomes necessary periodically to register the relevant anatomy. The first part of this paper describes a technique capable of 3-D registration at rates of 5–10 iterations/sec. Although other researchers have addressed this problem<sup>6,31</sup> to our knowledge none has demonstrated subsecond performance without the use of fiducial markers.

We have demonstrated the high speed registration capability by tracking the pose (position and orientation) of human faces. Though we have not yet applied the technique to a clinical problem, we believe that there is great potential for this method in medical applications. Three requirements for the use of this method are: 1) the ability to construct a polygonal mesh representation of the bounding surface of the relevant anatomy from presurgical data; 2) the ability to acquire, at high speed, 3-D data of the bounding surface of the anatomy during surgery; and 3) the ability to determine an approximate pose estimate for initialization. We have demonstrated the technique with a prototype high speed VLSI range sensor developed at Carnegie Mellon University (CMU).<sup>7</sup> As other high speed 3-D sensors capable of intrasurgical use become available (e.g., General Electric's interventional magnetic resonance imager, high speed radiographic imagers, real time range from focus sensors<sup>21</sup>), it should be possible to adapt our technique to such sensors.

The second topic addressed in this paper is the selection and acquisition of intrasurgical data used in 3-D registration. Sensors that have been used for intrasurgical data acquisition include coordinate measuring devices<sup>16,22,25</sup> and radiographic imagers.<sup>17</sup> These sensors vary in the costs associated with the acquisition of new data. Each additional unit of data acquired (i.e., 3-D data point, radiographic view) expends time and, in the case of radiographs, increases the radiation to which the patient is exposed. Therefore, minimizing the amount of intrasurgical data required to perform 3-D registration without sacrificing accuracy of the resulting pose estimate is desirable.

To achieve this goal, we have developed a technique for analyzing the geometric constraint between two data sets. We have demonstrated that there is a strong correlation between this geometric constraint and the accuracy that results from registering the data sets. To generate automatically data sets that result

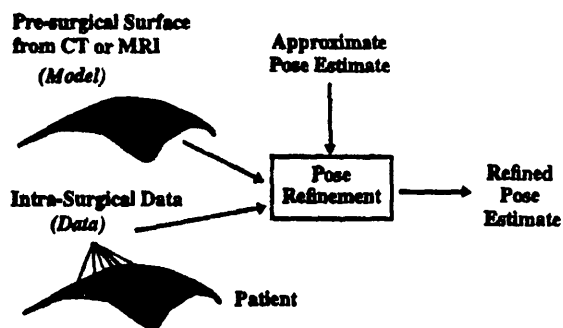


Fig 1 Surface based registration

in good registration accuracy, we have developed a synthesis technique which maximizes a measure of geometric constraint. We have empirically shown that the registration accuracy resulting from synthesized data sets is comparable to that resulting from the best manually selected data.

Recently two research groups have described systems that employ surface-based registration techniques for an orthopedic application. Lavalée et al.<sup>16</sup> and Nolte et al.<sup>22</sup> both describe systems for planning and executing the insertion of screws into the pedicle component of human vertebrae. Both employ registration techniques similar to that described in this paper. In particular, they register 3-D surfaces extracted from presurgical computed tomography (CT) to discrete point data from a coordinate measuring device. In addition, Nolte et al.<sup>22</sup> perform an excellent validation of the errors resulting from registration by comparing their surface based results to ground truth. It is our hope that the data selection technique presented in this paper will ultimately be useful for improving the registration accuracies in applications such as these.

## SURFACE-BASED REGISTRATION

A framework for surface based intrasurgical registration is outlined in Figure 1. The goal is to determine the best possible alignment between a surface extracted from presurgical volumetric data and a set of data collected during surgery. The intrasurgical data considered in the following discussion are discrete 3-D points, such as those collected by a coordinate measuring device or range sensor. The registration technique, however, can easily be generalized to other types of intrasurgical data.

For Figure 1, we assume that an approximate pose estimate is available during surgery via coarse anatomical landmark correspondence. This estimate is used as a starting point in the registration process. Thus, we refer to the mechanism for performing registration as pose refinement.

Most approaches to geometric pose refinement attempt to minimize a least square error metric such as

$$\min_{R, T} \sum_i \|M_i - (RD_i + T)\|^2 \quad (1)$$

where  $D_i$  represent points in the data set,  $M_i$  represent points in the model set, and  $R$  and  $T$  are a rotation and translation, respectively which minimize the expression. In this paper, the  $D_i$  correspond to the discrete 3 D points collected during surgery whereas the  $M_i$  correspond to 3 D points on the presurgical surface.

In fiducial based approaches to registration, the correspondences between the  $D_i$  and  $M_i$  are assumed to be known. Each  $(D_i, M_i)$  pair corresponds to the same fiducial. Given this correspondence there are several techniques for finding  $R$  and  $T$  that minimize the least square error in Equation 1.<sup>9,11</sup>

In approaches to registration without fiducials the  $(D_i, M_i)$  correspondences are unknown a priori. An approach for estimating pose despite these unknown correspondences was introduced in a paper by Besl and McKay.<sup>2</sup> Below is an overview of the iterative closest point (ICP) algorithm presented in that paper.

- 1) For each point  $D_i$  in the data set, compute the closest point (Euclidean distance)  $M_i$  lying on the surface of the model set.
- 2) Using the correspondences from step 1, find  $R$  and  $T$ , which minimize Equation 1 via the method described by Faugeras and Hebert.<sup>3</sup>
- 3) Apply the incremental transformation from step 2 to all points in the data set.
- 4) If the relative changes in  $R$  and  $T$  are less than a threshold,  $\epsilon$ , terminate, else goto 1.

The ICP algorithm works quite well especially when an approximate pose estimate is available for initialization. In general, there is no guarantee that ICP will converge to the global minimum however, we have found convergence to be very good in practice. Techniques exist for finding the global minimum when nonglobal convergence is a problem.<sup>2</sup> When outliers are present in the data (i.e., points in the data set for which there is no correspondence in the model) additional processing may be necessary.<sup>18,32</sup> We have employed outlier detection similar to that described by Zhang<sup>32</sup> for our high speed registration work.

The ICP algorithm has a basic pose refinement capability which we have used in our work on high speed registration as well as in the validation of our intrasurgical data selection techniques. One benefit of the ICP algorithm is that the approach is indepen-

dent of data representation. The only data representation requirement is the ability to calculate the closest points between the two data sets. Thus it should be straightforward to modify our implementation of ICP to handle other data types (e.g., registering bounding contours to surfaces).

### SPEED ENHANCEMENTS TO SURFACE-BASED REGISTRATION

Because of the simplicity of the ICP algorithm, it is well suited to high speed implementation. In particular unlike the case with some other pose refinement methods<sup>10</sup> time-consuming gradient calculations are not required. For this reason, we have been able to use ICP as the core component of a system for pose tracking of arbitrarily shaped 3 D surfaces at rates up to 10 Hz. To perform pose tracking at high speeds several speed enhancements were added to the basic ICP algorithm. Each of these enhancements, kd trees, closest point caching, fast surface point computation and acceleration, are described below.

#### kd-Trees

The most computationally expensive step in the ICP algorithm is finding the closest point sets. In general if there are  $N_D$  points in the data set and  $N_M$  geometric entities (i.e., points, lines, triangles) in the model set, then the complexity of a single closest point query is  $O(N_D N_M)$ . However, as suggested by Besl and McKay<sup>2</sup> and demonstrated by Zhang<sup>32</sup> this complexity can be reduced to  $O(N_D \log N_M)$  by the use of a  $k$ -dimensional binary tree, or simply kd tree.<sup>1</sup> The use of kd trees for closest point computation allows the decision at each node of a binary tree on which side of a hyperplane the closest point will lie. Thus large regions of the search space can be pruned at each level in the search. We have implemented a closest point algorithm based on the kd tree.<sup>4</sup> As demonstrated below, the use of kd trees was the most significant factor in improving the speed of ICP execution.

#### Closest Point Caching

A second small speed improvement was realized by caching closest points. Referring to the model set as  $M$  and the data set as  $D$ , points in  $M$  and  $D$  which are proximal at iteration  $k$ , are highly likely to be proximal at iteration  $k + 1$ . Thus, rather than finding the single closest point in  $M$  for a given point  $D_i[k]$  we can find  $n$  closest points in  $M$  and cache these points together with the point  $D_i[k]$ . There is little overhead involved in finding  $n$  closest points when  $n$  is a small number such as 5. On the next iteration since the point  $D_i[k + 1]$  is likely to be close to the

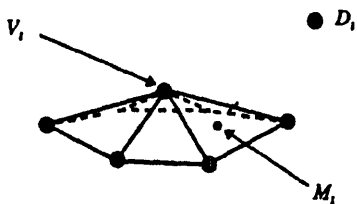


Fig 2 Closest surface point computation

point  $D_i[k]$ , it is also likely that the closest point in  $M$  to  $D_i[k + 1]$  will be one of the points cached on the previous iteration. It is possible to determine conclusively whether the closest point is contained in the cached set by performing a simple test. This test compares the magnitude of the previous incremental transformation to the distance between the closest cached point and the  $n$ th closest cached point (where  $n$  is the number of cached points). A variation on this test can also determine whether the closest point at iteration  $k + 1$  is the same as the closest point at iteration  $k$ . The overall result of caching is that closest points can often be found without requiring a full search of the kd tree. Rather, only the points in the cached set must be tested.

A similar caching technique can be applied to spatially (rather than temporally) adjacent points. If two data points  $D_i[k]$  and  $D_{i+1}[k]$  are spatially proximal, then it is likely that their corresponding closest points  $M_i[k]$  and  $M_{i+1}[k]$  will also be spatially proximal. An analogous caching technique can be applied to this situation, however, we have not yet implemented caching for spatially adjacent points.

### Fast Surface Point Computation

Since the model set is a triangular mesh surface, computation of the point requires an additional step. The output of the kd tree based point algorithm will return the vertex  $V_i$ , which is closest to the data point  $D_i$ , as shown in Figure 2. Given  $V_i$ , the closest model point  $M_i$  will lie within, or on the border of, one of the triangles to which the vertex belongs. (This is not strictly true, insofar as there are pathological cases for which  $M_i$  will lie in a totally different triangle. In our experience, we found that we can ignore such cases.) In order to find  $M_i$ , it is necessary to project  $D_i$  into the planes defined by each of these triangles. The resulting projected points will lie either inside or outside a given triangle. For each triangle, if the projected point lies inside the triangle, call this point  $C_k$ , where  $k$  is the triangle's index. For projected points lying outside the triangle,  $C_k$  is defined as the closest point between the border of the triangle and the projected point. Finally,  $M_i$  is

found as the point  $C_k^*$ , which is closest to the  $D_i$  among all  $C_k$ . In order to perform these computations quickly, once  $D_i$  is projected into each of the planes, all computations are performed in two dimensions (2D) rather than three. Thus, during initialization, each triangle must be stored in both its 2D and its 3D representations.

### Acceleration

A final speed improvement was realized using a modified version of the accelerated ICP algorithm described by Besl and McKay<sup>2</sup>. The accelerated ICP algorithm adds the following step to the basic algorithm (after step 2): 2b) If the incremental transformations ( $R, T$ ) at iterations  $k - 1, k - 2,$  and  $k - 3$  are well aligned, extrapolate the current incremental transformation.

The well aligned condition described above tests that the solution has been moving in an approximately constant direction. Extrapolation is performed by scaling the current incremental transformation. The scale factor is a function of the least square error and the magnitude of the incremental transformations at the previous three iterations.

Besl and McKay<sup>2</sup> calculate a single acceleration scale factor for both translation and rotation. We achieved better results by decoupling the acceleration of translation and rotation. There are two rea-

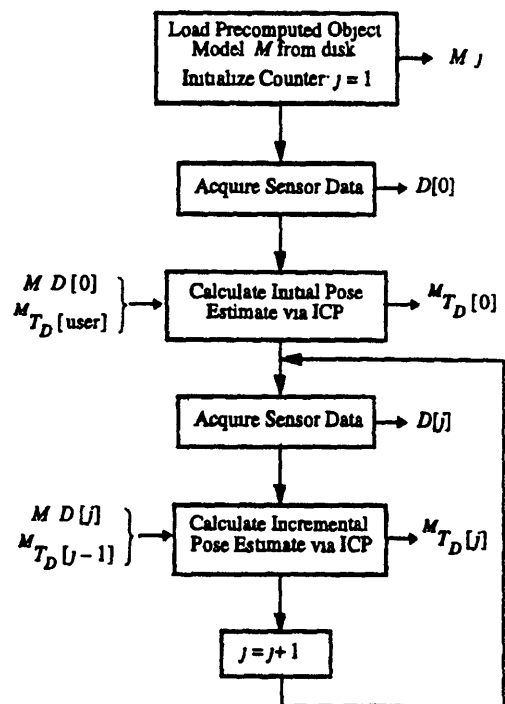


Fig 3 Tracking algorithm

Table 1 Enhancement Comparisons\*

Type	Time	%Time	Iterations	Rot Acc	Trans-Acc
None	908.8	100.0	122	0	0
a	261.2	28.7	35	11	11
kd	62.2	6.8	122	0	0
kd/a	18.0	2.0	35	11	11
kd/a/d	13.1	1.4	25	13	7
kd/a/d/c	11.9	1.3	25	13	7
kd/a/d/c/2d	8.3	0.9	25	13	7

\*Type indicates the enhancements used: none, no speed enhancements; a, coupled acceleration; kd, kd tree based closest point computation; d, decoupled acceleration; c, closest point caching; 2d, fast surface point computation. Time is the total ICP execution time in seconds. %Time is the percentage of time relative to the slowest time. Iterations is the number of ICP iterations. Rot Acc and Trans Acc are the number of iterations for which rotation and translation have been accelerated respectively.

sons for doing this. First, in the Besl and McKay approach, the well aligned condition described above is tested once for both rotation and translation. Thus, for example, if rotation was well aligned but translation was not, no acceleration would be performed. However, an acceleration on rotation alone seems desirable in this situation. A second reason for decoupling is related to the scale factor used in extrapolation. Besl and McKay used the same scale factor to extrapolate both rotation and translation components. This scale factor is designed to extrapolate the solution as much as possible in a single step without overshoot. In the coupled version, the size of the scale factor is governed by the component (translation or rotation) which would cause the solution to overshoot first. The other component could usually be accelerated further. By decoupling translation and rotation, they are independently accelerated as much as possible without overshoot.

### ENHANCEMENT RESULTS

Four speed enhancements have been described: closest point computation via kd trees, closest point caching, fast surface point computation, and decoupled acceleration. The results of applying each of these enhancements to a single registration problem are summarized in Table 1. In this problem,  $D$  was a point set containing 2,432 points and  $M$  was a triangular mesh containing 4,860 facets. The initial pose error was a rotation of roughly  $10^\circ$  about each axis, and a translation of roughly 10% of the object size along each axis. The ICP termination threshold  $\epsilon$  was small. (The magnitude of  $\epsilon$  determines the amount of "fine tuning" performed by the ICP algorithm. Smaller values of  $\epsilon$  result in pose estimates closer to the local minima.)

The speed improvements shown in Table 1 give an idea of the relative utility of each of the described enhancements. The actual relative utility

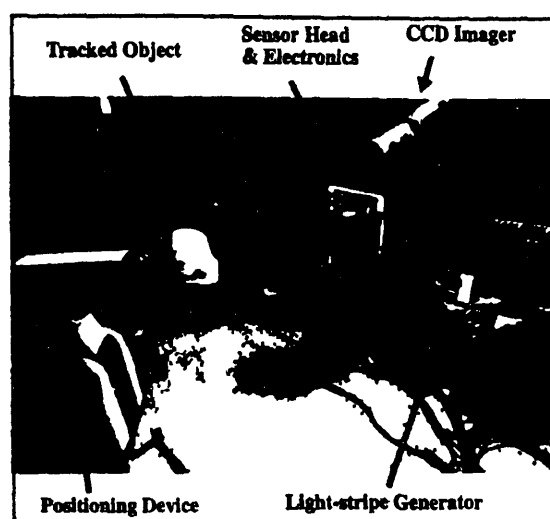


Fig. 4 Pose tracking apparatus

is a function of the underlying data, the initial pose and the termination threshold. Acceleration and kd tree search are always the two most important enhancements. The relative utility of kd tree search increases with the number of points in the data set. Caching is useful when the termination threshold is small, since the number of cache hits will be large during fine tuning.

We believe that additional speed improvements are possible via a multiprocessor implementation of the ICP algorithm. The closest point computation is easily calculated in a parallel manner, and doing so should result in speed improvements roughly proportional to the number of processors. We plan to address this issue in future work.

### THE TRACKING ALGORITHM

An outline of the tracking algorithm is shown in Figure 3. Each box in the diagram represents a processing step, and the processing sequence is indicated by the large headed arrows. Inputs to a processing step are indicated by the quantities to the left of each box, while outputs are indicated by the quantities to the right.

During initialization, a precomputed triangular mesh model  $M$  is loaded into memory and a kd tree is built from  $M$ . After a range image  $D[0]$  is acquired from the sensor, an initial transformation between the model and the initial object pose can be calculated. This transformation,  ${}^M T_D[0]$ , can be found in several seconds using the ICP algorithm with a starting transformation provided by the user. (A fully automated initialization that does not require user input would be possible by applying one of the tech

niques for solving the global pose estimation problem discussed by Besl and McKay<sup>2</sup>) In practice using the face data discussed below, we have found that initial pose errors as large as 15° of rotation about each axis and 50% of the surface size in translation will typically converge to the global minimum Once  ${}^M T_D[0]$  has been calculated, it is used to transform the model to the initial object position Thus, all future pose estimates are measured with respect to this initial starting pose

After initialization the algorithm enters the tracking loop Within the loop data are acquired by the sensor and the object pose is estimated via the ICP algorithm in roughly 0.1–0.3 sec These high speeds are possible for two reasons First, the difference in object position between iterations  $j$  and  $j - 1$  is typically small For example translational velocities of 10 cm/sec and rotational velocities of 20°/sec lead to incremental object pose discrepancies of roughly 2 cm and 4° Thus, since the ICP algorithm uses  ${}^M T_D[j - 1]$  as the starting point when finding  ${}^M T_D[j]$  registration can be performed in a small number of iterations, typically 3–10 Second the resolution of the range data used in our experiments was usually  $16 \times 16$  Thus the number of closest point computations required (256) was significantly less than that required when using the full sensor resolution ( $32 \times 32$ )

During each data acquisition cycle two preprocessing steps are performed on the range data First it is necessary to eliminate noisy data For the CMU VLSI range sensor noisy data are associated with poor reflection from the object of the projected light Thus noisy range data can be eliminated by thresholding reflected intensity values Second, it is necessary to determine which range data points lie on the surface of the object to be tracked Since our experiments were performed in an uncluttered environment range data on the object surface can be distinguished by thresholding the Z component of the range data Although this simple operation works well for our experiments a more sophisticated approach would be required in a cluttered environment

Using  ${}^M T_D[j - 1]$  as the starting point for incremental pose estimation works well when object motion is erratic and unpredictable In some situations, however object motion may be smooth and continuous and thus easier to predict For such motions, improved results are possible using an extrapolation scheme such as a Kalman filter Though we have not implemented a Kalman filter for this purpose we have implemented both first and second order extrapolation Since the extrapolated pose is often closer to the true pose than  ${}^M T_D[j - 1]$ , the cycle time is reduced

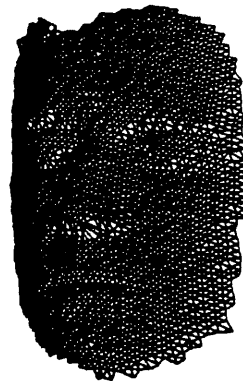


Fig 5 Surface mesh of the first author's face

## TRACKING RESULTS

The primary hardware component of the pose tracker is the CMU high speed VLSI range sensor<sup>7</sup> The sensor consists of two main components, the sensor head and light stripe generator as shown in Figure 4 The current version of this sensor can acquire  $32 \times 32$  cell range images in as little as 1 msec Range data are acquired at 10 bits of resolution and are accurate to 0.1% along the direction of range measurement As currently configured, the sensor workspace is roughly a cube 15 cm on each side

Using a precision positioning device to provide ground truth we characterized the static accuracy of the pose tracker All accuracy tests were performed using the same physical object a small bust of a human face In these tests the average translation error was found to be 0.9 mm (about 1% of the object size) and the average rotation error was 1.4° Until recently, it had not been possible to measure the system's dynamic accuracy, because our positioning device was not capable of generating accurately calibrated dynamic trajectories The recent acquisition of a high speed, fiducial based pose tracker<sup>24</sup> will allow us to characterize dynamic accuracy We have, however, been able to characterize the dynamic repeatability of the tracker Object trajectories with maximum velocities of 100 mm/sec and 22°/sec were reliably tracked with repeatability of roughly 1° in rotation and 1 mm in translation Additional system performance results were given by Simon et al<sup>28</sup>

We have demonstrated the high speed tracker by estimating the pose of real human faces The polygonal mesh surface model of one of these faces is seen in Figure 5 The data in this figure were acquired using a conventional light stripe range finder<sup>25</sup> Although the face tracking demonstrations were not performed under clinical conditions, we plan to evalu

ate our techniques to track the head during neurosurgery

The high speed tracking method we have demonstrated is independent of the particular sensor used to acquire intrasurgical data. The sensor must be able to acquire 3 D data on the surface of the relevant anatomy at rates and densities sufficient for the application. The tracking method is also independent of the particular anatomical region being tracked. The anatomy to be tracked must be rigid and its surface must be visible to the selected sensor during surgery.

This concludes the first part of the paper on high speed pose tracking. The second part of the paper discusses the problem of the selective acquisition of intrasurgical pose refinement data.

#### POSE REFINEMENT DATA SELECTION

In general there is a strong relationship between the accuracy resulting from surface based pose refinement and the quantity of the available intrasurgical data. Large quantities of high quality intrasurgical data tend to result in better accuracy. Unfortunately, there are often high costs associated with the acquisition of large quantities of intrasurgical data. Two such costs are the time needed to acquire the data and the patient's exposure to radiation. Minimizing acquisition time is particularly important because of the high monetary costs of operating room use and the risk of patient infection with increased operating time. The fundamental trade off between data quantity and pose refinement accuracy motivates our work in the selection of intrasurgical data. The goal of this work is to generate and execute a plan for intrasurgical data acquisition to minimize the amount of data acquired while ensuring pose refinement accuracy requirements.

A method for selecting and acquiring intrasurgical data is outlined in Figure 6, the shaded portion which is identical to Figure 1. The first step in the approach is intrasurgical data selection. This step uses the presurgical surface model as input and outputs a set of desired intrasurgical data specified in the reference frame of the presurgical data. The criterion for data selection is the maximization of geometric constraint between presurgical and intrasurgical data.

The next step is selective data acquisition. This step requires as input the desired intrasurgical data and a current estimate of the object's pose. This step acquires the desired data using a sensor of choice. Because of uncertainty in the pose of the patient, it is impossible to collect the desired data precisely (If we could collect this data precisely then we would already know the pose that we are seeking!) Therefore it is necessary to have an estimate of the patient's pose to aid in the acquisition process. Initially an approximate pose estimate is available to guide the acquisition process via coarse anatomical landmark correspondence. After some intrasurgical data have been acquired, an incremental pose refinement can be calculated and fed back to the data acquisition module to aid in the collection of subsequent data. The order of data acquisition can be planned to ensure that the earliest data collected are the least sensitive to precise localization of the patient, and data collected during the later stages require a fairly good estimate of patient pose.

The actual acquisition process could be performed either by a device, such as a robot or manually by a surgeon. When a robot is used, the pose estimate can be fed back directly to the robot's controller. When a surgeon acquires the data manually,

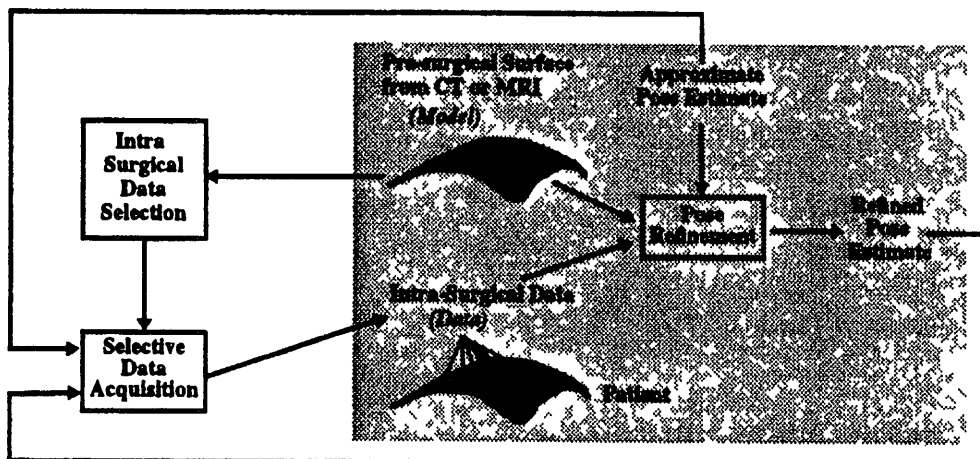


Fig 6 Data selection and acquisition

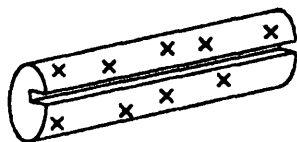


Fig 7 Localization of a slotted cylinder

pose feedback can be in the form of a 3 D graphical display of the relevant anatomy with the desired data overlain on this display While we have not yet used this technique clinically we plan to do so shortly in the area of orthopedic surgery

**GEOMETRIC CONSTRAINT MOTIVATING EXAMPLES**

To gain a better appreciation for the role of geometric constraint in pose refinement, consider the situation in Figure 7 Assume that the goal is to estimate the pose of a slotted cylinder using a coordinate measuring device to collect data on its surface If data were collected only at points indicated by an X it would be impossible to determine orientation about the central axis or translation along it Additional data collected in the disk shaped end regions and within the slot would allow determination of translation and rotation respectively The problem with the data configuration shown in Figure 7 is that there are freedoms in the geometric constraint between the surface of the cylinder and the discrete points shown Such freedoms result in multiple solutions to  $R$  and  $T$  in Equation 1

As a second example of the role of geometric constraint in pose refinement, imagine that we are trying to localize a cube (disregarding the symmetries) using data sampled from each of its faces Figure 8 shows three sampling configurations on a cube C1 has 25 points per face for a total of 150 points, and C2 and C3 have 4 points per face for a total of 24 points If we were to perform pose refinement using each of these sampling configurations assuming noisy data, which one would we expect to result in the best accuracy?

To answer this question, we performed a simple experiment For each sampling configuration, we performed pose refinement 100 times from random initial poses Zero mean gaussian noise was added to each discrete point in the data set Figure 9 shows the resulting pose refinement errors from Equation 1 normalized for the number of points and plotted relative to the error for configuration C1 As might be expected the configuration C1 results in the best pose refinement accuracy This agrees with the intuition that larger quantities of data will result in better

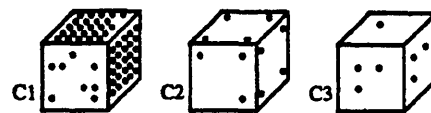


Fig 8 Localization of three cubes

pose refinement accuracies The results for each of the 24 point configurations are less intuitively obvious and an explanation will be delayed until the next section Note that despite the same number of data points configuration C2 clearly provides better accuracy than configuration C3

**GEOMETRIC CONSTRAINT ANALYSIS**

We begin the description of geometric constraint analysis by posing the following question Given a discrete point lying on a surface, how does the distance between the point and the surface vary as the point is perturbed by a small amount about its resting position?

The distance between a point,  $x$  and a surface is defined as the length of the shortest line between the point and the surface In general, there is no closed form analytical expression for this distance given an arbitrary surface however, the following local approximation has been proposed<sup>29</sup>

$$D(x) = \left\| \frac{F(x)}{\nabla F(x)} \right\| \tag{2}$$

where  $F(x) = 0$  is the implicit equation of the surface  $\|\nabla F(x)\|$  is the magnitude of the gradient to the surface,  $x$  is a point that may or may not lie on the surface, and  $D(x)$  is the approximate distance It can be shown that  $D(x)$  is a first order approximation to the true point to surface distance

Assume that there exists a point,  $x$ , which lies on the surface This point can be perturbed with respect

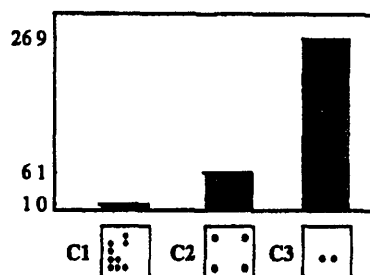


Fig 9 Cube pose refinement errors

to the surface by applying a differential transformation,  $T$ , to the point  $T$  can be represented by a homogeneous transformation which is a function of six parameters  $(t_x, t_y, t_z, \omega_x, \omega_y, \omega_z)$  where  $(\omega_x, \omega_y, \omega_z)$  are rotations about the  $X, Y$  and  $Z$  axes respectively and  $(t_x, t_y, t_z)$  are translations along the newly rotated  $X, Y$  and  $Z$  axes respectively. Define

$$t = [t_x, t_y, t_z, \omega_x, \omega_y, \omega_z]^T \quad (3)$$

as the 6 vector of parameters. As a first step in the analysis consider the gradient of  $D$  with respect to each of the parameters of  $t$ . It can be shown that the resulting 6 vector  $V(x_s)$  is defined as

$$V(x_s) = \frac{\partial}{\partial t} D(T(x_s)) = \begin{bmatrix} n \\ x_s \times n \end{bmatrix} \quad (4)$$

where  $n$  is the unit normal to the surface evaluated at the point  $x_s$ .  $V(x_s)$  relates a small transformation specified by a vector  $dt$  to a corresponding change in distance between the point and the surface. In other words

$$D(T(x_s)) = V^T(x_s) dt \quad (5)$$

Until this point we have considered how the distance between a single point and a surface changes as a function of an arbitrary small rigid transformation. The goal is to analyze the constraint imposed by a collection of points upon the underlying surface. Squaring Equation 5 results in

$$D^2(T(x_s)) = dt^T V(x_s) V^T(x_s) dt = dt^T M(x_s) dt \quad (6)$$

where  $M(x_s)$  is a symmetric positive semidefinite  $6 \times 6$  matrix. Summing the quantity in Equation 6 over points within a region of the surface  $R$  results in the sum of squared distance errors

$$E_R(T(x_s)) = dt^T \left[ \sum_{x_s \in R} M(x_s) \right] dt = dt^T \Psi_R dt \quad (7)$$

where  $\Psi_R$  is the sum of the  $M(x_s)$  matrices evaluated at each point in the region  $R$ . The matrix  $\Psi_R$  is a scatter matrix which contains information about the distribution of the original  $V(x_s)$  vectors over the re-

gion  $R$ . After performing principal component analysis,  $\Psi_R$  is transformed into an expression that is more easily interpreted

$$E_R(T(x_s)) = dt^T Q \Lambda Q^T dt = \sum_{i=1}^6 \lambda_i (dt^T q_i)^2 \quad (8)$$

where  $E_R$  is the least square error over the region  $R$ .  $\Lambda$  is a diagonal  $6 \times 6$  matrix containing the eigenvalues of  $\Psi_R$ .  $Q$  is a  $6 \times 6$  matrix whose columns are the eigenvectors of  $\Psi_R$ .  $\lambda_1 \geq \lambda_2 \geq \lambda_3 \geq \lambda_4 \geq \lambda_5 \geq \lambda_6$  are the eigenvalues of  $\Psi_R$  and  $q_i$  are the corresponding eigenvectors. Each eigenvector  $q_i$  can be interpreted as a differential transformation represented as a 6 vector: the first three elements are the translation components and the last three elements are the rotation components. We should note that this result is similar to one presented by Menq et al.<sup>19</sup>

From Equation 8 it can be seen that the eigenvector  $q_1$ , corresponding to the largest eigenvalue represents the direction of maximum constraint. Perturbing the points in the region  $R$  in the direction of  $q_1$  will result in the largest possible change in  $E_R$  from among all possible directions of perturbation. Similarly the differential transformation represented by the eigenvector  $q_6$  corresponds to the direction of maximum freedom. Perturbing the points in this direction will result in the smallest possible change in  $E_R$  from among all possible directions of perturbation. In general an eigenvalue  $\lambda_i$  is proportional to the rate of change of  $E_R$  induced by a differential transformation in the direction  $q_i$ .

A special situation occurs when some of the  $\lambda_i$  are close to or equal to zero. For each such eigenvalue a singularity exists such that perturbing the points in the direction of the corresponding eigenvector will result in no change in  $E_R$ . Clearly such

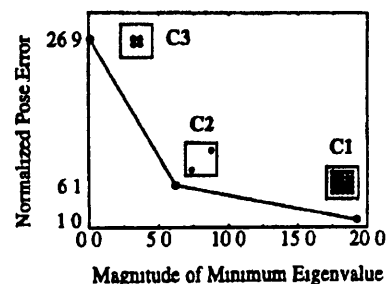


Fig 10 Accuracy vs minimum eigenvalue cube



singularities complicate pose refinement because it becomes impossible to localize the pose in the direction(s) of the singularity. The slotted cylinder example of Figure 7 has two zero eigenvalues, one corresponding to a rotation about the central axis and the other corresponding to a translation along it.

We now have a basis for understanding the pose refinement accuracy results from the cubes of Figure 9. For each of the cube sampling configurations (C1, C2, and C3), we performed the constraint analysis presented above. Figure 10 plots the magnitude of the smallest eigenvalue for each configuration vs the pose refinement errors plotted in Figure 9. The trend from this plot is clear, large magnitudes of the minimum eigenvalue result in better pose refinement accuracies. This agrees with the intuition suggested by Equation 8 for data configurations with small minimal eigenvalues: there are perturbations about the global minimum that result in only small changes in error. For the cubes of Figure 10, a small rotation has a much larger effect on the error in Equation 1 for the points in configuration C2 than for those in configuration C3. This allows the cube to be localized more accurately using the points in configuration C2.

In Figure 10, the magnitude of the minimum eigenvalue can be thought of as a criterion measure that evaluates the 'goodness' of a particular sampling configuration. In general, a variety of possible criterion measures could be used for this purpose. We are currently investigating several such measures including a measure of isotropy proposed by Kim and Khosla<sup>14</sup>

$$6 \frac{\sqrt[6]{\lambda_1 \lambda_2 \lambda_3 \lambda_4 \lambda_5 \lambda_6}}{\lambda_1 + \lambda_2 + \lambda_3 + \lambda_4 + \lambda_5 + \lambda_6} \quad (9)$$

and the following measure suggested by Nahvi<sup>20</sup>

$$\frac{\lambda_6^2}{\lambda_1} \quad (10)$$

A discussion of the implications of criterion measure selection for a related problem can be found in Kim and Khosla<sup>14</sup>

### GEOMETRIC CONSTRAINT SYNTHESIS RESULTS

The constraint analysis method described in the previous section provides a criterion for performing intrasurgical data selection as outlined in Figure 6. The goal of geometric constraint synthesis is to gen-

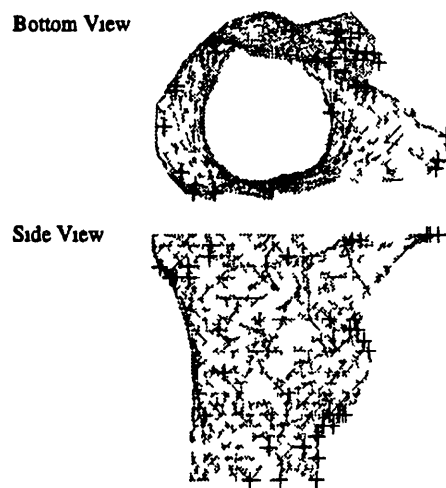


Fig 11 Synthesized data set for femur

erate data configurations for a given surface that maximize the smallest eigenvalue (or other criterion) resulting from constraint analysis. We have developed a technique for performing constraint synthesis for fixed size, discrete point data sets. Although the synthesized data configurations are not provably optimal, we have verified empirically that the resulting pose refinement accuracy is similar to the best data sets generated by local human experts. Since this work is research in progress, the results presented in this section should be viewed as preliminary.

To demonstrate the capabilities of constraint synthesis, we ran the algorithm on a surface model generated from CT images of the proximal end of a human femur. Figure 11 shows a synthesized data set containing 37 points superimposed on the surface model of the femur. Generation time for this set was about 30 min on a Sparc 10 workstation. In order to evaluate the synthesized data set, we compared it to 21 manually selected data sets of the same size. These sets were selected by seven

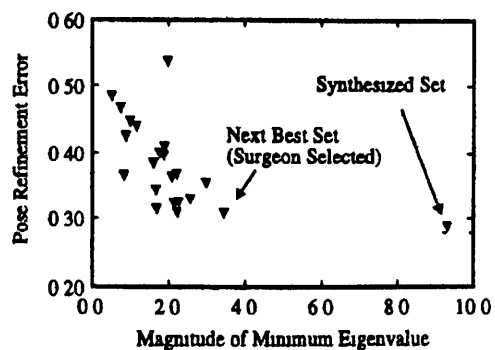


Fig 12 Accuracy vs minimum eigenvalue femur

people including one surgeon with training as an engineer, three experts in 3-D computer vision, and three graduate students in robotics. We performed 1,000 iterations of pose refinement using each of the synthesized data sets. Starting poses were determined randomly with maximum initial pose errors of 30 mm in translation and  $15^\circ$  in rotation. On each iteration, zero mean, gaussian noise with a standard deviation of 1.0 mm was added to each point in the data sets. Figure 12 shows the results of this experiment. The graph shows the magnitude of the minimal eigenvalue from constraint analysis for each of the 22 data sets vs. the pose refinement error of Equation 1 averaged over 1,000 iterations. Each point in the graph represents a different data set.

Several observations should be made from Figure 12. First, the magnitude of the minimum eigenvalue is related to the variance in pose refinement error. Data sets with small minimal eigenvalues may have large pose refinement errors, whereas those with larger minimal eigenvalues all have small errors. This suggests a relation between the magnitude of the minimum eigenvalue for a given data set and an upper bound on the resulting pose refinement error. Second, the data set with the largest minimal eigenvalue and smallest pose refinement error was the one synthesized automatically by our algorithm. The average transformation errors for the synthesized data set are 0.4 mm in translation and  $0.2^\circ$  in rotation. Third, note that calculating the magnitude of the minimal eigenvalue is a very fast operation (roughly 1 ms on a Sparc 10), whereas calculating the average pose refinement error is much slower (about 5 min on a Sparc 10). It is the low cost of calculating the minimal eigenvalue that allows us to synthesize near optimal data sets.

The results presented in Figures 11 and 12 implicitly assume that acquisition of the indicated intrasurgical data is both clinically and technically feasible. In general, certain regions of the underlying structure (e.g., femur) may be inaccessible to intrasurgical data acquisition. Furthermore, diseased or damaged regions of the anatomy may result in inaccurate presurgical and intrasurgical data. For example, it is very difficult to build accurate surface models of an arthritic femoral head from presurgical CT data. Such model inaccuracies will ultimately result in registration errors. To deal with this problem, clinical application of constraint synthesis will require the demarcation of accessible and nondiseased anatomical regions. The synthesis process can then be constrained to generate data that lie within these regions.

We have repeated the experiment described above on a few other surfaces, with similar results. In particular, when synthesizing data points for the cube using 24 discrete points, the technique reliably finds the provably optimal configuration—a distribution similar to configuration C2 with points located as close to the corners as possible. We are currently in the process of a more thorough investigation of the synthesized data sets. In particular, we are performing a series of experiments designed to validate our results using physical (nonsimulated) registration experiments. Using fiducial based registration to provide ground truth, we are investigating the accuracy that results from surface based registration with and without the use of the synthesized 'optimal' data.

The constraint synthesis algorithm finds near optimal configurations for fixed amounts of data; the number of data points is an input to the algorithm. The overall goal of data selection is not only to determine good configurations, but also to minimize the amount of data required. To achieve this goal, we are currently investigating methods for selecting minimally sized data sets. As input, our proposed method uses bounds on the acceptable accuracy and estimates of the uncertainty in the intrasurgical sensor data, the presurgical surface model, and the initial pose. The success of this method will depend on our ability to develop realistic noise models for the sensor and presurgical surface.

Accurate surface based registration relies on the ability to build precise surface models from presurgical data. Although techniques for generating surface models from CT data have been available for several years, the resulting models are typically used for visualization applications in which model accuracy is not crucial. We are currently investigating accuracy issues in surface model generation by analytically comparing generated surface models to a known ground truth.<sup>22</sup> In addition, we are studying the sensitivity of surface based pose refinement to errors in the underlying surface models.

We believe that the methods presented in this part of the paper will become useful tools in the area of intrasurgical pose refinement. Geometric constraint analysis will be useful not only to provide a criterion for data selection, but also to allow the study and evaluation of manually created data sets. Geometric constraint synthesis will be useful for automatically generating near optimal data sets without input from a human expert. In addition to applying constraint synthesis on a per patient basis, it could also be useful to study data generation for entire classes of objects (i.e., all femurs).

## CONCLUSIONS

In this paper we have presented two novel techniques with application to medical robotics and computer assisted surgery. First, we have demonstrated a high speed pose tracking capability with application to intrasurgical use. The technique is independent of the particular sensor used and of the anatomical region to which it is applied. Although this technique has not yet been demonstrated in clinical application we believe that it has significant promise for clinical use. Second we have presented a method for selecting near optimal intrasurgical pose refinement data. The goal of the selection process is to minimize the amount of data acquired for pose refinement while maintaining good accuracy.

There are several directions in which the work is proceeding. With the high speed tracker we are currently working on a multiprocessor implementation that would parallelize the closest point computation. The goal is to increase both the rate at which pose tracking can be performed as well as the amount of data that can be processed at high speeds. We are also investigating an extension to the technique that would allow tracking of articulated objects, such as human hands. Finally, we are planning to evaluate the high speed pose tracker on head tracking for neurosurgery.

In intrasurgical data selection there are several avenues of ongoing work. First intrasurgical data selection currently requires manual specification of data size. We are extending this method to generate minimally sized data sets automatically. Second intrasurgical data selection currently generates discrete point data sets. We are extending the method to generate bounding contours such as those that could be derived from radiographs or CT images. Third in intrasurgical registration it is not always necessary for pose accuracy to be isotropic. Accuracy in certain directions may be more critical than in others. Given such nonisotropic accuracy requirements, we would like to generate data sets that make the best possible use of limited data. Finally we are planning to apply the data selection method to a clinical problem in the area of orthopedic surgery.

## ACKNOWLEDGMENTS

The authors thank Robert O Toole for his insightful comments on this paper. Andy Gruss provided help using the CMU VLSI range sensor. Dr Anthony DiGioria applied his clinical expertise to the selection of discrete point data to which we compared our synthesis results. This work was supported in part by a National Challenge grant from the National Science Foundation (award ECS 9422734).

## REFERENCES

- 1 Bentley JL (1975) Multidimensional binary search trees used for associative searching. *Commun ACM* 18: 509-517
- 2 Besl PJ, McKay ND (1992) A method for registration of 3-D shapes. *IEEE Trans Pattern Anal Machine Intelligence* 14: 239-256
- 3 Faugeras OD, Hebert M (1986) The representation, recognition and locating of 3-D objects. *Int J Robotics Res* 5: 27-52
- 4 Friedman JH, Bentley JL, Finkel RA (1977) An algorithm for finding best matches in logarithmic expected time. *ACM Trans Math Software* 3: 209-226
- 5 Galloway RL, Maciunas RJ (1990) Stereotactic neurosurgery. *Crit Rev Biomed Eng* 18: 181-205
- 6 Grimson WEL, Lozano Perez T, Wells WM, Ettinger GJ, White SJ, Kikinis R (1994) Automated registration for enhanced reality visualization in surgery. *Proceedings of the First International Symposium on Medical Robotics and Computer Assisted Surgery*, pp 82-89
- 7 Gruss A, Tada S, Kanade T (1992) A VLSI smart sensor for fast range imaging. *International Conference on Intelligent Robots and Systems (IROS '92)*, Piscataway NJ: IEEE, pp 349-358
- 8 Gueziec A, Ayache N (1992) Smoothing and matching of 3-D space curves. *Proceedings of the Conference on Visualization in Biomedical Computing*, pp 259-273
- 9 Haralick RM, Joo H (1988) 2D/3D pose estimation. *Proceedings of the Ninth International Conference on Pattern Recognition*, Piscataway NJ: IEEE Computer Society Press, pp 385-391
- 10 Hauser DL, Taylor DL (1990) Optimal alignment of geometric models for comparison. *Proceedings of the First Conference on Visualization in Biomedical Computing*, Los Alamitos, CA: IEEE Computer Society Press, pp 426-431
- 11 Horn BKP (1987) Closed form solution of absolute orientation using unit quaternions. *J Optical Soc Am A* 4: 629-642
- 12 Jiang H, Robb RA, Holton KS (1992) A new approach to 3-D registration of multimodality medical images by surface matching. *Vis Biomed Comput SPIE* 1808: 196-213
- 13 Kendall MG, Stuart A (1977) Canonical variables. In Kendall MG, Stuart A (Eds) *Advanced Theory of Statistics*, 4th ed. London: C Griffin, pp 320-369
- 14 Kim J, Khosla PK (1991) Dexterity measures for design and control of manipulators. *Proceedings of the International Workshop on Intelligent Robots and Systems*, Piscataway NJ: IEEE, pp 758-763
- 15 Kwok YS, Hou J, Jonckheere EA, Hayati S (1988) A robot with improved absolute positioning accuracy for CT guided stereotactic brain surgery. *IEEE Trans Biomed Eng* 35: 153-160
- 16 Lavallee S, Sautot P, Troccaz J, Cinquin P, Merloz P (1994) Computer assisted spine surgery: A technique for accurate transpedicular screw fixation using CT data and a 3-D optical localizer. *Proceedings of the First International Symposium on Medical Robotics and Computer Assisted Surgery*, pp 315-322

- 17 Lavalley S Szeliski R, Brunie L (1991) Matching 3 D smooth surfaces with their 2 D projections using 3 D distance maps SPIE Proceedings Geometric Methods in Computer Vision pp 322-336
- 18 Masuda T Yokoya N (1994) A robust method for registration and segmentation of multiple range images Proceedings of the Second CAD-Based Vision Workshop Piscataway NJ IEEE pp 106-113
- 19 Menq CH Yau HT Lai GY (1992) Automated precision measurement of surface profile in CAD Directed inspection IEEE Trans Robotics Automation 8 268-278
- 20 Nahvi A (1995) Identification and control of the redundant linear drives of two anthropomorphic robots M Eng thesis McGill University
- 21 Nayar SK Watanabe M Noguchi M (1994) Real Time Focus Range Sensor Technical Report CUCS 028 94 New York Department of Computer Science Columbia University
- 22 Nolte LP Zamorano LJ Zhaowei J Wang Q Langlotz F Arm E Visarius H (1994) A novel approach to computer assisted spine surgery Proceedings of the First International Symposium on Medical Robotics and Computer Assisted Surgery pp 323-328
- 23 O Toole RV Simon DA Jaramaz B Ghattas O Blackwell MK Kallivokas L Morgan F Visnic C DiGirola AM Kanade T (1995) Towards more capable and less invasive robotic surgery in orthopaedics Proceedings of the First International Conference on Computer Vision Virtual Reality and Robotics in Medicine New York NY Springer Verlag
- 24 Radermacher K Staudte HW Rau G (1994) Computer assisted orthopedic surgery by means of individual templates—Aspects and analysis of potential applications Proceedings of the First International Symposium on Medical Robotics and Computer Assisted Surgery pp 42-48
- 25 Rohling R, Munger P Hollerbach J Peters T (1994) Comparison of relative accuracy between a mechanical and an optical position tracker for image guided neurosurgery Proceedings of the First International Symposium on Medical Robotics and Computer Assisted Surgery pp 277-282
- 26 Sato K, Inokuchi S (1987) Range imaging system utilizing nematic liquid crystal mask. Proceedings of the ICCV pp 657-661
- 27 Schweikard A Tombropoulos R, Adler JR, Latombe J (1994) Planning for image guided radiosurgery Applications of Computer Vision in Medical Image Processing AAAI pp 96-101
- 28 Simon DA Hebert M Kanade T (1994) Real time 3 D pose estimation using a high speed range sensor Proceedings of IEEE International Conference on Robotics and Automation pp 2235-2241
- 29 Taubin G (1991) Estimation of planar curves surfaces and nonplanar space curves defined by implicit equations with applications to edge and range image segmentation IEEE Trans Pattern Anal Machine Intelligence 13 1115-1138
- 30 Taylor RH Mittelstadt BD Paul HA Hanson W Kazanzides P Zuhars JF Williamson B Musits BL Glassman E Bargar WL (1994) An image directed robotic system for precise orthopaedic surgery IEEE Trans Robotics Automation 10 261-275
- 31 Yamamoto M (1993) Direct estimation of range flow on deformable shape from a video rate range camera IEEE Trans Pattern Anal Machine Intelligence 15 82-89
- 32 Zhang Z (1994) Iterative point matching for registration of free form curves and surfaces Int J Comput Vis 13 119-152

analyses J

s) Biocera  
merica 1988  
tu G Prob-  
behavior in  
d Sawai K  
iyaku Euro-

for surgical  
1988 87 vol  
can Society

te for surgi  
85 88 vol  
can Society

n oxide for  
Document  
phia Amer  
1989  
and Jarcho  
rd hydroxy  
engths and  
aterials J

Engineers  
v 1971

ceedings of  
ioceramics

als Evalua

# Dislocation After Total Hip Arthroplasty

## Causes and Prevention

DONALD E. MCCOLLUM, M.D., AND WILLIAM J. GRAY, M.D.

In this prospective study, a technique of positioning the acetabulum by bony landmarks of the pelvis in the standing position was developed using a standing lateral preoperative roentgenogram with the X ray tube centered over the trochanter. Since 1984, 441 total hip arthroplasties (THAs) were done through the posterior approach with a 1.14% dislocation rate through 1988 and no dislocations in 1989. To prevent impingement and dislocation, it was determined that the safest range for cup position was 30°–50° abduction and 20°–40° flexion from the horizontal. To measure postoperative cup position, a standing true lateral roentgenogram of the operated hip allowed direct measurement of cup flexion and was reproducible within 10°. No special instruments are necessary for this technique, which can be used with any THA system.

Despite many recent advances in total hip arthroplasty (THA), dislocation remains the most common postoperative complication and is second only to loosening as a cause for reoperation. Although most orthopedists agree that dislocation rates decrease with experience, many series still report a dislocation incidence of 3%–5%.<sup>17,19</sup> The factors that are most likely to cause dislocation after THA are surgical approach, restoration of tissue tension, prosthetic design, and orientation of components.

From Duke University Medical Center, Durham, North Carolina.

Presented at the 18th Open Scientific Meeting of the Hip Society, New Orleans, Louisiana, February 11, 1990.

Reprint requests to Donald E. McCollum, M.D., Duke University Medical Center, Box 2919, Durham, NC 27710.

Received April 23, 1990.

### SURGICAL APPROACH

A comparison of THAs as reported in the orthopedic literature revealed a much higher incidence of dislocation in patients who had THAs with a posterolateral approach in the lateral position than in patients who had THAs with anterior and transtrochanteric approaches in the supine position (Table 1).

Many orthopedists believe the advantages of the posterior approach, which include a shorter operating time, diminished blood loss, and decreased morbidity, outweigh the disadvantages of hip dislocation. When THA is done with the patient in the supine position through the anterolateral or the transtrochanteric approach, both anterior superior spines are available for orientation of the acetabulum. In the supine position, lumbar lordosis is decreased and the pelvic flexion is increased. In the postoperative period when the patient sits or stands, pelvic flexion is decreased, the acetabulum becomes more horizontal, and anterior dislocation is less likely to recur. The short external rotators are intact and prevent posterior dislocation. Dislocations after the anterior approach occur in extension and external rotation.

When the patient is placed in the lateral position for a posterolateral THA approach, the lumbar lordotic curve is flattened and the pelvis may be flexed as much as 35°. If the lumbosacral angle in the preoperative standing lateral roentgenogram is compared with the lumbosacral angle on the operating table with the patient in the lateral position, the

TABLE 1 Comparison of THA Approach and Rate of Hip Dislocation

Study	Year	Approach	Dislocation
<b>Supine Position</b>			
McKer <sup>20</sup>	1969	Anterolateral	2.00%
Charnley <sup>3</sup>	1971	Transtrochanteric	0.80%
Eftekhari <sup>7</sup>	1972	Transtrochanteric	0.50%
Pellici <i>et al</i> <sup>25</sup>	1979	Transtrochanteric	0.47%
Woo & Morrey <sup>32</sup>	1982	Anterolateral	2.30%
Vicar & Coleman <sup>31</sup>	1984	Anterior and Transtrochanteric	2.20%
<b>Lateral Position</b>			
Coventry <sup>5</sup>	1974	Transtrochanteric	3.00%
Fackler & Poss <sup>11</sup>	1980	Posterolateral	2.40%
Robinson <i>et al</i> <sup>28</sup>	1980	Posterior	7.50%
Woo & Morrey <sup>32</sup>	1982	Posterior	5.80%
Vicar & Coleman <sup>31</sup>	1984	Posterior	9.50%

pelvis is flexed 30° more relative to the table from the standing position. A series of standing preoperative lateral roentgenograms were compared with intraoperative lateral roentgenograms of the pelvis taken with the patient in the lateral position on the operating table. It was found that the lumbar lordosis decreased from the standing position by as much as 20°–35°. If the prosthetic cup was oriented in 15°–20° flexion to the longitudinal axis of the body, when the patient stood up the postoperative lumbar lordosis was regained, the pelvis extended, and the cup was retroverted as much as 10°–15°. This retroversion, combined with detachment of the short external rotators, tends to promote posterior dislocation when the hip is flexed. In addition, if the prosthetic cup is not flexed sufficiently with the patient in the upright position, impingement of the neck occurs against the anterior rim, levering the head backward out of the cup.

The lateral position not only makes positioning the prosthetic cup in the proper degree of flexion difficult but also causes the degree of abduction of the prosthetic cup to be less accurate. In a series of anteroposterior (AP) pelvic roentgenograms taken with the patient in the lateral position on the operating table, it was found that the superior acetabulum was adducted toward the foot of the table consistently between 10° to 15°. If the

cup was placed in a position of 45° of horizontal abduction to the table with the pelvis in an adducted position, when the patient stood up the cup was abducted an additional 10°–15°, placing it in 55°–60° of abduction, which is an unstable position. Correct abduction of the prosthetic cup was made more difficult because the opposite anterior superior spine was not available for orientation, and the surgeon, assuming that the pelvis was perpendicular to the operating table, must orient the cup in relationship to the table.

#### TISSUE TENSION

Charnley<sup>3</sup> believed that restoration of tissue tension was the most important consideration for preventing dislocation after THA. He routinely advanced the greater trochanter 1 cm to increase tissue tension on the abductor. He also recommended restoring the center of the femoral head to the level of the tip of the trochanter, and even recommended lengthening the extremity 1 cm, if necessary, to restore proper tissue tension. Fackler and Poss<sup>11</sup> found that 75% of their patients with recurrent dislocations had severe medical or neurologic problems that resulted in poor tissue tension. They also found in their series of 1443 THAs that dislocation was two and one-half times as common in patients who were operated upon without a trochanteric

osteotomy  
characteristic  
position the  
tension  
0.4%, with  
reported  
technique  
measure  
pin insert  
the great  
preoper  
this dist  
tension

The ir  
tion is m  
In a ser  
their dis  
THAs a  
Eftekhari  
curred in  
by Evan  
had prev  
dislocati  
loss of co

FIG 1  
sure pre  
mann's p  
a drill bit  
is resecte  
is replac  
trochant  
ing is ad  
the pins

Dislocation

2 00%
0 80%
0 50%
0 47%
2 30%
2 20%
3 00%
2 40%
7 50%
5 80%
9 50%

of horizon-  
 pelvis in an  
 nt stood up  
 al 10°-15°  
 n, which is  
 duction of  
 re difficult  
 erior spine  
 nd the sur-  
 perpendic-  
 orient the

ion of tis  
 t consider  
 fter THA  
 rochanter  
 he abduc  
 oring the  
 vel of the  
 mended  
 necessary  
 ickler and  
 ents with  
 edical or  
 a poor tis  
 r series of  
 two and  
 ents who  
 chanteric

osteotomy The supine position with a trochanteric osteotomy allowed Charnley to position the cup accurately and restore tissue tension, thus reducing his dislocation rate to 0.4%, which is the lowest rate of any series reported. In the present series,<sup>3,9</sup> the two-pin technique was used before head resection to measure the distance between a Steinmann's pin inserted in the ilium and a pin inserted in the greater trochanter (Fig 1). The amount of preoperative shortening was then added to this distance to restore leg length and tissue tension.

The incidence of postoperative hip dislocation is much higher after a previous surgery. In a series reported by Fackler and Poss,<sup>11</sup> their dislocation rate was 5.5% in revision THAs and only 1.8% in primary THAs. In Eftekhar's<sup>7</sup> series, 75% of dislocations occurred in revisions, and in the series reported by Evanski *et al*,<sup>10</sup> 80% of the patients had had previous surgery. The high incidence of dislocation may be due to fibrosis and the loss of contractility of the abductor muscle or

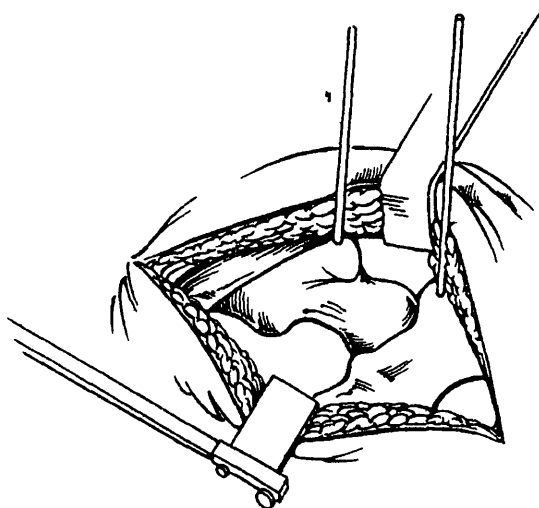


FIG 1 The two-pin technique is used to measure preoperative leg length by placing a Steinmann's pin in the ilium above the acetabulum and a drill bit in the greater trochanter before the head is resected. During the trial reduction the drill bit is replaced in the same drill hole in the greater trochanter. The preoperative amount of shortening is added to the initial measurement between the pins to restore leg length and tissue tension.

to damage to the innervation of these muscles.

### PROSTHETIC DESIGN

Amstutz and Markolf<sup>2</sup> demonstrated that prosthetic design is important in preventing dislocation. They described three modes of dislocation. In the first mode, because of poor tissue tension, the prosthetic head climbs the socket wall and slips over the rim of the socket without the neck impinging on the rim of the socket. They discovered that for this mode of dislocation, the larger head size was more stable since it had farther to travel before it slipped over the rim of the socket (Fig 2). In the second mode, the neck impinges on the socket wall at extremes of flexion, extension, or abduction and levers the head from the socket. They found that the head-to-neck ratio was most important in preventing this type of dislocation. With the cup flexed 20°, comparing the Charnley with a head-to-neck ratio of 1.74, impingement occurred at 80° hip flexion, whereas in the T28 prosthesis with a ratio range from 2.01 to 3.24, impingement did not occur until hip flexion reached 114°. The larger head-to-neck ratio was also more stable in flexion, abduction, and external rotation. The third mode of dislocation was that of impingement of the neck on a bony prominence, which occurs most often in hyperextension when a bony shelf is left behind the acetabular component.

Amstutz and Markolf<sup>2</sup> believed that prosthetic stability was affected by the size of the femoral head, the coverage provided by the socket, and orientation of the components.

### ORIENTATION OF COMPONENTS

Most orthopedists agree that the femoral component should be anteverted 15°-20° as is the anatomic neck of the femur.<sup>6,8,14,22,24,30,32</sup> Increased anteversion beyond this point may result in anterior subluxation of the femoral head when the hip is in extension and external rotation. Retrover-

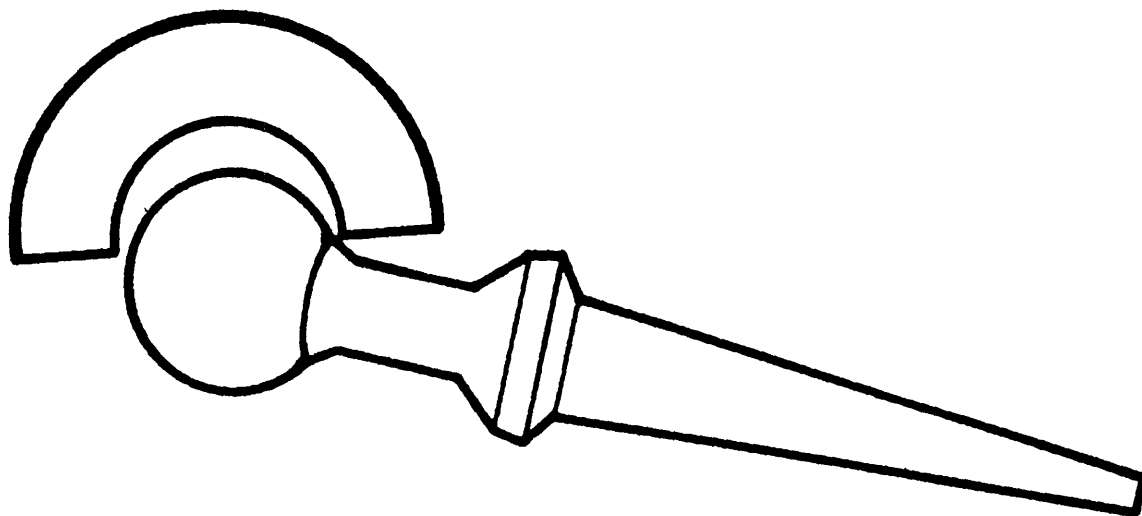


FIG 2 With the cup in the horizontal position, impingement occurs in this diagram at 75° flexion. Note that a smaller head to neck ratio would cause earlier impingement.

sion of the femoral component to 0° or more may cause posterior dislocation when the hip is internally rotated. Orientation of the femoral component is much less complex than orientation of the acetabulum. The femoral component in the normal hip can be oriented to bisect the neck of the femur, and anteversion can be checked easily by comparing the angle of the femoral component to the plane of motion of the knee joint. Orientation of the femoral component is easier to accomplish from the posterior approach than from the anterior approach because the greater and lesser trochanter are more clearly visible.

Orientation of the femoral component is much less critical than orientation of the acetabular component. This is because head coverage by the acetabulum changes very little with internal and external rotation of the femoral prosthesis. It is only with extreme external rotation (anteversion) of the femoral neck that impingement of the femoral neck occurs against the posterior rim of the acetabular component in full extension.

Orientation of the acetabular component is much more complex for the reasons previously mentioned: the pelvis is flexed when the patient lies on the operating table in the lateral position, and the superior bony ac-

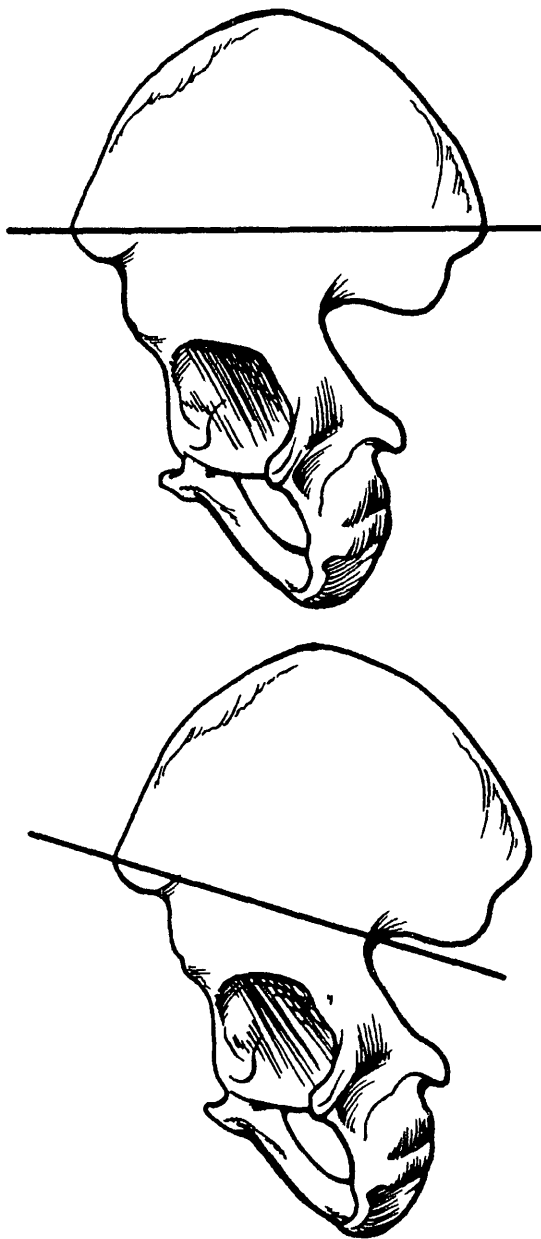
etabulum lies in a position of 15° adduction in relationship to the horizontal plane with the patient in the lateral position. Most of the acetabular positioning guides that are commercially available are designed to place the cup in 30°–45° abduction relative to the horizontal plane and in 15°–20° flexion relative to the long axis of the patient's trunk. Only one type of guide attempts to orient the acetabulum by bony landmarks. The protocol for this guide recommends drawing a line on the drapes between the posterior superior spine and the anterior superior spine, assuming that the line in the standing position is tilted downward from back to front 20° from the horizontal. To that line 35° is added, which should place the acetabulum in a position of 15° flexion relative to the horizontal with the patient in a standing position. This line was measured in 100 preoperative patients by taking a lateral standing roentgenogram. The line between the posterior superior spine and the anterior superior spine varied from -12° to +40°. It was not a reliable bony landmark for positioning the acetabulum (Fig 3).

Sellergren, in Turner and Arnold,<sup>30</sup> recommended that the position of the normal bony acetabulum was the best guide for positioning

FIGS  
line betw  
superior  
+12° (E  
and the  
+40°

the pros  
lum was  
dysplas  
previou  
ported t  
lum wa





FIGS 3A AND 3B (A) In the standing position a line between the posterior superior and anterior superior spine in 100 patients varied from  $-40^{\circ}$  to  $+12^{\circ}$  (B) A line drawn between the sciatic notch and the anterior superior spine ranged from  $0^{\circ}$  to  $+40^{\circ}$

the prosthetic acetabulum if the bony acetabulum was not distorted by osteophytes, was not dysplastic or had not been deformed by previous surgery Nordin and Frankel<sup>24</sup> reported that the position of the normal acetabulum was  $60^{\circ}$  abduction and  $40^{\circ}$  anteversion,

which places the normal bony acetabulum in considerably more abduction and flexion than recommended by most hip surgeons<sup>16</sup> The normal hip is stable with the acetabulum in this position because the femoral head is much larger than the prosthetic femoral head and the supporting capsule has not been disturbed Engh and Bobyn<sup>8</sup> recommended placing the cup in slightly greater anteversion and abduction than the anatomic acetabular rim A thorough search of the literature revealed no biomechanical study that demonstrated the position of the prosthetic acetabulum as the most stable throughout a physiologic range of motion (ROM)<sup>18,21,23,25-29</sup>

#### TECHNIQUE OF CUP POSITIONING

Before 1984, the anterolateral approach described by Muller<sup>22</sup> was used for primary THA Initially, the postoperative dislocation rate was 4.5% Following the anterior approach it was found that the most common cause of dislocation was malposition of the acetabulum, most often in too much flexion or abduction

Using the posterior approach, it was discovered that the position of the pelvis changed from the standing to the lateral recumbent position, to help position the prosthetic acetabulum, each preoperative patient had a standing lateral roentgenogram of the pelvis centered over the greater trochanter (Fig 4) A line was drawn on this roentgenogram between the sciatic notch and the anterior superior spine and its angle from the horizontal was measured In these same 100 patients this line was found to range from  $0^{\circ}$  to  $+40^{\circ}$  Subsequently with the patient in the lateral recumbent position after the incision was made one finger was placed in the sciatic notch and one finger on the anterior superior spine With methylene blue, a line was drawn on the drapes between these two points If this line measured  $20^{\circ}$  on the preoperative standing roentgenogram the cup was flexed so that the face of the cup was parallel to this line on the drapes, thus flexing the cup  $20^{\circ}$  If the line measured  $10^{\circ}$ , one line was drawn



flexion Note

adduction plane with most of the are com- place the o the hori- on relative ank Only at the ace- protocol a line on superior e assum osition is  $20^{\circ}$  from s added, in a posi- orizontal ion This ative pa- entgeno- or supe- pine vari- i reliable acetabu

recom- tal bony sitioning

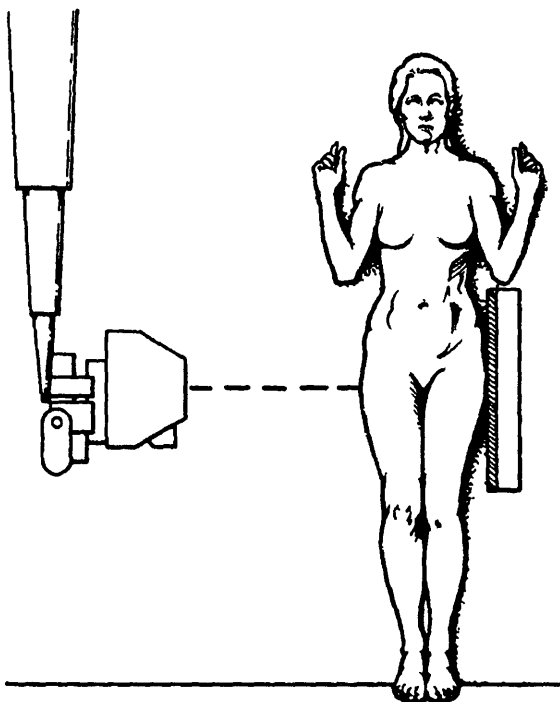


FIG 4 Sketch of how the angle of the line between the sciatic notch and the anterior superior spine is determined for orientation of the acetabulum. A preoperative standing, lateral roentgenogram was made of each patient with the X ray tube centered over the greater trochanter.

between the sciatic notch and anterior spine on the drapes and a second line was drawn and flexed an additional 10°. The cup was oriented to the second line, which would place it in 20° to the horizontal with the patient in the standing position (Fig 5). After a biomechanical study, cup flexion increased to 30°.

In the above technique, the McKee<sup>20</sup> cup positioner was used, which has 30° abduction and neutral flexion. With the short arm of the McKee cup positioner in the vertical position and the short handle aligned with the 20° line on the drapes, the face of the acetabulum should approximate 30° abduction and 20° flexion.

With the advent of the porous-coated acetabulum, the anterolateral approach did not afford an exposure wide enough to insert the prosthetic cup, and insertion of a straight-

stem femoral component was also difficult through this approach. Initially, for porous-coated prostheses, the direct lateral approach described by Hardinge<sup>13</sup> was used. However, it was time consuming, hemorrhage was increased, and postoperative limp was more common. When using the direct lateral approach, the acetabular cup was oriented in flexion by using the line between the posterior superior spine and the anterior superior spine as a reference point and adding 35° to this line (Fig 3). Cup position was not consistent because the line between the posterior spine and the anterior spine varied from -12° to +40°.

In the same 100 patients in whom the line between the posterior superior spine and the anterior spine was evaluated, a more consistent line was looked for that would be easier to observe on the roentgenogram and easier to palpate in the operating room. A line was found between the anterior spine and the sciatic notch in these roentgenograms that ranged from 0° to +40° (Fig 3).

Based on recommendations in the literature and prior success using the anterior approach, the cup was positioned in 30° abduction and 20° flexion, and it was decided to place the prosthetic acetabulum in this position through the posterior approach using the bony landmarks of the sciatic notch and the anterior superior spine.

When the cup was positioned in 20° flexion, impingement was occasionally noticed with the hip flexed to 90° and internally rotated to 90°. To eliminate impingement of the prosthetic neck against the prosthetic cup, flexion was increased to 30°. This position of 45° abduction and 30° flexion allowed flexion of the hip to 90° and internal rotation to 90° without impingement. The hips remained stable in full extension and external rotation with the cup in this position (Fig 5).

When the cup was abducted below 30°, impingement occurred in flexion. When the cup was abducted more than 50°, the head



FIGS notch a horizon flexion acetabu 30° flex short h handle was ins flexion

tended climb ductio (Fig 6 Alth ticed 1) flexion creasin tion A termin cup fle that tl would pingen cup w

also difficult for porous-coated approach. However, a change was made in the approach was more oriented in the posterior superior position, adding 35° to the posterior angle from

from the line and the more consistent and easier. A line was drawn and the diagrams that

the literature anterior approach 30° abduction decided to use this position using the approach and the

in 20° flexion, ly noticed externally rotation of prosthetic. This position and internal rotation and external position

below 30°, When the head

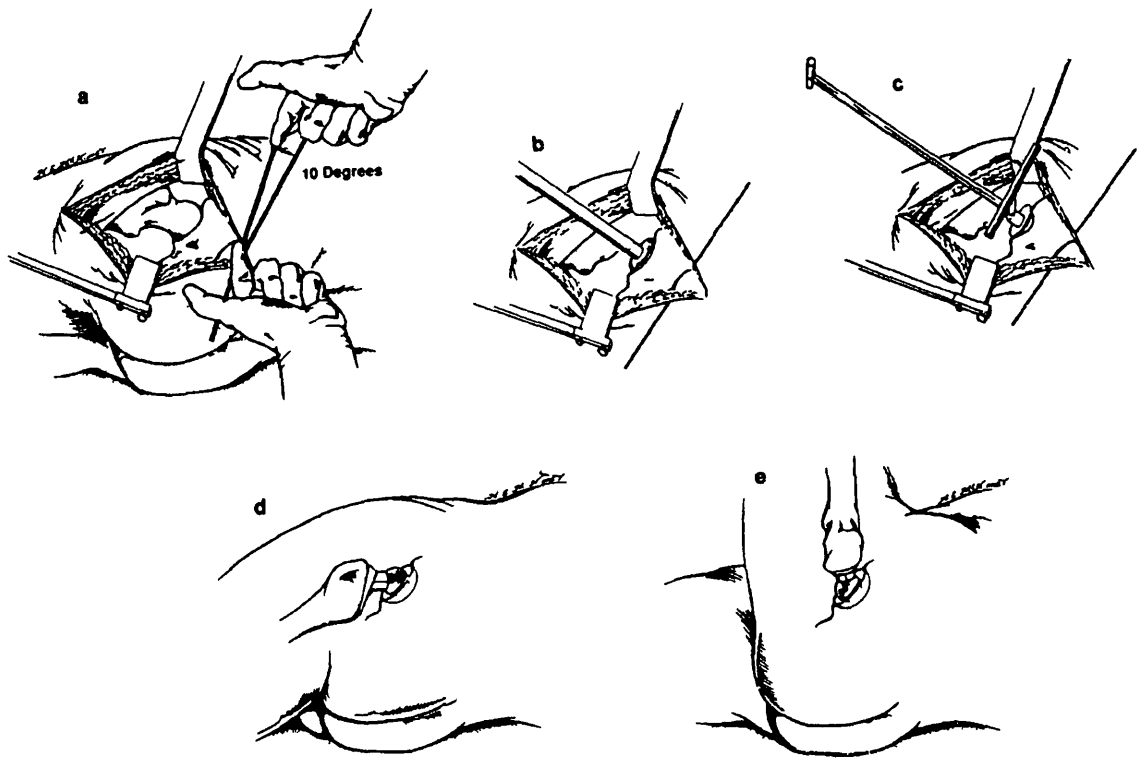


FIG. 5A-5E Sketch of cup positioning (A) With the incision open one finger was placed in the sciatic notch and one finger was placed on the anterior superior spine. If this line measured 20° from the horizontal on the standing preoperative lateral roentgenogram the other line was drawn in 10° more flexion to place the cup at 30° flexion. This line was drawn on the drapes with methylene blue. (B) The acetabulum was reamed with the shaft of the reamer perpendicular to this line and the cup was placed at 30° flexion to the horizontal in the standing position. (C) The McKee<sup>20</sup> cup positioner was used with the short handle in the upright position to place the cup at approximately 30°-40° of abduction. The long handle was perpendicular to the line on the drapes and the short handle was parallel. After the prosthesis was inserted stability was tested with the hip in (D) full extension and external rotation and in (E) full flexion and internal rotation to determine that impingement was not occurring.

tended to sublux out of the acetabulum by 'climbing the wall'. The safe range for abduction of the cup in 30° flexion is 30°-50° (Fig 6)

Although no anterior subluxation was noticed in the operating room with increasing flexion of the cup there was concern that increasing flexion might cause anterior dislocation. A biomechanical study was done to determine the safe range for cup abduction and cup flexion. The results of this study showed that the safe range for cup abduction that would allow physiologic ROM without impingement was 30°-50° abduction when the cup was in 30° flexion. It was also found that

the safe range for cup flexion that would allow physiologic ROM without impingement when the cup was fixed in 30° abduction was 20°-40° (Figs 7 and 8)<sup>15</sup>

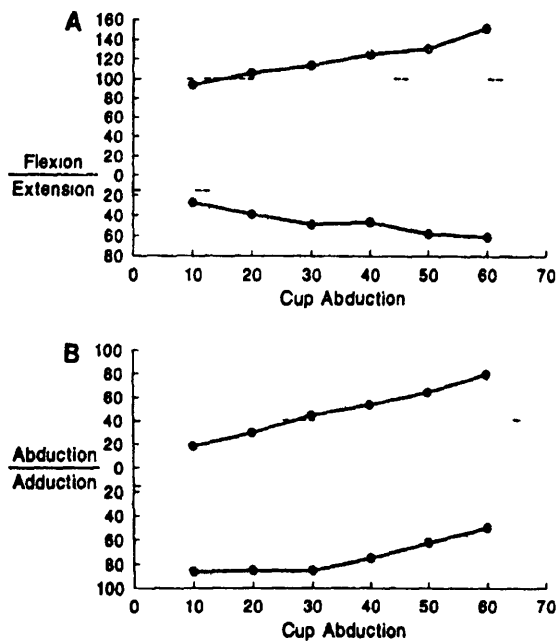
#### POSTOPERATIVE EVALUATION OF CUP POSITION

Many orthopedists have reported that the true lateral or cross-table lateral roentgenogram for measuring flexion of the acetabulum is not accurate.<sup>16,11-14,32</sup> It was found that the position of the cup in the lateral roentgenogram varied with the degree in which the uninvolved hip was flexed. When

the uninvolved hip is flexed beyond a right angle, the pelvis tends to flex making flexion of the cup greater than that present in the standing position. On repeated cross table lateral roentgenograms, a variation of as much as 20° was found in the position of the cup in the same patient on serial roentgenograms. Ackland *et al*'s technique of measuring flexion was satisfactory in the radiolucent cups but was not feasible with metal-backed cups and was cumbersome and time consuming. Abduction of the cup was measured directly on the AP roentgenogram of the pelvis centered over the pubis. Flexion of the cup was measured by taking a true lateral roentgenogram of the postoperative hip with the pa-



FIG 6 A biomechanical study was done measuring the safe range for cup abduction when the cup was fixed in 30° flexion. A similar study was done measuring the safe range for cup flexion with the cup fixed in 30° abduction.



FIGS 7A AND 7B With the acetabulum fixed in 30° flexion the amount of abduction is varied (A) This graph shows the range of flexion and extension in each position until the point of neck to cup impingement (B) This graph shows the range of abduction and adduction until impingement. In these graphs when the cup was abducted above 50° dislocation occurred by climbing the wall. When the cup was abducted less than 30° impingement occurred in flexion and abduction. The safe range for abduction of the cup in 30° flexion was 30°-50°.

tient standing and the uninvolved hip flexed to 90° by resting the foot on a foot rest (Fig 9). In the cross-table lateral roentgenogram of patients who had more than one set of roentgenograms, the roentgenographic variation was as great as 20°. Variation in the standing true lateral roentgenogram was within 10° each time. In the 100 patients who had both cross table and standing true lateral roentgenograms flexion in the standing roentgenogram was 15°-20° greater than in the recumbent roentgenogram (Table 2).

RESULTS

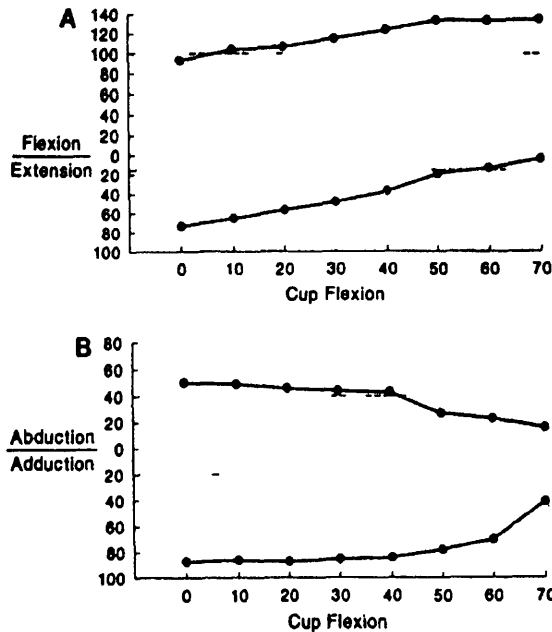
From 1984 to 1989, 441 THAs were performed through the posterior approach using the technique of positioning the cup by bony

A 14  
12  
10  
8  
6  
4  
2  
Flexion  
Extension 2  
4  
6  
E  
1C

B  
Abduction  
Adduction

FIGS 8  
30° abdu  
This gra  
sion in e  
impinge  
abductio  
these gra  
cup fixe  
20° cup  
Above 4  
extensio  
flexion  
20°-40°

landma  
ative la  
searche  
hospita  
return  
recorde  
not ma  
phone  
locatio  
Five  
None o  
postop  
locatio  
there w  
patient  
the tim  
Patie



FIGS 8A AND 8B With the acetabulum fixed in 30° abduction the amount of flexion is varied (A) and extension in each position until the point of neck to cup impingement (B) This graph shows the range of flexion and extension in each position until the point of neck to cup impingement (B) This graph shows the range of abduction and adduction until impingement In these graphs the safe range for cup flexion with the cup fixed in 30° abduction was 20°-40° Below 20° cup flexion impingement occurred in flexion Above 40° cup flexion impingement occurred in extension and abduction The safe range for cup flexion with the cup fixed in 30° abduction was 20°-40°

landmarks with the aid of a standing preoperative lateral roentgenogram Records were searched for any dislocations reported at the hospital, and all patients were questioned on return visits regarding any other dislocations recorded at other facilities Patients who had not made return visits were contacted by telephone and questioned specifically about dislocations

Five patients in this series had dislocations None of the dislocations occurred during the postoperative hospitalization period All dislocations were posterior in direction, and there were extenuating circumstances in each patient, all of whom hyperflexed the hip at the time of dislocation (Table 3)

Patient 1 had a posterior dislocation three

weeks postoperatively while sitting and leaning forward in a recliner chair The Porous Coated Anatomic cup (Howmedica Rutherford, New Jersey) shifted from a position of 30° flexion at the time of surgery to -4° retroversion at the time of his readmission Patient 2 dislocated six months postoperatively when he fell from a sitting position and hyperflexed his hip Patient 3 dislocated posteriorly with hyperflexion and adduction while sitting in the front seat of a car Patient 4 dislocated two weeks postoperatively when she sat on a low seat Patient 5 had avascular necrosis from steroids given for polymyositis Muscle tone was poor He dislocated while sitting on steps and adducted his hip The cup was oriented outside the safe range for abduction After a second dislocation, the cup was revised to a position of 40° abduction and 30° flexion with advancement of the trochanter, after which no further dislocations occurred His was the only hip that required revision The other four were treated with a short single spica cast for six weeks, and no further dislocations occurred

After a biomechanical study indicated that the safe range of flexion of the cup was be-

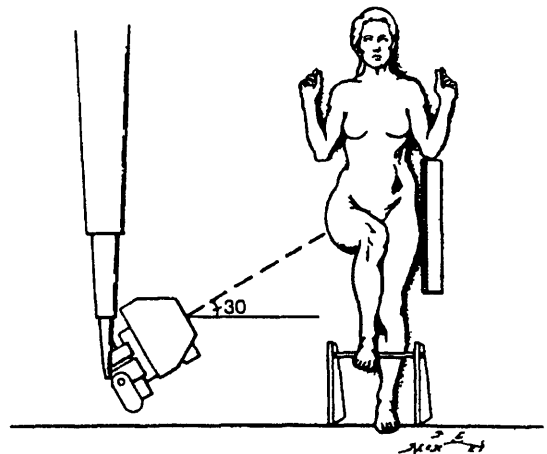


FIG 9 Sketch of postoperative cup flexion evaluated by a standing lateral roentgenogram The patient stands on the operated hip and the uninvolved hip is flexed to 90° The X ray tube is angled upward 30° and the beam is centered on the acetabulum The patient stands against a standard wall mounted Bucky diaphragm

TABLE 2 Postoperative Cup Position in 100 Patients

Position	Degrees	n	Position	Degrees	n
Flexion (max)	50 0°	1	Abduction	55 0°	2
Flexion (min)	20 0°	6	Abduction	30 0°	1
Safe range	20 0°-40 0°	93	Safe range	30 0°-50 0°	97
Mean	30 0°	52	Mean	42 0°	37
SD	5 5°		SD	4 4°	

SD standard deviation

tween 20° and 40°, which allowed physiologic ROM without dislocation, it was decided to increase flexion to 30°. Since that time, of 130 THAs done in 1989, no dislocations have occurred.

## DISCUSSION

Dislocation after THA is painful, prolongs hospital stay, and requires bracing and, frequently, a second operative procedure. The increasing use of porous ingrowth cups makes revision for malposition extremely difficult.

Based on experience with the anterior approach, it is believed that the major cause of dislocation is malposition of the acetabular component. When the patient is in the lateral position, the pelvis is flexed; if the cup is oriented in only 20° flexion to the longitudinal axis of the patient, when the patient stands, the lumbar lordosis recurs, the pelvis is extended, and the acetabulum may well be retroverted in the standing position. The hip dislocates in flexion as the neck impinges on the anterior rim.

Also, it must be remembered that with the patient in the lateral position, the operative side of the pelvis is tilted toward the foot of the table, and the cup should be abducted less than is apparent when the cup is oriented to the horizontal. Otherwise, if the cup is abducted 45° relative to the floor or the table, when the patient stands, abduction will approach 55° to 60°, which approaches an unstable position of abduction for the acetabulum.

Other unpublished data collected by McCollum and coworkers do not support the concept that the stable position for the cup should be 15°-20° flexion. The present study indicates that the most stable range of position for the cup is 30°-50° abduction and 20°-40° flexion. In this position, the hip remains stable while allowing a physiologic ROM. In this safe range, anterior dislocations did not occur, even when the anterior hip capsule was released. When using the posterior approach without a trochanteric osteotomy, no late subluxations or dislocations were noted during a six-year follow-up period.

TABLE 3 Dislocations in 441 Hips, 1984-1989 (1.14%)<sup>a</sup>

Patient	Date of Surgery	Postoperative Dislocation	Cup Position (ABD/FLX)
1	1986	3 weeks	35°/-4 0°
2	1987	6 months	35°/35 0°
3	1987	3 weeks	55°/20 0°
4	1988	2 weeks	50°/20 0°
5	1988	4 months	55°/20 0°

All of these patients had a posterior approach THA in the lateral position.  
ABD abduction FLX flexion

It h  
cup u  
roentg  
in 30°  
closely  
mal be  
of pati  
crepar  
previo  
the ac  
teoph  
*et al*<sup>6</sup>  
the an  
the ac  
line w  
the an  
in line  
tabulu  
has no  
phyte  
overgi  
roentg  
entati  
mal be  
abduc  
prosl  
range  
Wh  
is pro  
attain  
entry  
to ten  
bilizir  
the fr  
crease  
Rev  
this st  
techn  
tabul  
hips I  
plasty  
defor  
entati  
align  
able  
that f  
cated  
of the

n
2
1
97
37

t with the  
operative  
the foot of  
ucted less  
ented to  
up is ab  
the table,  
tion will  
proaches  
r the ace

cted by  
pport the  
the cup  
nt study  
of posi-  
ion and  
e hip re-  
siologic  
disloca  
anterior  
the pos  
costeot  
ocations  
-up pe-

BD/FLX)

0°  
10°  
20°  
30°  
40°

It has been noted that when positioning the cup using the preoperative standing lateral roentgenogram for orientation with the cup in 30° flexion and 45° abduction, it very closely approximates the position of the normal bony acetabulum in approximately 80% of patients. The patients in whom a wide discrepancy was noted were those who had previous surgery, some degree of dysplasia of the acetabulum, or marked overgrowth of osteophytes involving the acetabular rim. Dorr *et al*<sup>6</sup> stated that osteophytes seldom involve the anterior rim of the acetabulum and that the acetabulum can be oriented accurately in line with the old acetabulum by positioning the anterior rim of the prosthetic acetabulum in line with the bony anterior rim of the acetabulum. The anterior rim of the acetabulum has not been found to be devoid of osteophytes, and in the circumstance of marked overgrowth of bone, the standing lateral roentgenogram is necessary for accurate orientation. In addition, abduction of the normal bony acetabulum approximates 60°, and abduction in this alignment will place the prosthetic acetabulum outside the stable range of abduction.<sup>24</sup>

When the cup is malpositioned and the hip is protected for six weeks, stability may be attained by capsular healing. However, Coventry's<sup>4</sup> finding of 0.4% late dislocations five to ten years after surgery suggests that the stabilizing capsule may stretch out in time, and the frequency of late dislocations will increase.

Revision arthroplasty was not included in this study. However, since 1984, the same technique has been used for orienting the acetabular component in previously operated hips. Previous hip surgery such as cup arthroplasty, intertrochanteric osteotomy, or THA deforms the normal acetabulum, making orientation of the prosthetic acetabulum and alignment with the bony acetabulum unreliable. In a study by Fackler and Poss<sup>11</sup> of hips that had had a previous THA, 20.8% dislocated after a second surgery. Eighty percent of the dislocations in Evanski *et al*'s<sup>10</sup> series

had had previous surgery. In the present series of 155 revisions done since 1984 using this technique, eight postoperative dislocations occurred for a dislocation rate of 5.2%. These figures suggest that the high rate of dislocation in other series may be due to malposition of the acetabulum rather than to poor tissue tension. The bony landmarks of the pelvis vary with the individual patient's degree of lumbar lordosis, and a preoperative standing roentgenogram is helpful to detect this variation from the mean. Accurate positioning of the cup by these bony landmarks at the time of surgery is crucial in preventing postoperative dislocation. The standing true lateral roentgenogram is helpful in measuring the true degree of flexion of the metal-backed prosthetic cup. Accurate evaluation of cup position is necessary to identify the patient at risk for early or late dislocation.

#### REFERENCES

- 1 Acklind M, Bourne W, and Uthoff H. Anteversion of the acetabular cup. Measurement of angle after total hip replacement. *J Bone Joint Surg* 68B:409, 1986.
- 2 Amstutz H C and Markolf K L. Design features in total hip replacement. In Harris W H (ed) *Proceedings of the Second Open Scientific Meeting of the Hip Society*. New York: C V Mosby, 1974.
- 3 Charnley J. *Low Friction Arthroplasty of the Hip: Theory and Practice*. Berlin: Springer, 1979.
- 4 Coventry M B. Late dislocations in patients with Charnley total hip arthroplasty. *J Bone Joint Surg* 67A:832, 1985.
- 5 Coventry M B, Beckenbaugh R D, Nolan D R, and Ilstrup D. 2012 total hip arthroplasties: A study of postoperative and early complications. *J Bone Joint Surg* 56A:273, 1974.
- 6 Dorr L D, Wolf A W, Chandler R, and Conaty J P. Classification and treatment of dislocations of total hip arthroplasty. *Clin Orthop* 173:151, 1983.
- 7 Eftekhari N S. Dislocation and instability complicating low friction arthroplasty of the hip joint. *Clin Orthop* 121:120, 1976.
- 8 Engh C A and Bobyn J D. *Biological Fixation in Total Hip Arthroplasty*. Thorofare, New Jersey: Slack, 1985.
- 9 Etienne A, Cupic Z, and Charnley J. Postoperative dislocation after Charnley low friction arthroplasty. *Clin Orthop* 132:19, 1978.
- 10 Evanski P M, Waugh T R, and Orofino C F. Total hip replacement with the Charnley prosthesis. *Clin Orthop* 95:69, 1972.
- 11 Fackler C D and Poss R. Dislocation in total hip arthroplasties. *Clin Orthop* 151:169, 1980.

- 12 Goergen T G and Resnick D Evaluation of acetabular anteversion following total hip arthroplasty. Necessity of proper centering. *Br J Radiol* 48:259 1975
- 13 Hardinge K The direct lateral approach to the hip. *J Bone Joint Surg* 64B:17 1982
- 14 Herrlin K, Selvik G and Pettersson H Space orientation of total hip prosthesis. *Acta Radiologica* 27:619 1986
- 15 Herrlin K, Selvik G, Pettersson H, Kesek P, Onnerfalt R and Ohlin A Position orientation and component interaction in dislocation of the total hip prosthesis. *Acta Radiologica* 29:441 1981
- 16 Johnston R C and Smidt, G L Hip motion measurements for selected activities of daily living. *Clin Orthop* 72:205 1970
- 17 Khan A, Brakenbury P and Reynolds I Dislocation following total hip replacement. *J Bone Joint Surg* 63B:214 1981
- 18 Lewinnek G, Lewis J, Tarr R, Compere C and Zimmerman J Dislocations after total hip replacement arthroplasties. *J Bone Joint Surg* 60A:217 1978
- 19 Lindberg H, Carlsson A, Gentz C and Pettersson H Recurrent and non recurrent dislocation following total hip arthroplasty. *Acta Orthop Scand* 53:947 1982
- 20 McKee G K Total prosthetic replacement for advanced coxarthrosis. In: *Proceedings of the SICOT Meeting Tenth International Congress of Orthopedics and Traumatology Paris 1967*
- 21 McLaren R H Prosthetic hip angulation. *Radiology* 107:705 1973
- 22 Müller M E Total hip prostheses. *Clin Orthop* 72:46 1970
- 23 Nolan D R, Fitzgerald R H and Beckenbaugh R D Complications of total hip arthroplasty treated by reoperation. *J Bone Joint Surg* 57A:977 1975
- 24 Nordin M and Frankel B H *Basic Biomechanics of the Musculoskeletal System* ed 2 Philadelphia: Lea & Febiger 1989
- 25 Pellici P M, Salvati E A, and Robinson A J Mechanical failures in total hip replacement requiring reoperation. *J Bone Joint Surg* 61A:28, 1979
- 26 Pettersson H, Gentz, C, Lindberg, H and Carlsson A Radiologic evaluation of the position of the acetabular component of the total hip prosthesis. *Acta Radiologica* 23:259 1982
- 27 Ritter M A Dislocation and subluxation of the total hip replacement. *Clin Orthop* 121:92 1976
- 28 Robinson R P, Robinson H J Jr and Salvati E A Comparison of the transtrochanteric and posterior approaches for total hip replacement. *Clin Orthop* 147:143 1980
- 29 Seradge H, Nagle K R and Miller R J Analysis of version in the acetabular cup. *Clin Orthop* 166:152 1982
- 30 Turner R H and Arnold D *Revision Total Hip Arthroplasty* New York: Grune & Stratton 1982
- 31 Vicar A J and Coleman C R A comparison of the anterolateral transtrochanteric and posterior surgical approaches in primary total hip arthroplasty. *Clin Orthop* 188:152 1984
- 32 Woo R and Morrey B Dislocations after total hip arthroplasty. *J Bone Joint Surg* 64A:1295 1982

C

SAM

Surgic  
have be  
resultu  
losis I  
ated by  
abrasiv  
bone lo  
presum  
tulate  
erally b  
ine the  
out th  
compre  
less hi  
Ti-6Al  
molecu  
Specim  
pseudo  
artical  
knees  
technic  
electro  
plants  
surrou  
year sl  
tive of  
noviur

From  
Health  
materna  
Univers  
Prese  
Hip So  
1990  
Recip  
Repri  
den Av  
Recei



Real-time 3-D Pose Estimation  
Using a High-Speed Range Sensor

David A. Simon, Martial Hebert and Takeo Kanade

CMU-RI-TR-93-24

Robotics Institute  
Carnegie Mellon University  
Pittsburgh, Pennsylvania 15213

November 1993

© 1993 Carnegie Mellon University

## Table of Contents

1 0	Introduction	1
2 0	Registration	2
2 1	The ICP Algorithm	2
2 2	Speed Enhancements to ICP	4
2 2 1	Kd trees	4
2 2 2	Closest Point Caching	4
2 2 3	Closest Surface Point Computation	4
2 2 4	Acceleration	5
2 2 5	Enhancement Results	5
3 0	The Tracking Algorithm	6
4 0	Experimental Setup	8
5 0	Pose Estimation Results	9
5 1	Static Accuracy Results	10
5 2	Dynamic Tracking Results	12
6 0	Conclusions	12

## Abstract

This report describes a system which can perform full 3-D pose estimation of a single arbitrarily shaped, rigid object at rates up to 10Hz. A triangular mesh model of the object to be tracked is generated offline using conventional range sensors. Real-time range data of the object is sensed by the CMU high speed VLSI range sensor. Pose estimation is performed by registering the real-time range data to the triangular mesh model using an enhanced implementation of the Iterative Closest Point (ICP) Algorithm introduced by Besl and McKay. The method does not require explicit feature extraction or specification of correspondence. Pose estimation accuracies on the order of 1mm in translation and 1 degree in rotation have been measured.

## 1.0 Introduction

The problem of determining the 3-D pose of a rigid object at high speed has been approached by a number of researchers [10][12]. However, there are few systems capable of full 3-D pose estimation of arbitrarily shaped objects in real-time. There are three reasons why this goal has been difficult to attain. First, the 2-D data provided by conventional video cameras lacks the sensitivity required for *accurate* 3-D pose estimation of arbitrarily shaped objects. Second, many approaches to 3-D pose estimation require two operations which are difficult to perform: feature extraction and correspondence specification. Third, in order to perform 3-D pose estimation in real-time, each step in the underlying algorithm must be computationally efficient.

Direct use of 3-D data simplifies the pose estimation problem by providing shape structure which would otherwise need to be inferred from 2-D data. As noted in [12], while 2-D data is useful for estimating object motion in planes normal to a camera's optical axis, it is less sensitive to motions which deviate from these planes. Direct use of 3-D data should provide more precise object pose estimates, especially for general 3-D motions.

Many previous approaches to 3-D pose estimation are feature based [8][10][12]. Such approaches, however, suffer from some common difficulties. Typically, the steps in feature based pose estimation are: 1) extract features such as points or lines from the underlying data, 2) specify correspondence between data and model features, 3) compute the pose estimate from the derived correspondence. Unfortunately, the extraction of reliable features from images of real-world objects is difficult. Even when such features can be found, solution of the correspondence problem can be complex and computationally expensive.

In our approach, raw range data points which lie on the surface of the tracked object are matched to the underlying object surface model using an iterative least squares technique (the ICP algorithm). This approach eliminates the need to perform any feature extraction, or to specify feature correspondence.

To our knowledge, no previous approaches have succeeded in combining both high speed acquisition of 3-D data with high speed 3-D pose computation. Several researchers have utilized range data in the 3-D pose estimation problem [8][13]. Yamamoto [13] discusses a system for estimating the shape and pose of deformable objects using a video rate range camera, but the required computations are not performed at high speed.

The remainder of this paper is organized as follows. Section 2.0 describes the Iterative Closest Point algorithm and enhancements which allow it to be used for real-time pose estimation. Section 3.0 outlines the algorithm for real-time pose estimation. Section 4.0 describes the experimental setup used to demonstrate the approach. Section 5.0 contains experimental results, and Section 6.0 contains the conclusion.

## 2.0 Registration

The registration algorithm used in this system is strongly motivated by the work of Besl and McKay [2]. Their paper describes a general purpose method for the registration of rigid 3-D shapes which they refer to as the Iterative Closest Point algorithm. Zhang [14] has independently developed a similar algorithm which is better at handling outliers and occlusions in the data. Since these were not a major concern in our work, the formulation presented below parallels that of Besl and McKay.

### 2.1 The ICP Algorithm

Suppose that we have two independently derived sets of 3-D points which correspond to a single shape. We will call one of these sets the *model* set  $M$ , and the other the *data* set  $D$ . Assume that for each point in the data set, the corresponding point in the model set is known. The problem is to find a 3-D transformation which when applied to the data set  $D$ , minimizes a distance measure between the two point sets. The goal of this problem can be stated more formally as follows:

$$\min_{R, T} \sum_i \|M_i - (RD_i + T)\|^2 \quad (1)$$

where  $R$  is a 3x3 rotation matrix,  $T$  is a 3x1 translation vector, and the subscript  $i$  refers to corresponding elements of the sets  $M$  and  $D$  as shown in Figure 1. Efficient, non-iterative solutions to this problem, both employing unit quaternions, were presented in two papers, one by Faugeras and Hebert [4] and the other by Horn [7].

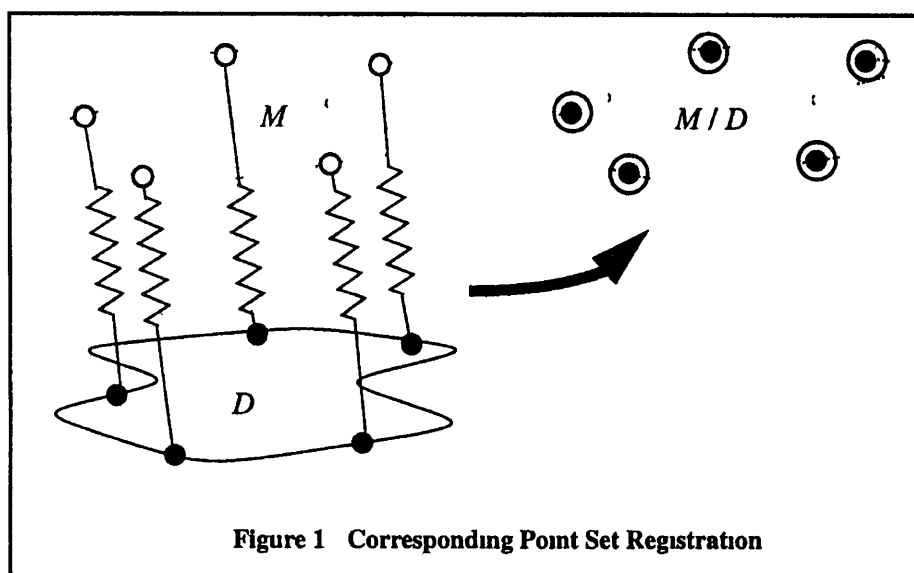


Figure 1 Corresponding Point Set Registration

The general 3-D shape registration problem that we address here, however, differs from the corresponding point set registration problem in two important regards. First, the point correspondence which was assumed to be known in the above problem is unknown in the general

case Second, general 3-D shapes to be registered are not necessarily represented as point sets [2]

Suppose that we are again given two sets  $M$  and  $D$  corresponding to a single shape, where  $D$  is a set of 3-D points and  $M$  is a triangular faceted surface. Assume that the correspondence between points in the two sets is initially unknown. As seen in Figure 2, for each point  $D_i$  from the set  $D$ , there exists at least one point on the surface of  $M$  which is closer to  $D_i$  than all other points in  $M$ . This is the *closest point*,  $M_i$ .

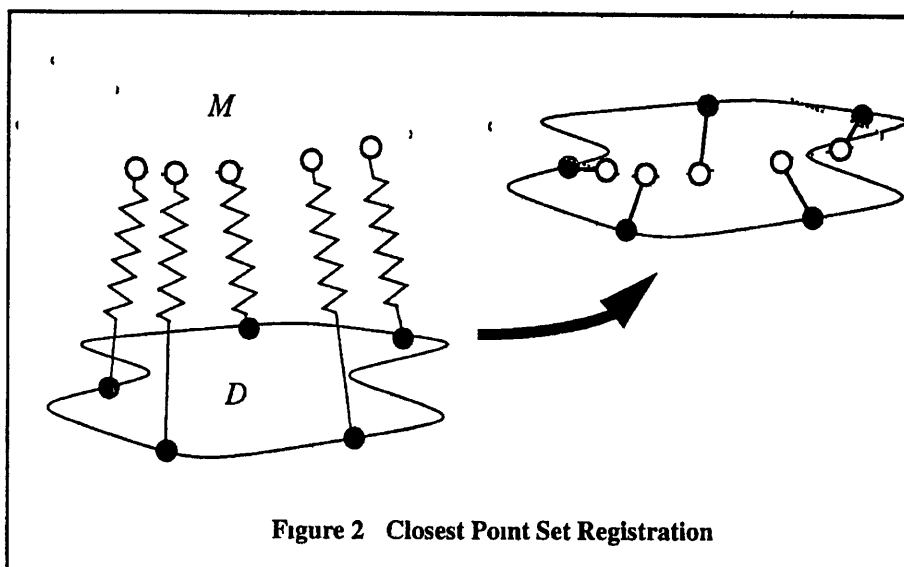


Figure 2 Closest Point Set Registration

The basic idea behind the ICP algorithm is that under certain conditions the point correspondence provided by sets of closest points is a reasonable approximation to the true point correspondence. Besl and McKay proved that if the process of finding closest point sets and then solving equation (1) is repeated, the solution is guaranteed to converge to a *local* minimum. The ICP algorithm can now be stated

- 1 For each point in  $D$ , compute the closest point in  $M$
- 2 With the correspondence from step 1, compute the incremental transformation  $(R, T)$  [equation (1)]
- 3 Apply the incremental transformation from step 2 to the data  $D$
- 4 Compute the change in total mean square error. If the change in error is less than a threshold,  $\epsilon$ , terminate. Else goto step 1

While the ICP algorithm is only guaranteed to converge to a local minima, there is no guarantee that this local minima will correspond to the actual global minima. How well the algorithm performs is a function of the initial pose estimate and the characteristics of the shape being registered. Besl and McKay discuss in detail the problem of finding the global minimum in situations where initial pose error is large. We have found that the ICP algorithm converges to the global minimum even with fairly large initial pose discrepancies. For the purposes of the system described in this paper, the initial pose discrepancies are usually small.

## 2.2 Speed Enhancements to ICP

A basic implementation of the ICP algorithm lacks the speed required to perform pose estimation in real-time. We have implemented several enhancements: kd-trees, closest point caching, efficient point to surface computation, and acceleration.

### 2.2.1 Kd-trees

The most computationally expensive step in the ICP algorithm is finding the closest point sets. In general, if there are  $N_D$  points in the data set and  $N_M$  geometric entities (i.e. points, lines, triangles) in the model set, then the complexity of the closest point computation is  $O(N_D N_M)$ . However, as suggested in [2] and demonstrated in [14], this complexity can be reduced to  $O(N_D \log N_M)$  by the use of a k-dimensional binary tree, or simply kd-tree [1]. The use of kd-trees for closest point computation allows us at each node of a binary tree to decide which side of a hyperplane the closest point will lie on. Thus, large regions of the search space can be pruned at each level in the search. We have implemented a closest point algorithm based on the kd-tree [5]. We have found that the actual performance improvement approaches that predicted by theory.

### 2.2.2 Closest Point Caching

A second small speed improvement was realized by caching closest points. Points in the sets  $M$  and  $D$  which are proximal at time  $k$  are highly likely to be proximal at time  $k+1$ . Thus, rather than finding the single closest point in  $M$  for a given point  $D_i[k]$ , we can find  $n$  closest points in  $M$  and cache these points together with the point  $D_i[k]$ . Note that there is little overhead involved in finding  $n$  closest points when  $n$  is a small number like 5. On the next iteration, since the point  $D_i[k+1]$  is likely to be close to the point  $D_i[k]$ , it is also likely that the closest point in  $M$  to  $D_i[k+1]$  will be one of the points cached on the previous iteration. It is possible to determine conclusively whether the closest point is contained in the cached set by performing a simple test. This test compares the magnitude of the previous incremental transformation to the distance between the closest cached point and the  $n$ th closest cached point (where  $n$  is the number of cached points). A variation on this test can also determine whether the closest point at time  $k+1$  is the *same* as the closest point at time  $k$ . The overall result of caching is that closest points can often be found without requiring a full search of the kd-tree. Rather, only the points in the cached set must be tested.

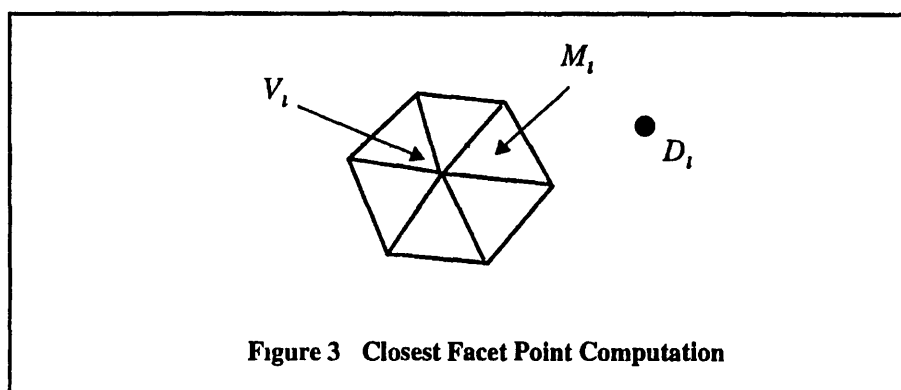
A similar caching technique can be applied to *spatially* (rather than *temporally*) adjacent points. If two data points  $D_i[k]$  and  $D_{i+1}[k]$  are proximal, then it is likely that their corresponding closest points  $M_i[k]$  and  $M_{i+1}[k]$  will also be proximal. An analogous caching technique can be applied for this situation, however we have not yet implemented caching for spatially adjacent points.

### 2.2.3 Closest Surface Point Computation

When  $M$  is a triangular faceted surface, computation of the closest point requires an additional step. The output of the kd-tree based closest point algorithm will return the closest *vertex*  $V_i$  on the surface of  $M$ , as shown in Figure 3. Given  $V_i$ , the closest point  $M_i$  will lie within, or on the border of, one of the triangles to which the vertex belongs<sup>1</sup>. In order to find  $M_i$ ,  $D_i$  is

<sup>1</sup> This is not strictly true as there are pathological cases for which  $M_i$  will lie in a totally different triangle. In our experience, we found that we can ignore such cases.

projected into the plane of each triangle, and the closest point between  $D_i$  and that triangle is computed. This is repeated for all triangles containing  $V_i$ , and the overall closest point is selected. In order to perform these computations quickly, once  $D_i$  is projected into the plane, all computations are performed in 2-D rather than 3-D. Thus, during initialization each must triangle be saved in both its 2-D and 3-D representations.



#### 2.2.4 Acceleration

A final speed improvement was realized using a modified version of the *accelerated* ICP algorithm described in [2]. The accelerated ICP algorithm adds the following step to the basic algorithm (after step 2)

- 2b) If the incremental transformations ( $R$ ,  $T$ ) at times  $k-1$ ,  $k-2$ , and  $k-3$  are *well aligned*, extrapolate the current incremental transformation.

The well aligned condition above tests that the solution has been moving in an approximately constant direction. Extrapolation is performed by scaling the current incremental transformation. The scale factor is a function of the mean square error and the magnitude of the incremental transformations at the previous three iterations.

Besl and McKay calculate a single acceleration scale factor for both translation and rotation. We achieved better results by decoupling the acceleration of translation and rotation. There are two reasons for doing this. First, in Besl's approach, the well aligned condition above is tested once for both rotation and translation. Thus, for example, if rotation was well aligned but translation was not, no acceleration would be performed. However, an acceleration on rotation alone seems desirable in this situation. A second reason for decoupling is related to the scale factor used in extrapolation. Besl and McKay used the same scale factor to extrapolate both rotation and translation components. This scale factor is designed to extrapolate the solution as much as possible in a single step without overshoot. In the coupled version, the size of the scale factor is governed by the component (translation or rotation) which would cause the solution to overshoot first. The other component could usually be accelerated further. By decoupling, translation and rotation are independently accelerated as much as possible without overshoot.

#### 2.2.5 Enhancement Results

Four speed enhancements were described in this section: closest point computation via kd-trees, closest point caching, efficient computation of closest facet points, and decoupled acceleration. The results of applying each of these enhancements to a single registration problem are summarized in Table 1. In this problem,  $D$  was a point set containing 2432 points and



$M$  was a triangular mesh containing 4860 facets. The initial pose error was roughly 10 degrees of rotation about each axis, and about 10% of object size in each translation. The ICP termination threshold,  $\epsilon$ , was small<sup>1</sup>

Type	Time	%T	Iter	R-Acc	T-Acc
none	908.8	100.0	122	0	0
a	261.2	28.7	35	11	11
kd	62.2	6.8	122	0	0
kd/a	18.0	2.0	35	11	11
kd/a/d	13.1	1.4	25	13	7
kd/a/d/c	11.9	1.3	25	13	7
kd/a/d/c/2d	8.3	0.9	25	13	7

**Table 1 Enhancement Comparisons**

In the table, *Type* indicates the enhancements used: a - coupled acceleration, kd - kd-tree search, d - decoupled acceleration, c - closest point caching, 2d - 2d calculation of closest facet points. *Time* is the total ICP execution time in seconds. *%T* is percentage of time relative to the slowest time. *Iter* is the number of ICP iterations. *R-Acc* and *T-Acc* are the number of accelerations for rotation and translation respectively.

The speed improvements shown in Table 1 give an idea of the relative utility of each of the described enhancements. The actual relative utility is a function of the underlying data, the initial pose, and the termination threshold. Acceleration and kd-tree search are always the two most important enhancements. The relative utility of kd-tree search increases with the number of points in the data set. Caching is useful when the termination threshold is small, since the number of cache hits will be large during fine-tuning.

### 3.0 The Tracking Algorithm

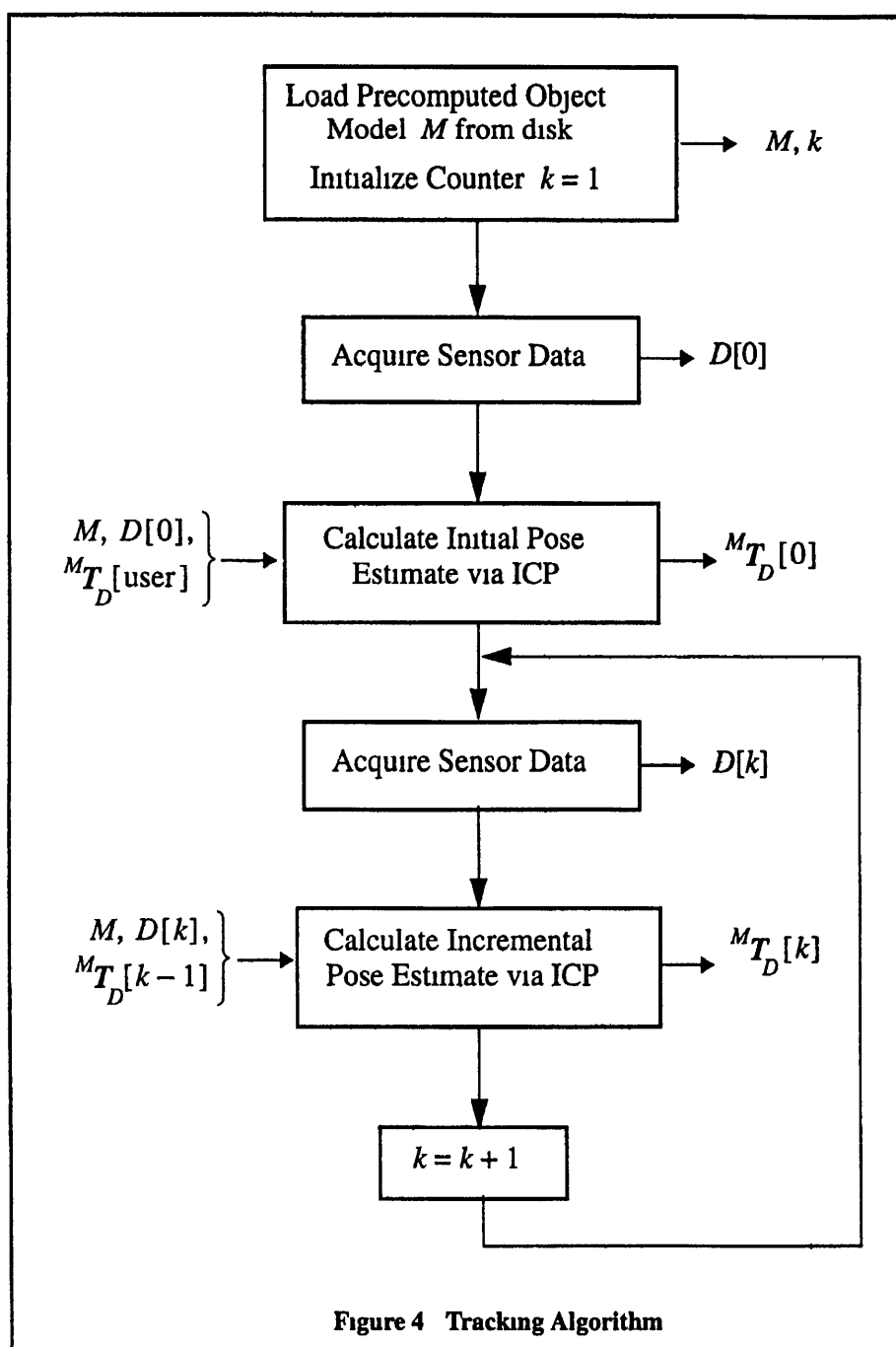
An outline of the tracking algorithm is shown in Figure 4. Each box in the diagram represents a processing step, and the processing sequence is indicated by the large-headed arrows. Inputs to a processing step are indicated by the quantities to the left of each box, while outputs are indicated by the quantities to the right.

During initialization, a precomputed triangular mesh model,  $M$ , is loaded into memory, and a kd-tree is built from  $M$ . For our experiments,  $M$  is constructed offline using a technique based on deformable surfaces [3]. This technique can fuse range data collected from multiple views into a single triangular mesh surface model. The range data used to create  $M$  is provided by several commercially available light-stripe range finders [11]. These sensors have been calibrated so that all data points are expressed in a single, world-centered coordinate frame.

To initialize the tracking algorithm, the transformation between the model,  $M$ , and the initial object pose  $D[0]$ , must be calculated. This transformation,  ${}^M T_D[0]$ , can be found in several seconds using the ICP algorithm with a starting transformation provided by the user<sup>2</sup>. In prac-

<sup>1</sup> The magnitude of  $\epsilon$  determines the amount of fine tuning performed by the ICP algorithm. Smaller values of  $\epsilon$  result in pose estimates closer to the local minima.

<sup>2</sup> A fully automated initialization which does not require user input would be possible by applying one of the techniques for solving the global pose estimation problem discussed in [2].



tice, we have found that initial pose errors as large as 15 degrees of rotation about each axis, and 50% of the object size in any translation will typically converge to the global minimum. Once  ${}^M T_D[0]$  has been calculated, it is used to transform the *model*,  $M$  to the initial object position. Thus, all future pose estimates are measured with respect to this initial starting position.

After initialization, the algorithm enters the tracking loop. Within the loop, data are acquired by the high speed range sensor, and the object pose is estimated via the ICP algorithm in roughly 0.1 - 0.3 sec. These high speeds are possible for two reasons. First, the difference in

object position at time  $k$  and time  $k-1$  is typically small. For example, translational velocities of 10cm per second and rotational velocities of 20 degrees per second lead to incremental object pose discrepancies of roughly 2cm and 4 degrees. Thus, since the ICP algorithm uses  ${}^M T_D [k-1]$  as the starting point when finding  ${}^M T_D [k]$ , the algorithm can perform the registration in a small number of iterations, typically 3-10. Second, the resolution of the range data used in the tracking loop, usually  $16 \times 16$ , is less than the full sensor resolution of  $32 \times 32$ . The reduced number of data points in the set  $D[k]$  results in a faster calculation of the pose estimate.

During each data acquisition cycle, two simple preprocessing steps are performed on the range data. The first step eliminates noisy range data. For the CMU high speed range sensor, noisy data is associated with poor reflection of the projected light from the object. Thus, noisy range data can be eliminated by thresholding the reflected intensity values. Since each cell in the range sensor has circuitry for measuring intensity, this is a trivial operation. The second preprocessing step determines which range data points lie on the surface of the object to be tracked. Since our experiments are performed in an uncluttered environment, range data on the object surface can be distinguished by thresholding the Z component of the range data. While this simple operation works well for our experiments, a more sophisticated approach would be required if the object were in a cluttered environment.

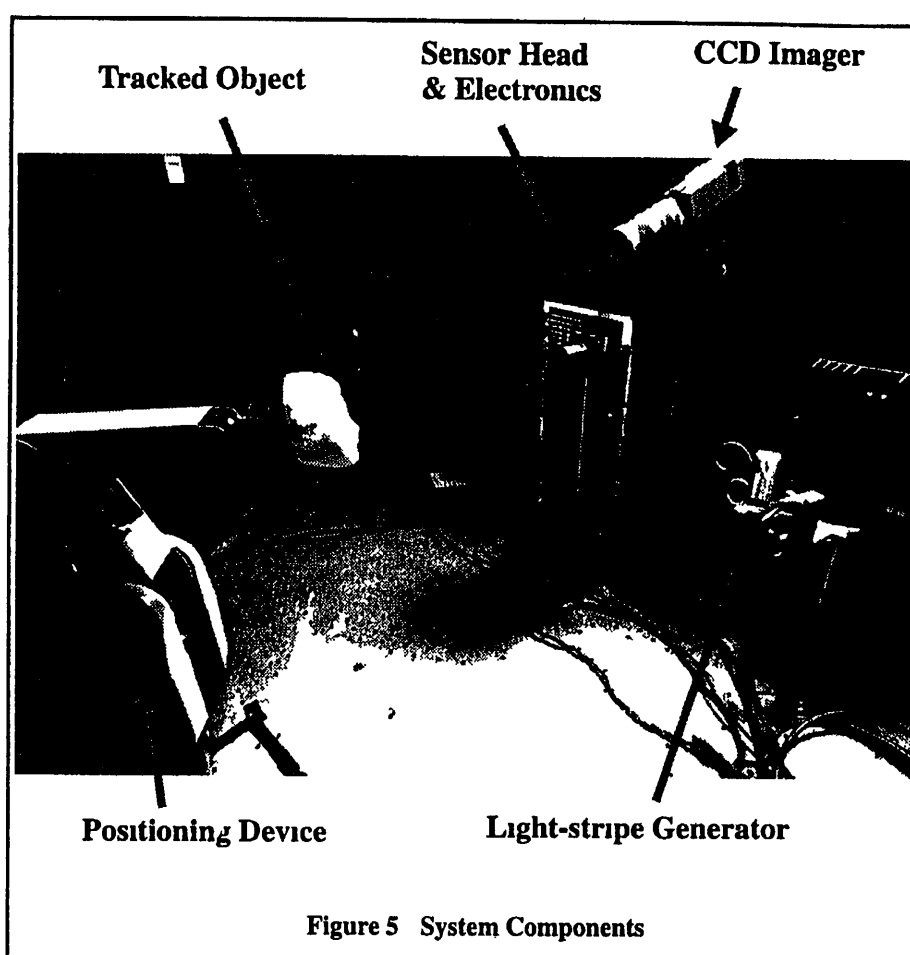
Using  ${}^M T_D [k-1]$  as the starting point for incremental pose estimation works well when object motion is erratic and unpredictable. In some situations, however, object motion may be smooth, continuous and thus easier to predict. For such motions, improved results are possible using an extrapolation scheme such as a Kalman filter. While we have not implemented a Kalman filter for this purpose, we have implemented both first and second order extrapolation. Since the extrapolated pose is often closer to the true pose than  ${}^M T_D [k-1]$ , the time required to compute the pose is reduced.

## 4.0 Experimental Setup

The experimental setup is shown in Figure 5. The CMU high speed VLSI range sensor developed by Gruss, Tada and Kanade [6] consists of two primary components: the sensor head and the light stripe generator. The tracked object, in this case a small bust of the Greek goddess Venus, is mounted on the end effector of a Microbot robot. The CCD imager is not a primary component of the system, but is used for display purposes only. Not shown is a Sparc-10 workstation used for computing the pose estimate, and for graphically displaying a 3-D model of the tracked object. The pose of the graphical 3-D model is updated at high speed to reflect the current object pose estimate.

The CMU high speed range sensor is based on a modified version of the traditional light-stripe range imaging technique known as the cell-parallel light-stripe method. The primary advantage of the cell-parallel method is that range image acquisition time is made independent of the number of data points in each frame.

The current version of the CMU range sensor can acquire a complete  $32 \times 32$  cell range image in as little as one millisecond. The range data is acquired at 10 bits of resolution, and is accurate to 0.1% or better (0.5mm at 500mm). The sensor workspace is shaped like a four sided pyramid. As currently configured, at a distance of 55cm from the sensor along the optical axis, a cross section of the workspace is an 11.5cm square. Thus, the sensor resolution at this distance is about 2.8 range measurements per cm in each direction.



All of the results presented below were collected using the face object shown in Figure 6. This object was manufactured directly from a triangular mesh CAD model using a stereolithographic process [9]. The advantage of this approach is that the physical object is very accurately represented by the corresponding CAD model. Thus, for purposes of characterizing system accuracy, errors caused by differences between the physical object and the CAD model are minimized.

All pose estimates presented below are specified in an object centered coordinate system as shown in Figure 6. The object itself is roughly 8cm x 10cm x 6cm in the X, Y, and Z directions respectively.

## 5.0 Pose Estimation Results

There are two results presented in this section. The first demonstrates the ability of our system to *accurately* estimate the pose of stationary, or slowly moving objects. The second demonstrates the ability to track complex motions in a highly *repeatable* manner. Currently, we do not have the ability to generate complex and accurately calibrated dynamic trajectories which are precisely known at each point along the trajectory. Therefore, we can not currently demonstrate that our system can *accurately* track *high speed* motions.

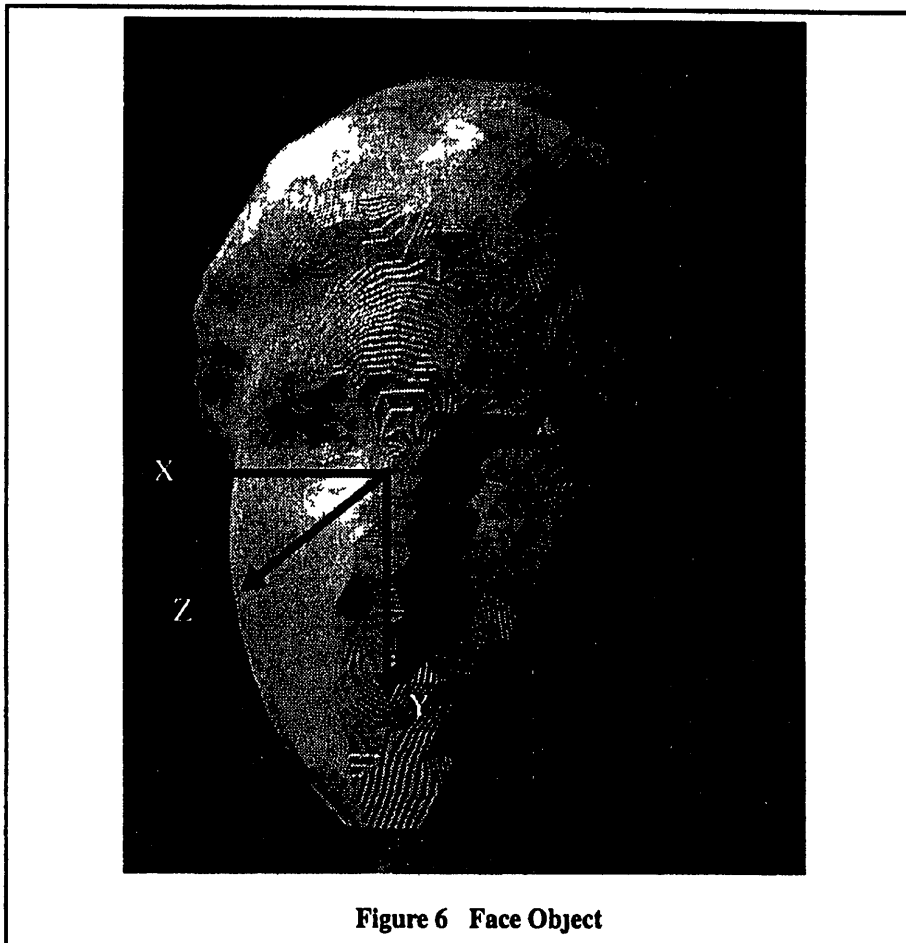


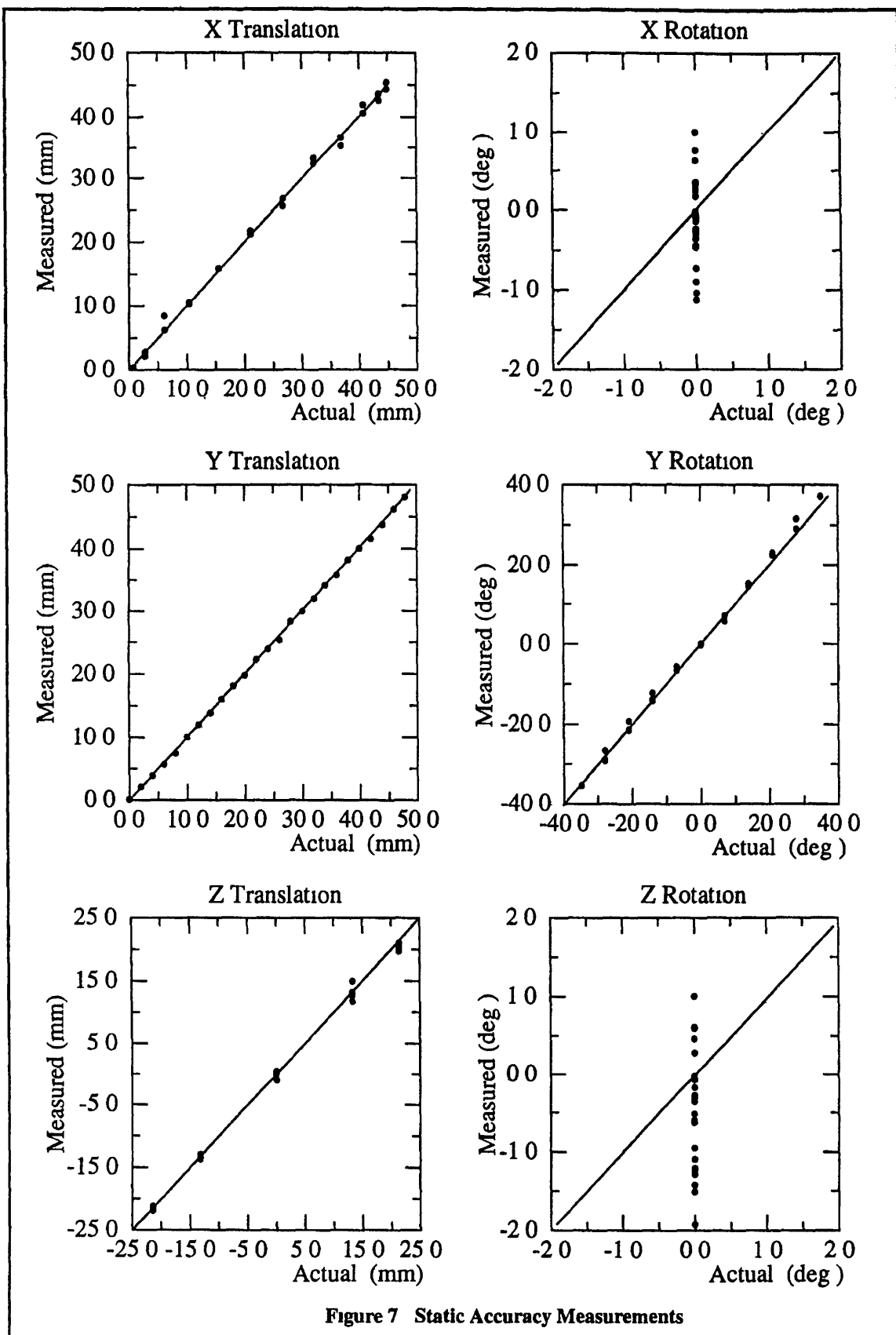
Figure 6 Face Object

### 5.1 Static Accuracy Results

The graphs in Figure 7 demonstrate the absolute accuracy of the system when the object is assumed to be stationary. To collect this data, the object was manually positioned to selected points along a trajectory using a high precision positioning device. At each point, 100 pose estimates were computed, and corresponding mean and standard deviation values were calculated. Each data point in the graphs compares the object's ground truth position to the mean of the corresponding estimated position. The solid line represents the zero error case, and vertical deviations from this line can be interpreted as error.

The object trajectory for these experiments consisted of coupled translations along each axis, and rotations about the Y axis. We were unable to generate rotations about the X and Z axes due to limitations in our apparatus. The average error between ground truth and estimated positions is 0.93mm in the translation components and 1.4 degrees in the rotation components. The standard deviation of each position estimate is less than 0.06mm in translation and 0.1 degree in rotation.

The results of Figure 7 demonstrate that the system can generate accurate pose estimates for stationary or slowly moving objects. In these experiments, the full resolution of the sensor was used, and the ICP termination threshold,  $\epsilon$ , was small. In the current implementation, the system is only capable of tracking very slowly moving objects using these parameter settings. When tracking faster motions, such as those described in Section 5.2, the sensor resolution is typically decreased by a factor of 2, while the ICP termination threshold is increased.



## 5.2 Dynamic Tracking Results

Figure 8 contains plots of estimated pose as the object is moved through a complex trajectory by the Microbot. Pose estimates are specified with respect to the object's initial pose at time 0. Maximum object velocities are roughly 100 mm/sec in translation and 22 degrees/sec in rotation.

Each graph in these figures actually contains 2 overlaid data sets corresponding to 2 different executions of the trajectory. Furthermore, each single execution of the trajectory is periodic with a period of 2. It is evident from these graphs that the *repeatability* of the pose estimation system is quite good. These results also demonstrate that the system can perform pose estimation fast enough to track object motion at the velocities specified above. The average cycle time in these experiments was about 0.3 seconds (3.3Hz), with variation between about 0.1 seconds (10Hz) and 0.5 seconds (2Hz). This variation in cycle time reflects the variation in the initial pose estimate  $M_{T_D}[k-1]$  relative to the actual pose. Large transformations between initial and actual pose result in an increased number of cycles required by the ICP algorithm, and thus a longer overall cycle time. Thus, faster object velocities typically lead to longer cycle times, while slower velocities lead to shorter cycle times.

## 6.0 Conclusions

We have described and demonstrated an approach for performing full 3-D pose estimation of arbitrarily shaped rigid objects at speeds up to 10Hz. The approach utilizes a high speed VLSI range sensor capable of acquiring 32x32 cell range images in 1 millisecond or less.

Three fundamental difficulties in real-time pose estimation have been addressed by the current work. First, the direct use of 3-D range data circumvents the need to infer depth information from 2-D data. Second, direct matching of object surface data avoids the need to solve the feature extraction and correspondence problems. Third, computationally efficient algorithms allow fast computation of the 3-D pose.

Real-time 3-D pose estimation would be useful in a variety of situations. In manufacturing environments, it could be used in feedback control loops to allow a mechanism (i.e. a robot) to perform an operation (i.e. grasping) on a moving part. In the area of Human Computer Interaction (HCI), real-time pose estimation could be useful for tracking movements of a body part for subsequent interpretation as input to a computer. In medicine, a variety of problems involve the need to register pre-operative, volumetric data with the corresponding anatomy of the actual patient. The approach described in this paper may be useful in these cases.

## Acknowledgments

The authors would like to thank Kazunori Higuchi for supplying the triangular mesh CAD models, Mark Wheeler for providing the code to implement the kd-tree search, Andy Gruss and Shige Tada for providing assistance with the high speed range sensor, and Lee Weiss and Kevin Hartmann for producing the stereolithographed object.

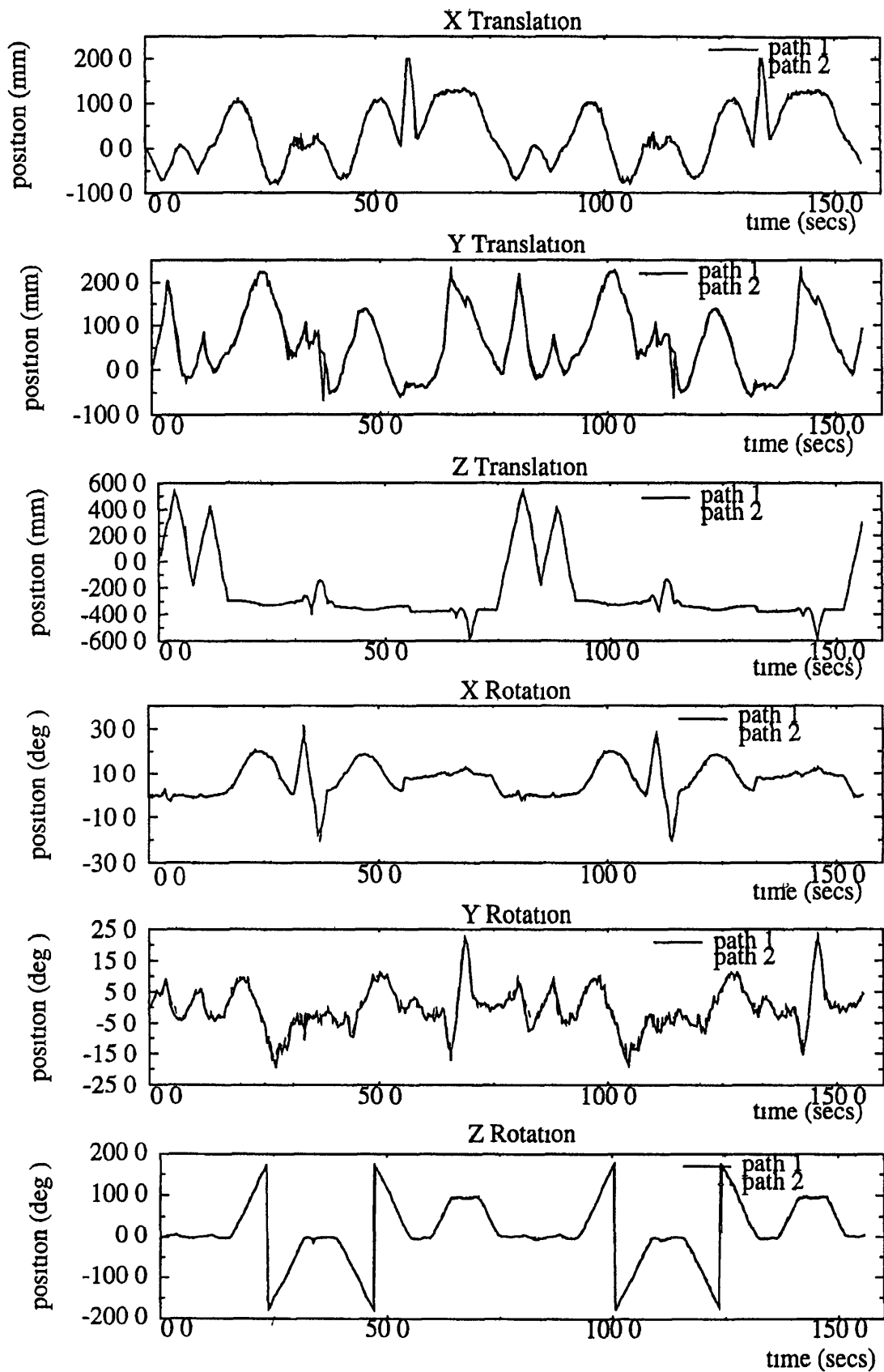


Figure 8 Dynamic Repeatability Measurements



## References

- [1] Bentley, J L Multidimensional binary search trees used for associative searching *Communications of the ACM* 18(9) 509-517, September, 1975
- [2] Besl, P J and McKay, N D A method for registration of 3-D shapes *IEEE Transactions on Pattern Analysis and Machine Intelligence* 14(2) 239-256, February, 1992
- [3] Delingette, H , Hebert, M and Ikeuchi K Shape representation and image segmentation using deformable surfaces *Image and Vision Computing* 10(3) 132-144, April, 1992
- [4] Faugeras, O D and Hebert, M The representation, recognition, and locating of 3-D objects *The International Journal of Robotics Research* 5(3) 27-52, Fall, 1986
- [5] Friedman, J H , Bentley, J L and Finkel, R A An algorithm for finding best matches in logarithmic expected time *ACM Transactions on Mathematical Software* 3(3) 209-226, 1977
- [6] Gruss, A , Tada, S and Kanade, T A VLSI smart sensor for fast range imaging *International Conference on Intelligent Robots and Systems (IROS '92)*, pages 349-58 IEEE, Raleigh, NC, July, 1992
- [7] Horn, B K P Closed-form solution of absolute orientation using unit quaternions *Journal of the Optical Society of America A* 4(4) 629-642, April, 1987
- [8] Kehtarnavaz, N and Mohan, S A framework for estimation of motion parameters from range images *Computer Vision Graphics, and Image Processing* 45(1) 88-105, January, 1989
- [9] Marcus, H and Bourell, D Solid free form fabrication *Advanced Materials and Processes* 144(3) 28-35, September, 1993
- [10] Papanikolopoulos, N P, Nelson, B and Khosla, P K Full 3-D tracking using the controlled active vision paradigm *Proceedings of the International Symposium on Intelligent Control* IEEE, Glasgow, Scotland, U K , August, 1992
- [11] Sato, K and Inokuchi, S Range-imaging system utilizing nematic liquid crystal mask *Proc ICCV*, pages 657-661 London, UK, 1987
- [12] Wang, J and Wilson, W J 3D relative position and orientation estimation using Kalman filter for robot control *Proceedings of IEEE International Conference on Robotics and Automation*, pages 2638-2645 IEEE, Nice, France, May, 1992
- [13] Yamamoto, M Direct estimation of range flow on deformable shape from a video rate range camera *IEEE Transactions on Pattern Analysis and Machine Intelligence* 15(1) 82-89 January, 1993
- [14] Zhang, Z Iterative point matching for registration of free-form curves and surfaces *The International Journal of Computer Vision* To Appear

FEM L HEAD CONTAINMENT IN TOTAL HIP ARTHROPLASTY  
STANDARD VS EXTENDED LIP LINERS

MAXIAN TA BROWN TD PEDERSEN DR AND CALLAGHAN JJ

Departments of Orthopaedic Surgery and Biomedical Engineering  
The University of Iowa Iowa City IA 52242

INTRODUCTION

Acetabular cup extended lip liners were developed in order to reduce the dislocation rate for total hip arthroplasty. In these designs, however, the polyethylene liner extends considerably beyond the edge of the metal backing, setting up a potential region of stress concentration at the supported edge. Previous work [1] has shown that the metal backing can have potentially deleterious effects in standard lip components. To evaluate the severity of stress concentrations in extended lip liners, we used a three-dimensional dual interface contact finite element (FE) formulation to study polyethylene stresses up to the point of head dislocation.

MATERIALS AND METHODS

Two zonings representing 28 mm components<sup>1</sup> were created from manufacturer blueprint specifications. Each liner (Figure 1) was comprised of 800 elements in four layers with an elastic modulus of 1400 MPa corresponding to oxidized polyethylene [2]. A perfectly conforming cobalt chrome backing was represented by a rigid Bézier surface, as was the femoral head. Thus the contact problem was formulated in terms of two interfaces: one between the metal backing and the liner, and the other between the liner and the femoral head. Rigid body contact modeling allows for large displacement and separation in three-dimensions. Nodes within the liner located at the approximate site of the retaining ring were constrained. To investigate the effects of friction between the metal backing and the polyethylene liner, the coefficient of friction at this contact interface was modeled as 0.0 (frictionless), 0.5, and 1.0 (no slip). The contact interface between the femoral head and acetabular bearing surface was assumed frictionless.

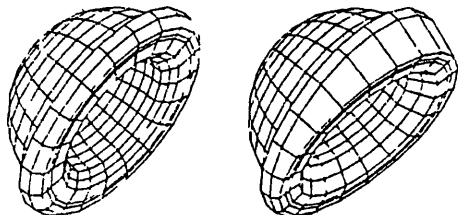


Figure 1 The standard and extended lip FE models

The acetabular components were positioned in neutral version, inclined 45° in the coronal plane. A 3.0 kN force was applied to the center of the femoral head vertically, and then in a succession of more laterally oriented directions until the integrated reaction force no longer equaled the applied force value, a condition indicative of incipient dislocation of the femoral head. To investigate the importance of the backing/liner contact interface, two otherwise matching models but with only a single contact surface between the liner and femoral head were also created. The metal backing in these models had an elastic modulus of 210 GPa and was assumed to be rigidly supported at its external surface.

RESULTS

Under all load directions and frictional conditions, peak polyethylene stresses were slightly lower in the extended compared to the standard liner (Figure 2), apparently due to the extended lip liner's slightly larger contact area. The limit of stability for the femoral head was 39° from the vertical for the standard liner and 50° for the extended lip liner, regardless of frictional conditions. There was no evidence of stress concentrations due to bending at the edge of the cantilever support in the extended lip. As the coefficient of friction between the metal backing and liner was increased, peak polyethylene stresses increased only slightly, as loading

appeared to shift from the component rims to the cup body. The single interface contact models followed the same trends as the dual interface contact models, with peak stresses differing 1-10% from the frictionless solution and 1-5% from the no slip solution.

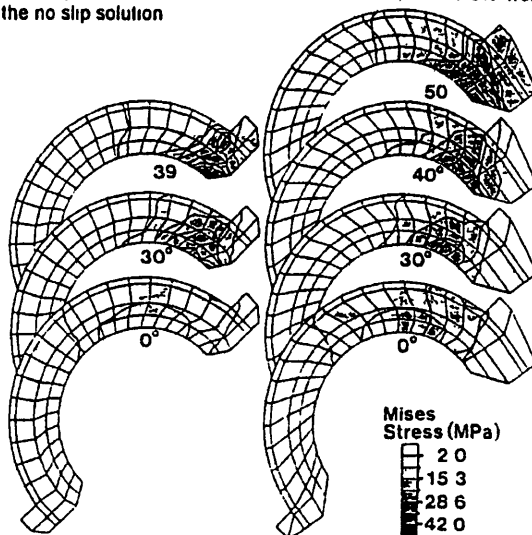


Figure 2 Coronal midsection von Mises stresses (with frictional coefficient = 0.5) for the standard (left) and extended lip (right) liners

DISCUSSION

The present data suggest that in terms of polyethylene articulation stresses, extended lip liners may actually be preferable to standard liners. The extended lip liners were able to maintain femoral head engagement over about an 11° larger range of force directions than the standard liners, thus providing the increased stability for which they were designed. At any given loading angle within the mutual range of stability, however, polyethylene stresses differed little between the two types of acetabular liners. The relatively small differences between the single- and double-interface contact solutions suggests that the incorporation of the second contact interface and frictional effects may be unnecessary for this particular class of problems.

<sup>1</sup>Duroloc DePuy Warsaw IN

REFERENCES

- 1) Kurtz *et al* (1993) *Trans ORS* 434
- 2) Rimnac *et al* (1994) *Trans ORS* 175

ACKNOWLEDGMENTS

Financial support received from DePuy Inc.

- One or more of the authors have received something of value from a commercial or other party related directly or indirectly to the subject of my presentation.
- The authors have not received anything of value from a commercial or other party related directly or indirectly to the subject of my presentation.

FULL Name Address Phone Fax and E Mail Numbers of Corresponding Author

Thomas D Brown Ph D  
Orthopaedic Biomechanics Laboratory  
2432 Steindler Building  
University of Iowa Iowa City IA 52242  
(319) 335-7528 FAX (319) 335-7530  
tom.brown@uiowa.edu

## FINITE ELEMENT MODELING OF DISLOCATION PROPENSITY IN TOTAL HIP ARTHROPLASTY

MAXIAN TA BROWN TD PEDERSEN DR AND CALLAGHAN JJ

Departments of Orthopaedic Surgery and Biomedical Engineering  
The University of Iowa Iowa City IA 52242

### INTRODUCTION

Dislocation rates of 5% following primary total hip arthroplasty (THA) and 10% following revision arthroplasty are commonly reported [1]. The use of modular components to include extended lip liners various acetabular bearing surface geometries and various modular taper head and neck geometries create numerous potential design variables responsible for component stability and instability in the THA construct. While neck impingement is predictable simply on kinematic grounds the dislocation process per se is far more complex and depends also on the ratio of articular contact force to external moment as well as upon elastic deformation of the component lip. Previous laboratory investigations of dislocation have used experimental models which evaluated bony impingement in combination with acetabular and femoral component design considerations [2]. To investigate the contribution of various component design variables to inherent component dislocation propensity we have developed a novel 3-D large displacement finite element (FE) technique.

### MATERIALS AND METHODS

Three 28 mm metal backed acetabular components were considered: a hemispherical polyethylene liner with a standard chamfered lip, a greater than hemispherical component with a non-chamfered lip, and an extended lip component (Figure 1).

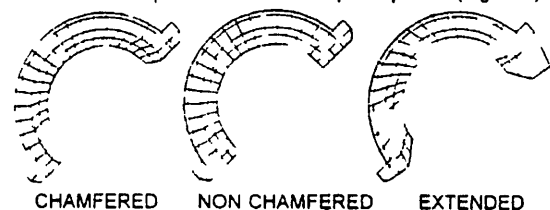


Figure 1 Coronal sections of the 3-D meshes

In each case the acetabular component was represented by an FE mesh with linear elastic material properties. Each acetabular component was then coupled with two different femoral component designs: one with a neck-trunion diameter of 16.3 mm (N1) and the second with 15.5 mm (N2). The tapers on each neck were the same, but because the proximal neck diameters were different the first component had a thicker neck than the second. The femoral components were represented by rigid Bezier surfaces and could undergo large three-dimensional motions. In each case the metal backing was rigidly supported. The acetabular components were oriented in neutral version with 45° of inclination. The extended lip component was oriented symmetric to the coronal plane. The femoral components were initially oriented perpendicular to the plane of the opening of the metal backing. Contact between the femoral and acetabular components was assumed to be frictionless. The femoral head was brought into contact under displacement control, generating a 1000 N medially directed force. The direction of this containment load was allowed to rotate clockwise during femoral component rotation. To cause dislocation the femoral component was rotated clockwise until solution instability occurred (the system matrix became non-positive definite, i.e. had negative eigenvalues). When instability occurred the dislocation moment was recovered from the current loads on the femoral head and the distance from the center of the femoral head to the point of highest contact stress on the acetabular component. The dislocation angle was the angular displacement from start position to instability (Figure 2).

### RESULTS

The extended lip component had only slightly higher dislocation angles and moments than the chamfered standard

lip component for the tested loading conditions. The alternative neck diameters had little effect on dislocation propensity for a given acetabular component geometry.

Table 1 Dislocation angles and moments

	Chamfered		Non chamfered		Extended	
	N1	N2	N1	N2	N1	N2
Imp Angle (°)	55	56	47	48	59	60
Dis Angle (°)	66	62	53	53	64	63
Moment (Nm)	17	17	13	13	18	18

Imp = Impingement Dis = Dislocation

The non-chamfered standard lip component had the worst performance of the component designs tested. This type of component impinged and became unstable 10° sooner than the other components with a dislocation moment roughly 25% less than the other two components. Peak contact stresses encountered during dislocation series-wide (15 MPa and up) imply that plastic deformation would occur during dislocation.

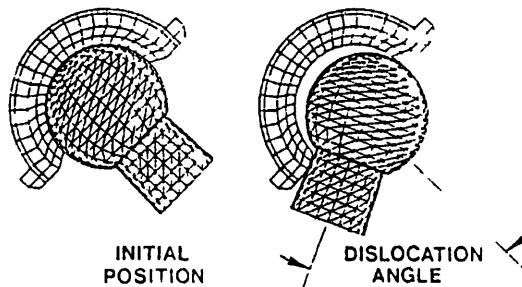


Figure 2 The initial and unstable positions

### DISCUSSION

This study demonstrates that the design of the acetabular component plays as great a role in dislocation propensity as that of the femoral neck. Under the tested conditions the extended lip component appeared to be no more stable than the chamfered standard lip one. The non-chamfered standard lip component impinged and became unstable much more readily than the other two acetabular component geometries. This modeling technique should allow for efficient evaluation of various design considerations independently and in combination to identify the choices and compromises associated with stability in the THA construct.

### REFERENCES

- 1) Woo *et al* (1982) *J BJS* 64A 1295-1306
- 2) Krushnell *et al* (1991) *J Arthroplasty* 6 S53-S58

### ACKNOWLEDGMENTS

Financial support DePuy Inc

- One or more of the authors have received something of value from a commercial or other party related directly or indirectly to the subject of my presentation
- The authors have not received anything of value from a commercial or other party related directly or indirectly to the subject of my presentation

FULL Name Address Phone Fax and E Mail Numbers of Corresponding Author

Thomas D Brown Ph D  
Orthopaedic Biomechanics Laboratory  
2432 Steindler Building  
University of Iowa Iowa City IA 52242  
(319) 335 7528 FAX (319) 335 7530  
tom.brown@uiowa.edu

## Computer-Assisted Knee Anterior Cruciate Ligament Reconstruction *First Clinical Tests*

Vincent Dessenne, M ScI , Stephane Lavalley, Ph D , Remi Julliard, M D ,  
Rachel Orti, M ScI , Sandra Martelli, Ph D , and Philippe Cinquin, Ph D , M D  
TIMC-IMAG, Faculte de Medecine de Grenoble La Tronche, France (VD, SL, RO, SM, PC),  
Clinique Mutualiste, Grenoble, France (RJ)

**ABSTRACT** Anterior cruciate ligament reconstruction is a delicate task. The procedure of choice is the patellar tendon bone autograft, but an anisometric position of this tendon often leads to failure. We propose a method that allows positioning of the central part of the ligament graft at the least anisometric sites. The system uses a workstation and a three-dimensional optical localizer to create images that represent knee kinematics. The surgeon uses these images to guide the surgery. This technique has been validated on eight cadavers and 12 patients. *J Image Guid Surg* 1 59-64 (1995)  
©1995 Wiley-Liss, Inc

---

**Key words** knee reconstruction, cruciate ligament, anterior cruciate ligament, patellar tendon graft

---

### INTRODUCTION

The treatment of an injury to the anterior cruciate ligament (ACL) is difficult. To replace a severed ligament, the surgeon creates two tunnels, one in the femoral notch and one in the tibia, and inserts and attaches a graft inside these tunnels. The procedure of choice is the patellar tendon graft (Fig. 1).

This surgical procedure can be performed in a classical open surgery or under arthroscopy. The success of the reconstruction depends on both the selection of the intraarticular graft position and the initial graft tension. If the insertion sites, initial tension, geometry, and mechanical properties of the normal ACL can be restored during reconstructive surgery, the long-term complications of an ACL injury can be greatly reduced. To determine the optimal placement of an ACL graft, the concept of isometry has been advocated by many authors.<sup>1-4</sup> This is a controversial approach, but in our opinion, using this criterion is a good start towards a rational and optimal surgery.

The graft is attached at two points, F and T, on the femur and the tibia, respectively. A perfect isom-

etry implies that there are no changes in the distance between F and T during flexion and extension of the knee (Fig. 2). Conversely, an anisometry is said to exist when there is a change in the distance during knee flexion/extension. With weak anisometry, the graft is subjected to nearly constant tensile forces. Therefore, the risk of rupture because of excessive tensile force in extension or in flexion is reduced, and knee stability is improved. In reality, the graft is not of uniform diameter; it approximates the form of a cylinder that widens at its extremities. However, if the centers of the femoral and tibial attachment sites are nearly isometric, then at least the central part of the graft is subjected to constant forces. Therefore, in our model, our optimal criterion corresponds to the minimal anisometry between the centers of the ends of the tunnels created by the surgeon on the femoral notch and the tibia.

There is a great deal of controversy over the employment of different surgical techniques for positioning. Many of these techniques strive to obtain near-isometric graft placements. To our knowledge,

---

Received original February 10, 1995; accepted February 16, 1995.

Address correspondence/reprint requests to Vincent Dessenne, TIMC-IMAG, Faculte de Medecine de Grenoble, 38706 La Tronche, France; e-mail: vincent.dessenne@imag.fr

©1995 Wiley-Liss, Inc

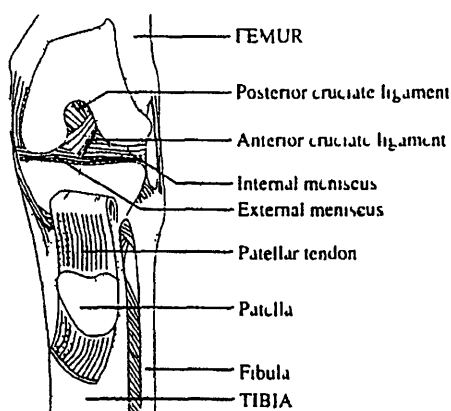


Fig 1 Anatomy of the anterior cruciate ligament in the intact knee

there is no easy fast and accurate technique to find the least anisometric insertion sites T and F. For instance in the well known technique of Rosenberg<sup>7</sup> the surgeon places a thin wire at some point F that appears to be the most isometric. By measuring the length variation of the candidate wire using a standard mechanical isometer the surgeon then selects another attachment point. This procedure is repeated until the anisometry is below a given threshold (typically  $\pm 1$  mm) or until the least anisometric point is found. We propose a system that interactively predicts in real time the anisometry and the profile of the length variation of the graft as a function of flexion angles for any point on the femoral notch surface.

### MATERIALS AND METHODS

The system we propose uses only intraoperative components. Radiographs, computed tomography and magnetic resonance imaging are not required. The entire system is installed on a cart and includes a workstation (DEC 5000 running Unix) and a three dimensional (3-D) optical localizer (Optotrak Northern Digital Fig 3).

The optical localizer consists of three linear charge coupled device (CCD) cameras that detect the position of infrared emitting diodes with an accuracy of  $\pm 0.3$  mm. The localizer can compute in real time the position and orientation of rigid bodies made of six diodes. The four rigid bodies are waterproof and can be sterilized with ethylene oxide plasma or liquid sterilization chemicals (Fig 4).

In the current version of the system the surgeon drills the tibial tunnel without using the computer system (see below). The system is used to optimize the placement of the femoral tunnel only.

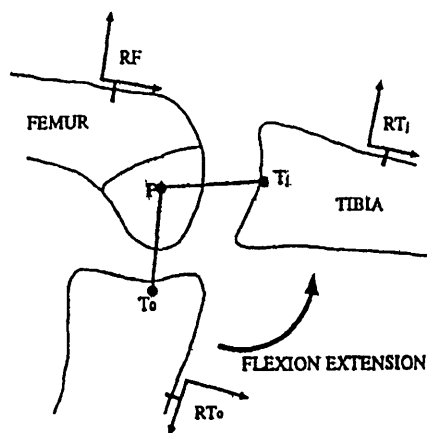


Fig 2 Attachment points of a graft F and T on the femur and the tibia respectively. During a flexion/extension of the knee the variation of the distance between F and  $T_0$ .  $T_j$  is called anisometry. If the trajectory of T belongs to a sphere centered in F the graft is perfectly isometric.

The method can be divided into four steps as detailed below.

#### Step 1 Passive Flexion-Extension

At the beginning of the surgical procedure the surgeon firmly fixes two optical rigid bodies to the femur and the tibia. These rigid bodies are used as reference coordinate systems, namely RF for the femur and RT for the tibia. A passive flexion/extension is then applied to the knee by the surgeon (Fig 5). For about 20-50 knee positions ranging from maximal extension to maximal flexion the surgeon presses a foot switch and the location of the coordinate system RT with respect to RF is computed and stored. This gives a set of matrices  $RT_j$  ( $j = 1 \dots M$ ) ordered by the knee flexion angle (Fig 2).

#### Step 2 3-D Points Acquisition

The surgeon uses the third rigid body i.e. RP (rigid body pointer) interactively to collect surface points arthroscopically on the femur. This 3-D pointer is easily calibrated in approximately 10 sec using a pivot technique by placing the pointer tip at a fixed location (with respect to another reference rigid body) and rotating the pointer around that fixed point (Fig 6).

The XYZ coordinates of the pointer tip are then computed in RP by locating the most invariant point along these motions (with a least squares approximation). With this 3-D optical pointer the surgeon collects several data points by placing the tip in contact with the surface and pressing a foot switch for each point (Fig 7).

**Tibial Attachment Point**

Once the tibial tunnel has been developed the center of its intraarticular extremity  $T_{drilled}$  is digitized with the pointer. An adjusted sharp rod is inserted into the tunnel to provide an accurate central point to digitize

**Femoral Notch Surface**

The surgeon acquires surface points on the femoral notch in an area that corresponds to all the possible candidate points for the femoral attachment site (typically a region of less than 15 mm x 15 mm). A set of 20-100 points  $P_i = (x_i, y_i, z_i) \quad i = 1 \dots N$  is acquired in less than 2 min

**Step 3 Anisometry maps computation**

At this stage all the data necessary to meet our criterion have been acquired. Three data modeling steps are necessary before the result can be utilized by the surgeon. They are performed within 1 min of the acquisition of the surface point data

**Reconstruction of the 3-D trajectory of T**

Step 1 above gives a set of positions  $RT_j$  of the coordinate system RT in the femur coordinate system RF. Step 2 above gives the coordinates of the tibial attachment point  $T_{drilled}$  in the coordinate system RT. Simple matrix products give a set of point positions  $T_j \quad j = 1 \dots M$  in RF. The trajectory of the tibial point  $T_{drilled}$  is roughly a portion of a circle. This a posteriori computation makes it possible to perform step 1 and step 2 in any order

**Spline Interpolation of the Femoral Notch Surface**

The set of femoral surface points  $P = (x, y, z)$  is interpolated by a bicubic spline surface. To represent the surface we have chosen a parametric representation of the type  $z = f(x, y)$  where  $f$  is a spline function. We initially compute the least squares plane fitting the set of points  $P_i$  so that two vectors  $x$  and  $y$  belonging to that plane define a new intrinsic surface coordinate system  $(x, y, z)$ . We call  $[H]$  the corresponding 3 x 4 coordinate transformation matrix between  $(x, y, z)$  and  $(r, s, z)$ . All the points  $P$  are first transformed in the intrinsic coordinate system before all the resulting points  $P$  are interpolated by a spline  $f$

$$(x, y, z) = [H] \cdot (r, s, f(r, s))$$

This parameterization is simple and reliable since the surface is digitized in a small area in which only one spline patch of the form  $z = f(x, y)$  is necessary to represent the whole surface

**Computation of Anisometry Maps**

For each point F of the interpolated femoral spline surface the system can now compute the predicted ligament length variation curve (in function of flexion angles) and the anisometry criterion ANI(F) which is computed as the maximal length variation

$$ANI(F) = \frac{MAX_{T_j} distance(F, T_j)}{MIN_{T_j} distance(F, T_j)}$$

By forming a regular grid in  $x$  and  $y$  (which are the  $x$  and  $y$  coordinates of the femoral surface points in the intrinsic surface coordinate system) we obtain a grid of femoral points given in RF by the equation given above. Therefore, we can write ANI as a function of  $r$  and  $s$

$$ANI(r, s) = \frac{MAX_{T_j} distance([H] \cdot (r, s, f(r, s)), T_j)}{MIN_{T_j} distance([H] \cdot (r, s, f(r, s)), T_j)}$$

By varying  $r$  and  $s$  in the region of interest the result is an anisometry map on the femoral surface that can be presented to the surgeon as a pseudocolor image. A different color is associated with each mm of  $r$  value (Fig 8)

**Step 4 Interactive Placement of the Femoral Tunnel**

The surgeon can now locate the most isometric point on the femoral surface using any standard surgical tool equipped with a fourth rigid body. For instance if we equip a drill it is calibrated easily and quickly by repeating the pivot calibration technique described in step 2 above for two points along the drill axis. While the surgeon is moving the drill the system computes in real time the intersection point  $I$  between the spline femoral surface and the drill axis. For that purpose a standard gradient conjugate method iteratively searches for the coordinates  $r$  and  $s$  such that the distance between the point  $(r, s, f(r, s))$  and the drill axis line given at a time  $t$  is zero. The point  $I$  is displayed on the anisometry map and the anisometry value ANI(I) is displayed in millimeters. The anisometry profile which is the curve of length variation along the flexion angles is also displayed in real time. The surgeon can then easily adjust the position of the tool until it is in a satisfactory region of the anisometry map and then drill a 2 mm femoral tunnel at that point. The surgeon always has the system prediction available in real time in case the drill slips

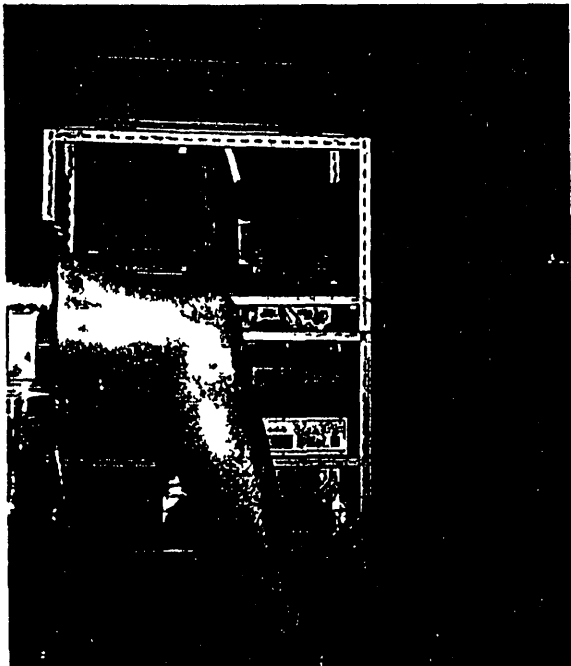


Fig 3 Workstation and 3 D localizer installed on a cart

slightly on the surface. Such an error can be corrected when using larger drill diameters (the final tunnel is about 10 mm in diameter). It is also possible to equip a standard guiding system in which the drill is introduced (Fig 9).

### CLINICAL VALIDATION

#### Validation on Eight Cadaver Knees

The system has been successfully tested on eight cadaveric specimens. In all cases, anisometry was less than 2 mm. Anatomical results were detailed by Lavallee et al. During this study, we compared the passive flexion/extension motions of the knee before any intervention and after cutting the ligament. Both trajectories were almost identical for all cases, with differences less than 1 mm. Therefore, for patients with fresh ruptures of the ACL, it is reasonable to assume that a passive flexion/extension of the knee performed at the beginning of the operation represents the kinematics of the normal knee.

#### Validation in 12 Patients

The system has been successfully tested with 12 patients in open surgery for three patients and under arthroscopy for nine patients (Fig 10). For the first patients, we used a conservative approach in which the surgeon employed standard technique, namely the method of Morgan et al.<sup>4</sup> while the system was used simply to measure and study the residual anisometry obtained. For ethical reasons, we did not

use the technique directly without preliminary validation. The position of the femoral site was acquired with the optical pointer, with anisometry ranging from 1.5 to 6.8 mm and a mean value of 3.0 mm and standard deviation of 1.7 mm. From these preliminary results, we conclude that the technique we used provides good anisometry on average, but placements with large anisometry still occur in some patients. Insofar as standard devices are not adapted to each individual patient, these results were not unexpected. Our results reinforce the interest in our computer-assisted technique; therefore, the active use of our system on a larger scale can now be planned.

### DISCUSSION

#### Cost vs Benefit

Because the purpose of our method is to improve a standard technique, only a long-term study can definitely demonstrate that this new technique is better than previous ones. However, cost and expected benefit can be analyzed.

#### General Cost

Time is a critical factor in ACL reconstruction, since the leg tourniquet must be removed as soon as possible (the time limit is 2 hr). Our method requires less than 10 min during surgery and about 15 min for preparation before surgery.

The system adds cumbersome new equipment in the operating room, and it may be difficult to use initially. However, the whole system is contained in a cart that is easily brought into or removed from the operating room. The cart can be moved at any time without affecting accuracy, because all coordinates are acquired in relative coordinate systems. The sys-

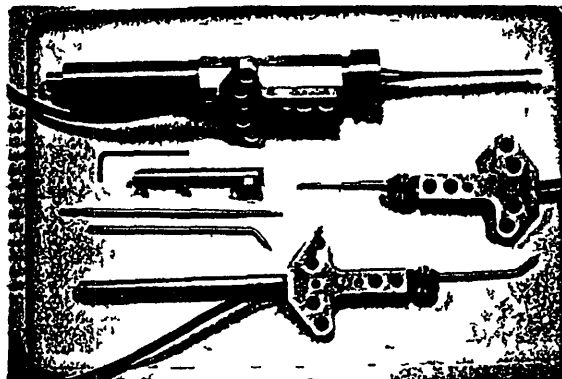


Fig 4 Optical rigid bodies, each made of six infrared diodes. Two rigid bodies are fixed on the tibia and femur; one rigid body is a pointer to collect 3-D data points, and another one locates any existing surgical drill or guide.

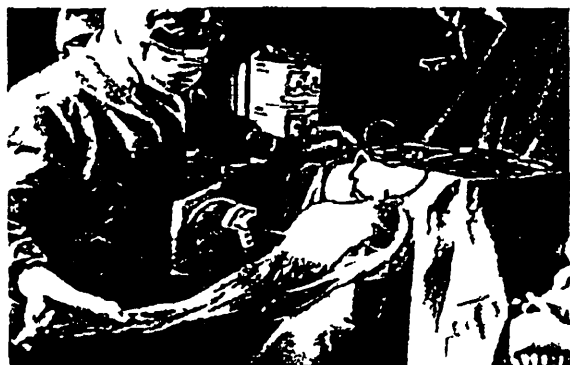


Fig 5 Two optical rigid bodies each with six infrared diodes are attached to the femur (RF) and the tibia (RT). A passive motion from flexion to extension is applied to the knee. The system records the positions of the coordinate systems during that motion.



Fig 7 The surgeon uses a 3 D pointer fixed to an optical rigid body. This allows collection of coordinates of specific points or surface points in RF or in RT.

tem is also strongly interactive and easy to understand. The acquisitions with the optical localizer must be performed when the field between the cameras and the rigid bodies is free, but that constraint has to be met for only a few seconds. Importantly, the surgeon can continue with the standard technique and material and use the new system as an additional aid.

Adding any equipment in the orthopedics surgical room increases the risks of infection. Special care must be taken regarding sterilization techniques.

In terms of cost, the new method requires only a standard computer and a 3 D optical localizer. The hardware components of these systems are now expensive. Over time, cost efficacy will improve as the price of the surgical device decreases.

#### Expected Benefit

For each patient, the system helps in obtaining an optimal placement of the graft. Unlike many currently used techniques, the system is not operator dependent.



Fig 6 The surgeon places the pointer tip at a fixed location and rotates the pointer around that fixed point.

Outcome depends more on the characteristics of the knee than on the quality of the surgery. Obviously, the new system does not remove the need for surgical expertise, but it is an additional tool that promotes minimal graft anisometry. We assume that this will improve the stability of the knee while increasing the lifetime of the graft. Our system should help surgeons to acquire experience and knowledge rapidly to perform successful ACL reconstruction.

#### Optimization of the Tibial Attachment Point

The significance of the position of the tibial tunnel vs the femoral point in anisometry is debated.<sup>15</sup> We have found that changing the location of the tibial

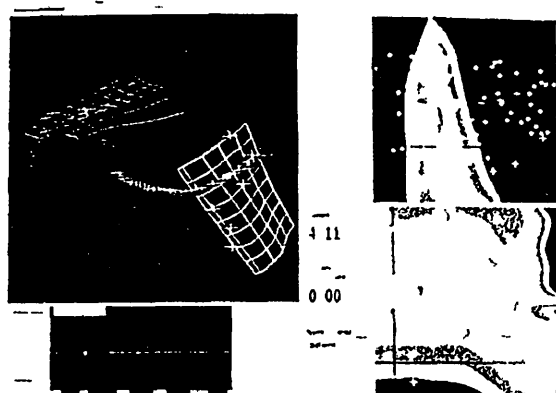


Fig 8 Typical anisometry map. A pseudocolor presentation of the predicted anisometry on the femoral surface is displayed as an image. An interactive 3 D view allows observation of the tibial point trajectory, the spline notch surface, and the anisometry map on the latter surface. For any candidate point F, the user interface presents the predicted anisometry values and profiles.





Fig 9 Any surgical tool can be equipped with an optical rigid body so that the position of the tool is displayed in real time on the anisometry map

tunnel in the tibia significantly moves the location of the least anisometric corresponding point on the femur. Indeed, for all the tibial insertion sites of a reasonable area, the anisometry maps on the femur have similar shapes and values, but they are translated.<sup>3</sup> Thus, for any tibial insertion site (in a reasonable area), there exists a femoral insertion point with a correct anisometry (below 2 mm).

However, an extended version of the system performs some optimization on the tibia. It is important to avoid notch impingement collisions between the ligament graft and the femoral notch at maximal extension. Therefore, this new version requires acquisition of surface points on the tibia and then allows prediction of collision for two given points T and F.

#### Towards an Easy Single-Tunnel Technique

The single tunnel technique advocated by some authors is difficult to perform. The technique we propose makes the single tunnel technique easy, fast, and accurate. A user interface is being developed to help the surgeon make a direct straight tunnel into the tibia and the femur, respecting the collision-free constraint mentioned above, and still optimizing the anisometry.



Fig 10 The surgeon uses an arthroscope (shown in the left hand) to locate points or to digitize surfaces inside the knee. The very end of the tip fixed to the optical rigid body (shown in the right hand) appears on the screen and clearly demonstrates the digitization to the surgeon.

#### CONCLUSIONS

ACL reconstruction is a delicate task for which many techniques have been advocated. The system we propose is accurate, is not operator dependent, and optimizes a defined criterion. It is based on affordable technology that does not require radiographs or preoperative imaging. The surgery is based on images that are created intraoperatively to represent complex dynamic data in a simple way. In that sense, the surgery is image guided. The system is very interactive and simple to use. It could readily be applied to other ligaments for which isometry is desired.

To facilitate further development, a realistic model of the ACL is needed. This would allow the use of criteria more exacting than the relatively simple central isometry criterion. Therefore, we are developing an elastic model of the ACL as a part of a more complex model of the whole knee.

#### REFERENCES

- 1 Champlébois G (1991) Utilisation des fonctions splines pour la mise au point d'un capteur tridimensionnel sans contact. Quelques applications médicales (in French). PhD thesis, Grenoble University.
- 2 Fleming B, Brynnon BD, Johnson RJ, McLeod WD, Pope MH (1993) Isometric versus tension measurements: A comparison for the reconstruction of the anterior cruciate ligament. *Am J Sports Med* 21: 82-88.
- 3 Lavalée S, Julliard R, Orti R, Cinquin P, Carpentier E (1994) Reconstruction du ligament croisé antérieur. Détermination du meilleur point isométrique femoral assistée par ordinateur (in French). *Eur J Orthop Surg Traumatol* 4: 87-92.
- 4 Morgan CD, Garrett JC (1993) Trans tibial Single Incision Anterior Cruciate Ligament Reconstruction. *Arthroscopy*.
- 5 Muncia T, Yamamoto H, Sakai H, Ishibashi T, Furuya K (1993) Relationship between changes in length and force in in vitro reconstructed anterior cruciate ligament. *Am J Sports Med* 21: 299-304.
- 6 Odensten M, Guillequist J (1985) Functional anatomy of the anterior cruciate ligament and a rationale for reconstruction. *J Bone Joint Surg Am* 67: 257-261.
- 7 Rosenberg D (1991) Technique Endoscopique de Reconstruction du Ligament Croisé Antérieur à l'Aide du Guide Pro Trac. Note Technique. Mansfield, MA: Acuflex Microsurgical Inc.

# Anatomy-based Registration for Computer-integrated Surgery

Ali Hamadeh<sup>1</sup>, Stephane Lavallee<sup>1</sup>, Richard Szeliski<sup>2</sup>,  
Philippe Cinqun<sup>1</sup>, Olivier Peria<sup>1</sup>

<sup>1</sup> TIMC IMAG

IAB, Faculte de Medecine de Grenoble, 38 706 La Tronche, France  
e-mail Stephane.Lavallee@imag.fr

<sup>2</sup> Digital Equipment Corporation, Cambridge Research Lab  
One Kendall Square, Bldg 700, Cambridge MA 02139

**Abstract** In Computed integrated Surgery (CIS), the registration between pre- or intra operative images, anatomical models and guiding systems such as robots or passive systems is a crucial step. In our methodology, rigid or elastic transformations are estimated using non linear least squares minimization of euclidean distances computed on data that can be 3D surfaces or 2D projections. This paper shows the variety of results that is achieved with this framework on several clinical applications.

## 1 Introduction

In Computer integrated Surgery (CIS), the registration of the whole information available for a given patient is an essential step [TLBM95]. See [Lav95] for a review of standard methods. Several kinds of data may have to be registered:

- *Pre operative data*: medical images such as CT, MRI, TEP, SPECT, or models such as brain atlases (usually the basis for the surgical planning)
- *Intra operative data*: medical images provided by low cost systems (X-rays, echography, microscopes or endoscopes), or positioning information provided by various sensors (optical, ultrasonic, mechanical, or electro-magnetic 3D localizers, range imaging systems). Guiding systems that can be passive 3D localizers or active robots have also to be registered with the images on which the surgical planning has been defined and updated. For that purpose, the guiding systems have often to be calibrated with intra operative sensors, which are in turn registered with the whole information.
- *Post operative data*: similar to pre-operative data. They have to be registered to measure the efficiency of an intervention and to update the models.

A typical application will have to register pre operative CT images with a 3D passive or active manipulator during surgery [LST+94]. In most of standard registration techniques used in CIS, material structures such as reference pins or balls have to be fixed to the patient. For several years, our group has been working on the concept of anatomy based registration according to which some reference anatomical structures of the patient provide sufficient features for registration. See [Lav95, LSB95] for a description of our methodology.

## 2 Registrati

In this section, we surface model  $S$  w sary to precomput model  $S$ . This dis minimum signed  $\phi$   $q$  inside a boundin positive for a point inside it. Therefore representation of  $S$  of 3-D points lying which is a 3D adap near the surface, se

### Rigid 3D-3D

In most of appl cedure applied to  $P$  can be represented of a second series c surface points (e.g. segmentation, or th

In this case we 6 components vectc the surface  $S$  know (we make the assum look for the param squares of distances by  $T(p)$  in the 3D

$E(p)$

where  $\bar{d}(T(p), q, S)$  the data point  $q$ ,  $t$  variance of the nois function is performe bust estimation is a given threshold and

### Rigid 3D 2D r

Sensor data may registered with a 3D the first step is to u the projection lines contour of the projec

## 2 Registration method

In this section, we briefly present the algorithms that enable us to register a 3D surface model  $S$  with various sensor data. For all these algorithms, it is necessary to precompute and store a 3D distance map associated with the 3D surface model  $S$ . This distance map is a function that gives an approximation of the minimum signed euclidean distance  $\tilde{d}$  to the 3D surface model  $S$  from any point  $q$  inside a bounding volume  $V$  that encloses  $S$ . This signed distance function is positive for a point located outside the surface  $S$  and negative for a point located inside it. Therefore, the zero of the 3D distance function gives a unique implicit representation of  $S$ . The distance map that we use is built from just a collection of 3D points lying on the surface  $S$  and it is represented by an octree-spline which is a 3D adaptive and continuous distance map whose resolution increases near the surface, see [LSB91] for more details.

### Rigid 3D-3D registration algorithm

In most of applications, the 3D model is the result of a segmentation procedure applied to MRI or CT images of a reference structure and sensor data can be represented by a collection of 3D points obtained through segmentation of a second series of 3D images (CT, MRI, ...), through manual digitization of surface points (e.g., using an optical pointer), through 2D ultrasound image segmentation, or through range image acquisition.

In this case we look for the rigid transformation  $T(p)$ , that depends on a 6 components vector  $p$  (3 translation components and 3 Euler angles), between the surface  $S$  known in  $Ref_{3D}$  and a set of  $M_P$  points  $q_i$  known in  $Ref_{sensor}$  (we make the assumption that most of the points  $q_i$  match to the surface). We look for the parameters  $p$  that minimize an error function given by the sum of squares of distances between the surface  $S$  and the 3D sensor points transformed by  $T(p)$  in the 3D reference system. The criterion to minimize is

$$E(p) = \sum_{i=1}^{M_P} \frac{1}{\sigma_i^2} [e_i(p)]^2 = \sum_{i=1}^{M_P} \frac{1}{\sigma_i^2} [\tilde{d}(T(p) q_i, S)]^2 \quad (1)$$

where  $\tilde{d}(T(p) q_i, S)$  is the minimum signed distance between the surface  $S$  and the data point  $q_i$  transformed by  $T(p)$  in the 3D reference system.  $\sigma_i^2$  is the variance of the noise of the measurement  $e_i(p)$ . The minimization of the error function is performed using the Levenberg Marquardt algorithm [PFTV92]. Robust estimation is also performed by simply removing the outliers exceeding a given threshold and starting again new series of iterations.

### Rigid 3D 2D registration algorithm

Sensor data may be also 2D X ray or video projection images that have to be registered with a 3D surface model [LS95]. To perform such 3D 2D registration, the first step is to use the result of sensor calibration to calculate in  $Ref_{sensor}$  the projection lines  $L_i$  associated with some pixels  $P_i$  that lie on the external contour of the projections of the reference structure. We then use a least squares

formulation similar to the previous one, except that the criterion (1) is now replaced by

$$E(p) = \sum_{i=1}^{M_P} \frac{1}{\sigma_i^2} [\bar{d}_i(l_i(p), S)]^2, \quad (2)$$

where  $\bar{d}_i(l_i(p), S)$  is the minimum, along the projection line  $l_i(p)$ , of the distance, computed in the octree-spline distance map, to the surface  $S$ .  $l_i(p)$  is the result of transformation  $T(p)$  applied to the projection line  $L_i$ .

#### Non rigid 3D-3D registration algorithm

The data can also correspond to a structure slightly different from the model (e.g., registration of a patient's brain with an Atlas, or tracking of deformations). For such non rigid registration, we extend the rigid 3d-3d registration algorithm by a significant modification of the transformation  $T$ . Instead of 6 parameters, we have now hundreds of parameters  $p$  that describe the transformation between  $Ref_{3D}$  and  $Ref_{sensor}$ . Although we match surfaces, we represent the deformation as a volumetric transformation, that is represented by a second octree-spline. The coarsest level of the deformation encodes the global (e.g., affine) transformation between the two surfaces, while finer levels encode smooth local displacements which bring the two surfaces into closer registration. A 3D displacement vector is associated with each corner of each cube of the octree-spline built on the 3D data points. The xv coordinates of all these vectors constitute the parameters we are looking for. For any point  $q_i$  in  $Ref_{sensor}$ , the transformed point  $r_i = T(q_i, p)$  is computed in  $Ref_{3D}$  by interpolating the displacement vectors located at the corners neighboring the point  $q_i$ . Therefore, the parameters  $p$  can be seen as the coefficients of an adaptive 3D spline. The energy that we minimize in this problem is given by

$$E(p) = \sum_{i=1}^N \frac{1}{\sigma_i^2} [d(r_i, S)]^2 + \mathcal{R}_m(p), \quad (3)$$

where  $d(r_i, S) = d(T(q_i, p), S)$  is the minimum Euclidean distance from the point  $r_i$  to the model surface  $S$ . Compared to equation (1), we have added a regularization term  $\mathcal{R}_m(p)$  that makes the problem well posed (the solution is unique). This term is a combination of 0th and 1st order stabilizers that tend to minimize and smooth the amount of deformations. The minimization of this energy is much more complex than the previous one, and the use of the Levenberg Marquardt algorithm now requires to solve a very large sparse system. Therefore we have chosen to use a single step of preconditioned conjugate gradient descent using also hierarchical basis preconditioning techniques to make this process converge faster [SL94].

### 3 Results of registration algorithms in various clinical cases

#### MRI CT registration using 3D scalp surface

In this app MRI and CT surfaces. The Once this registered CT in

The applic an intermedia

#### Registrat

Using an surface points can acquire so points are reg accuracy is be which has been convergence b of this verteb patients [LST

#### Registrat

It is also possible to acquire 3D sition of the u ultrasound presence structure several image of planar curv itization and registered with been successful positioning i

#### Registra

The techn surfaces intera segmented on case less the technically va results obtain

#### 3D 3D e

To demon range data ac sitions, the d 10° (Fig 5a)

In this application the scalp surface of a patient has been segmented on both MRI and CT images. The 3D/3D registration algorithm is applied on these two surfaces. The convergence takes only one second on a DEC-alpha workstation. Once this registration has been performed, for each MR image, the corresponding resliced CT image is computed and superimposed as we can see on Fig. 1.

The application of the same algorithm for SPECT/MRI registration using an intermediary Range Imaging Sensor is also presented in [PLC+93].

#### Registration using a manual digitization of surface points

Using an optical 3D localizer makes it possible and easy to collect a set of surface points manually. For example, during an operation on spine, a surgeon can acquire some surface points lying on the posterior part of the vertebra. These points are registered with a CT surface model of the same vertebra. The overall accuracy is better than 1mm. This technique helps the surgeon drill a trajectory which has been defined on pre-operative CT images. Fig. 2 shows the algorithm convergence between 3D surface points of a vertebra and the 3D surface model of this vertebra. This technique has been applied for open spine surgery on 6 patients [LST+94].

#### Registration using an ultrasound probe (2.5D ultrasound pointer)

It is also possible to replace a simple 3D digitizing probe by an ultrasound probe to acquire 3D data points during an operation. The idea is to measure the position of the ultrasound probe in space by adding a sensor on top of a standard ultrasound probe. On each image, some points that lie on the edge of a reference structure such as a bone are segmented, and this process is repeated for several images. The result is a set of 3D points in  $Ref_{sensor}$ , arranged in pieces of planar curves. The whole system that encompasses the ultrasound image digitization and segmentation is named *2.5D ultrasound pointer*. Such data can be registered with a 3D surface model as in previous examples. This technique has been successfully used for percutaneous spine surgery [BTML93] and for patient positioning in external radiotherapy [TMB+94] (see Fig. 3).

#### Registration of a 3D Surface with 2D projections

The technique of 3D/2D registration has been tested on vertebra and skull surfaces interactively segmented on a pair of calibrated X-rays and semi-automatically segmented on CT data. Independent error measurements were obtained for both cases: less than 1mm for the vertebra, 2mm for the skull. This method has been technically validated for percutaneous spine surgery [SCLT92]. Fig. 4 shows the results obtained on a skull.

#### 3D/3D elastic registration between two faces

To demonstrate the local non-rigid matching we use two different sets of range data acquired with a Cyberware laser range scanner. In their initial positions the data sets overlap by about 50% and differ in orientation by about  $10^\circ$  (Fig. 5a). Here, the octree spline distance map is computed on the larger of

the two data sets (*george1*), and the smaller of the two data sets is deformed (*heid1*). After 8 iterations of rigid matching and 8 iterations of non-rigid affine matching, the registered data sets appear as in Fig 5b. We then perform 8 iterations at each level of the local displacement spline for 1 through 5 levels. The octree spline has a total of 5728 cubes for a total of about 17000 degrees of freedom. Even with our large number of parameters, the algorithm converges very quickly, because it is always in the vicinity of a good solution (a typical iteration at the finest level takes about 2 seconds). From Fig 5c, we see that the two data sets are registered well, except for the eyebrows.

#### 4 Conclusions

In this paper, we have presented the application of quite simple registration techniques that we developed in the past five years for the domain of Computer-integrated Surgery. We have shown on real examples that a methodology based on distance minimization between anatomical reference structures can be used efficiently with many different types of data (3D images, range images, 3D points digitized manually, 3D points extracted on 2.5D ultrasound images, X-ray projections, models). All the results presented in this paper were obtained in a few seconds on DEC-Alpha workstations. The accuracy required for the specific applications was obtained in all cases.

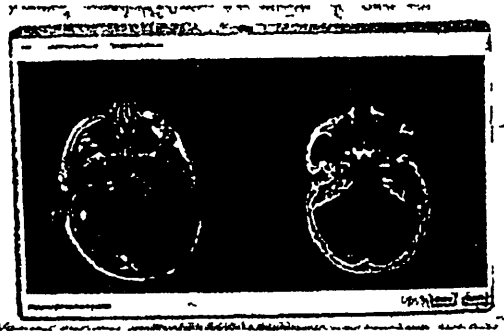


Fig 1 superimposition of MRI and resliced CT images after rigid 3D registration using the scalp surface. The result is visually perfect.

#### References

- [BTML93] C Barbe, J Troccaz, B Mazier, and S Lavalée. Using 2.5D echography in computer assisted spine surgery. In *IEEE* pp 160-161. San Diego 1993. IEEE Engineering in Medicine and Biology Society Proceedings.
- [Lav95] S Lavalée. Registration for Computer Integrated Surgery methodology, state of the art. In R Taylor, S Lavalée, G Burdea and R Mosges editors. *Computer Integrated Surgery (to appear)*. MIT Press 1995.



Fig 2 Rigid acquired manual vertebra segment



Fig 3 Rigid with a 2.5D ultrasound bone segment

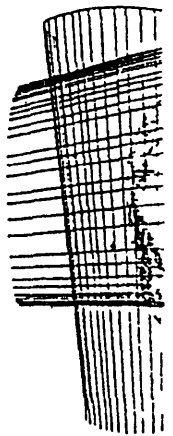


Fig 4 Conversion of a pair of lambda rays

sets is deformed  
 f non-rigid affine  
 en perform 8 it-  
 through 5 levels  
 ut 17000 degrees  
 orithm converges  
 lution (a typical  
 , we see that the

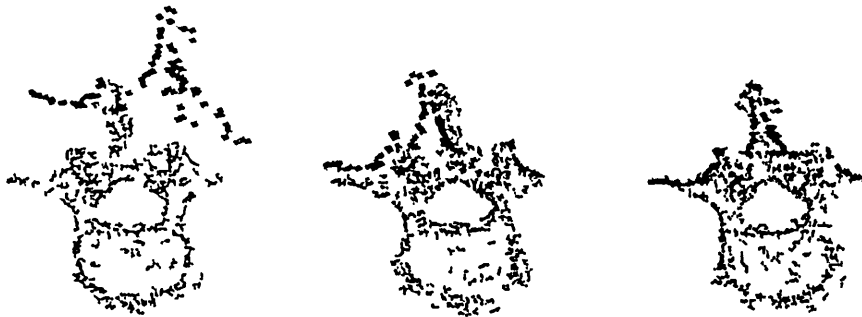


Fig 2 Rigid 3 D / 3 D registration during spine surgery, a set of surface points acquired manually with an optical 3D localizer converges towards the 3 D model of the vertebra segmented on pre-operative CT images

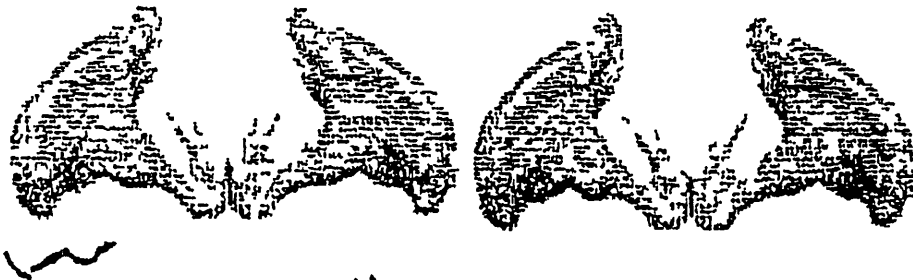


Fig 3 Rigid 3-D / 3 D registration during an operation 3D data points are acquired with a 2 5D ultrasound pointer and they are registered with a 3D model of the pelvis bone segmented on CT images This method gives a millimetric accuracy

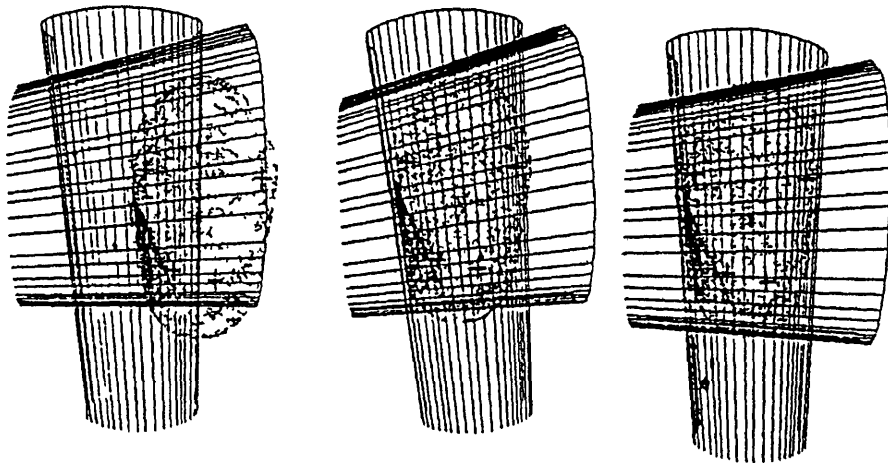


Fig 4 Convergence of 3 D / 2 D algorithm A set of projection lines issued from a pair of X rays of the skull converges towards the skull surface segmented on CT images

multiple registration  
 use of Computer-  
 methodology based  
 images can be used  
 images, 3D points  
 images, X ray pro-  
 ce obtained in a  
 d for the specific

D 3D registration

2 5D echography  
 San Diego, 1993  
 proceedings  
 ry methodology  
 id R. Mosges, edi-  
 s 1995

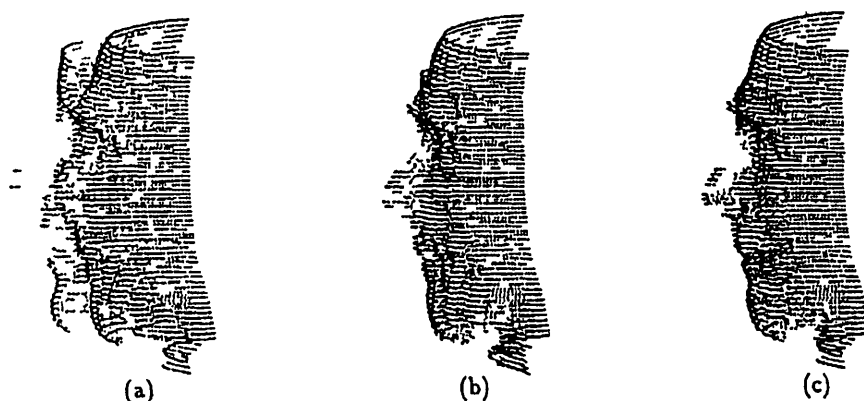


Fig 5 Elastic registration (a) initial position (b) affine registration (c) final result

- [LS95] S Lavallee and R Szeliski Recovering the position and orientation of free-form objects from image contours using 3-D distance maps *IEEE PAMI (Pattern Analysis and Machine Intelligence)*, to appear 1995
- [LSB91] S Lavallee, R Szeliski, and L Brunie Matching 3 D smooth surfaces with their 2 D projections using 3 D distance maps In *SPIE Vol 1570 Geometric Methods in Computer Vision*, pp 322-336, San Diego, CA 1991
- [LSB95] S Lavallee, R Szeliski, and L Brunie Anatomy based registration of 3-D medical images range images X ray projections 3 D models using octree-splines In R Taylor S Lavallee, G Burdea and R Moges editors *Computer Integrated Surgery (to appear)* MIT Press, Cambridge 1995
- [LST<sup>+</sup>94] S Lavallee P Sautot, J Troccaz P Cinquin and P Merloz Computer Assisted Spine Surgery a technique for accurate transpedicular screw fixation using CT data and a 3D optical localizer In *First International Symposium on Medical Robotics and Computer Assisted Surgery (MRCAS94)*, pp 315-322 Pittsburgh Pennsylvania, USA september 1994
- [PFTV92] W H Press B P Flannery S A Teukolsky, and W T Vetterling *Numerical Recipes in C The Art of Scientific Computing* Cambridge University Press Cambridge England second edition, 1992
- [PLC<sup>+</sup>93] O Perna S Lavallee G Champleboux, A F Joubert, J F Lebas, and P Cinquin Millimetric registration of SPECT and MR images of the brain without headholders In *IEEE EMBS Conf* pp 14-15 San Diego 1993
- [SCLT92] P Sautot, P Cinquin S Lavallee, and J Troccaz Computer assisted spine surgery a first step towards clinical application in orthopaedics In *14th IEEE RMBS Conf* pp 1071-1072 Paris November 1992
- [SL94] R Szeliski and S Lavallee Matching 3 D anatomical surfaces with non rigid deformations using octree-splines In *IEEE Workshop on Biomedical Image Analysis* Seattle June 1994 IEEE Computer Society
- [TLBM95] R H Taylor S Lavallee G C Burdea and R W Mosges *Computer integrated surgery (to be published)* MIT PRESS 1995
- [TMB<sup>+</sup>94] J Troccaz Y Menguy M Bolla, P Cinquin, P Vassal, N Laleb and S D Soglio Patient set up optimization for external conformal radiotherapy In A DiGioia T Kanade and R Taylor editors, *MRCAS 94 Medical Robotics and Computer Assisted Surgery* pp 306-313 Pittsburgh PA, september 1994

C

J B Ant

St

Abst  
image  
deriv  
the p  
In th  
ages  
based  
featu  
result

Keywords  
ometry, edg

## 1 Intro

Modern me  
gle patient  
informatio  
focus on th  
useful for e

Medical  
marking de  
which have  
latter categ

Matchin  
ilarity mea  
grey value  
to objects  
in image r  
Object bas  
based ima  
first, which  
not withou  
features fo  
ture measu  
applied to

When C  
forms a rid  
If a 'ridge  
feature im  
since the s  
suted for r  
have less v  
present to  
paper to cc



COMPUTER ASSISTED ORTHOPEDIC  
SURGERY BY MEANS OF  
INDIVIDUAL TEMPLATES  
ASPECTS AND ANALYSIS OF  
POTENTIAL APPLICATIONS

K Rademacher<sup>1</sup> H W Staudte<sup>2</sup> G Rau<sup>1</sup>

<sup>1</sup> Helmholtz Institute for Biomedical Engineering Aachen  
University of Technology Germany

<sup>2</sup> Department for Orthopedic Surgery District Hospital  
Marienhöhe Würselen Germany

**ABSTRACT** The paper discusses aspects of the concept of a computer integrated coupling of planning and execution in orthopedic surgery by means of individual templates. This preoperative non invasive procedure and technique for identification, localization and treatment of bone structures permits intraoperatively a geometrically exact reproduction of the workstrategy defined in the preoperative phase of surgical planning. After the general feasibility has been demonstrated in some exemplary applications, a detailed analysis of specific clusters of potential applications must be performed. This is an essential base for the ergonomic system design and synthesis of standardized solutions with practical relevance within clinical routine. General aspects as well as experiences concerning two exemplary in vitro and in vivo applications are discussed.

## I INTRODUCTION

There are many technologies in civil industrial environment which would be useful as tools within the surgical workprocess (concerning its primary effects). This exactly was the idea of Kwok et al. /5/ one of the pioneers in the field of medical robotics. Recent research activities concentrated on the related problems of multimodality, information processing, safety and sensor concepts as well as adequate robot control strategies /2, 3, 4, 12/.

An ergonomic analysis of the workprocess shows that the intraoperative process cannot be supported efficiently by simply planting high tech components into the complex workprocess of a surgical intervention.

One problem occurring in the course of surgical interventions is the matching of multidimensional information and action represented in different reference systems (geometries, forces, ...). In Orthopedic Surgery the motivation for translating an geometrically exact preoperative planning into the exact reproduction in relation to the reference system of the bone structures within the operating site is, for example, the necessity

- to aim a target point like a cystic cavity (defined entry point and trajectory)
- to omit sensitive structures like nerves or vessels
- to circumscribe relevant structures like marrow cavities or tumors
- to reconstruct optimal biomechanical conditions (e.g. by the definition of a first exact reference tibial cut in the case of knee TEP)
- to get a defined fit between implant and bone (e.g. hip TEP) or fragments of bone (e.g. craniofacial surgery)

The complexity concerning planning and execution for each of these criteria differs very much and depends on the requirements of each specific application.

The need for a better technical support results in the goals to reach

- higher precision, accuracy and efficiency
- shorter time of intervention and anesthesia with less blood loss
- reduction of stress and strain for the patient as well as for the operating team
- quality standardisation on an expert level even for a broad clinical application and last but not least
- the possibility to develop new less invasive operative strategies using new support systems /10/

Working on rigid bone structures, the problem of deformation or dislocation as it occurs in the case of soft tissue targeting is not relevant. But many problems remain.

If we want to profit from the possibility arising from digital imaging and 3D reconstructions, we have to provide functionalities and user interfaces which allow the surgeon as a non technical user to integrate his medical knowledge. He must be able to perform the surgical planning at least as efficient as he is used to do it in the conventional way. Then we have to provide a possibility to store this planning and to transfer it into the operating room. Also this step must be designed taking into account ergonomic aspects and the boundary conditions of clinical routine. Finally, the exact reproduction of the planned work on bone has to be supported. The surgeon must be able to control the intraoperative work on bone anytime. All effects of a technical solution must be compared with each of the goals mentioned above. Higher precision should not necessarily result, e.g. in a higher intraoperative workload. We have to investigate how and in which sequences and applications advanced technical means could improve surgical therapy. Generally holds that a simple and robust (not necessarily computerbased) solution providing an optimal therapeutic result is the best one.

## II THE PRINCIPLE OF INDIVIDUAL TEMPLATES

The intraoperative workprocess should not be loaded additionally by time consuming interactions with complex technical system components. Starting with this preliminary essence of our ergonomic worksystem analysis, we developed the concept of individual templates replacing the *intraoperative* robot by a *preoperative* NC milling machine. Individual templates are provided to store the information defined during the preoperative surgical planning in a way that it can be used intraoperatively in a very simple and even familiar manner.

In orthopedic surgery, standard templates and toolguides exist mainly for interventions in the area of extremities. But their positioning and orientation in spatial relation to bone is not exactly defined and reproducible according to the preoperative planning. In most cases, averaged geometrical relations of anatomical landmarks are assumed. As an exact positioning in spatial relation to the bone can be crucial to achieve, for example, physiological biomechanical conditions, this seems to be really suboptimal. For pathologically deformed bone

structures and for many interventions in the area of spine or pelvis (mainly implant independent interventions) no toolguides are available

But templates are familiar tools in orthopedic surgery. In principle the only missing information is the exact correlation between the reference systems of the bone structure, the surgical planning and the toolguides. Additionally individual geometries like backside contours or other 3D structures defined by the individual surgical planning should be reproducible (for example for limiting cutting depth). This bottleneck can be opened providing individual templates.

The idea of individual templates is to add the missing information and to provide an easy to use "hardware based 3D/3D surface matching between the reference systems of the operating site, the computerbased model and the planning of the intervention.

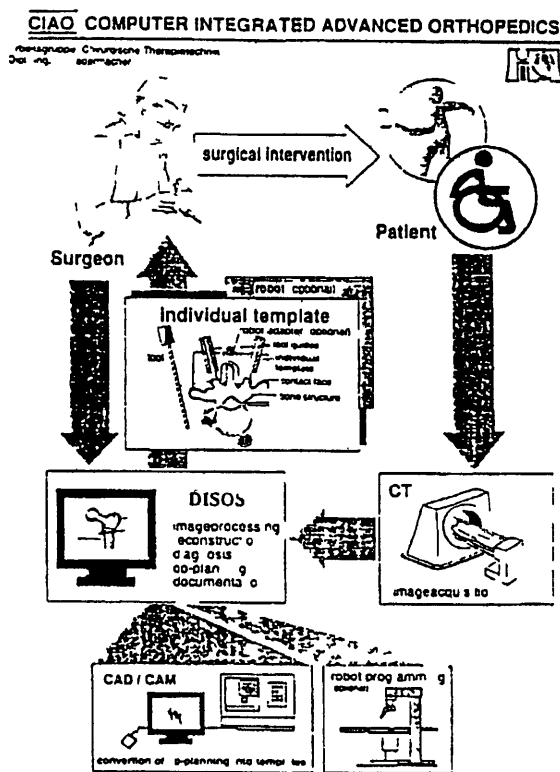


Fig 1 The concept of computer assisted orthopedic surgery by means of individual templates

Individual templates are generated on the base of 3D reconstructions of the bone structures extracted from CT image data and depending on the individual preoperative surgical planning. Negative hardcopies of small segments of the natural surface of bone normally prepared by the surgeon in the course of a conventional operation are defined and manufactured preoperatively by means of CAD/CAM technology. The contactfaces are milled in small semi finished plastic blocs of PMMA or PC adapted to the standard size of the surgical portal depending on the kind of intervention. Apart from these contactfaces already simple

toolguides like jig bushes, sawguides and even 3D-copying devices can be adapted or fixed in or onto this basic body of the individual template. Intraoperatively the spatial relation of bores, cuts or milling to the bone structure defined by the preoperative planning can be reproduced simply by putting the template formclosed on bone. In this way the surgeon is guided intraoperatively according to his preoperative planning, reducing time for execution and freehand work to minimum and increasing precision and accuracy. Of course this principle could also be used to define the correlation between the reference system of any bone structure and the tool coordinate system of a robot or passive manipulator such as described in [7].

Until now we investigated and improved the technical and medical feasibility of our concept with a series of in vitro experiments and in vivo investigations. The interventions could be performed already satisfactorily by means of the intraoperatively easy to use individual templates with integrated tool guides, so that an application of robotic solutions seems not to be evidently indicated until yet. In the next section we want to give some examples illustrating the concept of individual templates.

### III. EXAMPLES OF POTENTIAL APPLICATIONS

For our initial experiments with anatomical preparations we choose the example of a transpedicular drilling in a vertebra necessary for the fixation of pedicle screws, e.g. in the course of scoliosis therapy. Conventionally drilling is piloted by first introducing a thin metal probe into the estimated bone channel. The positioning is controlled by intraoperative biplanar x-ray imaging. The fixation of the screws in cortical bone of the pedicles as well as of the vertebral body is essential for a good anchoring. But the screws should not break through the ventral surface of vertebral body. The direct neighborhood of the spinal cord, roots and of blood vessels imply quite a high risk.

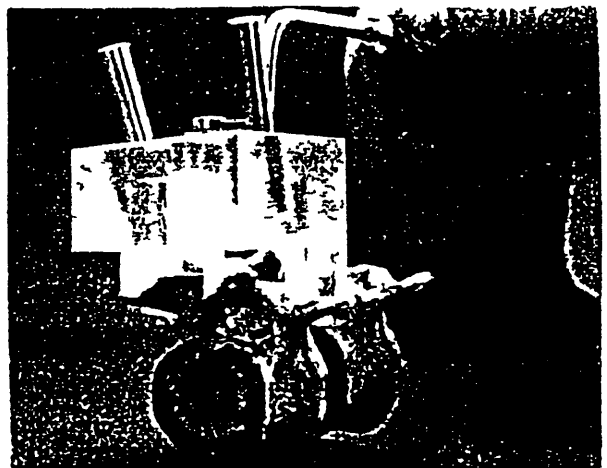


Fig 2 3D/3D matching of the computerbased model and the operating site can be reached by simply putting the template on bone.

Based on the 3D reconstruction of a vertebra and in consideration of the mentioned medical boundary conditions

we defined an individual template with contactfaces reflecting segments of the bone surface normally prepared in the course of conventional scoliosis surgery

Jig bushes integrated into this individual template defined exactly position orientation and depth of the transpedicular bore according to the surgical planning within a tolerance of less than 1 mm

There are many other examples for this "1D" application consisting in the preoperative definition of a linear trajectory between an entry and a target point. As a second potential application we simulated the puncture and refilling of a cystic cavity in femoral head. In this case a repositioning osteotomy can be necessary for turning the cystic region out of weight bearing area. Using individual templates the cystic cavity can be aimed precisely and the osteotomies can be reproduced according to the surgical planning.

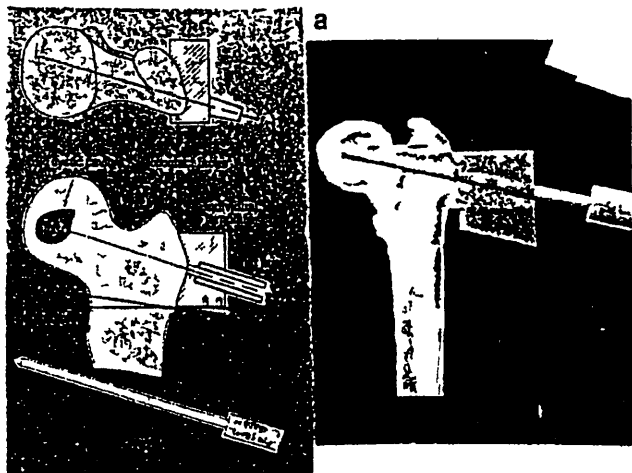


Fig 3 a) The principle of a puncture of a cystic cavity in femoral bone combined with repositioning osteotomies b) CAD simulation //

In total knee arthroplasty an initial cut in tibial bone serves as a reference for the succeeding steps of work on bone. Its exact positioning in spatial relation to the bone axes is crucial for the optimal success of therapy. Furthermore cutting depth should be limited to the backside surface of bone to conserve the posterior cruciate ligament as well as nerves and vessels going through the hollow of the knee.

Figure 4 shows an individual template for this category of interventions. The cutplane is defined by a sawguide fixed onto the basic body of template.

The individual template with its contactfaces is adapted to the surgical portal as well as to the specific medical and technical boundary conditions (e.g. concerning the importance of the axis of bone).

Additionally a 2D copying device limits cutting depth according to the backside contour of the tibial bone. A known geometry and kinematic of the saw (e.g. a TUKE saw) as well as a calibrated copying cam have to be assumed. Whereas the conventional templates working on the base of intramedullary nails are suitable in the case of undeformed bone, this new technique is useful especially in the case of pathologically deformed bone structures.

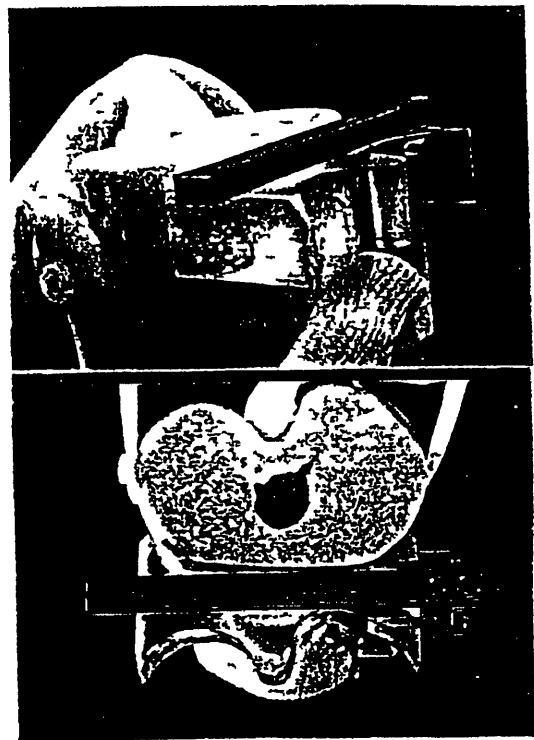


Fig 4 Individual template for the total knee arthroplasty

But this technique also opens new doors towards new concepts and strategies in therapy. For example we investigated the possibility to perform the correction of a scoliosis up to 45° COBB angle by means of repositioning osteotomies of the vertebral bodies without a lasting stiffening of spine. Individual templates would be necessary to reproduce intraoperatively the position orientation and depth of the osteotomies as well as of the transpedicular bores which have to be performed uniquely through a ventral portal //

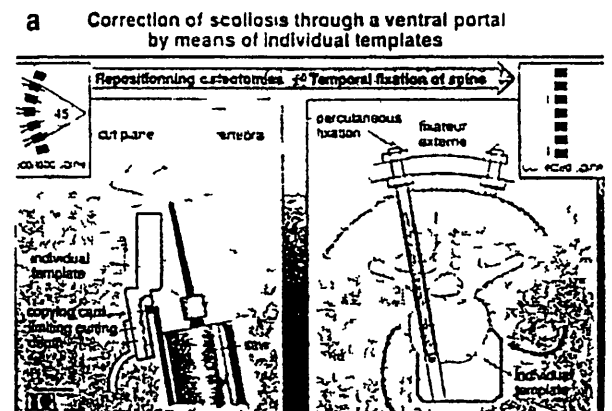


Fig 5 a) The principle of a scoliosis therapy by means of repositioning osteotomies //



Fig 5 b) individual template with a contactface to vertebral bone and a copying device limiting cutting depth to the backside surface of vertebral body

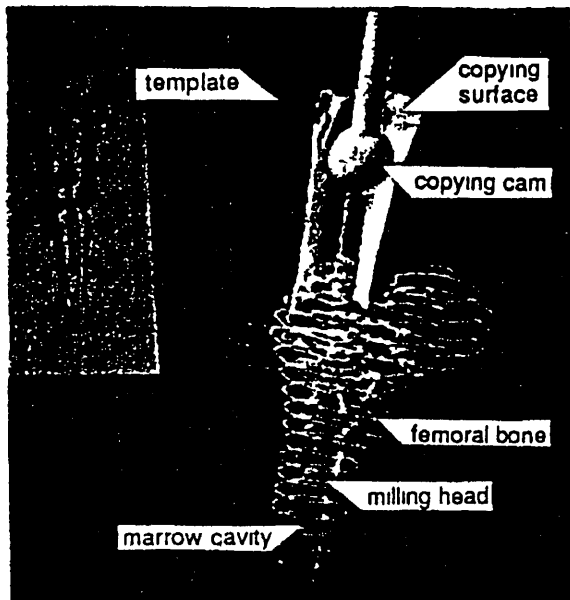


Fig 6 Principle and CAD Simulation of the 3D preparation of the marrow cavity in femoral bone

Last but not least individual templates can be used for the intraoperative reproduction of 3D work on bone. Fig 6 shows a CAD simulation of the preparation of an implant cavity in femoral bone. A 3D copying device representing the relevant geometries (like e.g. the shape of an implant shaft) is rigidly adapted to the basic body of an individual template. The milling tool is equipped with a compact parallel guide and a copying cam. Through the defined spatial relation of this individual template to bone, the surgeon is guided according to his preoperative planning by simply moving the copying cam (together with the milling tool) within this copying pot.

In the following we want to point out some more general aspects. We discuss two very different but nevertheless very typical examples for the analysis of potential applications being an essential part of our recent work.

#### IV GENERAL ASPECTS AND ANALYSIS OF POTENTIAL APPLICATIONS TWO EXAMPLES

To be of some relevance and benefit for the clinical routine, technical solutions are of limited value only. But the problems to solve for getting standardized solutions with necessary and sufficient functionalities practicable within clinical routine are highly interdependent and complex. Task allocation (man/man as well as man/machine), information flow, user interaction, quality assurance, manufacturing devices and infrastructures are only some aspects of an ergonomic system design. The exact *analysis* of potential applications and related work systems as an essential base of an ergonomic design approach is one main subject of our ongoing research [9].

Starting with analysis of complication reports, intraoperative work processes as well as in interviews with medical experts, we identify an increasing number of possible applications. The suitability and the requirements concerning geometries, accuracy, topologies, materials, etc. must be clarified. At least the ratio of costs to benefit will decide about the extent of application within clinical routine. For the delimited applications, we must analyse and characterize exactly the medical and technical boundary conditions, interdependences and bottlenecks, conventional tools, infrastructures and techniques concerning surgical planning and intervention. In a second step, the results must be classified and transformed into clusters of similar templates which have to be standardized concerning their geometries, accuracies, topology, material, and relating toolguides. In consequence, the related chain of image (geometrie) acquisition, surgical planning, and finally the design and manufacturing of the individual templates as well as the related manufacturing devices, semifinished material, and infrastructures can be standardized.

Concerning, for example, the standardisation of surgical planning and computer-assisted design of individual templates for specific interventions, we investigated the example of a puncture and refilling of a cystic cavity in femoral head. As a work platform, we used a conventional CAD/CAM system. For the definition of the contact faces, two cutplanes and one bore [7] as well as the design and preparation of the NC program generation for manufacturing the corresponding individual template, a proficient user needs about 50 to 60 minutes. Through the standardisation and makroprogramming of semifinished templates (3 sizes), toolguides, workviews, functionalities, and user interaction sequences, the same procedure performed by a nontechnical user takes about 3-5 minutes without any restriction concerning the required result.

But the complexity of individual templates and toolguides as well as the related functionalities, user interaction sequences, and possibilities of standardisation strongly depend on the requirements of each specific intervention.

In a second step, the delimited functionalities can be implemented into our desktop 3D surgical planning system DISOS [7, 8] (fig 7). We are designing with special respect to the surgeon as a non-technical user.

Apart from pages for data management, diagnosis, image

processing and a general planning page with basic tools for simulating and planning work on bone structures. DISOS will provide separate workpages optimized for specific interventions with individual templates. The system represents a workplatform for the evaluation and selection of concepts and solutions by means of in vitro and in vivo investigations.



Fig 7 DISOS (Desktop Imageprocessing System for Orthopedic Surgery) definition of a cutplane on the general planning page

Concerning the question of task allocation between man/man and man/machine one aim is to reach an optimal level of automation and to standardize as well as to integrate as far as possible (and reasonable) technical CAD/CAM features within the planning system.

We want to present two typical examples for our actual investigations.

a) Tripleosteotomy of pelvic bone by means of individual templates

The first surgical intervention with individually designed and manufactured templates has been a tripleosteotomy for repositioning glenoid cavity of the hip joint. It already confirmed the concept [7] (Fig 8). We used three independent templates for the three osteotomies and one bore. The intervention was planned by the surgeon with DISOS and the data was transmitted to the CAD/CAM device. The intraoperative x ray control showed that the cutplanes and the bore defined by the templates were exact 3D reproductions of surgical planning. An ongoing clinical evaluation of this approach will include about 20 cases of this (not very frequent) intervention.

In the meantime we are working out a detailed characterisation and standardisation of this intervention. CT scan is already today a standard imaging modality to perform surgical planning. It can be standardized by means of anatomical landmarks concerning ROI limitation and standard bone image reconstruction algorithms with low mAs products. To minimize radiation we are investigating the use of larger slice distances up to 8 mm. Three cuts (os pubis, os iliacus, os ischiaticus) and one bore (to fix a

handle for manipulating the isolated fragment of glenoid cavity) have to be performed. The pubis cut is not critical and can be carried out freehand. The intraoperative three-dimensional reproduction of the other cuts and the bore is much more difficult because of the very small independent surgical portals, the complex geometry of pelvic bone and the necessity to omit sensitive structures like the glenoid cavity and obturatorius nerves. Conventionally this is performed in time-consuming iterative procedures under repeated or permanent X-ray control. Position and orientation of each cut and of the bore is defined individually but under consideration of certain standards concerning anatomical landmarks, topographies and spatial relationships.

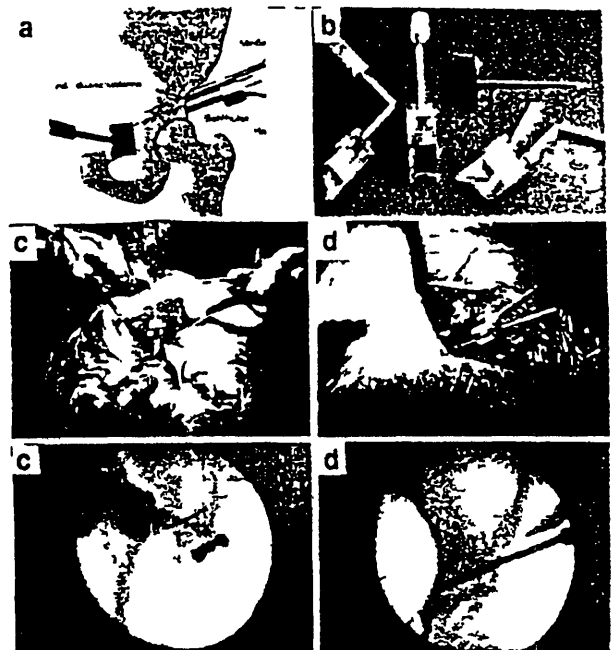


Fig 8 Tripleosteotomy of pelvic bone by means of individual templates: a) the principle, b) the templates, c) d) intraoperative use and x-ray control on os ischiaticus (c) and os iliacus (d).

The semifinished templates have very simple geometries which could be provided in 2 or 3 sizes typical for each cut. A jig bush (only its length must remain variable) is integrated into the template defining the cut on iliac bone. Thus design and manufacturing of these templates is easy to standardize. In consequence we are working on concepts for a low cost, easy to use manufacturing device specialized and adapted more efficiently to the specific process of manufacturing various standardized templates. Our investigations concerning manufacturing modalities for individual templates also included methods like stereolithography or solid modelling. But these methods do not seem to be adequate solutions concerning a rational, accurate and economic manufacturing.

Finally the individual templates are sterilized and transmitted to the operating room together with the conventional surgical instruments. The reproduction of the preoperative planning is performed by putting templates formclosed on bone. X-ray imaging normally is only necessary for a single

final check and for documentation

#### b) Decompression in cervical spine

The second very different example is a decompression in cervical spine. This intervention is much more delicate concerning the ergonomic design of the necessary and sufficient functionalities and tools for the preoperative planning as well as the intraoperative execution. Mainly the aspect of quality assurance gets much more important. 2D and 3D copying devices must be provided for limiting cutting depth. The required accuracy is at the limit of CT image resolution. Intraoperative control of the work on bone is much more difficult. The performance of decompression procedures relies on CT scan and MRI imaging techniques. However, after diagnosis/staging of stenosis, the execution of the intervention has to be carried out freehand moving drills, burrs and other tools. Our technique of creating individual templates for the work on bone guided by the preoperative surgical planning could facilitate tasks in the vulnerable region near the medulla. The analysis and optimization of this intervention is one subject of our actual work. After the analysis of the conventional methods and the delimitation of its bottlenecks, exemplary solutions for the following steps of process have been generated to be able to perform a first simulation and evaluation of this approach:

- image acquisition (CT)
- evaluation of degree of stenosis (DISOS)
- planning of the amount of decompression necessary dorsally or ventrally (DISOS)
- precising details of drilling and cutting (DISOS) (fig 9)
- exemplary design of templates (CAD) (fig 9)
- manufacturing of individual templates (CAM)
- intraoperative recalibration of the milling tool
- simulation of an intervention with application of templates reducing freehand work to minimum (OR) (fig 9)
- evaluation of accuracy, delimitation of points to optimize and of necessary functionalities concerning CT, DISOS, CAD/CAM and OR

The techniques of both a dorsal open-door decompression (a Hirabayashi type) and an anterior transcorporeal decompression have been demonstrated on cadaver material [11]. The individual templates with its contactfaces and 3D copying faces are manufactured of PC (Polycarbonate), thus being suitable to be sterilized by conventional steam. A circular jig plate (fig 7) aids the surgeon to maintain a perpendicular mode of cutting. A small copying cam is fixed onto the mill (fig 7). After assembly, the template finds its position on the surface of the cervical spine. An initial bore was used to check and recalibrate the length of the milling tool in relation to the copying cam. This bore was guided already by the individual template, but the milling head was advanced very carefully until the vertebral lamina was slidely perforated without an injuring of the dura.

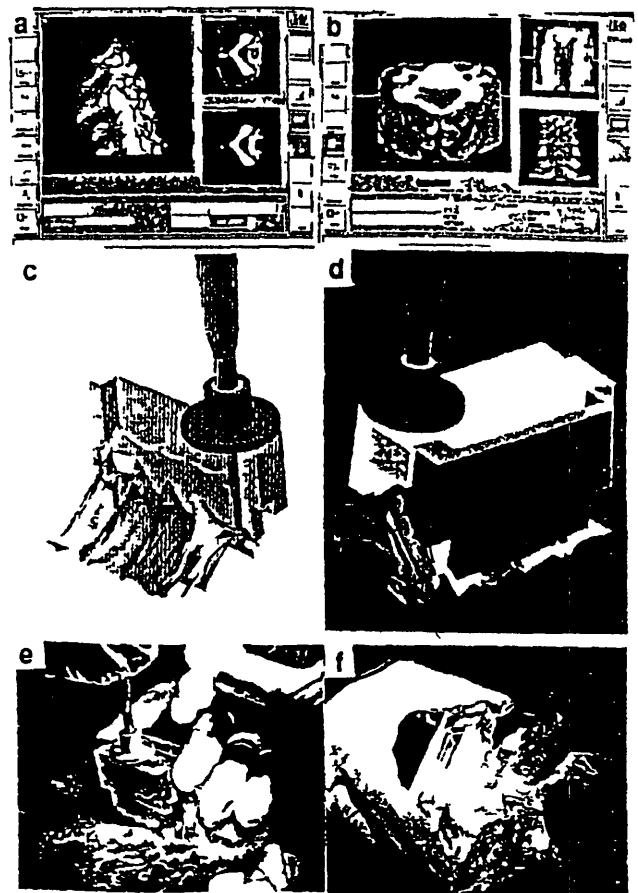


Fig 9 a) evaluation of degree of stenosis (DISOS)  
b) Planning of an open-door laminaectomy with DISOS (C3-C6 from dorsal)  
c) CAD simulation demonstrating the principle of 3D-depth limitation  
d) template for an intervention through a dorsal portal after assembly  
e) intraoperative application  
f) intraoperative application of a template for a transcorporeal decompression through a ventral portal

The length of the milling tool and the position of the copying cam on the copying surface was checked. After this recalibration, both sides of the laminaectomy could be performed very quickly. The milling tool is moved perpendicular to the template and is guided by the profile of the copying profile or surface respectively. Several layers of bone are subsequently removed to less than 1 mm on the left and about 1 mm on the right (leaving the anterior cortical layer intact) according to the preoperative planning. The milling tool perforated at two points of the planned path (without damaging dura) on the left lamina. Further improvements concerning the shape of templates, the topography of contactfaces, manufacturing of templates as well as the intraoperative technique for repositioning of spine and recalibration (final check) of the milling tool during intervention have to be performed. After this fundamental work has been done, this category of intervention should run into the process of standardization.

#### IV CONCLUSION

Our concept of a computer based coupling of the preoperative planning and the intraoperative execution in orthopedic surgery based on the procedure of individual templates has been successfully tested in various in vitro experiments and in vivo applications until now /6 7/ The number and complexity of potential applications as well as the aim to integrate solutions into the related work processes require a fundamental ergonomic system design approach An exact analysis modelling and simulation of delimited applications the related work processes and systems combined with the evaluation of exemplary solutions within simulation environments or in field test are fundamental elements of an synthesis and integration of complex technical solutions like computer assisted surgery systems within the surgical work process We identified many potential applications for the technique of individual templates Together with other approaches in the area of computer assisted orthopedic surgery it may become one element of the orthopedic toolbox of technical means But to be of some relevance and benefit for clinical routine we have to provide a certain level of standardization and rational integration of system components In this sense the detailed analysis of the medical and technical boundary conditions procedures and technical means for each specific application of individual templates is an essential part of our actual work.

#### V ACKNOWLEDGEMENTS

We would like to thank Dr A Stargart Departement of Radiology Aachen University Hospital as well as Dr A Prescher and Dominik Broers Institute for Anatomy Aachen University of Technology for the friendly and helpful cooperation

#### VI REFERENCES

- /1/ Bernotat R and G Rau Ergonomics in Medicine " In Perspectives in biomechanics (Reul Ghista Rau eds) Harwood Acad Publ NY 1980 381 398
- /2/ Cinquin P J Demongeot J Troccat St Lavallée G Champlébourg L Brunie F Leitner P Sautot B Mazier A Perez M Djaid T Fortin M Chenin and A Chapel "IGOR Image Guided Operating Robot Methodology Medical Applications Results Innovation et Technologie en Biologie et Médecine Vol 13 No 4 1992 374 393
- /3/ Davies B L R D Hibberd W S Ng A G Timoney and J E A Wickham Mechanical Constraints The Answer to Safe Robotic Surgery ? Innovation et Technologie en Biologie et Médecine Vol 13 No 4 1992 426 436
- /4/ Fadda M S Martelli M Dario M Marcacci A Visani and S Zaffagnini First Steps towards Robot Assisted Discectomy and Arthroplasty Innovation et Technologie en Biologie et Médecine Vol 13 No 4 1992 395 408
- /5/ Kwok Y S J Hou E A Jonckheere S A Hayati A Robot with improved Absolute Positioning accuracy for CT guided Stereotactic Brain Surgery IEEE Transactions on Biomedical Engineering Vol 35 No 2 Feb 1988
- /6/ Radermacher K Rau G Staudte H W CIAO Computer Integrated Advanced Orthopedics to appear in Proceedings of the 2nd European Conference in Engineering and Medicine Stuttgart Germany April 25 28 1993
- /7/ Radermacher K Rau G Staudte H W Computer Integrated Orthopedic Surgery Connection of planning and execution in surgical intervention in Taylor R Lavallée St Burdea G C Moesges R Computer Integrated Surgery MIT Press Cambridge MA (in press)
- /8/ Radermacher K H W Staudte G Rau Computer Assisted Matching of Planning and Execution in Orthopedic Surgery 15th Annual International Conference IEEE EMBS Seite 946 947 San Diego 1993
- /9/ Rau G K Radermacher B Thull C v Pichler Aspects in ergonomic system design applied to medical work systems in Taylor R Lavallée St. Burdea G C Moesges R Computer Integrated Surgery MIT Press Cambridge MA (in press)
- /10/ Rau G K Radermacher Minimal invasive surgery using advanced technologies Medical Technology International Cornhill 1993 pp 65-69
- /11/ Staudte H W K Radermacher G Rau Technique for better execution of CT scan planned decompression in the cervical spine to appear in Proc 4th Common Meeting of the Cervical Spine Research Society June 29 July 2 1994 Rome Italy
- /12/ Taylor R H H A Paul C B Cutting B Mittelstadt W Hanson P Kazanzides B L Musits Y Y Kim A Kalvin B Haddad D Khoramabadi and D Larose Augmentation of Human Precision in Computer Integrated Surgery Innovation et Technologie en Biologie et Médecine Vol 13 No 4 1992 451 468



## A Novel Approach to Computer Assisted Spine Surgery

Lutz-P Nolte\*, Lucia J Zamorano<sup>†</sup>, Zhaowei Jiang<sup>†</sup>, Qinghai Wang<sup>†</sup>,  
Frank Langlotz\*, Erich Arm\* Heiko Visarius\*

\* M E Müller Institute for Biomechanics, University of Bern, Bern, Switzerland

<sup>†</sup> Department of Neurological Surgery, Wayne State University, Detroit, MI, USA

**Introduction** Surgical techniques and precision often rely on the identification of predefined targets with the help of anatomic landmarks and on intra-operative use of image intensifiers. However, because there is no direct link between the image information, the accessible anatomy and the action of surgical instruments, several potential problems and possible complications are still involved. Our novel approach to this problem enables the real-time intra-operative image localization of surgical instruments. This was achieved by combining image-guided stereotaxis with advanced opto-electronic position sensing techniques. Several software modules allowing efficient image data processing, surgical planning and visualization of various intra-operative procedures have been developed.

The basic principles of stereotaxis have already been introduced early this century (Clarke and Horsley 1906). However, without recent advances in three-dimensional image reconstruction (Hounsfield et al 1973) and computer science, this technique could not be applied effectively to clinical problems. Since the end of the seventies, several systems for stereotactic tumor neurosurgery have been developed and clinically established (Kelly 1991). Although applications in the field of neurosurgery are still being developed, relatively few attempts have been made to apply this technique to orthopaedic surgery in general (Matsen et al 1993, Paul et al 1992) and to spine surgery in particular (Sautot et al 1993).

Spine surgery is frequently performed using a posterior approach. The spinal anatomy allows exposure of the bony posterior elements only, although several surgical procedures involve the anterior vertebral body as well. The insertion of pedicle screws through the pedicle and into the vertebral body for posterior spinal fixation is one clinically relevant example. Pilot holes are prepared and screws are inserted without any direct visual control. Image intensification is used but due to the associated radiation and difficulty of use, this system cannot be applied during the entire screw insertion period. The variability in width, height, and spatial orientation of pedicles consequently leads to a considerable rate of misplaced screws (Krag 1991). This not only limits anchoring potential but might endanger the integrity of the surrounding anatomy, i.e. spinal cord, nerve roots, and abdominal vessels (Esses et al 1993). A reliable and accurate system which allows real-time linkage of medical images and the operation field will minimize these surgical risks.

**Description of the system** The aim of the present study is to introduce a new system for pre-operative planning and simulation and for intra-operative guidance during spinal surgery. For this purpose, stereotactic concepts based on three-dimensional tomographic image reconstruction have been combined with a space digitizing system.

As usual, all stereotactic components, surgical instruments (drill pointer, probes, etc.), all anatomic structures, e.g. the vertebrae, and their medical images are treated as rigid bodies. The location and orientation of a rigid body in space can be completely defined when the location of three or more non-collinear points on the body with respect to a global space-fixed coordinate system (COS) are known. In practice, the orientation and origin location of a body-fixed COS with respect to the global COS are used to describe rigid body positions.

Various technologies exist to track and/or control rigid bodies in space. In medical applications, for example articulated arms or robots as well as infrared and acoustic space digitizing systems are currently in use (Kelly 1991, Matsen et al 1993, Paul et al 1992, Sautot et al 1993, Zamorano et al 1993a & 1993b).

During the design of our stereotactic system, the following requirements for the space digitizer were defined: (a) established surgical procedures should not be principally affected or significantly altered, (b) the existing surgical tool set should not be altered but only slightly modified, (c) the system's accuracy should be at least one order of magnitude better than the desired overall accuracy, and (d) it should be fast enough to allow real-time instrument control and visualization in the medical image.

Based on these criteria, we selected an opto-electronic space digitizer. The contactless system can track up to 256 pulsed infrared light-emitting diode markers (LED) with a maximum sampling rate of about 3200 markers per second. The camera can locate each LED with an accuracy of 0.15 mm within a field of view of 1.0 m x 1.2 m and a distance of 2.0 m. By attaching at least three markers onto each rigid body using so-called probes, the rigid body's location and orientation in space can be determined.

For the real-time display of a rigid body within a medical image, the position of the rigid body in the image COS is necessary. For example, it is necessary to display the drill tip during the drilling of a pilot hole through a pedicle. To accomplish this, the rigid body is "transformed" from the global COS to the image COS (Goldstein 1980). This matching of a COS in the operation theatre to a COS of a



tomography is termed 'skeletal registration'. In general matching methods can be divided into four categories (van den Elsen et al 1993) (a) control point or paired point methods (point to point matching) (b) moment based methods, (c) structure based methods, and (d) similarity optimization based methods

We chose a point-to-point method using a nonlinear iterative algorithm in combination with a surface matching refinement with intermediate visual checks resulting in a four step procedure of skeletal registration. The point-to-point step is based on four to six characteristic anatomic landmarks points which are digitized in both the CT/MRI image and on the vertebra. The resulting coordinate transformation may lack accuracy due to digitization errors in both systems and to difficulty in precisely identifying anatomical locations. However, this rough solution can be used as a starting vector for the iterative surface matching refinement. Intra-operatively, any 20 to 60 points on the vertebral bony surface are digitized and pre-operatively the vertebral surface had been detected from the tomographic image data and a minimum distance analysis in the voxel world had been carried out. Nonlinear matching algorithms (Jiang et al 1992) are then used to provide the required coordinate transformation.

Pre-operative data acquisition, image reconstruction, operation planning and simulation and real-time display of the location of surgical instruments were accomplished using the modified Neurological Surgery Planning System NSPS (Jiang et al 1993, Nolte et al 1993 & 1994, Zamorano et al 1993a & 1993b). The modified program will be referred to as OSPA (Orthopaedic Surgery Planning System). Data from tomographic images (MRI and CT) and projective images (X-ray, angiography) can be utilized as basis for the planning. Multi-modality abilities allow the use of all possible image sources simultaneously.

**Surgical Procedure** As a first clinical application, the proposed system for computer-assisted surgery was utilized for the insertion of spinal pedicle screws. This procedure involves distinct pre-operative and an intra-operative phases. *Pre-operatively* the OSPA Basic Module reconstructs and displays three-dimensional vertebral images or multiple two-dimensional views, i.e. frontal, sagittal and transverse sections from tomographic image data (MRI or CT) of the vertebrae to be operated on. This enables planning of the surgical intervention.

An approximate insertion axis for the pedicle screw is defined by digitizing its entry and target points. Equidistant sections perpendicular to the trajectory axis are generated and displayed. The chosen trajectory can then be interactively optimized and re-defined. This procedure is not mandatory but was found to be particularly helpful for planning the alignment of the overall fixation construct. In this procedure all intended pedicle have their optimized with respect to one another.

For the definition of body-fixed COSs on the vertebra and the surgical instruments, custom marker probes were designed (Fig 1).

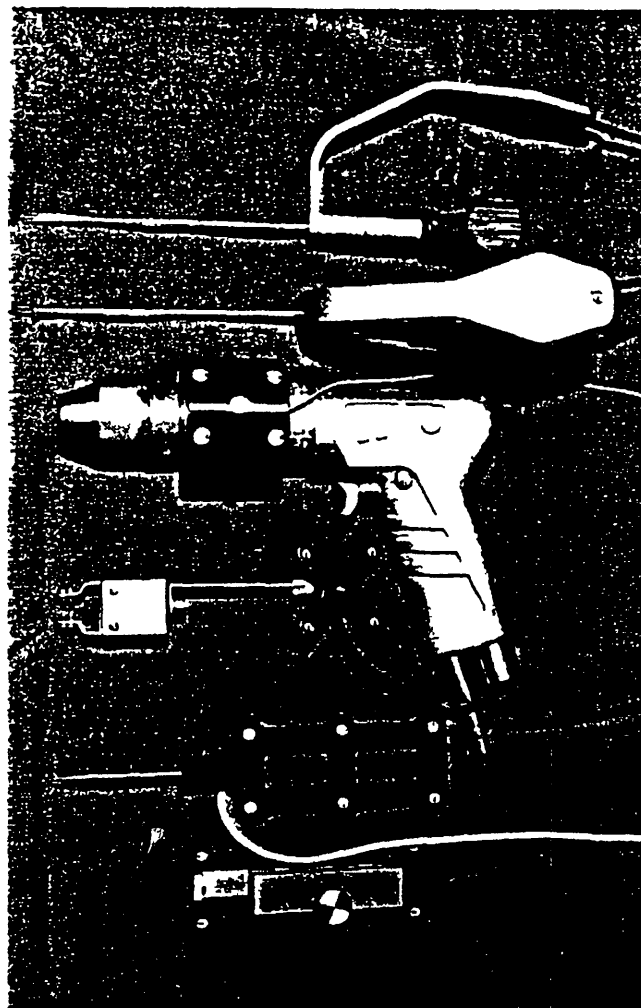


Figure 1

All *intra-operative* digitizations are then performed with respect to the local vertebral COS defined by the so-called Dynamic Reference Base (DRB).

The surgical situs is exposed in a standard posterior approach. The spinous process provides a secure anchoring point for the DRB carrying four markers. A space pointer with six markers is used to digitize specific anatomic landmarks on the accessible posterior elements. These points are located in the CT/MRI image accordingly in order to perform a point-to-point matching between the "real world" (vertebra) and the "virtual world" (image). Points on the dorsal aspect of the transverse processes, the facet joints and the spinous process usually provide a sufficiently accurate matching result. However, a refined surface matching digitizing any 20-40 points on the bony surfaces of the posterior elements is available and is performed in cases of inadequate accuracy of the point-to-point matching.

For control and security purposes the OSPA tracking module automatically displays any point being digitized on the vertebral surface in real-time in the tomographic image.

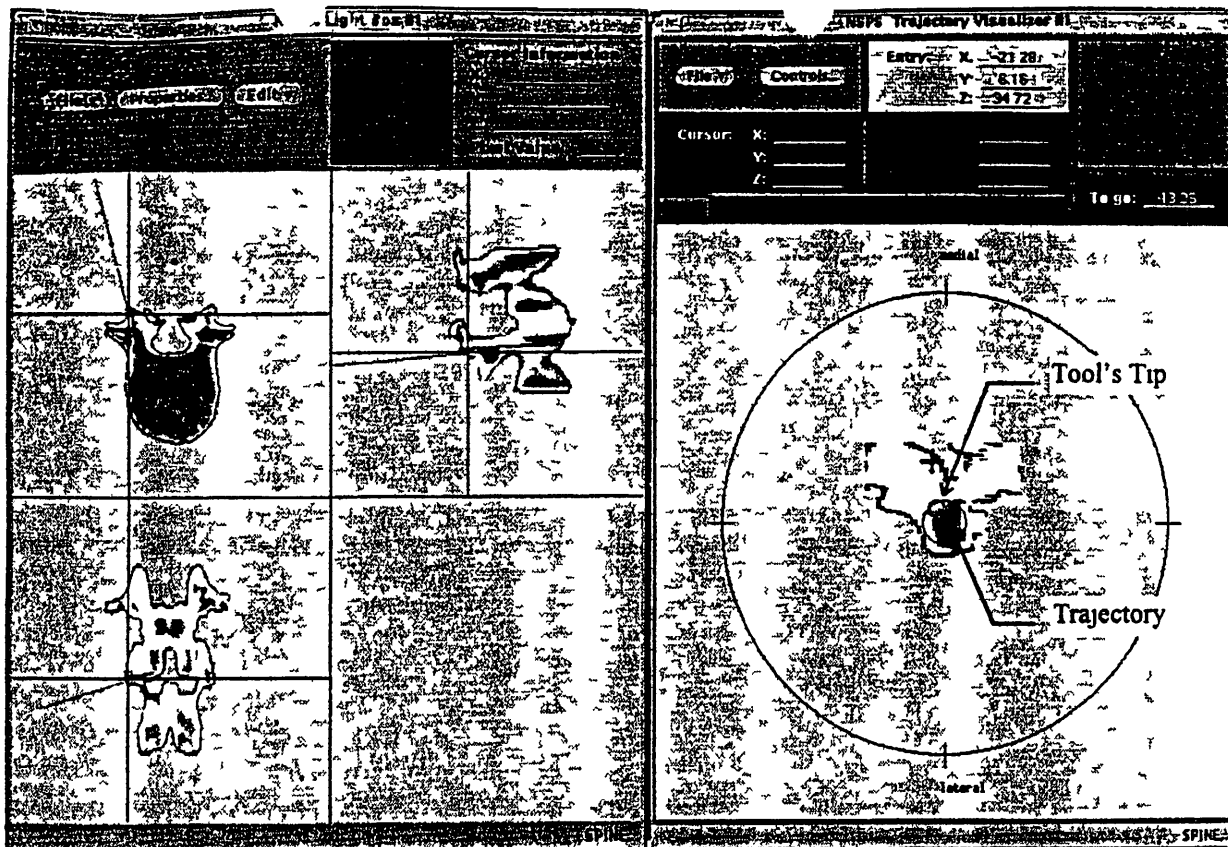


Figure 2

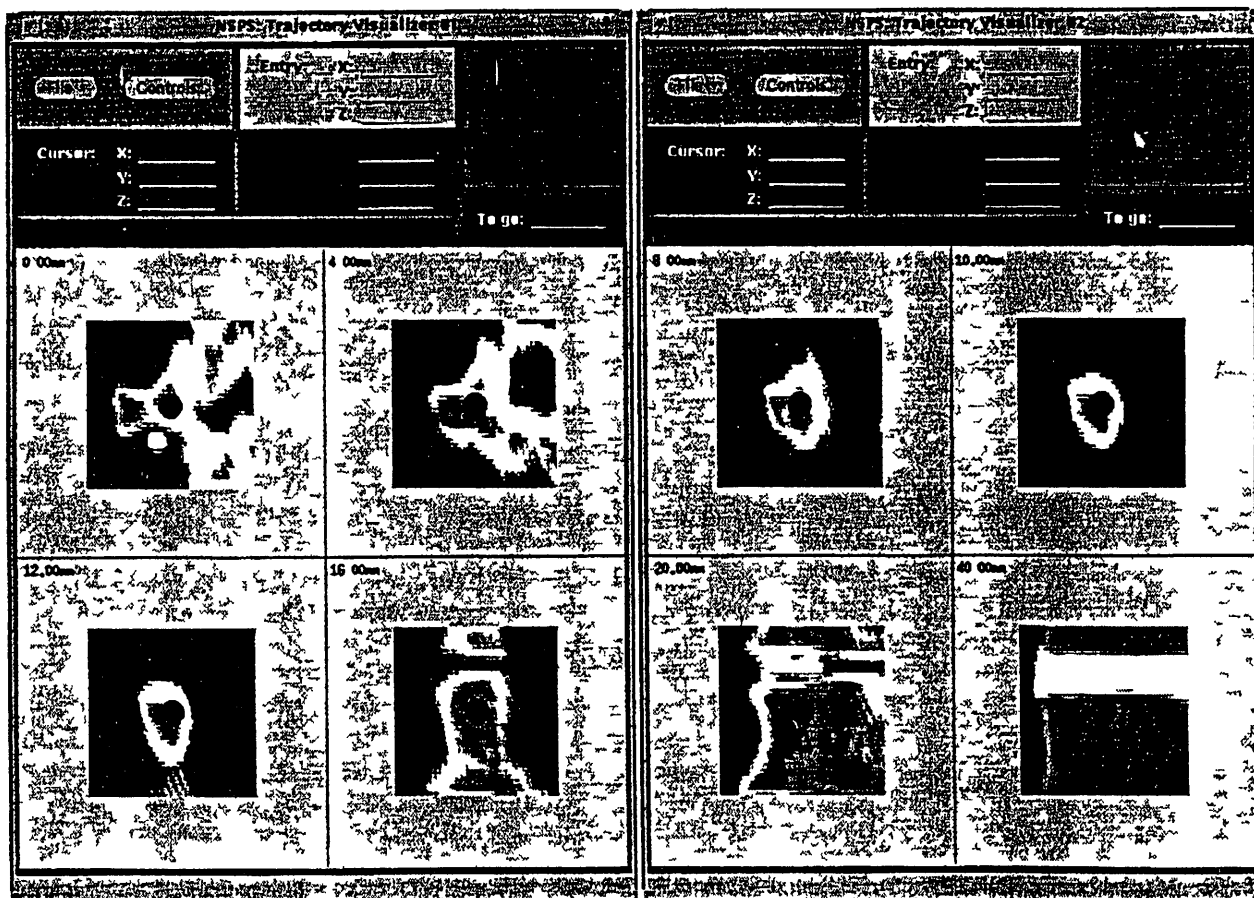


Figure 3

This provides a safe method to identify inaccurate transformations, i.e. when displayed and digitized points do not correspond

Once a sufficiently exact solution is found the location of any instrumented and calibrated surgical tool can be transformed into the coordinates of the tomographic image and displayed on screen in the image. The necessary calibration is done with one custom calibration device for all instruments

The surgeon may choose from various options of real-time visualization of the pedicle hole preparation. The instrument used can be displayed as a line in the above mentioned multiple two-dimensional views (Fig 2, left). Simultaneously the section perpendicular to the trajectory's axis with a circle representing the position of the instrument may be shown together with graphical guide lines for proper adjustment of the instrument (Fig 2, right). This view is the so-called Pedicle Navigator. Both options adjust the plane of their display, in real time, to the position of the instrument's tip. Furthermore multiple sections along the axis of intended pedicle hole preparation can be calculated and displayed according to the instrument's orientation in relation to the pedicle. This option may eliminate the need to perform the pre-operative planning and is termed the Real time Intraoperative Planning Option (Fig 3)

These tools guide the surgeon during pedicle hole preparation. The loss in operation time during the matching procedure is usually offset by faster hole preparation

**Validation of the System** For the evaluation of the entire cascade of errors a complex validation study has been performed

To justify the quality of a transformation or a digitization the coordinates of corresponding points in each relevant COS are required. For this purpose six precise polished titanium spheres were attached to a demineralized vertebra to provide a set of exactly defined reference points. The centers of the spheres were measured with a LASER measuring device (accuracy  $<5\mu\text{m}$ ). The resulting coordinates in the COS of the LASER device ( $\text{COS}^L$ ) were termed "exact". The vertebra was CT-scanned with slice distances of 1mm and 2mm. On-screen digitization of the sphere centers in the reconstructed CT data and digitization of the spheres using the 3D space pointer on the vertebra resulted in three additional sets of coordinates in the  $\text{COS}^{\text{CT}}$  and  $\text{COS}^V$ . The manual digitizations were performed several times by various observers to evaluate how accurate a point in the  $\text{COS}^{\text{CT}}$  and  $\text{COS}^V$  can be digitized. Table 1 shows the associated mean digitizing errors

Within the range of this accuracy the means of all coordinates were adjusted to match the exact results more precisely. Criteria for more precise matching were all possible distances between any two points out of the sets of six compared to the exact values. If, for example, the distance between spheres #1 and #4 was 43.543mm ( $d^L$ ) in  $\text{COS}^L$  and 43.525mm ( $d^V$ ) in  $\text{COS}^V$ ,  $d^V$  had to be enlarged by 0.018mm moving #1<sup>V</sup> and/or #4<sup>V</sup>. Using a non-linear

algorithm all centers in  $\text{COS}^V$  and  $\text{COS}^{\text{CT}}$  were shifted to minimize the differences from  $\text{COS}^L$ . In order to preserve

	RMS digitizing error [mm]
$\text{COS}^V$	0.15
$\text{COS}^{\text{CT}1\text{mm}}$	0.20
$\text{COS}^{\text{CT}2\text{mm}}$	0.22

Table 1

the validity of this procedure adjustments were kept less than the average digitization error in the relevant COS. The resulting coordinates were termed "nearly exact". Table 2 summarizes the performed adjustments

Sphere #	Displacements [mm]		
	$\text{COS}^V$	$\text{COS}^{\text{CT}1\text{mm}}$	$\text{COS}^{\text{CT}2\text{mm}}$
1	0.034	0.215	0.260
2	0.026	0.227	0.000
3	0.024	0.171	0.212
4	0.036	0.199	0.150
5	0.013	0.199	0.212
6	0.017	0.250	0.260

Table 2

These four sets of coordinates were then used to check the quality of the transformations. Assuming the skeletal registration would result in an exact transformation  $\text{COS}^V \rightarrow \text{COS}^{\text{CT}}$ , applying this transformation to points in  $\text{COS}^V$  would exactly transfer them to their corresponding points in  $\text{COS}^{\text{CT}}$ . If however, the transformation is inaccurate, the transformed points will differ from the correct points in  $\text{COS}^{\text{CT}}$ . The transformation error therefore can be defined as the space distance between the nearly exact points of  $\text{COS}^{\text{CT}}$  and the transformation of the corresponding nearly exact points of  $\text{COS}^V$  into  $\text{COS}^{\text{CT}}$  (Fig 4)

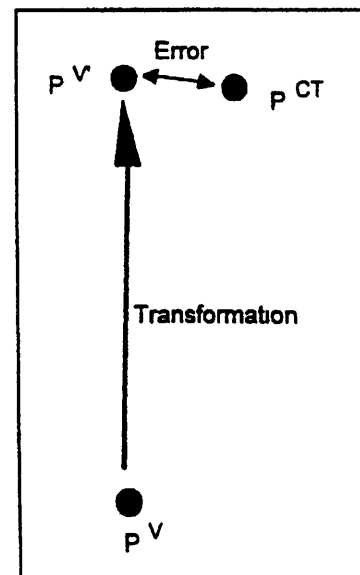


Figure 4

This value includes digitization errors in both COSs as well as numerical inaccuracies of the transformation algorithm. Table 3 gives an overview of this overall system's accuracy for different CT slice distances.

	Transformation error [mm]	
	COSCT1mm	COSCT2mm
RMS	0.71	1.74
SEM	0.07	0.41

Table 3

To further prove the accuracy and reliability of the system, 20 pedicle screw hole preparations were performed on human lumbar vertebra specimens in an *in vitro* setting. Based on 1mm CT scans, the trajectories were defined as described above. Using a standard 3.6mm drill bit in an instrumented pneumatic hand drill, pilot holes for pedicle screw insertion were prepared. Only the real-time display of the drill bit in the CT image was used as an aid for guidance to match the pre-operatively defined trajectory. Aluminum cylinders were inserted into the holes, and the 20 pedicles were cut into 77 histological sections perpendicular to the cylinder axes. Each section was classified into one of the following groups: (I) cylinder centered in pedicle, (II) cylinder touches cortex, (III) cylinder engages cortex, and (IV) cylinder perforates cortex. Figure 5 summarizes the results of the *in vitro* study.

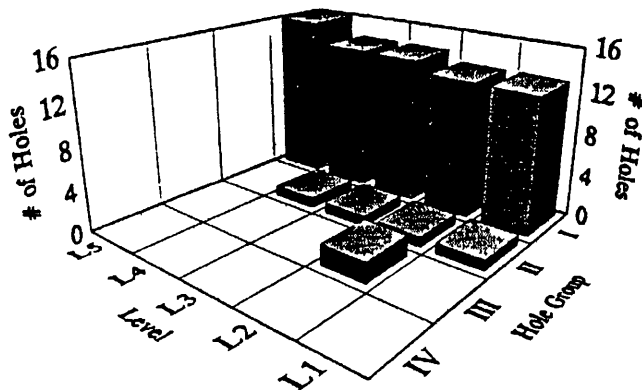


Figure 5

**Clinical Application** So far, six patients underwent posterior fixation of degenerative lumbar spinal segments using the system (Fig. 6). No complications occurred; post-operative radiological evaluation confirmed accurate placement of the pedicle screws. The introduction of the system into the surgical world is still occurring, however, basic concepts like tool handling and marker carrier design, are already optimized.



Figure 6

**Conclusions** The concept of the presented technique can be applied to a variety of surgical procedures. Image data reconstruction and manipulation modules provide powerful tools for pre-operative planning and simulation. Intra-operatively, a four-step procedure helps to perform an accurate skeletal registration, the basis for an accurate and safe tracking of surgical tools. Finally, the real-time display of the motion of any surgical instrument together with the corresponding tomographic image enables the surgeon to follow exactly the pre-operatively planned procedure. Early clinical results give reason to expect improved surgical outcome and might lead to new frontiers in orthopaedic surgery.

#### References

- 1 Clarke RH, Horsley, V (1906) On a method of investigating the deep ganglia and tracts of the central nervous system (cerebellum) Br Med J 2: 1799-1800

- 2 van den Elsen PA, Pol E, Viergever MA (1993) Medical image matching - a review with classification IEEE proceedings on medicine and biology 26-39
- 3 Esses SI, Sachs BL, Dreyzin V (1993) Complications associated with the technique of pedicle screw fixation a selected survey of ABS members Spine 15 2231-2239
- 4 Goldstein H (1980) Classical Mechanics, 2nd Ed Addison Wesley
- 5 Heilbrun MP (1988) Stereotactic Neurosurgery, Vol 2 Concepts in Neurosurgery Williams & Wilkins
- 6 Hounsfield GN, Ambrose J, Berry BJ, et al (1973) Computerized transverse axial scanning (tomography) Br J Radiol 46 1016-1051
- 7 Jiang H, Robb RA, Holton KS (1992) A new approach to three-dimensional registration of multimodality medical images by surface matching SPIE 1808 196-206
- 8 Jiang Z, Zamorano L, Kadi AM (1993) Neurological surgery planning system Proceedings of Clinical Application of Modern Imaging Technology, SPIE 1984 203-207
- 9 Kelly PJ (1991) Tumor stereotaxis Philadelphia W B Saunders Company
- 10 Krag MH (1991) Biomechanics of thoracolumbar spinal fixation a review Spine 16 84-99
- 11 Matsen FA, Garbini JL, Sidles JA, et al (1993) Robotic assistance in orthopaedic surgery Clin Orthop 296 178-186
- 12 Nolte LP, Zamorano L, Govindarajulu M, Jain GM, Visarius H (1993) An advanced biomechanical study of transpedicular screw fixation using stereotactic concepts Transactions of the Annual Meeting of the International Society for the Study of the Lumbar Spine Marseilles, France 46
- 13 Nolte LP, Zamorano LJ, Jiang Z, Wang Q, Langlotz F, Berlemann U (1994) Image guided insertion of transpedicular screws - a laboratory set-up Spine (accepted for publication)
- 14 Paul HA, Mittelstadt B, Bargar W, et al (1992) A surgical robot for total hip replacement surgery IEEE proceedings on robotics and automation 606-611
- 15 Sautot P, Cinquin P, Lavallée S, Troccaz J (1993) Computer assisted spine surgery a first step toward clinical application in orthopaedics IEEE proceedings in medicine and biology 1071-1072
- 16 Zamorano LJ, Nolte LP, Kadi AM, Jiang Z (1993) Interactive intraoperative localization using an infrared-based system J Neurol Res 15 290-298
- 17 Zamorano L, Nolte LP, Jiang Z, Kadi AM (1993) Image guided neurosurgery frame based and frameless approaches In Wilkins RH ed Neurological operative atlas Rengachary S S, Williams & Wilkins

## Comparison of Relative Accuracy Between a Mechanical and an Optical Position Tracker for Image-Guided Neurosurgery

Robert Rohling, Patrice Munger, John M. Hollerbach, and Terry Peters  
*Department of Biomedical Engineering, McGill University, Montreal, Quebec, Canada (R.R., P.M., T.P.),  
Department of Computer Science, University of Utah, Salt Lake City, Utah (J.M.H.)*

**ABSTRACT** An essential component in the execution of image-guided surgery is a hand-held probe whose spatial position is tracked during the procedure and displayed on a three-dimensional operative workstation. This paper describes an experiment performed in order to compare the accuracy of a mechanically linked pointing device (FARO surgical arm) and an optical position tracker (OPTOTRAK) against a "gold standard" *J Image Guid Surg* 1 30-34 (1995) ©1995 Wiley Liss Inc.

---

**Key words** FARO surgical arm, OPTOTRAK, position tracking

---

### INTRODUCTION

The rapidly growing field of computer assisted image guided neurosurgery has provided a way to improve surgical procedures. Image guided surgery provides a surgeon with two-dimensional (2 D) and three dimensional (3 D) diagnostic images typically acquired using computed tomography or magnetic resonance imaging along with a visual representation of a pointing device in the same imaging space.

The Viewing Wand (I S G Technologies Mississauga Ontario Canada) system currently used at Montreal Neurological Institute uses the FARO surgical arm (FARO Medical Technologies Orlando FL) as a pointing device i.e. as a means to transmit the coordinates of points in space to a computer. A number of types of 3-D pointing devices are available including mechanical (such as the FARO arm) optical [such as the OPTOTRAK (Northern Digital Inc Waterloo Ontario Canada)] ultrasonic and magnetic. These different types of localizing devices have been compared extensively by Maciunas.<sup>4</sup>

#### The FARO Surgical Arm

The FARO arm is a 6 degrees of freedom articulated aluminum device.<sup>3</sup> The probe is a 200 mm cylinder

with a thin shaft at the end (Fig 1). The articulated arm is passive allowing the surgeon (or an assistant) to adjust it manually to the desired position. The analog signals produced by the six joint angle potentiometers on the arm are digitized by an analog to digital (A/D) converter mounted on a personal computer (PC). A program provided by FARO is run on the same PC to convert the digitized readings of the joints potentiometers into a set of six numbers representing the position and the orientation of the probe holder with respect to a coordinate system attached to the base of the arm. Further calculations which depend on the type of probe must then be performed to determine the tip position of the probe. Errors in the calculated tip position of the probe are expected to arise primarily from potentiometer noise nonlinearity and drift, kinematic model parameter inaccuracies, joint wobble and hysteresis, and probe bending. The observed accuracy of the FARO surgical arm is about 1 mm.

#### The OPTOTRAK Position Tracker

The OPTOTRAK is a position tracking device which tracks infrared light emitting diodes (LEDs) by three

---

Received original February 3 1995 accepted February 20 1995

Address reprint requests to Robert Rohling Dept Biomedical Engineering McGill University 3775 University Street Montreal Quebec Canada H3A 2B4 e mail rohling@biorobotics.mcgill.ca

©1995 Wiley Liss Inc

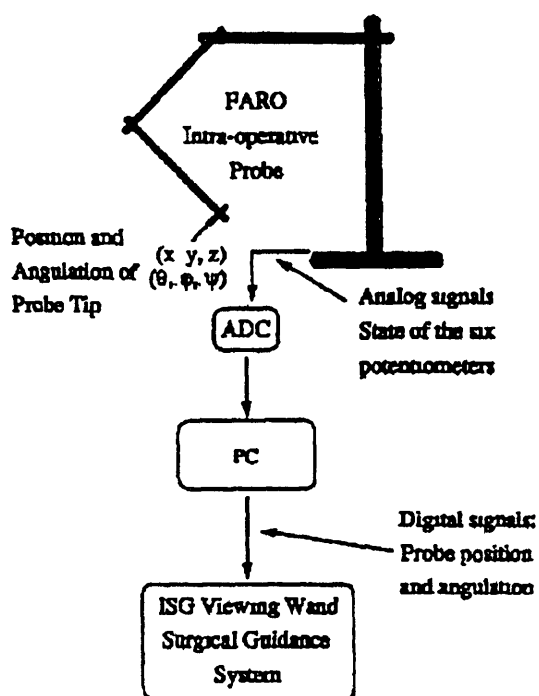


Fig 1 The FARO arm and the Viewing Wand system

fixed CCD cameras<sup>5</sup> The OPTOTRAK has a stated accuracy of 0.15 mm and a resolution of 0.01 mm at a distance of 2.5 m between the LED and the cameras. Low noise levels during tests yield a resolution of slightly greater than 0.01 mm. When multiple LEDs are used the OPTOTRAK samples them nearly simultaneously (~1000 Hz bandwidth) at a user selectable sampling rate.

**Goals**

The original goal of the experiment was to compare the accuracy of the two localizing devices dynamically, i.e. with the tip of the probe moving along an arbitrary path in space. However, it was impossible to synchronize the data acquisition of the OPTOTRAK and the limited sampling rate of the FARO arm. A static study of the relative accuracy was therefore done by comparing the distances between fixed points in space measured by both devices. These measurements are related to a third measurement we could consider as the gold standard. A metal block built for that purpose is described below.

**MATERIALS AND METHODS**

**Reference Block**

Holes 15 mm deep and spaced 10 mm apart were drilled into an aluminum bar with a Matsuura MC

510V (Elliott Machinery Canada, Ltd.) numerically controlled milling machine. Each hole was carefully milled to the same diameter as the probe tip such that after the probe was pressed into the hole no movement was detected. The 15 mm depth of the hole was enough that the probe tip could descend until an increase in the width limited further travel. This milling process ensured that the probe tip would descend the same amount for each hole. The accuracy of the milling machine is ±0.005 mm.

**Probe Setup**

LEDs were attached to the probe to track the probe position by first mounting the LEDs to a small aluminum plate using cyanoacrylate glue. A hole with the diameter of the probe shaft was then reamed into the plate, and the plate was attached to the probe shaft and secured by threaded fasteners (see Fig. 5).

**FARO Arm Data Acquisition**

The proprietary program running on the PC does not allow writing the probe holder position information directly into a text file. The software used by the Viewing Wand was modified to perform this task, which required moving the entire Viewing Wand system to the experimental location.

**Experimental Protocol**

The base of the articulated arm, the calibration bar and the OPTOTRAK cameras were all placed in rigid mounts, as illustrated in Figure 2. Three calibration trials were undertaken. Each trial was done with the calibration bar at a different position and orientation with respect to the FARO arm and OPTOTRAK to include different areas of the arm's workspace. Each trial followed the following procedure: 1) Place the probe tip in hole 1. 2) Take hands off the probe for a few seconds. 3) Move probe into the next hole and

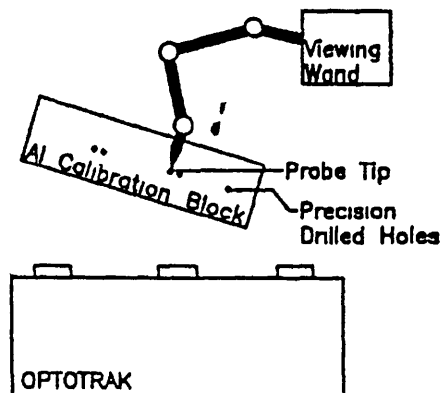


Fig 2 Overview of the measurement apparatus

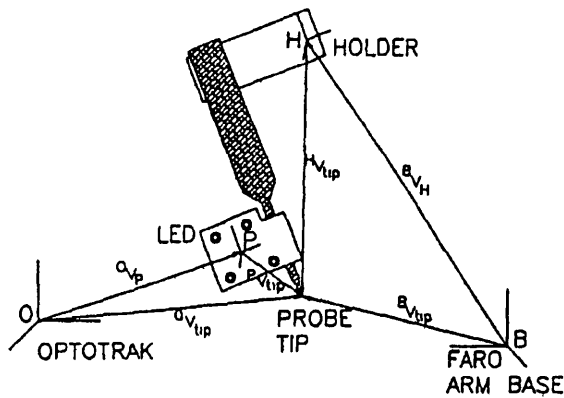


Fig 3 The probe tip with respect to the LED and the OPTOTRAK coordinate systems The following notation is used O OPTOTRAK coordinate system P probe coordinate system H probe holder coordinate system B FARO arm base

repeat During each trial the Viewing Wand program sampled the probe at approximately 50 Hz and the OPTOTRAK sampled at 100 Hz

RESULTS

Stationary Calibration Data Extraction

Fifty samples of FARO arm data for the position of each hole are extracted from the stationary portions of the calibration data with the operator's hands removed from the probe Fifty samples of OPTOTRAK data from each of the four LEDs are extracted in a similar manner

Conversion of OPTOTRAK Calibration Data

To compare the measurements of the OPTOTRAK to the measurements of the FARO arm the endpoint of the probe tip must be calculated from LED data The probe tip position ( ${}^O v_{tip}$ ) can be determined with respect to the OPTOTRAK coordinate system (O) if the fixed relationship ( ${}^P v_{tip}$ ) between the LED locations (P) and the probe tip is known (Fig 3) This vector was determined by a separate procedure briefly outlined below

1 Determination of vector  ${}^P v_{tip}$  The probe was rotated about a fixed endpoint (i.e.  ${}^O v_{tip}$  is constant) and 500 measurements were taken For each sample the centroid of the LEDs ( ${}^O v_p$ ) was calculated A least squares fit was performed to find the radius and center of the sphere that fits best this set of points The vector  ${}^O v_{tip}$  was found by using the center of this sphere

The next step was to establish the LED coordinate system P with an origin at the centroid ( ${}^O v_p$ ) of LEDs The principle axes ( ${}^O x_p, {}^O y_p, {}^O z_p$ ) of the

coordinate system were then determined by solving the eigenvalue problem outlined by An et al<sup>1</sup>

By using a homogeneous transformation matrix the transformation between  ${}^O v_{np}$  and  ${}^P v_{np}$  can then be written

$$\begin{bmatrix} {}^O v_{np} \\ 1 \end{bmatrix} = {}^O T_P \begin{bmatrix} {}^P v_{np} \\ 1 \end{bmatrix} \quad (1)$$

where

$${}^O T_P = \begin{bmatrix} {}^O x_p & {}^O y_p & {}^O z_p & {}^O v_p \\ 0 & 0 & 0 & 0 \end{bmatrix} \quad (2)$$

${}^P v_{np}$  was then determined from the inverse of Equation 1

$$\begin{bmatrix} {}^P v_{np} \\ 1 \end{bmatrix} = ({}^O T_P)^{-1} \begin{bmatrix} {}^O v_{np} \\ 1 \end{bmatrix} \quad (3)$$

2 Determination of the probe tip position in the OPTOTRAK frame After the constant vector  ${}^P v_{np}$  was found a similar procedure was used to find the vectors  ${}^O v_{np}$  from the position data of the four LEDs taken when the probe was moved to different calibration block positions

For the each calibration measurement calculate the centroid of LEDs ( ${}^O v_p$ ) Determine the coordinate system on the probe by finding the principal axes ( ${}^O x_p, {}^O y_p, {}^O z_p$ ) Use Equation 1 to determine  ${}^O v_{tip}$

Conversion of FARO Arm Calibration Data

As was previously mentioned the FARO arm data describe the location  ${}^B v_H$  of the probe holder (H) together with its orientation ( $\phi, \theta, \psi$ ) with respect

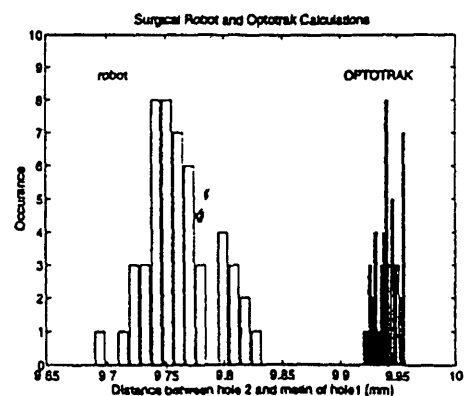


Fig 4 Examples of histograms of the robot (FARO arm) and OPTOTRAK measurement distributions The data shown correspond to the first data set from trial 1



to a coordinate system attached to the base of the arm (B). The angles correspond to the Euler's angles in the  $z-x-z$  convention.<sup>2</sup> The tip position vector  ${}^B v_{tip}$  in the arm's base (B) coordinate system is given by

$${}^B v_{np} = [R(\psi)R_x(\theta)R(\phi)]^{-1} {}^H v_{tip} + {}^B v_H \quad (4)$$

$$= R^{-1} {}^H v_{np} + {}^B v_H \quad (5)$$

where

$$R(\alpha) = \begin{bmatrix} \cos \alpha & \sin \alpha & 0 \\ -\sin \alpha & \cos \alpha & 0 \\ 0 & 0 & 1 \end{bmatrix} \quad (6)$$

and

$$R(\alpha) = \begin{bmatrix} 1 & 0 & 0 \\ 0 & \cos \alpha & \sin \alpha \\ 0 & -\sin \alpha & \cos \alpha \end{bmatrix} \quad (7)$$

The homogeneous matrix is written with a notation similar to that used in the previous section

$${}^B T_H = \begin{bmatrix} R^{-1} {}^H v_{np} \\ 0 & 0 & 0 & 1 \end{bmatrix} \quad (8)$$

A separate set of measurements taken as the probe was rotated about a fixed endpoint was acquired in the same manner as described above under Probe Setup. In this way the vector  ${}^H v_{np}$  was found by minimizing the standard deviation of the set of tip positions calculated using the inverse of the equation

$$\begin{bmatrix} {}^B v_{np} \\ 1 \end{bmatrix} = {}^B T_H \begin{bmatrix} {}^H v_{tip} \\ 1 \end{bmatrix} \quad (9)$$

This value of  ${}^H v_{np}$  was then used in Equation 9 to find the position of the probe's tip ( ${}^B v_{np}$ ) from the probe holder position and orientation measurements taken when the probe was moved to different calibration block positions.

#### Relative Accuracy Comparison

For each of the calculated OPTOTRAK vectors  ${}^O v_p$  and FARO arm vectors  ${}^B v_p$ , the mean vector to the hole 1 location is determined as the mean of its 50 samples. The 50 samples for hole 2 are sub-

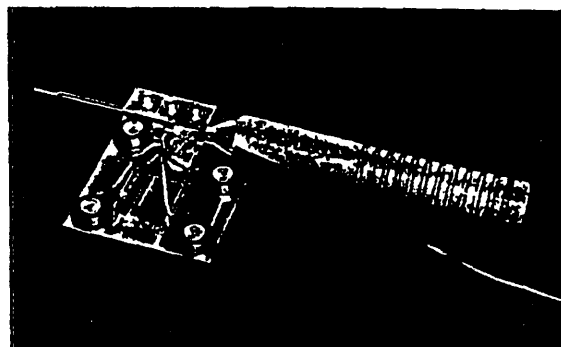


Fig 5 Four OPTOTRAK LEDs mounted on a plate are attached to the surgical probe

tracted from the hole 1 mean vector to get the vectors between holes 1 and 2. The norms of each of the 50 difference vectors are determined to obtain the magnitude of the distance between holes. This procedure is repeated for all holes measured during each trial.

The difference in the measured distances of hole 2 from hole 1 in trial 1 is plotted in Figure 4. Both the OPTOTRAK and the FARO arm yield distributions close to the true 10 mm spacing. The first point of interest in Figure 4 is that the OPTOTRAK distribution has a mean closer to the true (within the milling machine's 0.005 mm accuracy) 10 mm spacing than the FARO arm distribution mean. Second, the distribution of the OPTOTRAK measurements has a smaller standard deviation than the FARO arm distribution. The means of each of the OPTOTRAK and FARO arm distributions are listed in Table 1, along with the spread of each distribution.

The 50 measurements from the OPTOTRAK and the FARO arm of each hole were taken with a stationary probe, i.e., the orientation of the probe was constant and the LEDs directly faced the cameras. Independent tests by Northern Digital<sup>6</sup> on a larger six LED digitizing probe showed a similar level of accuracy for similar tests (maximum error of 0.11 mm and standard deviation of 0.02 mm). Northern Digital reported that the maximum error increased to 0.57 mm with a standard deviation of 0.06 mm when the orientation was continuously varied (30 roll, 120 pitch, and 160 yaw) about a fixed endpoint position. The main source of the increase in error was stated to be nonisotropic behavior of the markers; the marker is not a perfect point source and the center shifts as the marker is viewed at different angles. The calculated endpoint errors of the FARO arm are also expected to increase if the ori-

Table 1 Calculations of the Distances Between Holes\*

Distance from hole 1 (mm)	Machining Precision (mm)	OPTOTRAK measured distance [spread] (mm)	FARO arm distance [spread] (mm)
Trial 1			
10	0.005	9.942 [0.037]	9.762 [0.144]
20	0.005	—	—
30	0.005	—	—
40	0.005	39.826 [0.123]	39.434 [0.226]
Trial 2			
10	0.005	10.074 [0.152]	10.108 [0.491]
20	0.005	20.038 [0.088]	20.001 [0.349]
30	0.005	30.082 [0.039]	29.942 [0.162]
40	0.005	40.042 [0.048]	39.985 [0.166]
50	0.005	50.117 [0.034]	50.008 [0.241]
60	0.005	60.115 [0.040]	59.926 [0.195]
Trial 3			
10	0.005	9.940 [0.129]	9.718 [0.333]
20	0.005	19.868 [0.326]	19.638 [0.369]
30	0.005	29.944 [0.187]	29.624 [0.196]
40	0.005	39.955 [0.189]	39.456 [0.128]
50	0.005	49.823 [0.183]	49.511 [0.545]

The OPTOTRAK and FARO arm measured distances represent the mean of the norms of the measured vectors between the holes. The spread indicates the maximum subtracted from the minimum norm of the vectors between the holes. A dash indicates no measurement.

\*These data are plotted in Figure 4.

entation is dynamically varied. The OPTOTRAK based probe would still retain a slightly higher accuracy than the FARO arm.

## CONCLUSIONS

The OPTOTRAK gives results closer to the true 10 mm spacing than the FARO arm. It also has smaller spreads for each hole. The accuracy of the OPTOTRAK data closely matches the manufacturer's specifications. The FARO arm data are also within the manufacturer's specifications. Generally the FARO arm determinations of hole spacing are within 0.5 mm and have spreads of 0.5 mm. However, some distances are determined more accurately. 0.1 mm is not uncommon. This level of accuracy is sufficient to give confidence in its use in a neurosurgical environment.

We would stress the fact that the overall system accuracy in image guided neurosurgery is the

result of a number of factors, many of which add more inaccuracy to the overall result than those relating to the localization device. For example, we have found the major source of inaccuracy in such a system to be related to the registration of images to objects. Given the expected overall accuracy of such systems, both mechanically and optically based localizing devices are appropriate for use in image guided neurosurgery.

## ACKNOWLEDGMENTS

We thank B. L. K. Davey for his work on the modification of the Viewing Wand routine and for his assistance during the data acquisition. We also acknowledge the valuable help provided by R. M. Comeau. Support for this research was provided by the Office of Naval Research (grant N00014-90 J-1849) by the Natural Sciences and Engineering Research Council (NSERC) Network Centers of Excellence Institute for Robotics and Intelligent Systems (IRIS) and by Medical Research Council of Canada Operating and University/Industry grants. Personal support for J. M. H. was provided by the NSERC/Canadian Institute for Advanced Research (CIAR) Industrial Chair in Robotics and for R. R. and P. M. by NSERC Postgraduate Scholarships.

## REFERENCES

1. An, C. H., Atkeson, C. G., Follerbach, J. M. (1988) Model Based Control of a Robot Manipulator. Cambridge, MA: MIT Press.
2. Goldstein, H. (1981) Classical Mechanics. Reading, MA: Addison Wesley.
3. ISG Technologies Inc. (1993) Viewing Wand Operator's Guide. Mississauga, Canada: ISG Technologies Inc.
4. Maciunas, R. J. (1993) Interactive Image Guided Surgery. Chicago: American Association of Neurological Surgeons.
5. Northern Digital Inc. (1991) Technical Product Description: OPTOTRAK. Waterloo, Canada: Northern Digital Inc.
6. Northern Digital Inc. (1992) The OPTOTRAK System: Accuracy of Various Digitizing Probes. Waterloo, Canada: Northern Digital Inc.

# Automated Registration for Enhanced Reality Visualization in Surgery

E Grimson,<sup>1</sup> T Lozano-Perez,<sup>1</sup> W Wells,<sup>1,2</sup> G Ettinger,<sup>1,3</sup> S White,<sup>3</sup> R Kikinis<sup>2</sup>

## Abstract

There is a need for frameless guidance systems to aid neurosurgeons in planning the exact location of a craniotomy, to define the margins of tumors and to precisely locate neighboring critical structures. We have developed an automatic technique for registering clinical data, such as segmented MRI or CT reconstructions, with the actual head of the patient on the operating table. A second method calibrates the position of a video camera relative to the patient. The combination allows a visual mix of live video of the patient with the segmented 3D MRI or CT model. This registration enables us to employ enhanced reality techniques for planning and guiding neurosurgical procedures by merging live video images with the 3D reconstructions, and to interactively view extracranial or intracranial structures in a non-intrusive manner.

## 1 Motivating Problem

Neurosurgical procedures, such as biopsy or tumor ablation, require highly precise localization on the part of the surgeon, in order to attain the desired extraction of diseased tissue while minimizing damage to adjacent structures. The problem is exacerbated by the fact that the localization is three dimensional in nature, and often requires isolating a structure deeply buried within the cranium. While methods exist (e.g. MRI, CT) for imaging and displaying the 3D structure of the head, this still leaves the surgeon with the problem of relating what she sees on the 3D display with the actual anatomy of the patient.

Current solutions typically involve presurgically attaching a stereotactic frame to the patient's skull, then imaging the skull and frame as a unit. This allows the surgeon to locate the tumor or other target relative to a coordinate system attached to the stereotactic frame, and thus to the patient's head. Unfortunately, stereotactic frames are cumbersome, involve considerable discomfort to the patient, and have limited flexibility, especially should surgical plans have to change in the middle of the procedure.

<sup>1</sup>Artificial Intelligence Laboratory, Massachusetts Institute of Technology, Cambridge MA

<sup>2</sup>Department of Radiology, Brigham and Women's Hospital, Harvard Medical School, Boston MA

<sup>3</sup>The Analytic Sciences Corporation, Reading MA

## 1.1 An Ideal Solution

An ideal system would automatically register 3D data sets, and track changes in the position of a data set over time, without requiring the attachment of any devices to the patient. Such an ideal system should support real-time, adaptive, enhanced reality patient visualizations in the operating room, dynamic image-guided surgical planning and surgical procedures, such as biopsies or minimally-invasive therapeutic procedures, and registered transfer of *a priori* surgical plans to the patient in the OR.

While our group is actively developing all aspects of such a system, this paper focuses on one key component of such a system, the registration of different data sources to determine relevant coordinate frame transformations.

## 1.2 Contributions to the Ideal Solution

We have created a system that performs the registration of clinical image data with the position of the patient's head on the operating table at the time of surgery, using methods from visual object recognition. The method has been combined with an enhanced reality technique [11] in which we display a composite image of the 3D anatomical structures with a view of the patient's head. This registration enables the transfer to the operating room of preoperative surgical plans, obtained through analysis of the segmented 3D preoperative data [4], where they can be graphically overlaid onto video images of the patient. Such transfer allows the surgeon to mark internal landmarks used to guide the progression of the surgery. Extensions of our method include adaptively re-registering the video image of the patient to the 3D anatomical data, as the patient moves, or as the video source moves, as well as other surgical applications such as image-guided biopsy, or focused therapeutic procedures such as laser disc fusion or tumor ablation. We have also recently demonstrated the use of our system in clinical settings, by registering data sets acquired over extended time periods, thereby enabling the detection of changes in anatomy over time.

## 2 An Example Scenario

The following scenario describes the use of our methods:

(1) A patient requiring surgical therapy is scanned by a 3D, high-resolution scanner, such as MRI or CT.

(2) The scan is segmented into tissue type in a semi-automatic manner, typically by training an intensity classifier on a user-selected set of tissue samples.

(3) Prior to draping, the patient is scanned by a laser range scanner. The 3D locations of any table landmarks are also calculated, relative to the patient.

(4) The MRI or CT scan is automatically registered to the patient skin surface depth data from the laser ranger. This provides a transformation from MRI/CT to patient.

(5) The position and orientation of a video camera relative to the patient is determined, by matching video images of the laser points on an object to the actual 3D laser data. This provides a transformation from patient to camera.

(6) The registered internal anatomy is displayed in enhanced reality visualization [11] to "see" inside the patient, i.e., the two computed transformations are used to transform the 3D model into the same view as the video image of the patient, so that video mixing allows the surgeon to see both images simultaneously.

(7) The patient is draped and surgery is performed. The enhanced reality visualization does not interfere with the surgeon, but provides her with additional visualization information to greatly expand her limited field of view.

(8) The location of table landmarks can be continually tracked to identify changes in the position of the patient's attitude, relative to the visualization camera. Viewer location can also be continually tracked to identify any changes. Visualization updates are performed by updating the patient to viewer transformation.

(9) In general, the surgery is executed with an accurately registered enhanced visualization of the entire relevant patient anatomy, and thus with reduced side effects.

### 3 Details of Our Approach

Part 1 of this scenario is standard practice. Methods exist for Part 2 [4]. Parts 8-9 are part of our planned future work. Here, we focus on parts 3-7, where the key step is the registration of data obtained from the patient in the operating room with previously obtained data.

We use a multi stage matching and verification of a 3D data set acquired at the time of the surgery with 3D clinical data sets acquired previously. The central ideas are to use a laser striping device to obtain 3D data from the patient's skin, and to use a sequence of recognition techniques to match this data to segmented skin data from the MRI or CT reconstruction. These techniques allow us to accurately register the clinical data with the current position of the patient, so that we can display a superimposed image of the 3D structures overlaid on a view of the patient.

The basic steps of our method are outlined below.

#### 3.1 Model input

We obtain a segmented 3D reconstruction of the patient's anatomy, for example using CT or MRI. The segmentation is typically done by training an intensity classifier on a user selected set of tissue samples, where the operator uses knowledge of anatomy to identify the tissue type. Once initial training is completed, the rest of the scans can be automatically classified on the basis of intensities in the scanned images, and thus segmented into tissue types [4]. Automatically removing gain artifacts from the sensor data can be used to improve the segmentation [12].

This 3D anatomical reconstruction is referred to as the model, and is represented relative to a model coordinate frame. For simplicity, the origin of the coordinate system can be taken as the centroid of the points.

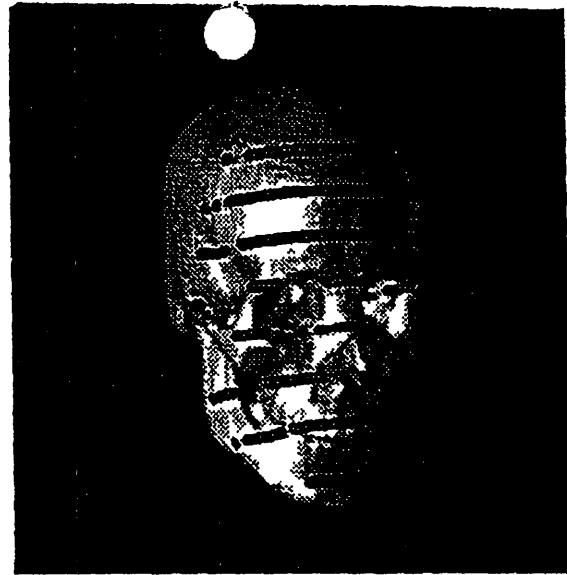


Figure 1 Example of registered laser data (shown as large dots) overlaid on CT model.

#### 3.2 Data input

We obtain a set of 3D data points from the surface of the patient's skin by using a laser striping device. For our purposes, the laser simply provides a set of accurate 3D point measurements, obtained along a small (5-10) set of planar slices of the object (roughly 240 points per slice). This information is referred to as the data, and is represented in a coordinate frame attached to the laser, which reflects the position of the patient in a coordinate frame that exists in the operating room. Our problem is to determine a transformation that will map the model into the data in a consistent manner.

#### 3.3 Matching data sets

We match the two data sets using the following steps:

(1) First, we sample a set of views of the model. For each view, we use a z-buffer method to extract a sampled set of visible points of the model. For each such model, we execute the matching process described below.

(2) Next, we separate laser data of the patient's head from background data. Currently we do this with a simple user interface. Note that this process need not be perfect, we simply want to remove gross outliers from the data. From this data, we find three widely separated points that come from the head.

(3) We use constrained search [6] to match triples of visible sampled model points to the three selected laser points. The method finds all such matches consistent with the relative geometry of each triple, and for each we compute the coordinate frame transformation that maps the three laser points into their corresponding model points. These transformations form a set of hypotheses. Note that due to sampling, these hypothesized transformations are at best approximations to the actual transformation.

In examples such as Figure 1, there are typically  $\approx 1000$  laser sample points, and the model has typically 40,000

sample points. Given a view, and a coarsely sampled z-buffer, there are typically 1000 model points in the sampled view. In principle, there are  $\approx 10^{15}$  possible hypotheses, but using simple distance constraints, there are usually  $\approx 100,000$  possible hypotheses that remain.

(4) We use the Alignment Method [7] to filter out those hypotheses, by transforming all the laser points by the hypothesized transformation, and verifying that the fraction of the transformed laser points without a corresponding model point within some predefined distance is less than some predefined bound. We discard those hypotheses that do not satisfy this verification.

(5) For each verified hypothesis, we refine as follows:

(5.1) Evaluate the current pose. Thus, if  $\ell_i$  is a vector representing a laser point,  $m_j$  is a vector representing a model point, and  $T$  is a coordinate frame transformation, then the evaluation function for a particular pose is

$$E_1(T) = \sum_i \sum_j e^{-\frac{|T\ell_i - m_j|^2}{\sigma^2}} \quad (1)$$

This objective function is similar to the posterior marginal pose estimation (PMPE) method used in [10]. This Gaussian weighted distribution is a method for roughly interpolating between the sampled model points to estimate the nearest point on the underlying surface to the transformed laser point. Because of its formulation, the objective function is generally quite smooth, and thus facilitates "pulling in" solutions from moderately removed locations in parameter space. As well, it bears some similarity to the radial basis approximation schemes used for learning and recognition in other parts of computer vision (e.g. [2]).

(5.2) Iteratively maximize this evaluation function using Powell's method. This yields an estimate for the pose of the laser points in model coordinates.

(5.3) Execute this refinement and evaluation process using a multiresolution set of Gaussians.

(5.4) Using the resulting pose of this refinement, repeat the pose evaluation process, now using a rectified least squares distance measure. In particular, perform a second sampling of the model from the current viewpoint, using a finer sampled z-buffer. Relative to this finer model, evaluate each pose by measuring the distance from each transformed laser point to the nearest model point, (with a cutoff at some predefined maximum distance). Evaluate the pose by summing the squared distances of each point. Minimize using Powell's method to find the least squares pose solution. Here the evaluation function is

$$E_2(T) = \sum_i \min_j \left\{ d_{\max}^2, \min_j |T\ell_i - m_j|^2 \right\} \quad (2)$$

where  $d_{\max}$  is some preset maximum distance. This objective function is essentially the same as the MAP matching scheme of [10], and acts much like a robust chamfer matching scheme (e.g. [8]). This second objective function is more accurate locally since it is composed of saturated quadratic forms, but it is also prone to sticking in local minima. Hence we add one more stage.

(5.5) To avoid local minima traps, randomly perturb the solution and repeat the least squares refinement. We continue, keeping the new pose if its associated RMS error is better than our current best. We terminate this process

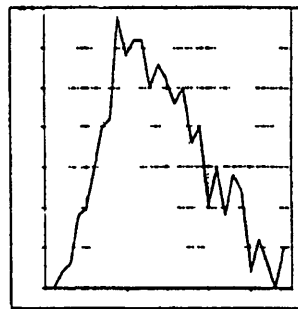


Figure 2 Histogram of residual errors for pose of Figure 1

when the number of such trials that have passed since the RMS value was last improved becomes larger than some threshold.

(5.6) The final result (Figure 1) is a pose, and a measure of the residual deviation of the fit to the model surface.

We collect such solutions for each verified hypothesis, over all legal view samples, and rank order them by smallest RMS measure. The result is a highly accurate transformation of the MRI data into the laser coordinate frame.

### 3.4 Camera Calibration

Once we have such a registration, it can be used for surgical planning. A video camera can be positioned in roughly the viewpoint of the surgeon, i.e. looking over her shoulder. If one can calibrate the position and orientation of this camera relative to the laser coordinate system, one can then render the aligned MRI or CT data relative to the view of the camera. This rendering can be mixed with the live video signal, giving the surgeon an enhanced reality view of the patient's anatomy [11]. This can be used for tasks such as planning a craniotomy or a biopsy, or defining the margins of an exposed tumor for minimal excision.

We have investigated two methods for calibrating the camera position and orientation, one using a calibration object of known size and shape, and one using an arbitrary object (such as the patient's head). In each case, matching 3D laser features against video images of those features allows us to solve for the position of the camera.

## 4 Testing the Method

We have run a series of controlled experiments, in which we have registered a CT reconstruction of a plastic skull with laser data extracted for a variety of viewpoints. In all cases, the system finds a correct registration, with typical residual RMS errors of 1.6 millimeters.

We have also run a series of trials with actual neurosurgery patients. An example registration of the laser data against an MRI model of the patient is shown in Figure 3. Note that in this case, while most of the scalp had been shaved for surgery, a patch of hair was left hanging down over the patient's temple. As a result, laser data coming from the hair cannot be matched against the segmented skin surface in the MRI model, and this shows up as a set of points slightly elevated above the patient's skin surface in the final registration. We can automatically remove these

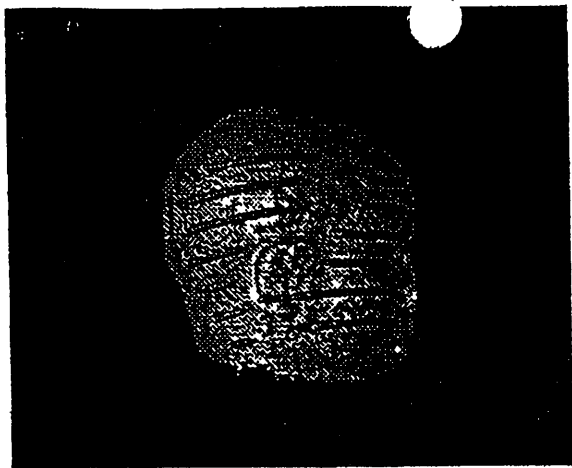


Figure 3 Example of registered laser data (shown as large dots) overlaid on an MRI model. This is a case of registration of an actual neurosurgical case with the patient fully prepped for surgery before the laser data is acquired.

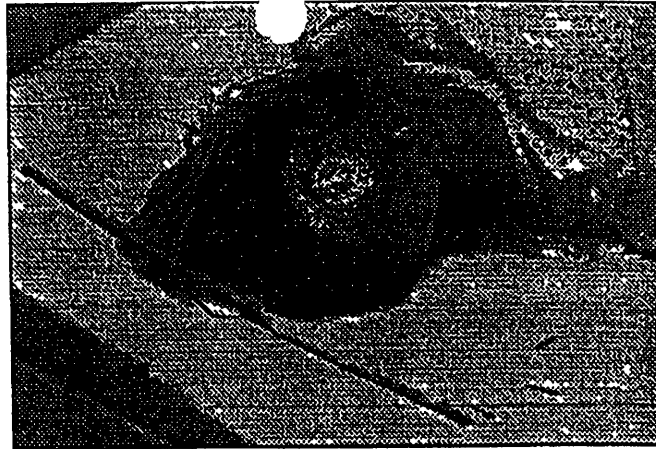


Figure 4 Using the results of Figure 3, and given a calibration of a video camera relative to the laser, we can overlay parts of the MRI model on top of a video view of the patient, providing an enhanced reality visualization of the tumor. In this figure the tumor is shown in green, and the ventricles are displayed as a landmark in blue.

points, and reregister the remaining data. Also displayed are the internal positions of the tumor and the ventricles. The RMS error in this case was 1.9mm. Finally, given the registration between the patient and the model (by matching the laser data in this manner) we can transform the model into the coordinate system of a second video camera, and overlay this model on top of the camera's video view. This is shown in Figure 4.

As mentioned earlier, the method has applications for surgical planning and guidance, including tumor excision and biopsy. The method has broader application, however, including the registration of multiple clinical data sets such as MRI versus CT. A companion paper [5] discusses the application of our method to change detection studies for tracking lesion growth in patients with multiple sclerosis.

## 5 Related Work

Several other groups have reported methods similar to ours. Of particular interest are three such approaches. Two other groups use alternative least squares minimization methods [9, 3] with some operator input to initialize and to guide the search. A third group [1] performs registration by matching ridge lines on surfaces.

## References

- [1] Ayache, N., J. D. Boissonnat, L. Cohen, B. Geiger, J. Levy, O. Monga, P. Sander, "Steps Toward the Automatic Interpretation of 3D Images", In *3D Imaging in Medicine*, edited by H. Fuchs, K. Hohne, S. Pizer, NATO ASI Series, Springer Verlag, 1990, pp. 107-120.
- [2] Brunelli, R. and T. Poggio, 1991, "HyberBF Networks for Real Object Recognition", *IJCAI*, Sydney, Australia.
- [3] Champloboux, G., Lavallee, S., Szeliski, R., Brunie, L., "From accurate range imaging sensor calibration to accurate model based 3D object localization", *IEEE Conf Comp Vis Patt Recog* 83-89, 1992.
- [4] Chue, H. E. and W. E. Lorensen and R. Kikinis and F. Jolesz, 1990, "Three Dimensional Segmentation of MR

Images of the Head Using Probability and Connectivity" *JCAT* 14(6) 1037-1045

- [5] Ettinger, G. J., W. E. L. Grimson, and T. Lozano-Peres, 1994, "Automatic 3D Image Registration for Medical Change Detection Applications", *AAAI 1994 Spring Symposium Series, Applications of Computer Vision in Medical Image Processing*.
- [6] Grimson, W. E. L., 1990, *Object Recognition by Computer: The role of geometric constraints*, MIT Press, Cambridge.
- [7] Huttenlocher, D. and S. Ullman, 1990, "Recognizing Solid Objects by Alignment with an Image," *Int J Comp Vis* 5(2) 195-212.
- [8] Jiang, H., R. A. Robb and K. S. Holton, 1992, "A New Approach to 3D Registration of Multimodality Medical Images by Surface Matching", in *Visualization in Biomedical Computing - SPIE* 196-213.
- [9] Pelizzari, C. A., Chen, G. T. Y., Spelbring, D. R., Weichselbaum, R. R., Chin, T. C., "Accurate three dimensional registration of CT, PET, and/or MR images of the brain", *JCAT* 13(1) 20-26, 1989.
- [10] Wells, W. M., 1993, *Statistical Object Recognition*, Ph.D. Thesis, MIT (MIT AI Lab TR 1398).
- [11] Wells, W. M., R. Kikinis, D. Altobelli, W. Lorensen, G. Ettinger, H. Chue, P. L. Gleason and F. Jolesz, 1993, "Video Registration using Fiducials for Surgical Enhanced Reality" *15th Conf IEEE Eng Med Biol Soc*.
- [12] Wells, W. M., R. Kikinis, F. A. Jolesz, and W. E. L. Grimson, 1993, "Statistical Gain Correction and Segmentation of Magnetic Resonance Imaging Data", in preparation.

## Computer-Assisted Spine Surgery: A Technique for Accurate Transpedicular Screw Fixation Using CT Data and a 3-D Optical Localizer

S Lavallee, Ph D, P Sautot, Ph D, J Troccaz, Ph D, P Cinqun, Ph D, M D, and P Merloz, M D  
Faculte de Medecine de Grenoble, TIMC-IMAG (S L, PS, J T, P C), La Tronche,  
France, Service de Chirurgie Orthopedique, CHU (P M), Grenoble, La Tronche, France

**ABSTRACT** The computer-assisted spine surgery system presented in this paper follows the basic ideas which have been developed for computer-assisted medical interventions (CAMI) in our lab since 1985. There are three steps to insert a linear tool inside vertebral pedicles. First, the surgeon defines an optimal trajectory on pre-operative computed tomography. Second, this trajectory is reported in the operating room coordinate system using an intra-operative sensor and a registration algorithm. Third, a guiding system helps the surgeon follow the selected trajectory. In this paper, we present an implementation of this method that uses only a 3-dimensional optical localizer. Results on cadaver specimens and on the first seven patients are presented. *J Image Guid Surg* 1 65-73 (1995)  
©1995 Wiley Liss Inc

---

**Key words** computed tomography, spinal surgery, surface registration, 3-dimensional optical localizer

---

### INTRODUCTION

The spine contains 24 articulated vertebrae. Instrumentation is used to fix spine segments to reduce deformities (e.g. scoliosis) or to treat fractures. Spinal surgery instrumentation consists of three basic implantable elements: the rod, the hook, and the screw (Fig. 1). The pedicle is the strongest part of the vertebral bone into which a screw can be driven. Unfortunately, it is not the widest part of the vertebra. The diameter of a lumbar or thoracic pedicle may vary from 3 mm to 10 mm.<sup>16</sup> Figure 2 demonstrates the anatomy of vertebrae. During spine surgery, the back part of the vertebra is exposed and the surgeon's anatomical knowledge guides the drilling direction. A slight error in direction may result in a significant error in the position of the tip of the screw. Drilling is performed at least twice, but sometimes ten or twelve times during surgery, with no direct visibility of the crucial structures, i.e. spinal cord, lung, vessels, and nerves. Even when the surgical instrument is inside the vertebra, the surgeon does not know the

location of the tip. Therefore, providing the surgeon with a 3-dimensional (3-D) representation of the vertebra during surgery would be a great improvement. Previous studies of surgical procedures have demonstrated an approximately 10% incorrect placement of the screws.<sup>17</sup> It is important to increase safety by more precise intervention. Presently, our technique is restricted to lumbar vertebrae (where the pedicle is larger), but a future application is for dorsal vertebrae. Finally, percutaneous screw placement would contribute to less invasive surgery, which could be also used for intra-vertebral disc punctures. In this paper, we focus on transpedicular screw fixation, but the method we propose has many related applications in orthopedics.

For several years, our group has been developing methods for computer-assisted surgery.<sup>3-5</sup> We have implemented several systems that follow the same methodology. The basic components of these systems are: 1) A user interface to plan the surgery using pre-

---

Received original February 14, 1995; accepted March 1, 1995.

Address reprint requests to Stephane Lavallee, TIMC, AB, Faculté de Médecine, 38706 La Tronche Cédex, France; email: stephane.lavallee@imag.fr

©1995 Wiley Liss Inc



Fig 1 Lateral and frontal radiographs of an instrumented spine

operative computed tomography (CT) 2) An intraoperative sensor to collect data. It can be a pair of radiographic images<sup>13</sup> a 3-D ultrasound probe spatially registered<sup>1</sup> or a 3-D pointer (described in this paper) 3) A registration algorithm to match intraoperative data with a model of the vertebra segmented on pre-operative CT images<sup>8</sup> And 4) A guiding system to perform the planned trajectory. It can be a simple mechanical guide—a laser beam positioned by a robot and aligned with the trajectory<sup>15,18</sup> or a passive localizer (described in this paper). See Lavallee et al<sup>9</sup> for an extensive description and comparison of these systems.

Recently a technique very similar to ours has been proposed by Nolte et al<sup>13</sup>. These authors report successful tests in clinical trials. Almost the same material components are used in this study confirming the need for an accurate localizer such as the Optotrak system. However a different user interface design was used in which CT images are displayed in almost real time during surgery. This might be preferable to avoid the pre-operative planning step. A major difference with our system is that we use a

surface registration instead of a simple point registration. The surface registration has the advantage of being easier for the surgeon since it requires only that some random 3-D points on the vertebra surface be digitized instead of digitizing specific landmarks on both CT images and real vertebrae. Surface registration is also more accurate than point matching. Since we are able to perform the registration technique using both 3-D surface points and radiographic images, our system also provides the possibility of using only radiographs, making possible percutaneous operations. Barbe et al<sup>1</sup> demonstrated that a percutaneous (non-invasive) registration can be also performed using ultrasound images.

This paper presents a passive system using only a 3-D optical localizer during surgery for both registration and guidance. After a description of the system and the method, results of studies with cadaveric specimens and with seven patients are described.

## METHODS

### Surgical Planning

Computed tomography provides 2-dimensional (2-D) images of the anatomy of interest (typically three or more vertebrae). Using a spiral CT, a set of 2 mm spaced slices is easily obtained. We are also investigating the use of magnetic resonance imaging (MRI).

Before operating, the surgeon chooses an optimal 3-D line in the volume of medical images. In the literature, several quantitative parameters are proposed to describe a vertebra<sup>16</sup>. These parameters can be related to direct measurements on CT scan images<sup>14</sup>. These reports have encouraged us to design a user interface to plan the position of a screw inside a pedicle (Fig 3). Three orthogonal re-sliced images are computed and interactively modified by the surgeon. The intersection of the two first planes corresponds to the trajectory axis. The third image pro-

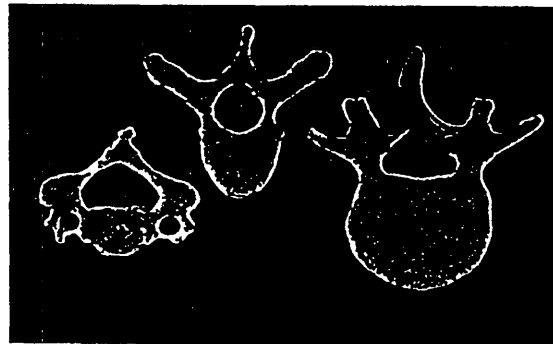


Fig 2 Vertebral anatomy. From left to right, cervical, thoracic and lumbar vertebra.



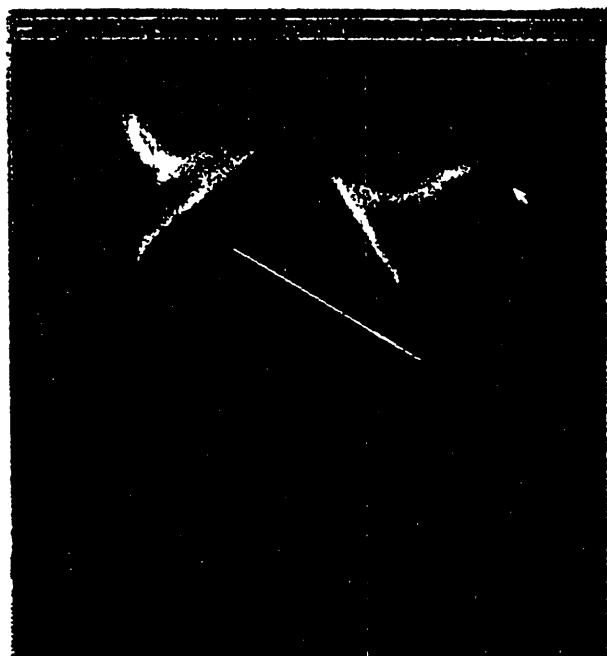


Fig 3 Surgical planning interactive definition of a line segment within the CT volume of data

duces a section orthogonal to the trajectory. At the end of this session the trajectory is defined by two points in the CT coordinate system  $P1_{CT} = (x1\ y1\ z1)$  and  $P2_{CT} = (x2\ y2\ z2)$ . The first point  $P1_{CT}$  defines the farthest extent of the screw to avoid perforation of the vertebral core. The diameter of the screw is also selected at this stage to insure that the screw is entirely inside the pedicle.

#### The Intra-Operative System

The system used in the operating room consists of a workstation DEC 5000, a 3-D optical localizer (Optotrak™ Northern Digital Toronto) and a set of 3 sterilizable rigid bodies each made of 6 infra red diodes (Fig 4). These components are integrated in a mobile cart. The optical sensor provides the position and orientation of the rigid bodies in real time with an accuracy of  $\pm 0.3$  mm.

A first rigid body is firmly fixed to the spinous process of the vertebra. It defines the intra-operative coordinate system  $Ref_{intra}$ .

A second rigid body  $Ref_{np}$  is equipped with a sharp tip to collect 3-D coordinates of points by a simple contact activated by a pedal switch. This 3-D pointer is easily calibrated using a pivot technique that takes about 10 seconds. The surgeon first places the pointer tip at a fixed location anywhere on the reference rigid body  $Ref_{intra}$  and then rotates the pointer around this fixed point. The intrinsic XYZ<sub>np</sub>

coordinates of the tool tip are then computed in the coordinate system  $Ref_{pointer}$  by calculating with a least squares approximation the most invariant point in these motions. The system accepts the calibration only if the mean residual error obtained in the least squares estimation is less than 0.5 mm. It is usually 0.2 mm. By simple matrix products each acquisition gives the position of the pointer tip in  $Ref_{intra}$ .

A third rigid body  $Ref_{drill}$  is mounted on a standard surgical drill. The drill chuck defines the mechanical axis and is calibrated by repeating the pivot calibration technique for two sharp drills of differ-

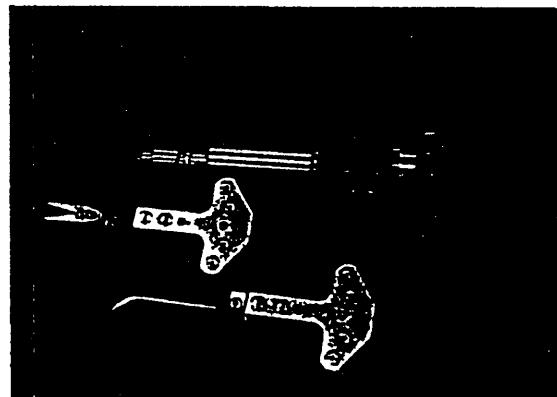


Fig 4 The material is made of 3 rigid bodies with 6 infra red markers that are attached to a pointer, a pin that will be fixed to the vertebra, and a standard drill.

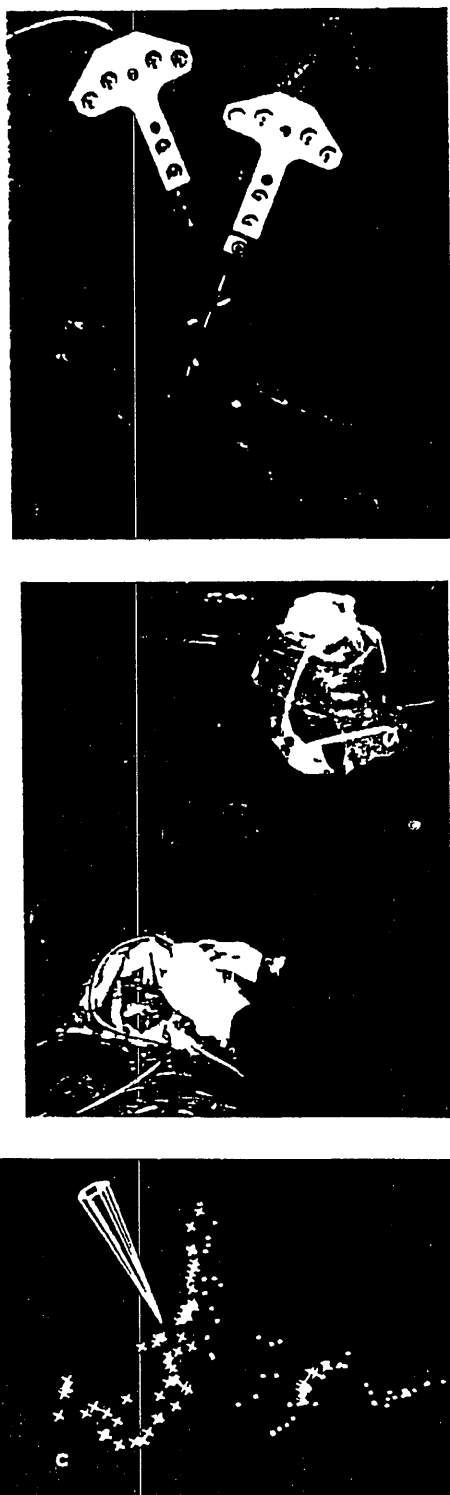


Fig 5 To collect a 3 D point the surgeon positions the pointer tip in contact with the vertebral surface and presses a foot pedal (a) Acquisition during in vitro experiments (b) Acquisition during actual surgery (c) The result is a set of 3 D surface points lying on the vertebral surface Motions of the vertebra are compensated through an internal coordinate system fixed to the spinous process

ent lengths Therefore for each coordinates acquisition the system yields the position of the drill tip A1 and a second point on the drill axis A2 both being computed in  $Ref_{intra}$

Using the 3 D pointer  $Ref_{pointer}$ , the surgeon collects a set of points lying on the surface of the exposed vertebra (Fig 5) Typically about 50 points are acquired in a few seconds The result is a set of 3 D coordinates of points  $M_i, i = 1 \dots m$  given in the intrinsic vertebral reference system Therefore any motion of the vertebra due to respiration or movements by the surgeon does not affect the precision of the acquisition

#### Pre-Operative and Intra-Operative Registration

Registration calculates the rigid-body transformation between the coordinate system associated with CT images, namely  $Ref_{CT}$ , and the intra operative coordinate system associated with the vertebra namely  $Ref_{intra}$

First we use the result of a segmentation process of the vertebral surface from CT images We have developed several deformable surface tools to model pre operative images with minimal interaction with the user<sup>10 11</sup> These tools create a dense set of surface points  $N_j, j = 1 \dots n$  in  $Ref_{CT}$  (typically  $n = 10000$ ) From such a set, a 3 D octree spline distance map is computed This is a pre processing step that speeds the intra operative registration<sup>8</sup> These steps are performed before the operation

During the surgery a 3 D/3 D registration algorithm matches the 3-D data points  $M_i$  with the octree spline distance map computed from the points  $N_j$  Beginning with a standard initial position the algorithm estimates the rigid body transformation  $RT_{CT}^{intra}$  between the CT coordinate system and the intra operative coordinate system To obtain this transformation the sum of squares of distances between the points  $M_i$  and the surface represented implicitly by the octree spline distance map is minimized Details can be found in Champeboux et al<sup>2</sup> and Lavallee et al<sup>6-8</sup>

Figure 6 shows a typical convergence of the registration algorithm At the end of this step the optimal trajectory can be computed in  $Ref_{intra}$

$$P_{i_{intra}} = RT_{CT}^{intra} P_{i_{CT}} \text{ for } i = 1 \dots 2 \quad (1)$$

#### Alignment of a Surgical Drill

This final step aligns the points A1 and A2 to define the drill axis with the optimal surgical line ( $P1_{intra}, P2_{intra}$ ) The drill is aligned with the optimal trajec

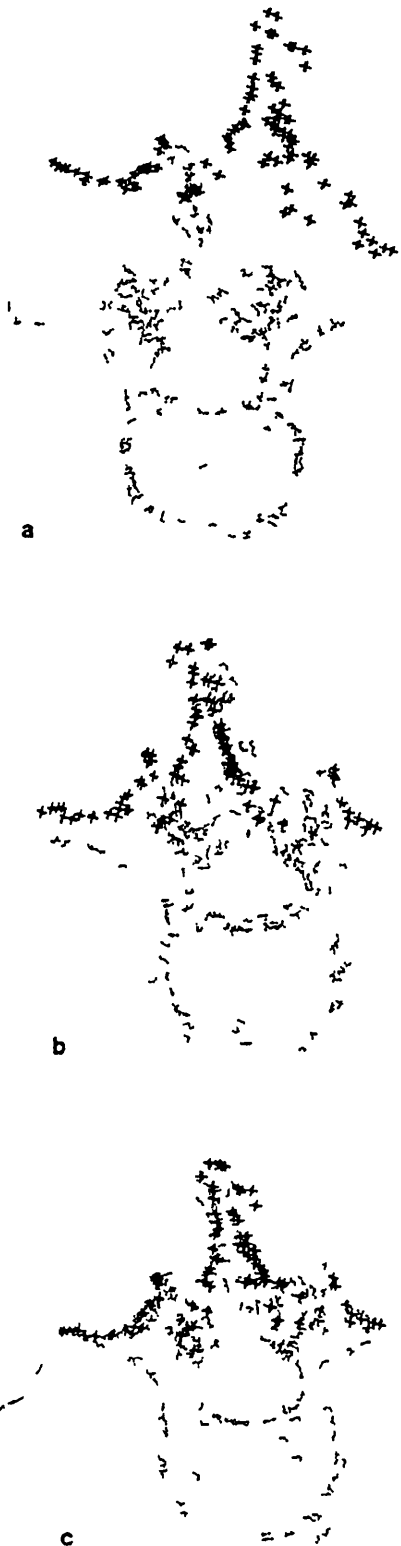


Fig 6 Iterative registration of 3 D data points with the surface model segmented in CT images (a) Initial position (b) Intermediate position (c) Final position The convergence is reached in about 2 sec on a DEC5000

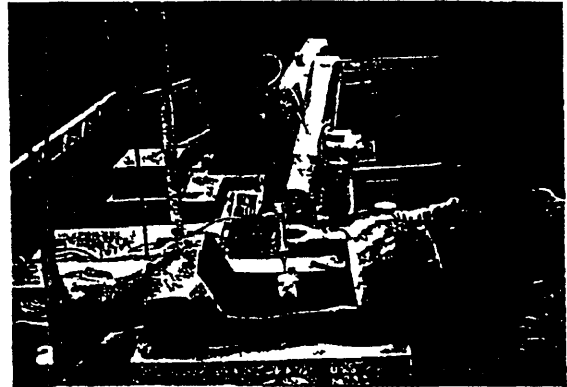


Fig 7 During in vitro experiments a 6 axis robot positions a laser beam at the location of the optimal trajectory with a submillimetric accuracy (a) A tool is aligned with the laser beam in simulated open surgery (b) The same technique can be used for percutaneous surgery

tory if and only if the distances between the drill points A1 and A2 and the optimal line are zero

A first possibility to perform of such an alignment is based on a robot that carries a laser beam. The robot positions the laser beam to coincide with the optimal trajectory. Then the surgeon aligns a tool with this laser beam<sup>15</sup>. Figure 7 shows such an alignment performed during in vitro experiments. However since this technique requires the use of a robot we have designed a less expensive technique using only the 3 D localizer. This approach is described below. In the future a possible strategy is to merge both approaches to gain ease of use and also safety by redundancy.

The technique using only the 3 D localizer is based on a specifically designed graphics user inter-

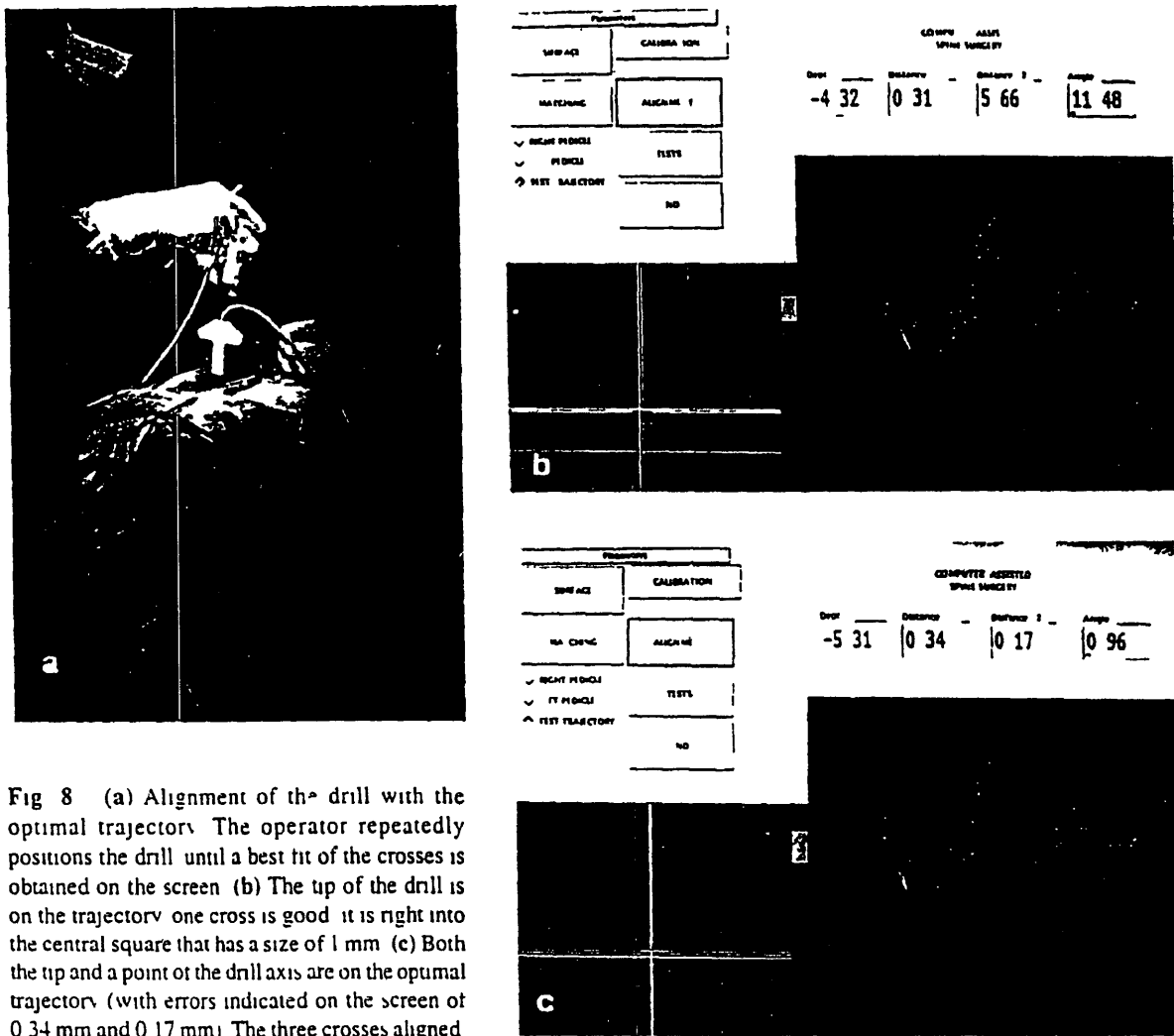


Fig 8 (a) Alignment of the drill with the optimal trajectory. The operator repeatedly positions the drill until a best fit of the crosses is obtained on the screen (b) The tip of the drill is on the trajectory, one cross is good, it is right into the central square that has a size of 1 mm (c) Both the tip and a point of the drill axis are on the optimal trajectory (with errors indicated on the screen of 0.34 mm and 0.17 mm). The three crosses aligned.

face. On the left part of the screen, we compute a view which is orthogonal to the optimal line. On that view, the optimal line ( $P1_{\text{tra}}$ ,  $P2_{\text{tra}}$ ) is reduced to a single point drawn as a red square in the middle of the image. In real time, the drill point A1 is projected on that view and drawn as a green cross. The drill point A2 is projected on that view as well and drawn as a blue cross. For an arbitrary position of the drill, the three crosses are distinct. The corresponding window is scaled to 10 mm, therefore a motion of one pixel on the screen corresponds to 0.02 mm, which ensures sufficient sensitivity. The position of the drill is acquired and displayed at a frequency more than 10 Hz.

A two steps method is used to easily align the crosses. First, the surgeon locates the tip of the drill on the optimal trajectory by aligning the green and red crosses. The distance between the tip point A1 and the optimal line is computed and displayed in millimeters. Second, the surgeon adjusts the orientation of

the drill by aligning the blue and red crosses. The distance between the axis point A2 and the optimal line is computed and displayed in millimeters (Fig 8).

Other features are useful to display for the surgeon. First, the angle between the drill axis and the optimal line is computed and displayed in degrees. But more importantly, the distance between the tip of the drill A1 and the limit point  $P1_{\text{tra}}$  is computed and displayed in millimeters. Moreover, the amplitude of this depth is also represented by a vertical color bar.

Finally, on the right part of the screen, a 3D view represents the vertebral surface points, the optimal trajectory, and a drawing of the current position of the drill as an arrow. Although we can interactively change the point of view and the scale of this view, we find it useful for global representation and checking of abnormalities, but not as useful as the simple view with crosses which allows for an accurate and easy alignment.

This alignment procedure is actually very intuitive and accurate. Using a rough pre alignment between the screen and the surgeon the motions from left to right in reality coincide with motions from left to right on the screen. Typically a sub millimetric alignment is performed in a few seconds. The only drawback of this method is that the surgeon has to look at the screen and the vertebra at the same time. However the screen can be quite close to the operating field.

#### VALIDATION

##### In Vitro Studies

This method was first validated with in vitro experiments. An isolated vertebra is pierced with two 3 mm holes in the right and left pedicles. A 3-D CT of this vertebra is acquired and the positions of the axes of the holes are defined interactively using the user interface presented above. We then acquire surface points and register the CT and intra-operative coordinate systems. Finally a drill is inserted inside the holes made in the pedicles. The system then computes the distances between the planned trajectory and the actual position of the drill axis. For all experiments submillimetric distances were obtained.

In a second series of experiments the surgeon actually drilled the pedicles of cadaver specimens using the complete system. Then we acquired lateral and frontal radiographs to check that the drilled axis was in the middle of the pedicle. The result was very satisfactory according to the surgeon (Fig 9).

##### Clinical Studies

Clinical studies were begun in May 1994. Thus far the system has been used with 7 patients. Figure 5 shows the surgeon digitizing surface points before they are registered with the CT model of the vertebra. The cart that carries the workstation and the 3 cameras of the optical localizer are seen in the background behind a sterile plastic cover.

During these first studies on patients the system was not used completely for safety and ethical reasons. The surgeon drills the pedicle of a vertebra as usual but the trajectory chosen by the surgeon is compared with the trajectory indicated by the system. A drill equipped with a rigid body is inserted in the hole made by the surgeon to measure the errors by looking at the offset positions of the 2 crosses described above.

During these studies we also check the accuracy of the system by taking a pair of calibrated radiographs of the vertebra. In Figure 10 a calibration plate is positioned between the X ray intensifier and the vertebra. This plate is located in the sensor coordinate system by the use of a fourth infra-red rigid body mounted on the plate. Radiographs are then digitized from the video output of the X-ray system. A technique of 3-D/2-D registration is applied between the CT model of the vertebra and the pair of calibrated radiographs to estimate the transformation between the CT coordinate system and the intra-operative reference system.<sup>8</sup> This transformation is compared with the transformation obtained with the technique described in this paper to check the coherence between two systems. In the future we hope that this percutaneous registration will replace the registration using 3 D surface points. So far the latter technique has proven to be more reliable.



Fig 9 In vitro experiment lateral radiograph of a vertebra after the pedicle has been drilled according to the complete method. The drill is in the middle of the pedicle.

For all patients a difference of a few millimeters was found between the trajectory made manually and the trajectory indicated by the surgeon. This corresponds to the error made by the surgeon when the operation is performed without computer assistance (Fig 11). Such a comparison verifies if the system is working well in clinical conditions and also provides the surgeon with experience of the technique. Because of the positive results in these preliminary studies we are planning a full clinical trial.

CONCLUSION

In conclusion the system we propose for computer assisted surgery is simple to use and very accurate. It has been tested in clinical conditions in the operating room. Successful results with in vitro experiments and positive tests in vivo let us plan an extensive clinical trial of the system. The clinical benefits of this system are first to provide reliable and optimal transpedicular fixations on lumbar vertebrae and second to make possible and easy the transpedicular fixation of vertebrae higher than the lumbar region.



Fig 10 Acquisition of calibrated x rays during the operation

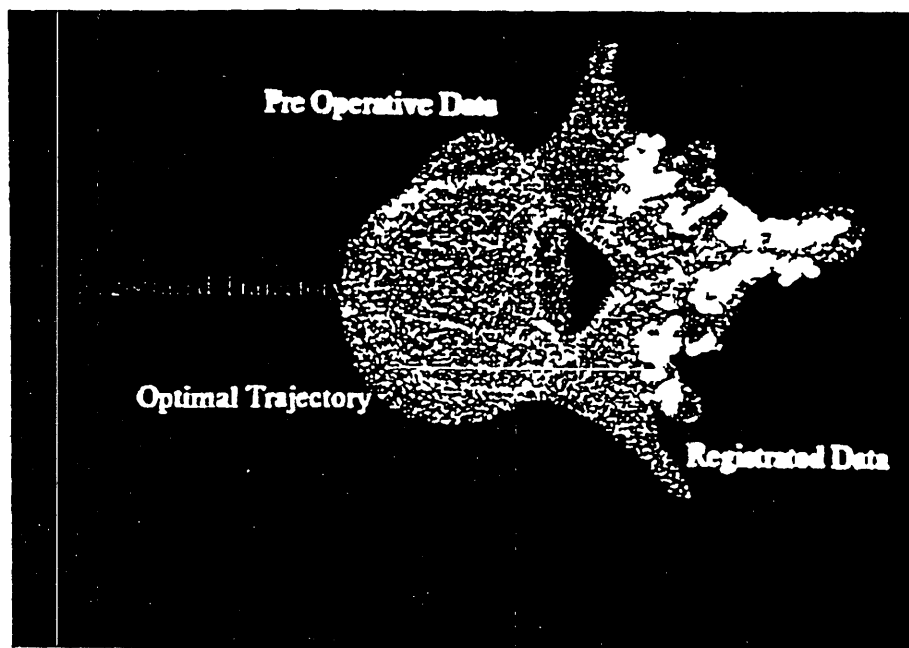


Fig 11 Typical difference between the optimal trajectory and the trajectory selected by the surgeon

## REFERENCES

- 1 Barbe C Troccaz J Mazier B Lavallée S (1993) Using 2.5D echography in computer assisted spine surgery IEEE Engineering in Medicine and Biology Society Proceedings pp 160-161
- 2 Champlébourg G Lavallee S Szeliski R Brunie L (1992) From accurate range imaging sensor calibration to accurate model based 3D object localization IEEE Computer Society Conference on Computer Vision and Pattern Recognition (CVPR 92) pp 83-89
- 3 Cinquin P (1994) Gestes Médico-Chirurgicaux Assistés par Ordinateur Annales de Radiologie (in French) 36 386-406
- 4 Lavallée S (1989) A new system for computer assisted neurosurgery IEEE Engineering Medicine Biology Society (EMBS) pp 926-927
- 5 Lavallée S Cinquin P (1990) Computer assisted medical interventions In Hohne KH (ed) NATO ARW 3D Imaging in Medicine Berlin Springer Verlag pp 301-312
- 6 Lavallee S Cinquin P Szeliski R Pena O Hamadeh A Champlébourg G Troccaz J (1995) Building a hybrid patient's model for Augmented Reality in Surgery A registration problem Comput Biol Med (in press)
- 7 Lavallee S Szeliski R (1995) Recovering the position and orientation of free form objects from image contours using 3D distance maps IEEE PAMI (Pattern Analysis and Machine Intelligence) (in press)
- 8 Lavallee S Szeliski R Brunie L (1991) Matching 3D smooth surfaces with their 2D projections using 3D distance maps SPIE Geometric Methods in Computer Vision 1570 332-336
- 9 Lavallée S Troccaz J Sautot P Mazier B Cinquin P Merloz P Chirossel JP (1995) Computer assisted spine surgery using anatomy based registration In Taylor R Lavallee S Burdea G Mosges R (ed) Computer Integrated Surgery Cambridge MIT Press (in press)
- 10 Leitner F Cinquin P (1993) From Splines and Snakes to SNAKES SPLINES In Laugier C (ed) Geometric Reasoning From Perception to Action Berlin Springer Verlag pp 264-281
- 11 Leitner S Marque I Lavallee S Cinquin P (1991) Dynamic segmentation Finding the edge with spline snakes In Laurent PJ (ed) Curves and Surfaces Chamonix Academic Press pp 279-284
- 12 Mazier B Lavallée S Cinquin P (1990) Computer assisted interventionist imaging Application to the vertebral column surgery 12th IEEE Engineering in Medicine and Biology Conference pp 430-431
- 13 Nolte LP Zamorano L Jiang Z, Wang Q Langlotz F Arm E Visarius H (1994) A novel approach to Computer Assisted Spine Surgery MRCAS Proceedings pp 323-328
- 14 Olsewski JM Simmons EH Kallen FC Mendel FC Severin CM Berens DL (1990) Morphometry of the lumbar spine Anatomical perspectives related to transpedicular fixation J Bone Joint Surg AM 72 541-548
- 15 Sautot P Cinquin P Lavallée S Troccaz J (1992) Computer assisted spine surgery A first step towards clinical application in orthopaedics 14th IEEE Engineering in Medicine and Biology Conference pp 1071-1072
- 16 Scoles PV Linton AE Latimer B Levy ME Giovanni BF (1987) Vertebral body and posterior element morphology in the normal adult spine 4th Proceeding of the International Congress on Cotrel Dubousset Instrumentation pp 151-156
- 17 Sim E (1993) Location of transpedicular screws fixation of the lower thoracic and lumbar spine Acta Othop Scand 64 28-32
- 18 Troccaz J Lavallee S Sautot P Cinquin P Mazier B Chirossel JP (1993) Robot assisted spine surgery Medimicroelectronics International Workshop Malaga English Ministry pp 1-11

# An Image-Directed Robotic System for Precise Orthopaedic Surgery

Russell H Taylor, Fellow IEEE Brent D Mittelstadt, Howard A Paul,  
William Hanson, Peter Kazanzides, Member IEEE Joel F Zuhars, Member IEEE  
Bill Williamson, Bela L Musits, Edward Glassman, and William L Bargar

**Abstract**—We have developed an image-directed robotic system to augment the performance of human surgeons in precise bone machining procedures in orthopaedic surgery, initially targeted at cementless total hip replacement surgery. The total system consists of an interactive CT based presurgical planning component and a surgical system consisting of a robot, redundant motion monitoring, and man machine interface components. In vitro experiments conducted with this system have demonstrated an order-of magnitude improvement in implant fit and placement accuracy, compared to standard manual preparation techniques. The first generation system described in this paper was used in a successful veterinary clinical trial on 26 dogs needing hip replacement surgery. It was the basis for subsequent development of a second-generation system that is now in human clinical trials.

## I INTRODUCTION AND BACKGROUND

### A Augmentation of Human Skill in Surgery

THE RESEARCH reported in this paper represents a step in an evolving partnership between humans (surgeons) and machines (computers and robots) that seeks to exploit the capabilities of both to do a task *better* than either can do alone. Recent advances in medical imaging technology (CT MRI PET etc) coupled with advances in computer based image processing and modelling capabilities have given physicians an unprecedented ability to model and visualize anatomical structures in live patients and to use this information quantitatively in diagnosis and treatment planning. Further, advances in CAD/CAM technology have made it practical to use this data to design and precisely fabricate custom surgical implants for individual patients.

One result is that the precision of image based presurgical planning often greatly exceeds the precision of surgical execution. Typically, geometrically precise surgery has been limited to procedures (such as brain biopsies) for which a suitable stereotactic frame is available. The inconvenience and restricted applicability of these devices has led many

researchers to explore the use of robotic devices to augment a surgeon's ability to perform geometrically precise tasks planned from computed tomography (CT) or other image data.

The pioneering work in the use of general purpose robots for surgery was that of Kwok *et al* [1] who used a six axis industrial robot to replace a stereotactic frame in neurosurgery. In this case the robot was mounted in a known position relative to the table of a CT scanner and suitable geometric calibrations were performed. During surgery, the patient was CT-scanned and a desired placement for a biopsy needle probe was determined from the image data. The robot then positioned a passive needle guide appropriately, brakes were applied and power was turned off. Finally, the surgeon inserted the needle through the guide into the patient's brain. The principal benefit gained was the greater convenience and faster positioning possible with the robot compared to the use of a stereotactic frame. A number of similar systems have been developed subsequently. The most successful to date is that of Lavalée *et al* ([2] [3]) who used a stereo pair of intraoperative radiographs to register the robot to the patient's CT data (and to the patient) and to plan needle paths that avoid blood vessels. Over three hundred cases have been performed although (again) the robot is turned off while the needle is inserted. Kelly *et al* [4] [5] have implemented a specialized motorized stereotactic system for laser neurosurgery in which an XYZ table is used to reposition the patient's head relative to the focal point of a surgical microscope. More recently Drake Goldenberg *et al* [6] have reported several cases in which a general purpose robot moved while in contact with the patient although the motions were very simple and highly constrained. Further these cases were performed on an exception basis in which the surgeon had no practical alternative despite somewhat more limited safety checking than would have been desirable for more routine use. Several other neurosurgery robots are in various stages of development (e.g. [7]).

A number of active robotic systems for augmentation of non neurosurgical procedures have also been proposed or developed. For example Davies *et al* have developed a specialized robotic device to assist in laparoscopic prostatectomies [8] which has been used clinically. A number of groups (e.g. [9]–[12]) have developed a variety of other telerobotic devices for endoscopic and laparoscopic surgery. McEwen *et al* have developed and marketed a clinically qualified voice controlled limb positioning system for orthopaedics [13]. Several groups (e.g. [14], [15]) have demonstrated *in vitro* robotic systems for

Manuscript received December 16 1991 revised March 14 1994

R. H. Taylor and E. Glassman are with the IBM T. J. Watson Research Center Yorktown Heights New York 10598 USA.

B. D. Mittelstadt, P. Kazanzides, J. F. Zuhars, B. Williamson, B. L. Musits and W. L. Bargar are with Integrated Surgical Systems Sacramento California 95834 USA.

H. A. Paul deceased was with Integrated Surgical Systems Sacramento California 95834 USA.

W. Hanson was with the IBM Palo Alto Science Center Palo Alto CA 95834 USA. He is now with Loral Federal Systems Gaithersburg MD 20879 USA.

IEEE Log Number 9403327



positioning passive instrument guides for knee replacement surgery. Of these applications, that of Davies comes closest to ours in the sense that it uses an active automatic device to perform a tissue removal operation. Important differences include an order of magnitude difference in the accuracy required for the application, the greater complexity of the shapes to be cut, the use of a general purpose manipulator rather than a specialized device, and the greater degree of safety and consistency checking built into our system, which must move safely in a much less constrained volume.

### B. Precise Orthopaedic Surgery

Orthopaedic applications represent a particularly promising domain for the integration of image and model based presurgical planning, CAD/CAM technology, and precise robotic execution. For example, about half of the 300,000 total hip replacement operations performed each year use cementless implants. In these procedures, accurate preparation of the femoral cavity to match the implant shape and accurate placement of the cavity relative to the femur can significantly affect stress transfer, implant stability, and restoration of proper biomechanics, which in turn are important factors affecting efficacy. For example, Sandborn *et al.* [16] have reported that the size of gaps between bone and implant significantly affects bone ingrowth. Furthermore, the present manual broaching method<sup>1</sup> for preparing the femoral cavity leaves considerable room for improvement. In one recent study, Paul Hayes *et al.* [17] found that only about 20% of the implant actually touches bone when it is inserted into a manually broached hole. The average gap between the implant and the bone was commonly 1–4 mm, and the overall hole size was 36% larger than the broach. Furthermore, the exact placement of the implant cavity relative to the bone (which affects restoration of biomechanics) depends on the surgeon's ability to line up the broach manually and to drive it the right distance into the femur. Driving the broach too far can split the femur.

These considerations have led us to explore the use of robotic machining to prepare the femoral cavity for the implant. Initial feasibility studies by Paul Mittelstadt *et al.* [18] demonstrated that a robot could successfully machine shapes in human cadaver bones and that preoperatively implanted calibration pins could be used to accurately register CT image and robot coordinates for a femur.

Following these studies, we developed a complete planning and execution system suitable for use in an actual operating room. *In vivo* experiments with this first generation system demonstrated an order of magnitude improvement in surgical precision compared to manual broaching. One of the authors (Dr. Paul) conducted a veterinary clinical trial on dogs needing hip replacement surgery. This experience provided the basis for development of a second generation system that is now in human clinical trials [19]–[22].

Subsequent sections of this paper will summarize the presurgical planning and surgical procedure followed for robotic

<sup>1</sup>Fig. 1 shows a typical cementless implant and the corresponding broach used to make the hole for it. Fig. 2 shows the use of a broach on a human patient. The procedure in a dog is essentially the same.

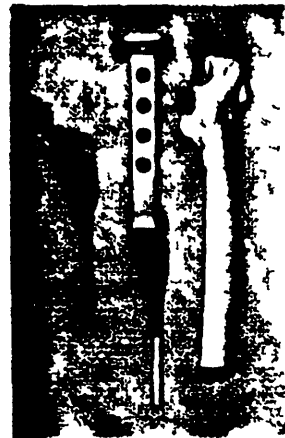


Fig. 1. Typical cementless hip implant and instrumentation. This shows a typical cementless hip implant together with the broach used to produce a corresponding hole in the patient's thigh in conventional hip surgery. Proper placement of the implant socket relative to the femur and accurate reproduction of the socket shape are very important to a successful uniform stress transfer and restoration of the proper biomechanics.



Fig. 2. Manual broaching procedure. This figure shows the use of a broach in a human cementless hip replacement. The procedure in a dog is essentially the same. One study found that only about 20% of the implant actually touches bone when it is inserted into a manually broached hole. The average gap between the implant and the bone was commonly 1–4 mm, and the overall hole size was 36% larger than the broach.

hip replacement surgery and will discuss the requirements for robotic systems intended to augment human precision in surgery. After providing a brief overview of the system architecture, we will provide a fuller discussion of several key aspects of the system, including the image-based presurgical planning, geometric calibration, shape cutting, and safety checking mechanisms. Finally, we will discuss experience of the system in actual clinical use (on dogs) and will discuss some of the lessons learned.

## II. SUMMARY OF PROCEDURE

Before surgery, three titanium pins are implanted through small skin incisions into the greater trochanter and condyle of the patient's femur. A CT scan is made of the leg. The presurgical planning system automatically locates the pin relative to the coordinate system of the CT images. The sur-

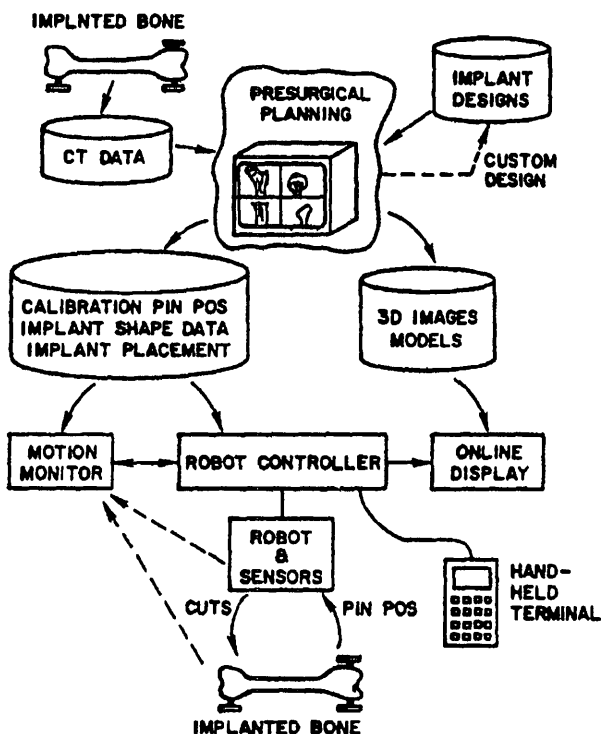


Fig 3 Architecture of hip replacement surgery system. The system consists of a presurgical planning component and a surgical component. In the system used for the veterinary clinical trial, the motion monitoring and robot control functions are subsumed within the robot controller.

geon interactively selects an implant model and determines its desired placement relative to CT coordinates. This information is written to a diskette for use in surgery.

Key steps of the intraoperative procedure are shown in Fig 5 for an *in vitro* test on a cadaver femur. Fig 6 shows the operating room scene during the first canine clinical trial in May 1990. Briefly, the procedure is as follows:

- 1) The robot is brought into the operating room and powered up. A sterile cutting tool is attached to a tool interface just below the force sensor, and the robot is covered with a sterile drape. The patient data diskette is loaded into the robot controller, and the robot is placed in a standby mode.
- 2) The patient is prepared and draped in the normal manner. Surgery proceeds normally until the acetabular component of the implant is implanted and the ball of the femur is removed.
- 3) The robot is brought up to the operating table, and the femur is rigidly attached to the robot base, using a specially designed fixator. The three titanium pins are exposed manually.
- 4) A ball probe/cutter bit is inserted into the collet of the cutting tool. The top center of each pin is then located by a combination of manual guiding and autonomous tactile search by the robot. Although several modes of manual guiding are available, the most commonly used is force compliance. The surgeon simply pulls on the shaft of the cutter; the robot controller senses the forces exerted on the tool and moves the robot in the indicated direction.

- 5) The robot controller uses the pin location information to compute an appropriate transformation from CT coordinates to robot coordinates. The ball probe is replaced by a standard cutting bit, and the robot cuts out the desired implant shape at the planned position and orientation relative to the pins. The surgeon monitors progress both by direct observation of the robot and patient and by looking at a graphical display depicting successive cuts.
- 6) When cutting is complete, the femur is unclamped from the fixator, and the robot is moved out of the way. The rest of the procedure proceeds in the normal way with the added step of removing the locator pins from the patient.

### III REQUIREMENTS AND ISSUES

#### A Human Machine Interaction in a Surgical Situation

Our goal is not to replace the surgeon. Instead, we are concerned with developing a surgical tool that can assist the surgeon by precisely executing a tissue removal task under the surgeon's supervision. Although the robot's geometric accuracy is much greater than the surgeon's, the surgeon's understanding of the total situation is clearly much greater than any computer's, and he or she is responsible for what goes on in the operating room. Suitable interfaces must be provided to allow the surgeon to monitor the robot's actions, to pause execution at any time, initiate error recovery actions, and provide positional guidance to the robot. There is also the related problem of human-computer interaction in presurgical planning. Convenient and naturally understood interfaces must be provided to allow the surgeon to specify what implant shape is to be cut and where it is to go. Furthermore, the interfaces used intraoperatively to report progress of the surgery should be as consistent as possible with those used to plan it.

#### B Registration of Plan Data with Intraoperative Reality

The surgical plan is based on anatomical information derived from CT images taken prior to surgery. Reliable and accurate methods to locate the corresponding anatomical structures relative to the robot are essential if the plan is to be executed successfully.

#### C Verification

It is very important to verify that the greater potential geometric accuracy offered by the use of a robotic surgical system is in fact achieved in practical use. Suitable methods must be developed for verifying the performance of individual system components and of the system as a whole.

#### D Operating Room Compatibility and Sterility

It must be easy to incorporate the robot into a hospital's normal routine. It may be difficult for a hospital to dedicate an operating room to robotic surgery, and even if it does so, it is important that maintenance not be disruptive.<sup>2</sup> Gener-

<sup>2</sup>These considerations led us to rule out some configurations (such as a Cartesian manipulator suspended from the ceiling) that might otherwise have been attractive.

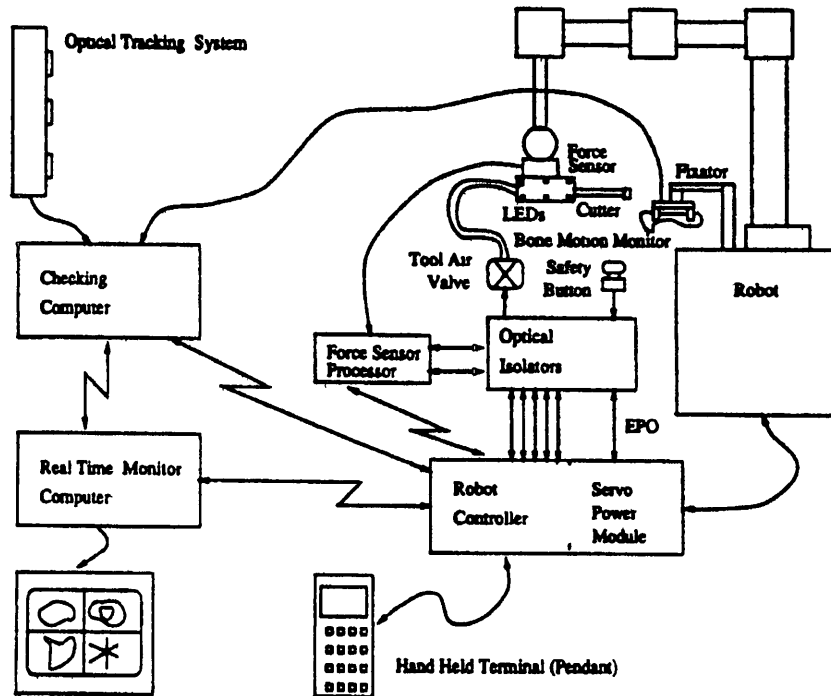


Fig 4 Operating room system architecture The operating room system consists of 1) a surgical robot with its associated controller tooling and safety interlocks 2) a fixator to hold the bone securely to the robot 3) a redundant motion-monitoring subsystem consisting of a checking computer optical tracking system and bone motion detector and 4) a human-machine interface with an online display computer and a hand held terminal interfaced to the robot controller

ally the system should be easily brought into the operating room and set up as part of the normal presurgical routine. Similarly, removal, sterilization, and reattachment of the end effector and other critical components should be easy and suitable. Sterile drapes must be developed for the manipulator arm and other structural components that cannot be easily sterilized.

#### E Safety Error Recovery and Backup

Clearly, redundant safety mechanisms are very important both for the protection of the patient and of the surgeon. Manual pause and emergency power off functions are essential. Wherever possible, potential error conditions must be anticipated and checked for, and adequate recovery procedures must be available. Although the robot often may be able to continue with the procedure following a pause, it is also prudent to provide a reliable means of stopping the robot, removing it from the surgical field, and continuing the operation with manual backup.

Since the surgeon must rely on the precision of the robot, it is extremely important that no single failure cause an undetected loss of accuracy. The system must monitor the position of the robot's cutting tool relative to the shape that it is supposed to cut and stop cutting if it strays out of the desired volume for any reason. It is especially important that systematic shifts (such as might arise from the bone slipping relative to the fixator) be detected promptly. A single misplaced cut can usually be repaired, but it may be much harder to correct for misplacing the entire cavity.

#### IV SYSTEM ARCHITECTURE

The system (Fig 3) consists of a presurgical planning component and an intraoperative (surgical) component. These components are summarized below and discussed at greater length in subsequent sections.

##### A Presurgical Planning

This component [23] implemented on an IBM workstation permits the surgeon to select an implant model and size and to specify where the corresponding shape is to be machined in the patient's femur.

The system maintains a library of computer-aided design (CAD) models of implant designs and accepts computed tomography data for individual patients. It automatically determines the CT coordinates of the preoperatively implanted locator pins and provides a variety of interactive graphics tools for the surgeon to examine the CT data, to select an appropriate model and size from the implant design library, and to manipulate the position and orientation of the selected implant shape relative to CT coordinates.<sup>3</sup> The output consists of files containing 1) patient identification data, 2) the position of the locator pins relative to CT coordinates, 3) the implant specification, 4) the desired implant placement relative to CT coordinates, and 5) processed image and model data that will be used for a real-time animation of the progress of the surgery.

<sup>3</sup>In the future, we anticipate the use of computer optimization techniques to assist the surgeon in determining the best implant placement and also in the design of custom implants.

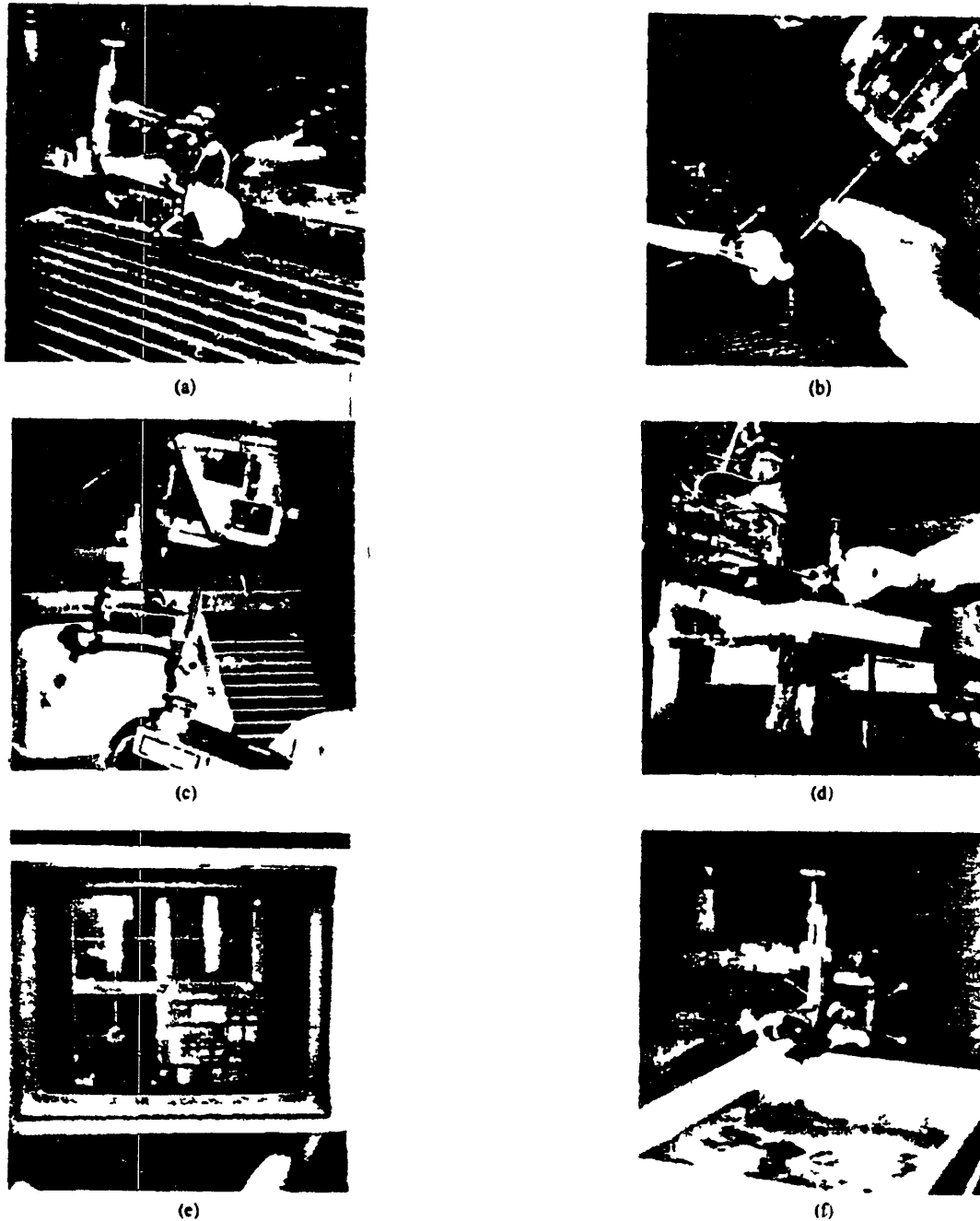


Fig 5 Surgical procedure for hip surgery (a) Fixated cadaver bone (b) Manual guiding to approximate pin position (c) Tactile search for a pin (d) Cutting the shape (e) Online display (f) Final result

### B Operating Room System

The operating room system (illustrated in Fig 4) consists of several components. The five axis robot is an IBM 7576 SCARA manipulator with an added pitch axis six degree of freedom force sensor and a standard high speed surgical cutting tool. During surgery all but the robot's cutting tool is covered by a sterile drape; the cutting tool is separately sterilized. A sterile fixation rigidly attached to the robot's base holds the bone during the robotic part of the procedure. The robot controller provides servocontrol, low level monitoring, sensor interfaces, and higher level application functions implemented in the AML/2 language. During surgery the force sensor is

used to support redundant safety checking: tactile search to find the locator pins and compliant motion guiding by the surgeon.

The *redundant motion monitoring subsystem* [24] is implemented on an IBM PC/AT with specialized IO hardware. It relies on independent sensing to track the position and orientation of the robot end effector during the cutting phase of the surgery and checks to verify that the cutter tip never strays more than a prespecified amount outside of the defined implant volume. It also monitors strain gauges that can detect possible shifts of the bone relative to the fixation device. If either condition is detected a freeze motion signal is sent to the robot controller. After motion is stopped application

code in the robot controller queries the motion monitoring system for more information and then enters an appropriate error recovery procedure under the surgeon's supervision.

The *human machine interface* includes an *online display* system that combines data generated in presurgical planning with data transmitted from the robot controller to show progress of the cutting procedure superimposed on the CT derived image views used in planning. A gas sterilized *hand held terminal* allows the surgeon to interact with the system during the course of the operation. This terminal supports manual guiding, motion enable, emergency power on/off, and menu selection functions. It may also be used to pace transitions from one major application step to the next and to select appropriate pre-programmed error recovery procedures should the need arise. Each of the major control components (robot control and motion checker) is able to freeze all robot motion or to turn off manipulator and cutter power in response to recognized exception conditions. If this happens the surgeon must explicitly re-enable motion from the hand held terminal.

## V. PRESURGICAL PLANNING SYSTEM

### A. Input Processing

One mundane but nevertheless essential task is to load the image data into the computer. The CT scanner used for the veterinary clinical trial of this system produced images on magnetic tape in GE 9800 format. The voxel size for typical scans was  $0.39 \times 0.39 \text{ mm} \times 1.5 \text{ mm}$  thick. Multiple cross-sectional images spaced 3 mm apart were taken throughout the proximal femur. In the vicinity of the locator pins, the images were spaced only 1.5 mm apart (i.e. they were contiguous). The input software includes facilities for tape reading, previewing image slices, selecting a region of interest to reduce the size of data sets, maintaining patient information, etc.

### B. Pin Location Algorithms

A key problem is determining the location of the top center point of each locator pin relative to CT coordinates. This is by no means trivial. Although the density of the pins is much higher than that of bone, simple segmentation based on thresholding is complicated by blooming and other artifacts associated with the image formation process, so that the images are rather noisy. In particular, edge information is very unreliable.<sup>4</sup> The pins are not nicely aligned with the CT slices, and the CT voxels are not cubes. Even in the absence of noise, CT cross sections that pass through the screw threads, hexagonal drive hole, and the pin head and shaft can produce images that are rather difficult to analyze. To overcome these problems, a robust three-phase method has been developed.

In the first phase, simple density thresholding is used to distinguish the metallic pin voxels from surrounding tissue.

<sup>4</sup>Experiments by one of the authors [18], [25] with various materials showed that titanium and ceramic yielded the best contrast without excessive blooming. However, the resulting images were still far from clean. Titanium was chosen for reasons of biocompatibility and because it is more commonly used in orthopaedic implants than titanium.



Fig. 6. Operating room scene from first canine clinical trial in May 1980. The surgeon is Dr. Paul. The patient was a family pet needing hip replacement surgery.

voxels. Unfortunately, blooming causes many tissue voxels to be mislabeled as pin, giving the pins a ragged, starburst appearance. These artifacts are cleaned up by first dilating and then eroding the binary thresholded image with standard 3D morphology filters using spherical structural elements. This process also smooths out the screw threads and fills in the drive socket of the pin image.

In the next phase, the approximate position and orientation of the pin are determined by calculating the first and second moments of the binary pin image.

$$m_1 = \frac{\sum_j p_j}{\sum_j 1}$$

and

$$M_2 = \frac{\sum_j (p_j - m_1)(p_j - m_1)^T}{\sum_j 1}$$

where the  $p_j$  are the coordinates of all voxels  $j$  classified "pin." Since the pin is cylindrically symmetric, two of the eigenvectors of  $M_2$  will be practically equal. The other eigenvector,  $a$ , represents the principal axis of the pin.<sup>5</sup>

<sup>5</sup>This method would not work if the length of the pin shaft was such that all three eigenvectors had the same length. In this case, it would be necessary to use higher order moments to disambiguate the axes. However, our locator pin design precludes this possibility.

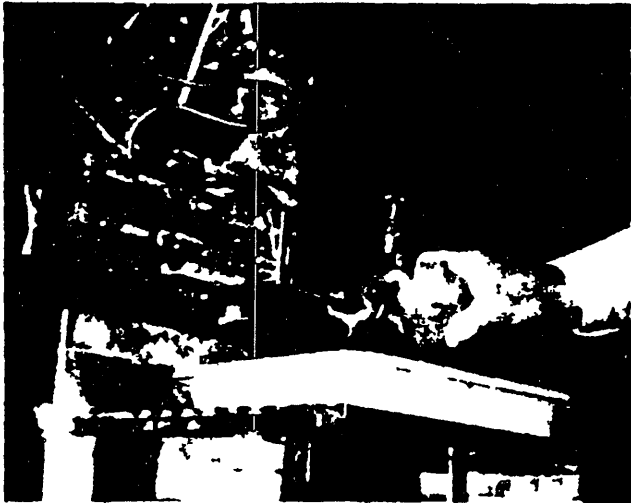


Fig 7 Robot's wrist during shape cutting experiment. The LED beacon plates used by the motion monitoring system are clearly visible. The force sensor is just visible behind the top of the plates.

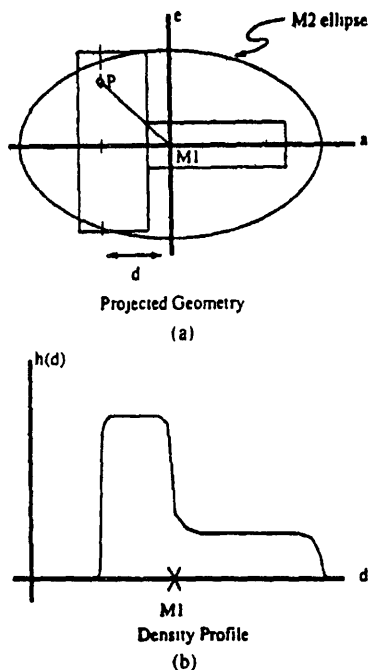


Fig 8 Projected pin profile. (a) Projected geometry. (b) Density profile.

In the third phase a cross sectional volume profile  $h(d)$  is computed as a function of the distance  $d$  along the axis  $m_1 + da$  (Fig 8). The intercept  $d_0$  of the leading edge of the pin profile is computed and the top center point  $p_{tc}$  of the pin is then readily computed from

$$p_{tc} = m_1 + d_0a$$

### C Interactive Docking Subsystem

The interactive docking subsystem integrates 3D image display and computer graphics techniques to support positioning of a 3D CAD model of the desired prosthesis shape relative to the CT image of the patient's anatomy. Since 3D perspective projections inherently distort distance and shape we chose to use orthogonal 2D cross sections to represent the 3D

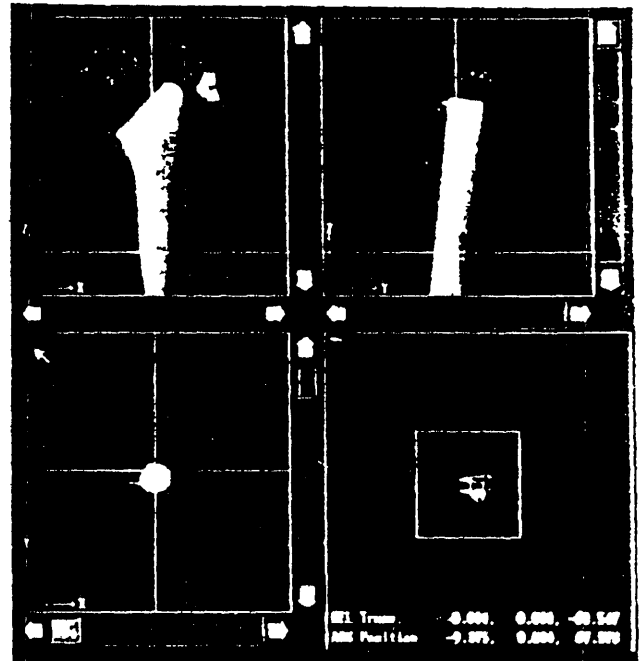


Fig 9 Presurgical planning display.

information. The interactive display screen is shown in Fig 9. Three orthogonal sections through the CT data set representing the bone are shown together with a simple graphic view showing the location of the three cutting planes relative to the data set. Standard resampling techniques are used to generate undistorted cross sectional images which may be displayed in one of three modes. Grey-scale mode simply displays the CT densities of each (resampled) voxel. Color map mode uses different hues (red, blue, etc.) to represent different tissue classes (cortical bone, trabecular bone, etc.) which are presently computed by relatively simple intensity thresholding techniques.<sup>6</sup> Surface contour mode shows a graphic representation of boundaries between tissue types. This graphic data can be manipulated very quickly and is most useful when the surgeon is identifying the desired cross sectional views through the CT data.

In use the surgeon typically selects boundary mode and uses the mouse to position and orient the cutting planes relative to the CT data. The surgeon then selects either grey scale or color map mode. Again using the mouse the surgeon selects the desired implant model from a library of available designs and manipulates the position and orientation of the implant relative to the CT coordinate system. As he does this the computer automatically generates the cross sections corresponding to the selected orthogonal cross sections and displays them superimposed on the corresponding 2D images. All manipulations, whether of the implant or of the cross sectional CT views are specified relative to one of the three 2D views. Thus complex 6D reorientations are accomplished by breaking them down into a sequence of simpler transfor

<sup>6</sup>The threshold values used to distinguish between different bone classes were qualitatively determined by the co author who is a surgeon (Dr Paul) and reflect his best judgement as to what is useful. Any such distinction are to some extent arbitrary.

mations When the surgeon is satisfied, the coordinates of each locator pin, the implant specification, and the desired implant position and orientation relative to CT coordinates are written to a file

In the future we expect that the computer will assist the surgeon by computing and displaying appropriate goodness of fit measures and eventually proposing optimized positions and custom implant designs Even in its present state of development however this system has proved to be very effective and quite easy to use The 2D cross sectional displays are intuitively attractive to and easily learned by the orthopaedic surgeons who are the targeted end users The restriction to one 2D rotation or translation at a time has similarly proved to be inconsequential since our users tend to think of rotations and translations that are easily perceivable in a single display—namely the ones that the system allows on a single interaction,

## VI GEOMETRIC CALIBRATION

Geometric calibration (e.g. [26]–[28]) is a crucial component of any practical robotic application especially one in which geometrically accurate paths are an important factor This is equally true of surgical applications At the same time it is important to define methods that are simple robust do not require elaborate equipment and are appropriate for the accuracies required by the task In this section we will describe our approach to these tradeoffs

### A Find Pin Routine

The methods used in the calibration and in the actual surgical execution are very similar to methods earlier used in training a robot to copy pilot hole positions for automatic drilling of aircraft wing panels [29] A ball probe cutter is inserted into the collet of the cutting tool and the force sensor is used to determine points of contact with the object being located (typically a cylindrical pin) Points of contact are located by moving the ball to the proximity of the surface and then executing a slow guarded motion in a specified direction As soon as the force exceeds a specified threshold the motion is stopped Since there may be an unpredictable amount of overshoot a sequence of very small steps  $x_i$  are then taken in the reverse direction and the forces  $f_i$  along the motion direction are measured at each point The apparent compliance is estimated by a straight line approximation

$$f_i = K(x_i - x_0)$$

The point  $x_0$  where the force goes to 0 is assumed to be the contact point Experience has shown that this method while somewhat tedious is in practice very robust Repeatabilities of the order of 25  $\mu\text{m}$  are routinely obtained A cylindrical object like a pin or cup is then easily located by locating three points on the top surface and three points on the side

### B Kinematic Model

As stated earlier, the robot is a modified SCARA manipulator augmented by an extra pitch axis which (in turn) carries a

six degree-of freedom force sensor and a high speed revolute surgical cutter The nominal kinematics are given by

$$p_{\text{tool}} = p_{\text{wrist}} + R(x, \theta_4)R(y, \theta_5)v_c$$

where  $R(a, \theta)$  is a rotation by angle  $\theta$  about axis  $a$  and

$$p_{\text{wrist}} = R(x, \theta_1)(l_1x + R(x, \theta_2)l_2x) + \theta_3z$$

$l_1$  = length of first link

$l_2$  = length of second link

$\theta_1$  = first joint rotation

$\theta_2$  = second joint rotation

$\theta_3$  = sliding joint displacement

$\theta_4$  = roll joint rotation

$\theta_5$  = pitch joint rotation

$v_c$  = cutter displacement vector

There are of course a number of error terms corresponding to link dimensional variations encoder offsets etc The calibration performed by the robot manufacturer characterizes these values quite well and the local accuracy of the basic SCARA has proved to be sufficient for our purposes<sup>7</sup> However we were somewhat more concerned about the pitch motor and end effector and therefore decided to develop an additional calibration procedure for these distal parts of the system The crucial factor is the position of the tool tip which is given by

$$p_{\text{tool}} = p_{\text{wrist}} + R(x, \theta_4 + \Delta\theta_4) \cdot (\alpha x + v_{\text{distal}})$$

where

$$v_{\text{distal}} = R(x, \beta) \cdot (R(y, \theta_5 + \Delta\theta_5)(v_c + \Delta v_c))$$

$\Delta\theta_4$  = rotational misalignment of joint 4 with joint 5

$\alpha$  = displacement of pitch axis from roll axis

$\beta$  = pitch axis tilt error term

$\Delta\theta_5$  = combined pitch offset & shaft alignment error

$\Delta v_c$  = cutter shaft displacement vector uncertainty

Tool orientation is relatively less important and no special efforts were required to calibrate it aside from determining the angular offsets  $\Delta\theta_4$  and  $\Delta\theta_5$

### C Parameter Estimation

Our present calibration method uses a single vertical post rigidly mounted to robot's base Essentially the calibration works by repeatedly executing the find pin routine to measure the apparent position of the post for a number of different roll and pitch orientations Since the post does not move the post location and the unknown kinematic parameters  $\alpha$   $\beta$   $\Delta\theta_4$   $\Delta\theta_5$  and  $\Delta v_c$  may be found by least squares regression

<sup>7</sup>The specified repeatability of the robot we used is  $\pm 0.05$  mm in the  $\{x, y\}$  plane and  $\pm 0.02$  mm in  $Z$  The robot's specified  $\{x, y, z\}$  region accuracy is 0.2 mm over a 250 mm square Over the rather shorter distances involved in machining a canine implant the accuracy rapidly approaches the repeatability which in our experience was actually better than the specified value

on the linearized relation

$$\begin{aligned} p_{\text{post}} \cong & p_{\text{wrist}} + R_4 \cdot R_5 \cdot (v_c + \Delta v_c) \\ & + \beta R_4 \cdot (x \times R_5 \cdot v_c) \\ & + \Delta \theta_4 R_4 \cdot (z \times R_5 \cdot v_c) \\ & + \Delta \theta_5 (y \times (R_4 \cdot R_5 \cdot v_c)) + \alpha R_4 x \end{aligned}$$

where

$$\begin{aligned} R_4 &= R(z, \theta_4) \\ R_5 &= R(y, \theta_5) \end{aligned}$$

Our experience with this calibration procedure has been quite good. A typical calibration run consisted of 28 poses with roll angles varying through  $\pm 90^\circ$  and pitch angles varying from  $2^\circ$  to  $60^\circ$ . After reduction of the data, the average residual variation in the apparent position of  $p_{\text{post}}$  was typically about 0.1 mm. Over a series of 9 calibration runs made during the canine clinical trial, the average residual variation ranged from 0.08 mm to 0.12 mm and the maximum residual magnitude ranged from 0.16 mm to 0.33 mm, which is well within the required accuracy for this application. Further, since the wrist orientation does not change during the shape cutting phase, any remaining wrist calibration error simply causes the position of the hole to be shifted slightly in the patient's femur and does not affect the actual shape being cut.

## VII SHAPE CUTTING

At present we use a constant orientation cutting strategy. The shape is cut as follows:

- 1) An end mill (typically 7–9 mm in diameter) is placed in the collet of the cutting tool.
- 2) The cutter is oriented parallel to the long axis of the implant.
- 3) Successive transverse pockets (typically about 2.5 mm deep) are cut to produce the rough shape of the implant. At the conclusion of this stage, the implant shape has a stair case appearance.
- 4) Successive longitudinal cuts are made to remove the excess material in the stair cases. Although this produces a slightly scalloped surface finish, in practice it is easy to approximate the desired surface with a relatively small number of cuts. The residual height  $\delta h$  of any scallop will be given by

$$\delta h = r_{\text{cutter}} - \sqrt{r_{\text{cutter}}^2 - \frac{d^2}{2}}$$

where  $r_{\text{cutter}}$  is the cutter radius and  $d$  is the distance between cuts. Solving for  $d$  gives

$$\begin{aligned} d &= \sqrt{4r_{\text{cutter}}\delta h - 2(\delta h)^2} \\ &\cong 2\sqrt{r_{\text{cutter}}\delta h} \quad \text{for small } \delta h \end{aligned}$$

Thus  $r_{\text{cutter}} = 5$  mm and  $\delta h = 0.05$  mm would require the finishing cuts to be 1 mm apart. These cuts are made without changing the cutter orientation.

- 5) If necessary, the end mill is replaced with a smaller diameter ball cutter and additional finishing cuts are

made to sharpen the corners of the implant hole. Obtaining proper clearance for these cuts requires the cutter orientation to be changed slightly. Changes in the implant designs during veterinary clinical testing rendered this step unnecessary.

One advantage of a constant orientation cutting strategy is that it substantially eliminates the effect of unmodeled kinematic errors in the distal parts of the robot on the shape of the hole being cut, although they do still affect the location of the hole relative to the bone. Since the shape dimensional tolerances are in fact somewhat tighter than the positioning tolerances, maintaining a constant orientation is indeed valuable. More complex implant shapes of course will require full five axis trajectories.

## VIII INTRAOPERATIVE DISPLAY

The presurgical planning system is also used in the operating room to provide displays showing the progress of the cutting phase of the surgery. During surgery, the planning system is connected to the robot controller via a standard serial communication line and rechristened the real time monitor. Three orthogonal cross sections through the 3D CT data set used to plan the surgery are displayed together with corresponding cross sections of the shape to be cut, just as in presurgical planning. As each successive cutting stroke is made, the robot controller sends short messages to the display computer, which then changes the color of the portions of the cross sectional images corresponding to the cutting stroke. Once a complete layer is cut out, that entire portion changes color yet again.

## IX SAFETY CHECKING SUBSYSTEMS

### A Requirements

Safety was a primary consideration in designing the system. The principal requirements were defined by the co-authors of this paper who are surgeons (Dr Paul and Dr Bargar). These included

- 1) *The robot must never run away.* No single mode hardware (or system) error may cause the application software to lose control of its motions. Furthermore, the application software must request only proper motions.
- 2) *The robot must never exert excessive force on the patient.* If forces on the cutter exceed expected values by more than a predefined threshold amount, then something may be wrong, and the robot must stop moving immediately.
- 3) *The robot's cutter must stay within a prespecified positional envelope relative to the volume being cut.* For hip replacement surgery, the main goal is to prevent a systematic shift in the placement or shape of the hole. A single gouge is generally reparable, although undesirable. Of course, other surgical procedures (like brain surgery) may be less forgiving.
- 4) *The surgeon must be in charge at all times.* This is of course, the fundamental dilemma. The surgeon has to trust the system to some extent. Nevertheless, the system must provide the surgeon with timely information.



about its status and the surgeon must be able to pause motion at any time. Once robot motion is stopped he or she must be able to further query the robot's status to manually guide it to select an appropriate recovery procedure to continue the surgery or to completely terminate use of the robot and continue manually.

### B Robot Controller Checks

The robot controller routinely performs many safety and consistency checks including monitoring position and velocity limits in the joint servos and monitoring of external signals. In addition to a basic power-enable relay (external to the controller) controller software provides facilities for disabling manipulator power for freezing or pausing motion, for resuming interrupted motions and for transferring control to application software recovery procedures. A safety time out monitor turns off arm power if the controller does not affirmatively verify system integrity every 18 ms.

Many conditions (externally signalled consistency checks, force thresholds, pushbutton closures, etc.) interrupt the application program, pause motion or drop power under certain conditions. The surgeon can then use the hand held terminal to query system status to select local actions (such as manual guiding or withdrawal of the cutting tool) to continue the present motion to discontinue or repeat the present step of the procedure or to restart from an earlier stage of the procedure. One very common case is a simple surgeon initiated pause to allow the surgical team to perform some housekeeping function like replacing an irrigation bottle or to allow the surgeon to satisfy himself or herself that all is well.

### C Force Monitor Checks

The microprocessor interface to a wrist mounted force sensor computes forces and torques at the cutter tip. If any tip force component greater than approximately 1.5 kgf is detected the controller is signalled to pause motion. Forces greater than about 3 kgf cause arm power to be dropped. Experiments in which a sudden large motion is commanded in the middle of cutting confirm that these checks are quite effective in detecting run away conditions. They are also effective in detecting such conditions as the cutter stalling or being impeded by improperly retracted soft tissue.

### D Independent Motion Monitoring Checks

We developed an independent checking subsystem to verify that the cutter step stays within a defined safe volume relative to the bone essentially corresponding to the implant shape and an approach region. The checking system is implemented on a separate PC/AT computer from the robot controller, in order to minimize the chances of common mode failures. The check requires two steps: 1) verification that the bone does not move relative to the fixator, which is rigidly attached to the robot's base, and 2) verification that the end effector never strays from a defined volume in space.

We devised a strain gauge system for detecting motions of the bone relative to the fixator. Bench experiments demonstrated that motions on the order of 0.1 mm could be detected. However, experiments with the fixator indicated that even

rather large forces (5 kgf) produced only negligible (16  $\mu$ m) motion and the bone motion monitor was not used in any clinical tests.

To verify end effector motion we used a Northern Digital Optotrak™ 3D digitizer which is capable of tracking light emitting diodes to an accuracy of better than 0.1 mm at a rate of approximately 1000 positions/second. We fabricated a rigid PC card with eight such beacons and affixed it to the robot's wrist as shown in Fig. 7. An arbitrary coordinate system for the PC card was defined from the beacon positions and the positions  $b_r$  of the beacons relative to this coordinate system were measured. The Optotrak measures the positions  $b_o$  of these beacons in space, and computes a best estimate of the plate position  $F_p$  by regression from the relationship

$$b_o \cong F_p \cdot b_p$$

The robot to-Optotrak and plate to-cutter transformations  $T_{ro}$  and  $T_{pc}$  are computed by ordinary least squares estimation from data taken with the robot in various known positions using appropriate linearized models. Using these transformations an estimate of the cutter coordinates  $F_{rc}$  relative to the robot may be obtained from the relationship

$$F_{rc} = T_{ro}^{-1} \cdot F_p \cdot T_{pc}$$

Constructive solid geometry (CSG) tree check volumes corresponding to implant and cutter selection were constructed from primitives bounded by quadric surfaces

$$p_c^T \cdot Q_i \cdot p_c + q_i \cdot p_c + d_i \leq 0$$

located one millimeter outside the furthest nominal excursions of the cutter when the shape is cut. Intraoperative checking is performed by reading the beacon plate coordinates from the Optotrak, computing the corresponding cutter position and then checking to see if this position falls outside the check volume. If so the checking subsystem signals an out of bounds condition through an optically isolated digital port to the robot controller which pauses motion and then obtains more detailed information through a serial communications line.

To verify the performance of this system we deliberately moved the cutter in a succession of very small steps through the boundary of the checking volume. We found that the system could detect when a motion crossed a threshold to approximately 0.2 mm precision with constant orientation and approximately 0.4 mm with cutter reorientation. Checking rates of approximately 3-4 Hz were obtained using a slow (6 MHz 286) PC/AT. At typical cutter speeds the total excursion before motion is frozen is about 2 mm after accounting for all latencies.

## X EXPERIENCE AND DISCUSSION

### A In Vitro

Extensive tests were conducted on plastic and cadaver bones and on foam test blocks in order to verify basic system accuracy and to gain confidence in overall system behavior [25]. Fig. 11 shows typical cross sections produced

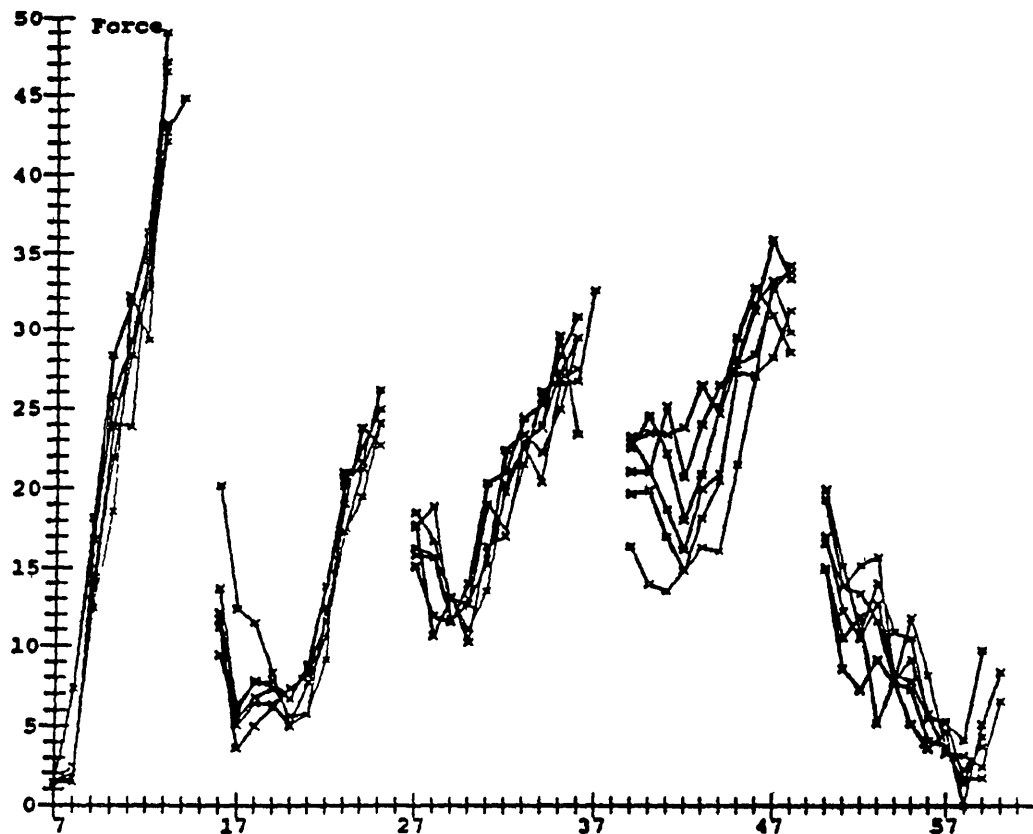


Fig 10 Cutting force on cadaver dog bone. This figure shows a plot of the magnitude of the force on the cutter tip for five typical to the actual cut. In this plot 40 force units correspond to one pound (0.45 kgf).

by manual broaching and robotic machining. In one bottom line experiment three pins were implanted into a test fixture and located on CT images of the fixture. A number of foam blocks were then successively (and repeatably) clamped into a socket in the test fixture which was placed at various poses within the workspace of the robot. Test shapes were cut in the foam blocks using steps 3 through 5 of the surgical procedure. The positions of these shapes and of the pins were then measured on a coordinate measuring machine with an accuracy of approximately 0.0125 mm (0.0005 inches). In a typical test run the three blocks were cut for each of four separate poses (all combinations of "left leg/right leg and 0 degrees/15 degrees fixator pitch) for each of three separate CT scans for a total of  $3 \times 4 \times 3 = 36$  blocks. The total placement error of the test shapes was found to be 0.5 mm for a test fixture with pins placed at the distances they would be on a human. Similarly the dimensions of test shapes machined in cadaver bone were measured with calipers accurate to 0.02 mm. Dimensional errors were less than 0.05 mm. Further tests in which actual implant shapes were cut in both foam blocks and canine cadaver bones and an implant was then inserted into the hole were also conducted. Although a dimensional study similar to [17] was not performed the fit achieved was qualitatively very good. The implant slipped into the hole with little effort and fit snugly. No gaps could be seen if the foam block was split longitudinally after insertion of the implant.

Cutting forces for bone machining were also measured. Typical results are shown in Fig 10. The greatest force which

seldom exceeded 0.5 kgf typically was encountered when the cutter moved from the center plunge position to the first corner of a rectangular section of bone being removed. Forces would then drop off substantially as the cutter began moving along edges of the section building up to somewhat smaller local maxima (about 0.3-0.4 kgf) as successive corners of the shape were reached.

Except for bone motion detection the redundant checking mechanisms discussed above were all integrated into the prototype surgical system and used in *in vivo* testing on cadaver bones. The most common error condition detected during these tests was excessive cutting force when the cutter plunged into unusually hard bone which caused the controller to pause robot motion. Continuation from this condition was easily achieved by backing up the cutter 1-2 mm and restarting the current cut.

Both the real time monitor and the motion tracking system proved to be surprisingly useful in application debugging. Even though the display was essentially an animation it provided useful information about exactly where the robot should be and what the controller thought it was doing. The motion tracker provided a useful consistency check to the calibration procedures. It also caught a real bug in the shape cutting code that might otherwise have been very hard to find.

#### B In Vivo

A clinical trial on 26 dogs needing hip replacement surgery was conducted from May 1990 through September 1991. All



Fig. 11. Comparative cross section. This figure shows sections of human cadaver bone (top) prepared with a manual broach and (bottom) machined with a robot. The measured midline dimensions of the machined sections are within 0.05 to 0.1 mm of nominal. Some surface irregularities are seen where the machined surface intersect cancellous bone, other chipping arises from the bone sectioning process.

procedures were successful with no intraoperative complications or infections. There were no intraoperative or postoperative cracks or fractures, and (in the opinion of the surgeon) the implants were easily inserted and provided more mechanical stability than would normally be experienced with manual broaching of the femur. In contrast, cracking<sup>8</sup> was experienced in 5 out of 15 cases in a manually broached control group and the implant placement was not as good. Radiographs were used to compare placement of the implant in the femur for 15 cases in which the robot was used to prepare the femur with 15 cases in which conventional manual broaching was done. It was found that for the Techmedica cementless canine implants used in the study, conventional broaching often resulted in the proximal end of the implant was often tilted more toward the medial direction of the femur (i.e. more in a varus orientation) than the surgeon judged to be optimal. Because of this possibility, the surgeon tended to select a slightly smaller implant design than he otherwise would have. In contrast, robotic machining consistently matched the implant axis with

<sup>8</sup> Fixed by wrapping cerclage wire around the affected bone.

the axis of the proximal femur, enabling the surgeon to select the implant size that best matched the patient's initial bone geometry.

In surgery, the system worked very well. Although no systematic effort was made to compare surgical execution times, the total time of surgery was roughly comparable to that for manual broaching. Anecdotally, it was observed that the time required for robot machining was more consistent from case to case than the time required for manual broaching. There were very few glitches, and that there was no actual use of any of the error recovery capabilities of the system. This is as it should be. The force monitor occasionally froze motion when the cutter encountered an unusually thick section of cortical bone at the proximal end of the femur. In these cases, the surgeon simply restarted motion with the hand held terminal. On two other occasions, where the force monitor stopped motion (once when the cutter became entangled in some suture material and once when it got stuck in an assistant's glove), it was necessary for the robot to withdraw from the bone. The surgical team cleared the entanglement and resumed the procedure with only a few seconds of motion being repeated.

The veterinary surgeon (Dr. Paul) relied on the force monitor to provide positional status information in conjunction with his other senses. By listening to the force monitor, he could tell when the cutter was in contact with hard tissue. When he heard a change in pitch, he would look at the force monitor to verify that what he was hearing was consistent with what the robot was cutting. One interesting possibility for future work would be to automate such multisensory cross checks.

The separate motion checking system was used *in vivo* for dogs. The surgical field is rather cluttered since the technician must constantly irrigate the bone while the robot is cutting it. It proved to be very difficult to place the vision system sensors in the veterinarian's operating room so that they would always have a clear view of the end effector. One possibility would have been to mount the camera overhead. Another would have been to use the system for occasional *spot checks* of the robot. However, one consequence of the confidence gained from the *in vivo* tests was that the surgeon concluded that the additional redundancy gained was not worth the added complexity for veterinary cases. A different sensing solution altogether based on monitoring redundant joint encoders was consequently adopted for the final *in vivo human qualified* second generation system [19]-[22].

## XI CONCLUSIONS

The system described in this paper demonstrated the feasibility of adapting a general purpose manipulator to use as a precise surgical tool. We were able to demonstrate an order-of-magnitude improvement in the precision with which a surgeon can execute a critical step in hip replacement surgery.

Beyond this, it may be worthwhile to recap how the system has addressed the general requirements discussed at the beginning of the paper. We found that even very simple human-machine interaction technology can be surprisingly effective, although further improvements are desirable. This is

of hands on force compliant guiding for positioning the robot has been especially successful since it enables the surgeon to position the robot in a way that is natural and intuitively simple. An animated information display showing the progress of the surgical procedure was useful although this is again an area where considerable improvement can be made both in the presentation of information to the surgeon and in the incorporation of realtime sensing. One ultimate system might be some sort of heads up display showing the surgical plan superimposed on the actual patient with the display being updated based on a combination of position tracking, cutter force data, acoustic sensing and intraoperative imaging.

Model reality registration was accomplished in this case by the use of landmark pins which could be located easily in both CT images and in physical reality. Although their use in this particular surgery is acceptable, less invasive methods may often be desirable. One obvious choice is to register intraoperative radiographs to features on CT-derived models. Another would be to use a 3D digitizer such as the Optotrak to point out anatomical features and then to provide realtime tracking of markers placed on the patient at the time of surgery (see e.g. [30]).

Verification of robot performance and of the methods chosen to register the plan to reality was an important issue, one that required as much time and effort as any other aspect of the system development and is discussed more fully in [25]. In this regard, experimental measurement of individual error sources and the bottom line experiments described above went hand in hand. Similarly, the optical endpoint check, though ultimately not used in the operating room, proved very useful in debugging the shape cutting software.

The related issue of safety was also paramount. The fact that our application required a robot to move a tool in contact with a patient motivated us to implement a number of redundant consistency checking mechanisms which proved quite valuable both in application debugging and in actual surgery.

In implementing these redundant checking mechanisms we encountered an important tradeoff with the realities of operating room compatibility for a complex piece of equipment. The area around the patient is crowded and it is often awkward to maintain a clear field of view required for optical checking equipment. This led the surgeon in this particular application to conclude that whatever extra safety may be gained by a completely independent visual check compared to checks on the robot's encoders does not justify the extra system and operating room complexity involved.<sup>9</sup> In other applications where an optical system is also taking a more active role, for example in tracking the patient's anatomy, it may be desirable to permit its use for redundant safety checking as well.

In any case, it is clear that the system reported here represents only a step in the evolution of a man-machine partnership in the operating room in which the complementary abilities of robotic devices and humans are exploited under the human's supervision to help provide a better result for the patient. Indeed, this process has continued for the hip

surgery augmentation system that we have described. The experience gained with veterinary patients provided the basis for development of a second generation system [19]–[21] for use on humans.

#### ACKNOWLEDGMENT

We wish to thank many people and groups who have contributed to this effort. Those deserving special mention include Techmedica Inc (implants), Bill Anspach of The Anspach Effort Inc (cutter tools), Steve Lamb of OSI Inc (fixation system), Micro Techmedical Corp (sterile draping), Ken Honeycutt and Kip Harris of IBM Manufacturing Systems Products (robot consultation), Bob Olyha and Tony Castellano of IBM Research (interface electronics) and Jerry Krist and Leon Kehl of Northern Digital (optical tracking).

#### REFERENCES

- [1] Y S Kwok, J Hou, E Jonckheere and S Havati. A robot with improved absolute positioning accuracy for CT guided stereotactic surgery. *IEEE Trans Biomed Eng* pp 153–161 February 1988.
- [2] S Lavallee. Gestes medico-chirurgicaux assistés par ordinateur. Application à la neurochirurgie stéréotaxique. Ph.D. thesis, University of Grenoble, 1989.
- [3] S Lavallee. A new system for computer assisted neurosurgery. in *Proc 11th IEEE Engineering in Medicine and Biology Conf*, Seattle, Nov 1989, pp 926–927.
- [4] Bruce A Kall, Patnck J Kelly and Stephan J Goers. Interactive stereotactic surgical system for the removal of intracranial tumors utilizing CO<sub>2</sub> laser and CT-derived database. *IEEE Trans Biomed Eng* pp 112–116 February 1985.
- [5] Patnck J Kelly, Bruce A Kall, Stephan Goerss and Franklin Eames. Computer assisted stereotaxic laser resection of intra axial brain neoplasms. *J Neurosurg* pp 427–439 March 1986.
- [6] James M Drake, Michael Joy, Andrew Goldenberg and David Kreindler. Robotic and computer assisted resection of brain tumors. in *Proc Fifth Int Conf on Advanced Robotics*, Pisa, June 1991, pp 888–892.
- [7] D Glauser, P Flury, N Villotte and C W Burckhardt. Conception of a robot dedicated to neurosurgical operations. in *Proc Fifth Int Conf on Advanced Robotics*, Pisa, June 1991, pp 899–904.
- [8] B L Davies, R D Hibberd, A Timoney and J Wickham. A surgeon robot for prostatectomies. in *Proc Fifth Int Conf Advanced Robotics*, Pisa, June 1991, pp 871–875.
- [9] K Ikuta, M Tsukamoto and S Hirose. Shape memory alloy servo actuator system with electric resistance feedback and application for active endoscopes. in *IEEE Robotics and Automat Conf*, 1988.
- [10] R H Sturges and S Laowattana. A flexible tendon controlled device for endoscopy. in *Proc IEEE Robotics and Automation Conference*, Sacramento, CA, 1991.
- [11] Philip Green. Advanced teleoperator technology for enhanced minimally invasive surgery. in *Proc Medicine Meets Virtual Reality Conference*, San Diego, June 4–7, 1992.
- [12] Yulan Wang. Robotically enhanced surgery. in *Proc Medicine Meets Virtual Reality II*, San Diego, Jan 27–30, 1994.
- [13] J A McEwen, C R Bussani, G F Auchinleck and M J Breault. Development and initial clinical evaluation of pre robotic and robotic retraction systems for surgery. in *Proc Second Workshop on Medical and Health Care Robots*, pp 91–101, Newcastle-on Tyne, Sept 1989.
- [14] J L Garbini, R G Kauria, J A Sidles, R V Larson and F A Matson. Robotic instrumentation in total knee arthroplasty. in *Proc 33rd Annual Meeting Orthopaedic Research Society*, San Francisco, January 1987, p 413.
- [15] Thomas C Kienzie, S David Stulberg, Michael Peshkin, Arthur Quaid and Chi-haur Wu. An integrated CAD robotics system for total knee replacement surgery. in *Proc 1993 IEEE Conf Robotics Automat*, Atlanta, May 1993, pp 889–894.
- [16] P M Sandborn, S D Cook, W Spies and M Koster. Tissue response in porous coated implants locking initial bone apposition. *J of Arthroplasty*, December 1988.
- [17] H A Paul, D E Hayes, W L Baer and B D Mittelstadt. Accuracy of canal preparation in total hip replacement surgery using custom

<sup>9</sup>As mentioned earlier, the next generation robot [22] incorporates an additional, independent set of encoders to provide further redundancy.

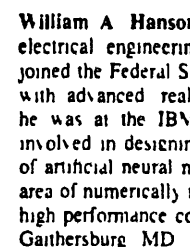
- broaches in *Proc First International Symposium on Custom Made Prostheses* Dusseldorf October 1988
- [18] H A Paul B D Mittelstadt B L Musits W L Bargar and D E Hayes Application of CT and robotic technology to hip replacement surgery in *Proc First International Symposium on Custom Made Prostheses* Dusseldorf October 1988
- [19] H Paul B Mittelstadt W Bargar B Musits R Taylor P Kazanzides J Zuhars B Williamson and W Hanson A surgical robot for total hip replacement surgery in *Proc IEEE Conference on Robotics and Automation* Nice May 1992
- [20] P Kazanzides J Zuhars B Mittelstadt P Cain F Smith L Rose and B Musits Architecture of a surgical robot in *Proc 1992 IEEE Conf on Syst Man Cyber* Chicago August 1992
- [21] Brent Mittelstadt, Peter Kazanzides Joel Zuhars Phil Cain and Bill Williamson "Robotic surgery Achieving predictable results in an unpredictable environment" in *Proc Sixth Int Conf on Advanced Robotics* Tokyo Nov 1-2 1993
- \* [22] B D Mittelstadt, P Kazanzides J Zuhars B Williamson P Cain F Smith and W Bargar The evolution of a surgical robot from prototype to human clinical use in *Computer Integrated Surgery* R Taylor S Lavallee G Bardea and R Moesges Eds Cambridge MA MIT Press To appear
- [23] W H Hanson, H A Paul, Bill Williamson and Brent Mittelstadt Orthodock A Computer System for Presurgical Planning in *Proc 17th IEEE Medicine & Biology Conf* Phila 1990
- [24] Russell H Taylor Peter Kazanzides Brent D Mittelstadt and Howard A Paul Redundant consistency checking in a precise surgical robot in *Proc 17th IEEE Medicine & Biology Conf* Phila November 1990
- [25] B D Mittelstadt Ph.D thesis University of California at Davis in preparation
- [26] John M Hollerbach Advances in robot calibration in *Proc Sixth ISRR* Cambridge MA MIT Press 1993
- [27] L J Everett "Models for diagnosing robot error sources" in *Proc 1993 IEEE Conf on Robotics and Automation* Atlanta May 1993 pp 11155-159
- [28] A Goswami A Quaid and M Peshkin Complete parameter identification of a robot from partial pose information in *Proc 1993 IEEE Conf on Robotics and Automation* Atlanta May 1993 pp 1168-173
- [29] Russell H Taylor Method and apparatus to teach a robot the position and orientation of hole centerlines US Patent 4 4485 453 filed 1982 issued Nov 27 1985
- [30] Russell H Taylor Court B Cutting Yong Gil Kim Alan D Kalvin David Larose Betsy Haddad Deljou Khoramabadi Marilyn Noz Robert Oliva Nik Braun and Dieter Grimm "A model based optimal planning and execution system with active sensing and passive manipulation for augmentation of human precision in computer integrated surgery" in *Proc 1991 Int Symposium on Experimental Robotics* Toulouse France June 25-27 1991 New York Springer Verlag 1991



**Brent Mittelstadt** received a degree in electrical engineering from the University of Arizona and received the Ph.D degree in biomedical engineering from the University of California at Davis in 1988. He is currently a biomedical engineering research fellow and is working on the ROBODOC program as a research fellow. He is responsible for the development work on the robot.



**Howard A Paul** received the Veterinary Degree from the Ecole Nationale Vétérinaire D'Alfort France and completed his M.D. at the University of California at Davis School of Veterinary Medicine. Dr Paul was a faculty member and Chairman of Integrated Surgical Systems. He had extensive research experience in orthopaedic devices including joint replacement implants.



**William A Hanson** (S 74-M 85) received the B.S. in electrical engineering from Rensselaer Polytechnic Institute in 1966. In 1966 he joined the Federal Systems Division of IBM in Owego, New York where he worked with advanced real time signal processing systems. From 1965 to 1971 he was at the IBM Palo Alto Scientific Center where he was involved in designing a language and simulation environment for the simulation of artificial neural networks. Subsequently he worked in the area of numerically intensive computing. Since 1992 he has been a leading high performance computing effort at Loral Federal Systems, Gaithersburg MD.

Mr Hanson's research interests include high performance computing, information theory, digital image processing (particularly medical image processing), visualization and artificial neural networks. He is an IBM Certified Architect and a member of the IEEE. He is available at the time of publication.



**Russell H Taylor** (S 68-M 77-SM 87-F 94) received the B.E.S. degree from Johns Hopkins University in 1970 and a Ph.D. in Computer Science from Stanford in 1976. He joined IBM Research in 1976 where he developed the AML language. Following a two-year assignment in Boca Raton he managed robotics research activities at IBM Research from 1982 until returning to full time technical work in late 1988. Since March 1990 he has been manager of Computer Assisted Surgery.

His research interests include robot systems programming languages, model based planning and (most recently) the use of imaging model-based planning and robotic systems to augment human performance in surgical procedures.

Dr Taylor is Editor Emeritus of the *IEEE Transactions on Robotics and Automation*, a Fellow of the IEEE, a member of the IEEE Robotics and Automation Society, AdCom co chair of the IEEE Robotics and Automation Society Technical Committee on Medical Robotics, and a member of various other honorary societies, panels, program committees, and advisory boards.



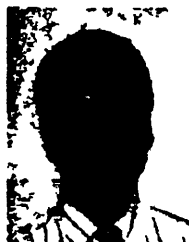
**Peter Kazanzides** (S 82-M 88) received the Ph.D. degree in electrical engineering from Johns Hopkins University. He joined the ROBODOC program as a postdoctoral fellow in the IBM Robotics Laboratory and is responsible for the development of the base systems. His research interests include robot control and programming.



**Joel Zuhars** (M 92) received the M.S. in electrical and computer engineering from the University of California at Davis. He was employed by the John Hopkins University Physics Lab. He is currently a faculty member in the Integrated Surgical Systems. He is interested in the possibility of developing the next generation of



Bill Williamson is a Senior Software Engineer for Integrated Surgical Systems Inc. He developed the user interface for the preoperative planning workstation. He is responsible for researching and developing new imaging applications.



Edward Glassman received the B.S. degree in biomechanics from the Massachusetts Institute of Technology in 1982 where he developed a microprocessor controlled adaptive above knee prosthesis. From 1982 through 1990 he was a researcher at the IBM T. J. Watson Research Center where he focused on the development and application of high performance sensor based robotic systems for a wide variety of tasks ranging from semiconductor manufacturing to robotic surgical assistant. Currently he is a member of the IBM Consulting

Group specializing in Healthcare. Particular areas of interest continue to be the assessment and application of new technologies that fundamentally change the way a business operates.



Bela Musits received the B.S. and M.S. degrees in engineering and the M.B.A. degree in marketing from Rensselaer Polytechnic Institute. He is currently the President of Integrated Surgical Systems Inc. Prior to joining Integrated Surgical Systems Inc. he managed the ROBODOC project within IBM and collaborated with Dr. Paul and Dr. Bargar.



William L. Bargar received the M.D. degree from Ohio State University. He completed his residency at Case Western Reserve University and his fellowship in joint replacement at UCLA Medical Center. Currently he has a private practice at Sutter General Hospital in Sacramento, CA. Dr. Bargar is a specialist in joint reconstructive surgery and was the first surgeon to perform ROBODOC assisted surgery on a human patient.



**UNITED STATES DEPARTMENT OF COMMERCE**  
**Patent and Trademark Office**  
 Address COMMISSIONER OF PATENTS AND TRADEMARKS  
 Washington D.C. 20231

# 2

APPLICATION NUMBER	FILING/RECEIPT DATE	FIRST NAMED APPLICANT	ATTORNEY DOCKET NO /TITLE
--------------------	---------------------	-----------------------	---------------------------

00 / 00 / 00    00 / 00 / 00    0000000    A    0000

EDWARD J. JENNIFER  
 LAW FIRM & CONSULTANTS  
 1500 DEWEY BUILDING  
 PITTSBURGH PA 15

NOT ASSIGNED

DATE MAILED

2411

00 / 00 / 00

**NOTICE TO FILE MISSING PARTS OF APPLICATION**  
**Filing Date Granted**

An Application Number and Filing Date have been assigned to this application. However, the items indicated below are missing. The required items and fees identified below must be timely submitted ALONG WITH THE PAYMENT OF A SURCHARGE for items 1 and 3-6 only of \$ 130.00 for a  large entity  small entity in compliance with 37 CFR 1.27. The surcharge is set forth in 37 CFR 1.16(e). Applicant is given TWO MONTHS FROM THE DATE OF THIS NOTICE within which to file all required items and pay any fees required above to avoid abandonment. Extensions of time may be obtained by filing a petition accompanied by the extension fee under the provisions of 37 CFR 1.136(a).

If all required items on this form are filed within the period set above, the total amount owed by applicant as a  large entity  small entity (verified statement filed), is \$ 130.00

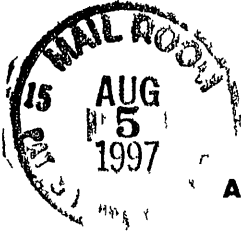
- 1 The statutory basic filing fee is
  - missing
  - insufficient
 Applicant must submit \$ \_\_\_\_\_ to complete the basic filing fee and/or file a verified small entity statement claiming such status (37 CFR 1.27)
- 2 Additional claim fees of \$ \_\_\_\_\_ including any multiple dependent claim fees are required. Applicant must either submit the additional claim fees or cancel additional claims for which fees are due.
- 3 The oath or declaration
  - is missing
  - does not cover the newly submitted items
  - does not identify the application to which it applies
  - does not include the city and state or foreign country of applicant's residence
 An oath or declaration in compliance with 37 CFR 1.63 including residence information and identifying the application by the above Application Number and Filing Date is required.
- 4 The signature(s) to the oath or declaration is/are
  - missing
  - by a person other than inventor or person qualified under 37 CFR 1.42, 1.43 or 1.47
 A properly signed oath or declaration in compliance with 37 CFR 1.63 identifying the application by the above Application Number and Filing Date is required.
- 5 The signature of the following joint inventor(s) is missing from the oath or declaration.
 

An oath or declaration listing the names of all inventors and signed by the omitted inventor(s) identifying this application by the above Application Number and Filing Date is required.
- 6 A \$ \_\_\_\_\_ processing fee is required since your check was returned without payment (37 CFR 1.21(m)).
- 7 Your filing receipt was mailed in error because your check was returned without payment.
- 8 The application does not comply with the Sequence Rules. See attached Notice to Comply with Sequence Rules 37 CFR 1.821-1.825.
- 9 OTHER

Direct the response and any questions about this notice to Attention: Box Missing Parts

**A copy of this notice MUST be returned with the response**

Customer Service Center  
 Initial Patent Examination Division (703) 308 1202



Attorney's Docket No 97012

PATENT

**IN THE UNITED STATES PATENT AND TRADEMARK OFFICE**

In re application of Anthony M DiGirola III et al

Serial No 08 / 803,993 Group No

Filed February 21, 1997 Examiner

For APPARATUS AND METHOD FOR FACILITATING THE IMPLANTATION OF ARTIFICIAL COMPONENTS IN JOINTS

Box Missing Part  
Assistant Commissioner for Patents  
Washington, D C 20231

**COMPLETION OF FILING REQUIREMENTS**

*(check and complete this item, if applicable)*

I  This replies to the Notice to File Missing Parts of Application (PTO-1533) mailed 6/5/97

NOTE If these papers are filed before the office letter issues adequate identification of the original papers should be made e.g. in addition to the name of the inventor and title of invention the filing date based on the Express Mail procedure the serial number from the return post card or the attorney's docket number added

A copy of the Notice to File Missing Parts of Application—Filing Date Granted (Form PTO-1533) is enclosed

NOTE The PTO requires that a copy of Form PTO 1533 be returned with the response to the notice to file missing parts to the application

**CERTIFICATE OF MAILING/TRANSMISSION (37 C F R 1 8a)**

I hereby certify that this correspondence is on the date shown below being

**MAILING**

**FACSIMILE**

deposited with the United States Postal Service with sufficient postage as first class mail in an envelope addressed to the Assistant Commissioner for Patents Washington D C 20231

transmitted by facsimile to the Patent and Trademark Office

Signature \_\_\_\_\_

Date \_\_\_\_\_

(type or print name of person certifying)

(Completion of Filing Requirements [5 1]—page 1 of 6)



## DECLARATION OR OATH

- II  No declaration or oath was filed Enclosed is the original declaration or oath for this application

OR

- The declaration or oath that was filed was determined to be defective A new original oath or declaration is attached

NOTE 37 C F R 1 41(a) points out that Full names must be stated including the family name and at least one given name without abbreviation together with any other given name or initial

NOTE For surcharge fee for filing declaration after filing date complete item VI(3) below

NOTE Acceptable minimums in the declaration for identification of the specification to which it applies are the name of the inventor and (1) serial number (2) attorney docket number which was on the application as filed and the filing date (3) title of the invention and filing date (4) title of invention and reference to a specification which is attached to the declaration at the time of execution and filed with the declaration or (5) title of invention and a statement by a registered attorney that the application filed in the PTO is the application which the inventor executed by signing the declaration If identification (4) is used it must be accompanied by a statement that the attached specification is a copy of the specification and any amendments thereto which were filed in the PTO to obtain the filing date such a statement must be a verified statement if made by a person not registered to practice before the PTO Notice of September 12 1983 (1035 O G 3)

NOTE Another minimum found acceptable in the declaration is the filing date (i e date of express mail) and the express mail number useful where the serial number is not yet known But note the practice where the express mail deposit is a Saturday Sunday or holiday within the District of Columbia 37 C F R 1 10(c)

(complete (c) or (d) if applicable)

Attached is a

- (c)  Statement by a registered attorney that the application filed in the PTO is the application that the inventor executed by signing the declaration
- (d)  Statement that the "attached" specification is a copy of the specification and any amendments thereto that were filed in the PTO to obtain the filing date

## AMENDMENT CANCELLING CLAIMS

- III  Cancel claims \_\_\_\_\_ inclusive

## TRANSMITTAL OF ENGLISH TRANSLATION OF NON-ENGLISH LANGUAGE PAPERS

- IV  Submitted herewith is a verified English translation of the non-English language application papers as originally filed It is requested that this translation be used as the copy for examination purposes in the PTO

NOTE For fee processing a non English application complete item VI(5) below

NOTE A non English oath or declaration in the form provided or approved by the PTO need not be translated 37 C F R 1 69(b)

NOTE The translation for a regular application filed in a foreign language must be verified 37 C F R 1 52(d)

(Completion of Filing Requirements [5 1]—page 2 of 6)

**SMALL ENTITY STATUS**

V (Two verified statements are)

A verified statement that this filing is by a small entity

NOTE If an original verified statement and a refund request is filed within two months of the date of payment of a fee then the excess fee paid will be refunded on request 37 C F R 1 28(a)

(check and complete applicable items)

are is attached

A separate refund request accompanies this paper

was filed on \_\_\_\_\_ (original)

**COMPLETION FEES**

VI

WARNING Failure to submit the surcharge fees where required will cause the application to become abandoned 37 C F R 1 53(d)

NOTE The filing fees fees for claims and surcharge fees listed below in items 1 2 and 3 are reduced by 50% where proof of a small entity status is established on or before the date the fee is paid If the full fee was paid but a verified statement is filed within 2 months of the date of timely payment of a fee then the excess fee paid will be refunded on request 37 C F R 1 28(a)

1 Filing fee

original patent application  
(37 C F R 1 16(a)—\$770 00, Small entity—\$385 00) \$ \_\_\_\_\_

design application  
(37 C F R 1 16(f)—\$320 00 small entity—\$160 00) \$ \_\_\_\_\_

\$ \_\_\_\_\_

2 Fees for claims

each independent claim in excess of 3  
(37 C F R 1 16(b)—\$80 00 small entity—\$40 00) \$ \_\_\_\_\_

each claim in excess of 20  
(37 C F R 1 16(c)—\$22 00, small entity—\$11 00) \$ \_\_\_\_\_

multiple dependent claim(s)  
(37 C F R 1 16(d)—\$260 00, small entity—\$130 00) \$ \_\_\_\_\_

3 Surcharge fees

late payment of filing fee

and/or

late filing of original declaration or oath  
(37 C F R 1 16(e)—\$130 00 small entity—\$65 00) \$ 65 00

NOTE Even where a facsimile declaration or oath signed by the inventor(s) was part of the originally filed papers the surcharge fee is required

NOTE If both the filing fee and declaration or oath were missing from the original papers only one surcharge fee for both need be paid 37 C F R 1 16(e)

(Completion of Filing Requirements [5 1]—page 3 of 6)

- 4  Petition and fee for filing by other than all the inventors or a person not the inventor (37 C F R 1 17(h) and 1 47—\$130 00) \$ \_\_\_\_\_
- 5  Fee for processing an application filed with a specification in a non-English language (37 C F R 1 17(k) and 1 52(d)—\$130 00) \$ \_\_\_\_\_
- 6  Fee for processing and retention of application (37 C F R 1 21(l) and 1 53(d)—\$130 00) \$ \_\_\_\_\_
- 7  Assignment (See 'ASSIGNMENT COVER SHEET')

NOTE 37 C F R 1 21(l) establishes a fee for processing and retaining any application which is abandoned for failing to complete the application pursuant to 37 C F R 1 53(d) and this as well as the changes to 37 C F R 1 53 and 1 78 indicate that in order to obtain the benefit of a prior U S application either the basic filing fee or the processing and retention fee of § 1 21(1) within 1 year of notification under §1 53(d) must be paid

Total completion fees \$ 65 00

### EXTENSION OF TIME

#### VII

(complete (a) or (b) as applicable)

The proceedings herein are for a patent application and the provisions of 37 C F R 1 136(a) apply

- (a)  Applicant petitions for an extension of time the fees for which are set out in 37 C F R 1 17(a)-(d) for the total number of months checked below

Extension (months)	Fee for other than small entity	Fee for small entity
<input type="checkbox"/> one month	\$ 110 00	\$ 55 00
<input type="checkbox"/> two months	\$ 390 00	\$195 00
<input type="checkbox"/> three months	\$ 930 00	\$465 00
<input type="checkbox"/> four months	\$1 470 00	\$735 00

Fee \$ \_\_\_\_\_

If an additional extension of time is required, please consider this a petition therefor

(check and complete the next item, if applicable)

- An extension for \_\_\_\_\_ months has already been secured, and the fee paid therefor of \$ \_\_\_\_\_ is deducted from the total fee due for the total months of extension now requested

Extension fee due with this request \$ \_\_\_\_\_

or

- (b)  Applicant believes that no extension of term is required. However, this conditional petition is being made to provide for the possibility that applicant has inadvertently overlooked the need for a petition and fee for extension of time

(Completion of Filing Requirements [5 1]—page 4 of 6)

**TOTAL FEE DUE**

VIII

The total fee due is

Completion fee(s) \$ 65 00

Extension fee (if any) \$ - 0 -

Total Fee Due \$ 65 00

**PAYMENT OF FEES**

IX

Enclosed is a check in the amount of \$ 65,00

Charge Account No \_\_\_\_\_ in the amount of \$ \_\_\_\_\_

A duplicate of this request is attached

NOTE Fees should be itemized in such a manner that it is clear for which purpose the fees are paid 37 C F R 1 22(b)

**AUTHORIZATION TO CHARGE ADDITIONAL FEES**

X

**WARNING** Accurately count claims especially multiple dependant claims to avoid unexpected high charges if extra claims are authorized

The Commissioner is hereby authorized to charge the following additional fees that may be required by this paper and during the pendency of this application to Account No 11-1110

37 C F R 1 16(a) (f) or (g) (filing fees)

37 C F R 1 16(b) (c) and (d) (presentation of extra claims)

NOTE Because additional fees for excess or multiple dependent claims not paid on filing or on later presentation must only be paid or these claims cancelled by amendment prior to the expiration of the time period set for response by the PTO in any notice of fee deficiency (37 C F R 1 16(d)) it might be best not to authorize the PTO to charge additional claim fees except possibly when dealing with amendments after final action

37 C F R 1 16(e) (surcharge for filing the basic filing fee and/or declaration on a date later than the filing date of the application)

37 C F R 1 17 (application processing fees)

**WARNING** While 37 C F R 1 17(a) (b) (c) and (d) deal with extensions of time under § 1 136(a) this authorization should be made only with the knowledge that Submission of the appropriate extension fee under 37 C F R 1 136(a) is to no avail unless a request or petition for extension is filed (Emphasis added) Notice of Nov 5 1985 (1060 O G 27)

37 C F R 1 18 (issue fee at or before mailing of Notice of Allowance pursuant to 37 C F R 1 311(b))

NOTE Where an authorization to charge the issue fee to a deposit account has been filed before the mailing of a Notice of Allowance the issue fee will be automatically charged to the deposit account at the time of mailing the notice of allowance 37 C F R 1 311(b)

NOTE 37 C F R 1 28(b) requires Notification of any change in loss of entitlement to small entity status must be filed in the application prior to paying or at the time of paying issue fee From the wording of 37 C F R 1 28(b) (a) notification of change of status must be made even if the fee is paid as other than a small entity and (b) no notification is required if the change is to another small entity

(Completion of Filing Requirements [5 1]—page 5 of 6)

Reg No 39,094

Tel No (412) 355-8375



SIGNATURE OF ATTORNEY

Michael C Antone

*(type or print name of attorney)*

Kirkpatrick & Lockhart LLP

P O Address 1500 Oliver Building  
Pittsburgh, PA 15222

(Completion of Filing Requirements [5 1]—page 6 of 6)



**PATENT**

**IN THE UNITED STATES PATENT AND TRADEMARK OFFICE**

In re application of Anthony M DiGirola III et al

Serial No 08 /803 993

Group No

Filed February 21 1997

Examiner

For APPARATUS AND METHOD FOR FACILITATING THE IMPLANTATION OF ARTIFICIAL COMPONENTS  
IN JOINTS

**Commissioner of Patents and Trademarks**

**Washington, D C 20231**

**EXPRESS MAIL CERTIFICATE**

"Express Mail label number EH437667898US

Date of Deposit August 5, 1997

I hereby certify that the following attached paper or fee

COMPLETION OF FILING REQUIREMENTS  
PTO FORM 1533  
COMBINED DECLARATION AND POWER OF ATTORNEY  
STATEMENT BY ATTORNEY  
(TWO) VERIFIED STATEMENTS NON PROFIT ORGANIZATIONS  
CHECK PAYABLE TO PTO (For late filing of Oath & Declaration)

is being deposited with the United States Postal Service Express Mail Post Office to Addressee service  
under 37 CFR 1 10 on the date indicated above and is addressed to the Commissioner of Patents  
and Trademarks Washington D C 20231

Beth H Retort

(Typed or printed name of person mailing paper or fee)

(Signature of person mailing paper or fee)

**NOTE** Each paper must have its own certificate and the Express Mail label number as a part thereof or  
attached thereto When as here the certification is presented on a separate sheet that sheet  
must (1) be signed and (2) fully identify and be securely attached to the paper or fee it  
accompanies Identification should include the serial number and filing date of the application as  
well as the type of paper being filed e g complete application specification and drawings  
responses to rejection or refusal notice of appeal etc If the serial number of the application is  
not known the identification should include at least the name of the inventor(s) and the title of the  
invention

**NOTE** The label number need not be placed in each page It should however be placed on  
the first page of each separate document such as a new application amendment  
assignment and transmittal letter for a fee along with the certificate of mailing by  
Express Mail Although the label number may be on checks such a practice is not  
required In order not to deface formal drawings it is suggested that the label number be  
placed on the back of each formal drawing or the drawings be accompanied by a set of  
informal drawings on which the label number is placed

**(Express Mail Certificate [8-3])**





ATTORNEY'S DOCKET NO 97012

**PATENT**

COMBINED DECLARATION AND POWER OF ATTORNEY  
(ORIGINAL DESIGN NATIONAL STAGE OF PCT SUPPLEMENTAL DIVISIONAL  
CONTINUATION OR C I P)

As a below named inventor, I hereby declare that

**TYPE OF DECLARATION**

This declaration is of the following type

(check one applicable item below)

- original
- design
- supplemental

**NOTE** If the declaration is for an International Application being filed as a divisional continuation or continuation in-part application do not check next item check appropriate one of the last three items

- national stage of PCT

**NOTE** If one of the following 3 items apply then complete and also attach ADDED PAGES FOR DIVISIONAL CONTINUATION OR C I P

- divisional
- continuation
- continuation in part (C I P)

**INVENTORSHIP IDENTIFICATION**

**WARNING** If the inventors are each not the inventors of all the claims an explanation of the facts including the ownership of all the claims at the time that the last claimed invention was made should be submitted

My residence post office address and citizenship are as stated below next to my name I believe that I am the original first and sole inventor (*if only one name is listed below*) or an original, first and joint inventor (*if plural names are listed below*) of the subject matter that is claimed and for which a patent I sought on the invention entitled

**TITLE OF INVENTION**

APPARATUS AND METHOD FOR FACILITATING THE IMPLANTATION OF ARTIFICIAL COMPONENTS IN JOINTS

5  
1  
2  
3  
4  
5  
6  
7  
8  
9  
10  
11  
12  
13  
14  
15  
16  
17  
18  
19  
20  
21  
22  
23  
24  
25  
26  
27  
28  
29  
30  
31  
32  
33  
34  
35  
36  
37  
38  
39  
40  
41  
42  
43  
44  
45  
46  
47  
48  
49  
50



**SPECIFICATION IDENTIFICATION**

the specification of which

(complete (a) (b) or (c))

(a)  is attached hereto

**NOTE** The following combinations of information supplied in an oath or declaration filed on the application filing date with a specification are acceptable as minimums for identifying a specification and compliance with any one of the items below will be accepted as complying with the identification requirement of 37 CFR 1.63

(1) name of inventor(s) and reference to an attached specification which is both attached to the oath or declaration at the time of execution and submitted with the oath or declaration on filing

(2) name of inventor(s) and attorney docket number which was on the specification as filed or

(3) name of inventor(s) and title which was on the specification as filed "

Notice of July 13, 1995 (1177 O G 60)

(b)  was filed on February 21, 1997 as Serial No 08/803,993

(c) or  \_\_\_\_\_ and was amended on \_\_\_\_\_ (if applicable)

**NOTE** Amendments filed after the original papers are deposited with the PTO that contain new matter are not accorded a filing date by being referred to in the declaration. Accordingly the amendments involved are those filed with the application papers or in the case of a supplemental declaration are those amendments claiming matter not encompassed in the original statement of invention or claims. See 37 CFR 1.67

**NOTE** "The following combinations of information supplied in an oath or declaration filed after the filing date are acceptable as minimums for identifying a specification and compliance with any one of the items below will be accepted as complying with the identification requirement of 37 CFR 1.63

(1) name of inventor(s) and application number (consisting of the series code and the serial number e.g. 08/123 456)

(2) name of inventor(s) serial number and filing date

(3) name of inventor(s) and attorney docket number which was on the specification as filed

(4) name of inventor(s) title which was on the specification as filed and filing date

(5) name of inventor(s) title which was on the specification as filed and reference to an attached specification which is both attached to the oath or declaration at the time of execution and submitted with the oath or declaration or

(6) name of inventor(s) title which was on the specification as filed and accompanied by a cover letter accurately identifying the application for which it was intended by either the application number (consisting of the series code and the serial number e.g. 08/123 456) or serial number and filing date. Absent any statement(s) to the contrary it will be presumed that the application filed in the PTO is the application which the inventor(s) executed by signing the oath or declaration

Notice of July 13 1995 (1177 O G 60)

(Declaration and Power of Attorney [1-1]-page 2 of 7)

DECLARATION

# File History Content Report

The following content is missing from the original file history record obtained from the United States Patent and Trademark Office. No additional information is available.

Document Date - 1997-08-05

Document Title - Oath or Declaration filed

Page(s) - 3 of 7

This page is not part of the official USPTO record. It has been determined that content identified on this document is missing from the original file history record.

**PRIOR FOREIGN/PCT APPLICATION(S) FILED WITHIN 12 MONTHS  
(6 MONTHS FOR DESIGN) PRIOR TO THIS APPLICATION  
AND ANY PRIORITY CLAIMS UNDER 35 U S C § 119(a)-(d)**

COUNTRY (OR INDICATE IF PCT)	APPLICATION NUMBER	DATE OF FILING (day month, year)	PRIORITY CLAIMED UNDER 37 USC 119	
			<input type="checkbox"/> YES	NO <input type="checkbox"/>
			<input type="checkbox"/> YES	NO <input type="checkbox"/>
			<input type="checkbox"/> YES	NO <input type="checkbox"/>
			<input type="checkbox"/> YES	NO <input type="checkbox"/>
			<input type="checkbox"/> YES	NO <input type="checkbox"/>

**CLAIM FOR BENEFIT OF PRIOR U S PROVISIONAL APPLICATION(S)  
(34 U S C § 119(e))**

I hereby claim the benefit under Title 35 United States Code § 119(e) of any United States provisional application(s) listed below

**PROVISIONAL APPLICATION NUMBER**

**FILING DATE**

\_\_\_\_\_  
\_\_\_\_\_  
\_\_\_\_\_

\_\_\_\_\_  
\_\_\_\_\_  
\_\_\_\_\_

**CLAIM FOR BENEFIT OF EARLIER US/PCT APPLICATION(S)  
UNDER 35 U S C 120**

- The claim for the benefit of any such applications are set forth in the attached **ADDED PAGES TO COMBINED DECLARATION AND POWER OF ATTORNEY FOR DIVISIONAL, CONTINUATION OR CONTINUATION IN PART (C I P) APPLICATION**

ADDED PAGES TO COMBINED DECLARATION AND POWER OF ATTORNEY FOR DIVISIONAL, CONTINUATION OR CONTINUATION IN PART (C I P) APPLICATION

**ALL FOREIGN APPLICATION(S), IF ANY, FILED MORE THAN 12 MONTHS  
(6 MONTHS FOR DESIGN) PRIOR TO THIS U S APPLICATION**

---

---

**NOTE** *If the application filed more than 12 months from the filing date of this application is a PCT filing forming the basis for this application entering the United States as (1) the national stage or (2) a continuation divisional or continuation-in part then also complete ADDED PAGES TO COMBINED DECLARATION AND POWER OF ATTORNEY FOR DIVISIONAL CONTINUATION OR C I-P APPLICATION for benefit of the prior U S or PCT application(s) under 35 U S C § 120*

**POWER OF ATTORNEY**

I hereby appoint the following attorney(s) and/or agent(s) to prosecute this application and transact all business in the Patent and Trademark Office connected therewith

Michael C Antone Reg No 39 094 Tara C Cacciabaudo Reg No 40 935, George D Dickos Reg No 30 048, Thomas J Edgington Reg No 34,324, Christine R Ethridge, Reg No 30 557 Jason D Haislmaier, Reg No 40 300, James R Kyper Reg No 27 346 Mark R Leslie Reg No 36 360 Franklin B Molin Reg No 37 397 Jonathan C Parks Reg No 40,120 Edward L Pencoske Reg No 29 688 Darren E Wolf Reg No 36 310 and Robert D Yeager Reg No 25 047

Attached as part of this declaration and power of attorney, is the authorization of the above named attorney(s) to accept and follow instructions from my representative(s)

SEND CORRESPONDENCE TO  
(Name)

*Michael C Antone, Esq  
Kirkpatnck & Lockhart LLP  
1500 Oliver Building  
Pittsburgh, Pennsylvania 15222*

DIRECT TELEPHONE CALLS TO  
(Name and telephone number)

*Michael C Antone, Esq  
(412) 355-8645*

**DECLARATION**

I hereby declare that all statements made herein of my own knowledge are true and that all statements made on information and belief are believed to be true and further that these statements were made with the knowledge that willful false statements and the like so made are punishable by fine or imprisonment or both under Section 1001 of Title 18 of the United States Code and that such willful false statements may jeopardize the validity of the application or any patent issued thereon

(Declaration and Power of Attorney [1-1]- page 5 of 7)

**SIGNATURE(S)**

NOTE Carefully indicate the family (or last) name as it should appear on the filing receipt and all other documents

Full name of sole or first inventor

Anthony M DiGioia III  
(GIVEN NAME) (MIDDLE INITIAL OR NAME) FAMILY (OR LAST NAME)  
Inventor's signature *Anthony M DiGioia III*  
Date June 30, 1997 Country of Citizenship USA  
Residence Pittsburgh, PA 15232  
Post Office Address 5200 Westminister Place  
Pittsburgh, PA 15232

Full name of second joint inventor if any \_\_\_\_\_

David A Simon  
(GIVEN NAME) (MIDDLE INITIAL OR NAME) FAMILY (OR LAST NAME)  
Inventor's signature *David A Simon*  
Date 6/27/97 Country of Citizenship USA  
Residence Boulder, CO 80303 1238  
Post Office Address 1424 Patton Drive  
Boulder, CO 80303-1238

Full name of third joint inventor if any \_\_\_\_\_

Branislav \_\_\_\_\_ Jaramaz  
(GIVEN NAME) (MIDDLE INITIAL OR NAME) FAMILY (OR LAST NAME)  
Inventor's signature *Branislav Jaramaz*  
Date 6/27/97 Country of Citizenship Croatia  
Residence Pittsburgh, PA 15217  
Post Office Address 5162 Beeler Street  
Pittsburgh, PA 15217

(Declaration and Power of Attorney [1 1]--page 6 of 7)

(check proper box(es) for any of the following added page(s) that form a part of this declaration)

**Signature for fourth and subsequent joint inventors** *Number of pages added*  
2

\* \* \*

**Signature by administrator(trix) or legal representative for deceased or incapacitated inventor** *Number of pages added* \_\_\_\_\_

\* \* \*

**Signature for inventor who refuses to sign or cannot be reached by person authorized under 37 CFR 1 47** *Number of pages added* \_\_\_\_\_

**Added page for signature by one joint inventor on behalf of deceased inventor(s) where legal representative cannot be appointed in time (37 CFR 1 47)**

**Added pages to combined declaration and power of attorney for divisional continuation or continuation-in part (C-I P) application**

**Number of pages added** \_\_\_\_\_

\* \* \*

**Authorization of attorney(s) to accept and follow instructions from representative**

\* \* \*

*(if no further pages form a part of this Declaration then end this Declaration with this page and check the following item)*

**This declaration ends with this page**

(Declaration and Power of Attorney [1-1] page 7 of 7)











I hereby declare that rights under contract or law have been conveyed, and remain with, the nonprofit organization with regard to the above identified invention

If the rights held by the nonprofit organization are not exclusive, each individual concern or organization having rights to the invention is listed below\* and no rights to the invention are held by any person other than the inventor who could not qualify as a small business concern under 37 CFR 1.9(d) or by any concern that would not qualify as a small business concern under 37 CFR 1.9(d), or a nonprofit organization under 37 CFR 1.9(e)

*NOTE: Separate verified statements are required from each named person concern or organization having rights to the invention averaging to their status as small entities (37 CFR 1.27)*

NAME \_\_\_\_\_

ADDRESS \_\_\_\_\_

INDIVIDUAL       SMALL BUSINESS CONCERN       NONPROFIT ORGANIZATION

NAME \_\_\_\_\_

ADDRESS \_\_\_\_\_

INDIVIDUAL       SMALL BUSINESS CONCERN       NONPROFIT ORGANIZATION

I acknowledge the duty to file in this application or patent, notification of any change in status resulting in loss of entitlement to small entity status prior to paying or at the time of paying the earliest of the issue fee or any maintenance fee due after the date on which status as a small entity is no longer appropriate (37 CFR 1.28(b))

I hereby declare that all statements made herein of my own knowledge are true and that all statements made on information and belief are believed to be true and further that these statements were made with the knowledge that willful false statements and the like so made are punishable by fine or imprisonment or both, under Section 1001 of Title 18 of the United States Code and that such willful false statements may jeopardize the validity of the application any patent issuing thereon or any patent to which this verified statement is directed

NAME OF PERSON SIGNING Susan Burkett

TITLE IN ORGANIZATION Associate Provost

ADDRESS OF PERSON SIGNING Carnegie Mellon University  
5000 Forbes Avenue, Pittsburgh, Pennsylvania 15213

SIGNATURE 

Date 30 July 99

(Small Entity—Non Profit [7 3]—page 2 of 2)

11-11-99-1003-1003



Attorney's Docket No 97012 **PATENT**

Applicant or Patentee Anthony M DiGiola III et al

Application or Patent No 08 / 803,993

Filed or Issued February 21, 1997

For APPARATUS AND METHOD FOR FACILITATING THE IMPLANTATION OF ARTIFICIAL COMPONENTS IN JOINTS

**VERIFIED STATEMENT (DECLARATION) CLAIMING SMALL ENTITY STATUS (37 CFR 1 9(f) and 1 27(d))—NONPROFIT ORGANIZATION**

I hereby declare that I am an official empowered to act on behalf of the nonprofit organization identified below

NAME OF ORGANIZATION Shadyside Hospital

ADDRESS OF ORGANIZATION 5200 Centre Avenue

Pittsburgh, PA 15232

**TYPE OF ORGANIZATION**

- UNIVERSITY OR OTHER INSTITUTION OF HIGHER EDUCATION
- TAX EXEMPT UNDER INTERNAL REVENUE SERVICE CODE (26 USC 501(a) and 501(c)(3))
- NONPROFIT SCIENTIFIC OR EDUCATIONAL UNDER STATUTE OF STATE OF THE UNITED STATES OF AMERICA  
(NAME OF STATE \_\_\_\_\_)  
(CITATION OF STATUTE \_\_\_\_\_)
- WOULD QUALIFY AS TAX EXEMPT UNDER INTERNAL REVENUE SERVICE CODE (26 USC 501(a) and 501(c)(3)), IF LOCATED IN THE UNITED STATES OF AMERICA
- WOULD QUALIFY AS NONPROFIT SCIENTIFIC OR EDUCATIONAL UNDER STATUTE OF STATE OF THE UNITED STATES OF AMERICA IF LOCATED IN THE UNITED STATES OF AMERICA  
(NAME OF STATE \_\_\_\_\_)  
(CITATION OF STATUTE \_\_\_\_\_)

I hereby declare that the nonprofit organization identified above qualifies as a nonprofit organization, as defined in 37 CFR 1 9(e) for purposes of paying reduced fees under Sections 41(a) and (b) of Title 35 United States Code with regard to the invention entitled APPARATUS AND METHOD FOR FACILITATING THE IMPLANTATION OF ARTIFICIAL COMPONENTS IN JOINTS

by inventor(s) Anthony M DiGiola III, David A Simon, Branislav Jaramaz,

Michael K Blackwell, Frederick M Morgan, Robert V O'Toole  
described in and Takeo Kanade

- the specification filed herewith
- application no 08 / 803 993 filed February 21, 1997
- patent no \_\_\_\_\_, issued \_\_\_\_\_

(Small Entity—Non Profit [7 3]—page 1 of 2)

40#EEU-26022000

I hereby declare that rights under contract or law have been conveyed and remain with the nonprofit organization, with regard to the above identified invention

If the rights held by the nonprofit organization are not exclusive, each individual, concern or organization having rights to the invention is listed below\* and no rights to the invention are held by any person other than the inventor who could not qualify as a small business concern under 37 CFR 1 9(d), or by any concern that would not qualify as a small business concern under 37 CFR 1 9(d) or a nonprofit organization under 37 CFR 1 9(e)

NOTE Separate verified statements are required from each named person concern or organization having rights to the invention avering to their status as small entities (37 CFR 1 27)

NAME \_\_\_\_\_

ADDRESS \_\_\_\_\_

INDIVIDUAL       SMALL BUSINESS CONCERN       NONPROFIT ORGANIZATION

NAME \_\_\_\_\_

ADDRESS \_\_\_\_\_

INDIVIDUAL       SMALL BUSINESS CONCERN       NONPROFIT ORGANIZATION

I acknowledge the duty to file in this application or patent notification of any change in status resulting in loss of entitlement to small entity status prior to paying or at the time of paying the earliest of the issue fee or any maintenance fee due after the date on which status as a small entity is no longer appropriate (37 CFR 1 28(b))

I hereby declare that all statements made herein of my own knowledge are true and that all statements made on information and belief are believed to be true and further that these statements were made with the knowledge that willful false statements and the like so made are punishable by fine or imprisonment or both, under Section 1001 of Title 18 of the United States Code and that such willful false statements may jeopardize the validity of the application any patent issuing thereon or any patent to which this verified statement is directed

NAME OF PERSON SIGNING Stanley J Milavec, Jr  
TITLE IN ORGANIZATION Acting Vice President & General Counsel

ADDRESS OF PERSON SIGNING Shadyside Hospital  
Room 104, School of Nursing, 5200 Centre Avenue, Pittsburgh, PA  
15232

SIGNATURE 

Date 8/1/97

40 FEB - 2000



BEST COPY

UNITED STATES DEPARTMENT OF COMMERCE  
Patent and Trademark Office

Address COMMISSIONER OF PATENTS AND TRADEMARKS  
Washington D C 20231

*Handwritten initials*

APPLICATION NUMBER	FILING DATE	FIRST NAMED APPLICANT	ATTORNEY DOCKET NO
--------------------	-------------	-----------------------	--------------------

08/903 993    11/21/97    DIGIOIA    A    97012

EXAMINER

LM21/UE24

MICHAEL C ANTONE  
KIRKPATRICK & LOCKHART  
1500 OLIVER BUILDING  
PITTSBURGH PA 15222

ART UNIT	PAPER NUMBER
----------	--------------

2763

6

DATE MAILED

06/24/99

This is a communication from the examiner in charge of your application  
COMMISSIONER OF PATENTS AND TRADEMARKS

**NOTICE OF ALLOWABILITY**

All claims being allowable, PROSECUTION ON THE MERITS IS (OR REMAINS) CLOSED in this application. If not included herewith (or previously mailed) a Notice of Allowance and Issue Fee Due or other appropriate communication will be mailed in due course.

This communication is responsive to IDS RECEIVED 5-20-97

The allowed claim(s) is/are 1-24

The drawings filed on \_\_\_\_\_ are acceptable

Acknowledgement is made of a claim for foreign priority under 35 U.S.C. § 119(a) (d)

All  Some  None of the CERTIFIED copies of the priority documents have been

received

received in Application No. (Series Code/Serial Number) \_\_\_\_\_

received in this national stage application from the International Bureau (PCT Rule 17.2(a))

\*Certified copies not received \_\_\_\_\_

Acknowledgement is made of a claim for domestic priority under 35 U.S.C. § 119(e)

A SHORTENED STATUTORY PERIOD FOR RESPONSE to comply with the requirements noted below is set to EXPIRE THREE MONTHS FROM THE DATE MAILED\* of this Office action. Failure to timely comply will result in ABANDONMENT of this application. Extensions of time may be obtained under the provisions of 37 CFR 1.136(a).

Note the attached EXAMINER'S AMENDMENT or NOTICE OF INFORMAL APPLICATION PTO 152, which discloses that the oath or declaration is deficient. A SUBSTITUTE OATH OR DECLARATION IS REQUIRED.

Applicant MUST submit NEW FORMAL DRAWINGS

because the originally filed drawings were declared by applicant to be informal

including changes required by the Notice of Draftperson's Patent Drawing Review PTO 948 attached hereto or to Paper No. \_\_\_\_\_

including changes required by the proposed drawing correction filed on \_\_\_\_\_ which has been approved by the examiner

including changes required by the attached Examiner's Amendment/Comment

Identifying indicia such as the application number (see 37 CFR 1.84(c)) should be written on the reverse side of the drawings. The drawings should be filed as a separate paper with a transmittal letter addressed to the Official Draftperson.

Note the attached Examiner's comment regarding REQUIREMENT FOR THE DEPOSIT OF BIOLOGICAL MATERIAL

Any response to this letter should include in the upper right hand corner the APPLICATION NUMBER (SERIES CODE/SERIAL NUMBER). If applicant has received a Notice of Allowance and Issue Fee Due the ISSUE BATCH NUMBER and DATE of the NOTICE OF ALLOWANCE should also be included.

**Attachment(s)**

Notice of References Cited PTO 892

Information Disclosure Statement(s) PTO 1449 Paper No(s) 4

Notice of Draftperson's Patent Drawing Review PTO 948

Notice of Informal Patent Application PTO 152

Interview Summary PTO-413

Examiner's Amendment/Comment

Examiner's Comment Regarding Requirement for Deposit of Biological Material

Examiner's Statement of Reasons for Allowance

*Handwritten signature of Vincent N. Trans*

VINCENT N TRANS  
PRIMARY EXAMINER

Serial Number 08/803,993

2

Art Unit 2763

1 The following communication is in response to applicant's filing on 21-February-1997

2 An Examiner's Amendment to the record appears below Should the changes and/or additions be unacceptable to applicant, an amendment may be filed as provided by 37 C F R § 1 312 To ensure consideration of such an amendment, it **MUST** be submitted no later than the payment of the Issue Fee Authorization for this Examiner's Amendment was given by Christine Ethridge (Reg No 30,557) on 11-June-1998

**EXAMINER'S AMENDMENT**

3 In the Claims

claim 11 ✓ line 3 ✓ Insert --to-- between "attached" and "the"

claim 14 ✓ line 2 ✓ Delete [and a] and insert --and an--

claim 24 ✓ line 2 ✓ Change "comprise" to --comprises--

**REASONS FOR ALLOWANCE**

4 The following is an Examiner's Statement of Reasons for the indication of allowable subject matter The invention describes a method and apparatus for determining an implant position for at least one artificial component in a patient's joint, wherein models of the patient's joint and the artificial component are created for use in calculating a range of motion based on simulating movement of the joint with the artificial component in a test position,

Serial Number 08/803,993

3

Art Unit 2763

whereby an implant position for the artificial component is determined based on a predetermined range of motion and the calculated range of motion. The claims also contain "means-plus-function language." According to 35 USC § 112, sixth paragraph, "An element in a claim for a combination may be expressed as a means or step for performing a specified function without recital of structure, material, or acts in support thereof, and such claim shall be construed to cover the corresponding structure, material, or acts described in the specification and equivalents thereof" (see In re Donaldson Company, Inc., CAFC (2/14/94) 29 USPQ2d 1845, and PTO Notice on Means or Step Plus Function Limitation Under 35 USC § 112, 6th paragraph, C E Van Horn, 20 April 1994 (1162 OG 59 published May 17, 1994))

The Examiner has established this notice of allowance based upon the interpretation of 35 USC § 112, 6th paragraph "means or step plus function" limitation in the claims as limited to the corresponding structure, material or acts described in the specification and equivalents thereof which is found at least at <page 10, line 17 through page 21, line 20, and Figures 1-10(b)>. The art of record fails to teach, suggest, or render obvious the <computer-assisted means for determining the implant position of an artificial component utilizing a predetermined range of motion and a calculated range of motion determined from the simulated movement of joint and component models from a test position> having the corresponding structure which is disclosed in the specification. In view of the foregoing, the claims of the present application are found to be patentable over the prior art.



Serial Number 08/803,993

4

Art Unit 2763

5 Any comments considered necessary by applicant **MUST** be submitted no later than the payment of the Issue Fee and, to avoid processing delays, should preferably accompany the Issue Fee. Such submissions should clearly be labeled "Comments on Statement of Reasons for Allowance"

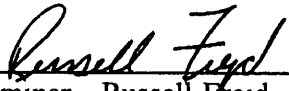
6 Any response to the Examiner in regard to this allowance should be

**directed to** Russell Frejd, telephone number (703) 305-4839, Monday-Friday from 0630 to 1500 ET, or the examiner's supervisor, Kevin Teska, telephone number (703) 305-9704. Any inquiry of a general nature or relating to the status of this application should be directed to the Group receptionist, telephone number (703) 305-3900

**mailed to** Commissioner of Patents and Trademarks  
Washington, D C 20231

**or faxed to** (703) 308-9051 (for formal communications intended for entry), or (703) 308-5357 (for informal or draft communications, please label "PROPOSED" or "DRAFT")

Hand delivered responses should be brought to Crystal Park II, 2121 Crystal Drive Arlington VA Sixth Floor (Receptionist)

  
\_\_\_\_\_  
Examiner Russell Frejd  
Date 19-June-1998



VINCENT N TRANS  
PRIMARY EXAMINER

# File History Content Report

The following content is missing from the original file history record obtained from the United States Patent and Trademark Office. No additional information is available.

Document Date - 1998-06-24

Document Title - List of references cited by examiner

BEST COPY



UNITED STATES DEPARTMENT OF COMMERCE  
Patent and Trademark Office

**NOTICE OF ALLOWANCE AND ISSUE FEE DUE**

LM21/0624

MICHAEL C ANTONE  
IRKPATRICK & LOUHART  
1500 OLIVER BUILDING  
PITTSBURGH PA 15222

APPLICATION NO	FILING DATE	TOTAL CLAIMS	EXAMINER AND GROUP ART UNIT	DATE MAILED
08/003,793	02/21/97	024	FREJD, R	2763 04/14/98
First Named Applicant	DIGIDIA ANTHONY M		III	

TITLE OF INVENTION: APPARATUS AND METHOD FOR FACILITATING THE IMPLANTATION OF ARTIFICIAL COMPONENTS IN JOINTS

ATTY'S DOCKET NO	CLASS SUBCLASS	BATCH NO	APPLN TYPE	SMALL ENTITY	FEE DUE	DATE DUE
0 17012	3e4-57s	000	F99 UTILITY	YES	\$660 00	09/24/98

**THE APPLICATION IDENTIFIED ABOVE HAS BEEN EXAMINED AND IS ALLOWED FOR ISSUANCE AS A PATENT PROSECUTION ON THE MERITS IS CLOSED.**

**THE ISSUE FEE MUST BE PAID WITHIN THREE MONTHS FROM THE MAILING DATE OF THIS NOTICE OR THIS APPLICATION SHALL BE REGARDED AS ABANDONED THIS STATUTORY PERIOD CANNOT BE EXTENDED.**

**HOW TO RESPOND TO THIS NOTICE**

I Review the SMALL ENTITY status shown above  
If the SMALL ENTITY is shown as YES, verify your current SMALL ENTITY status

If the SMALL ENTITY is shown as NO

A Pay FEE DUE shown above, or

B File verified statement of Small Entity Status before or with payment of 1/2 the FEE DUE shown above

A If the status is changed pay twice the amount of the FEE DUE shown above and notify the Patent and Trademark Office of the change in status or

B If the status is the same, pay the FEE DUE shown above

II Part B Issue Fee Transmittal should be completed and returned to the Patent and Trademark Office (PTO) with your ISSUE FEE Even if the ISSUE FEE has already been paid by charge to deposit account, Part B Issue Fee Transmittal should be completed and returned. If you are charging the ISSUE FEE to your deposit account, section "4b" of Part B Issue Fee Transmittal should be completed and an extra copy of the form should be submitted.

III All communications regarding this application must give application number and batch number  
Please direct all communications prior to issuance to Box ISSUE FEE unless advised to the contrary

**IMPORTANT REMINDER** Utility patents issuing on applications filed on or after Dec 12, 1980 may require payment of maintenance fees It is patentee's responsibility to ensure timely payment of maintenance fees when due

PATENT AND TRADEMARK OFFICE COPY



**UNITED STATES DEPARTMENT OF COMMERCE  
Patent and Trademark Office**

Address COMMISSIONER OF PATENTS AND TRADEMARKS  
Washington D C 20231

APPLICATION NO	FILING DATE	FIRST NAMED INVENTOR	ATTORNEY DOCKET NO
05/503,993	02/21/97	DIGIDIA	A 97012

MICHAEL C ANTONE  
KIRKPATRICK & LOCHART  
1500 OLIVER BUILDING  
PITTSBURGH PA 15222

LMC1/0625

EXAMINER  
FREJIA R

ART UNIT	PAPER NUMBER
2763	

DATE MAILED 06/25/97

**Please find below and/or attached an Office communication concerning this application or proceeding**

**Commissioner of Patents and Trademarks**

Attorney's Docket No 9,012

PATENT

**IN THE UNITED STATES PATENT AND TRADEMARK OFFICE**

In re application of Anthony M Digioia, III et al

Serial No 08/803,993

Group No 2700

Filed February 21, 1997

Examiner Frejd, R

For APPARATUS AND METHOD FOR FACILITATING THE IMPLANTATION OF ARTIFICIAL COMPONENTS IN JOINTS

Batch No F89

Assistant Commissioner for Patents  
Washington, D C 20231  
ATTENTION Box Issue Fee

**TRANSMITTAL OF PAYMENT OF ISSUE FEE (37 C F R. 1 311)**

1 Applicant hereby pays the issue fee for the attached Issue Fee Transmittal PTOL-85

2 Fee (37 C F R. 1 18(a) and (b))

Application status is

	<u>Regular</u>	<u>Design</u>
<input checked="" type="checkbox"/> small business entity-fee	<input checked="" type="checkbox"/> \$660 00	<input type="checkbox"/> \$225 00
<input type="checkbox"/> verified statement attached		
<input checked="" type="checkbox"/> verified statement filed on <u>8/5/97</u>		
<input type="checkbox"/> other than a small entity-fee	<input type="checkbox"/> \$1,320 00	<input type="checkbox"/> \$450 00

3 Payment of fee

Enclosed please find check for \$ 690.00

Charge Account 11-1110 for any fee deficiency

Charge Account \_\_\_\_\_ the sum of \$ \_\_\_\_\_

A duplicate of this request is attached

  
SIGNATURE OF ATTORNEY

Jonathan C. Parks  
(type or print name of person certifying)

Reg No 40,120

Tel No (412) 355-6288

Kirkpatrick & Lockhart, LLP  
1500 Oliver Building  
Pittsburgh, PA 15222-2312

**CERTIFICATE OF MAILING/TRANSMISSION (37 C F R. 1 8a)**

I hereby certify that this correspondence is on the date shown below being

MAILING	FACSIMILE
<input type="checkbox"/> deposited with the United States Postal Service with sufficient postage as first class mail, in an envelope addressed to the Assistant Commissioner for Patents, Washington, D C 20231	<input type="checkbox"/> transmitted by facsimile to the patent and Trademark Office

Date \_\_\_\_\_

\_\_\_\_\_  
Signature  
(type or print name of person certifying)

PATENT

IN THE UNITED STATES PATENT AND TRADEMARK OFFICE

In re application of Digioia, III et al

Serial No 08/803,993

Group No 2700

Filed February 21, 1997

Examiner Frejd, R

For APPARATUS AND METHOD FOR FACILITATING THE IMPLANTATION OF ARTIFICIAL COMPONENTS IN JOINTS

Box Issue Fee  
Assistant Commissioner of Patents  
Washington, D C 20231

EXPRESS MAIL CERTIFICATE

Express Mail label number EE687588703US

Date of Deposit September 22, 1998

I hereby certify that the following attached paper or fee

TRANSMITTAL OF PAYMENT OF ISSUE FEE  
PTO FORM 85B  
CHECK PAYABLE TO PTO

is being deposited with the United States Postal Service Express Mail Post Office to Addressee service under 37 CFR 1 10 on the date indicated above and is addressed to Box Issue Fee the Assistant Commissioner of Patents Washington D C 20231

Beth H Refort

(Typed or printed name of person mailing paper or fee)

(Signature of person mailing paper or fee)

NOTE Each paper must have its own certificate and the Express Mail label number as a part thereof or attached thereto When as here the certification is presented on a separate sheet that sheet must (1) be signed and (2) fully identify and be securely attached to the paper or fee it accompanies Identification should include the serial number and filing date of the application as well as the type of paper being filed e g complete application specification and drawings responses to rejection or refusal notice of appeal etc If the serial number of the application is not known the identification should include at least the name of the inventor(s) and the title of the invention

NOTE The label number need not be placed in each page It should however be placed on the first page of each separate document such as a new application, amendment assignment and transmittal letter for a fee along with the certificate of mailing by Express Mail Although the label number may be on checks such a practice is not required In order not to deface formal drawings it is suggested that the label number be placed on the back of each formal drawing or the drawings be accompanied by a set of informal drawings on which the label number is placed

(Express Mail Certificate [8-3])

PI-51495 01

BR

PART B—ISSUE FEE TRANSMITTAL

Complete and mail this form, together with the appropriate fees, to Box ISSUE FEE Assistant Commissioner for Patents Washington, D C 20231

242-6660  
561-30

**MAILING INSTRUCTIONS** This form should be used for transmitting the ISSUE FEE Blocks 1 through 4 should be completed where appropriate. All further correspondence including the Issue Fee Receipt the Patent advance orders and notification of maintenance fees will be mailed to the current correspondence address as indicated unless corrected below or directed otherwise in Block 1 by (a) specifying a new correspondence address and/or (b) indicating a separate FEE ADDRESS for maintenance fee notifications

Note: The certificate of mailing below can only be used for domestic mailings of the Issue Fee Transmittal. This certificate cannot be used for any other accompanying papers. Each additional paper, such as an assignment or formal drawing, must have its own certificate of mailing.

Certificate of Mailing

I hereby certify that this Issue Fee Transmittal is being deposited with the United States Postal Service with sufficient postage for first class mail in an envelope addressed to the Box Issue Fee address above on the date indicated below

CURRENT CORRESPONDENCE ADDRESS (Note: Legibly mark-up with any corrections or use Block 1)

MICHAEL C ANTONI  
IRI PATRICK & LOCKHART  
1500 OLIVER BUILDING  
PITTSBURGH PA 15222

LM21/0624

RECEIVED  
Publishing Division  
SEP 22 1998

(Depositor's name)

(Signature)

(Date)

APPLICATION NO	FILING DATE	TOTAL CLAIMS	EXAMINER AND GROUP ART UNIT	DATE MAILED
1127E03 997	02/21/97	024	FREJD, R	2763 06/24/98
First Named Applicant	DIGIOIA ANTHONY M		III	

TITLE OF INVENTION: APPARATUS AND METHOD FOR FACILITATING THE IMPLANTATION OF ARTIFICIAL COMPONENTS IN JOINTS

ATTY'S DOCKET NO	CLASS-SUBCLASS	BATCH NO	APPLN TYPE	SMALL ENTITY	FEE DUE	DATE DUE
11 97012	364-570 000	F59	UTILITY	YES	\$650 00	11/7/95

1 Change of correspondence address or indication of Fee Address (37 CFR 1.363) Use of PTO form(s) and Customer Number are recommended but not required

2 For printing on the patent front page list (1) the names of up to 3 registered patent attorneys or agents OR alternatively (2) the name of a single firm (having as a member a registered attorney or agent) and the names of up to 2 registered patent attorneys or agents. If no name is listed no name will be printed

1 Kirkpatrick & Lockhart LLP  
2  
3

- Change of correspondence address (or Change of Correspondence Address form PTO/SB/122) attached
- Fee Address indication (or Fee Address Indication form PTO/SB/47) attached

3 ASSIGNEE NAME AND RESIDENCE DATA TO BE PRINTED ON THE PATENT (print or type) **RELEASE NOTE** Unless an assignee is identified below no assignee data will appear on the patent. Inclusion of assignee data is only appropriate when an assignment has been previously submitted to the PTO or is being submitted under separate cover. Completion of this form is NOT a substitute for filing an assignment.

(A) NAME OF ASSIGNEE: Carnegie Mellon University  
(B) RESIDENCE (CITY & STATE OR COUNTRY): Pittsburgh, PA 15213

Please check the appropriate assignee category indicated below (will not be printed on the patent)  
 Individual  corporation or other private group entity  government

4a The following fees are enclosed (make check payable to Commissioner of Patents and Trademarks)

Issue Fee  
 Advance Order # of Copies: 10

4b The following fees or deficiency in these fees should be charged to DEPOSIT ACCOUNT NUMBER 11-1110 (ENCLOSE AN EXTRA COPY OF THIS FORM)

Issue Fee  
 Advance Order # of Copies: 10

The COMMISSIONER OF PATENTS AND TRADEMARKS IS requested to apply the Issue Fee to the application identified above

(Authorized Signature)

(Date)

[Signature]

9/22/98

NOTE: The Issue Fee will not be accepted from anyone other than the applicant, a registered attorney or agent, or the assignee or other party in interest as shown by the records of the Patent and Trademark Office.

**Burden Hour Statement** This form is estimated to take 0.2 hours to complete. Time will vary depending on the needs of the individual case. Any comments on the amount of time required to complete this form should be sent to the Chief Information Officer, Patent and Trademark Office, Washington, D C 20231. DO NOT SEND FEES OR COMPLETED FORMS TO THIS ADDRESS. SEND FEES AND THIS FORM TO: Box Issue Fee, Assistant Commissioner for Patents, Washington D C 20231.

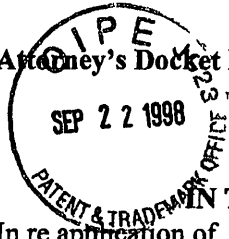
Under the Paperwork Reduction Act of 1995 no persons are required to respond to a collection of information unless it displays a valid OMB control number.

01 FC 242  
20 FC 561  
10/02/1998 BSTERMART 00000053 08803933

TRANSMIT THIS FORM WITH FEE

Attorney's Docket No 97012

PATENT



Serial No 08/803,993  
Batch No F89

IN THE UNITED STATES PATENT AND TRADEMARK OFFICE

In re application of Anthony M DiGirola, III et al

Serial No 08/803,993

Group No 2700

Filed February 21, 1997

Examiner Frejd, R

For APPARATUS AND METHOD FOR FACILITATING THE IMPLANTATION OF ARTIFICIAL COMPONENTS IN JOINTS

Assistant Commissioner for Patents  
Washington, D C 20231

TRANSMITTAL OF FORMAL DRAWINGS

In response to the NOTICE OF ALLOWABILITY mailed on June 24, 1998  
(date)

attached please find

(a) the formal drawing(s) for this application

Number of Sheets 11

NOTE Identifying indicia if provided should include the application number or the title of the invention inventor's name docket number (if any) and the name and telephone number of a person to call if the Office is unable to match the drawings to the proper application This information should be placed on the back of each sheet of a drawing a minimum distance of 1.5 cm (5/8 inch) down from the top of the page 37 C.F.R. 1.84(c)

Each sheet of drawing indicates the identifying indicia suggested in § 1.84(c) on the reverse side of the drawing

(b) a copy of the NOTICE OF ALLOWABILITY

Reg No 40,120

SIGNATURE OF ATTORNEY  
Jonathan C. Parks  
(type or print name of person certifying)

Tel No (412) 355-6288

Kirkpatrick & Lockhart, LLP  
1500 Oliver Building  
Pittsburgh, PA 15222

CERTIFICATE OF MAILING (37 C.F.R. 1.8(a))

I hereby certify that this paper (along with any paper referred to as being attached or enclosed) is being deposited with the United States Postal Service on the date shown below the sufficient postage as first class mail in an envelope addressed to the Commissioner of Patents and Trademarks, Washington, D C 20231

Date \_\_\_\_\_

\_\_\_\_\_  
(type or print name of person mailing paper)

\_\_\_\_\_  
(Signature of person mailing paper)

(Transmittal of Formal Drawings In Response to Notice of Informal Drawings [9-16 1])





IN THE UNITED STATES PATENT AND TRADEMARK OFFICE

In re application of Digioia, III et al

Serial No 08/803,993

Group No 2700

Filed February 21, 1997

Examiner Frejd, R

For APPARATUS AND METHOD FOR FACILITATING THE IMPLANTATION OF ARTIFICIAL COMPONENTS IN JOINTS

Assistant Commissioner of Patents  
Washington, D C 20231

EXPRESS MAIL CERTIFICATE

Express Mail label number EE687588685US

Date of Deposit September 22, 1998

I hereby certify that the following attached paper or fee

TRANSMITTAL OF FORMAL DRAWINGS  
ELEVEN SHEETS OF FORMAL DRAWINGS  
COPY OF NOTICE OF ALLOWABILITY

is being deposited with the United States Postal Service Express Mail Post Office to Addressee service under 37 CFR 1 10 on the date indicated above and is addressed to the Assistant Commissioner of Patents Washington D C 20231

Beth H. Retort

(Typed or printed name of person mailing paper or fee)

(Signature of person mailing paper or fee)

NOTE Each paper must have its own certificate and the Express Mail' label number as a part thereof or attached thereto When as here the certification is presented on a separate sheet that sheet must (1) be signed and (2) fully identify and be securely attached to the paper or fee it accompanies Identification should include the serial number and filing date of the application as well as the type of paper being filed e g complete application specification and drawings responses to rejection or refusal notice of appeal etc If the serial number of the application is not known the identification should include at least the name of the inventor(s) and the title of the invention

NOTE The label number need not be placed in each page It should however be placed on the first page of each separate document, such as a new application, amendment assignment and transmittal letter for a fee along with the certificate of mailing by Express Mail Although the label number may be on checks such a practice is not required In order not to deface formal drawings it is suggested that the label number be placed on the back of each formal drawing or the drawings be accompanied by a set of informal drawings on which the label number is placed

(Express Mail Certificate [8 3])

PI-51495 01

CLASS	OP	PK
REF	CLASS	SUBCLASS

5880976

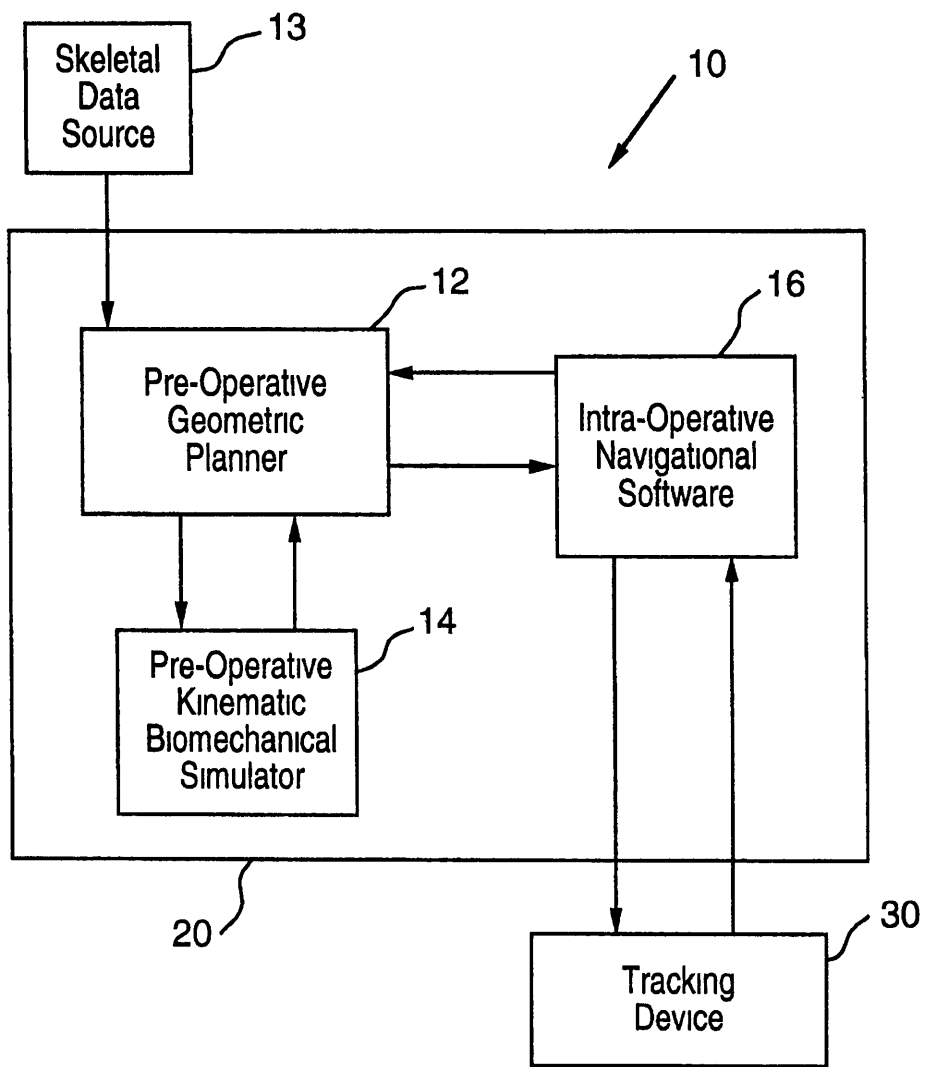


FIG. 1

APPROVED	DATE	BY	REVISION
	08/13		
DRAFTED			

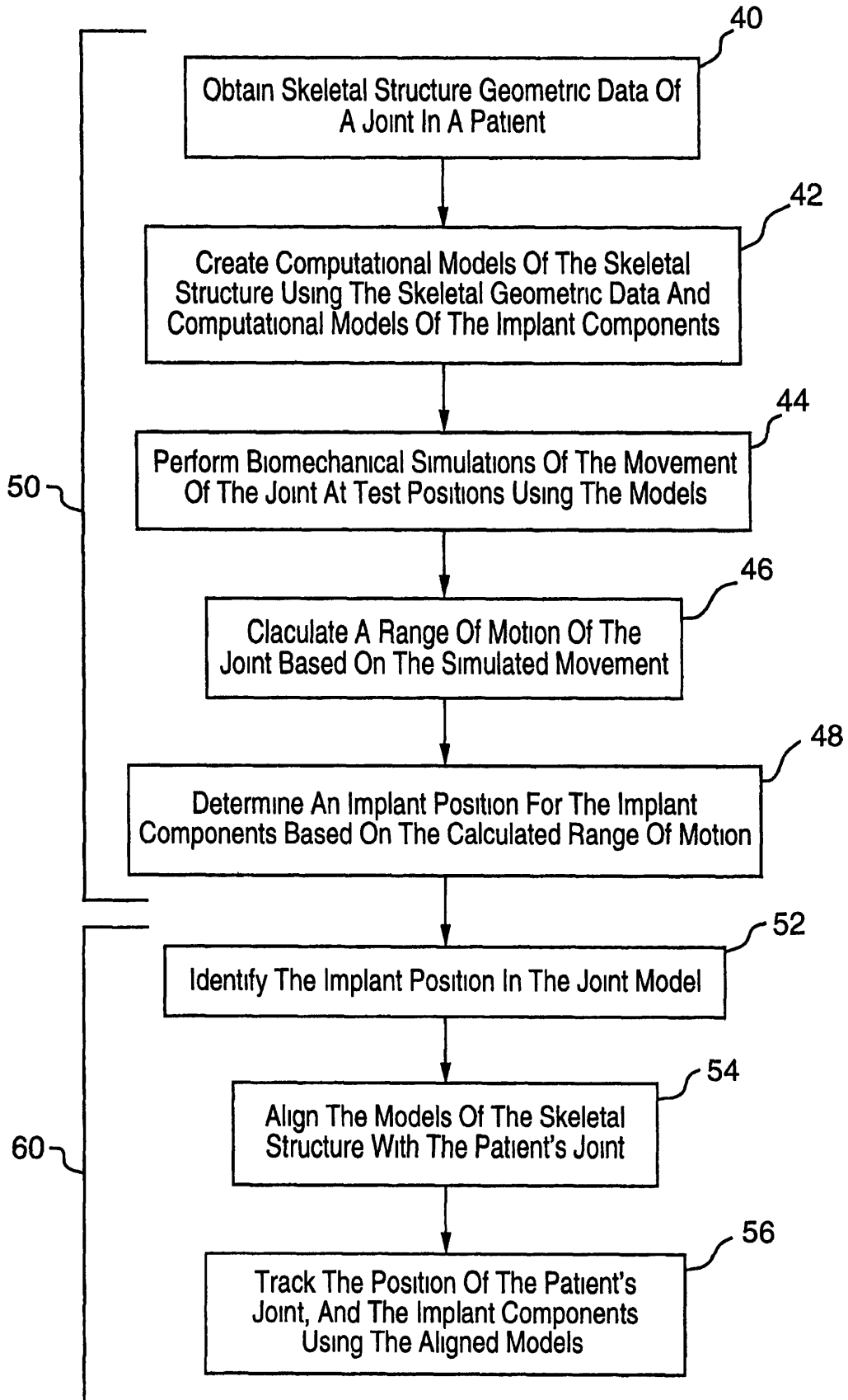


FIG. 2

APPROVED	O. H.	
BY	CLASS	SUBCLASS
DRAWN BY		

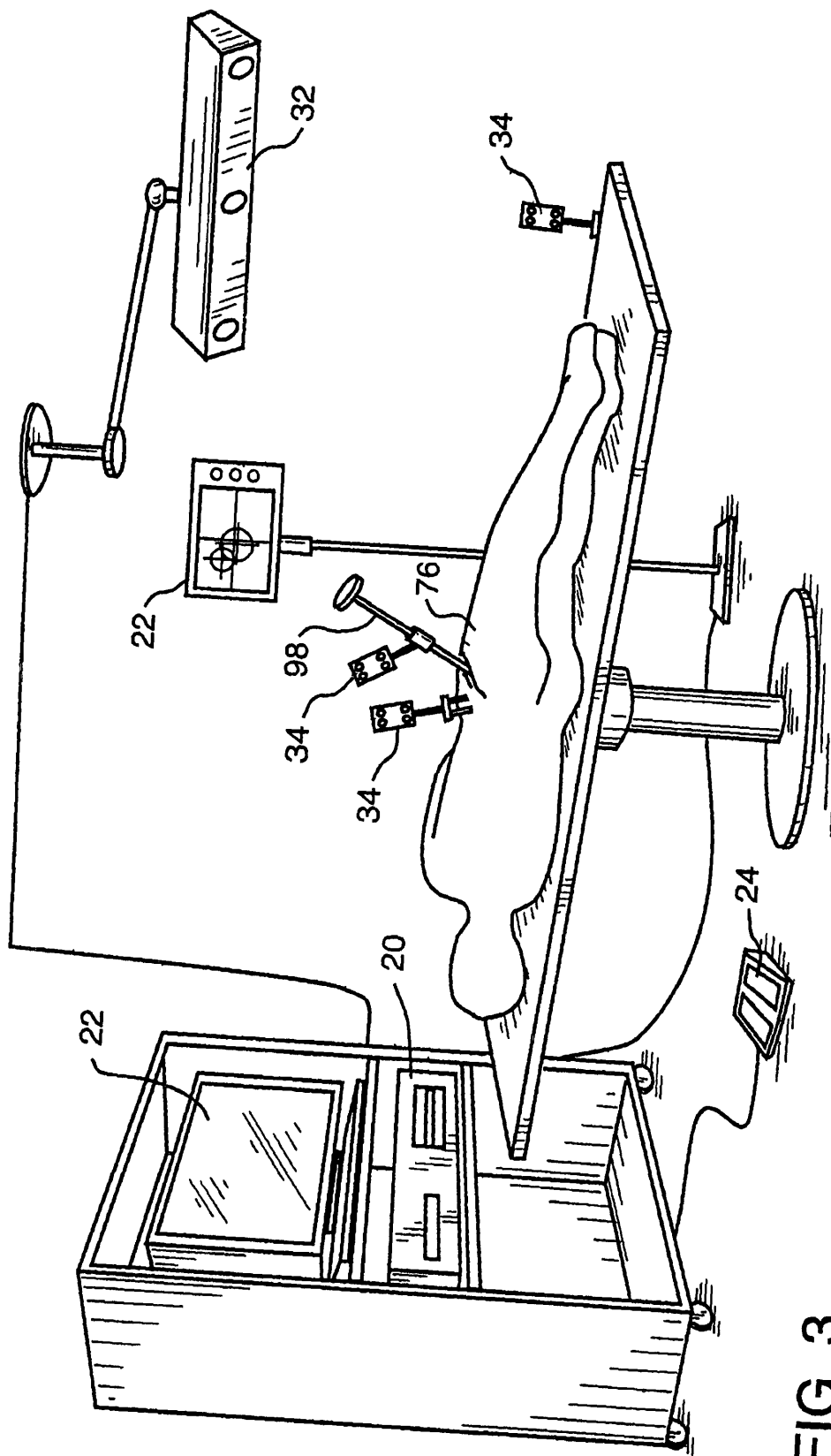


FIG. 3

DATE	FILE
BY	CLASS (SUBCLASS)
CHARACTER	

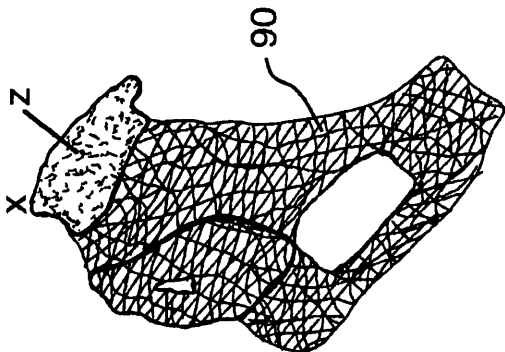


FIG. 4C

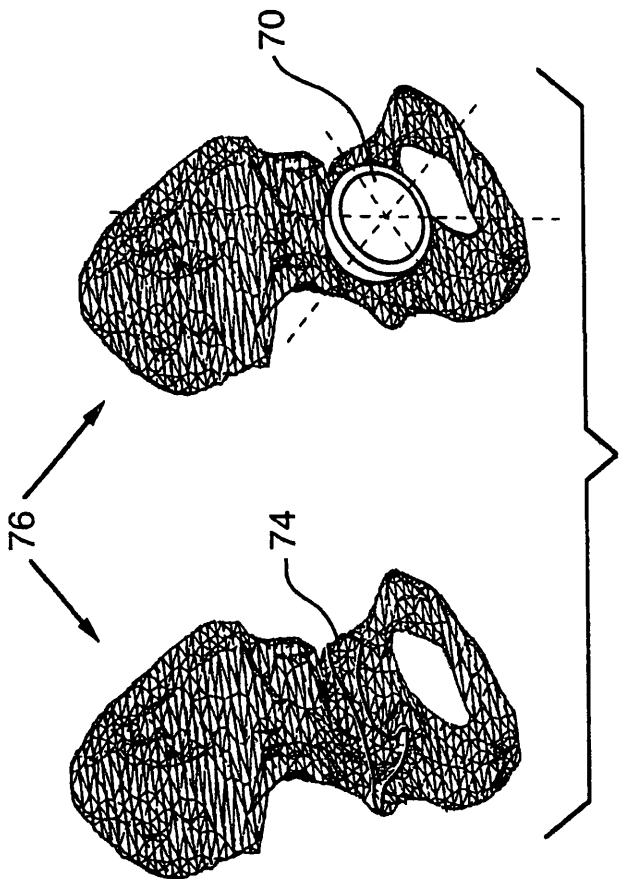


FIG. 4b

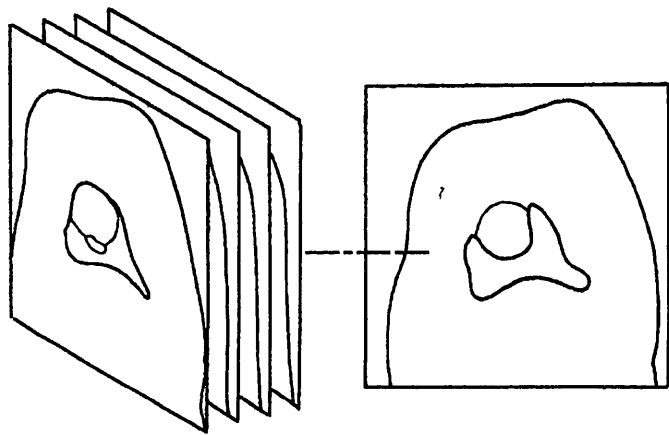


FIG 4a

APPROVED	OFFICE	FIG.
BY	CLASS	SUBCLASS
DATE		

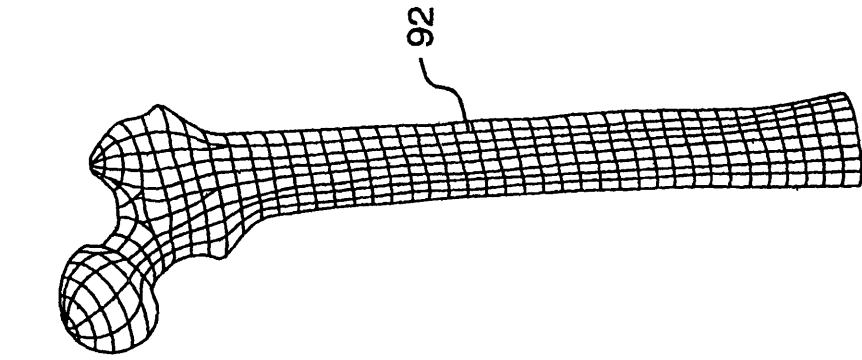


FIG. 5c

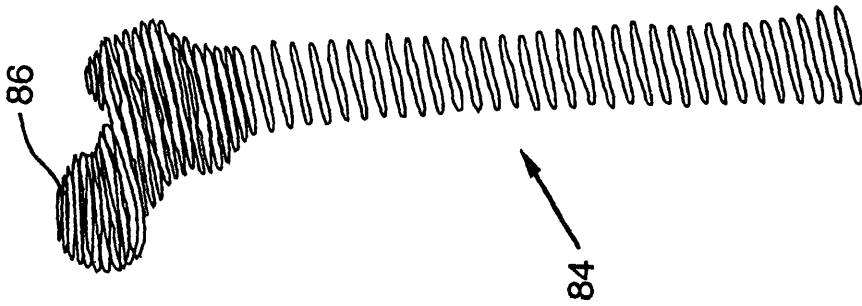


FIG. 5b

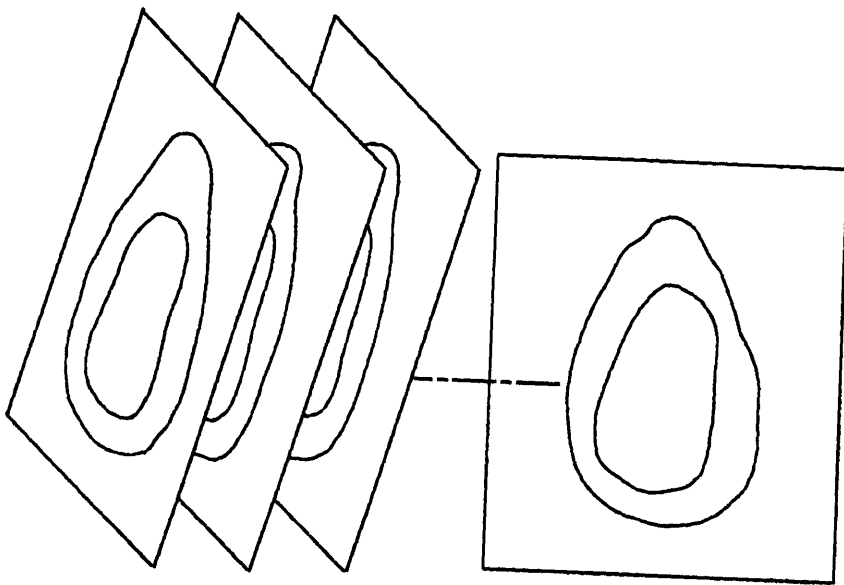


FIG. 5a

APPROVED	OG 111	
BY	CLASS	SUBCLASS
DRAFTSMAN		

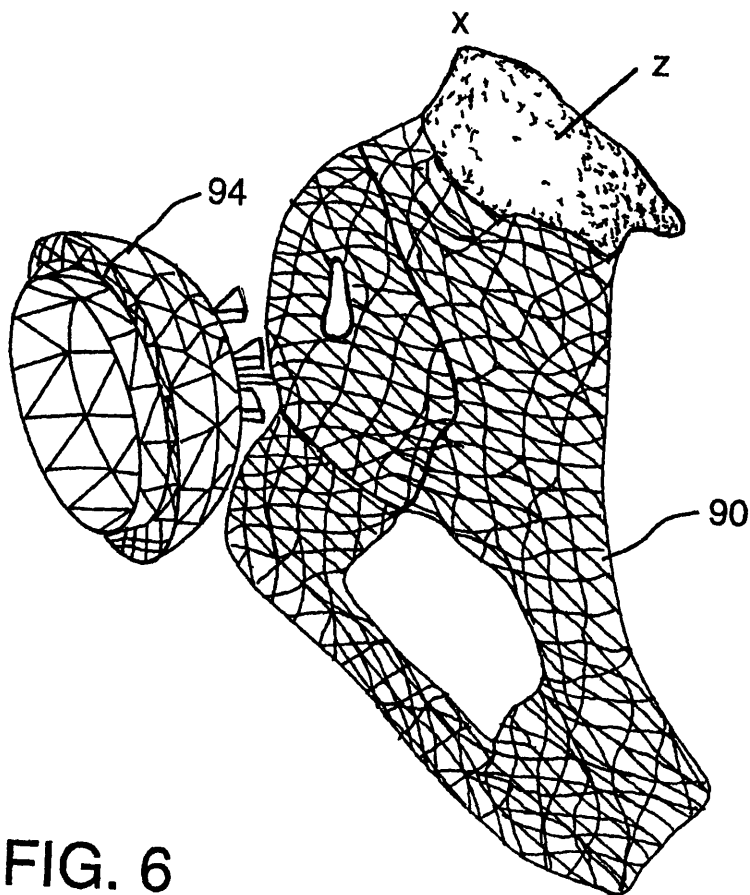


FIG. 6





APPROVED BY	CLASSIFIED	DATE
BY	CLASS	UNCLASS
DATE		

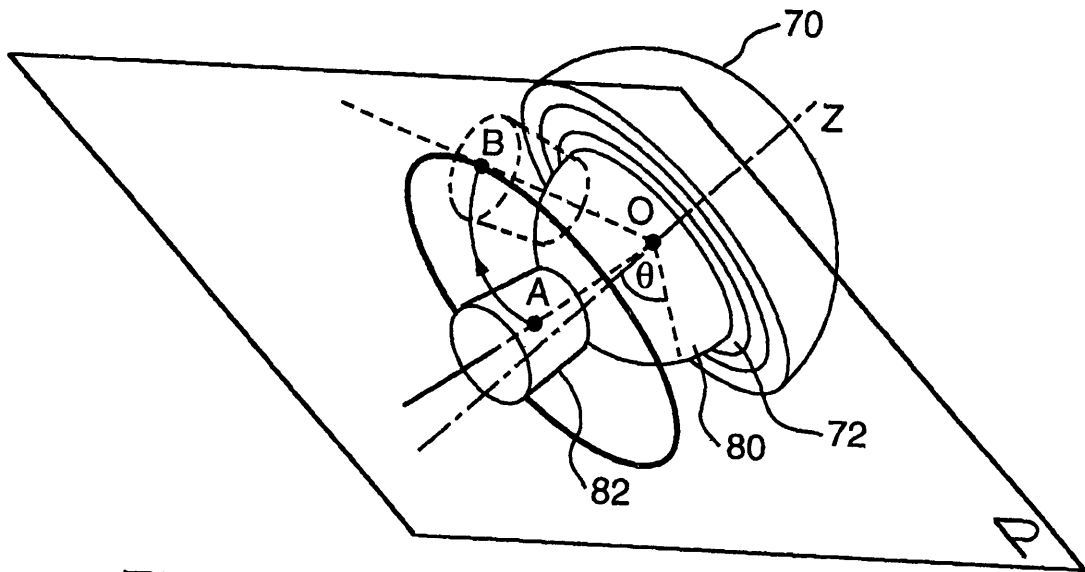


FIG. 8

APPROVED	O. P. J.	
BY	CLAS.	SUBCLASS
DRAFTS' AN		

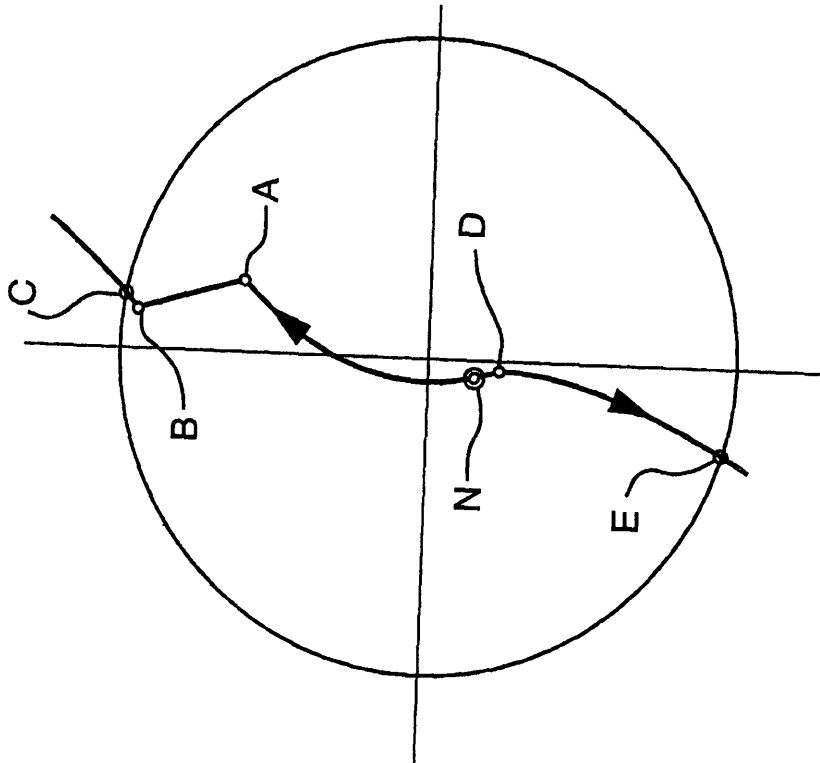


FIG 9a

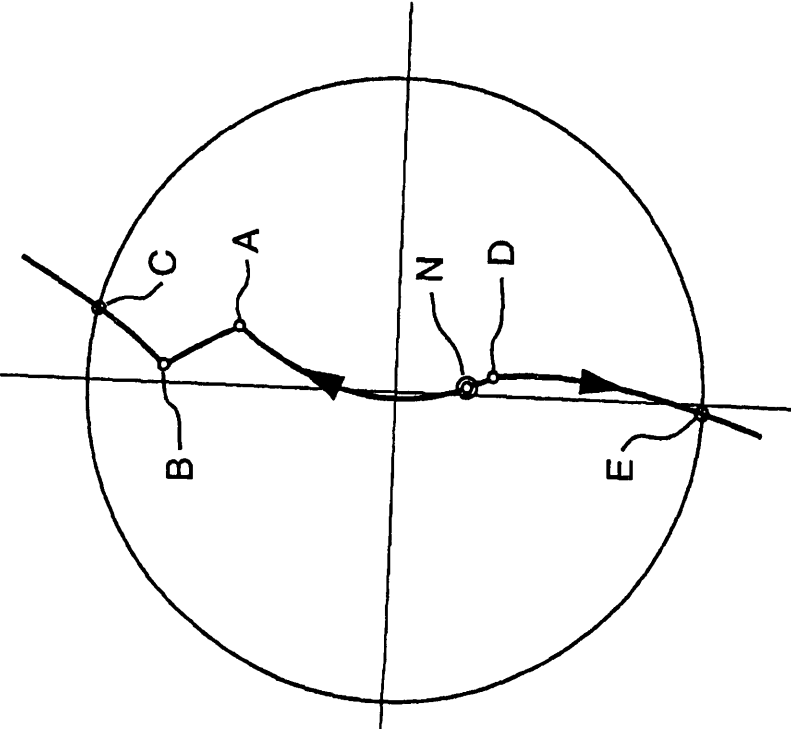


FIG. 9b

APR 11 1971	BY	ALIES	SUBCLASS
DR 11/1/71			

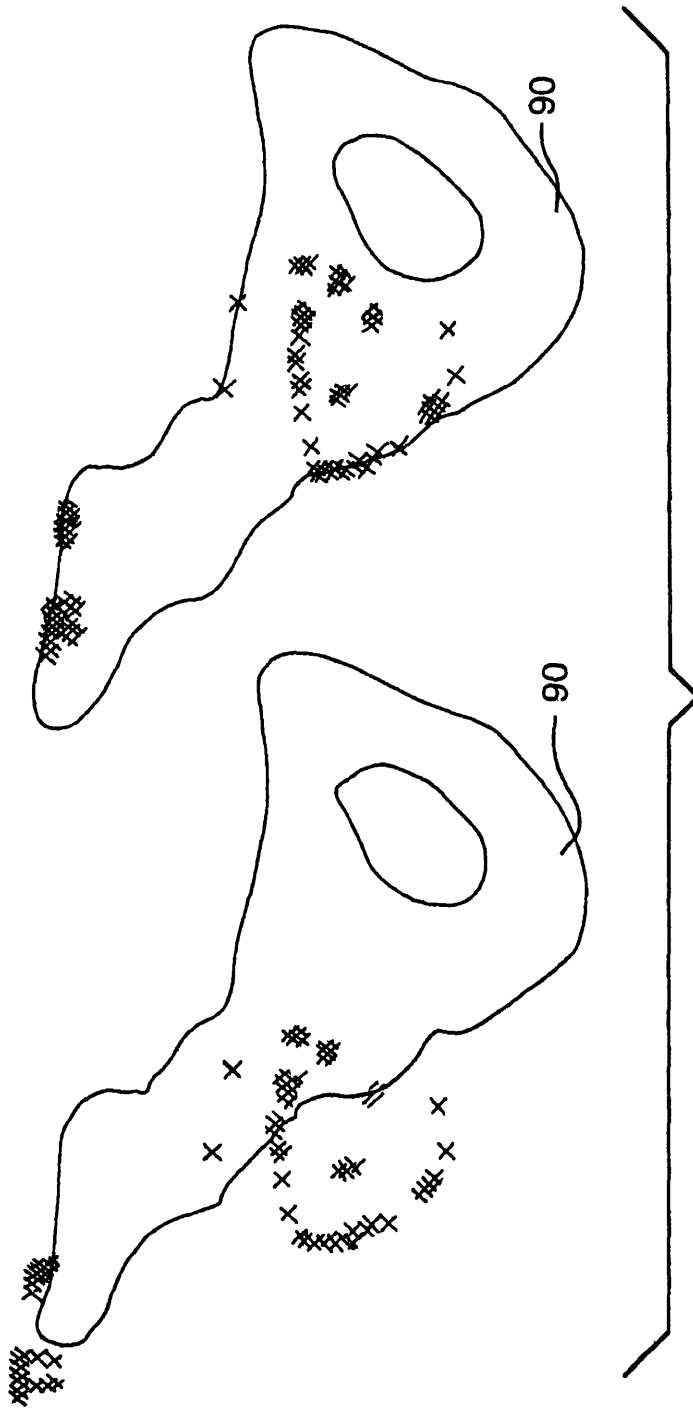


FIG. 10a

DATE	TIME	BY	REMARKS

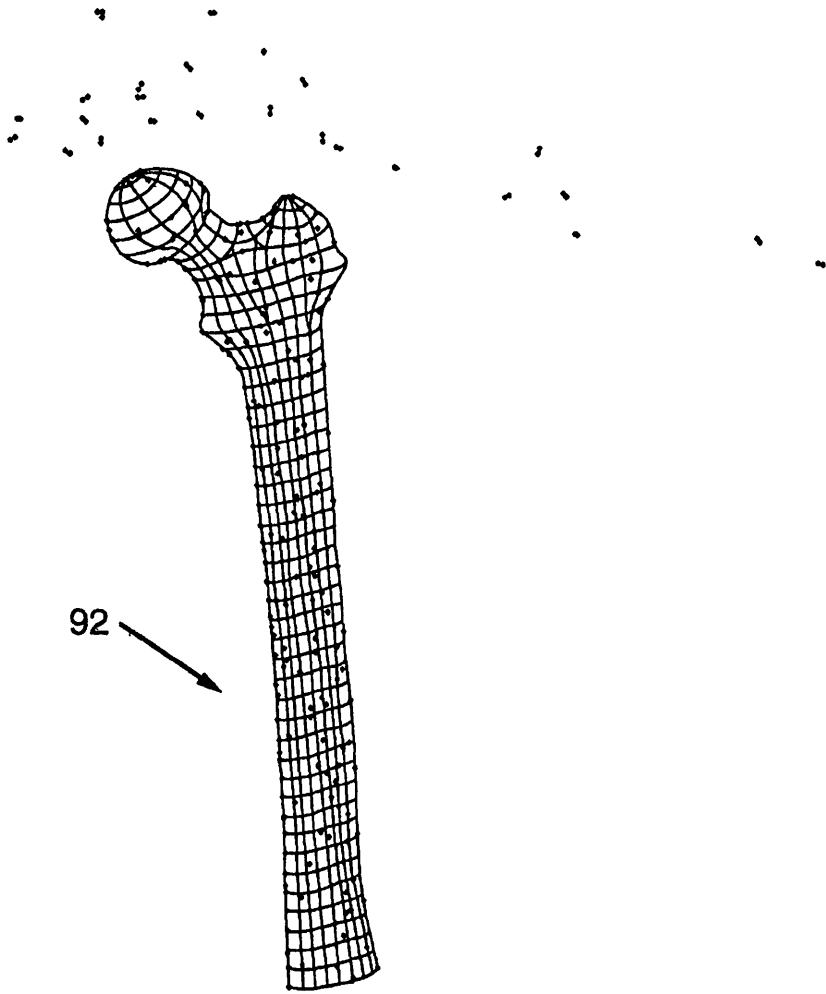


FIG. 10b

Transaction History Date 1999-03-09  
Date information retrieved from USPTO Patent  
Application Information Retrieval (PAIR)  
system records at [www.uspto.gov](http://www.uspto.gov)

PTO UTILITY GRANT

Paper Number 9

The  
United  
States  
of  
America



**The Commissioner of Patents  
and Trademarks**

*Has received an application for a patent for a new and useful invention. The title and description of the invention are enclosed. The requirements of law have been complied with, and it has been determined that a patent on the invention shall be granted under the law.*

*Therefore, this*

**United States Patent**

*Grants to the person(s) having title to this patent the right to exclude others from making, using, offering for sale, or selling the invention throughout the United States of America or importing the invention into the United States of America for the term set forth below, subject to the payment of maintenance fees as provided by law.*

*If this application was filed prior to June 8, 1995, the term of this patent is the longer of seventeen years from the date of grant of this patent or twenty years from the earliest effective US filing date of the application, subject to any statutory extension.*

*If this application was filed on or after June 8, 1995, the term of this patent is twenty years from the US filing date, subject to a statutory extension. If the application contains a specific reference to an earlier filed application or applications under 35 U.S.C. 120, 121 or 365(c), the term of the patent is twenty years from the date on which the earliest application was filed, subject to any statutory extension.*

*Bruce Lehman*  
Commissioner of Patents and Trademarks

*Starna Cooper*  
Attest

# File History Content Report

The following content is missing from the original file history record obtained from the United States Patent and Trademark Office. No additional information is available.

Document Date - 1999-10-07

Document Title - Applicant Communication Re Small Entity Statement

**PATENT APPLICATION FEE DETERMINATION RECORD**  
Effective October 1, 1996

Application or Docket Number

**CLAIMS AS FILED - PART I**

(Column 1) (Column 2)

**SMALL ENTITY** OR

**OTHER THAN SMALL ENTITY**

FOR	NUMBER FILED	NUMBER EXTRA
BASIC FEE		
TOTAL CLAIMS	minus 20 =	*
INDEPENDENT CLAIMS	minus 3 =	*
MULTIPLE DEPENDENT CLAIM PRESENT		

RATE	FEE
	385 00
x\$11=	
x40=	
+130=	
TOTAL	

RATE	FEE
	770 00
x\$22=	
x80=	
+260=	
TOTAL	

\* If the difference in column 1 is less than zero enter 0 in column 2

**CLAIMS AS AMENDED - PART II**

(Column 1) (Column 2) (Column 3)

**SMALL ENTITY** OR

**OTHER THAN SMALL ENTITY**

AMENDMENT A	CLAIMS REMAINING AFTER AMENDMENT		HIGHEST NUMBER PREVIOUSLY PAID FOR	PRESENT EXTRA
	Total	*	Minus	**
Independent	*	Minus	***	=
FIRST PRESENTATION OF MULTIPLE DEPENDENT CLAIM				

RATE	ADDITIONAL FEE
x\$11=	
x40=	
+130=	
TOTAL ADDIT FEE	

RATE	ADDITIONAL FEE
x\$22=	
x80=	
+260=	
TOTAL ADDIT FEE	

(Column 1) (Column 2) (Column 3)

AMENDMENT B	CLAIMS REMAINING AFTER AMENDMENT		HIGHEST NUMBER PREVIOUSLY PAID FOR	PRESENT EXTRA
	Total	*	Minus	**
Independent	*	Minus	***	=
FIRST PRESENTATION OF MULTIPLE DEPENDENT CLAIM				

RATE	ADDITIONAL FEE
x\$11=	
x40=	
+130=	
TOTAL ADDIT FEE	

RATE	ADDITIONAL FEE
x\$22=	
x80=	
+260=	
TOTAL ADDIT FEE	

(Column 1) (Column 2) (Column 3)

AMENDMENT C	CLAIMS REMAINING AFTER AMENDMENT		HIGHEST NUMBER PREVIOUSLY PAID FOR	PRESENT EXTRA
	Total	*	Minus	**
Independent	*	Minus	***	=
FIRST PRESENTATION OF MULTIPLE DEPENDENT CLAIM				

RATE	ADDITIONAL FEE
x\$11=	
x40=	
+130=	
TOTAL ADDIT FEE	

RATE	ADDITIONAL FEE
x\$22=	
x80=	
+260=	
TOTAL ADDIT FEE	

\*\* If the entry in column 1 is less than the entry in column 2 write 0 in column 3  
 \*\*\* If the "Highest Number Previously Paid For" IN THIS SPACE is less than 20 enter "20"  
 \*\*\*\* If the "Highest Number Previously Paid For" IN THIS SPACE is less than 3 enter "3"  
 The Highest Number Previously Paid For" (Total or Independent) is the highest number found in the appropriate box in column 1





Table of Contents

---

1. US5880976A Apparatus and method for facilitating the implantation of artificial components in joints
-

**Family 1/1**

**4 record(s) per family**

**Record 1/4** US5880976A Apparatus and method for facilitating the implantation of artificial components in joints

**Publication Number:** US5880976A 19990309

**Title:** Apparatus and method for facilitating the implantation of artificial components in joints

**Title - DWPI:** Computer based artificial component implant position determining system for total hip replacement

**Priority Number:** US1997803993A

**Priority Date:** 1997-02-21

**Application Number:** US1997803993A

**Application Date:** 1997-02-21

**Publication Date:** 1999-03-09

**IPC Class Table:**

IPC	Section	Class	Subclass	Class Group	Subgroup
A61B001715	A	A61	A61B	A61B0017	A61B001715
A61F000246	A	A61	A61F	A61F0002	A61F000246
A61B000506	A	A61	A61B	A61B0005	A61B000506
A61B0005107	A	A61	A61B	A61B0005	A61B0005107
A61B001700	A	A61	A61B	A61B0017	A61B001700
A61B001900	A	A61	A61B	A61B0019	A61B001900
A61F000230	A	A61	A61F	A61F0002	A61F000230
A61F000232	A	A61	A61F	A61F0002	A61F000232
A61F000234	A	A61	A61F	A61F0002	A61F000234
A61F000236	A	A61	A61F	A61F0002	A61F000236
A61F000238	A	A61	A61F	A61F0002	A61F000238
A61F000240	A	A61	A61F	A61F0002	A61F000240
A61F000242	A	A61	A61F	A61F0002	A61F000242

**IPC Class Table - DWPI:**

IPC - DWPI	Section - DWPI	Class - DWPI	Subclass - DWPI	Class Group - DWPI	Subgroup - DWPI
A61B001714	A	A61	A61B	A61B0017	A61B001714
A61F000246	A	A61	A61F	A61F0002	A61F000246
A61B001715	A	A61	A61B	A61B0017	A61B001715
A61B001700	A	A61	A61B	A61B0017	A61B001700
A61B001900	A	A61	A61B	A61B0019	A61B001900
A61B000506	A	A61	A61B	A61B0005	A61B000506
A61B0005107	A	A61	A61B	A61B0005	A61B0005107
A61F000230	A	A61	A61F	A61F0002	A61F000230
A61F000232	A	A61	A61F	A61F0002	A61F000232
A61F000236	A	A61	A61F	A61F0002	A61F000236
A61F000238	A	A61	A61F	A61F0002	A61F000238
A61F000242	A	A61	A61F	A61F0002	A61F000242
A61F000234	A	A61	A61F	A61F0002	A61F000234
A61F000240	A	A61	A61F	A61F0002	A61F000240

**Assignee/Applicant:** Carnegie Mellon University,Pittsburgh,PA,US

**JP F Terms:**

**JP FI Codes:**

**Assignee - Original:** Carnegie Mellon University

**Any CPC Table:**

Type	Invention	Additional	Version	Office
Current	<b>A61B 19/5244</b>	A61B 5/06	20130101	EP
Current	A61B 17/15	A61B 5/1075	20130101	EP
Current	A61B 17/155	A61B 5/4528	20130101	EP
Current	A61F 2/46	A61B 19/50	20130101	EP
Current	A61F 2/4657	A61B 2017/00716	20130101	EP
Current		A61B 2019/502	20130101	EP
Current		A61B 2019/505	20130101	EP
Current		A61B 2019/507	20130101	EP
Current		A61B 2019/5255	20130101	EP
Current		A61B 2019/5272	20130101	EP
Current		A61B 2019/5276	20130101	EP

Current		A61B 2019/564	20130101	EP
Current		A61F 2/32	20130101	EP
Current		A61F 2/34	20130101	EP
Current		A61F 2/36	20130101	EP
Current		A61F 2/38	20130101	EP
Current		A61F 2/3804	20130101	EP
Current		A61F 2/40	20130101	EP
Current		A61F 2/4202	20130101	EP
Current		A61F 2/4225	20130101	EP
Current		A61F 2/4241	20130101	EP
Current		A61F 2/4261	20130101	EP
Current		A61F 2/468	20130101	EP
Current		A61F 2002/30945	20130101	EP
Current		A61F 2002/30948	20130101	EP
Current		A61F 2002/30952	20130101	EP
Current		A61F 2002/3611	20130101	EP
Current		A61F 2002/3625	20130101	EP
Current		A61F 2002/3631	20130101	EP
Current		A61F 2002/4633	20130101	EP
Current		A61F 2002/4668	20130101	EP
Current		G05B 2219/45166	20130101	EP
Current		G05B 2219/45168	20130101	EP
Current		Y10S 623/914	20130101	EP

**ECLA:** A61B001715 | A61B001715K2 | A61B001952H12 | A61F000246 | A61F000246M | K61B000506 | K61B0005107H | K61B001700Q6P | K61B001950 | K61B001950B2 | K61B001950B4 | K61B001950D | K61B001952H12B6 | K61B001952H12F | K61B001952H14 | K61B001956D | K61F000230M2A2 | K61F000230M2B | K61F000230M2C | K61F000232 | K61F000234 | K61F000236 | K61F000236C1 | K61F000236C2 | K61F000236C2G | K61F000238 | K61F000238B | K61F000240 | K61F000242A | K61F000242F | K61F000242H | K61F000242W | K61F000246D2 | K61F000246M6 | K61F000246R | S05B021945166 | S05B021945168 | K61B000545K

**Abstract:**

Apparatuses and methods are disclosed for determining an implant position for at least one artificial component in a joint and facilitating the implantation thereof. The apparatuses and methods include creating a joint model of a patient's joint into which an artificial component is to be implanted and creating a component model of the artificial component. The joint and artificial component models are used to simulate movement in the patient's joint with the artificial component in a test position. The component model and the joint model are used to calculate a range of motion in the joint for at least one test position based on the simulated motion. An implant position, including angular orientation, in the patient's joint is determined based on a predetermined range of motion and the calculated range of motion. In a preferred embodiment, the implant position can be identified in the joint model and the joint model aligned with the joint by

registering positional data from discrete points on the joint with the joint model. Such registration also allows for tracking of the joint during surgical procedures. A current preferred application of the invention is for determining the implant position and sizing of an acetabular cup and femoral implant for use in total hip replacement surgery.

**Language of Publication:** EN

**INPADOC Legal Status Table:**

Gazette Date	Code	INPADOC Legal Status Impact
2010-09-09	FPAY	+
Description: FEE PAYMENT		
2006-09-11	FPAY	+
Description: FEE PAYMENT		
2002-09-25	REMI	-
Description: MAINTENANCE FEE REMINDER MAILED		
2002-09-06	FPAY	+
Description: FEE PAYMENT		
1997-08-06	AS	-
Description: ASSIGNMENT CARNEGIE MELLON UNIVERSITY, PENNSYLVANIA ASSIGNMENT OF ASSIGNORS INTEREST; ASSIGNORS: DIGIOIA, ANTHONY M., III; SIMON, DAVID A.; JARAMAZ, BRANISLAV; AND OTHERS; REEL/FRAME: 008642/0243 1997-07-17		
1997-08-06	AS	-
Description: ASSIGNMENT SHADYSIDE HOSPITAL, PENNSYLVANIA ASSIGNMENT OF ASSIGNORS INTEREST; ASSIGNORS: DIGIOIA, ANTHONY M., III; SIMON, DAVID A.; JARAMAZ, BRANISLAV; AND OTHERS; REEL/FRAME: 008642/0243 1997-07-17		

**Post-Issuance (US):**

**Reassignment (US) Table:**

Assignee	Assignor	Date Signed	Reel/Frame	Date
CARNEGIE MELLON UNIVERSITY, PITTSBURGH, PA, US	DIGIOIA, ANTHONY M., III	1997-07-17	008642/0243	1997-08-06

SHADYSIDE  
HOSPITAL, PITTSBURGH, PA  
, US

Conveyance: ASSIGNMENT OF ASSIGNORS INTEREST (SEE DOCUMENT FOR DETAILS). | ASSIGNMENT OF  
ASSIGNORS INTEREST (SEE DOCUMENT FOR DETAILS).

Corresponent: KIRKPATRICK & LOCKHART LLP MICHAEL C. ANTONE, ESQ. 1500 OLIVER BUILDING PITTSBURGH, PA  
15222 | KIRKPATRICK & LOCKHART LLP MICHAEL C. ANTONE, ESQ. 1500 OLIVER BUILDING PITTSBURGH, PA 15222

Maintenance Status (US):

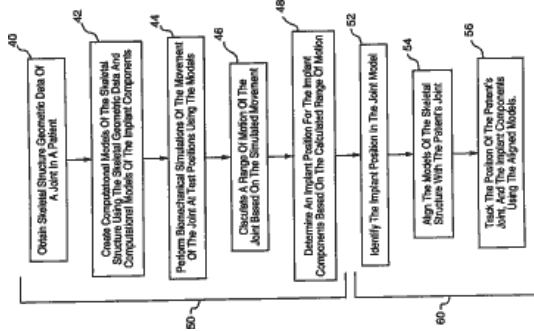
Litigation (US):

Opposition (EP):

License (EP):

EPO Procedural Status:

Front Page Drawing:



**Record 2/4** US5995738A Apparatus and method for facilitating the implantation of artificial components in joints

**Publication Number:** US5995738A 19991130

**Title:** Apparatus and method for facilitating the implantation of artificial components in joints

**Title - DWPI:** Computer assistant artificial component implant position determining system during total hip replacement, arthroplasty operations

**Priority Number:** US1997803993A

**Priority Date:** 1997-02-21

**Application Number:** US1998190740A

**Application Date:** 1998-11-12

**Publication Date:** 1999-11-30

**IPC Class Table:**

IPC	Section	Class	Subclass	Class Group	Subgroup
A61B001715	A	A61	A61B	A61B0017	A61B001715
A61F000246	A	A61	A61F	A61F0002	A61F000246
A61B000506	A	A61	A61B	A61B0005	A61B000506
A61B0005107	A	A61	A61B	A61B0005	A61B0005107
A61B001700	A	A61	A61B	A61B0017	A61B001700
A61B001900	A	A61	A61B	A61B0019	A61B001900
A61F000230	A	A61	A61F	A61F0002	A61F000230
A61F000232	A	A61	A61F	A61F0002	A61F000232
A61F000234	A	A61	A61F	A61F0002	A61F000234
A61F000236	A	A61	A61F	A61F0002	A61F000236
A61F000238	A	A61	A61F	A61F0002	A61F000238
A61F000240	A	A61	A61F	A61F0002	A61F000240
A61F000242	A	A61	A61F	A61F0002	A61F000242

**IPC Class Table - DWPI:**

IPC - DWPI	Section - DWPI	Class - DWPI	Subclass - DWPI	Class Group - DWPI	Subgroup - DWPI
A61B001714	A	A61	A61B	A61B0017	A61B001714
A61F000246	A	A61	A61F	A61F0002	A61F000246
A61B001715	A	A61	A61B	A61B0017	A61B001715

A61B001700	A	A61	A61B	A61B0017	A61B001700
A61B001900	A	A61	A61B	A61B0019	A61B001900
A61B000506	A	A61	A61B	A61B0005	A61B000506
A61B0005107	A	A61	A61B	A61B0005	A61B0005107
A61F000230	A	A61	A61F	A61F0002	A61F000230
A61F000232	A	A61	A61F	A61F0002	A61F000232
A61F000236	A	A61	A61F	A61F0002	A61F000236
A61F000238	A	A61	A61F	A61F0002	A61F000238
A61F000242	A	A61	A61F	A61F0002	A61F000242
A61F000234	A	A61	A61F	A61F0002	A61F000234
A61F000240	A	A61	A61F	A61F0002	A61F000240

**Assignee/Applicant:** Carnegie Mellon University,Pittsburgh,PA,US

**JP F Terms:**

**JP FI Codes:**

**Assignee - Original:** Carnegie Mellon University

**Any CPC Table:**

Type	Invention	Additional	Version	Office
Current	<b>A61B 19/5244</b>	A61B 5/06	20130101	EP
Current	A61B 17/15	A61B 5/1075	20130101	EP
Current	A61B 17/155	A61B 5/4528	20130101	EP
Current	A61F 2/46	A61B 19/50	20130101	EP
Current	A61F 2/4657	A61B 2017/00716	20130101	EP
Current		A61B 2019/502	20130101	EP
Current		A61B 2019/505	20130101	EP
Current		A61B 2019/507	20130101	EP
Current		A61B 2019/5255	20130101	EP
Current		A61B 2019/5272	20130101	EP
Current		A61B 2019/5276	20130101	EP
Current		A61B 2019/564	20130101	EP
Current		A61F 2/32	20130101	EP
Current		A61F 2/34	20130101	EP
Current		A61F 2/36	20130101	EP
Current		A61F 2/38	20130101	EP
Current		A61F 2/3804	20130101	EP
Current		A61F 2/40	20130101	EP
Current		A61F 2/4202	20130101	EP
Current		A61F 2/4225	20130101	EP
Current		A61F 2/4241	20130101	EP
Current		A61F 2/4261	20130101	EP
Current		A61F 2/468	20130101	EP
Current		A61F 2002/30945	20130101	EP
Current		A61F 2002/30948	20130101	EP



Current		A61F 2002/30952	20130101	EP
Current		A61F 2002/3611	20130101	EP
Current		A61F 2002/3625	20130101	EP
Current		A61F 2002/3631	20130101	EP
Current		A61F 2002/4633	20130101	EP
Current		A61F 2002/4668	20130101	EP
Current		G05B 2219/45166	20130101	EP
Current		G05B 2219/45168	20130101	EP
Current		Y10S 623/914	20130101	EP

**ECLA:** A61B001715 | A61B001715K2 | A61B001952H12 | A61F000246 | A61F000246M | K61B000506 | K61B0005107H | K61B001700Q6P | K61B001950 | K61B001950B2 | K61B001950B4 | K61B001950D | K61B001952H12B6 | K61B001952H12F | K61B001952H14 | K61B001956D | K61F000230M2A2 | K61F000230M2B | K61F000230M2C | K61F000232 | K61F000234 | K61F000236 | K61F000236C1 | K61F000236C2 | K61F000236C2G | K61F000238 | K61F000238B | K61F000240 | K61F000242A | K61F000242F | K61F000242H | K61F000242W | K61F000246D2 | K61F000246M6 | K61F000246R | S05B021945166 | S05B021945168 | K61B000545K

**Abstract:**

Apparatuses and methods are disclosed for determining an implant position for at least one artificial component in a joint and facilitating the implantation thereof. The apparatuses and methods include creating a joint model of a patient's joint into which an artificial component is to be implanted and creating a component model of the artificial component. The joint and artificial component models are used to simulate movement in the patient's joint with the artificial component in a test position. The component model and the joint model are used to calculate a range of motion in the joint for at least one test position based on the simulated motion. An implant position, including angular orientation, in the patient's joint is determined based on a predetermined range of motion and the calculated range of motion. In a preferred embodiment, the implant position can be identified in the joint model and the joint model aligned with the joint by registering positional data from discrete points on the joint with the joint model. Such registration also allows for tracking of the joint during surgical procedures. A current preferred application of the invention is for determining the implant position and sizing of an acetabular cup and femoral implant for use in total hip replacement surgery.

**Language of Publication:** EN

**INPADOC Legal Status Table:**

Gazette Date	Code	INPADOC Legal Status Impact
2008-01-22	FP	-
Description: EXPIRED DUE TO FAILURE TO PAY MAINTENANCE FEE 2007-11-30		
2007-11-30	LAPS	-
Description: LAPSE FOR FAILURE TO PAY MAINTENANCE FEES		
2007-06-18	REMI	-

Description: MAINTENANCE FEE REMINDER MAILED		
2003-05-29	FPAY	+
Description: FEE PAYMENT		

Post-Issuance (US): EXPI Expiration 2007-11-30 2007 2008-01-22 2008 DUE TO FAILURE TO PAY MAINTENANCE FEES

Reassignment (US) Table:

Maintenance Status (US): E2

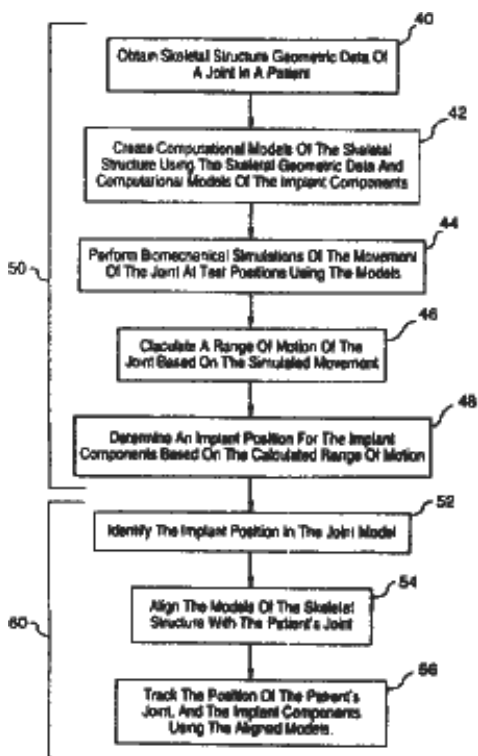
Litigation (US):

Opposition (EP):

License (EP):

EPO Procedural Status:

Front Page Drawing:



**Record 3/4** US6002859A Apparatus and method for facilitating the implantation of artificial components in joints | Apparatus and method facilitating the implantation of artificial components in joints

**Publication Number:** US6002859A 19991214

**Title:** Apparatus and method for facilitating the implantation of artificial components in joints | Apparatus and method facilitating the implantation of artificial components in joints

**Title - DWPI:** Computer assisted surgical implantation facilitating apparatus for artificial acetabular, femoral components during total hip replacement and revision procedures

**Priority Number:** US1997803993A

**Priority Date:** 1997-02-21

**Application Number:** US1998190893A

**Application Date:** 1998-11-12

**Publication Date:** 1999-12-14

**IPC Class Table:**

IPC	Section	Class	Subclass	Class Group	Subgroup
A61B001715	A	A61	A61B	A61B0017	A61B001715
A61F000246	A	A61	A61F	A61F0002	A61F000246
A61B000506	A	A61	A61B	A61B0005	A61B000506
A61B0005107	A	A61	A61B	A61B0005	A61B0005107
A61B001700	A	A61	A61B	A61B0017	A61B001700
A61B001900	A	A61	A61B	A61B0019	A61B001900
A61F000230	A	A61	A61F	A61F0002	A61F000230
A61F000232	A	A61	A61F	A61F0002	A61F000232
A61F000234	A	A61	A61F	A61F0002	A61F000234
A61F000236	A	A61	A61F	A61F0002	A61F000236
A61F000238	A	A61	A61F	A61F0002	A61F000238
A61F000240	A	A61	A61F	A61F0002	A61F000240
A61F000242	A	A61	A61F	A61F0002	A61F000242

**IPC Class Table - DWPI:**

IPC - DWPI	Section - DWPI	Class - DWPI	Subclass - DWPI	Class Group - DWPI	Subgroup - DWPI
A61B001714	A	A61	A61B	A61B0017	A61B001714
A61F000246	A	A61	A61F	A61F0002	A61F000246

A61B001715	A	A61	A61B	A61B0017	A61B001715
A61B001700	A	A61	A61B	A61B0017	A61B001700
A61B001900	A	A61	A61B	A61B0019	A61B001900
A61B000506	A	A61	A61B	A61B0005	A61B000506
A61B0005107	A	A61	A61B	A61B0005	A61B0005107
A61F000230	A	A61	A61F	A61F0002	A61F000230
A61F000232	A	A61	A61F	A61F0002	A61F000232
A61F000236	A	A61	A61F	A61F0002	A61F000236
A61F000238	A	A61	A61F	A61F0002	A61F000238
A61F000242	A	A61	A61F	A61F0002	A61F000242
A61F000234	A	A61	A61F	A61F0002	A61F000234
A61F000240	A	A61	A61F	A61F0002	A61F000240

**Assignee/Applicant:** Carnegie Mellon University,Pittsburgh,PA,US

**JP F Terms:**

**JP FI Codes:**

**Assignee - Original:** Carnegie Mellon University

**Any CPC Table:**

Type	Invention	Additional	Version	Office
Current	<b>A61B 19/5244</b>	A61B 5/06	20130101	EP
Current	A61B 17/15	A61B 5/1075	20130101	EP
Current	A61B 17/155	A61B 5/4528	20130101	EP
Current	A61F 2/46	A61B 19/50	20130101	EP
Current	A61F 2/4657	A61B 2017/00716	20130101	EP
Current		A61B 2019/502	20130101	EP
Current		A61B 2019/505	20130101	EP
Current		A61B 2019/507	20130101	EP
Current		A61B 2019/5255	20130101	EP
Current		A61B 2019/5272	20130101	EP
Current		A61B 2019/5276	20130101	EP
Current		A61B 2019/564	20130101	EP
Current		A61F 2/32	20130101	EP
Current		A61F 2/34	20130101	EP
Current		A61F 2/36	20130101	EP
Current		A61F 2/38	20130101	EP
Current		A61F 2/3804	20130101	EP
Current		A61F 2/40	20130101	EP
Current		A61F 2/4202	20130101	EP
Current		A61F 2/4225	20130101	EP
Current		A61F 2/4241	20130101	EP
Current		A61F 2/4261	20130101	EP
Current		A61F 2/468	20130101	EP

Current		A61F 2002/30945	20130101	EP
Current		A61F 2002/30948	20130101	EP
Current		A61F 2002/30952	20130101	EP
Current		A61F 2002/3611	20130101	EP
Current		A61F 2002/3625	20130101	EP
Current		A61F 2002/3631	20130101	EP
Current		A61F 2002/4633	20130101	EP
Current		A61F 2002/4668	20130101	EP
Current		G05B 2219/45166	20130101	EP
Current		G05B 2219/45168	20130101	EP
Current		Y10S 623/914	20130101	EP

**ECLA:** A61B001715 | A61B001715K2 | A61B001952H12 | A61F000246 | A61F000246M | K61B000506 | K61B0005107H | K61B001700Q6P | K61B001950 | K61B001950B2 | K61B001950B4 | K61B001950D | K61B001952H12B6 | K61B001952H12F | K61B001952H14 | K61B001956D | K61F000230M2A2 | K61F000230M2B | K61F000230M2C | K61F000232 | K61F000234 | K61F000236 | K61F000236C1 | K61F000236C2 | K61F000236C2G | K61F000238 | K61F000238B | K61F000240 | K61F000242A | K61F000242F | K61F000242H | K61F000242W | K61F000246D2 | K61F000246M6 | K61F000246R | S05B021945166 | S05B021945168 | K61B000545K

**Abstract:**

Apparatuses and methods are disclosed for determining an implant position for at least one artificial component in a joint and facilitating the implantation thereof. The apparatuses and methods include creating a joint model of a patient's joint into which an artificial component is to be implanted and creating a component model of the artificial component. The joint and artificial component models are used to stimulate movement in the patient's joint with the artificial component in a test position. The component model and the joint model are used to calculate a range of motion in the joint for at least one test position based on the simulated motion. An implant position, including angular orientation, in the patient's joint is determined based on a predetermined range of motion and the calculated range of motion. In a preferred embodiment, the implant position can be identified in the joint model and the joint model aligned with the joint by registering positional data from discrete points on the joint with the joint model. Such registration also allows for tracking of the joint during surgical procedures. A current preferred application of the invention is for determining the implant position and sizing of an acetabular cup and femoral implant for use in total hip replacement surgery.

**Language of Publication:** EN

**INPADOC Legal Status Table:**

Gazette Date	Code	INPADOC Legal Status Impact
2008-02-05	FP	-
Description: EXPIRED DUE TO FAILURE TO PAY MAINTENANCE FEE 2007-12-14		
2007-12-14	LAPS	-
Description: LAPSE FOR FAILURE TO PAY MAINTENANCE FEES		

2007-06-27	REMI	-
Description: MAINTENANCE FEE REMINDER MAILED		
2003-06-16	FPAY	+
Description: FEE PAYMENT		
2002-04-02	CC	-
Description: CERTIFICATE OF CORRECTION		

**Post-Issuance (US):** CORR-CERT Certificate of Correction 2002-04-02 2002 2002-04-23 2002 a Certificate of Correction was issued for this patent | EXPI Expiration 2007-12-14 2007 2008-02-05 2008 DUE TO FAILURE TO PAY MAINTENANCE FEES

**Reassignment (US) Table:**

**Maintenance Status (US):** CC | E2

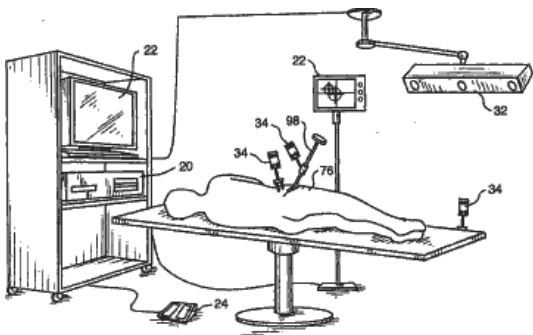
**Litigation (US):**

**Opposition (EP):**

**License (EP):**

**EPO Procedural Status:**

**Front Page Drawing:**



**Record 4/4 US6205411B1 Computer-assisted surgery planner and intra-operative guidance system**

**Publication Number:** US6205411B1 20010320

**Title:** Computer-assisted surgery planner and intra-operative guidance system

**Title - DWPI:** Computer assisted artificial joint component implantation guidance apparatus used in total hip replacement, has pre-operative kinematic biomechanical simulator to output position to implant artificial component

**Priority Number:** US1997803993A

**Priority Date:** 1997-02-21

**Application Number:** US1998189914A

**Application Date:** 1998-11-12

**Publication Date:** 2001-03-20

**IPC Class Table:**

IPC	Section	Class	Subclass	Class Group	Subgroup
A61B001715	A	A61	A61B	A61B0017	A61B001715
A61F000246	A	A61	A61F	A61F0002	A61F000246
A61B000506	A	A61	A61B	A61B0005	A61B000506
A61B0005107	A	A61	A61B	A61B0005	A61B0005107
A61B001700	A	A61	A61B	A61B0017	A61B001700
A61B001900	A	A61	A61B	A61B0019	A61B001900
A61F000230	A	A61	A61F	A61F0002	A61F000230
A61F000232	A	A61	A61F	A61F0002	A61F000232
A61F000234	A	A61	A61F	A61F0002	A61F000234
A61F000236	A	A61	A61F	A61F0002	A61F000236
A61F000238	A	A61	A61F	A61F0002	A61F000238
A61F000240	A	A61	A61F	A61F0002	A61F000240
A61F000242	A	A61	A61F	A61F0002	A61F000242

**IPC Class Table - DWPI:**

IPC - DWPI	Section - DWPI	Class - DWPI	Subclass - DWPI	Class Group - DWPI	Subgroup - DWPI
A61B001714	A	A61	A61B	A61B0017	A61B001714
A61F000246	A	A61	A61F	A61F0002	A61F000246

A61B001715	A	A61	A61B	A61B0017	A61B001715
A61B001700	A	A61	A61B	A61B0017	A61B001700
A61B001900	A	A61	A61B	A61B0019	A61B001900
A61B000506	A	A61	A61B	A61B0005	A61B000506
A61B0005107	A	A61	A61B	A61B0005	A61B0005107
A61F000230	A	A61	A61F	A61F0002	A61F000230
A61F000232	A	A61	A61F	A61F0002	A61F000232
A61F000236	A	A61	A61F	A61F0002	A61F000236
A61F000238	A	A61	A61F	A61F0002	A61F000238
A61F000242	A	A61	A61F	A61F0002	A61F000242
A61F000234	A	A61	A61F	A61F0002	A61F000234
A61F000240	A	A61	A61F	A61F0002	A61F000240

**Assignee/Applicant:** Carnegie Mellon University,Pittsburgh,PA

**JP F Terms:**

**JP FI Codes:**

**Assignee - Original:** Carnegie Mellon University

**Any CPC Table:**

Type	Invention	Additional	Version	Office
Current	<b>A61B 17/15</b>	A61B 5/06	20130101	EP
Current	A61B 17/155	A61B 5/1075	20130101	EP
Current	A61B 19/5244	A61B 5/4528	20130101	EP
Current	A61F 2/46	A61B 19/50	20130101	EP
Current	A61F 2/4657	A61B 2017/00716	20130101	EP
Current		A61B 2019/502	20130101	EP
Current		A61B 2019/505	20130101	EP
Current		A61B 2019/507	20130101	EP
Current		A61B 2019/5255	20130101	EP
Current		A61B 2019/5272	20130101	EP
Current		A61B 2019/5276	20130101	EP
Current		A61B 2019/564	20130101	EP
Current		A61F 2/32	20130101	EP
Current		A61F 2/34	20130101	EP
Current		A61F 2/36	20130101	EP
Current		A61F 2/38	20130101	EP
Current		A61F 2/3804	20130101	EP
Current		A61F 2/40	20130101	EP
Current		A61F 2/4202	20130101	EP
Current		A61F 2/4225	20130101	EP
Current		A61F 2/4241	20130101	EP
Current		A61F 2/4261	20130101	EP
Current		A61F 2/468	20130101	EP



Current		A61F 2002/30945	20130101	EP
Current		A61F 2002/30948	20130101	EP
Current		A61F 2002/30952	20130101	EP
Current		A61F 2002/3611	20130101	EP
Current		A61F 2002/3625	20130101	EP
Current		A61F 2002/3631	20130101	EP
Current		A61F 2002/4633	20130101	EP
Current		A61F 2002/4668	20130101	EP
Current		G05B 2219/45166	20130101	EP
Current		G05B 2219/45168	20130101	EP
Current		Y10S 623/901	20130101	EP

**ECLA:** A61B001715 | A61B001715K2 | A61B001952H12 | A61F000246 | A61F000246M | K61B000506 | K61B0005107H | K61B000545K | K61B001700Q6P | K61B001950 | K61B001950B2 | K61B001950B4 | K61B001950D | K61B001952H12B6 | K61B001952H12F | K61B001952H14 | K61B001956D | K61F000230M2A2 | K61F000230M2B | K61F000230M2C | K61F000232 | K61F000234 | K61F000236 | K61F000236C1 | K61F000236C2 | K61F000236C2G | K61F000238 | K61F000238B | K61F000240 | K61F000242A | K61F000242F | K61F000242H | K61F000242W | K61F000246D2 | K61F000246M6 | K61F000246R | S05B021945166 | S05B021945168

**Abstract:**

An apparatus for facilitating the implantation of an artificial component in one of a hip joint, a knee joint, a hand and wrist joint, an elbow joint, a shoulder joint, and a foot and ankle joint. The apparatus includes a pre-operative geometric planner and a pre-operative kinematic biomechanical simulator in communication with the pre-operative geometric planner.

**Language of Publication:** EN

**INPADOC Legal Status Table:**

Gazette Date	Code	INPADOC Legal Status Impact
2012-09-20	FPAY	+
Description: FEE PAYMENT		
2008-09-22	FPAY	+
Description: FEE PAYMENT		
2004-09-20	FPAY	+
Description: FEE PAYMENT		
1999-02-08	AS	-
Description: ASSIGNMENT CARNEGIE MELLON UNIVERSITY, PENNSYLVANIA ASSIGNMENT OF ASSIGNORS INTEREST; ASSIGNORS:DIGIOIA, ANTHONY M., III; SIMON, DAVID A.; JARAMAZ, BRANISLAV; AND OTHERS; REEL/FRAME:009747/0082 1999-01-31		

**Post-Issuance (US):  
Reassignment (US) Table:**

Assignee	Assignor	Date Signed	Reel/Frame	Date
CARNEGIE MELLON UNIVERSITY,PITTSBURGH, PA,US	DIGIOIA, ANTHONY M., III	1999-01-31	009747/0082	1999-02-08
	SIMON, DAVID A.	1999-01-31		
	JARAMAZ, BRANISLAV	1999-01-31		
	BLACKWELL, MICHAEL K.	1999-01-31		
	MORGAN, FREDERICK M.	1999-01-31		
	O'TOOLE, ROBERT V.	1999-01-31		
	KANADE, TAKEO	1999-01-31		
Conveyance: ASSIGNMENT OF ASSIGNORS INTEREST (SEE DOCUMENT FOR DETAILS).				
Correspondent: KIRKPATRICK & LOCKHART LLP JONATHAN C. PARKS 1500 OLIVER BUILDING PITTSBURGH, PA 15222				

**Maintenance Status (US):**

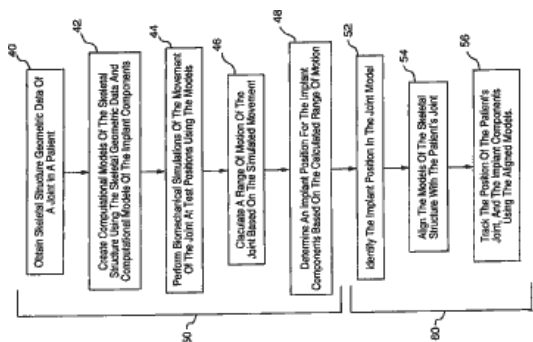
**Litigation (US):**

**Opposition (EP):**

**License (EP):**

**EPO Procedural Status:**

**Front Page Drawing:**



Copyright 2007-2014 THOMSON REUTERS

# USPTO Maintenance Report

Patent Bibliographic Data		09/03/2014 09:42 AM			
Patent Number:	5880976	Application Number:	08803993		
Issue Date:	03/09/1999	Filing Date:	02/21/1997		
Title:	APPARATUS AND METHOD FOR FACILITATING THE IMPLANTATION OF ARTIFICIAL COMPONENTS IN JOINTS				
Status:	4th, 8th and 12th year fees paid		Entity:	SMALL	
Window Opens:	N/A	Surcharge Date:	N/A	Expiration:	N/A
Fee Amt Due:	Window not open	Surchg Amt Due:	Window not open	Total Amt Due:	Window not open
Fee Code:					
Surcharge Fee Code:					
Most recent events (up to 7):	09/09/2010 09/11/2006 09/25/2002 09/06/2002	Payment of Maintenance Fee, 12th Yr, Small Entity. Payment of Maintenance Fee, 8th Yr, Small Entity. Maintenance Fee Reminder Mailed. Payment of Maintenance Fee, 4th Yr, Small Entity. --- End of Maintenance History ---			
Address for fee purposes:	MICHAEL C ANTONE KIRKPATRICK & LOCKHART 1500 OLIVER BUILDING PITTSBURGH PA 15222				